

Synthesis, optimization, and characterization of
chromen-4-one and 1,7-phenanthroline derivatives as
ligands for the orphan G protein-coupled
receptors 35 and 84

DISSERTATION

zur

Erlangung des Doktorgrades Dr. rer. nat.

der

Mathematisch-Naturwissenschaftlichen Fakultät

der

Rheinischen Friedrich-Wilhelms-Universität Bonn

vorgelegt von

Lukas Leopold Wendt

aus Villach

Bonn 2021

Angefertigt mit Genehmigung der Mathematisch-Naturwissenschaftlichen Fakultät der
Rheinischen Friedrich-Wilhelms-Universität Bonn

1. Gutachter: Prof. Dr. Christa E. Müller
2. Gutachter: Prof. Dr. Finn K. Hansen

Tag der Promotion: 14.06.2021

Erscheinungsjahr: 2021

Die vorliegende Arbeit wurde in der Zeit von November 2016 bis März 2021 am Pharmazeutischen Institut der Rheinischen Friedrich-Wilhelms-Universität Bonn unter der Leitung von Frau Prof. Dr. Christa E. Müller angefertigt.

Table of contents

Abstract	1
1 Introduction	5
1.1 G protein-coupled receptors	5
1.2 GPR35	12
1.2.1 GPR35 ligands	15
1.2.2 Synthetic GPR35 ligands	19
1.2.3 GPR35 antagonists	26
1.3 GPR84	31
1.3.2 GPR84 antagonists	39
2 Objectives of the study	43
2.1 Introduction	43
2.2 Compound design of GPR35 agonists	44
2.2.1 Chromen-4-one derivatives	44
2.2.2 Phenanthroline derivatives	47
2.3 Compound design of GPR84 antagonists	50
3 Results and Discussion	55
3.1 Synthesis of 1,7-phenanthroline derivatives	55
3.2 Synthesis of chromen-4-one derivatives	65
3.3 Synthesis of quinolone and indole derivatives	80
3.4 Pharmacological evaluation at GPR35	83
3.4.1 Introduction	83
3.4.2 Results	85
3.4.3 Structure-activity relationships	88
3.5 Pharmacological evaluation at GPR84	127
3.5.1 Introduction	127
3.5.2 Results	129
3.5.3 Structure-activity relationships	130
3.6 Selectivity studies	137
3.6.1 Introduction	137
3.6.2 Selectivity of GPR35 agonists	137
3.6.3 Selectivity of GPR84 antagonists	145
3.7 Drug metabolism and pharmacokinetics	151
3.7.1 Results	151
3.7.2 Discussion	152
4 Summary and outlook	155
4.1 Development of potent and selective ligands for orphan GPCRs	155
4.1.1 Synthesis	155

4.1.2 GPR35.....	160
4.1.3 GPR84.....	163
5 Experimental section	167
5.1 General remarks	167
5.2 Preparation of phenanthrolines, quinolones, and indole derivatives	168
5.2.1 General Procedures	168
Preparation of 68a	169
Preparation of 68b.....	170
Preparation of 68c	171
Preparation of 67d and 68d	172
Preparation of 68e	173
Preparation of 68f	174
Preparation of 68g.....	175
Preparation of 68h.....	176
Preparation of 68i (bufrolin)	178
Preparation of 67j and 68j.....	179
Preparation of 68k.....	180
Preparation of 67l and 68l.....	182
Preparation of 67m and 68m.....	183
Preparation of 68n.....	185
Preparation of 68o.....	187
Preparation of 68p.....	188
Preparation of 68q.....	190
Preparation of 67r and 68r	191
Preparation of 68s	192
Preparation of 68t.....	193
Preparation of 68u.....	195
Preparation of 68v	196
Preparation of 68w	198
Preparation of 68x.....	199
Preparation of 68y.....	200
Preparation of 68z.....	202
Preparation of 111	203
Preparation of 104 and 105	203
Preparation of 96a	204
Preparation of 96b.....	205
Preparation of 99.....	206
Preparation of 101 and 102	207
Preparation of 106, 107, and 108	208

Preparation of 109 and 110.....	209
5.3 Preparation of chromen-4-one derivatives.....	211
5.3.1 General Procedures.....	211
Preparation of 71b.....	212
Preparation of 88a.....	213
Preparation of 88b.....	214
Preparation of 88c.....	215
Preparation of 88d.....	216
Preparation of 88e.....	218
Preparation of 86a.....	219
Preparation of 80 and 87.....	220
Preparation of 86b.....	221
Preparation of 85a.....	222
Preparation of 85b.....	223
Preparation of 89b.....	224
Preparation of 89c.....	225
Preparation of 89g.....	227
Preparation of 89d.....	228
Preparation of 89e.....	229
Preparation of 89f.....	230
Preparation of 89h.....	231
Preparation of 90a.....	232
Preparation of 90b.....	234
Preparation of 73, 89a, 91b, 92b, and 93b.....	235
Preparation of 70, 92a, and 93a.....	238
5.3 Biological experiments.....	241
5.3.1 G protein-coupled receptor 35.....	241
5.3.2 G protein-coupled receptor 84.....	242
6 List of abbreviations.....	244
7 Literature.....	247
8 Acknowledgements.....	269

Abstract

G protein-coupled receptors (GPCRs) are ideal drug targets. Their characteristic tissue distribution, marked ligand specificity, and their roles in countless (patho)physiological processes are being exploited by more than a third of currently available pharmaceutical drugs. However, a substantial number of GPCRs is still underexplored. The so-called orphan receptors are promising new drug targets with unique properties and the potential to expand available treatment options. Unfortunately, the inadequate knowledge of their endogenous activators has hampered target validation studies and drug development as a consequence.

GPR35 and GPR84 are orphan receptors, and both have essential functions in health and disease. While GPR35 promotes anti-inflammatory activities and plays a role in cardiovascular diseases, energy metabolism, and immune regulation, and is predominantly expressed in the gastrointestinal tract, GPR84 was described as a pro-inflammatory receptor. It is mainly expressed on immune cells and upregulated during infection or stress. Efforts to identify the cognate ligands of these receptors have prompted disagreement in the scientific community, since no proposed ligand could convince regarding potency and selectivity.

Thus, synthetic ligands are necessary tools to study orphan receptors such as GPR35 and GPR84. Whereas only few surrogate ligands with high potency have been described for GPR84, many structurally diverse agonists are available for GPR35 - including well-known pharmaceutical drugs and excipients, such as cromolyn, furosemide, and pamoic acid. However, these ligands are notoriously inactive at the rat and especially mouse GPR35 orthologs, which prevents their use in animal studies and impedes preclinical drug development. Even the most potent chromen-4-one-based GPR35 agonists developed by our group were highly human-selective, and recent efforts to obtain derivatives with substantially increased rodent GPR35 activity were unsuccessful.

In the present study, we aimed to enhance our scaffold's activity at the rat and mouse receptor orthologs. Compounds **86b** and **88e** displayed markedly increased potency at the rat and mouse GPR35 compared to the previously reported **26** (PSB-21028)¹ (see **Figure A.1**), yet their activity at the human ortholog was still significantly stronger.

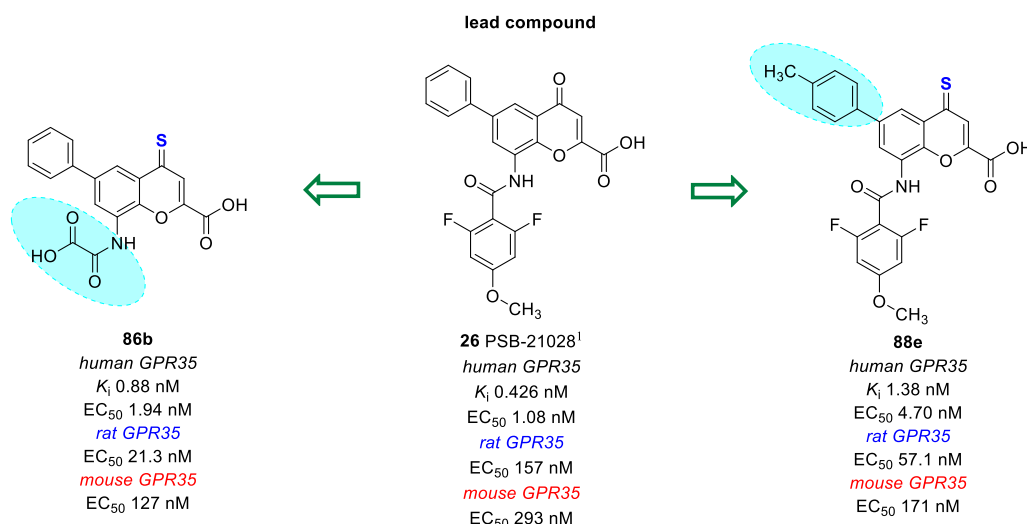


Figure A.1. Chromen-4-one derivatives showed considerable GPR35 ortholog selectivity.¹

Based on a report by MacKenzie et al.,² we also optimized the structure of bufrolin, a failed clinical candidate for the treatment of allergic asthma. It had shown high and equipotent activity at the human and rat GPR35, and by chemically introducing structural modifications, we successfully increased mouse receptor potency. The resulting compounds **68o** and **68p** are the first GPR35 agonists with single-digit nanomolar potency at the mouse receptor ortholog. Considering their equally high affinity and potency at the human and rat receptors, they represent the most useful GPR35 agonists for animal studies currently in existence (**Figure A.2**).

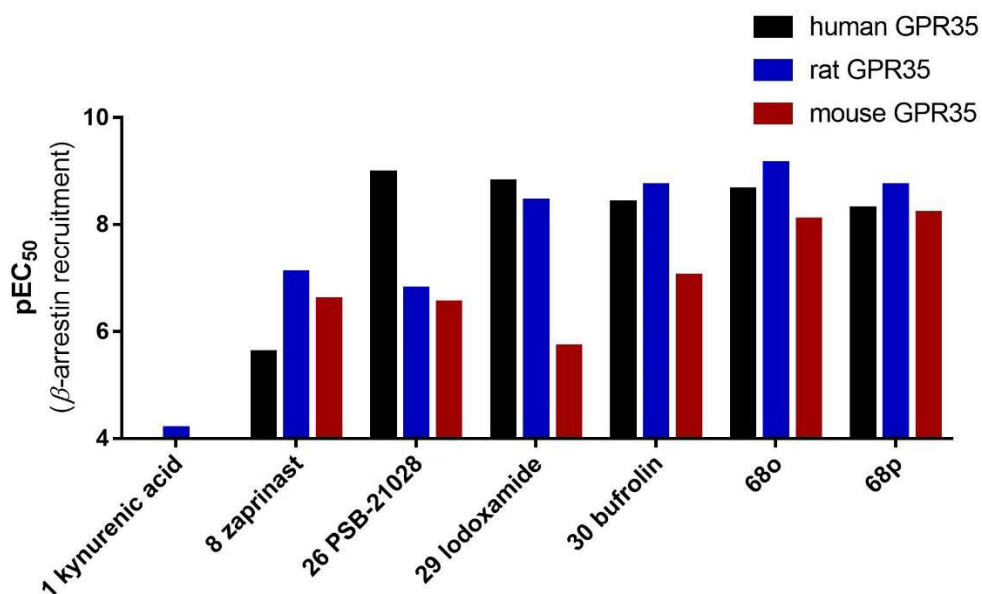


Figure A.2. Compounds **68o** and **68p** display low species selectivity compared to other GPR35 agonists.¹⁻³

The compounds were selective for GPR35 versus a variety of similar GPCRs, including the most closely related GPR55 (sequence similarity: 53%). Preliminary drug metabolism and pharmacokinetic studies demonstrated considerable metabolic stability in vitro, relatively high aqueous solubility, yet low membrane permeability. As such, the compounds are ideal for local application, e.g., in the lungs or the gastrointestinal tract, where GPR35 expression is high, minimizing systemic side effects.

The GPR84 antagonists discussed herein were based on the previously reported PSB-17138 (see **Figure A.3**),¹ which already exhibited nanomolar affinity for the receptor. Its physicochemical properties, on the other hand, were inadequate. The molecule's extremely high lipophilicity ($\log D_{7.4}$ 2.83) negatively affected its solubility and impeded clinical development. By introducing polar structural elements and carefully monitoring their effects on affinity and potency, we successfully increased the lead compound's polarity and significantly enhanced biological activity. Compound **89h** is dramatically less lipophilic than the lead compound ($\log D_{7.4}$ 1.00) and exhibited ~10-fold higher affinity for GPR84. It is also the most potent GPR84 antagonist currently in existence, which occupies the receptor's fatty acid binding site.

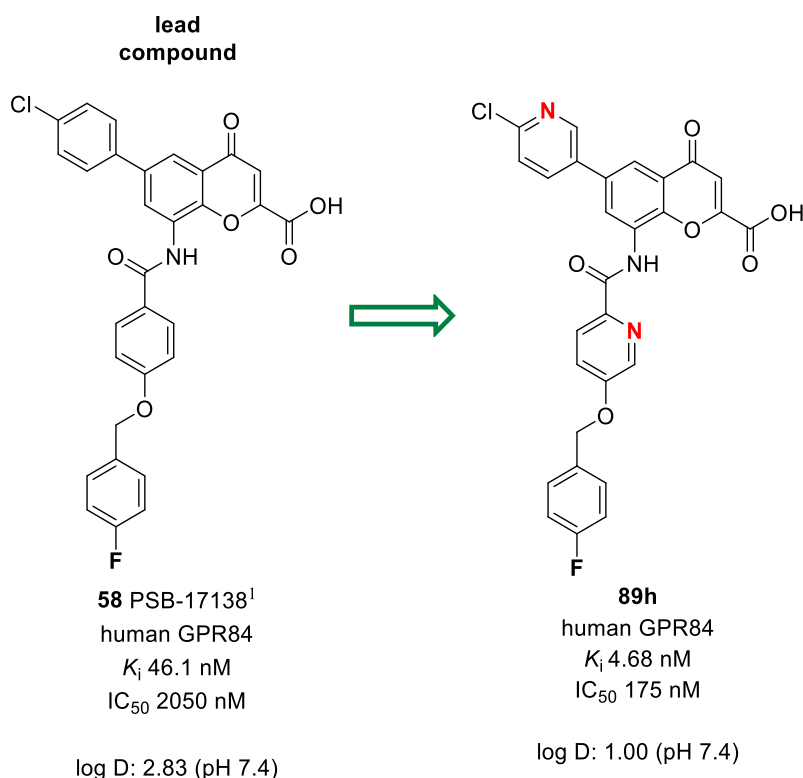


Figure A.3. Affinity, potency, and physicochemical properties of previous GPR84 antagonists could be improved considerably.

1 Introduction

1.1 G protein-coupled receptors

Among the many different biochemical processes ensuring a coordinated cellular response to countless external influences, G protein-coupled receptors (GPCRs) play an integral role. These transmembrane biomolecules are specialized proteins with the ability to be activated by a large variety of signaling molecules, ions, and even light.^{4,5} Upon engagement with its ligand, the receptor reacts to the received stimulus by changing its three-dimensional structure, which triggers a plethora of subsequent intracellular effects.^{6,7} Thus, GPCRs enable cells to react to the outside world and to communicate with each other. Since they control or influence physiological processes, such as blood pressure, heart rate, immune responses, cell differentiation, appetite, vision, and even our senses of taste and smell, it is not surprising that dysregulation can have dire consequences.⁸⁻¹¹

The important roles of GPCRs in major diseases, their extreme structural and functional diversity, their highly specific tissue distribution, their localization in cell membranes, and their specialized response to endogenous and exogenous ligands make them ideal targets for pharmacological intervention.^{9,11,12} Indeed, the first synthetic ligand intended for therapeutic use targeting a GPCR (propranolol, a blocker of β -adrenergic receptors) was developed back in 1964,¹³ before the concept of individual cellular receptor proteins had even been firmly established.^{9,14} Advances in protein purification, sequencing, and polymerase chain reaction (PCR) technology revealed unexpected sequence homology between the β_2 -adrenoceptor and rhodopsin (the protein responsible for visual phototransduction). Both proteins were predicted to incorporate seven transmembrane (7TM) regions giving rise to the idea of a large 7TM-receptor superfamily.^{15,16} Since then, ever more GPCRs have been discovered, studied, and exploited as drug targets. To date, at least 30% of all pharmaceutical drugs convey their effects by interacting with such a receptor.^{9,12}

The growing amount of information about their amino acid sequence allowed the grouping of receptors according to sequence identity and functional similarity. While different classification schemes have been proposed, the most common ones are the A-F system, which divides all GPCRs into six classes (classes A-F) based on their amino acid sequence (see **Figure 1.1**),¹⁷⁻¹⁹ and the GRAFS system, grouping vertebrate GPCRs into five families (Glutamate, Rhodopsin, Adhesion, Frizzled/taste, and Secretin) according to evolutionary characteristics.^{20,21} Class A

receptors are rhodopsin-like receptors and constitute the largest group of GPCRs with approximately 700 representatives. This group can be further divided into subfamilies (in the A-F system) or into so-called “branches” α - δ (in the GRAFS system). Thus, the GPCR superfamily forms the largest and most diverse group of membrane proteins, accounting for roughly 800 different members in humans (the exact number of distinct human GPCRs is not known).^{4,22} Although the classes or families share remarkably little of their sequence identity among each other (only 20-30%), all GPCRs appear to have their general 7TM architecture and intracellular signaling mechanisms in common.²³

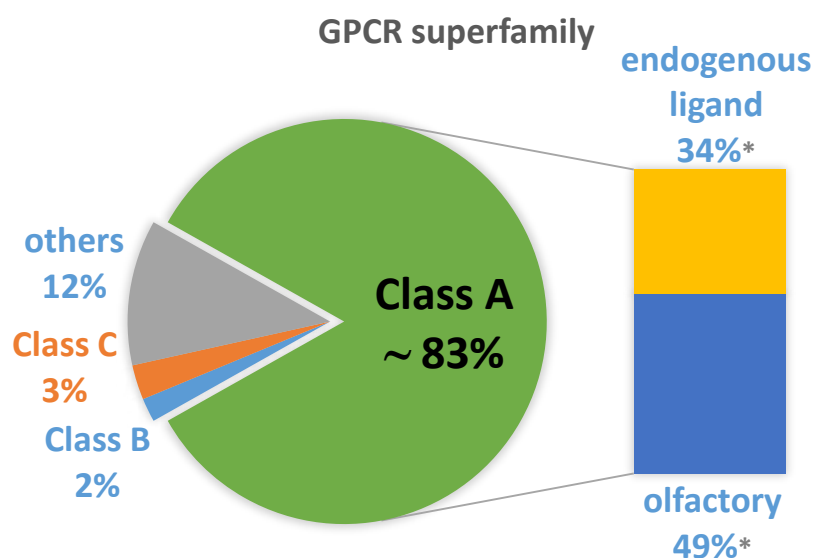


Figure 1.1. Classification of GPCR genes according to amino acid sequence.²⁴ (*predicted from sequence)

All GPCRs are believed to possess seven transmembrane α -helices (TM 1-7) that are connected by three intracellular (ICL 1-3) and three extracellular loops (ECL 1-3). **Figure 1.2** provides a schematic overview. The N-terminus is located outside of the cell, while the C-terminus is on the inside.^{5,25} Each receptor region plays an important role in signal transduction. The extracellular parts are responsible for guiding the correct ligand into the binding pocket, which can be located either deep inside the 7TM domain, at ECLs, or on the N-terminus. The TM bundle, on the other hand, is in charge of initiating conformational changes of its α -helices upon ligand binding. These alterations allow the intracellular domains to change their affinity for a variety of cytosolic proteins, causing different cellular effects.⁵ While extracellular regions are

highly variable among receptors, allowing for a large number and diversity of possible ligands,²³ the intracellular parts are rather conserved and possess multiple motifs or patterns that are associated with distinct biochemical tasks, such as protein stabilization or G protein activation.^{26,27}

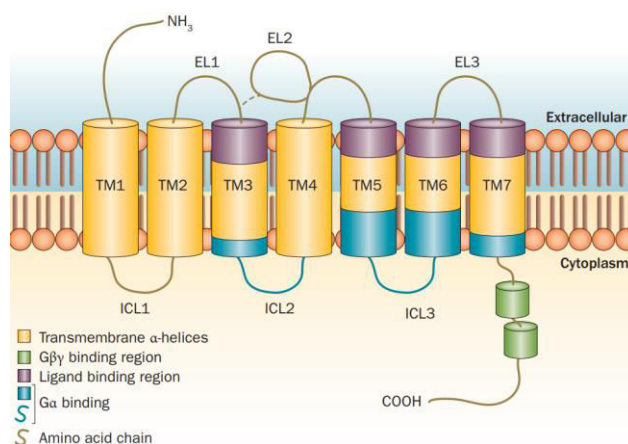


Figure 1.2. Schematic representation of a typical GPCR. EL, extracellular loop; ICL, intracellular loop; TM, transmembrane domain.²⁸

The idea of so-called “G proteins” (guanine nucleotide-binding proteins) being responsible for intracellular effects of some bioactive molecules (e.g. adrenaline) was suggested by Martin Rodbell and co-workers in the 1970s^{REF29} and soon afterwards corroborated by Alfred Gilman’s group, who succeeded in the purification of a G protein.³⁰ Nowadays, it is well-established that GPCRs elicit their actions via those heterotrimeric G proteins.⁶ They consist of three subunits (α , β , γ), however, it is the α -subunit that is responsible for guanosine triphosphate (GTP) or diphosphate (GDP) binding and for GTP hydrolysis. The β and γ subunits are tightly bound to each other forming the $\beta\gamma$ -complex, which is regarded as one functional unit.^{6,7,31} Interestingly, these subunits all belong to a relatively small gene family of only 16 different α , five β , and twelve γ isoforms. Compared to the extreme variability of GPCR genes, this underlines the high conservation of the intracellular signaling processes shared by all GPCRs.^{6,32}

Although both, α -subunit and $\beta\gamma$ -complex, can interact with a number of distinct effector systems, the nature of the α -subunit determines the classification of the entire G protein. There are four major types of G α protein subunits grouped together according to function: G α_s , G $\alpha_{i/o}$, G $\alpha_{q/11}$, and G $\alpha_{12/13}$ (see **Figure 1.3**).^{6,33} While the G α_s (or G $_s$) protein stimulates the enzyme

adenylate cyclase (AC) and thus the formation of 3',5'-cyclic adenosine monophosphate (cAMP), an important second messenger molecule, the $G_{\alpha_{i/o}}$ (or $G_{i/o}$) protein inhibits the enzyme, leading to a reduction of intracellular cAMP concentration. The $G_{\alpha_{q/11}}$ (or $G_{q/11}$) protein, instead, stimulates the enzyme phospholipase C (PLC), which cleaves the minor membrane phospholipid phosphatidylinositol 4,5-bisphosphate (PIP_2) into the two second messenger molecules inositol trisphosphate (IP_3) and diacylglycerol (DAG), ultimately triggering the release of Ca^{2+} into the cytoplasm among other effects. The initiation of the $G_{\alpha_{12/13}}$ (or $G_{12/13}$) pathway activates small GTPases, such as RhoA, which regulate cytoskeleton rearrangements necessary for cell migration.^{6,34–36}

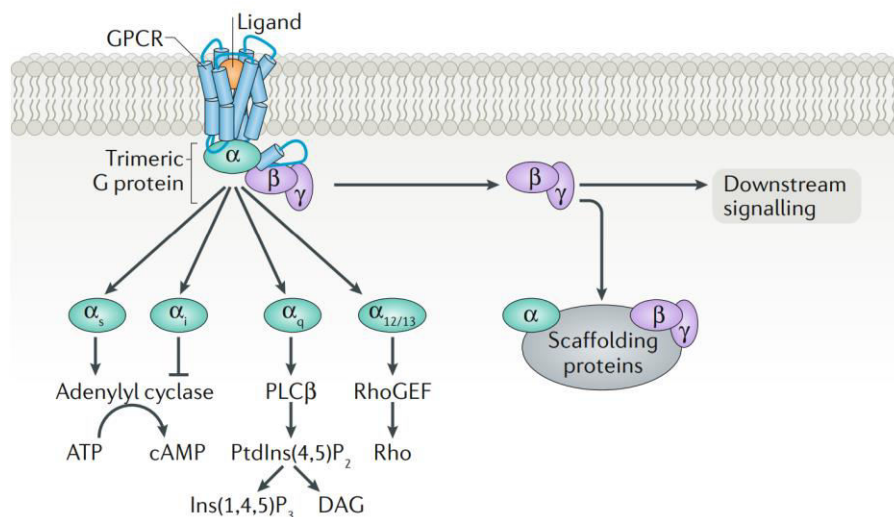


Figure 1.3. Overview of G proteins and their respective intracellular effectors.³⁷

The $G_{\beta\gamma}$ complex engages in its own intricate signaling, and – depending on subunit composition – it interacts with many effector proteins, including AC, PLC, ion channels, extracellular signal-regulated kinases (ERK), and G protein-coupled receptor kinases (GRKs), among others.^{38–40} GRKs are of particular significance for receptor desensitization via the recruitment of so-called arrestin proteins (or β -arrestins). These block the interaction of the GPCR with its G protein and also facilitate the internalization (endocytosis) of the receptor by their interaction with clathrin, for example.^{41,42} The $\beta\gamma$ -complex additionally stabilizes the $G\alpha$ subunit, increasing its affinity for GDP, which promotes the α subunit's inactive state. Thus, $G_{\beta\gamma}$ contributes to signal termination and the restoration of cellular equilibrium, but it is clearly also involved in other processes that are less straightforward.^{42,43}

or receptor desensitization via β -arrestins (for all receptors that recruit them). These assay systems are particularly important for the pharmacological characterization of new molecules in drug development and were used extensively to investigate new GPCR ligands of the present study (see below).

1.2 GPR35

In 1998, the human G protein-coupled receptor 35 (GPR35) was first described as an open reading frame on chromosome 2q35.3 coding for two different splice variants termed GPR35a and GPR35b.⁵⁰ While the former protein consists of 309 amino acids, the latter contains 31 additional amino acids at the extracellular N-terminus (see **Figure 1.5**).^{51,52} Although the significance of this extension is still unclear,^{51,53} there is evidence that the two isoforms have slightly different functions.^{2,52-54} It appears that the shorter form of the receptor is more abundant.^{52,55} Phylogenetically, GPR35 is most closely related to the cannabinoid- and lysophosphatidylinositol-activated GPR55 (30% sequence identity, 53% similarity) and to the lysophosphatidic acid receptor 4 (LPA₄, formerly GPR23, 32% sequence identity, 54% similarity). Thus, it belongs to the δ -branch of class A (rhodopsin-like) receptors.^{4,50,56}

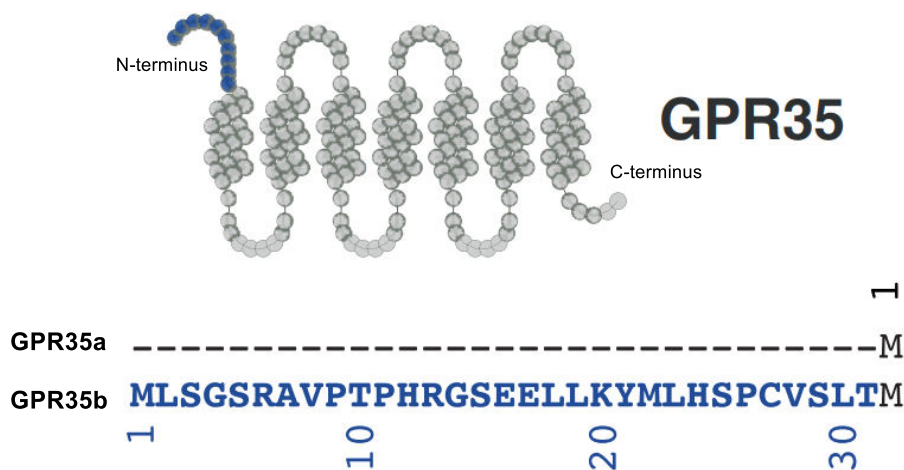


Figure 1.5. GPR35 is expressed as two distinct isoforms in humans: GPR35a and GPR35b.⁵¹

Orthologs of the receptor can be found in many other species, including apes, rodents, other mammals, amphibians, and even fish,⁵³ however, they generally share low sequence identity with the human GPR35. The mouse receptor ortholog, for example, shares only 73% of its amino acid sequence with the human GPR35a (82% similarity), and the rat receptor has only 72% sequence identity (81% similarity) with the human counterpart.^{53,57} Even among rodent receptor orthologs there is significant disparity, with mouse and rat GPR35 sharing only about 85% of their amino acid sequence (92% similarity).⁵⁷ Considering the importance of rodents as

model organisms for preclinical drug development, these differences have far-reaching implications for target validation, safety, and efficacy studies (see below).

Whereas initial studies had reported GPR35 signaling to be mediated by pertussis toxin sensitive G proteins lowering intracellular 3',5'-cyclic adenosine monophosphate (cAMP) concentrations (i.e. $G_{i/o}$),^{55,58-60} multiple later works suggested that pivotal G protein-mediated signaling occurs via the poorly characterized $G\alpha_{13}$.^{3,61-63} Using chimeric G proteins and the agonist zaprinast, Jenkins et al. showed that human and rat GPR35 coupled most effectively to $G\alpha_{13}$ and preferred it even over the related $G\alpha_{12}$.^{3,61} McCallum et al. demonstrated that GPR35-mediated cell migration was inhibited by selective Rho-kinase inhibitors, indicating the involvement of $G\alpha_{13}$, which regulates Rho-guanine exchange factors.⁶² More recently, Mackenzie et al. used clustered regularly interspaced short palindromic repeat (CRISPR)-Cas9 (CRISPR-associated protein-9) on human-GPR35-transfected human embryonic kidney 293 (HEK293) cells to eliminate the expression of G proteins. In transforming growth factor- α (TGF- α) shedding studies, the elimination of $G\alpha_{12}$ and $G\alpha_{13}$ prevented GPR35 agonist-mediated TGF- α shedding entirely, which is indicative of a major role of these G proteins for GPR35's signal transduction.⁶³ Other groups have observed a G_q -mediated elevation of calcium,^{64,65} which could not be corroborated later on.^{61,63}

While the exact roles of GPR35 in the human body are still largely unclear, early studies focused on single nucleotide polymorphisms (SNPs) in the receptor gene and their association with diseases. Multiple genome wide association studies have linked variations of the receptor to mostly inflammation-related diseases, including diabetes,⁶⁶ atherosclerosis,⁶⁷ inflammatory bowel diseases,⁶⁸⁻⁷¹ ankylosing spondylitis,^{70,72} and primary sclerosing cholangitis.⁶⁹ The disease-associated effects of individual receptor variants have been reviewed in detail.^{53,56}

Another path towards identifying a receptor's (patho)physiological functions is to investigate its expression pattern. Since its discovery, many groups have reported GPR35 mRNA expression in various tissues. Transcripts were most abundant in the digestive tract with significant expression in the stomach, small intestine,⁵⁰ colon, and rectum in both human and rodent tissues.^{57,73} Recently, Milligan and coworkers reported the generation of a transgenic knock-in mouse line in which a hemagglutinin (HA) epitope tag sequence was introduced in-frame with the C-terminus of mouse GPR35. Anti-HA staining was used to visualize the receptor and showed high expression throughout colonic crypts.⁵³ Previously, an extensive expression analysis of GPCRs had found GPR35 expression in mouse vagal afferent neurons innervating the gastrointestinal tract.⁷⁴ In 2018, the significance of GPR35 expression in the

gastrointestinal tract was tested in an experimental mouse model of ulcerative colitis.⁷⁵ GPR35 knockout mice showed massive pathological alterations including the complete loss of colonic crypts upon drinking dextran sulfate sodium (DSS)-containing water. Compared to wild type, lack of GPR35 significantly worsened the disease outcome. Thus, GPR35 could play an important role in the protection from colonic inflammation.⁷⁵ High receptor levels were also reported in cells associated with the immune system, including human, rat, and mouse splenic tissue,^{57,73} human thymus,⁷³ and on human monocytes, neutrophils, T cells, and dendritic cells,⁵⁷ as well as natural killer T cells.⁵⁸ GPR35 expression has fittingly been associated with certain types of cancer, including gastric,⁵² breast,⁷⁶ colon,⁵⁴ and lung cancer.⁷⁷ The receptor's role in cancer is ambiguous, since GPR35 agonists have been reported to reduce cancer growth,⁵³ but recently, Schneditz et al. showed that, conversely, GPR35 depletion reduced intestinal tumorigenesis in a mouse colon cancer model.⁷⁸ In humans and mice, the receptor is reportedly also highly expressed in adipose tissue.^{57,73} Although no receptor expression was detected in heart tissue under physiological conditions,⁵⁰ a study found significant receptor upregulation in myocardial tissue from heart failure patients compared with healthy control tissue, and artificial receptor overexpression led to cellular hypertrophy and reduced cellular survival.⁷⁹ The study also found a significant blood pressure increase in GPR35 knockout mice compared to wild type littermates.⁷⁹ Since hypoxia is at the root of many cardiac ailments, a group investigated the consequences of both acute and chronic hypoxia on mouse cardiomyocytes due to either myocardial infarction or chronic hypertension. Interestingly, the observed GPR35 overexpression was found well in advance of pathological cardiac hypertrophy and remodeling, which could be used to predict the development of heart failure or to monitor blood pressure management.⁸⁰ More recently, a group studying the effects of angiotensin II infusion upon GPR35 knockout and in wild type mice observed a protective effect of GPR35 depletion against hypertension and cardiac dysfunction.⁸¹ Taken together, these results indicate that GPR35 is involved in blood pressure regulation and may represent a novel drug target for the therapeutic intervention in hypertension. High receptor mRNA levels were also found in lung tissue, skeletal muscle, uterus, and dorsal root ganglion.^{57,59,73,82} The receptor was also present in brain tissues, including rat cerebrum,⁵⁷ mouse astrocytes,⁸³ and rat hippocampus.⁸⁴ The expression in dorsal root ganglia^{59,82,83,85,86} and the nervous system in general^{74,82,84,85} has offered an explanation for antinociceptive effects of various GPR35 agonists (see below).^{59,86–88}

1.2.1 GPR35 ligands

Most of the information about a receptor's physiological roles can be derived from in vitro and in vivo experiments with its natural agonist, characterizing its effects on receptor-expressing cells, tissues, or the entire organism. However, despite many attempts by the scientific community, the cognate ligand of GPR35 has not been satisfactorily identified thus far. Therefore, the receptor is officially still considered a so-called "orphan" receptor.⁸⁹

Kynurenic acid (**1**, **Figure 1.6**) was the first reported endogenously produced GPR35 agonist.⁷³ It was discovered in a screening of ~300 biochemical intermediates at the human GPR35, and it has since been confirmed by multiple studies to activate the receptor. Kynurenic acid is an important metabolite in the kynurenine pathway, which accounts for the metabolism of about 95% of free tryptophan.⁹⁰ Like GPR35, it is present in many tissues including the brain, pancreas, colon, spleen, and muscle,⁵⁶ but there are several problems with this receptor-ligand pairing. Firstly, the reported potencies for kynurenic acid at the human, rat, and mouse receptor orthologs (EC_{50} 39.2 μ M, 7.4 μ M, 10.7 μ M, respectively)⁷³ are too low to allow receptor activation in vivo, since such high kynurenic acid tissue concentrations are hardly present under physiological conditions (nanomolar kynurenic acid concentrations).^{55,91} An independent study observed even weaker potency at human and rat receptors (EC_{50} >100 μ M, 66 μ M, respectively) in bioluminescence resonance energy transfer (BRET) assays, using HEK293 cells transiently expressing C-terminally tagged forms of GPR35 and β -arrestin-2.⁶¹ Similar activity was determined in radioligand binding assays against the radioligand [³H]PSB-13253 (K_i 137 μ M) using membrane preparations of CHO cells recombinantly expressing the human GPR35.⁹² Moreover, multiple groups failed to produce a significant response for kynurenic acid in functional assays at the human receptor ortholog at all.^{64,92,93} Secondly, kynurenic acid is actually equally or more potent at other targets. Among other effects, it acts as a neuroprotective endogenous antagonist at the *N*-methyl-D-aspartate (NMDA)-receptor ion channel complex (IC_{50} 8-10 μ M), as a non-competitive antagonist at the α 7-nicotinic acetylcholine receptor (IC_{50} ~10 μ M), and has agonist activity at the arylhydrocarbon receptor (IC_{50} 1-10 μ M).^{56,90} Therefore, it remains controversial, whether kynurenic acid can be GPR35's cognate ligand, and how the compound's low potency, species preference, and lack of selectivity can be explained.^{53,56}

Other promising endogenously produced GPR35 agonists were reported by Oka et al.⁶⁴ The group demonstrated that lysophosphatidic acid (LPA) species, especially 2-oleoyl-LPA (**2**, **Figure 1.6**) and 2-linoleoyl-LPA, could stimulate [Ca^{2+}]_i mobilization in human-GPR35-

transfected HEK293 cells above the level observed for endogenously expressed LPA receptors. Subsequent *in vitro* assays measuring ERK_{1/2} phosphorylation (at 1 μM), RhoA protein activation (at 1 μM), and receptor internalization (at 10 μM) suggested similar involvement of GPR35.⁶⁴ Interestingly, LPA species have been associated with a number of diseases including cancer, obesity, impaired glucose tolerance, and pain, which is reminiscent of GPR35's pathophysiological profile (see above). However, there are some issues with the pairing of LPA species like 2-oleoyl-LPA and GPR35 as suggested by Oka et al. Firstly, GPR35 is not known to robustly couple to the $\text{G}\alpha_q$ pathway, and another group failed to observe recruitment of β -arrestin to the receptor upon stimulation with LPA.⁹⁴ This could indicate ligand bias of LPA species towards the $\text{G}\alpha_q$ pathway, which has not been described for other GPR35 agonists.⁹¹ Also, the study did not assess whether the measured effects could be blocked by GPR35 antagonists, leaving open the possibility that they were mediated via another mechanism. Considering that the original results could not be replicated by independent groups,⁵³ the currently available data do not support this receptor-ligand pairing.

Another interesting suggestion for the natural ligand of GPR35 was the cyclic nucleotide guanosine-3',5'-cyclic monophosphate (cGMP, **3**, **Figure 1.6**) proposed by Southern et al. The group screened 10,500 endogenous molecules at the human GPR35 using β -arrestin recruitment assays and identified cGMP and a number of synthetic derivatives as GPR35 agonists. The natural cGMP displayed only weak potency with an EC_{50} value of $\sim 130 \mu\text{M}$.⁹⁴ It has since been questioned whether cGMP could reach (extracellular) concentrations high enough to activate the receptor efficiently *in vivo*.

In a campaign to identify further endogenous GPR35 agonists, Deng et al. employed whole cell dynamic mass redistribution (DMR) assays in HT-29 cells (a human colorectal cancer cell line natively expressing GPR35) to screen multiple tyrosine metabolites for their activity.⁹³ Fluorescence resonance energy transfer (FRET)-based arrestin translocation assays with GPR35-transfected cells were used to confirm that, among others, 5,6-dihydroxyindole-2-carboxylic acid (DHICA, **4**, **Figure 1.6**), 3,3',5-triiodothyronine (T_3), and 3,3',5'-triiodothyronine (reverse T_3 , **5**) were GPR35 agonists with micromolar potency (EC_{50} 22.9 μM , 513 μM , and 108 μM , respectively). Reverse T_3 was the most potent endogenous agonist described in the study, generating DMR with an EC_{50} value of 5.89 μM ,⁹³ however, as with other suggested cognate ligands (see above), it is unlikely that either one of the reported molecules reaches sufficient tissue concentrations *in vivo* to activate GPR35. Nevertheless, it is possible that increased production of reverse T_3 under certain thyroid disorders leads to

GPR35 activation, thus contributing to the poorly understood nongenomic effects of thyroid hormones (e.g. stimulation of tumor cell proliferation).^{91,93,95}

More recently, Maravillas-Montero and coworkers reported that the orphan chemokine (C-X-C motif) ligand 17 (CXCL17) induced a robust calcium flux in the human-GPR35-transfected mouse pro-B cell line Ba/F3 and HEK293 cells in a dose-dependent manner.⁶⁵ The response was observed at nanomolar CXCL17 concentrations, which is within the physiologic range of this chemokine in vivo. The measured response of the human monocytic THP-1 cell line could be increased through pretreatment with prostaglandin E₂ (PGE₂), which elevated endogenous GPR35 expression by these cells confirmed via quantitative real-time polymerase chain reaction (qRT-PCR). Interestingly, the group reported strong downregulation of GPR35 in CXCL17 knockout mouse lung tissue compared to wild type, which was regarded as evidence of a receptor-ligand match. The authors went so far as to suggest renaming GPR35 CXCR8 (CXC chemokine receptor 8).⁶⁵ Other groups have since failed to corroborate these findings.^{96,97} Park and colleagues were able to confirm the agonist activity of a well-known synthetic GPR35 agonist in GPR35-transfected HEK293 cells, but failed to observe any GPR35-dependent effects upon stimulation with either mouse or human CXCL17 in alkaline phosphatase-tagged transforming growth factor- α (AP-TGF α) shedding assays.⁹⁶ Moreover, the group could show that GPR35 agonist-induced migration inhibition of THP-1 cells was efficiently blocked by a synthetic GPR35 antagonist or by silencing GPR35 expression via GPR35 siRNA transfection. In contrast, CXCL17 actually stimulated THP-1 cell migration and neither GPR35 antagonist treatment nor siRNA transfection could block this effect. This strongly suggests that – at least in THP-1 cells – the effects of CXCL17 are not mediated by GPR35. Binti Mohd Amir and coworkers also set out to investigate the connection between GPR35 and CXCL17.⁹⁷ While a synthetic GPR35 agonist induced significant β -arrestin recruitment to human, rat, and mouse GPR35 in transfected HEK293T cells, no effect could be observed for CXCL17 even at a high concentration of 100 nM. Since the lack of arrestin recruitment is not tantamount to being inactive, the group coexpressed human GPR35 alongside chimeric G α subunits in HEK293 cells. Again, synthetic GPR35 agonists produced a dose-dependent response, but CXCL17 failed to emulate this effect. Furthermore, the group employed an array of different assays of chemotaxis, calcium flux, and receptor endocytosis, using different cell lines and CXCL17 concentrations, yet the chemokine elicited no GPR35-dependent effects. Although PGE₂-treated THP-1 cells did in fact respond to a 10 μ M concentration of CXCL17 in a real-time assay of cell migration, the presence of 1 μ M GPR35 antagonist (ML145, IC₅₀ ~25 nM, for structure see next section) had no influence on cell migration.⁹⁷ In line with these findings, a

small study found that common synthetic GPR35 agonists implausibly counteracted the pain-inducing effects of CXCL17 in a mouse pain model.⁸⁷ Taken together, these data are overwhelming evidence that GPR35 is not involved in CXCL17-mediated effects.

The most recent report of natural substances acting as GPR35 agonists was published by Foata and colleagues.⁹⁸ They investigated the ability of human milk oligosaccharides (HMOs), a group of more than 100 related sugars present in human milk, to activate human G protein-coupled receptors. The group used a mixture of six distinct HMOs and screened a panel of 165 mostly deorphanized GPCRs for agonist activity in β -arrestin recruitment assays. Of all the GPCRs, only GPR35 was activated by the HMO mixture at 2 mM. Upon further investigation, only two out of the six HMOs were shown to be GPR35 agonists: lacto-*N*-tetraose (LNT, **6**, **Figure 1.6**) and 6'-*O*-sialyllactose (6'SL, **7**) were each able to activate the receptor with an EC₅₀ value of 2.18 mM. Interestingly, the evoked efficacy was higher when an equimolar mixture of LNT and 6'SL was used (69%) than with the individual HMOs (17% for **6**, 20% for **7**), which is indicative of a cooperative effect of multiple HMOs. Foata et al. could also show additive effects of LNT and 6'SL with kynurenic acid (**1**). The addition of 200 μ M of **1** increased the efficacy of HMOs at low concentrations without altering maximal effects, indicating a cooperative effect of the combination. The authors speculated that the effects of HMOs on GPR35 might also be mediated by pathways other than direct receptor activation. They showed that the presence of 2-*O*-fucosyllactose (2'FL) increased the concentration of kynurenic acid in fermented infant stool samples. With water being absorbed in the gastrointestinal (GI) tract, the concentrations of some HMOs like LNT or 6'SL in milk could reach active levels. Along with GPR35's strong expression in the intestine, this might play a role for the attenuation of abdominal pain in breastfed infants. Since the study only investigated six out of ~100 HMOs, and homologs of GPR35 are also present in non-mammalian animals,⁵³ more extensive research is needed to clarify the effect of milk oligosaccharides on GPCRs like GPR35. The fact that the receptor is also expressed on tissues outside of the GI tract and that the bioavailability of HMOs is below 1%⁹⁸ poses another challenge for this receptor-ligand match.

In conclusion, although many molecules have been proposed to be the natural ligand of GPR35, there is still no consensus in the scientific community about the identity of the receptor's cognate activator. While kynurenic acid (**1**, **Figure 1.6**), 2-oleoyl LPA (**2**), cGMP (**3**), DHICA (**4**), reverse T₃ (**5**), CXCL17, and HMO species (**6** and **7**) are the most intriguing suggestions, each of them disqualifies for one or more reasons (see above). Until more conclusive evidence is presented in future research, GPR35 still remains an orphan receptor.

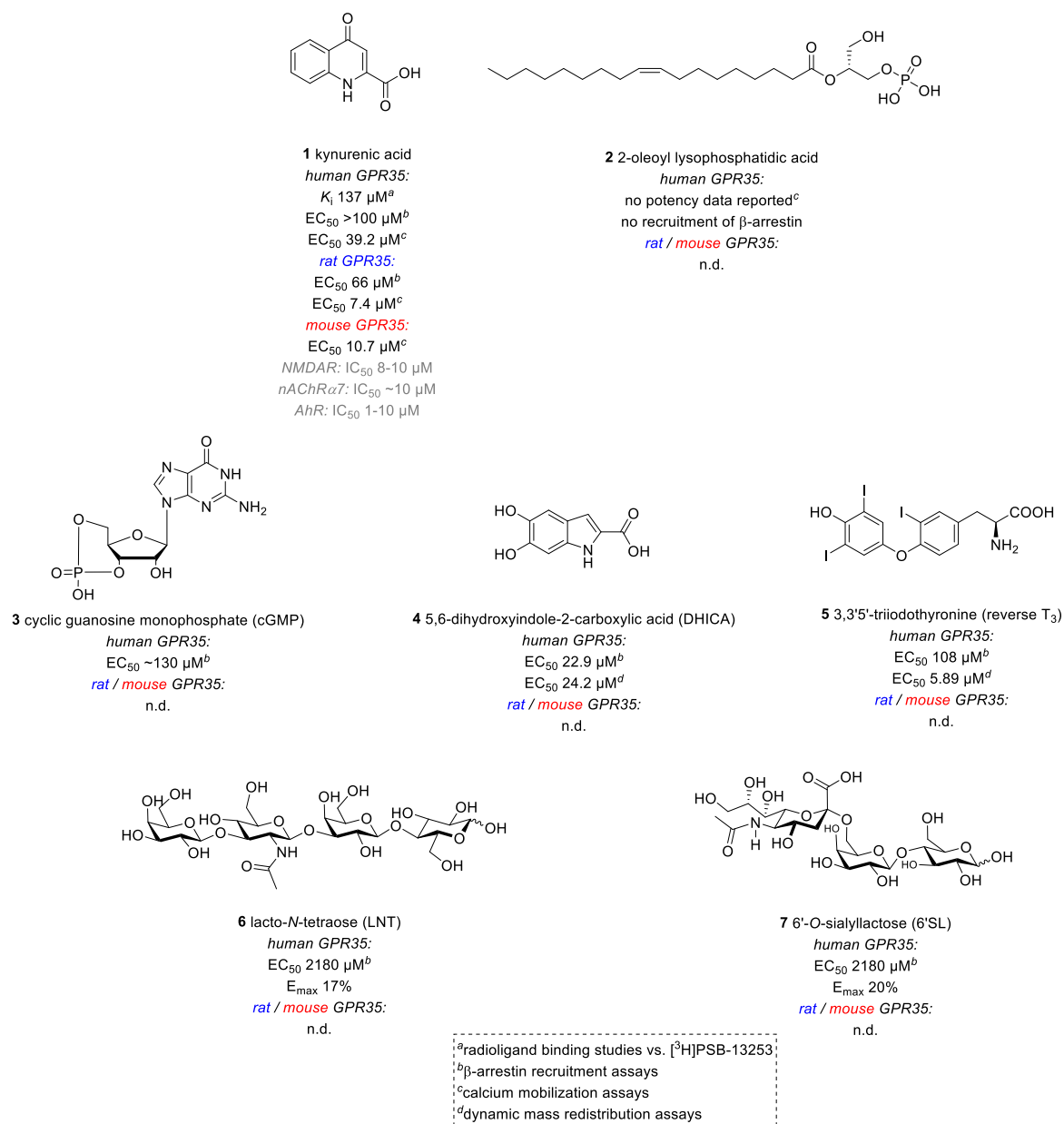


Figure 1.6. Proposed endogenous ligands for GPR35 with potency and affinity data determined in different assay systems.^{61,64,73,90,93,94,98} n.d., not determined.

1.2.2 Synthetic GPR35 ligands

While the elucidation of GPR35's natural agonist has been fruitless so far, the discovery of synthetic ligands has been more successful. Synthetic GPR35 agonists and antagonists have been vital for the characterization of the receptor, facilitating both in vitro and in vivo experiments. The first surrogate GPR35 agonist was described by Taniguchi et al.⁵⁷ Zaprinast (**8**, **Figure 1.7**), a phosphodiesterase (PDE) inhibitor and lead compound for the development

of sildenafil (**9**),⁹⁹ is a cyclic guanosine monophosphate (cGMP, **2**, **Figure 1.6**) derivative with moderate inhibitory potency at PDE5 ($IC_{50} \sim 0.5 \mu\text{M}$) and PDE6 ($IC_{50} 0.15 \mu\text{M}$).^{57,99} It is also an inhibitor of other PDEs with much lower potency.⁵⁷ Zaprinast was shown to raise intracellular calcium levels in calcium mobilization assays in HEK293 cells coexpressing the human or rat GPR35 and chimeric $G\alpha_q$ proteins and promiscuous G_{16} protein. In that system, zaprinast was found to be an agonist at the human GPR35 with an EC_{50} value of 840 nM and – like kynurenic acid (**1**, **Figure 1.6**) – it showed even higher potency at the rat receptor ortholog (EC_{50} 16 nM).⁵⁷ An independent group later confirmed that the compound activated the human, rat, and mouse GPR35 in BRET-based β -arrestin-2 recruitment assays as a full agonist (EC_{50} 2.51 μM , 80 nM, 250 nM) in transfected HEK293T cells.¹⁰⁰ The affinity of zaprinast for the human GPR35 was reported with a K_i value of 401 nM determined vs. the radioligand [^3H]PSB-13253 (see below) in competition binding experiments.⁹² Because of its reasonable potency across species and its high efficacy, zaprinast has since become the standard reference agonist for in vitro GPR35 assays.^{3,53,60,100} However, its value to investigate the receptor's pharmacology is limited by its activity at various PDE families.

A surprising discovery was reported by Zhao and colleagues in 2010.¹⁰¹ The hitherto believed to be entirely biologically inactive pharmaceutical excipient pamoic acid (**10**, **Figure 1.7**) was identified as a hit compound in a high-throughput screening at the human GPR35. The primary screen discovered oxantel pamoate and pyrantel pamoate (antihelmintic drugs in the form of their pamoic acid salts), yet pyrantel tartrate failed to activate the receptor in a follow up screen.¹⁰¹ Upon testing the excipient itself, pamoic acid (EC_{50} 79 nM) was significantly more potent than zaprinast (EC_{50} 1 μM) or kynurenic acid (EC_{50} 217 μM) in a β -arrestin assay at human GPR35. Remarkably, the once deemed biologically inactive supporting agent pamoic acid was discovered to be the most potent human GPR35 agonist at the time.^{3,101} While Zhao et al. initially also reported some activity of the compound at the mouse receptor,¹⁰¹ later studies could not corroborate these findings. An extensive follow-up study by Jenkins et al. demonstrated that pamoic acid is only a partial GPR35 agonist ($E_{\text{max}} \sim 55\%$ compared with **8** in BRET-based β -arrestin-2 interaction assays), highly selective for the human ortholog, and virtually inactive at mouse and rat GPR35 at the highest tested concentration (10 μM), limiting its usefulness in animal studies.¹⁰²

In the search for additional GPR35 agonists, Yang et al. screened a library of commercial drugs and discovered the widespread anti-asthma medicine cromolyn disodium (cromoglicic acid, **11**, **Figure 1.7**) to be a potent GPR35 agonist.¹⁰³ Aequorin assays measuring calcium flux were used to determine receptor activation in human, rat, or mouse GPR35- and Gq_5 -cotransfected

CHO cells. Cromolyn disodium (**11**) displayed similar potency as zaprinast (**8**) at the human receptor ortholog (EC_{50} 209 nM vs. 129 nM, respectively), but was significantly weaker at the rat and mouse receptors (**11**: EC_{50} 891 nM (rat), 1.55 μ M (mouse); **8**: EC_{50} 16 nM (rat), 24 nM (mouse)). Based upon their findings, they tested other mast-cell stabilizing drugs and discovered that nedocromil (**12**) was even more potent than **11** (EC_{50} 126 nM). However, its potency at rat and mouse receptors was in the micromolar range (rat GPR35: EC_{50} 2.8 μ M; mouse GPR35: EC_{50} 7.2 μ M).¹⁰³

Jenkins and coworkers also identified the mast-cell stabilizing drug cromoglicic acid (**11**, **Figure 1.7**) as well as the anticoagulant dicumarol (**13**) to be potent GPR35 agonists.³ They also reported agonist activity for the flavonoids quercetin (**14**) and luteolin (**15**) and the anti-inflammatory drug niflumic acid (**16**). Curiously, flumenamic acid (**17**), which differs from niflumic acid only by one nitrogen atom (see **Figure 1.7**), was entirely inactive at both human and rat GPR35.³

Other minor GPR35 agonists were discovered by Deng et al. who reported activity at the human GPR35 for their 2-(4-methylfuran-2-(5*H*)-ylidene)malononitrile and thieno[3,2-*b*]thiophene-2-carboxylic acid derivatives (**18** and **19**, respectively).¹⁰⁴ Those derivatives were more potent than zaprinast in dynamic mass redistribution (DMR) assays, but failed to potently induce β -arrestin recruitment (for EC_{50} values, see **Figure 1.7**). The study was among the first to highlight the importance of a carboxylic acid or bioisosteric group for efficient receptor activation.¹⁰⁴ The same group subsequently also optimized the structure of the proposed endogenous ligand DHICA (**4**, EC_{50} 23.6 μ M) developing derivative **20** (**Figure 1.7**) with increased potency in DMR assays (EC_{50} 160 nM). However, its potency in β -arrestin recruitment assays was considerably weaker (EC_{50} 46.5 μ M) and no activity was reported for other receptor orthologs.¹⁰⁵

A small study found the common loop-diuretic drugs furosemide (**21**, **Figure 1.7**) and bumetanide (**22**) to display activity at the human GPR35 in aequorin-based Ca^{2+} -assays (**21**: EC_{50} 6.17 μ M, **22**: EC_{50} ~10 μ M).¹⁰⁶ The authors speculated that the clinically observed antipruritic effects of furosemide and bumetanide¹⁰⁷ might be attributed to GPR35 activation, however, the relevance for patients remains to be clarified. The compounds displayed no noteworthy activity at rat or mouse GPR35.¹⁰⁶

In 2013, our group identified 8-benzamidochromen-4-one-2-carboxylic acids as potent and selective agonists for the human GPR35 ortholog.¹⁰⁸ The most potent agonists of the study were 6-bromo-8-(4-methoxybenzamido)-4-oxo-4*H*-chromene-2-carboxylic acid (**23a**, PSB-13253),⁹²

Figure 1.7) and 6-bromo-8-(2-chloro-4-methoxybenzamido)-4-oxo-4*H*-chromene-2-carboxylic acid (**24**). The former displayed EC₅₀ values of 12.1 nM and 1.40 μM at the human and rat receptors, respectively, but was inactive at the mouse ortholog. The latter (**24**) showed EC₅₀ values of 11.1 nM and 4.17 μM at the human and rat receptors, respectively, and was equally inactive at the mouse receptor ortholog. The most potent ligands were full agonists at the human receptor, yet only produced a partial response at the rat receptor compared with the standard agonist **8** (10 μM). Thus, like other described GPR35 agonists, the reported chromone derivatives displayed remarkable selectivity for the human receptor. Interestingly, the most potent derivatives were also examined at the N-terminally longer GPR35b isoform, but no significant differences in potency could be observed. The activity was determined in β-arrestin recruitment assays using CHO cells and the enzyme complementation technology.¹⁰⁸

In a subsequent study, our group developed the first GPR35 radioligand.⁹² [³H]PSB-13253 (**23b**) displayed high affinity (K_D 5.27 nM) for the human receptor and, for the first time, allowed affinity determinations of previously described agonists without relying on functional assays: the purported cognate ligand of GPR35, kynurenic acid (**1**, **Figure 1.6**), showed a K_i value of only 137 μM. Zaprinast (**8**, **Figure 1.7**) and cromolyn (**11**) exhibited mediocre affinity with K_i values of 0.401 μM and 2.34 μM, respectively. Pamoic acid (**10**), despite having been used for years as inactive excipient, had the highest affinity of the previously described “pharmaceuticals”. Consecutive syntheses and study of structure-activity relationships (SAR) of chromones led to the discovery of 6-bromo-8-(2,6-difluoro-4-methoxybenzamido)-4-oxo-4*H*-chromene-2-carboxylic acid (**25**, **Figure 1.7**). The compound showed the highest affinity (K_i 0.589 nM) of all examined derivatives, and it was highly potent in β-arrestin recruitment assays (EC₅₀ 5.54 nM). Binding experiments were conducted with membrane preparations of CHO cells recombinantly expressing human GPR35.⁹²

More recently, our group optimized the chromen-4-one scaffold and developed a compound with even greater potency and affinity than **25**. PSB-21028 (**26**) displayed an EC₅₀ value of 1.08 nM at the human GPR35 and retained some potency at the rat and mouse receptor orthologs (rat: EC₅₀ 157 nM, mouse: EC₅₀ 293 nM) in β-arrestin recruitment assays. It is the most potent human GPR35 agonist described to date. Similar to **25**, **26** shows a K_i value in the subnanomolar range (K_i 0.43 nM).¹

In addition to our group’s chromen-4-one derivatives, Wei et al. identified chromen-2-one derivatives as reasonably potent GPR35 agonists.¹⁰⁹ 6-Bromo-7-hydroxy-8-nitro-3-(1*H*-tetrazol-5-yl)-2*H*-chromen-2-one (**27**, **Figure 1.7**) was the most potent derivative to trigger

DMR (EC_{50} 5.8 nM), however, its potency in β -arrestin recruitment assays was considerably weaker (EC_{50} 197 nM). In a later publication, the group described **28** to potently trigger DMR as well (EC_{50} 41 nM), yet neither β -arrestin recruitment data nor activity at rodent receptor orthologs was reported.¹¹⁰

Based on the reports of mast cell stabilizers such as cromolyn (**11**, **Figure 1.7**) and nedocromil (**12**) being modest-potency GPR35 agonists, MacKenzie et al. identified the related compounds lodoxamide (**29**) and bufrolin (**30**) to be highly potent GPR35 agonists at the human receptor (EC_{50} 1.6 nM, 2.9 nM, respectively) determined in CHO-K1 cells using PathHunter β -arrestin recruitment assays.² In BRET-based β -arrestin interaction assays, **29** and **30** were similarly potent (EC_{50} 3.6 nM, 12.8 nM). In contrast to previously described ligands, both compounds retained activity at the rat receptor ortholog in the same assay system (**29**: EC_{50} 12.5 nM, **30**: EC_{50} 9.9 nM). The two antiallergenic drugs were shown to be the most equipotent agonists of the human and rat GPR35 ever described and served as lead structures for some of the new ligands discussed herein (see below). In addition to lodoxamide and bufrolin, the group reported agonist GPR35 activity for the antiallergenic amlexanox (**31**), doxantrazole (**32**) and pemirolast (**33**), however, all of those were significantly more potent at the rat receptor ortholog. The authors speculated that the inability of many antiallergic molecules to progress in clinical development might have a basis in their species selectivity at GPR35.²

Evidently, most reported GPR35 agonists display remarkable human receptor selectivity, while few show a preference for the rat receptor ortholog. Still fewer display activity at mouse GPR35. The most equipotent agonists at human and rat receptors, lodoxamide (**29**) and bufrolin (**30**), likewise showed dramatically weaker potency at the mouse receptor ortholog (EC_{50} ~1.9 μ M, 155 nM, respectively) in BRET-based β -arrestin interaction assays. Thus, lodoxamide had greater than 150-fold lower potency at the mouse than at the rat receptor, and bufrolin was 15-fold weaker.¹¹¹ Nevertheless, both compounds were remarkably equipotent at the human and rat receptors and showed some potency at the mouse receptor ortholog. Therefore, they were promising starting points for synthetic optimization, which is part of the present study.

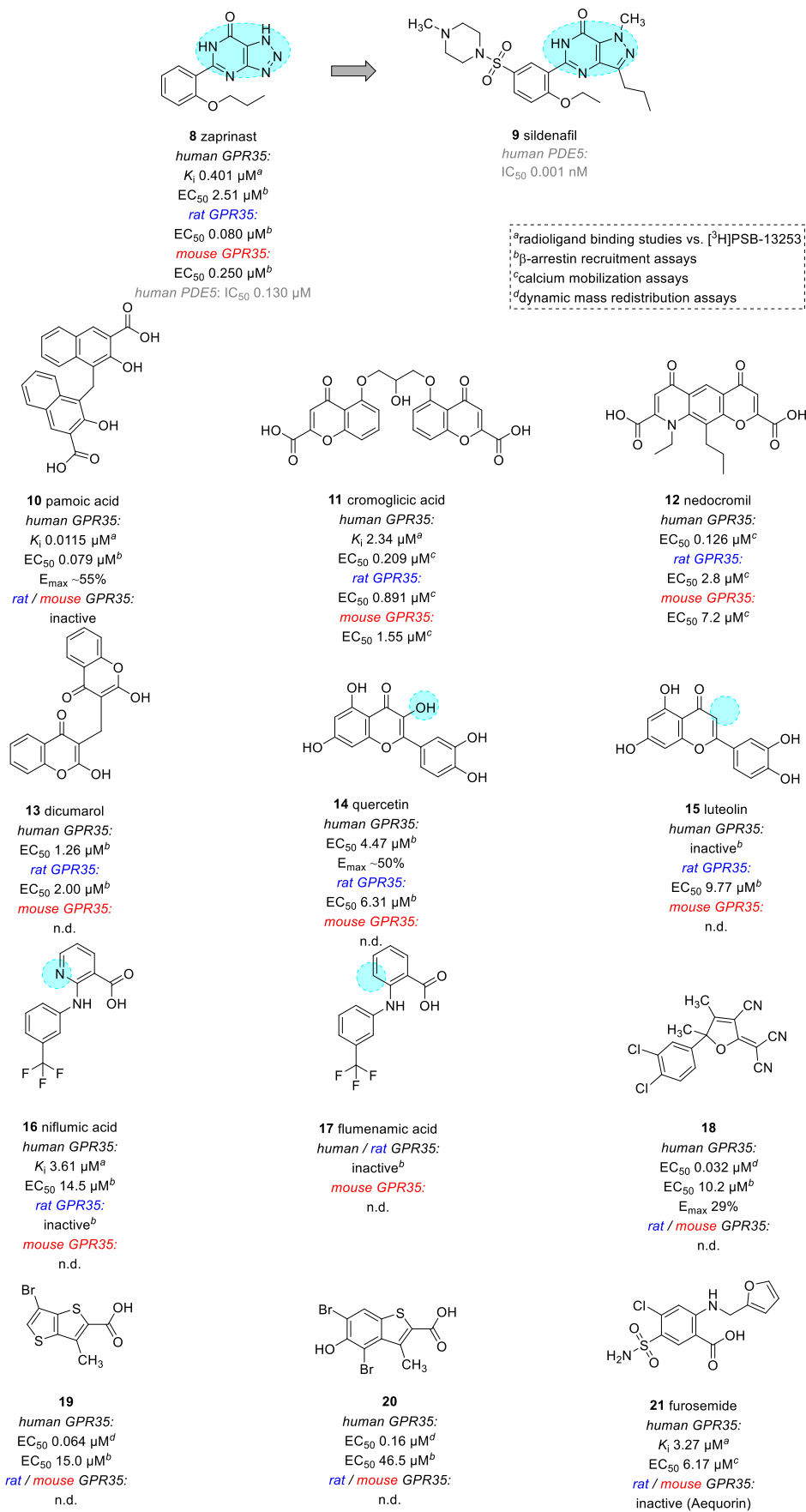
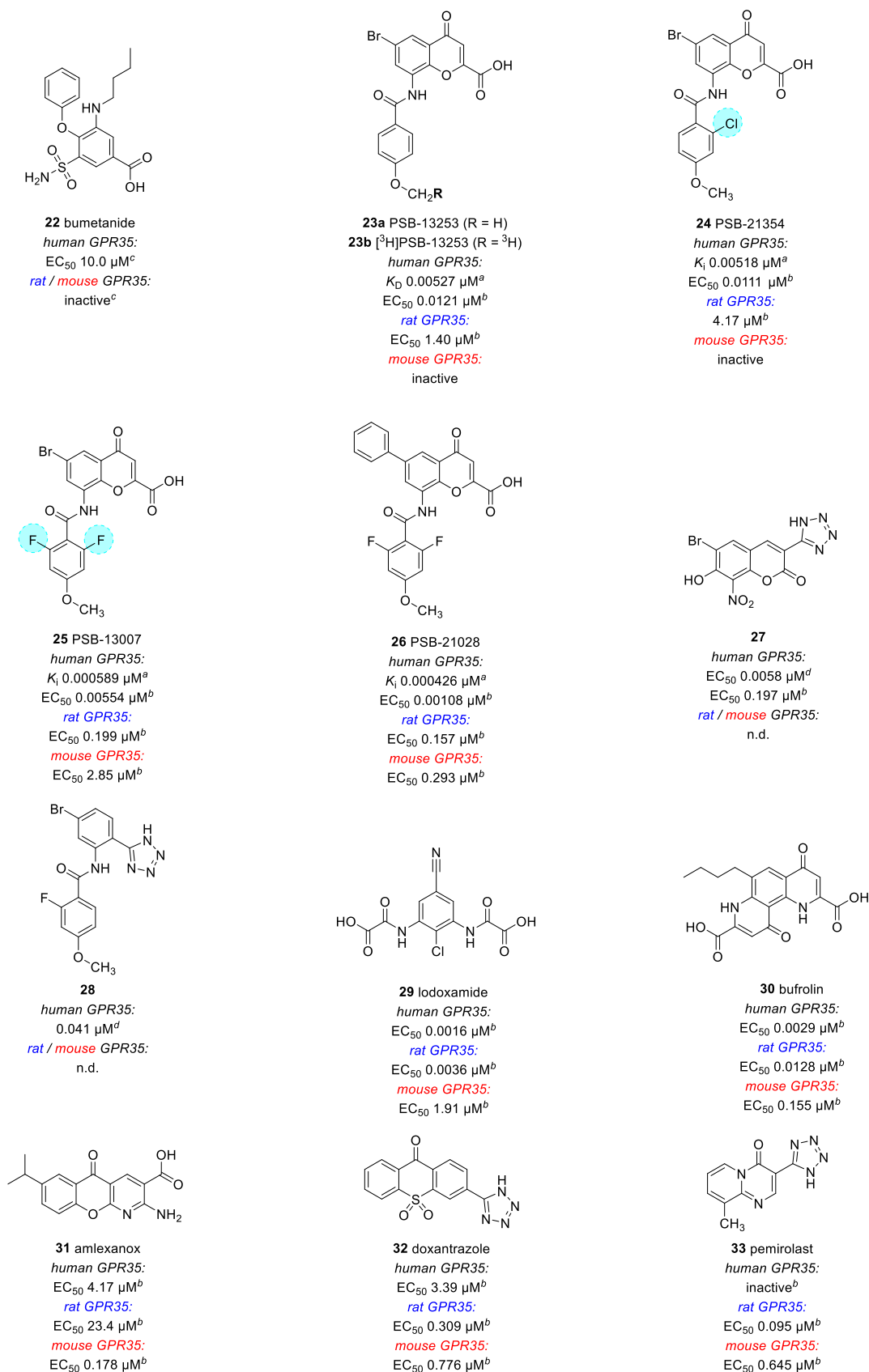


Figure 1.7. Synthetic GPR35 agonists with potency and affinity data (Part 1).



^aradioligand binding studies vs. [³H]PSB-13253
^b β -arrestin recruitment assays
^ccalcium mobilization assays
^ddynamic mass redistribution assays

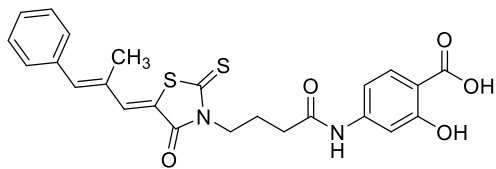
Figure 1.7. Synthetic GPR35 agonists with potency and affinity data (Part 2).^{1,2,92,106,108–111}

1.2.3 GPR35 antagonists

Only few GPR35 antagonists have been described in the literature and all of them were identified by Heynen-Genel et al. in a high-throughput screening of 291,994 compounds.^{112,113} The group initially reported CID2286812 (**34**, **Figure 1.8**, ML145) and CID1542103 (**35**, **Figure 1.8**, ML144) to possess antagonist activity at human GPR35 (IC_{50} 0.061 μ M and 4.72 μ M, respectively). Interestingly, their derivatives CID2286888 (**36**, IC_{50} 0.088 μ M) and CID1502520 (**37**, IC_{50} 5.01 μ M) were also active in β -arrestin assays in human GPR35-overexpressing osteosarcoma U2OS cells against the standard agonist zaprinast (**8**, **Figure 1.7**). Despite initial concerns over the rhodanine moiety in **34** and **36**, which represents a pan assay interference structure (PAINS), all compounds were selective versus the closely related GPR55 (**34**: ~1,080-fold; **35**: >15-fold) and the unrelated vasopressin receptor type IIa. It is therefore unlikely that the PAINS element of **34** and **36** was responsible for the antagonist activity at GPR35.¹¹² A later study confirmed that **34** displays high affinity for the human GPR35 in radioligand binding studies (K_i 0.00876 μ M vs. **23b**).⁹² In a second report, the group described CID2745687 (**38**, **Figure 1.8**, CID9581011, ML194), the structure of which is distinct from the aforementioned antagonists.¹¹³ It displayed an IC_{50} value of 0.160 μ M at the human GPR35 in β -arrestin recruitment assays and was 57-fold selective versus GPR55. Its affinity to the receptor was reported with a K_i value of 0.0422 μ M vs. **23b** (**Figure 1.7**).⁹² Interestingly, the *tert*-butyl group attached to the urea moiety could be replaced by other bulky substituents, such as *p*-Cl-phenyl (**39**, **Figure 1.8**: IC_{50} 0.171 μ M) and phenyl (**40**: IC_{50} 0.211 μ M), whereas the smaller methyl residue resulted in lower potency (**41**, IC_{50} 2.49 μ M).¹¹³

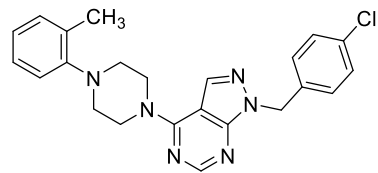
While initially nothing was known about the compounds' species selectivity, another group investigated their potency at rat and mouse GPR35. However, neither CID2286812 (**34**) nor CID2745687 (**37**) could inhibit the effects of zaprinast (**8**, **Figure 1.7**) or pamoic acid (**10**) at rat or mouse GPR35 orthologs in β -arrestin recruitment assays.¹⁰² Later studies confirmed that **34** and **37** were inactive at rat and mouse GPR35.^{53,63,111} Surprisingly, Zhao et al. reported that CID2745687 was able to block the effects of pamoic acid and zaprinast in mouse GPR35-transfected HEK293 cells.¹⁰¹ Similarly, Berlinguer-Palmini and co-workers showed that CID2745687 blocked the effects of kynurenic acid in mouse astrocytes,⁸³ and another group reported antagonist activity of the compound in a mouse model of DSS-induced colitis.¹¹⁴ Very recently, Kim et al. observed that CID2745687 reversed the anti-fibrotic effects of lodoxamide (**29**) in a mouse model of tetrachloromethane-induced hepatic fibrosis, despite both compounds' reported lack of activity at mouse GPR35.¹¹⁵ Moreover, Chen et al. found that

CID2745678 (but likely also CID2745687 (**37**) with the last two digits erroneously swapped)⁵³ could prevent anoxia-induced mitochondrial damage in neonatal mouse myocytes.¹¹⁶ It is currently unclear how the investigated GPR35 antagonists with in vivo activity in mouse models elicit their effects, without questioning their selectivity towards GPR35.⁵³



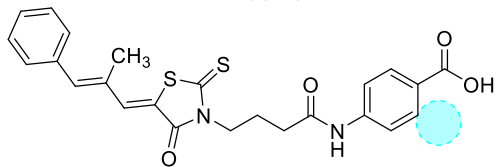
34 CID2286812 (ML145)

human GPR35:
 K_i 0.00876 μM^a
 IC_{50} 0.0201 μM^b
 rat / mouse GPR35:
 inactive^b



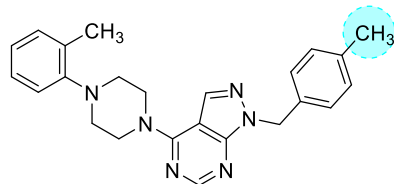
35 CID1542103 (ML144)

human GPR35:
 IC_{50} 2.22 μM^b
 rat / mouse GPR35:
 n.d.



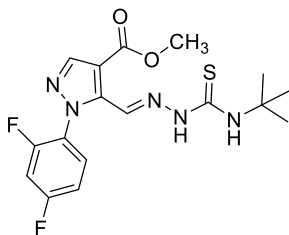
36 CID2286888

human GPR35:
 IC_{50} 0.100 μM^b
 rat / mouse GPR35:
 n.d.



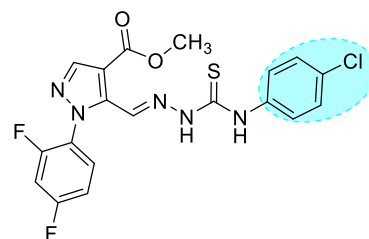
37 CID1502520

human GPR35:
 IC_{50} 2.65 μM^b
 rat / mouse GPR35:
 n.d.



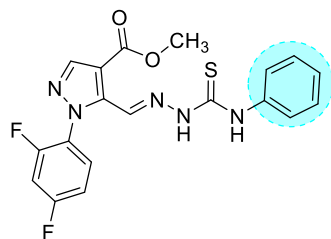
38 CID2745687 (ML194)

human GPR35:
 K_i 0.0422 μM^a
 IC_{50} 0.160 μM^b
 rat / mouse GPR35:
 inactive^b



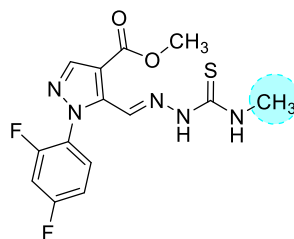
39

human GPR35:
 IC_{50} 0.171 μM^b
 rat / mouse GPR35:
 n.d.



40

human GPR35:
 IC_{50} 0.211 μM^b
 rat / mouse GPR35:
 n.d.



41

human GPR35:
 IC_{50} 2.49 μM^b
 rat / mouse GPR35:
 n.d.

^aradioligand binding experiments vs. [³H]PSB-13253
^b β -arrestin recruitment assays vs. zaprinast

Figure 1.8. GPR35 antagonists with potency and affinity data.^{92,102,112,113} n.d., not determined.

To conclude, both GPR35 agonists and antagonists show potential for the treatment of many diseases. Agonists have already shown promise in the treatment of inflammatory diseases, such as allergies with two GPR35-targeting anti-allergy medicines (lodoxamide and cromoglicic acid) already on the market.^{2,103} However, it is still unclear to what an extent their effects are mediated via GPR35.⁵³ Considering the receptor's extremely high expression in the gastrointestinal tract,⁵⁰ agonists might also be useful for the treatment of inflammatory bowel diseases, such as ulcerative colitis, which has been studied in animal models.⁷⁵ Antagonists, on the other hand, have been proposed for the treatment of cardiovascular diseases.⁹¹ As GPR35 knockout mice show decreased blood pressure⁷⁹ and are protected from angiotensin II-induced cardiac damage,⁸¹ blocking the receptor could have beneficial effects in the treatment of hypertension and heart failure. The increased GPR35 expression on certain types of tumor cells might contribute to accelerated cancer growth.⁷⁸ Antagonists have the potential to obstruct this process, and might therefore be useful chemotherapeutics as well. However, while various ligands for the receptor are available as tool compounds, none of them have reached clinical development. This is suspected to be due to most compounds' inability to activate rodent – and especially mouse – GPR35, since the overwhelming majority of agonists and all antagonists have no affinity for these receptor orthologs (see above). Even the most potent human GPR35 agonists are typically much weaker at the rat receptor ortholog and virtually inactive at the mouse receptor.^{1,92,108} Keeping in mind that these animals are generally used for preclinical target validation and efficacy studies, there is a need for compounds that activate human, rat, and mouse GPR35 with comparable and high potency.^{2,53} The development of such ligands is part of this study and will be discussed below.

1.3 GPR84

In 2001, the class A G protein-coupled receptor GPR84 was discovered by two independent teams, investigating immune cell receptor expression patterns.^{117,118} GPR84 is not closely related to any other GPCR, with its closest homolog being the dopamine D2 receptor which shows only 26% amino acid identity and 41% similarity. It is highly conserved among species with 85% identity (90% similarity) between human and mouse.^{117–120} GPR84 mRNA expression can be found in tissues related to immune function, such as bone marrow, leukocytes, activated microglia, spleen, and in the lungs.^{117,119,121–124}

Although basal GPR84 levels are generally low, the receptor's mRNA expression is markedly upregulated under inflammatory conditions, such as stimulation with lipopolysaccharides (LPS),¹²⁵ which also translated into higher receptor protein expression.¹²⁶ A transient increase of GPR84 mRNA transcripts was reported for human adipocytes following exposure to interleukin 33 (IL-33), tumor necrosis factor (TNF), or IL-1 β .^{127,128} In human and murine macrophages, GPR84 mRNA expression was increased under chronically elevated glucose concentrations and in the presence of oxidized LDL – both being low-grade inflammatory stimuli.¹²⁵

Wang et al. (2006) showed that the receptor is activated by medium-chain fatty acids (MCFAs) with chain lengths of 9 to 14 carbon atoms.¹²¹ Fatty acids with chain lengths above or below were inactive. Other groups confirmed that the carboxylic acid moiety of these ligands is necessary for GPR84 activation, since neither carboxamide nor ester derivatives displayed activity at the receptor.^{129,130} In the original work, decanoic acid (10 carbon atoms, also known as capric acid, see below) displayed an EC₅₀ value of 4.5 μ M and was the most potent MCFA in cAMP accumulation assays in GPR84-transfected CHO cells. Despite the apparent overlap in ligand recognition with free fatty acid receptors (FFARs), GPR84 does not appear to be related to them (see **Figure 1.9**).¹³¹

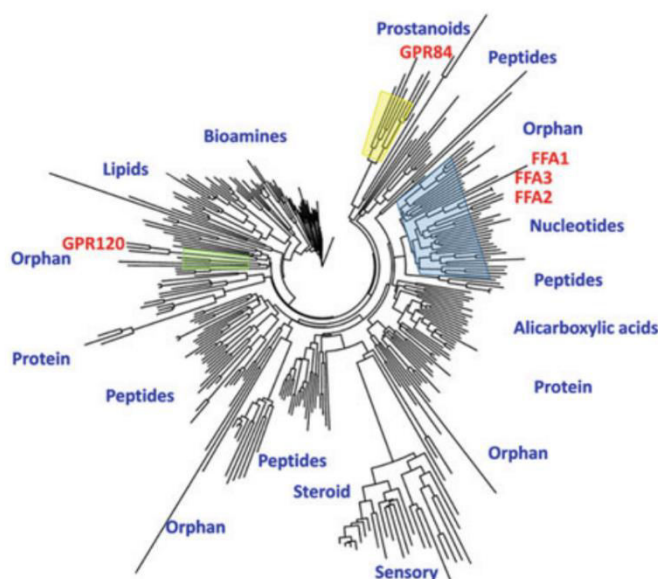


Figure 1.9. Phylogenetic tree of class A G protein-coupled receptors. Clusters containing fatty acid-activated receptors are highlighted.¹³²

It also appears to have different functions than FFARs, whose physiological roles are strongly linked to energy metabolism (see **Table 1.1**).¹³³

Table 1.1. G protein-coupled fatty acid receptors, their coupling, physiological functions, and ligands

receptor	G protein coupling	highlighted physiological role(s)	potent physiological agonists
FFAR1 (GPR40)	G _{q/11}	glucose-dependent insulin release, inhibition of osteoclastogenesis, ^{134,135} regulation of taste preference for fatty acids ¹³⁶	long chain: C12 – C18
FFAR2 (GPR43)	G _{q/11} , G _{i/o}	immune function, hematopoiesis, mast cell activity, adipogenesis ¹³⁷	short chain: C2 – C4
FFAR3 (GPR41)	G _{i/o}	pancreatic peptide YY secretion, glucagon-like peptide 1 secretion ¹³⁸	short chain: C3, C4 > C2
FFAR4 (GPR120)	G _{q/11}	glucagon-like peptide 1 secretion ¹³⁹	long chain: C12 – C16
GPR84 (GPCR4)	G _{i/o} , G _{12/13}	immunostimulation, ¹²¹ proinflammatory effects, ¹⁴⁰ defense against pathogens ¹²²	medium chain: C9 – C14

Not only MCFAs but also their natural 2- or 3-hydroxylated metabolites can activate GPR84.^{141,142} Whereas their activity generally depends on the chain lengths of investigated derivatives and the assay conditions, 2- and 3-hydroxy fatty acids have often shown superior affinity and potency to their non-hydroxylated relatives.^{49,143} The most comprehensive analysis of different hydroxy derivatives of lauric acid (dodecanoic acid) was reported by Kaspersen et al. The group examined all possible hydroxylauric acids in [³⁵S]GTPγS binding assays using

membrane preparations of cells expressing FLAG-human-GPR84-eYFP and found that only derivatives with a hydroxy group in positions 2, 3, 4, and 12 could activate the receptor (EC_{50} 12.9, 5.25, 38.0, 20.9 μ M, respectively). These results suggest that hydroxylation in position 3 is most influential. All other derivatives were found inactive at a high concentration of 100 μ M. Surprisingly, no [35 S]GTP γ S binding could be measured for non-hydroxylated lauric acid at 100 μ M.¹⁴² The only study that addressed possible differences between *S*- and *R*-enantiomers found no significant activity discrepancy between the enantiopure (*R*)-3-hydroxytetradecanoic acid and its racemic mixture in radioligand binding assays vs. [3 H]PSB-1584 (for structure, see below), or in cAMP and β -arrestin assays.⁴⁹ Although (hydroxy-)MCFAs can undoubtedly activate the receptor and are endogenously produced metabolites, their potential role as GPR84's cognate ligands is disputed for several reasons. Firstly, their potencies in recombinant cells and their affinities in radioligand binding assays are rather low.^{49,121} Consequently, high tissue concentrations are required for receptor activation, which might not be present under physiological conditions.¹⁴⁴ Furthermore, MCFAs are highly unselective ligands, interacting with a variety of other receptors.¹⁴⁵ (Hydroxy-)MCFAs could still be GPR84's sole natural ligand(s), but until more conclusive evidence is published, the receptor remains orphan.⁸⁹

The receptor's G protein specificity was investigated in two important studies.^{120,121} Wang and co-workers measured the response of recombinant GPR84-CHO cells to decanoic or undecanoic acid in the presence of small, promiscuous, chimeric G_q proteins, which convert all signaling into calcium mobilization. Only the G_{qi9} chimeric G protein produced significant signals. Moreover, MCFA-induced inhibition of forskolin-stimulated cAMP production was completely abolished upon preincubation with pertussis toxin (PTX), which is a specific inhibitor of $G_{i/o}$ proteins. These results suggest that, at least in transfected CHO cells, GPR84 signals via PTX-sensitive $G_{i/o}$ proteins.¹²¹ Gaidarov et al. reported $G_{i/o}$ - as well as $G_{12/13}$ -dependent signaling in recombinant HEK293 cells: in experiments with cells expressing GPR84 and chimeric G_s - G_{12} or G_s - G_{13} proteins, agonist treatment led to increased cAMP production indicating robust coupling not only to $G_{i/o}$ proteins, but also to the $G_{12/13}$ pathway. The effect was even more pronounced upon pretreatment with PTX, suppressing G_i -mediated signaling.¹²⁰ This provides a link to Rho/Rac signaling, subsequent modulation of the cytoskeleton, and cell migration. In human macrophages, the receptor mediated G_i protein-dependent Erk $_{1/2}$ and Akt phosphorylation, PI $_3$ kinase activation, and calcium influx.¹²⁰

The activation of GPR84 on immune cells, such as monocytes and neutrophils, generally leads to an increased immunological response involving the production of pro-inflammatory cytokines,¹²¹ and increased bacterial adhesion and phagocytosis.¹²⁵ The increased response was

absent in GPR84-deficient cells or those treated with a GPR84 antagonist.¹²⁵ Furthermore, GPR84 knockout macrophages produced lower levels of stress-response cytokines, such as IL-1, IL-6, and TNF.¹⁴⁶ Receptor activation has also been reported to trigger the release of reactive oxygen species in neutrophils and macrophages.¹⁴⁷ Thus, it appears to be justified to designate GPR84 as an immunostimulatory receptor.^{122,140,141,148,149}

Several studies have linked GPR84 to a variety of (mostly inflammation-related) diseases, including inflammatory bowel disease (IBD),¹⁵⁰ fibrosis,^{151,152} neuropathic pain,¹⁴⁶ reflux esophagitis,¹⁵³ obesity,¹⁴⁰ Alzheimer's disease (AD),¹⁵⁴ and atherosclerosis.¹²⁰ The receptor's role in leukemogenesis¹⁵⁵ and osteoclastogenesis¹⁵⁶ merits further investigation. However, in the absence of clearly defined pharmacology, the potential of orphan GPCRs as drug targets is often estimated by the effects of non-cognate ligands (for details see next section) or knock-out experiments. The GPR40 agonist and GPR84 antagonist fezagepras (PBI-4050, setogepram), for example, exhibited antifibrotic and anti-inflammatory effects in various mouse fibrosis models.¹⁵² The compound has also been investigated in clinical trials.¹⁵⁷ Anti-inflammatory properties of GPR84 antagonists were also studied in a clinical trial of GLPG1205 for the treatment of ulcerative colitis, however, the compound failed to reach the clinical endpoints for efficacy.¹⁵⁸ Nevertheless, GLPG1205 did reduce disease activity and neutrophil infiltration in an animal model for colitis.¹⁵⁹ This compound is currently being studied in a phase II trial as a treatment for idiopathic pulmonary fibrosis (NCT03725852). Antagonists of GPR84 have also been proposed for the treatment of chronic pain after reports of elevated receptor expression following nerve injury.^{124,146,160,161} Agonists of the receptor, instead, have powerful immunostimulatory effects, which could be exploited for the treatment of cancer (immunoncology) or infections by activating the endogenous immune response. However, GPR84 agonists could even elicit *anti*-inflammatory effects in patients by triggering receptor desensitization.¹⁶² Agonists have also been proposed for the prevention of atherosclerosis, possibly disrupting macrophage recruitment toward atherosclerotic plaques.¹²⁰ Audoy-Rémus and colleagues, on the other hand, demonstrated the receptor's complex role in the progression of AD, where GPR84 signaling protected dendrites from further decline. Thus, agonists could potentially slow down disease progression of AD and have a protective effect.¹⁵⁴ Multiple studies have investigated the receptor's role in obesity and energy metabolism and although they came to somewhat contradictory conclusions regarding glucose tolerance and body weight, GPR84 signaling appears to be important for mitochondrial function and reduces oxidative stress.^{163,164} Thus, activation of the receptor could improve energy metabolism in obese

patients.¹⁶¹ Taken together, both agonists and antagonists appear to have promising therapeutic applications.

1.3.1 GPR84 ligands

Although MCFAs, such as capric acid (**42**, for structures see **Figure 1.10**),¹²¹ and their hydroxylated derivatives^{141,142} are GPR84 agonists, their promiscuity and weak potency make them poor choices for studying isolated GPR84-related effects in vitro or in vivo. The story of the development of useful GPR84 tool compounds began in 2013, when the first potent surrogate agonist, 6-octylaminouracil (**43**, 6-OAU), was discovered by Suzuki and coworkers through a high-throughput screening (HTS) approach. The compound promoted [³⁵S]guanosine 5'-O-(γ -thio)triphosphate ([³⁵S]GTP γ S) binding in GPR84-transfected Sf9 cell membranes with an EC₅₀ value of 512 nM.¹⁴¹ The compound induced chemotaxis of granulocytes and macrophages and increased the production of various proinflammatory cytokines (e.g. CCL2, CCL5, CXCL1, IL-6, IL-8, IL-12B, and TNF α) in those cells.^{125,141,161} It has a fatty acid-like structure with a hydrophilic head group (uracil) and a lipophilic tail (octyl chain), and is predicted to share its GPR84 binding site with MCFAs.⁴⁹ 6-OAU is a non-biased agonist that does not have a particular preference for either G protein-mediated or β -arrestin pathways.¹⁶² The molecule's scaffold allowed a number of modifications, proving to be a valuable starting point for synthetic optimization.

The bioisosteric derivative 2-(hexylthio)pyrimidine-4,6-diol (**44**, ZQ-16) was reported in 2016 by Zhang et al. and had also been discovered by HTS. It was only a minor improvement (2.5-fold) compared to 6-OAU (**43**) with an EC₅₀ value of 134 nM for **44** vs. 341 nM for **43**, measured in cAMP assays in human-GPR84-transfected HEK293 cells.¹⁶⁵ The group optimized that compound, which led to the discovery of 6-nonylpyridine-2,4-diol (**45**, LY-237). This molecule differs only slightly from **44**, in that one nitrogen and one sulfur atom were each replaced by carbon, and the alkyl chain length was slightly elongated. However, its potency was ~400 times higher than that of **44** (**45**: EC₅₀ 0.352 nM vs. **44**: 144 nM) determined in cAMP assays in HEK293 cells.¹⁶⁶ Nevertheless, the increased potency did not translate into higher affinity determined in radioligand binding assays (**44**: K_i 0.219 nM, **45**: K_i 1.56 nM) vs. [³H]PSB-1584 (see below).⁴⁹ Compound **45** is still one of the most potent GPR84 agonist described in the literature to date.¹⁶¹

In a melanophore-based HTS of small molecules, Gaidarov and co-workers found the natural product embelin (**46**, **Figure 1.10**; previously disclosed in a patent)¹⁶⁷ to be a potent and reasonably selective GPR84 agonist (EC₅₀ 8 nM) in a melanophore aggregation assay. It is produced by *Embelia ribes* Burm.f. (“false black pepper”). Similar to the above-mentioned agonists, **46** has a hydrophilic head group (2,5-dihydroxy-*p*-benzoquinone) and a lipophilic alkyl tail (11 carbon atoms). Despite the compound’s many effects in biological systems,^{168–170} its only well-characterized molecular targets are GPR84 and X-linked inhibitor of apoptosis protein (XIAP). However, in a standard selectivity screening assay, the compound also showed affinity for the adenosine receptor A₃ (K_i 1.4 μM) and the CXCR2 receptor (K_i 93 nM).¹²⁰ Embelin inhibited forskolin-stimulated cAMP production in HEK293 cells expressing recombinant GPR84 in a concentration-dependent manner (EC₅₀ 89 nM). Upon pretreatment with pertussis toxin (PTX) the effect was abolished, indicating the involvement of the G_{i/o} pathway.^{120,167} The group explored the effect of varied alkyl chain lengths and found that only analogs with chain lengths between 4 and 14 carbon atoms were active. Shorter or longer chains led to inactive compounds. The optimal chain length was 7 (EC₅₀ 2 nM) and 8 carbon atoms (**47**, C8-embelin, EC₅₀ 1.6 nM). Similar results were observed in cAMP assays in macrophages. Experiments with HEK cells expressing mouse GPR84 yielded virtually identical structure-activity relationships (SARs), which is consistent with the high conservation of receptor orthologs (85% sequence identity, 90% similarity).¹²⁰

Pillaiyar, Köse, Müller et al. conducted chemical modifications based on the scaffold of the standard agonist 6-octylaminouracil (**43**).¹⁶² Reducing the alkyl chain length from octyl (8 carbon atoms) to hexyl (6 carbon atoms) resulted in PSB-1584 (**48**, 6-hexylaminouracil, **Figure 1.10**) with an EC₅₀ value of 5 nM (vs. 17 nM for **43**) determined in cAMP assays in recombinant human GPR84-expressing CHO cells. While this compound displayed equal potency in cAMP and β-arrestin assays (EC₅₀ 3.2 nM), demonstrating non-biased agonism, the group also described highly biased GPR84 agonists, e.g. 6-(4-chlorophenethyl)aminouracil (**49**, PSB-16434, cAMP assay: EC₅₀ 7.1 nM, β-arrestin assay: EC₅₀ 520 nM, 79-fold G_i-selective) and 6-(4-bromophenethyl)aminouracil (**50**, PSB-17365, cAMP assay: EC₅₀ 2.5 nM, β-arrestin assay: EC₅₀ 100 nM, 20-fold G_i-selective). The introduction of a *p*-halophenethyl group instead of the alkyl chain of **48** appears to be responsible for this shift in G protein preference. Biased ligands exhibit a different pharmacological profile from classical, non-biased compounds, which can have several advantages. They might be devoid of some side effects attributed to the omitted pathway,¹⁷¹ the desired effect may persist for an extended period of time due to the lack of receptor desensitization, or they might elicit a different response entirely by engaging an

opposed signaling cascade.^{148,162} In a follow-up study, the non-biased ligand PSB-1584 (**48**) was transformed into the high-affinity (K_D 2.08 nM) tritium-labeled radioligand [³H]PSB-1584 (**51**), which allowed – for the first time – direct affinity calculations at the receptor.⁴⁹ In contrast to the usual cell-based bioassays, radioligand binding is not dependent on secondary signaling cascades and thus provides better, comparable data. Affinity data also provide valuable insight into the binding modes of different ligands (see below).

Another biased GPR84 agonist was later discovered by Lucy et al.¹⁷² The compound 3-(2-((4-chloronaphthalen-1-yl)oxy)ethyl)pyridine 1-oxide (**52**, DL-175, **Figure 1.10**) was similarly potent as 6-OAU (**43**) in cAMP accumulation assays (EC_{50} 33 nM vs. 19 nM, respectively), but completely inactive in β -arrestin assays at a high concentration of 60 μ M in human-GPR84-transfected CHO cells. The structure of **52** is quite different from the abovementioned agonists, since it contains a pyridine-*N*-oxide moiety, likely acting as the hydrophilic head group. Additional experiments with this ligand demonstrated that certain cellular responses to GPR84 agonists like increased phagocytosis and chemotaxis can be separable from each other. Similar to other non-biased GPR84 agonists, the G-protein biased **52** increased phagocytosis in M1 polarized U937 macrophages. However, it failed to induce macrophage migration typical of non-biased GPR84 agonists. These results illustrate that different GPR84 agonists can produce distinct effects in human macrophages, which has important implications for drug development (see above).¹⁷²

Although the cognate ligand of GPR84 is still disputed, most authors consider the fatty acid binding site as the receptor's *orthosteric* binding site, and ligands such as MCFAs, 6-OAU, embelin, and their derivatives are often (inaccurately) referred to as “orthosteric ligands”.^{49,126,130,148} In that sense, there are also *allosteric* agonists of GPR84 interacting with a different binding pocket. The first one was described by Takeda and co-workers in 2003:¹⁷³ 3,3'-diindolylmethane (**53**, DIM) is a natural product and a major metabolite of indole-3-carbinol, a degradation product of glucobrassicin present in cruciferous vegetables.¹⁷⁴ In the original publication, its ability to promote [³⁵S]GTP γ S binding was reported with an EC_{50} value of 11 μ M in Sf9 insect cells transfected with the human GPR84,¹⁷³ yet its potency in cAMP assays was generally higher (e.g. EC_{50} 0.252 μ M).¹⁴⁸ In contrast to the aforementioned agonists, DIM does not resemble fatty acids and actually increased the affinity of the “orthosteric” radioligand [³H]PSB-1584 in binding assays, instead of competing with it. Its binding mode is therefore considered allosteric with respect to the lipid binding site, and it was characterized as an ago-allosteric modulator.⁴⁹

DIM is not regarded as a selective ligand, because it has other effects attributed to it that are likely unrelated to the activation of GPR84 (e.g. activation of the arylhydrocarbon receptor (AhR) and the estrogen receptor).¹⁷⁴⁻¹⁷⁷ It is also a partial agonist at the human cannabinoid receptor 2 (EC_{50} 1.7 μ M, determined in β -arrestin assays).¹⁷⁸ Pillaiyar, Köse, Müller et al. explored its SAR at GPR84 and discovered more potent derivatives. Some were biased towards G_i -mediated adenylate cyclase inhibition, whereas others predominantly induced β -arrestin recruitment. The most potent ago-allosteric modulator, PSB-16671 (**54**, 3,3'-di(5,7-difluoro-1*H*-indol-3-yl)methane), displayed an EC_{50} value of 0.0413 μ M in CHO cells transfected with the human GPR84 with a bias for cAMP inhibition vs. arrestin recruitment (EC_{50} 5.47 μ M) determined in the same cell line. The compound showed only negligible engagement with the AhR and was selective against a variety of other receptors.¹⁴⁸ Another group later confirmed that PSB-16671 produced most of its effects directly via GPR84 activation in human- and mouse-derived immune cell models. Nevertheless, some of its activity in mouse bone-marrow-derived neutrophils appeared to be due to off-target effects. This was shown by the compound's partially retained activity in the presence of an antagonist, as well as in GPR84-deficient cells.¹²⁶ The existence of further cellular targets for the DIM derivative is therefore a logical conclusion.

Presently, there appear to be at least three separate binding sites on the receptor, as the radiolabeled GPR84 antagonist [³H]G9543 (for structure see below) does not share its binding pocket with decanoic acid or DIM, nor is its affinity affected by the mutation of arginine 172, despite this residue playing an important role in the (supposedly) orthosteric ligand recognition of MCFAs.¹³⁰ So far, three studies have attempted to elucidate the exact binding modes of various ligands using mutagenesis and docking studies.^{49,129,130} However, the studies have reached somewhat contradictory conclusions, and further research, ideally including X-ray crystallography, is necessary to definitively answer this question.

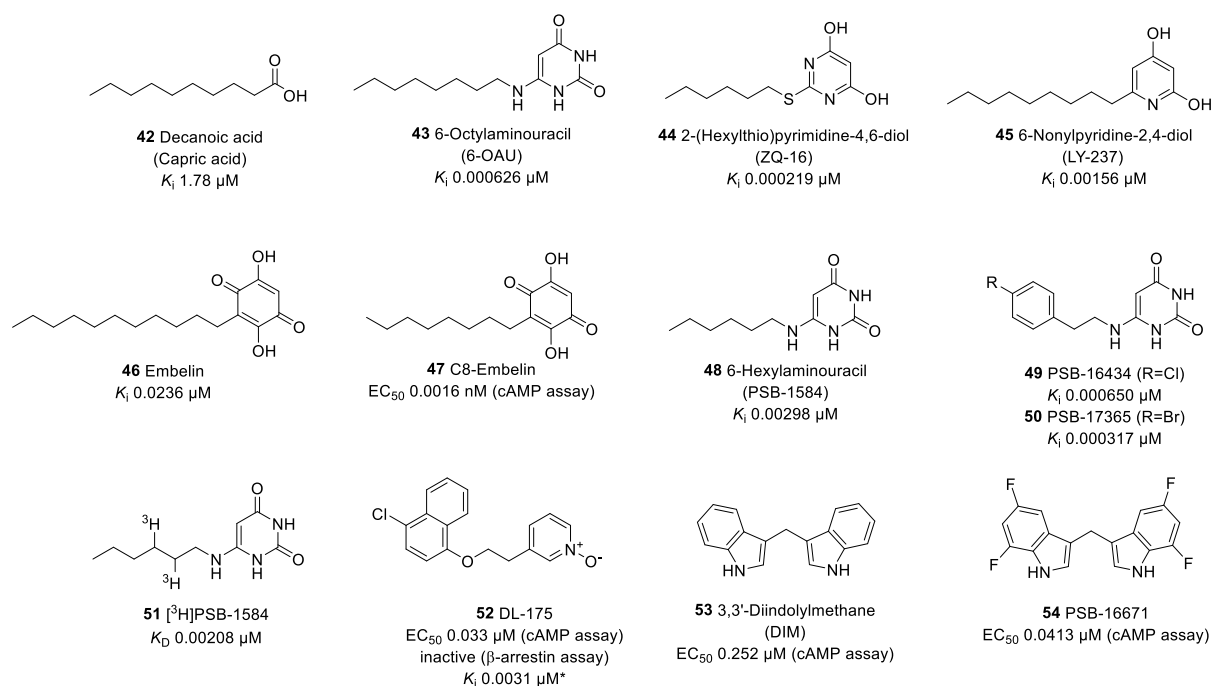


Figure 1.10. Structures of selected GPR84 agonists (**42-52**) and ago-allosteric modulators (**53,54**). (Affinities are provided for comparison and were determined in competition binding experiments vs. **54** (^3H]PSB-1584) by Köse et al.⁴⁹ If no K_i was determined, EC_{50} values are given adopted from Gaidarov et al.¹²⁰ for **47**, Lucy et al.¹⁷² for **52**, and Pillaiyar et al.¹⁴⁸ for **53** and **54**. *Affinity determined in-house in radioligand binding assays vs. **51**.)

1.3.2 GPR84 antagonists

While there are numerous potent GPR84 agonists described in the literature (*see above*), GPR84 antagonists are limited to few examples, belonging to three distinct classes: class I, dihydropyrimidinoisoquinolinones and derivatives,¹⁷⁹ class II, 3-alkylphenylacetic acid derivatives,¹⁵² and class III, 8-benzamidochromen-4-one derivatives¹ (for structures, see **Figure 1.11**).

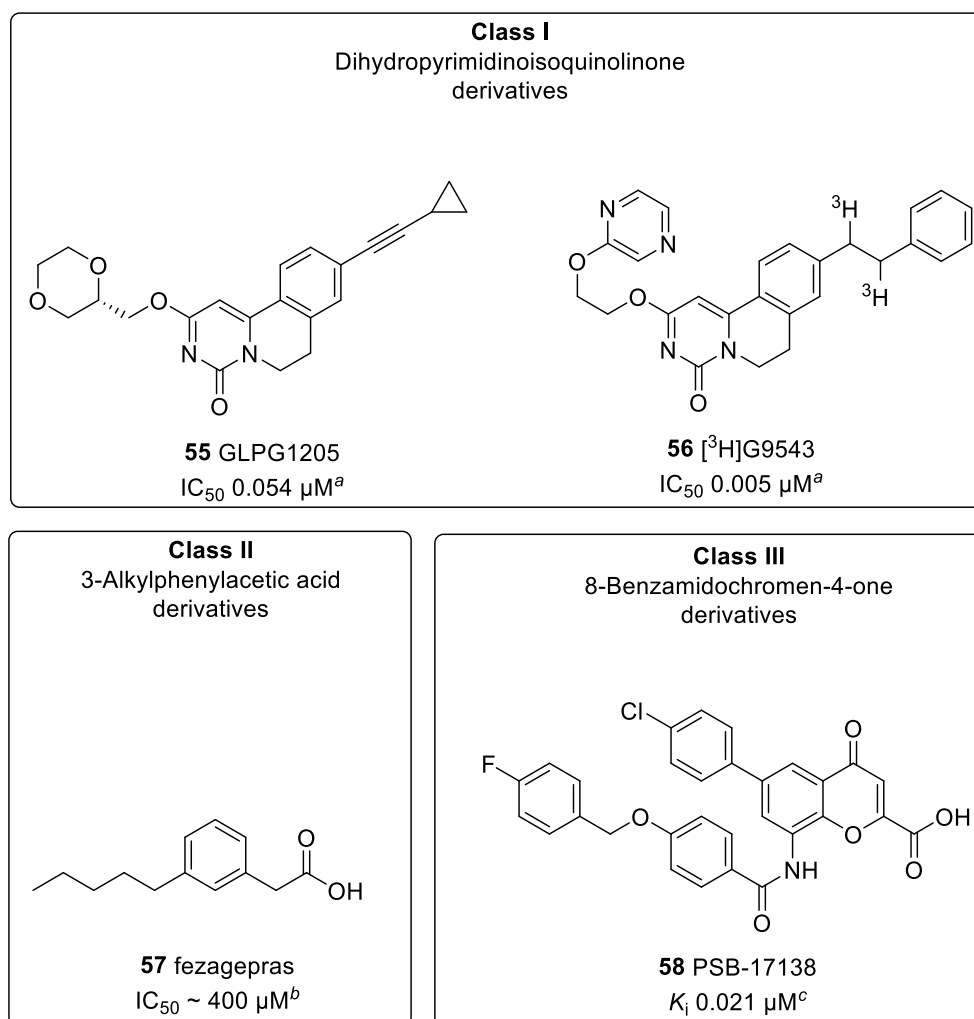


Figure 1.11. Selected GPR84 antagonists grouped into chemical classes. (IC₅₀ values determined in [³⁵S]GTPγS assay versus **53** (a)^{159,161} or BRET activation biosensor assay versus **42** (b)¹⁵². K_i value determined in competition binding experiments versus **51** (c).⁴⁹)

Class I antagonists include a large series of structurally related compounds originally disclosed in a patent (WO2013092791A1, Galapagos NV, Belgium), including GLP1205 (**55**, (S)-2-((1,4-dioxan-2-yl)methoxy)-9-(cyclopropylethynyl)-6,7-dihydro-4H-pyrimido[6,1-a]isoquinolin-4-one, **Figure 1.11**), the clinical candidate that is being investigated in a phase II pulmonary fibrosis trial (NCT03725852), after having failed to convince in a previous trial for ulcerative colitis.¹⁵⁸ In an animal model of artificially induced colitis, the compound had been promising being effective at reducing disease severity, including neutrophil infiltration.^{159,161} The original patent lists the activity of GLPG1205 with an IC₅₀ between 0.01-100 nM determined in [³⁵S]GTPγS binding assays (using DIM at its EC₈₀ concentration as an agonist). Recently, Marsango and Barki et al. reported an IC₅₀ value of 54 nM for the compound determined versus DIM (**53**, **Figure 1.10**) in the same assay system.¹⁶¹ This value was later confirmed by

Labéguère et al.¹⁵⁹ The radiolabeled antagonist [³H]G9543 (**56**, 9-(2-phenylethyl-1,2-*t*₂)-2-(2-(pyrazin-2-yloxy)ethoxy)-6,7-dihydro-4*H*-pyrimido[6,1-*a*]isoquinolin-4-one, **Figure 1.11**) is a tritiated derivative of class I antagonists. It displayed an IC₅₀ value of 5 nM in [³⁵S]GTPγS binding assays,¹⁵⁹ and its affinity was reported with a *K*_D value of 0.24 nM in membrane preparations expressing FLAG-human-GPR84-eYFP.¹³⁰ Al Mahmud et al. demonstrated a non-competitive binding mode for the examined derivatives, since neither lipid-like nor DIM-derived agonists could displace the radioligand.¹³⁰ Interestingly, these antagonists display markedly weaker affinity at the mouse GPR84 (20-70-fold) than at the human receptor ortholog, despite the high similarity between human and rodent receptors.^{126,159,161} The lack of insight into their binding mode and the compounds' failure to efficiently block rodent GPR84 reduces their usefulness for preclinical studies.

Only one representative of class II antagonists has been described. Fezagepras (**57**, PBI-4050, setogepram, **Figure 1.11**) is structurally related to decanoic acid but rigidified by the incorporation of a phenyl ring. It displayed weak inhibition of G_i activation in HEK293 cells transfected with human GPR84 and a G_{αi2} activation biosensor in a BRET assay (IC₅₀ ~ 400 μM) using decanoic acid as agonist.¹⁵² The compound additionally showed weak agonism at GPR40 (FFAR1) with an EC₅₀ value of ~1 mM determined in a BRET-based assay that allows the monitoring of β-arrestin recruitment in HEK293 cells.¹⁵² Grouix et al. demonstrated that the antifibrotic effect of fezagepras is also due to the modulation of other cellular targets: the compound activated liver kinase B1 (LKB1) as well as AMP-activated protein kinase (AMPK) and blocked mammalian target of rapamycin (mTOR). The effect on mTOR phosphorylation was most pronounced and could be observed at a dose of 250 μM in TGFβ-activated hepatic stellate cells, whereas an increase in LKB1 and AMPK phosphorylation was only measured at a 500 μM dose (Western blot analyses).¹⁸⁰ Furthermore, a group recently reported activity at the FFAR2 for that compound (unpublished results).¹⁶¹ Therefore, the antifibrotic activity of fezagepras, which is currently studied in clinical trials,¹⁵⁷ is likely due to a combination of these effects.

The first selective antagonists sharing the receptor's ("orthosteric") MCFAs binding site were recently developed by our group.¹ The series of 8-benzamidochromen-4-one derivatives (class III, **Figure 1.11**) was characterized in functional cellular assays (cAMP accumulation and β-arrestin recruitment assays in human GPR84-transfected CHO cells), as well as in radioligand binding studies vs. [³H]PSB-1584 (**51**, **Figure 1.9**). PSB-17138 (**58**, 6-(4-chlorophenyl)-8-(4-((4-fluorobenzyl)oxy)benzamido)-4-oxo-4*H*-chromene-2-carboxylic acid, **Figure 1.11**) was the most potent antagonist of the study with IC₅₀ values of 7.34 nM (cAMP assay) and 3.02 nM

(β -arrestin assay). The compound also showed the highest affinity among the examined derivatives with a K_i value of 46.1 nM determined vs. **51**. A summary of the most relevant SARs determined in the original work¹ is provided in **Figure 1.12**.

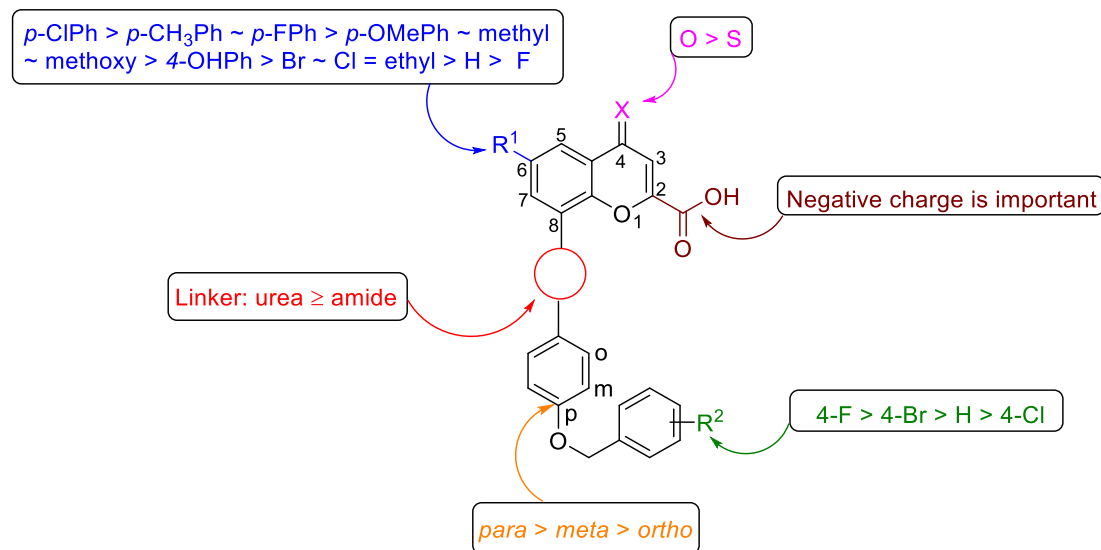


Figure 1.12. Structure-activity relationships for chromen-4-ones as GPR84 antagonists.

The most potent derivatives were tested for GPR84 selectivity against various related GPCRs (GPR17, GPR18, GPR35, GPR55, FFAR1, FFAR4), and found to display no noteworthy activity at those receptors. The optimization of this scaffold to reach even more powerful and drug-like – especially better soluble – GPR84 antagonist is part of the present study and will be discussed below.

2 Objectives of the study

The motivation of this study was to synthesize and characterize powerful new tool compounds for both GPR35 and GPR84 to facilitate drug development. We based our approach on the following rationales.

2.1 Introduction

The G protein-coupled receptors 35 and 84 are still underexplored potential drug targets despite their numerous (patho)physiological roles. GPR35 has powerful antiallergic and anti-inflammatory properties^{2,181} and is involved in blood pressure regulation,⁸¹ energy homeostasis,^{78,182} and chronic pain,^{59,91} among others. However, potent agonists at the human receptor are practically inactive at the rodent receptors complicating preclinical animal studies. The first objective of this work was the optimization of chromen-4-one-2-carboxylic acids, 1,7-phenanthroline-2,8-dicarboxylic acids, quinolone, and indole derivatives to develop new, highly potent, selective, and druggable ligands for GPR35 with activity at human, rat, and mouse receptors. GPR84 is an immunostimulatory receptor that is highly expressed on leukocytes and upregulated during infection and inflammation.¹⁶¹ Agonists have the potential to intensify the body's immune response to threats, including infection and cancer.¹²⁴ Inhibiting GPR84 signaling through antagonists could limit an excessive inflammatory response in autoimmune disorders, such as inflammatory bowel diseases and fibrosis, among others.^{152,158,183} However, only few potent antagonists have been described in the literature despite their promising applications. The second aim of this study was to optimize the physicochemical properties of our group's most powerful GPR84 antagonist (PSB-19138),¹ which displays unfavorable water solubility, without decrease in biological activity. The chosen strategy was the introduction of polar groups into the scaffold and examining their effects in biological assay systems. Furthermore, a synthetic route for the preparation of PSB-19138 more suitable for large scale synthesis than previous methods was devised.

2.2 Compound design of GPR35 agonists

Most GPR35 agonists display a clear preference for the human GPR35 ortholog (see Introduction). Only few scaffolds are active at the human and rat receptors and even fewer show activity at the mouse receptor in addition to the human and rat orthologs. The most potent scaffolds at these receptors have been discovered in previous works and are depicted in **Figure 2.1**. The 8-benzamidochromen-4-one derivative **25** was discovered by our group,⁹² whereas **29** and **30** were reported by Mackenzie et al.² The 1,7-phenanthroline-2,8-dicarboxylic acid derivative bufrolin (**30**) is the most potent derivative at all three species described in the literature so far, but its potency at the mouse receptor is still not satisfactory.^{53,111}

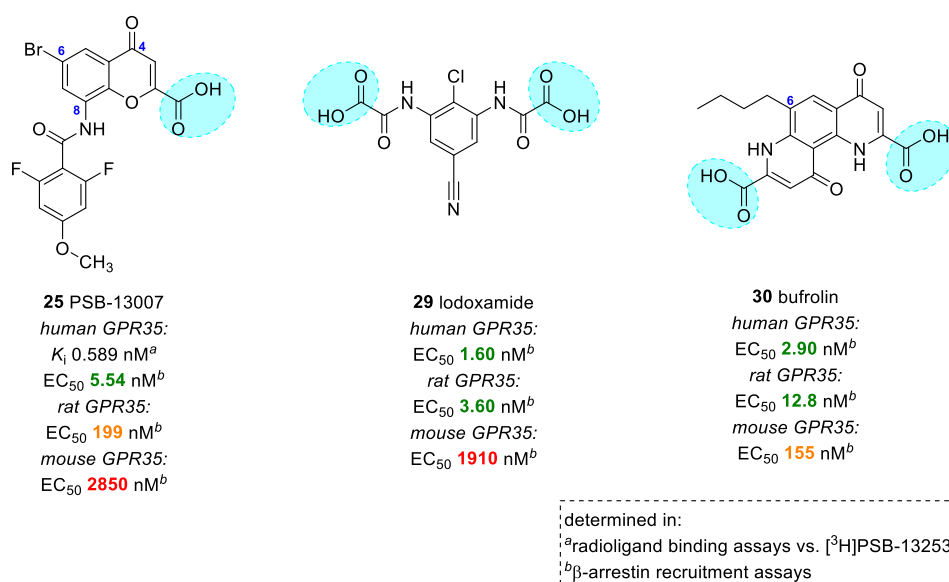


Figure 2.1. Most equipotent GPR35 agonists at the human, rat, and mouse receptors. EC_{50} values < 50 nM are printed green, <500 nM are printed orange, and >500 nM are printed red.

2.2.1 Chromen-4-one derivatives

The study conducted by my predecessor found that the rodent receptor activity of the chromen-4-one-2-carboxylic acid scaffold (as in **25**, **Figure 2.1**) could be increased by performing synthetic modifications at the 4-, 6-, and 8-positions of the scaffold. For detailed analyses of the structure-activity relationships of all the undertaken modifications, see the respective work.¹ In summary, the introduction of a phenyl moiety (**26**, **Figure 2.2**) in the 6-position led to a

significantly more potent compound at all receptor orthologs. Moreover, the human receptor tolerated the introduction of a second carboxylic acid in position 8 – as in **59** (**Figure 2.2**), which also led to an increased rat receptor potency. The combination of the two modifications provided a number of compounds with increased mouse receptor potency. For example, phenyl or butyl substitution in the 6-position combined with a second carboxylic acid moiety in position 8 led to compounds **60** and **61** (**Figure 2.2**), which displayed nanomolar potencies at all three receptor orthologs. Interestingly, **61** shows remarkable structural similarities with bufrolin (**30**, **Figure 2.1**). These substitution patterns led to the most potent derivatives at the human and rat receptors of the previous study, but failed to substantially increase mouse receptor activity. Upon alterations at position 4, however, a significant increase in mouse receptor activity was observed. The exchange of the 4-keto moiety to thioketone as in **62** (**Figure 2.2**) led to the most potent chromone derivative at the mouse receptor ortholog of my predecessor's work. Yet only one derivative of this kind was synthesized, and modifications at the other positions were left unaddressed. Therefore, one part of this study was to investigate additional substitution patterns of 8-carboxyformamidochromen-4-one derivatives, including 4-thio-substituted ones to discover an even more potent derivative for the mouse receptor ortholog.

Previous work:

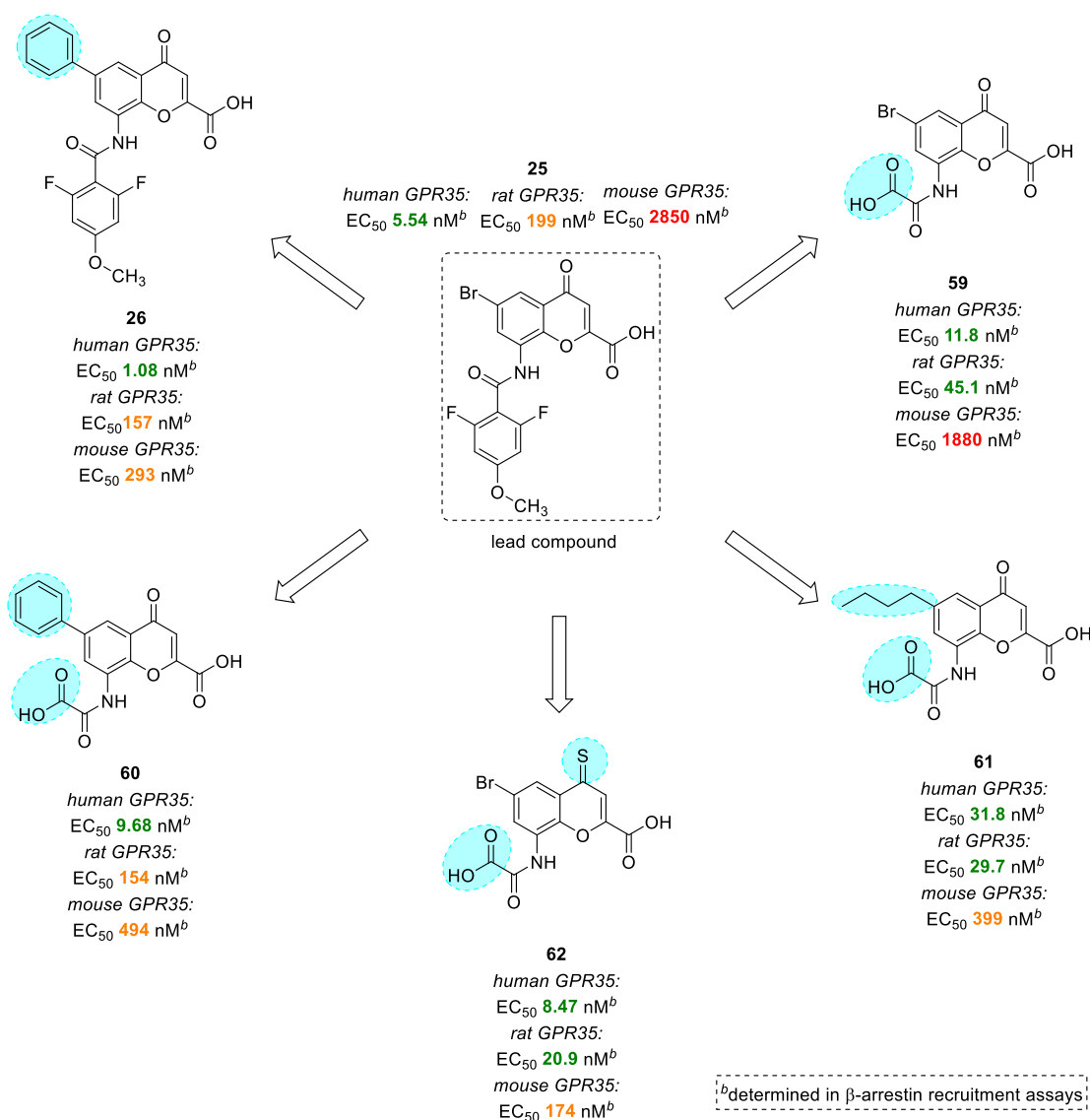


Figure 2.2. Previous optimization of chromen-4-one derivatives that increased potency at rodent receptor orthologs.

One of the aims of this study was to optimize the chromen-4-one scaffold for the mouse GPR35, since such compounds are essential to perform target validation studies in animal models of diseases. This was accomplished by varying the substitution pattern in positions 4, 6, and 8 (see **Figure 2.3**), introducing a number of different residues. Using β -arrestin recruitment assays in transfected CHO cells recombinantly expressing human, rat, or mouse GPR35 as described in earlier publications,^{92,108} the changes were carefully monitored to ensure persistent potency at human and rat GPR35. Considering that the thionation in the 4-position of the core scaffold had previously had such a dramatic impact on mouse potency, special focus lay on the preparation

of new chromen-4-thione derivatives. Likewise, previous studies had shown the distinguished potential of the 6-position for increasing overall potency. Large and lipophilic substituents had had a particularly positive effect and were therefore examined in more detail. Furthermore, a modification of the 3-position was to be explored, as well as the ester protection of the carboxylic acid moieties. Finally, we investigated the importance of the core chromone structure by replacing it with quinoline or indole rings and compared the resulting compounds' performance in cell-based assays with that of the original scaffold. **Figure 2.3** summarizes the chemical modifications of the chromen-4-one scaffold investigated in this work.

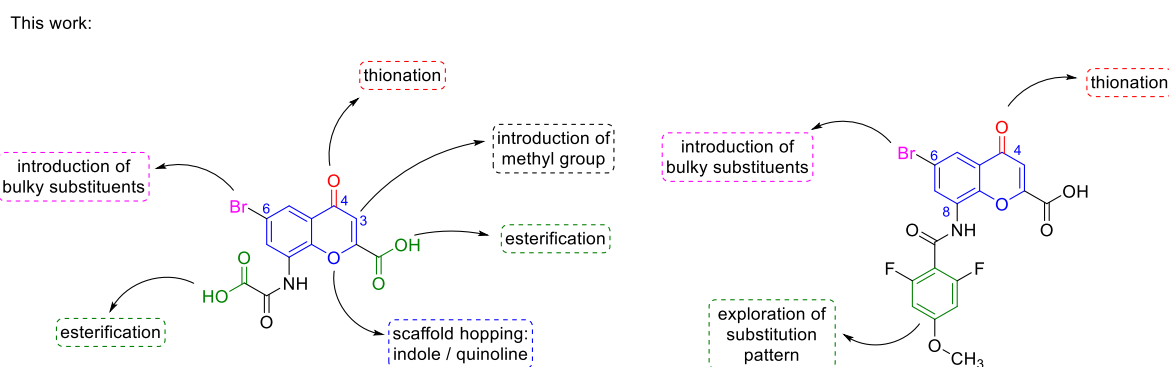


Figure 2.3. Chemical modifications of chromen-4-one-based GPR35 agonists to be investigated herein.

2.2.2 Phenanthroline derivatives

As mentioned above, the phenanthroline derivative bufrolin (**30**, **Figure 2.1**) was the most potent molecule at human, rat, and mouse GPR35.² Interestingly, the study by my predecessor featured one bufrolin-derived molecule (**63**),¹ which showed similar properties (see **Figure 2.4**).

Previous works:

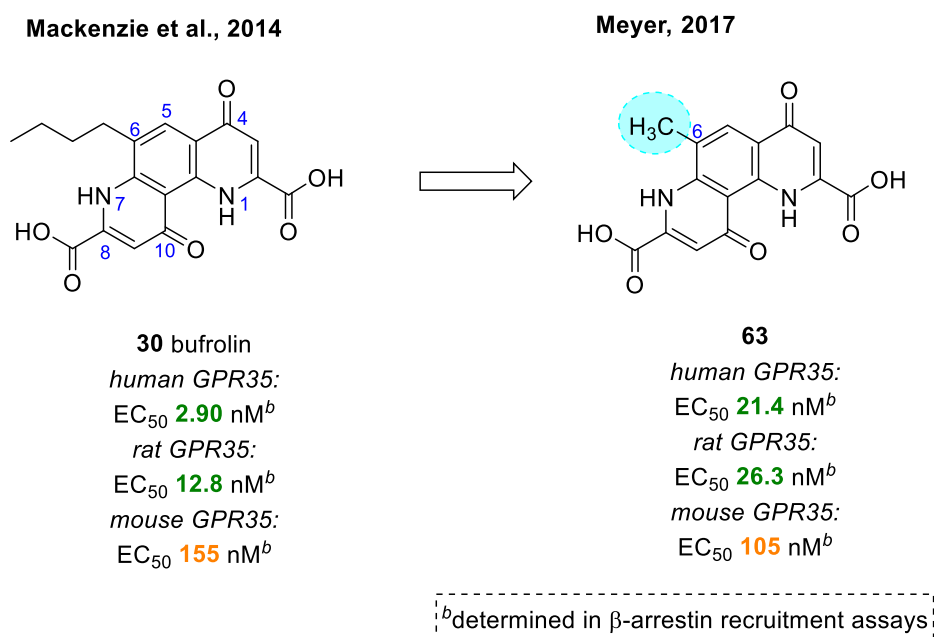


Figure 2.4. The most potent agonists at human, rat, and mouse GPR35 share a 1,7-phenanthroline scaffold.^{1,2}

Considering its favorable features, our aim was to explore the scaffold's structure-activity relationships in detail. To the best of our knowledge, the compound was first mentioned in a patent from 1974 that describes the antiallergic effect of pyridoquinoline dicarboxylic acid derivatives.¹⁸⁴ The authors listed bufrolin as a “particularly preferred compound” and suggested it for the treatment of asthma, for example, allergic asthma. In 1977, the compound's antiallergic potential was investigated in a rat passive cutaneous anaphylaxis (PCA) assay using rats passively sensitized to egg albumin.¹⁸⁵ Bufrolin elicited a 500-fold more potent anti-allergenic effect than the reference compound cromolyn and was the most potent 1,7-phenanthroline-2,8-dicarboxylic acid derivative of that study. At the time, however, the molecular target of bufrolin was unknown, and no structure-activity relationship analysis could be performed. Extrapolating from our own group's research on chromen-4-one-2-carboxylic acid derivatives,^{1,92,108} we decided that the most promising position for synthetic modification was the 6-position. Its modification, especially the introduction of bulky groups, such as halogens, aryl moieties, and alkyl chains, had previously increased their potency. Therefore, one of the aims was to extensively modify this position (**A**, **Figure 2.5**). Furthermore, the effect of an additional substituent in the 5-position was to be explored (**B**). The superiority of the 1,7-phenanthroline scaffold vs. other (pyrido)quinolines was studied (**C**, **D**). Moreover, the

significance of the carboxylic acid moieties in positions 2 and 8 was investigated. Thus, a series of compounds was esterified (**E**) and examined for agonist and antagonist activity, and the carboxylic acid groups were replaced by primary alcohol moieties (**F**). Finally, we wanted to probe the importance of the hydrogen-acceptor in position 4 (**G**). **Figure 2.5** provides an overview of modifications carried out at the phenanthroline scaffold.

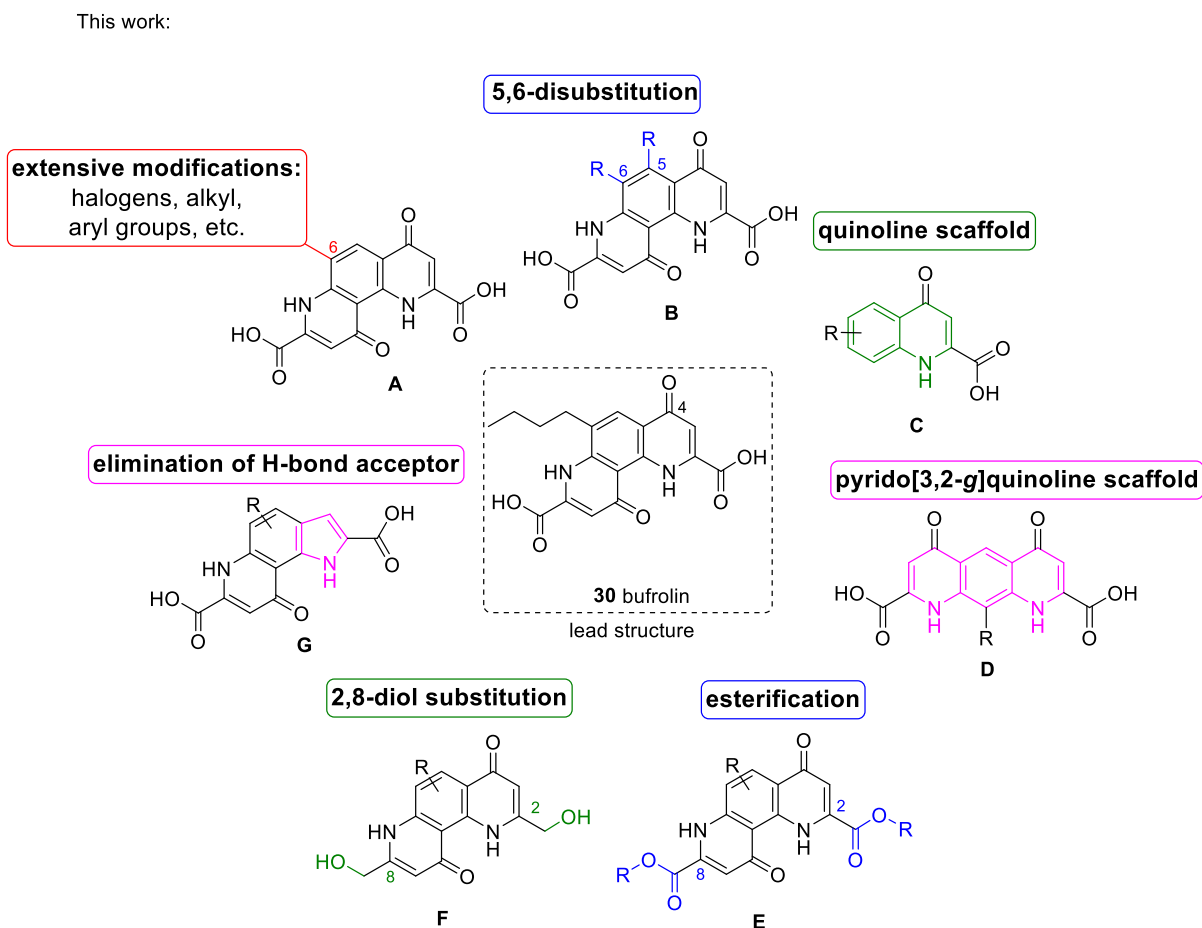


Figure 2.5. The lead structure bufrolin was extensively modified to increase rodent GPR35 activity.

One of the issues with existing GPR35 agonists that show activity at human, rat, and mouse receptor orthologs is their lack of selectivity for GPR35. Zaprinast (**8**, **Figure 1.7**, 1.2.2 *Synthetic GPR35 ligands*), for example, displays activity at all three receptor orthologs, however, it is also a relatively potent phosphodiesterase inhibitor. This limits its usefulness for animal studies (see Introduction). Therefore, apart from developing highly potent GPR35 agonists for the human, rat, and mouse receptor orthologs, our aim was to obtain compounds

with high selectivity versus other related targets. The most potent derivatives needed to be selective versus other GPCRs, such as the closely related GPR55 (30% sequence identity, 53% sequence similarity), GPR17 (identity 29%, similarity 47%), GPR18 (26% identity, 46% similarity), GPR84 (25% identity, 42% similarity), MRGPRX2 (identity 25%, similarity 50%), and MRGPRX4 (identity 29%, similarity 48%).*

Lastly, the metabolic and pharmacokinetic properties of selected representative compounds were to be tested to ensure sufficient metabolic stability, aqueous solubility, and membrane permeability, required for clinical development.

2.3 Compound design of GPR84 antagonists

The most potent GPR84 antagonists that occupy the receptor's lipid binding site were developed by our group.¹ PSB-17138 (**Figure 2.6**) displayed the highest potency in functional assays and the highest affinity in radioligand binding assays versus the agonist radioligand [³H]6-hexylaminouracil (PSB-1584). Therefore, it served as the lead compound for this work. However, the structure entailed a number of issues that are discussed in this section.

*Sequence identity and similarity determined using the U.S. National Library of Medicine's Basic Local Alignment Search Tool (BLAST) <https://blast.ncbi.nlm.nih.gov/Blast.cgi?page=Proteins>.

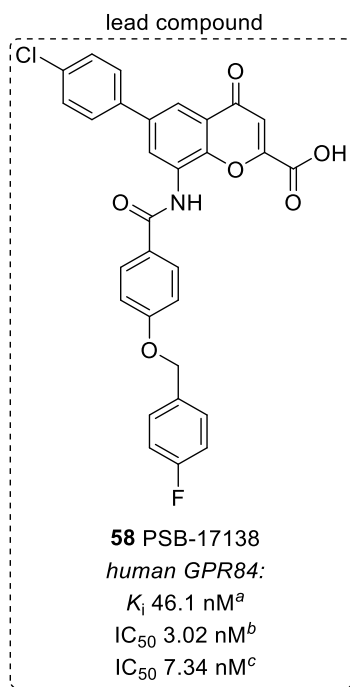


Figure 2.6. PSB-17138 served as the lead compound for this work. Determined in ^aradioligand binding assays versus [³H]PSB-1584, ^bβ-arrestin recruitment assays, and ^ccAMP accumulation assays.

Firstly, little of the compound was available for additional experiments and it needed to be resynthesized in a larger batch. However, the synthetic route that had been employed for its preparation in the previous work proved unsuitable for the generation of larger amounts of the molecule. So, the synthetic pathway needed to be optimized to increase yields and decrease reaction times. The purity of the final reaction product was generally low as well, which necessitated additional, inefficient purification procedures (by preparative HPLC), complicated by the compound's poor solubility in most solvents, especially in water/acetonitrile or water/methanol mixtures that are typically used for reverse-phase preparative HPLC or flash chromatography. The use of chromatographic purification techniques was therefore only suitable for small amounts in the range of few milligrams. One aim was, consequently, to prepare the lead compound and optimize its synthetic pathway to facilitate the production in a larger amount required for extensive biological studies.

Despite the good performance of PSB-17138 as GPR84 antagonist and its favorable selectivity profile,¹ the issue of its undesirable physicochemical properties, especially poor solubility, had to be addressed. Preliminary solubility measurements at a contract research laboratory (Pharmacelsus, Saarbrücken, Germany) were inconclusive due to insufficient dissolution in the

used solvent (data not shown). Considering that solubility and cell permeability are major factors for the success of drug development efforts, we carefully analyzed the reported structure-activity relationships of PSB-17138 in an attempt to introduce favorable functional groups into the structure to improve its properties without impairing its antagonistic potency at GPR84. Therefore, individual variations of the lead compound PSB-17138 had to be investigated in GPR84-dependent bioassays, before combining distinct structural modifications.

The existing SARs determined in the previous study provided important structural insight and served as a basis for possible modifications (see **Figure 2.7**). For instance, while *p*-chlorophenyl had been the best substituent at the 6-position of the chromone core, additional halogen substituents at this ring (C) had not been examined – nor had the ring been replaced with more polar heterocycles. Similarly, the carboxylic acid moiety in the 2-position of the core left room for improvement, since the bioisosteric replacement by a variety of functional groups had not been addressed. And while other important modifications had been described for the benzamide (D) and benzyl (E) rings, the focus had previously been on increasing receptor affinity, so their replacement with hydrophilic heterocycles had not been attempted. Likewise, only few modifications at ring E had been performed once *p*-fluoro had been identified to be the most beneficial substituent. The introduction of more polar substituents at the 4-position of ring E was therefore examined in this study.

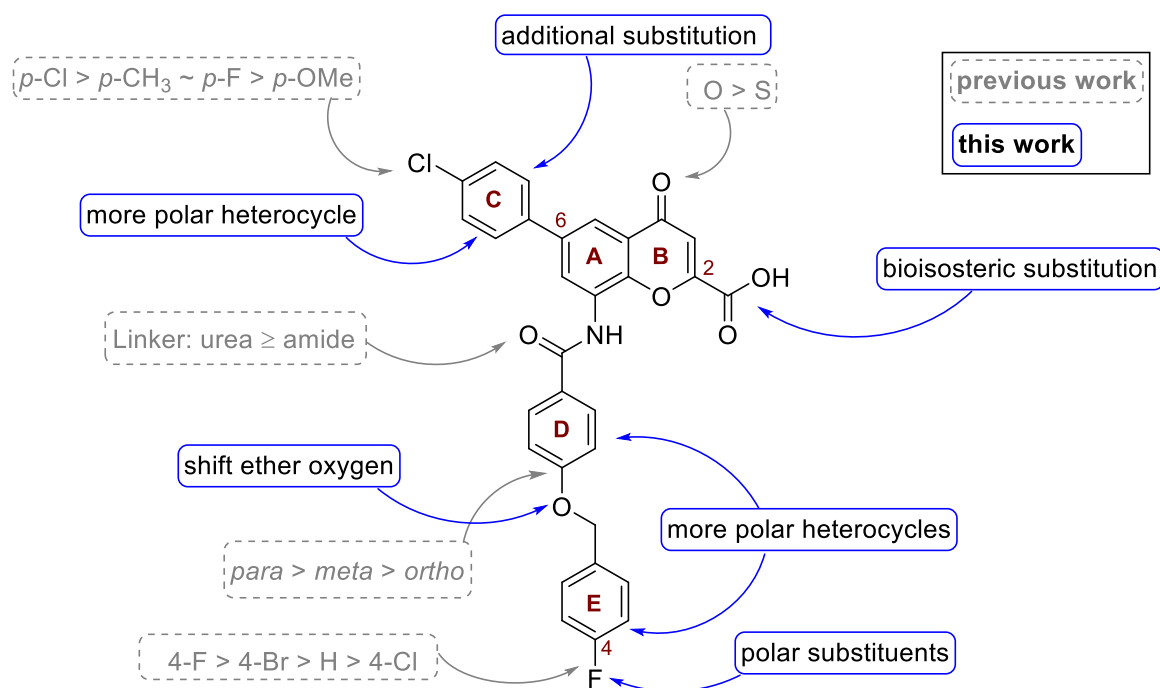


Figure 2.7. Possible modifications at the lead structure to increase polarity.

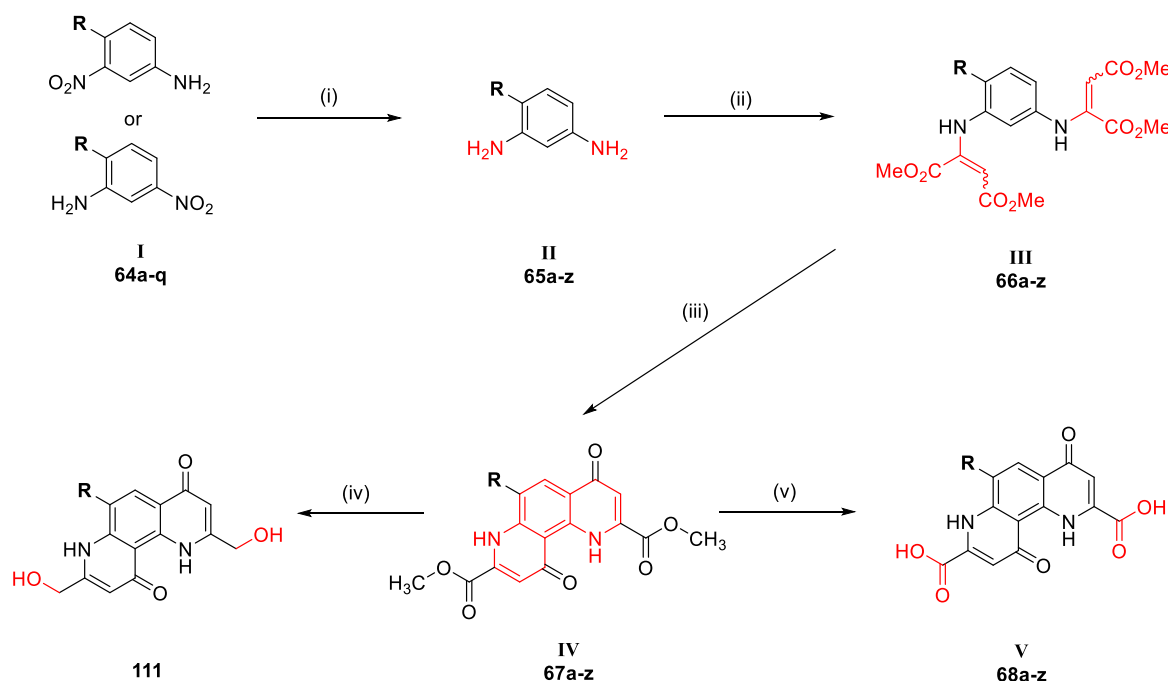
New compounds were to be tested in radioligand binding and functional assays as described in the previous work.¹ The aim was to discover beneficial or neutral modifications and to combine them, thus reaching new derivatives with increased polarity and solubility.

3 Results and Discussion

3.1 Synthesis of 1,7-phenanthroline derivatives

1,7-Phenanthroline derivatives were prepared as depicted in **Schemes 3.1** and **3.2**. Final compounds **68f**, **68i**, **68j** and their preparation have been described in the literature.^{1,184–186} In short, appropriately 4-substituted 1,3-phenylenediamines **II** (**65a-z**) were either commercially available (**65a-f**) or synthesized from appropriate nitroanilines **I** (**64a-q**) followed by catalytic reduction of the respective nitro group to the amine. They were then converted into enamine intermediates **III** (**66a-z**) that were subsequently cyclized in a Conrad-Limpach-like reaction to furnish **IV** (**67a-z**), followed by hydrolysis to afford 2,8-dicarboxylic acid derivatives **V** (**68a-z**). Compound **111** was afforded via the reduction of compound **67l**. For detailed synthetic procedures see individual compounds (*5.2 Preparation of Phenanthrolines, quinolines, and indole derivatives*).

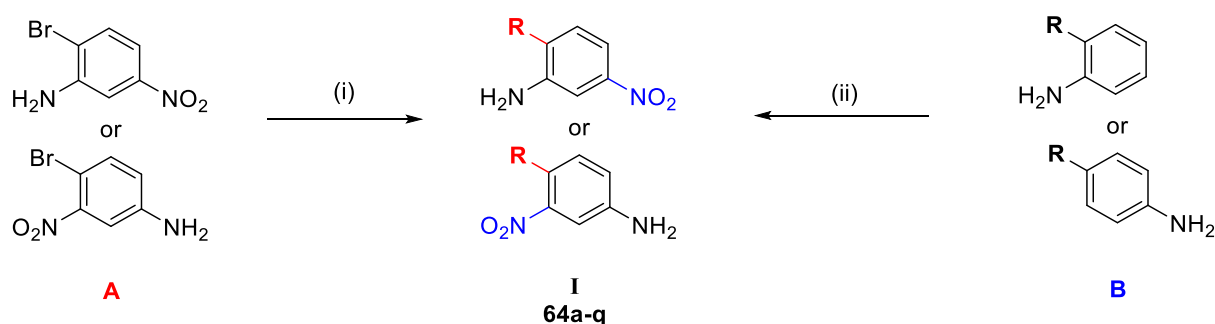
Scheme 3.1. Preparation of 1,7-phenanthroline derivatives.^a



^aReagents and conditions: (i) MeOH:THF (1:1), Pd/C (10%), H₂, 3.1 bar, rt, 2 h, 90-100% yield; (ii) DMAD, MeOH, rt, 12-24 h, Ar, 25-92% yield; (iii) Ph₂O, 250 °C, ~15 min, 4-67% yield; (iv) MeOH:DCM (1:1), NaBH₄, 0 °C, 2 h; rt, 2 h, 23% yield; (v) procedure A: NaOH aq, reflux, 1 h; HCl conc., 50-100% yield; procedure B: HCl (6M):HAc (1:1), reflux, 3-6 h, 65-100% yield. For R see **Tables 3.1-6**.

4-Aryl-1,3-phenylenediamines (**65u-y**) were prepared from 2-bromo-5-nitroaniline or 4-bromo-3-nitroaniline (**A**, **Scheme 3.2**) via the nitroaniline intermediates **I** in high yields using a Suzuki coupling protocol. 4-Alkyl-1,3-phenylenediamines (**65h-p**, **65r-t**) were prepared from commercially available 2- or 4-alkylanilines (**B**) in a selective nitration reaction under acidic conditions (**Scheme 3.2** and **Table 3.1**).

Scheme 3.2. Preparation of nitroanilines.^a



^aReagents and conditions: (i) boronic acid derivative, Pd(PPh₃)₄, K₂CO₃, toluene, DMF, 130°C, 3 h, 74-95% yield; (ii) HNO₃, H₂SO₄, -5°C, 15 min, 60-99% yield. For **R** see **Table 3.1**.

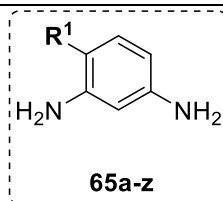
Table 3.1. Yields and purities of nitration and Suzuki coupling reactions for substituted nitroanilines I

		64a-j	64k-q				
I							
compd	R ¹	yield ^a [%]	purity ^b [%]	compd	R ¹	yield ^a [%]	purity ^b [%]
64a^c	pentyl	98	98.4	64k^c	propyl	64	99.1
64b^c	hexyl	80	98.0	64l^c	butyl	91	99.2
64c^c	heptyl	99	94.3	64m^c	<i>t</i> -butyl	76	90.0
64d^c	octyl	82	95.4	64n^d	thiophen-2-yl	86	99.1
64e^c	nonyl	75	94.4	64o^d	phenyl	95	98.1
64f^c	decyl	79	81.4	64p^d	<i>p</i> -tolyl	88	96.6
64g^c	dodecyl	60	94.8	64q^d	<i>t</i> -butylphenyl	74	97.1
64h^c	<i>sec</i> -butyl	99	98.2				
64i^c	cyclohexyl	85	98.7				
64j^d	4-butyl-phenyl	82	97.8				

^aPercentages reflect isolated yields. ^bPurity was determined by HPLC-UV (254 nm)-ESI-MS. ^cCompounds were synthesized via a selective nitration reaction. ^dCompounds were synthesized using a Suzuki coupling protocol.

This was followed by palladium-catalyzed hydrogenation at room temperature in a mixture of tetrahydrofuran and methanol that was found to dissolve alkylnitroanilines better than the individual solvents. The reduction was always completed in less than 2 hours, and the resulting phenylenediamines **65g-z** could be isolated in excellent yields (90-100%) following filtration (Table 3.2).

Table 3.2. Yields of catalytic reduction reactions affording 1,3-phenylenediamines II

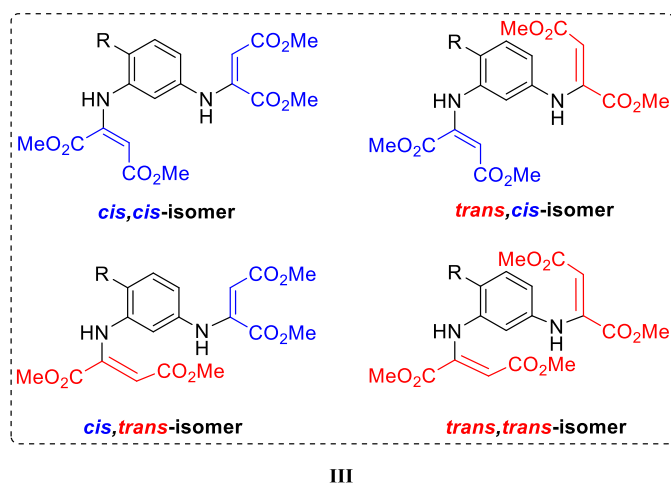


II

compd	R ¹	yield ^a [%]	compd	R ¹	yield ^a [%]
65a^b	H	-	65n	nonyl	100
65b^b	F	-	65o	decyl	98
65c^b	Cl	-	65p	dodecyl	100
65d^b	Br	-	65q	OCH ₃	100
65e^b	NO ₂	-	65r	<i>sec</i> -butyl	100
65f^{cb}	CH ₃	-	65s	<i>tert</i> -butyl	95
65g	ethyl	100	65t	cyclohexyl	100
65h	propyl	100	65u	thiophen-2-yl	100
65i	butyl	99	65v	phenyl	100
65j	pentyl	98	65w	<i>p</i> -tolyl	100
65k	hexyl	99	65x	<i>4-tert</i> -butylphenyl	100
65l	heptyl	99	65y	<i>4</i> -butylphenyl	90
65m	octyl	100	65z	5,6-dimethyl	100

^aPercentages reflect isolated yields. ^bCommercially available.

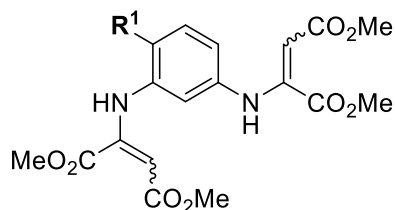
1,3-Phenylenediamines (**II**) were immediately reacted with dimethyl acetylenedicarboxylate (DMAD) under the exclusion of air, due to their rapid oxidation (brown discoloration) resulting in lower yields. Therefore, DMAD (or its diethyl derivative in the case of **66h**) was added dropwise at room temperature under an argon atmosphere. This hydroamination reaction afforded the appropriate enamine intermediates **III** in moderate yields (on average 60%, see Table 3.3) as isomeric mixtures (for structures, see Figure 3.1).



III

Figure 3.1. Four possible reaction products with different *cis-trans* isomerism.

In the literature,^{184,185} these mixtures were either used directly for the next reaction step or after extraction, however, we found that prior purification via column chromatography (petroleum ether/ethyl acetate, 4:1) increased yields and purities of the subsequent reaction products. Therefore, reaction mixtures were generally separated on column, collecting only the most lipophilic isomer fractions for subsequent reactions. All of these compounds were isolated as highly viscous, yellow oils miscible with most common organic solvents, including – in some cases – petroleum ether.

Table 3.3. Yields and purities of hydroamination intermediates III**III
66a-z**

compd	R ¹	yield ^a [%]	purity ^b [%]	compd	R ¹	yield ^b [%]	purity ^c [%]
66a	H	46	96.5	66n	nonyl	62	86.4
66b	F	60	98.4	66o	decyl	41	61.5
66c	Cl	66	96.5	66p	dodecyl	67	91.6
66d	Br	38	68.4	66q	OCH ₃	76	82.9
66e	NO ₂	68	80.4	66r	<i>sec</i> -butyl	62	91.2
66f	CH ₃	79	87.9	66s	<i>tert</i> -butyl	36	97.3
66g	ethyl	86	95.0	66t	cyclohexyl	70	91.0
66h^c	propyl	100	98.0	66u	thiophen-2-yl	25	87.2
66i	butyl	52	89.9	66v	phenyl	92	85.0
66j	pentyl	47	86.2	66w	<i>p</i> -tolyl	27	79.6
66k	hexyl	63	95.7	66x	4- <i>tert</i> -butylphenyl	37	n.d.
66l	heptyl	66	89.3	66y	4-butylphenyl	82	98.9
66m	octyl	69	88.9	66z	4,5-dimethyl	92	82.6

^aPercentages reflect isolated yields. ^bPurity was determined by HPLC-UV (254 nm)-ESI-MS. ^cCompound **66h** was synthesized with diethyl acetylenedicarboxylate and is a tetraethylester derivative. n.d., not determined.

Enamine intermediates (**III**) were cyclized to the appropriate 1,7-phenanthroline 2,8-diester derivatives in a 6- π -electrocyclization at high temperatures. High-boiling solvents like diphenyl ether or Dowtherm[®] A (26.5% biphenyl + 73.5% diphenyl ether) were employed to reach the necessary temperature of at least 245°C. Due to the extreme conditions, the reaction generally yielded many side products in addition to the desired product. Some of these side products were monocyclized quinolone derivatives (see **Figure 3.2**), some others were non-characterized decomposition products.

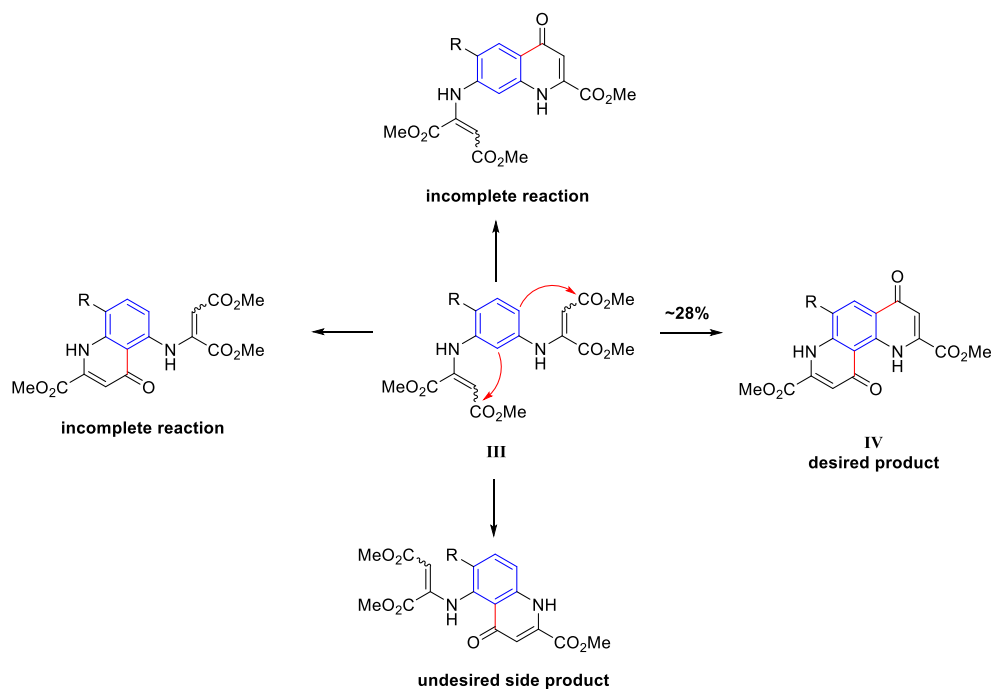
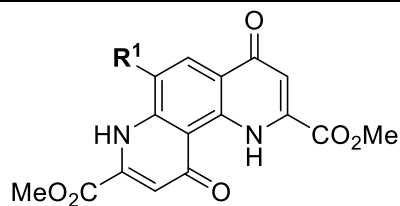


Figure 3.2. Cyclization reaction in high-boiling solvents yields variably cyclized (side) products.

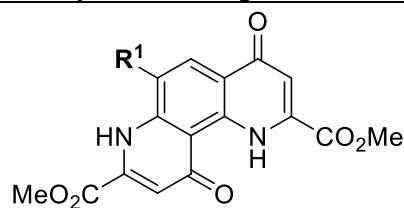
The reaction time was kept below 15 min to balance product formation and degradation. A simple glass tube served as reflux condenser to avoid deposition of solid diphenyl ether (melting point: ~ 27 °C). The isolation of the desired cyclized 1,7-phenanthroline derivatives was generally challenging due to the mentioned presence of multiple side products, their particular physicochemical properties (highly polar, yet poorly soluble), and the high boiling point of the solvent, diphenyl ether. However, purification could be achieved by exploiting the compounds' poor solubility in all common solvents except chlorinated hydrocarbons, like DCM or chloroform: first, the cooled reaction mixture was mixed with petroleum ether to precipitate the desired polar components. These were then collected by filtration and washed with more petroleum ether, removing remaining diphenyl ether. Subsequent washing with different solvents, especially acetone, was often sufficient to purify the compounds. In other instances, the precipitate had to be purified by column chromatography using a mixture of dichloromethane and methanol (e.g. 99:1) as solvent. The yields of these reactions were generally low (on average 28%, see **Table 3.4**).

Table 3.4. Yields and purities of cyclized intermediates IV**IV
67a-z**

compd	R ¹	yield ^a [%]	purity ^b [%]	compd	R ¹	yield ^a [%]	purity ^b [%]
67a	H	53	95.3	67n	nonyl	49	98.6
67b	F	7	99.1	67o	decyl	8	98.2
67c	Cl	30	93.1	67p	dodecyl	35	94.0
67d	Br	24	96.4	67q	OCH ₃	11	86.0
67e	NO ₂	4	92.6	67r	<i>sec</i> -butyl	7	98.2
67f	CH ₃	26	96.1	67s	<i>tert</i> -butyl	8	95.6
67g	ethyl	30	99.1	67t	cyclohexyl	47	93.7
67h^c	propyl	35	90.8	67u	thiophen-2- yl	28	96.5
67i	butyl	35	97.2	67v	phenyl	10	97.5
67j	pentyl	28	98.2	67w	<i>p</i> -tolyl	29	94.0
67k	hexyl	28	89.3	67x	<i>4-tert</i> - butylphenyl	67	97.3
67l	heptyl	38	97.6	67y	<i>4</i> -butyl- phenyl	11	98.2
67m	octyl	26	98.7	67z	<i>5,6</i> - dimethyl	41	92.4

^aPercentages reflect isolated yields. ^bPurity was determined by HPLC-UV (254 nm)-ESI-MS. ^cCompound **67h** is a 2,8-diethylester derivative.

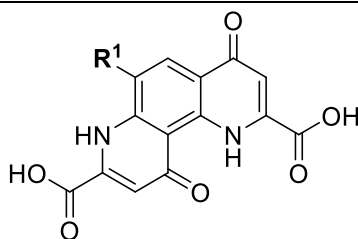
Some of the compounds were final products and further characterized in bioassays; for their melting points see **Table 3.5**.

Table 3.5. Melting points of 2,8-dimethyl ester compounds

compd	R ¹	m.p. ^a [°C]
67d	Br	>290
67j	pentyl	190-191 ^b
67l	heptyl	172-173
67m	octyl	169-170
67r	<i>sec</i> -butyl	198-199

^aMelting points are uncorrected. ^bLit. m.p.: 185 °C.

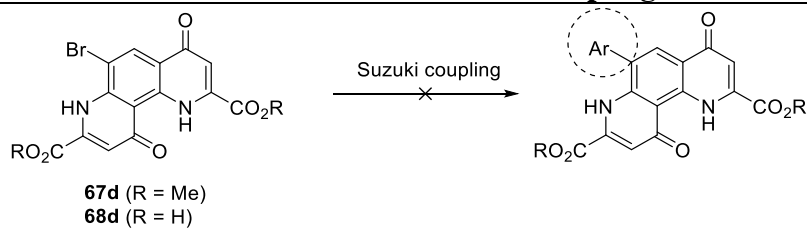
Phenanthroline-2,8-dicarboxylic acid ester derivatives were then hydrolyzed to their corresponding acids using aqueous sodium hydroxide solution either alone or in a mixture with methanol, followed by acidification with hydrochloric acid and filtration. Washing of the precipitate with water usually afforded the products in good yields and high purity (procedure A, see **Table 3.6**). Another method was an acidic hydrolysis procedure using a mixture of acetic acid and hydrochloric acid. In this case, the products precipitated from the reaction mixture, and could be isolated directly by filtration (procedure B, **Table 3.6**). The resulting 1,7-phenanthroline-2,8-dicarboxylic acid derivatives were usually poorly soluble in common solvents like DMSO, acetone, or methanol, but highly soluble in aqueous ammonia.

Table 3.6. Yields, purities, and melting points of final 1,7-phenanthroline-2,8-dicarboxylic acid derivatives**V**
68a-z

compd	R ¹	yield ^a [%]	purity ^b [%]	m.p. ^c [°C]	compd	R ¹	yield ^a [%]	purity ^b [%]	m.p. ^c [°C]
68a ^d	H	85	96.0	>300 ^f	68n ^e	nonyl	99	95.0	>300
68b ^d	F	72	99.8	>300	68o ^e	decyl	99	97.5	>300
68c ^d	Cl	50	99.3	>300	68p ^e	dodecyl	70	97.0	>300
68d ^d	Br	74	95.7	>300	68q ^d	OCH ₃	94	98.3	>300
68e ^d	NO ₂	72	99.6	>300	68r ^e	<i>sec</i> -butyl	65	98.9	>300
68f ^e	CH ₃	100	99.1	>300	68s ^d	<i>tert</i> -butyl	54	97.8	>300
68g ^e	ethyl	87	99.9	>300	68t ^d	cyclohexyl	97	96.4	>300
68h ^d	propyl	70	96.4	>300	68u ^e	thiophen-2-yl	86	95.0	>300
68i ^d	butyl	88	99.6	>300 ^g	68v ^d	phenyl	80	98.8	>300
68j ^e	pentyl	65	99.5	>300 ^h	68w ^e	<i>p</i> -tolyl	96	95.0	>300
68k ^e	hexyl	95	99.4	>300	68x ^e	<i>4-tert</i> -butylphenyl	82	98.4	>300
68l ^e	heptyl	65	98.2	>300	68y ^d	<i>4</i> -butylphenyl	98	99.0	>300
68m ^e	octyl	94	97.4	>300	68z ^d	5,6-dimethyl	100	95.0	>300

^aPercentages reflect isolated yields. ^bPurity was determined by HPLC-UV (254 nm)-ESI-MS. ^cMelting points are uncorrected. ^dAlkaline hydrolysis (procedure A). ^eAcidic hydrolysis (procedure B). ^fLit. m.p.: >320 °C. ^gLit. m.p.: 300 °C dec., ¹⁸⁴ 305-310 °C dec. ^hLit. m.p.: 297-300 °C dec., ¹⁸⁴ 300-305 °C dec. ¹⁸⁵

In early attempts to simplify the future preparation of 1,7-phenanthrolines and facilitate the rapid generation of differently 6-position-substituted derivatives, we tried to establish a Suzuki-coupling protocol, employing the 6-bromo derivatives **67d** and **68d** as starting materials. However, either due to the compounds' low solubility in the chosen solvent systems or their general lack of reactivity, no reaction could be observed under the tested conditions (see **Table 3.7**). Therefore, we decided to build the scaffold from the respective 1,3-phenylenediamine for each target compound as described above.

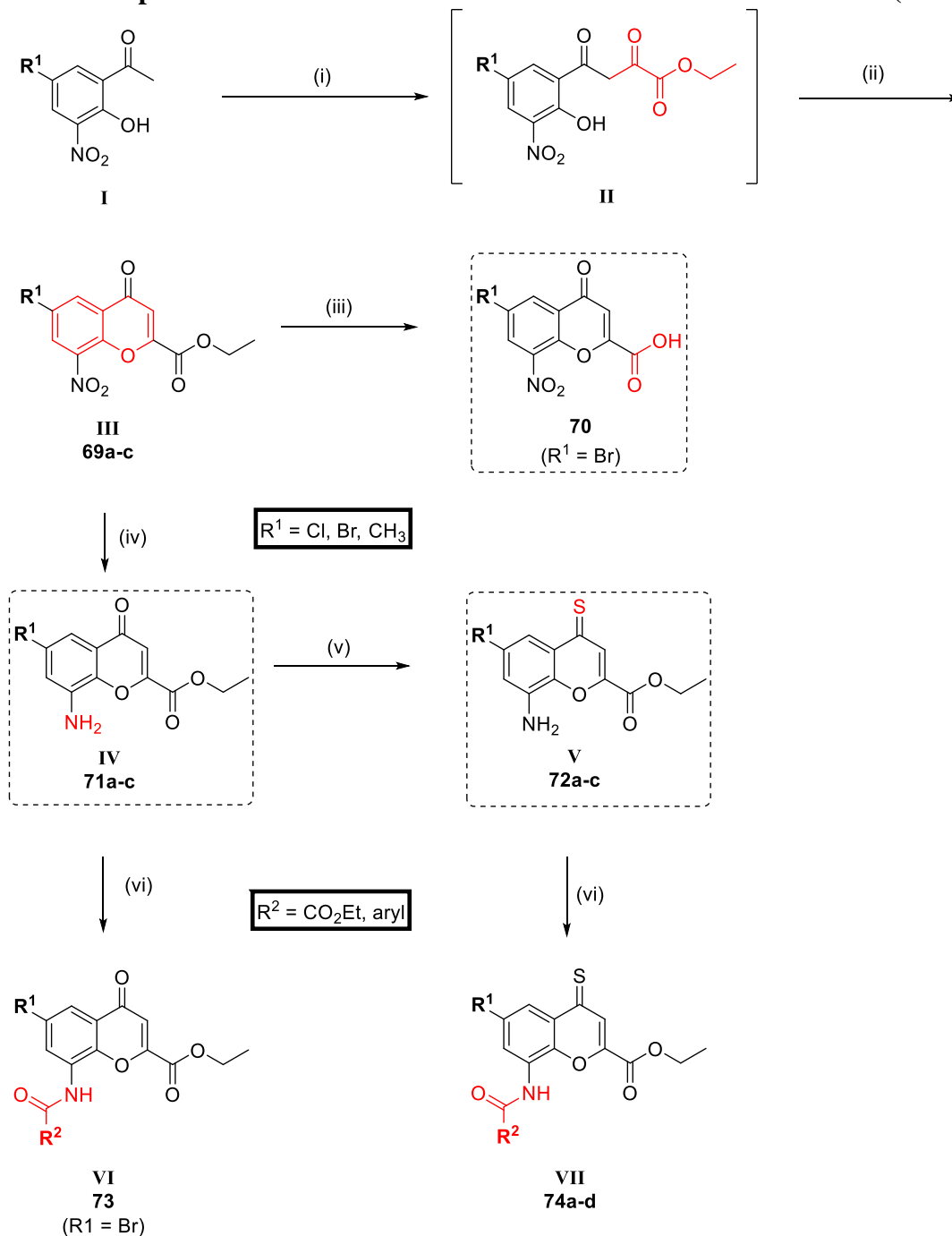
Table 3.7. Reaction conditions of unsuccessful Suzuki coupling reactions^a

starting material	boronic acid (2 eq.)	catalyst (0.1 eq.)	base (2 eq.)	solvent 1	solvent 2	temperature [°C]	time	yield [%]
67d	PhB(OH) ₂	Pd(PPh ₃) ₄	K ₂ CO ₃	toluene	DMF	130	3 h	0
67d	PhB(OH) ₂	Pd(dppf)Cl ₂	K ₂ CO ₃	dioxane	-	60-100	5 h	0
67d		Pd(PPh ₃) ₄	CS ₂ CO ₃	DMF	-	130	3 h	0
68d	PhB(OH) ₂	Pd(PPh ₃) ₄	K ₂ CO ₃	toluene	DMF	130	o.n.	0

^aProduct formation monitored by HPLC-UV (254 nm)-ESI-MS of crude reaction mixture. Ar, aryl; DMF, dimethylformamide; eq., equivalent; o.n., overnight; Pd(dppf)Cl₂, [1,1'-bis(diphenylphosphino)ferrocene]-palladium(II) dichloride; Pd(PPh₃)₄, tetrakis(triphenylphosphine)palladium(0); PhB(OH)₂, phenylboronic acid.

3.2 Synthesis of chromen-4-one derivatives

Chromone derivatives were synthesized according to **Schemes 3.3-8**. The final compound **70** as well as the intermediate compounds **IV** and **V** were important starting points for the preparation of most target compounds. Their synthesis is depicted in **Scheme 3.3**. The starting material for all herein described chromone derivatives (except for the 3-methyl substituted **80** and **87**; see below) were the commercially available 5'-position-substituted 2'-hydroxy-3'-nitroacetophenones (**I**). In a crossed Claisen condensation, these were reacted with diethyl oxalate under basic conditions, using potassium or sodium *tert*-butoxide, to form the diketone intermediates **II**. Contrary to dimethylformamide (DMF) being used in previous reports,^{1,92,108} tetrahydrofuran (THF) was employed as a solvent. This allowed for a much more rapid workflow because of THF's lower boiling point. The use of THF reduced reaction times for this step from 2.5 hours to 20 minutes. **II** could be isolated after the evaporation of solvent, acidic workup, and extraction. Due to the compounds' reported instability, they were immediately used for the subsequent step.

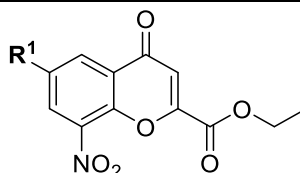
Scheme 3.3. Preparation of chromen-4-one and chromen-4-thione derivatives (Part 1).^a

^aReagents and conditions: (i) diethyl oxalate, KO^tBu, THF, 0 °C, 20 min; (ii) EtOH, HCl conc., reflux, 10 min, 62–84% yield for 2 steps; (iii) HCl (6M):HAc (1:1), reflux, 2 h, 80% yield; (iv) SnCl₂·2H₂O, HCl (2M), EtOH, 65 °C, 40 min, 79–100% yield; (v) Lawesson's reagent, toluene, reflux, 2 h, 17–58% yield; (vi) acid chloride, THF/DCM, DIPEA, 0 °C, 1 h, Ar; rt, 24 h, 34–75% yield.

An acid-catalyzed intramolecular condensation reaction in boiling ethanol, containing few milliliters of concentrated aqueous hydrochloric acid, afforded the cyclized chromen-4-one derivatives **III** (**69a-c**) in isolated yields of 62–84% over two steps. In contrast to previous reports,^{1,92,108} this reaction was usually completed within 10 minutes (instead of overnight). The

products crystallized from the solution and could be isolated by filtration (for yields and purities see **Table 3.8**).

Table 3.8. Yields and purities of 6-substituted 8-nitrochromen-4-one derivatives III



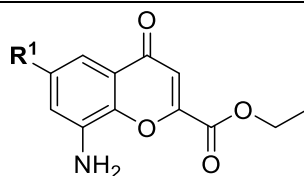
III
69a-c

compd	R ¹	yield ^a [%]	purity ^b [%]
69a	Cl	62	92.5
69b	Br	78	94.0
69c	CH ₃	84	99.4

^aPercentages reflect isolated yields over two reaction steps. ^bPurity was determined by HPLC-UV (254 nm)-ESI-MS.

Further purification was usually achieved by washing the solid with cold ethanol or recrystallization from ethanol. For the preparation of **70**, the 6-bromo derivative of **III** (**69b**) was hydrolyzed using a boiling mixture (1:1) of glacial acetic acid and aqueous hydrochloric acid (6M), which afforded the reaction product in great purity via crystallization upon cooling. This procedure avoided the formation of decomposition products, which often occur during basic hydrolysis of chromones,¹ and to our best knowledge has not been described in the literature for this compound before.

For the synthesis of various 8-benzamido- and 8-carboxyformamidochromen-4-ones with halogen- or methyl-substitution in position 6 (**VI**), as well as for their respective 4-thioxo derivatives (**VII**), compounds **IV** (**71a-c**) were important intermediates. Especially the 6-bromo-substituted **71b** was a valuable starting point that allowed the introduction of various functional groups (see below). Therefore, mild reduction of the nitro group in position 8 with tin(II) chloride dihydrate was used to prevent reductive elimination of the 6-bromo moiety usually encountered with more aggressive reducing agents. It afforded **IV** (**71a-c**) in very good to quantitative yields (79–100%) after a reported extraction procedure (for yields and purities see **Table 3.9**).^{1,108}

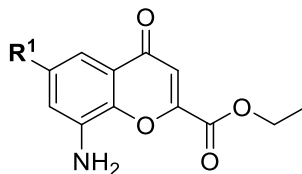
Table 3.9. Yields and purities of 6-substituted 8-aminochromen-4-one derivatives IV**IV**
71a-c

compd	R ¹	yield ^a [%]	purity ^b [%]
71a	Cl	79	95.7
71b	Br	100	97.4
71c	CH ₃	84	96.2

^aPercentages reflect isolated yields over two reaction steps. ^bPurity was determined by HPLC-UV (254 nm)-ESI-MS.

Compounds **IV** were either used directly in amide coupling reactions affording **VI** (**73**), or first transformed into their respective chromen-4-thione derivatives **V** (**72a-c**) by a thionation reaction in toluene using Lawesson's reagent (2,4-bis(4-methoxyphenyl)-1,3,2,4-dithiadiphosphetane-2,4-dithione). This reaction was generally completed within 2 hours, contrary to the reported 16 hours.¹ Yields for thionation reactions, in general, were low (17–58%), but did not increase with longer reaction times. In analogy to the synthesis of **VI**, amide coupling reactions thereafter afforded amides **VII** (**74a-d**).

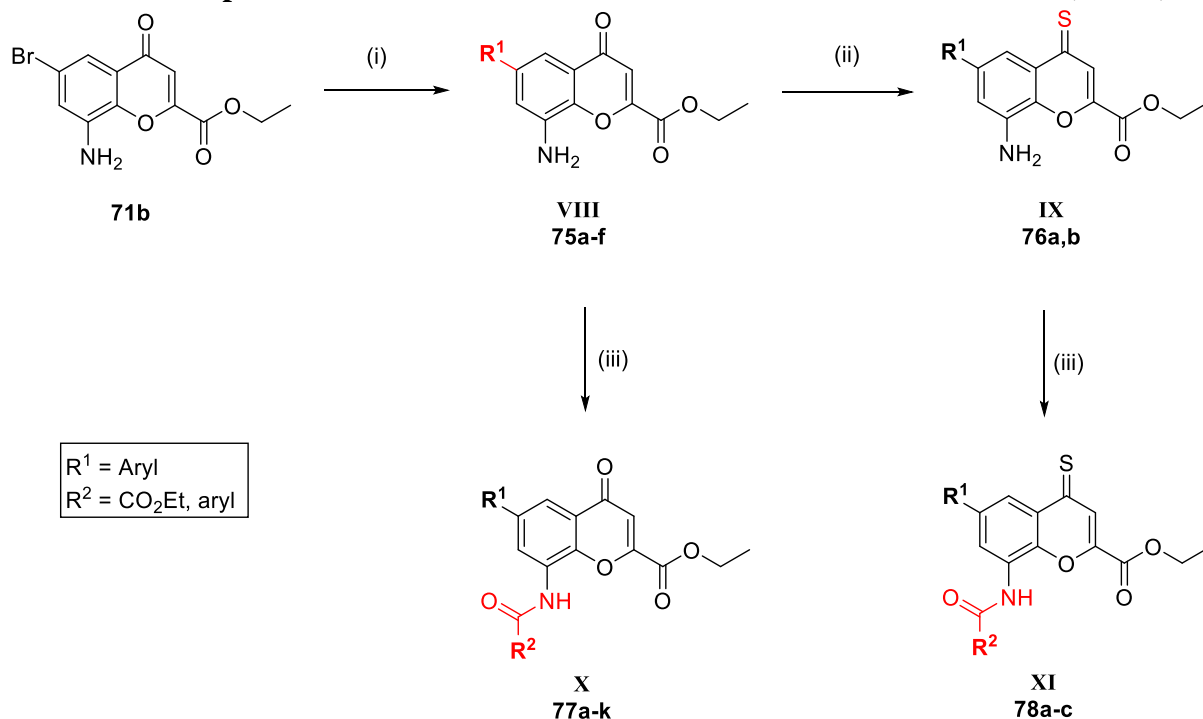
For the preparation of a number of 8-arylamido- and 8-carboxyformamidochromonen-4-ones with different aryl moieties in their 6-positions (**X**, **Scheme 3.4**), as well as for their respective 4-thio derivatives (**XI**), ethyl 8-amino-6-bromo-4-oxo-4*H*-chromene-2-carboxylate (**71b**) was used as starting material (see **Scheme 3.4**). First, **71b** was reacted with various boronic acid derivatives using a Suzuki coupling protocol previously described by our group.¹ Since chromone derivatives lack stability under basic conditions usually required for efficient Suzuki coupling, the weak base potassium carbonate and anhydrous solvents (toluene and DMF) were employed. The reaction was usually rapidly completed affording **VIII** (**75a-f**) in high yields (up to 96%) within 2-3 hours. However, depending on the boronic acid derivative used, reaction times could be longer and yields could be as low as 30% (see individual compounds and **Table 3.10**).

Table 3.10. Yields and purities of Suzuki coupling reactions affording VIII**VIII
75a-f**

compd	R ¹	yield ^a [%]	purity ^b [%]	compd	R ¹	yield ^a [%]	purity ^b [%]
75a	phenyl	96	96.0	75d	<i>p</i> -Cl-phenyl	55	94.1
75b	<i>p</i> -tolyl	81	95.9	75e	<i>o,p</i> -diCl-phenyl	80	91.3
75c	4-butyl-phenyl	80	94.5	75f	6-Cl-pyridin-3-yl	30	95.4

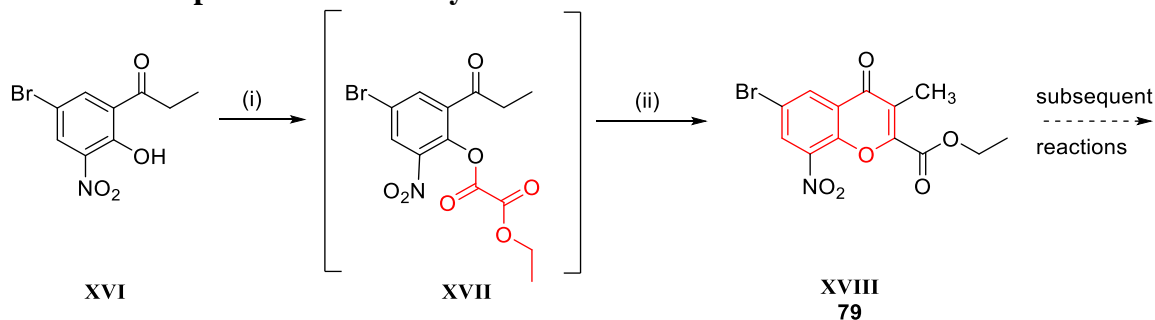
^aPercentages reflect isolated yields. ^bPurity was determined by HPLC-UV (254 nm)-ESI-MS.

In the next step, the Suzuki coupling products **VIII** (**Scheme 3.4**) were either directly used for amide coupling reactions yielding **X** (**77a-k**) in analogy to the preparation of **VI** (**Scheme 3.3**), or initially thionated affording **IX** (**76a,b**, **Scheme 3.4**) in analogy to the preparation of **V** (**Scheme 3.3**) and employed in amide coupling reactions thereafter, yielding **XI** (**78a-c**). See **Table 3.11** for purity data and reaction yields.

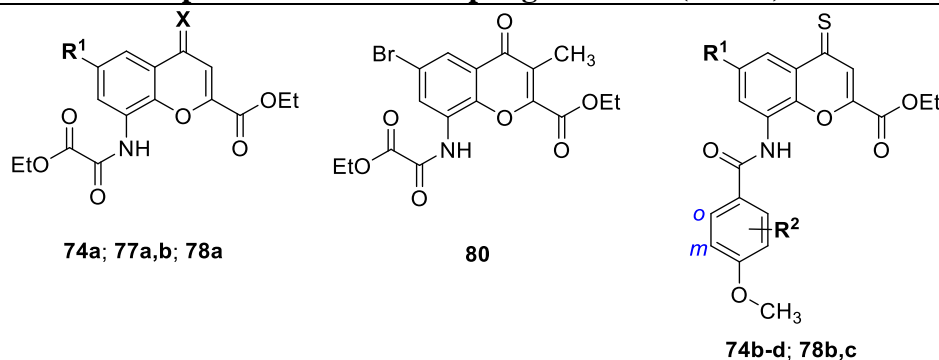
Scheme 3.4. Preparation of chromen-4-one and chromen-4-thione derivatives (Part 2).^a

^aReagents and conditions: (i) Boronic acid derivative, Pd(PPh₃)₄, K₂CO₃, toluene, DMF, 130°C, 3 h, 30-96% yield; (ii) Lawesson's reagent, toluene, reflux, 2 h, 33-56% yield; (iii) acid chloride, THF/DCM, DIPEA, 0 °C, 1 h, Ar; rt, 24 h, 48-91% yield.

3-Methyl-substituted chromen-4-one intermediates (for final compounds **80** and **87**) were synthesized in a Baker-Venkataraman rearrangement according to literature¹⁸⁷ (see **Scheme 3.5**), contrary to the related Claisen condensation that was employed for other herein described chromones. Compound **XVI** (1-(5-bromo-2-hydroxy-3-nitrophenyl)propan-1-one) was used as a commercially available starting material and reacted with ethoxalyl chloride in dry pyridine. The intermediate **XVII** was then cyclized in situ affording **XVIII** (**79**). Subsequent reactions were performed in analogy to above mentioned procedures.

Scheme 3.5. Preparation of 3-methylchromen-4-one derivatives.^a

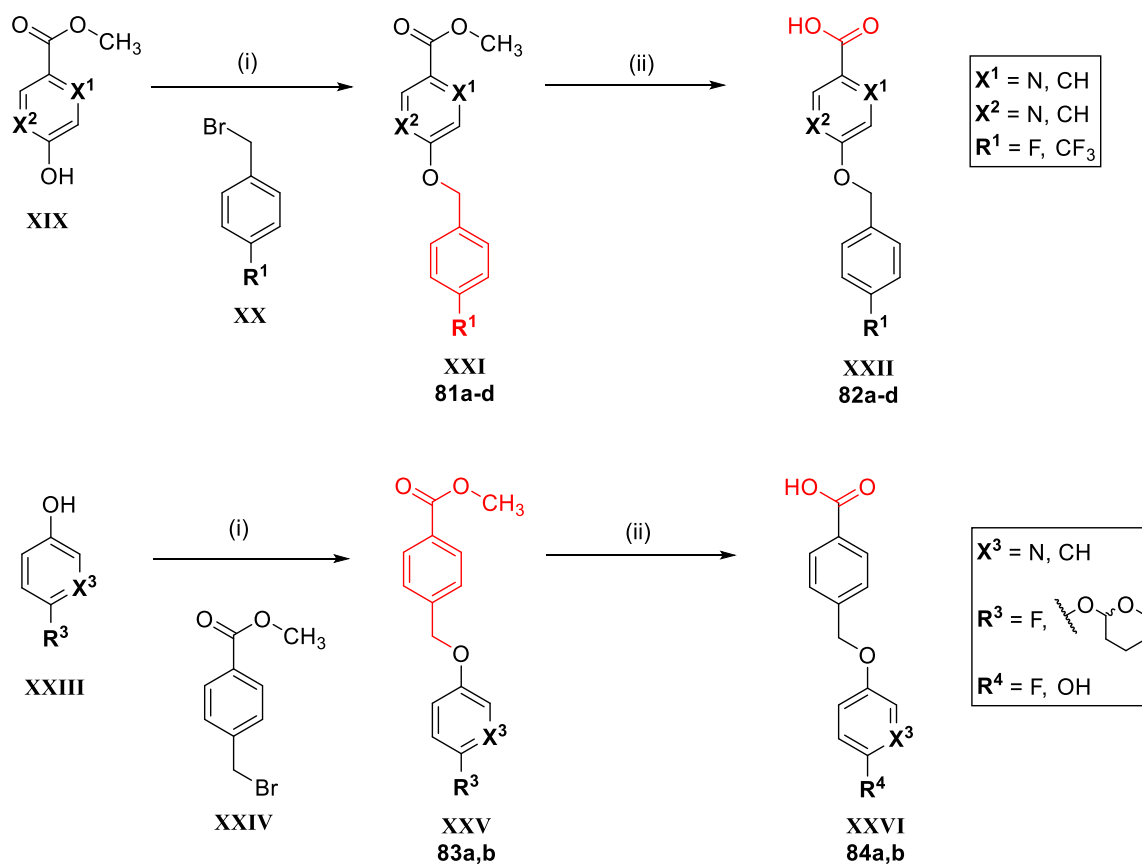
^aReagents and conditions: (i) ethoxalyl chloride, pyridine, rt, 5 min; (ii) pyridine, reflux, 6 h, 37% yield.

Table 3.11. Yields and purities of amide coupling reactions (Part 1)

compd	R ¹	X	yield ^a [%]	purity ^b [%]	compd	R ¹	R ²	yield ^a [%]	purity ^b [%]
77a	<i>p</i> -tolyl	O	71	97.4	74b	Br	<i>o</i> -diF	50	89.7
77b	butyl-phenyl	O	91	96.1	74c	Br	<i>m</i> -diF	34	72.2
74a	Cl	S	75	98.8	74d	CH ₃	<i>o</i> -diF	64	93.3
78a	phenyl	S	75	96.4	78b	phenyl	<i>o</i> -diF	48	85.1
80	-	-	85	97.1	78c	<i>p</i> -tolyl	<i>o</i> -diF	70	91.1

^aPercentages reflect isolated yields. ^bPurity was determined by HPLC-UV (254 nm)-ESI-MS.

8-Arylamidochromen-4-one derivatives were generally prepared by reacting variably substituted aromatic carboxylic acid chlorides with the appropriate 8-aminochromone derivative (as outlined in **Schemes 3.3** and **3.4**). Acid chlorides were synthesized from their respective carboxylic acids using thionyl chloride as chlorinating reagent. Due to their high reactivity, acid chlorides were prepared shortly before the amide coupling reactions (or, in one instance, generated in situ; see synthetic procedure of **77c**). While some aromatic carboxylic acid derivatives were commercially available, others had to be prepared beforehand. The synthetic procedure of these intermediates is laid out in **Scheme 3.6**.

Scheme 3.6. Preparation of 4-(benzyloxy)- and 4-(phenoxy)methylbenzoic acid derivatives.^a


^aReagents and conditions: (i) K_2CO_3 , acetone, reflux, 30 min; reflux 3 h, 55–99% yield; (ii) aq NaOH (10%), MeOH, H_2O , reflux, 30 min; HCl conc, 70–100% yield.

For the preparation of 4-(benzyloxy)benzoic acid derivatives **XXII (82a-d)**, the appropriate methyl *p*-hydroxybenzoate derivative (**XIX**) reacted with a benzyl bromide (**XX**) in a Williamson ether synthesis, affording **XXI (81a-d)** in acceptable to excellent yields (55–99%). Subsequent hydrolysis of the methyl ester yielded the desired acid **XXII (82a-d)**. For the preparation of 4-(phenoxy)methylbenzoic acid derivatives **XXVI (84a,b)**, phenol derivatives **XXIII** reacted with methyl 4-(bromomethyl)benzoate (**XXIV**), yielding **XXV (83a,b)** similar to the above described Williamson ether synthesis (for yields and purities see **Table 3.12**). Hydrolysis with sodium hydroxide followed by acidification with hydrochloric acid afforded the desired **XXVI (84a,b)**. The reactions generally progressed rapidly and supplied the required acid derivatives in high yields (see **Table 3.12**). The preparation of the 4''-hydroxy-substituted **90b** (see below) required the protection of free hydroxy groups of intermediates during etherification and the amide coupling reaction. Therefore, tetrahydropyran-2-yl-protected hydroquinone (deoxyarbutin) was employed as phenolic component for the synthesis of **83b**; and **84b** was acetylated prior to amide coupling reactions (for synthetic procedure, see

experimental section). When OH-protected derivatives were used, no product formation was observed.

Table 3.12. Yields and purities of ether syntheses and respective hydrolysis reactions

XXI 81a-d			XXV 83a,b			XXII 82a-d			XXVI 84a,b		
compd	R ¹	X ¹	X ²	yield ^a [%]	purity ^b [%]	compd	R ¹	X ¹	X ²	yield ^a [%]	purity ^b [%]
81a	F	CH	CH	55	97.9	82a	F	CH	CH	100	98.8
81b	CF ₃	CH	CH	99	97.4	82b	CF ₃	CH	CH	98	98.4
81c	F	N	CH	83	99.0	83c	F	N	CH	70	80.8
81d	F	CH	N	91	99.1	84d	F	CH	N	94	98.1
83a	F	N	-	90	97.6	84a	F	N	-	87	99.0
83b	O ^c	CH	-	n.d. ^d	n.d. ^d	84b	OH	CH	-	92	98.0

^aPercentages reflect isolated yields. ^bPurity was determined by HPLC-UV (254 nm)-ESI-MS. ^cTetrahydropyran-2-yl-protected. ^dReaction yields a mixture (see experimental section).

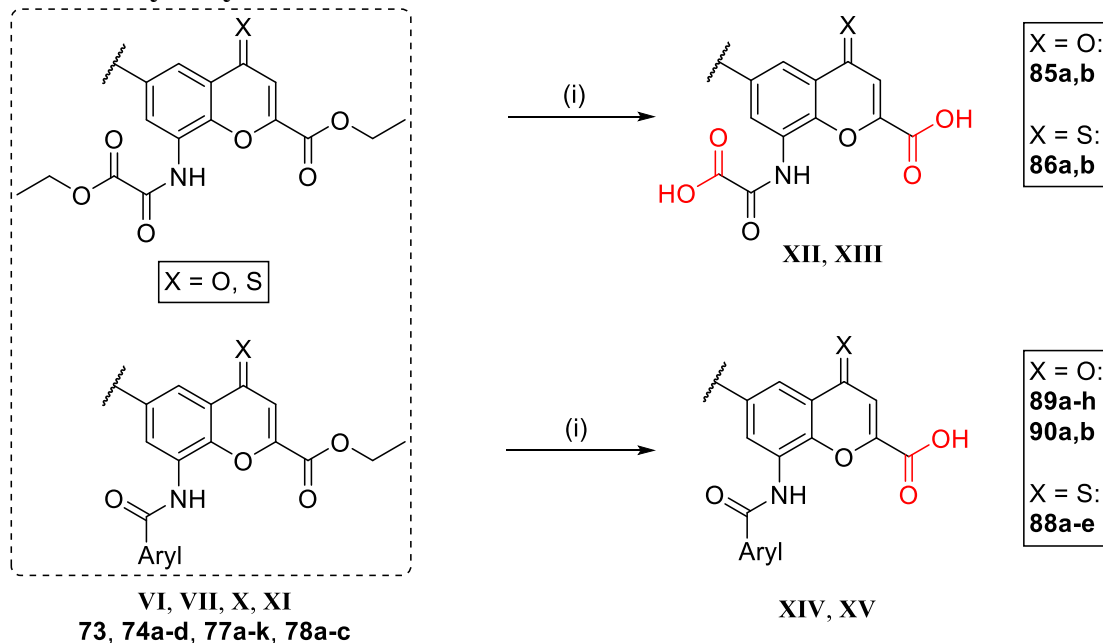
Amide coupling reactions of these benzoic acid ether derivatives with respective 6-position-substituted chromen-4-one derivatives were carried out in analogy to above mentioned amide couplings via the acid chloride using thionyl chloride as chlorinating agent. For yields and purities see **Table 3.13**. The resulting reaction products were generally poorly soluble in common solvents, including methanol, acetonitrile, and DMSO. Therefore, purity determination via HPLC was not possible for all of these compounds (i.e., **77c**, **77f**, **77i**, and **77k**).

Table 3.13. Yields and purities of amide coupling reactions (Part 2)

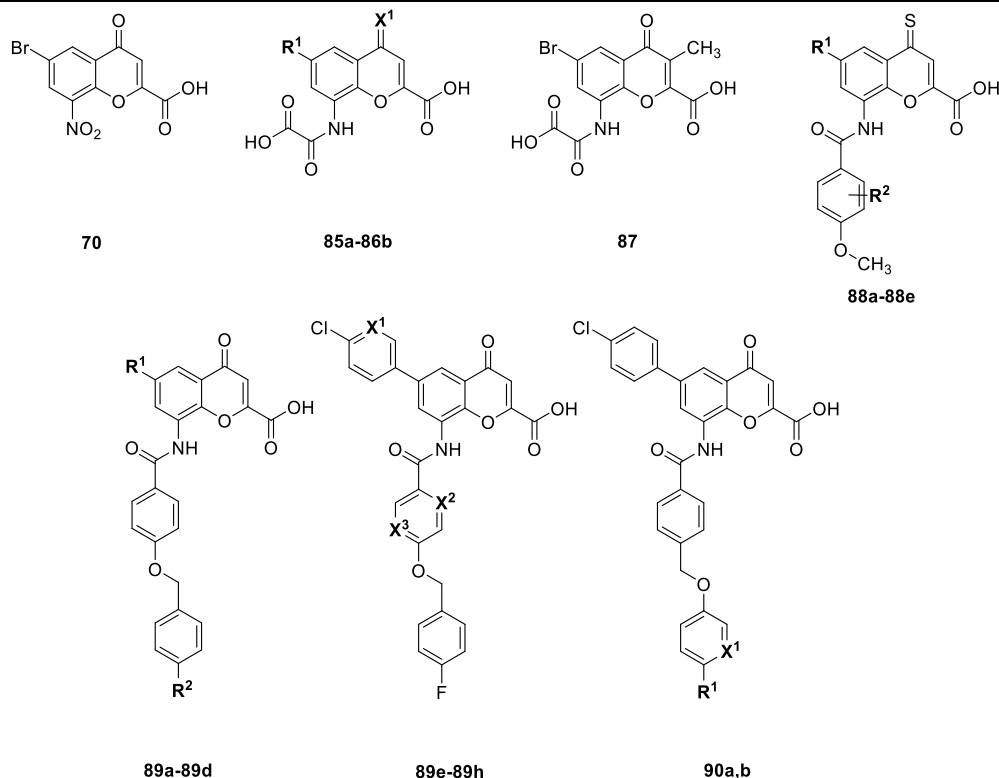
compd	substitution pattern					yield ^a [%]	purity ^b [%]
	R ¹	R ²	X ¹	X ²	X ³		
73^c	Br	F	-	-	-	61	98.0
77c	<i>p</i> -Cl-phenyl	F	-	-	-	18	n.d.
77d	<i>p</i> -Cl-phenyl	CF ₃	-	-	-	47	97.7
77e	2,4-dichloro-phenyl	F	-	-	-	31	90.0
77f	-	-	N	CH	CH	13	n.d.
77g	-	-	CH	N	CH	31	98.2
77h	-	-	CH	CH	N	53	99.6
77i	-	-	N	N	CH	39	n.d.
77j	F	-	N	-	-	87	97.6
77k	OAc	-	CH	-	-	98	n.d.

^aPercentages reflect isolated yields. ^bPurity was determined by HPLC-UV (254 nm)-ESI-MS. ^c**73** is a final compound, m.p. 223-224 °C. n.d., not determined (insoluble).

The final products, 6- substituted 8-carboxyformamidochromen-4-one (**XII**, **XIII**; **Scheme 3.7**) or 8-arylamidochromen-4-one derivatives (**XIV**, **XV**), were synthesized from their respective (di)ester precursors by a mild hydrolysis reaction, employing potassium carbonate as a base and a mixture of THF and water as solvent. Acidification with hydrochloric acid yielded the target compounds in acceptable yields upon filtration (see **Table 3.14**).

Scheme 3.7. Hydrolysis of chromen-4-one and chromen-4-thione derivatives.^a

^aReagents and conditions: (i) K₂CO₃, H₂O, THF, rt, 24 h, 45-99% yield.

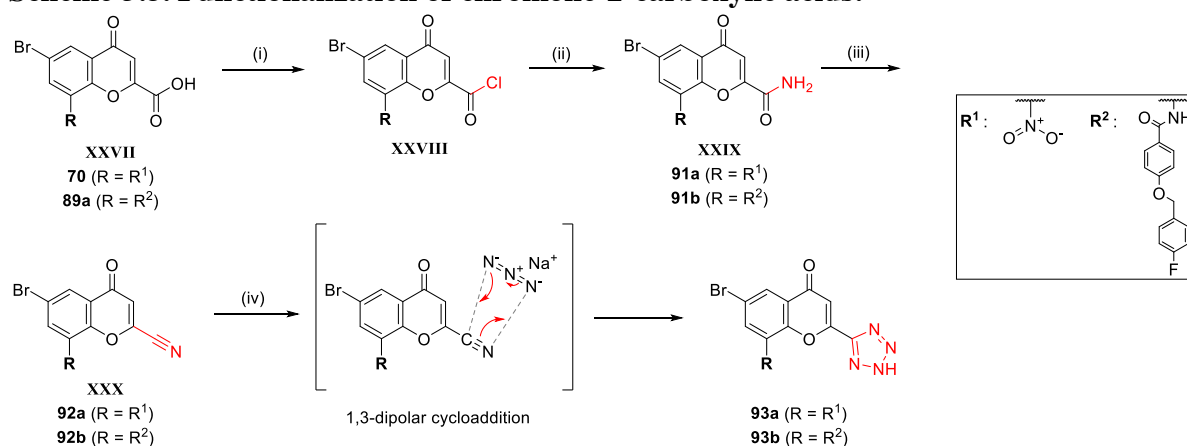
Table 3.14. Yields, purities, and melting points of hydrolysis reaction products

compd	substitution pattern					yield ^a [%]	purity ^b [%]	m.p. ^c [°C]
	R ¹	R ²	X ¹	X ²	X ³			
70	<i>see above for structure</i>					80	95.6	228-229
85a	<i>p</i> -tolyl	-	O	-	-	82	97.4	250-251
85b	4-butyl-phenyl	-	O	-	-	84	98.8	250-251
86a	Cl	-	S	-	-	60	95.6	231-232
86b	phenyl	-	S	-	-	99	96.4	250-251
87	<i>see above for structure</i>					90	98.8	243-244
88a	Br	<i>o</i> -diF	-	-	-	60	98.8	165-166
88b	Br	<i>m</i> -diF	-	-	-	45	96.5	240-241
88c	CH ₃	<i>o</i> -diF	-	-	-	93	97.6	250-251
88d	phenyl	<i>o</i> -diF	-	-	-	66	97.2	165-166
88e	<i>p</i> -tolyl	<i>o</i> -diF	-	-	-	90	97.3	166-167
89a	Br	F	-	-	-	95	98.9	252-253 ^d
89b	<i>p</i> -Cl-phenyl	F	-	-	-	69	98.1	265-266 ^e
89c	<i>p</i> -Cl-phenyl	CF ₃	-	-	-	84	97.1	282-283
89d	2,4-dichloro-phenyl	F	-	-	-	80	96.1	253-254
89e	-	-	N	CH	CH	45	96.7	290-291
89f	-	-	CH	N	CH	64	97.7	246-247
89g	-	-	CH	CH	N	79	96.3	>300
89h	-	-	N	N	CH	65	96.9	257-258
90a	F	-	N	-	-	91	98.2	269-270
90b	OH	-	CH	-	-	n.d.	97.1	272-273

^aPercentages reflect isolated yields. ^bPurity was determined by HPLC-UV (254 nm)-ESI-MS. ^cMelting points are uncorrected. ^dLit. m.p. 239-240 °C. ^eLit. m.p. 264-265 °C. ^fn.d., not determined.

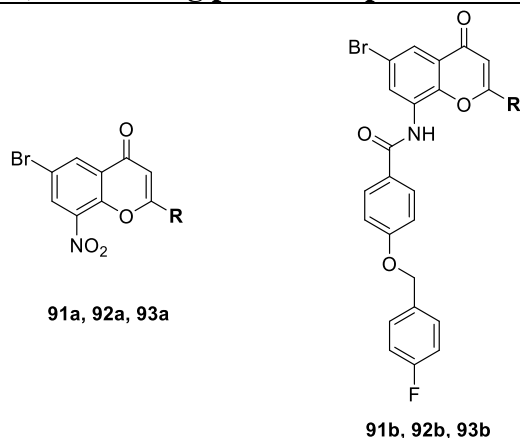
A number of final compounds was synthesized from suitable 6,8-disubstituted chromone-2-carboxylic acid derivatives to prepare corresponding derivatives with functionalized 2-positions (see **Scheme 3.8**). First, the carboxylic acid moiety of **XXVII** (**70**, **89**) was chlorinated with thionyl chloride, giving the acid chlorides **XXVIII**. An amide coupling reaction, employing gaseous ammonia both as reactant and as base, yielded the primary amides **XXIX** (**91a,b**). Subsequent dehydration with phosphoryl chloride provided the respective nitriles **XXX** (**92a,b**) in good yields (57-88%). The reaction of such nitriles with sodium azide and pyridinium hydrochloride gave the 2-(tetrazol-5-yl)-chromenones **93a** and **93b** via a 1,3-dipolar cycloaddition in excellent yields after filtration (84-94%).

Scheme 3.8. Functionalization of chromone-2-carboxylic acids.^a



^aReagents and conditions: (i) SOCl_2 , DCM, DMF cat., reflux, 1 h; (ii) NH_3 , DCM, 0 °C, 1 h, 50-56% yield (2 steps); (iii) POCl_3 , DMF, 0 °C, overnight, Ar, 57-88% yield; (iv) NaN_3 , pyridinium·HCl, DMF, 100 °C, 1 h, Ar; aq HCl (2M), 0 °C, 84-94% yield.

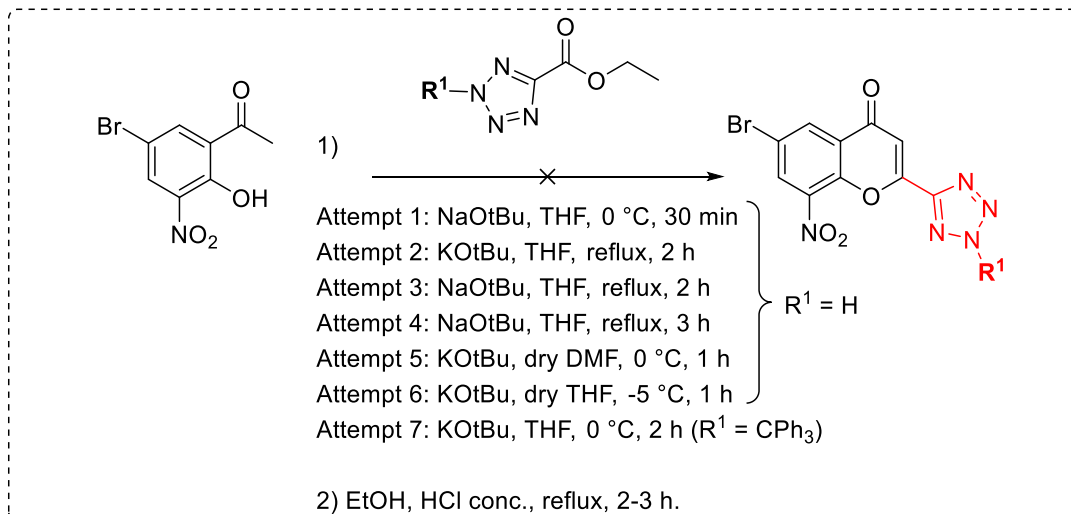
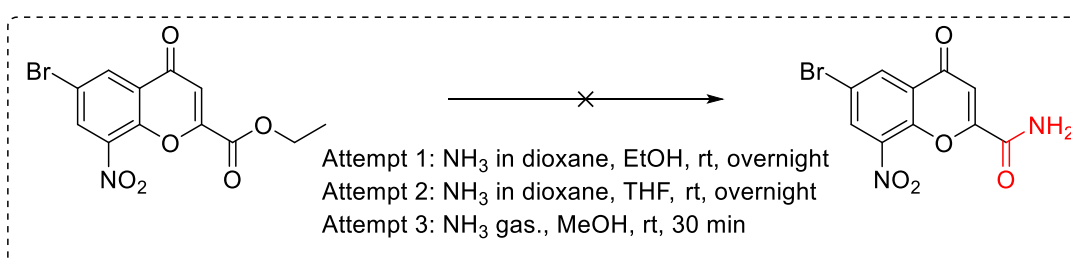
Some of these compounds were final products and characterized in biological assays. For reaction yields, compounds' purities, and their melting points, see **Table 3.15**.

Table 3.15. Yields, purities, and melting points of 2-position functionalization reactions

compd	R	yield ^a [%]	purity ^b [%]	m.p. ^c [°C]	compd	R	yield ^a [%]	purity ^b [%]	m.p. ^c [°C]
91a	CONH	56	96.1	n.d.	91b	CONH	50	96.6	295-296
92a	C≡N	88	97.8	150-151	92b	C≡N	57	97.3	229-230
93a		94	99.0	250-251	93b		84	98.4	230-231

^aPercentages reflect isolated yields. ^bPurity was determined by HPLC-UV (254 nm)-ESI-MS. ^cMelting points are uncorrected. n.d., not determined.

Prior to using the protocol described above, the preparation of chromen-4-one derivatives bearing a 2-tetrazol-5-yl moiety was attempted, using different synthetic pathways (see **Figure 3.3**). Firstly, 5'-bromo-2'-hydroxy-3'-nitroacetophenone was directly reacted with ethyl tetrazole-5-carboxylate instead of diethyl oxalate (Procedure A), which would have saved 5 additional reaction steps. Even the trityl-protection of the tetrazole ring had no effect. Procedure B, instead, aimed at reducing the number of reaction steps (from 5 to 3) by avoiding the initial hydrolysis and acid chloride formation, directly reacting esters with ammonia to give the corresponding amides according to the literature.¹⁸⁸ However, neither procedure yielded the desired product.

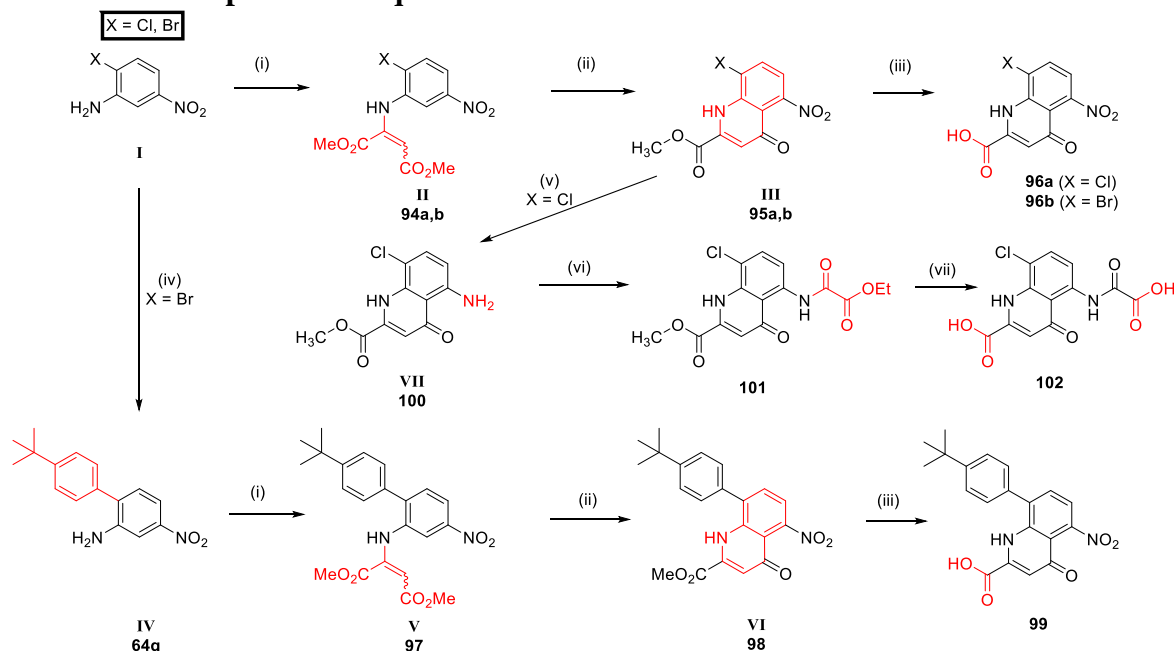
Procedure A:**Procedure B:****Figure 3.3.** Failed attempts to reduce reaction steps for the preparation of tetrazole compounds.

3.3 Synthesis of quinolone and indole derivatives

Quinolone derivatives were prepared from intermediate compounds of the syntheses above. Their preparation is outlined in **Scheme 3.9**. For the preparation of 8-chloro-5-nitro-4-oxo-1,4-dihydroquinoline-2-carboxylic acid (**96a**) and 8-bromo-5-nitro-4-oxo-1,4-dihydroquinoline-2-carboxylic acid (**96b**), 2-chloro-5-nitroaniline or 2-bromo-5-nitroaniline, respectively, were reacted with dimethyl acetylenedicarboxylate (DMAD), affording the enamine intermediates **II**. These were cyclized in a 6- π -electrocyclization (as described above) to give **III**. Subsequent hydrolysis afforded **96a** and **96b**. Starting from the Suzuki-coupled nitroaniline **IV** (**64q**), the reaction progressed in analogy via the enamine **V** and the cyclized **VI**, furnishing 8-(4-(*tert*-butyl)phenyl)-5-nitro-4-oxo-1,4-dihydroquinoline-2-carboxylic acid (**99**).

Methyl 8-chloro-5-nitro-4-oxo-1,4-dihydroquinoline-2-carboxylate could also be reduced to its 5-amino derivative **VII**. Amide coupling with ethoxalyl chloride afforded the amide **101**. A subsequent mild hydrolysis gave the dicarboxylic acid, 5-(carboxyformamido)-8-chloro-4-oxo-1,4-dihydroquinoline-2-carboxylic acid (**102**).

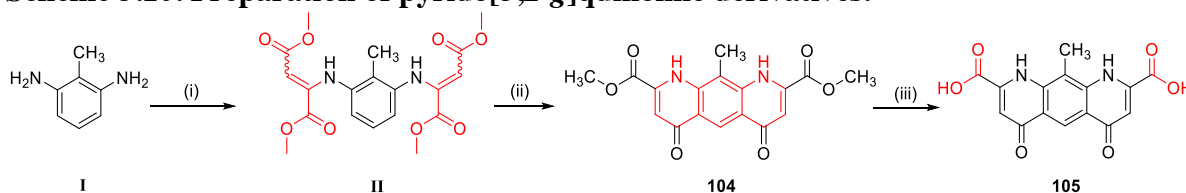
Scheme 3.9. Preparation of quinolone derivatives.^a



^aReagents and conditions: (i) DMAD, MeOH, rt, overnight, 42-100% yield; (ii) Ph₂O, ~250 °C, max. 15 min, 23-78% yield; (iii) aq NaOH (10%), MeOH, reflux, 30 min; HCl conc., 52-73% yield; (iv) boronic acid derivative, Pd(PPh₃)₄, K₂CO₃, toluene, DMF, 130°C, 3 h, 74% yield; (v) SnCl₂·2H₂O, EtOH, HCl (2M), 70 °C, 40 min, 70% yield; (vi) ethoxalyl chloride, Et₃N, DCM dry, 0 °C, 1 h, rt, 24 h, 80% yield; (vii) MeOH, aq NaOH (0.6M), 70 °C, 1 h; HCl conc., 86% yield.

The pyrido[3,2-*g*]quinoline derivatives **104** and **105** were synthesized from 2,6-diaminotoluene (**I**) in analogy to the preparation of 1,7-phenanthrolines (see above). The synthetic path is illustrated in **Scheme 3.10**. Compound **I** reacted with dimethyl acetylenedicarboxylate (DMAD), affording the intermediate **II** (**103**). Cyclization and subsequent hydrolysis yielded **104** and **105**, respectively.

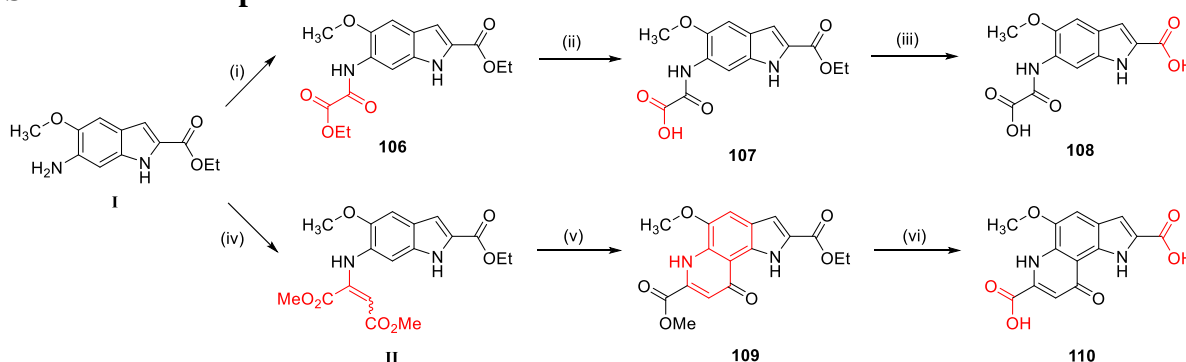
Scheme 3.10. Preparation of pyrido[3,2-*g*]quinoline derivatives.^a



^aReagents and conditions: (i) DMAD, MeOH, rt, overnight, 55% yield; (ii) Ph₂O, ~250 °C, 15 min, 44% yield; (iii) aq NaOH (10%), MeOH, reflux, 30 min; HCl conc., 98% yield.

A number of indole derivatives were prepared from the commercially available ethyl 6-amino-5-methoxy-1*H*-indole-2-carboxylate (**I**, see **Scheme 3.11**). Amide coupling with ethoxalyl chloride gave compound **106**, which could be partially hydrolyzed affording **107**. Hydrolysis of the other carboxylic acid gave **108**. Compound **I** was also reacted with dimethyl acetylenedicarboxylate (DMAD) to yield the enamine intermediate **II**. Cyclization (in analogy to reactions above) provided **109**. Subsequent hydrolysis afforded **110**.

Scheme 3.11. Preparation of indole derivatives.^a



^aReagents and conditions: (i) ethoxalyl chloride, Et₃N, DCM dry, 0 °C, 1 h; rt, 24 h, 67% yield; (ii) K₂CO₃, H₂O, THF, rt, 48 h, 100% yield; (iii) aq NaOH (1M), MeOH, 70 °C, 1 h; HCl conc., 96% yield; (iv) DMAD, MeOH, rt, overnight, 100% yield; (v) Ph₂O, ~250 °C, 15 min, 57% yield; (vi) aq NaOH (10%), MeOH, reflux, 30 min; HCl conc., 91% yield.

Purity data and melting points of final quinolone and indole compounds are summarized in **Table 3.16**.

Table 3.16. Purities and melting points of quinolone and indole derivatives

compd	substitution pattern		purity ^a [%]	m.p. ^b [°C]
	R ¹	R ²		
96a	Cl	-	99.7	>300
96b	Br	-	99.5	>300
99	4- <i>t</i> -butylphenyl	-	99.1	>300
101	ethyl	ethyl	97.7	254-255
102	H	H	99.9	270-271
104	methyl	-	97.7	>300
105	H	-	99.9	>300
106	ethyl	ethyl	99.3	234-235
107	ethyl	H	99.7	223-224
108	H	H	98.6	253-254
109	ethyl	methyl	99.3	240-241
110	H	H	99.6	>300

^aPurity was determined by HPLC-UV (254 nm)-ESI-MS. ^bMelting points are uncorrected.

3.4 Pharmacological evaluation at GPR35

3.4.1 Introduction

The pharmacology of some chromen-4-one derivatives at GPR35 has already been discussed in detail by Funke and Thimm in 2013 (see Introduction).^{186,189} The subsequent development of a radioligand by our group facilitated affinity measurements for GPR35 ligands.⁹² [³H]PSB-13253 was the first radioligand for the human GPR35 and enabled the generation of precise affinity data.⁹² However, the agonist radioligand - while displaying high affinity at the human receptor - was inactive at the rat and mouse receptor orthologs.⁹² This is the reason why affinity data are only available for the human, but not the rodent receptor orthologs. Dr. Anne Meyer continued to improve our group's chromen-4-one-derived GPR35 agonists.¹ One goal was to improve GPR35 activity of these agonists at the rodent receptors. The optimized molecules showed increased activity at the rat receptor, however, they still lacked substantial potency at the mouse receptor ortholog.¹ Therefore, our group decided to investigate other scaffolds to obtain derivatives with activity at that receptor as well. The phenanthroline-derived **63** was the most potent compound at the mouse receptor ortholog,¹ which was congruent with the findings by MacKenzie et al. who reported that the mast-cell stabilizer bufrolin, which had never reached the market, could activate the human and rat receptor ortholog with equal potency.² While the original publication did not discuss the compound's activity at the mouse receptor, later works confirmed that that receptor, too, was potently activated by bufrolin, albeit with >50-fold weaker activity in β -arrestin recruitment assays.¹¹¹ We therefore aimed at improving this scaffold in addition to the chromen-4-one derivatives of previous works.

The new compounds were investigated for their potency in β -arrestin recruitment assays at the human, rat, and mouse GPR35 as well as for their affinity at the human receptor versus the radioligand [³H]PSB-13253.⁹² β -Arrestin recruitment assays are the standard method for pharmacological evaluation of GPR35 agonists, and the validity and correlation with binding affinity of this method has been demonstrated in previous studies.^{3,60,92} The PathHunter β -arrestin recruitment assay was used in this study (see **Figure 3.4**).^{*} In short, the GPR35 ortholog to be investigated is C-terminally tagged with a fragment of the enzyme β -galactosidase. The complementary enzyme fragment is attached to the β -arrestin. If the receptor is activated by the presence of an agonist, the two enzyme fragments will join and form a functioning β -

^{*} Eurofins DiscoverX Products, LLC (<https://www.discoverx.com/technologies-platforms/enzyme-fragment-complementation-technology/cell-based-efc-assays/protein-protein-interactions/gpcrs-b-arrestin>)

galactosidase, which cleaves a substance into a chemiluminescent reaction product, whose emission can be measured. Light intensity is proportional to receptor activation at a given agonist concentration.

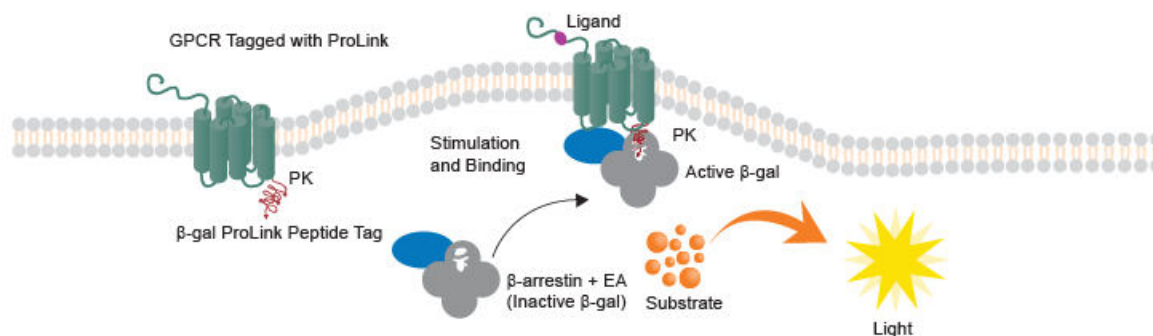


Figure 3.4. Principle of the PathHunter β -arrestin recruitment assay system. The figure was taken from www.discoverx.com. β -gal, β -galactosidase, EA, enzyme acceptor; PK, enzyme donor fragment (ProLinkTM).

Measurements at different concentrations can be used to determine EC_{50} values, which represent half-maximal effective concentrations. These EC_{50} values are then used to compare the activity of different compounds. The method is highly sensitive and not particularly prone to artifacts, since only the recruitment of β -arrestins by the investigated receptor results in chemiluminescence.¹⁰⁸ However, it is possible that some compounds are potent receptor agonists but biased for G protein signaling versus β -arrestin recruitment,⁴⁹ which would result in an underestimation of activity in the β -arrestin assay. Therefore, a second assay principle, such as radioligand binding, is helpful to confirm data from β -arrestin recruitment assays. Radioligand binding assays determine the ability of a compound to displace a radiolabeled ligand with known affinity for the receptor of interest from its binding pocket, which directly correlates to binding affinity. Measurements of radioactivity at different concentrations of the investigated compound result in concentration-inhibition curves, which can be used to determine inhibition constants (K_i values). Similar to EC_{50} values, K_i values are then used to compare different compounds.

3.4.2 Results

The EC_{50} and K_i values for potency and affinity of individual compounds determined at the human, rat, and mouse GPR35 are provided in **Tables 3.17-19**. Assays were performed by Dr. Dominik Thimm, M.Sc. Beatriz Büschbell, and Miriam Dieltz, respectively.

Table 3.17. Potency and affinity of chromen-4-one derivatives

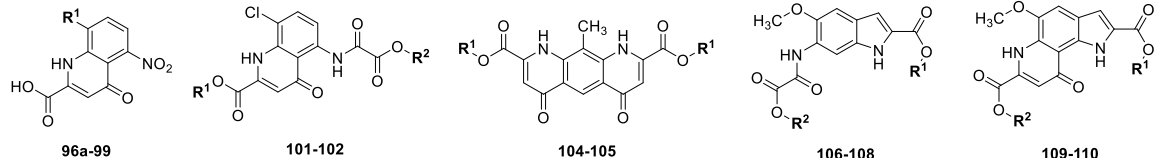
		R ²				radio-ligand binding assays ^a		β-arrestin recruitment assays ^b				
compd	R ¹	<i>m</i>	<i>e</i>	<i>t</i>	<i>para</i>	human GPR35		rat GPR35		mouse GPR35		
						K _i ± SEM (nM)	EC ₅₀ ± SEM (nM)	EC ₅₀ ± SEM (nM)	EC ₅₀ ± SEM (nM)	EC ₅₀ ± SEM (nM)	EC ₅₀ ± SEM (nM)	
						(% inhibition ± SEM)	(% effect ^c ± SEM)	E _{max} ^c	(% effect ^d ± SEM)	E _{max} ^d	E _{max} ^c	
standard agonists												
zaprinast ^e						401 ± 15	1960 ± 240	100	61.1 ± 6.1	100	1600 ± 40	100
cromolyn sodium ^e						2340 ± 40	1260 ± 170	-	986 ± 126	-	4840 ± 600	-
23a	PSB-13253 ^e	Br	H	H	OCH ₃	5.18	12.1	121	1400	88	(36 ± 1)	-
25 ^e		Br	di-F	H	OCH ₃	0.589 ± 0.076	5.54 ± 0.29	119	199 ± 39	98	2850 ± 410	106
26		phenyl	di-F	H	OCH ₃	0.426 ± 0.037	1.08 ± 0.11	113	157 ± 13	107	293 ± 43	96
112		Br	H	H	OCH ₃	1.25 ± 0.06	3.62 ± 0.66	118	552 ± 42	73	1310 ± 70	92
88a		Br	di-F	H	OCH ₃	1.09 ± 0.06	6.14 ± 0.48	116	520 ± 60	96	1800 ± 140	89
88b		Br	H	di-F	OCH ₃	11.8 ± 1.3	39.8 ± 6.6	113	1670 ± 160	60	2630 ± 350	81
88c		CH ₃	di-F	H	OCH ₃	0.662 ± 0.167	2.18 ± 0.32	115	615 ± 103	84	984 ± 24	91
88d		phenyl	di-F	H	OCH ₃	1.52 ± 0.10	5.28 ± 0.14	112	212 ± 28	89	169 ± 22	94
88e		<i>p</i> -tolyl	di-F	H	OCH ₃	1.38 ± 0.33	4.70 ± 0.43	119	57.1 ± 13.9	92	171 ± 28	101
113		H	-	-	-	396 ± 36	246 ± 17	106	779 ± 97	92	(37 ± 4)	-
114		F	-	-	-	42.6 ± 11.1	106 ± 11	104	263 ± 34	109	4760 ± 320	97
115		Cl	-	-	-	7.16 ± 0.12	29.3 ± 1.5	110	80.0 ± 3.1	98	1710 ± 460	104
59		Br	-	-	-	13.8 ± 1.5	11.8 ± 1.5	104	45.1 ± 6.5	112	1880 ± 440	124
116		CH ₃	-	-	-	63.5 ± 20.8	104 ± 3	113	406 ± 36	108	2380 ± 740	92
117		ethyl	-	-	-	17.9 ± 1.4	27.5 ± 2.5	111	75.0 ± 2.0	113	1000 ± 300	114
61		butyl	-	-	-	8.97 ± 1.50	31.8 ± 5.3	96	29.7 ± 4.0	109	399 ± 83	110
118		OCH ₃	-	-	-	33.5 ± 5.1	93.8 ± 8.7	115	851 ± 102	108	4710 ± 530	88
60		phenyl	-	-	-	3.19 ± 0.56	9.68 ± 0.48	109	154 ± 15	99	494 ± 83	95
85a		<i>p</i> -tolyl	-	-	-	0.892 ± 0.312	2.20 ± 0.13	111	142 ± 21	112	388 ± 27	107
85b		4-butyl-phenyl	-	-	-	4.50 ± 0.69	15.6 ± 0.9	105	132 ± 16	85	465 ± 82	97
80		ethyl	-	-	-	119 ± 30	680 ± 71	105	97.8 ± 6.2	98	1080 ± 80	108
87		H	-	-	-	51.6 ± 6.45	75.0 ± 14.6	110	12.2 ± 0.9	102	167 ± 33	104
86a		Cl	-	-	-	2.05 ± 0.52	8.04 ± 0.40	109	21.6 ± 1.9	102	249 ± 48	111
62		Br	-	-	-	2.71 ± 0.32	8.47 ± 0.72	126	20.9 ± 2.3	107	174 ± 19	118
86b		phenyl	-	-	-	0.883 ± 0.148	1.94 ± 0.14	108	21.3 ± 1.4	105	127 ± 7	102

^aAffinities were determined in competition binding experiments using 5 nM [³H]PSB-13253 and membrane preparations of CHO cells recombinantly expressing human GPR35. ^bPotencies were determined in functional β-arrestin recruitment assays using β-arrestin CHO cells (DiscoverX) recombinantly expressing the GPR35 orthologs. Screenings were performed at a concentration of 10 μM. Effects were normalized to the signal induced by 30 μM (human and mouse) or 10 μM zaprinast (rat), corresponding to the maximal response at the respective receptor. ^cResults were previously published.^{92,108} Compounds previously synthesized by another member of our group appear in gray.¹

Table 3.18. Potency and affinity of 1,7-phenanthroline derivatives

		radioligand binding assays ^a		β -arrestin recruitment assays ^b				
compd	R	human GPR35		rat GPR35		mouse GPR35		
		$K_i \pm \text{SEM}$ (nM) (% inhibition \pm SEM)	$\text{EC}_{50} \pm \text{SEM}$ (nM) (% effect ^c \pm SEM)	E_{max}^c	$\text{EC}_{50} \pm \text{SEM}$ (nM) (% effect ^d \pm SEM)	E_{max}^d	$\text{EC}_{50} \pm \text{SEM}$ (nM) (% effect ^c \pm SEM)	E_{max}^c
68a-68y								
68z								
67d-67m								
111								
68a	H	142 \pm 23	578 \pm 70	84	334 \pm 63	80	996 \pm 119	97
68b	F	38.7 \pm 10.8	186 \pm 17	100	170 \pm 11	111	3180 \pm 160	86
68c	Cl	2.16 \pm 0.63	8.98 \pm 0.94	111	21.6 \pm 3.8	104	427 \pm 40	96
68d	Br	1.82 \pm 0.16	3.32 \pm 0.48	115	9.69 \pm 2.65	100	268 \pm 27	93
68e	NO ₂	1.49 \pm 0.32	2.91 \pm 0.20	113	63.2 \pm 4.6	111	706 \pm 75	92
63	CH ₃	6.20 \pm 0.65	21.4 \pm 2.1	102	26.3 \pm 2.3	111	105 \pm 15	102
68g	ethyl	3.20 \pm 0.83	14.1 \pm 2.2	117	15.0 \pm 4.0	112	322 \pm 27	99
68h	propyl	1.08 \pm 0.25	3.70 \pm 0.60	107	3.22 \pm 0.62	105	31.6 \pm 5.1	118
68i (30), bufrolin	butyl	1.22 \pm 0.17	3.86 \pm 0.71	106	1.86 \pm 0.27	114	90.6 \pm 20.7	80
68j	pentyl	1.12 \pm 0.12	3.44 \pm 0.01	98	1.46 \pm 0.06	112	34.1 \pm 2.8	89
68k	hexyl	1.12 \pm 0.12	3.94 \pm 0.43	100	0.846 \pm 0.089	86	36.8 \pm 4.0	95
68l	heptyl	1.61 \pm 0.26	2.86 \pm 0.04	90	0.871 \pm 0.095	113	20.5 \pm 3.2	94
68m	octyl	1.44 \pm 0.39	3.36 \pm 0.24	98	0.780 \pm 0.066	105	14.3 \pm 0.8	97
68n	nonyl	1.49 \pm 0.22	4.31 \pm 0.21	102	0.671 \pm 0.082	104	11.7 \pm 2.1	95
68o	decyl	0.863 \pm 0.117	2.24 \pm 0.13	101	0.723 \pm 0.090	103	8.18 \pm 1.39	98
68p	dodecyl	1.48 \pm 0.09	5.05 \pm 0.75	102	1.87 \pm 0.16	118	6.12 \pm 0.53	95
68q	OCH ₃	12.2 \pm 2.9	63.1 \pm 10.6	105	283 \pm 27	116	1760 \pm 50	96
68r	sec-butyl	5.52 \pm 0.70	13.8 \pm 2.6	109	20.3 \pm 2.4	103	135 \pm 15	92
68s	<i>t</i> -butyl	68.3 \pm 10.3	281 \pm 67	98	68.2 \pm 9.3	93	381 \pm 49	110
68t	cyclohexyl	2.54 \pm 0.31	6.92 \pm 0.20	99	11.8 \pm 1.3	98	37.0 \pm 4.1	98
68u	thiophen-2-yl	2.25 \pm 0.35	6.05 \pm 0.14	105	5.90 \pm 0.50	106	51.7 \pm 2.0	90
68v	phenyl	2.12 \pm 0.70	9.49 \pm 1.53	114	31.7 \pm 3.2	103	121 \pm 18	94
68w	<i>p</i> -tolyl	2.07 \pm 0.24	3.87 \pm 0.13	102	12.0 \pm 2.1	93	74.8 \pm 1.6	89
68x	4- <i>t</i> -butyl-phenyl	3.47 \pm 0.42	5.30 \pm 1.06	94	39.2 \pm 10.8	98	292 \pm 44	78
68y	4-butyl-phenyl	1.69 \pm 0.28	1.96 \pm 0.29	113	7.81 \pm 0.27	91	60.2 \pm 5.5	89
68z	-	2.10 \pm 1.23	2.93 \pm 0.57	111	17.7 \pm 1.9	98	61.5 \pm 3.4	105
67d	Br	1450 \pm 370	1250 \pm 280	108	1450 \pm 300	100	3880 \pm 260	86
67r	sec-butyl	843 \pm 64	1090 \pm 90	123	499 \pm 70	110	849 \pm 18	109
67j	pentyl	232 \pm 40	209 \pm 25	106	65.0 \pm 8.1	97	588 \pm 86	122
67l	heptyl	102 \pm 22	239 \pm 43	64	63.0 \pm 9.8	86	881 \pm 136	135
67m	octyl	175 \pm 38	(38 \pm 2)	-	96.4 \pm 12.7	83	629 \pm 30	106
111	heptyl	(29 \pm 9)	(2 \pm 1)	-	(2 \pm 3)	-	(24 \pm 2)	-

^aAffinities were determined in competition binding experiments using 5 nM [³H]PSB-13253 and membrane preparations of CHO cells recombinantly expressing human GPR35. ^bPotencies were determined in functional β -arrestin recruitment assays using β -arrestin CHO cells (DiscoverX) recombinantly expressing the GPR35 orthologs. Screenings were performed at a concentration of 10 μ M. Effects were normalized to the signal induced by ^c30 μ M (human and mouse) or ^d10 μ M zaprinast (rat), corresponding to the maximal response at the respective receptor. Compounds previously synthesized by another member of our group appear in gray.¹

Table 3.19. Potency and affinity of indole and quinolone derivatives


compd	R ¹	R ²	radioligand binding assays ^a			β -arrestin recruitment assays ^b			
			human GPR35			rat GPR35		mouse GPR35	
			$K_i \pm$ SEM (nM) (% inhibition \pm SEM)	$EC_{50} \pm$ SEM (nM) (% effect ^c \pm SEM)	E_{max}^c	$EC_{50} \pm$ SEM (nM) (% effect ^d \pm SEM)	E_{max}^d	$EC_{50} \pm$ SEM (nM) (% effect ^c \pm SEM)	E_{max}^c
96a	Cl	-	918 \pm 186	4900 \pm 1340	101	1210 \pm 300	104	(38 \pm 8)	-
96b	Br	-	949 \pm 143	3800 \pm 320	90	550 \pm 85	102	4490 \pm 540	74
99	4- <i>t</i> -butyl-phenyl	-	1210 \pm 304	3420 \pm 410	72	974 \pm 159	66	2750 \pm 180	94
101	CH ₃	ethyl	98.0 \pm 25.7	42.2 \pm 3.2	112	377 \pm 73	90	3240 \pm 300	77
102	H	H	3.41 \pm 0.77	8.95 \pm 0.56	112	511 \pm 168	120	2930 \pm 310	112
104	CH ₃	-	111 \pm 36	56.5 \pm 12.7	97	498 \pm 103	89	1470 \pm 59	81
105	H	-	2.84 \pm 0.21	11.4 \pm 1.8	106	320 \pm 98	98	518 \pm 88	103
106	ethyl	ethyl	(19 \pm 4)	(8 \pm 0)	-	(41 \pm 3)	-	(5 \pm 3)	-
107	H	ethyl	991 \pm 406	5820 \pm 910	86	1130 \pm 280	83	4280 \pm 680	85
108	H	H	26.5 \pm 6.1	115 \pm 5	114	3930 \pm 390	98	5840 \pm 790	95
109	CH ₃	ethyl	(25 \pm 7)	(46 \pm 7)	-	740 \pm 87	84	(23 \pm 3)	-
110	H	H	2.40 \pm 0.51	4.48 \pm 0.52	109	423 \pm 33	110	2480 \pm 340	80

^aAffinities were determined in competition binding experiments using 5 nM [³H]PSB-13253 and membrane preparations of CHO cells recombinantly expressing human GPR35. ^bPotencies were determined in functional β -arrestin recruitment assays using β -arrestin CHO cells (DiscoverX) recombinantly expressing the GPR35 orthologs. Screenings were performed at a concentration of 10 μ M. Effects were normalized to the signal induced by ^c30 μ M (human and mouse) or ^d10 μ M zaprinast (rat), corresponding to the maximal response at the respective receptor.

3.4.3 Structure-activity relationships

Seeing as there is such a discrepancy between the three receptor orthologs it makes sense to discuss the results separately for the human, rat, and mouse GPR35. Also, there are rather large differences between the various scaffolds, so they will be discussed separately as well.

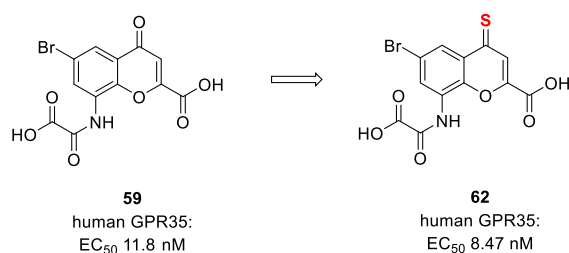
3.4.3.1 Human GPR35

Potency of chromen-4-one derivatives

Large libraries of chromen-4-one derivatives have been developed and evaluated at GPR35 (see 1.2.2 *Synthetic GPR35 ligands*) and various important considerations regarding their structure-activity relationships have been described in previous studies.^{1,92,108,186,189} However, the scaffold had been optimized for the human GPR35 and potency at rodent receptor orthologs

remained limited. While the most potent derivative described displayed nanomolar potency and subnanomolar affinity at the human GPR35, potency at rat and mouse GPR35 was still considerably lower.¹ In this study, the aim was to improve potency at rodent GPR35 orthologs via the introduction of favorable functional groups to the chromen-4-one scaffold. A reduction in human GPR35 potency was only accepted if it led to a considerable increase in potency at a rodent ortholog.

In a previous study, the thionation of 6-bromo-8-(carboxyformamido)-4-oxo-4*H*-chromene-2-carboxylic acid (**59**, EC₅₀ 11.8 nM) led to **62** (EC₅₀ 8.47 nM).¹ While the increase in potency was not significant at the human GPR35 ortholog, the compound showed greatly enhanced potency at the rat and mouse GPR35 compared to the unthionated **59** (see below). Therefore, we developed a series of chromen-4-thione derivatives to investigate the impact of thionation in the 4-position. In general, the human receptor tolerated thionated compounds well (see **Figure 3.5**).

previous work:¹

this work:

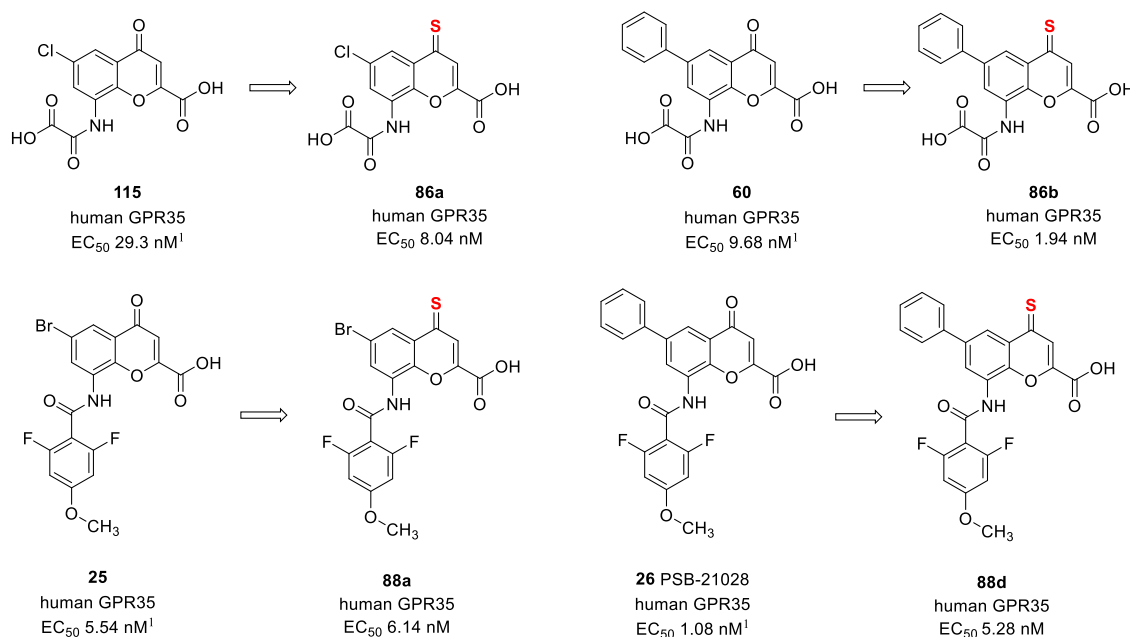


Figure 3.5. Thionation of the 4-position of chromen-4-one derivatives was tolerated by the human GPR35.¹

The 6-chloro-substituted 4-thio derivative **86a** (EC₅₀ 8.04 nM) displayed 3.6-fold increased potency compared to its forerunner **115** (ANM296, EC₅₀ 29.3 nM), and the thionated 6-phenyl derivative **86b** (EC₅₀ 1.94 nM) was almost 5-fold more potent than its 4-oxo counterpart **60** (EC₅₀ 9.68 nM). Incidentally, **86b** was the most potent chromone derivative at the human receptor of the present study. Thus, the potency of 8-carboxyformamidochromen-4-ones was reliably increased by thionation. Interestingly, the same did not hold true for the larger 8-benzamidochromen-4-one derivatives. The 6-bromo-substituted **88a** (EC₅₀ 6.14 nM) was slightly less potent than the unthionated **25** (EC₅₀ 5.54 nM), and **88d** (EC₅₀ 5.28 nM) was almost 5-fold less potent than **26** (EC₅₀ 1.08 nM). A similar relation was observed for the rat ortholog of GPR35. It is possible that the larger 8-benzamide residue exhausts the available space in the receptor binding pocket in combination with a 4-thio substitution.

Despite a small decrease in potency upon thionation of 8-benzamidochromen-4-ones compared to 8-carboxyformamidochromones, these compounds were still among the most active ones among the herein identified GPR35 agonists (see **Figure 3.6**). Curiously, the rank order of potency for these derivatives was slightly different from the previously determined one for analogous 4-oxo derivatives.¹ The most potent derivative was **88c**, which displayed an EC₅₀ value of 2.18 nM. This was followed by the 6-*p*-tolyl derivative **88e** (EC₅₀ 4.70 nM), which displayed equally high potency as **88d** (EC₅₀ 5.28 nM). The 6-bromo compound **88a** (EC₅₀ 6.14 nM) was only slightly less potent. We also examined the substitution pattern of the benzamide in the 8-position, however, 3,5-difluorination led to a compound with drastically decreased potency (**88b**, EC₅₀ 39.8 nM) compared to the 2,6-difluorinated **88a**.

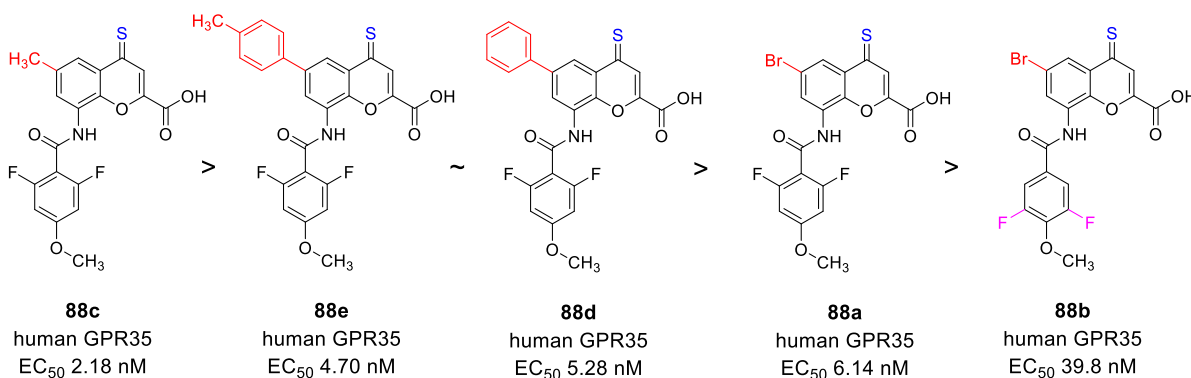


Figure 3.6. Rank order of potency of 8-benzamidochromen-4-thione derivatives at the human GPR35.

A series of non-thionated 8-carboxyformamidochromen-4-ones was described by Meyer et al.¹ Although those compounds showed high potency at the human receptor, their potency at rodent receptors was considerably lower. The 6-phenyl-substituted **60** (EC₅₀ 9.68 nM) was the most potent derivative of the previous study. We observed that its potency could be increased 4.4-fold by introducing a methyl group to the 6-phenyl moiety. The resulting **85a** displayed an EC₅₀ value of 2.20 nM and showed slightly increased activity at the rodent receptor orthologs as well (see below). Further elongation of the *para*-substituent led to the 6-butylphenyl derivative **85b** (EC₅₀ 15.6 nM). However, its potency was decreased compared to **60** at the human receptor (see **Figure 3.7**) and not significantly enhanced at rodent receptor orthologs (see below). We also modified the 3-position of the chromen-4-one scaffold, introducing a methyl group to the 6-bromo-substituted 8-carboxyformamidochromone **59** (EC₅₀ 11.8 nM). However, the resulting 3-methyl derivative **87** displayed >6-fold reduced potency (EC₅₀ 75.0 nM) at the human GPR35 (see **Figure 3.7**). Interestingly, the same modification led to a substantially increased rodent

receptor potency (see below). The rank order of potency of differently 6-position-substituted 8-carboxyformamidochromones at the human GPR35 is provided in **Figure 3.8**.

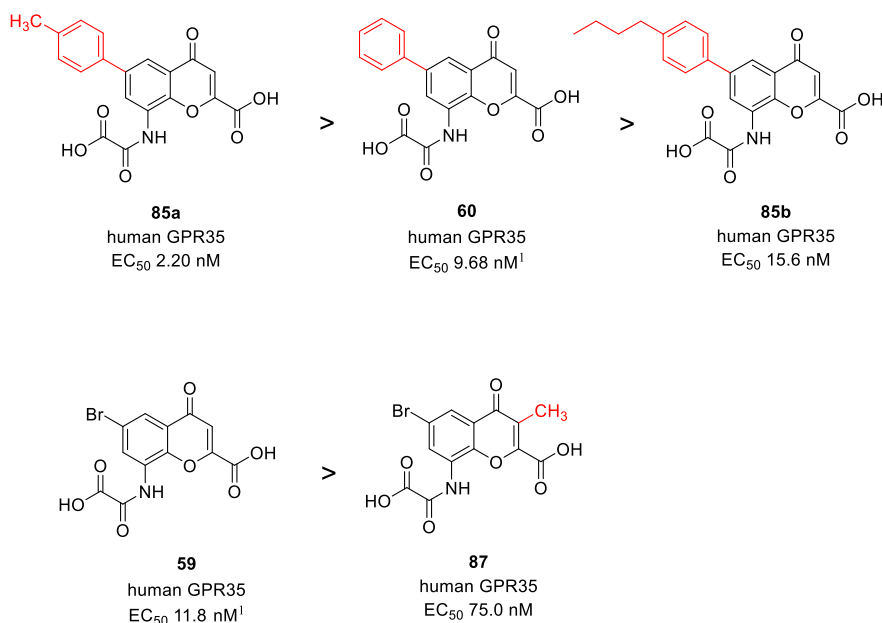


Figure 3.7. Effects of alkylation on potency of 8-carboxyformamidochromone derivatives at the human GPR35.¹

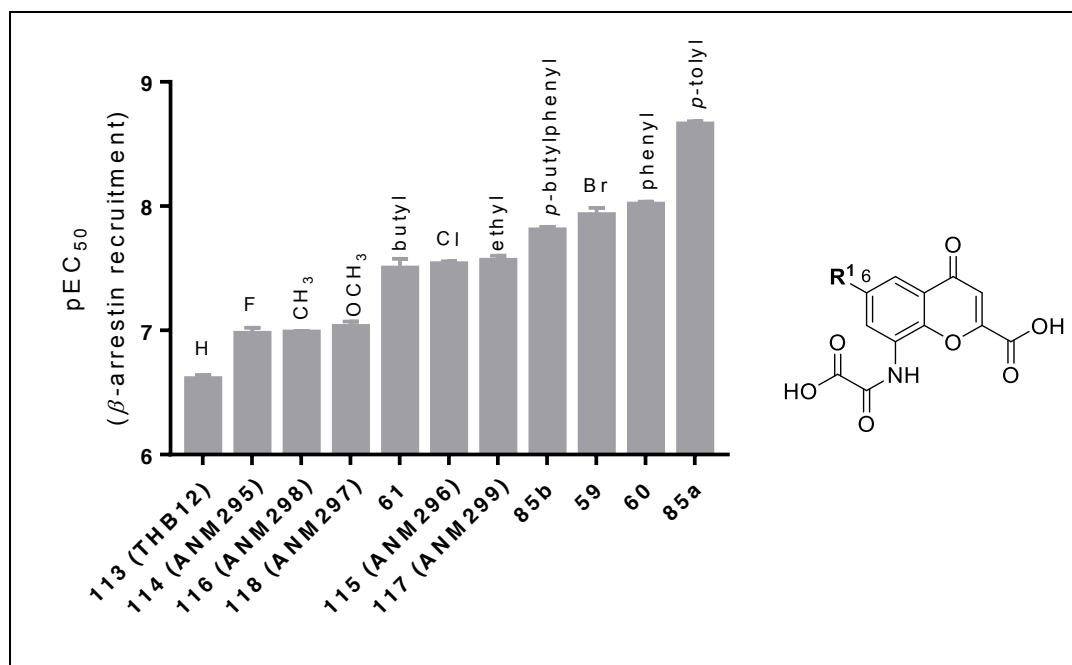


Figure 3.8. Structure-activity relationships of 8-carboxyformamidochromen-4-ones determined for the human GPR35.¹

Potency of 1,7-phenanthroline derivatives

Apart from chromen-4-one derivatives, the human GPR35 was also activated by molecules with a 1,7-phenanthroline scaffold. The lead compound bufrolin (**30**, **Figure 3.9**) activated the receptor with an EC_{50} value of 3.86 nM, yet its potency at the mouse receptor was 23-fold lower. Therefore, we introduced a variety of different substituents, which had various effects on potency. Interestingly, most modifications were tolerated exceptionally well by the human receptor, and only few residues led to a vastly decreased potency at this GPR35 ortholog.

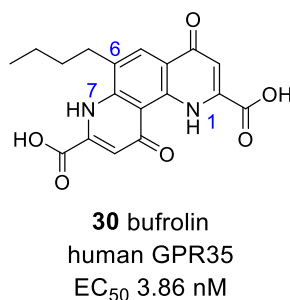


Figure 3.9. The lead compound bufrolin (**30**) already displayed high potency at the human GPR35.

At first, we removed the butyl group in the 6-position of our lead compound, replacing it with hydrogen. The resulting **68a** displayed remarkably decreased potency (~150-fold) with an EC_{50} value of 578 nM. It seemed that a lipophilic interaction of some sort was required in this position for efficient binding. Previous works regarding chromen-4-one-derived GPR35 agonists had shown that halogen substituents in the 6-position could increase potency.¹⁰⁸ Interestingly, already a 6-fluoro substitution increased potency by >3-fold compared to hydrogen (**68b**: EC_{50} 186 nM). A 6-chloro substituent increased potency further (**68c**: EC_{50} 8.98 nM). The 6-bromo-substituted **68d** showed the highest potency at the human GPR35 with an EC_{50} value of 3.32 nM (see **Figure 3.10**). As such, it was equally potent as the lead compound bufrolin, however, its potency at the murine orthologs was considerably lower (see below).

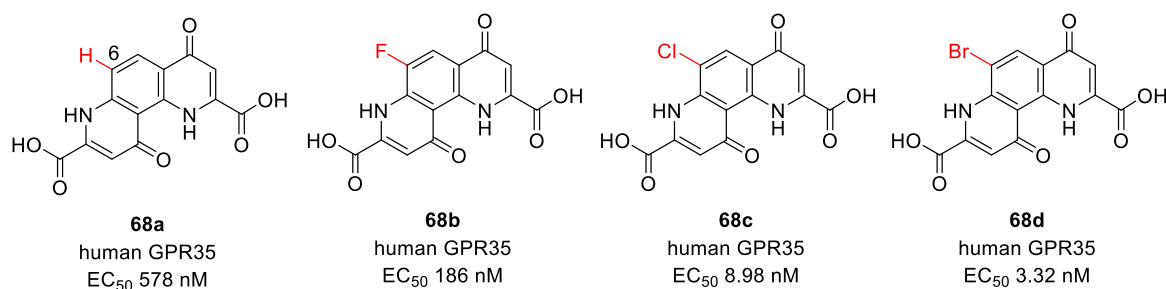


Figure 3.10. Large halogen atoms in the 6-position increased potency compared to hydrogen.

In a previous study, the butyl group in the 6-position of the lead compound bufrolin was truncated to a methyl group.¹ The resulting **63** (EC₅₀ 21.4 nM) displayed slightly lower potency than the lead structure.¹ In this study, we investigated the impact of 6-alkyl residues further. We therefore successively elongated the alkyl chain. However, we only found a weak correlation between chain length and potency. While the 6-ethyl derivative **68g** (EC₅₀ 14.1 nM) was significantly more potent than **63**,¹ the 6-propyl derivative **68h** (EC₅₀ 3.70 nM) was already as potent as the 6-butyl-substituted lead structure bufrolin (**30**: EC₅₀ 3.86 nM) and further elongation did not lead to a significantly increased potency at the human GPR35 (see **Figure 3.11**). The 6-decyl derivative **68o** displayed the highest potency of this series with an EC₅₀ value of 2.20 nM.

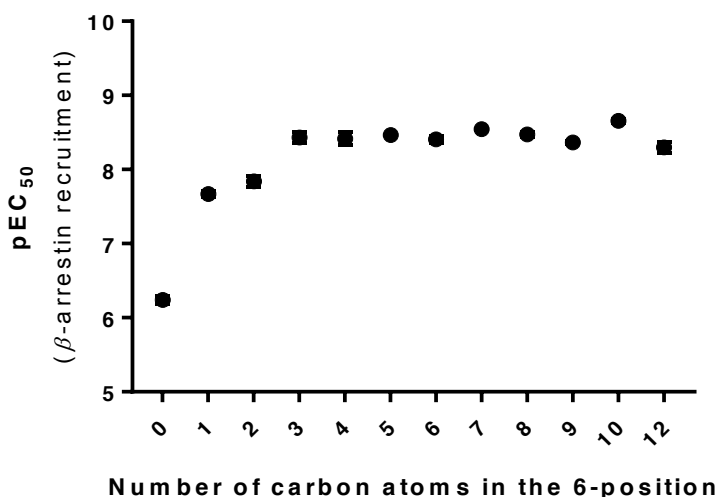


Figure 3.11. Potency of 6-alkyl-substituted 1,7-phenanthroline derivatives in relation to chain length.

We also investigated the impact of branched alkyl chains on potency by replacing the *n*-butyl group of the lead compound with related isomers and a cyclic residue, respectively (see **Figure**

3.12). The introduction of a bulky *tert*-butyl residue as in **68s** was not tolerated well. With an EC₅₀ value of 281 nM, it was among the weakest compounds with this scaffold. The *sec*-butyl residue, which is less bulky, was considerably better tolerated (**68r**, EC₅₀ 13.8 nM). The 6-cyclohexyl derivative **68t** displayed high potency (EC₅₀ 6.92 nM). However, none of the branched derivatives could quite match the potency of the linear lead compound (**30**: EC₅₀ 3.86 nM).

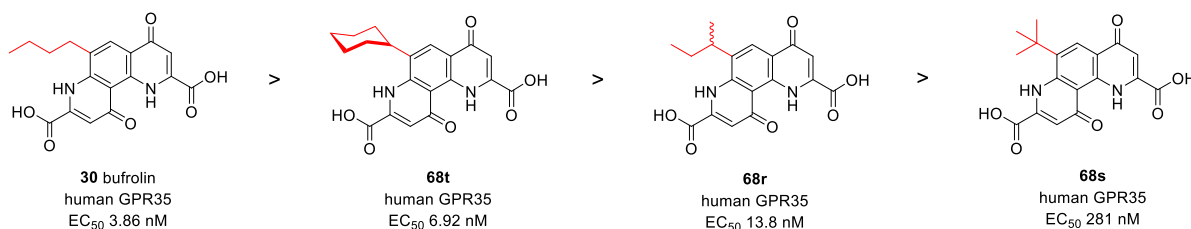


Figure 3.12. Linear alkyl chains were tolerated better by the human GPR35 than branched ones.

In accordance with previous findings for the chromen-4-one scaffold, the introduction of aryl moieties to the 6-position of 1,7-phenanthrolines was tolerated relatively well (see **Figure 3.13**). The 6-phenyl derivative **68v** (EC₅₀ 9.49 nM) displayed similar potency as the 6-chloro derivative **68c** (EC₅₀ 8.98) at the human GPR35. The bioisosteric 6-thiophen-2-yl-containing **68u** was even more potent with an EC₅₀ value of 6.05 nM. Interestingly, the introduction of a *tert*-butyl group to the *para*-position of a 6-phenyl moiety also showed increased potency (**68x**: EC₅₀ 5.30 nM) compared to the unsubstituted phenyl derivative **68v**. The 6-*p*-tolyl derivative **68w** was slightly more potent (EC₅₀ 3.87 nM). The most potent compound with an aryl moiety was the 6-*p*-butylphenyl-substituted **68y**, which displayed an EC₅₀ value of 1.96 nM. It was also the most potent of all investigated 1,7-phenanthroline derivatives at the human GPR35.

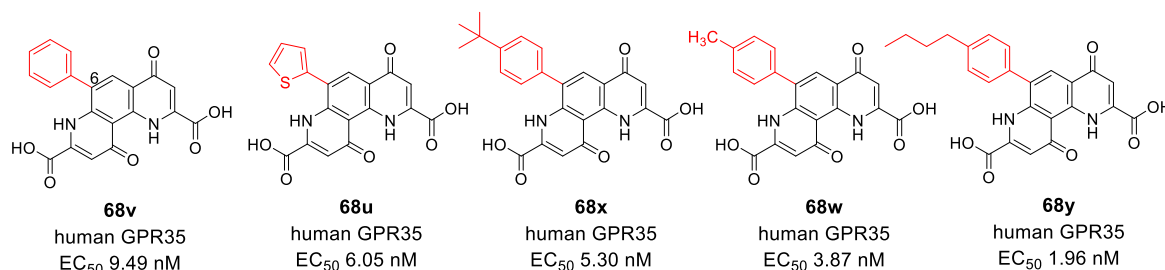


Figure 3.13. The alkylation of aryl residues in the 6-position was tolerated well by the human GPR35.

Other minor substituents that were introduced were a 6-methoxy moiety (**68q**) and a 6-nitro group (**68e**). The 6-methoxy derivative **68q** was among the least potent 1,7-phenanthroline

derivatives at the human GPR35 (EC_{50} 63.1 nM) and also at its murine orthologs (see below). Interestingly, however, the 6-nitro derivative **68e** displayed extremely high potency at the human receptor ortholog (EC_{50} 2.91 nM), but was 22-fold and 243-fold less potent at the rat and mouse GPR35 orthologs, respectively.

Apart from the 6-position, we also investigated the impact of modifications at the 2- and 8-positions, the effect of alkylation of the 5-position, and the removal of a hydrogen-bond acceptor in the 4-position. In general, esterification of the 2,8-dicarboxylic acid moieties was not tolerated well by the human receptor ortholog, since the esterified 6-bromo (**67d**: EC_{50} 1250 nM), 6-*sec*-butyl (**67r**: EC_{50} 1090 nM), 6-pentyl (**67j**: EC_{50} 209 nM), and 6-heptyl (**67l**: EC_{50} 239 nM) derivatives were markedly less potent than their free acid counterparts. The esterified 6-octyl derivative **67m** was inactive (see **Figure 3.14**). In addition to reduced potency, **67l** also displayed lower efficacy at the human GPR35 ortholog (E_{max} 64%) compared to the standard agonist zaprinast. Considering that the related 2,6-dihydroxy derivative **111** was completely inactive, it appears that a carboxylic acid moiety in these positions is a necessity for efficient receptor activation.

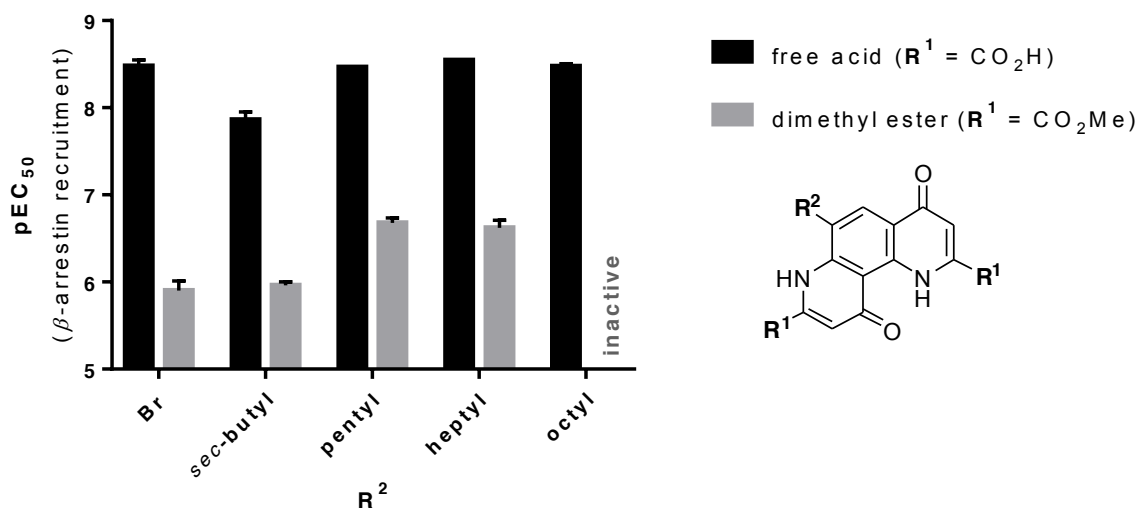


Figure 3.14. Esterification of carboxylic acid moieties resulted in decreased potency.

Alkylation of the 5-position, on the other hand, had a positive influence on potency. The 5,6-dimethylated **68z** displayed an EC_{50} value of 2.93 nM, which is a >7-fold increase compared to the 6-monomethylated **63** (see **Figure 3.15**).

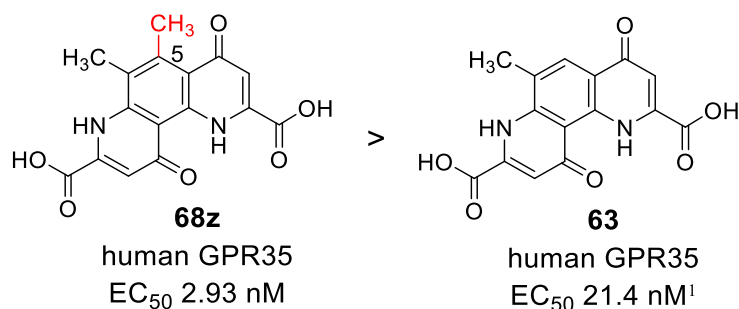


Figure 3.15. Methylation in the 5-position increased potency at the human receptor ortholog.

Lastly, we investigated the importance of the hydrogen-bond acceptor in the 4-position by removing the carbonyl oxygen, shrinking the A-ring from a 4-pyridone to a pyrrole ring (see **Figure 3.16**). The resulting **110** showed remarkably increased potency (EC_{50} 4.48 nM) compared to the equivalent phenanthroline (**68q**: EC_{50} 63.1 nM), which was 14-fold less potent. Therefore, it appears that an H-bond acceptor in that position is not a necessity for the human GPR35 ortholog.

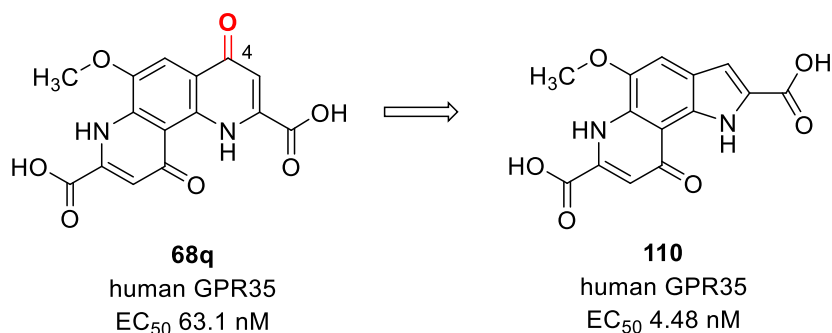


Figure 3.16. The elimination of a hydrogen bond acceptor in the 4-position of the 1,7-phenanthroline core was tolerated well by the human GPR35 ortholog.

Potency of further scaffolds

Similar to the pyrrolo[2,3-*f*]quinolone **110**, which is mentioned above, further investigated scaffolds showed comparably high potency at the human GPR35 (see **Figure 3.17**). The pyrido[3,2-*g*]quinolone **105** displayed an EC_{50} value of 11.4 nM. Thus, it was more potent than the equivalent phenanthroline derivative **63** (EC_{50} 21.4 nM).¹ Interestingly, the quinoline derivative **102** (EC_{50} 8.95 nM) exhibited almost identical potency to its 1,7-phenanthroline equivalent **68c** (EC_{50} 8.98 nM). However, its derivative **96a**, which differs from **102** only in the absence of a second carboxylic acid moiety in the 5-position, was barely active (EC_{50} 4900

nM). A similarly low potency was observed for the other quinolone derivatives. The 8-*tert*-butylphenyl derivative **99** (Table 3.19) was the most potent of these compounds with an EC₅₀ value of 3420 nM. The 8-bromo derivative **96b** (Table 3.19) was equally weak (EC₅₀ 3800 nM). The indole derivative **108** was relatively potent at the human receptor ortholog and in the potency range of its chromen-4-one and phenanthroline counterparts. A comparison between different scaffolds is provided in Figure 3.17.

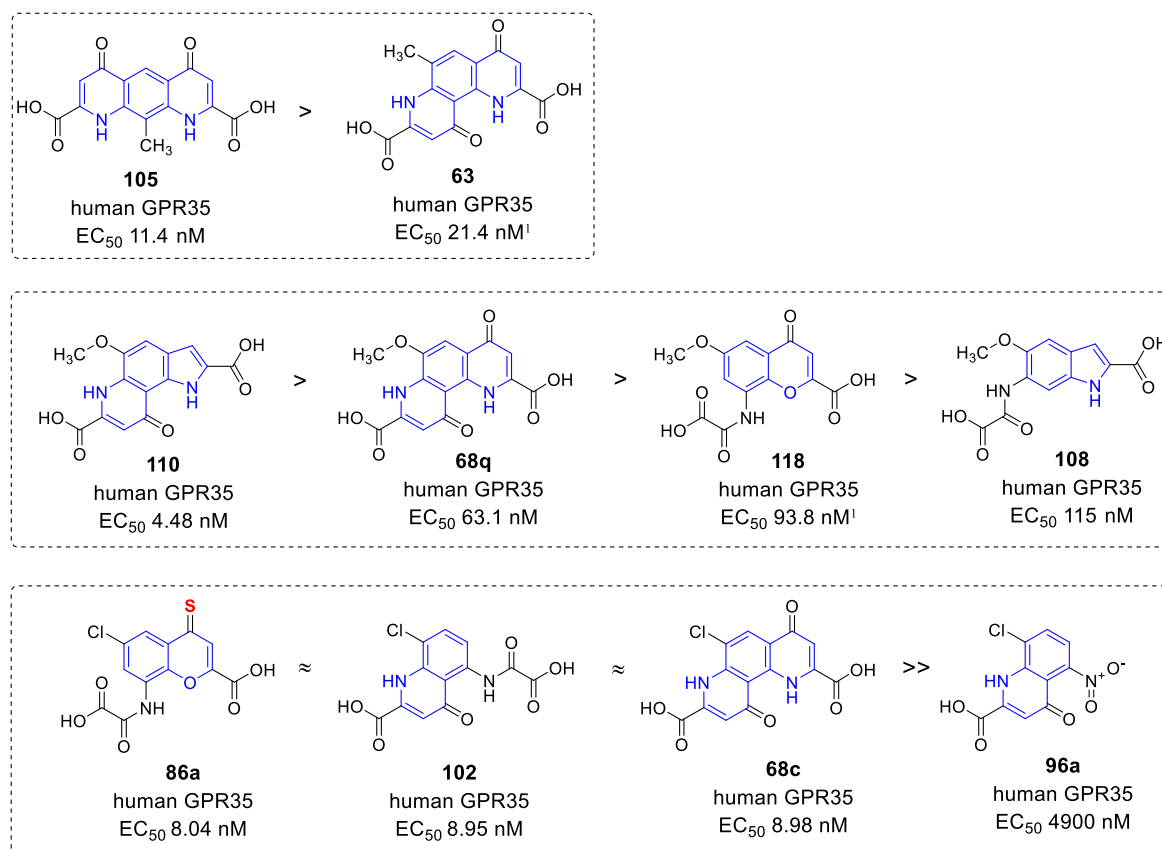


Figure 3.17. Comparison of different scaffolds at the human GPR35 ortholog.

Summary: Human GPR35

In general, all of the optimized compounds were full agonists at the human GPR35. The most potent chromen-4-one derivatives at the human GPR35 ortholog had large, lipophilic residues in their respective 6-positions, such as an alkyl chain, a bromine, or an aryl moiety. However, the human receptor tolerated a large variety of substituents in this position, and even substitution with smaller, more polar residues led to reasonably potent derivatives. The esterification of carboxylic acid moieties, on the other hand, was not tolerated and decreased potency in all cases. Neither was the alkylation of the 3-position tolerated. The thionation of the 4-position had mixed outcomes, which depended on the other substituents. It was generally

accepted, however. The best substituent in the 8-position was either a 2,6-difluorinated 4-methoxybenzamide or an oxalic acid monoamide. **Figure 3.18** provides a summary of important chromen-4-one structure-activity relationships at the human GPR35.

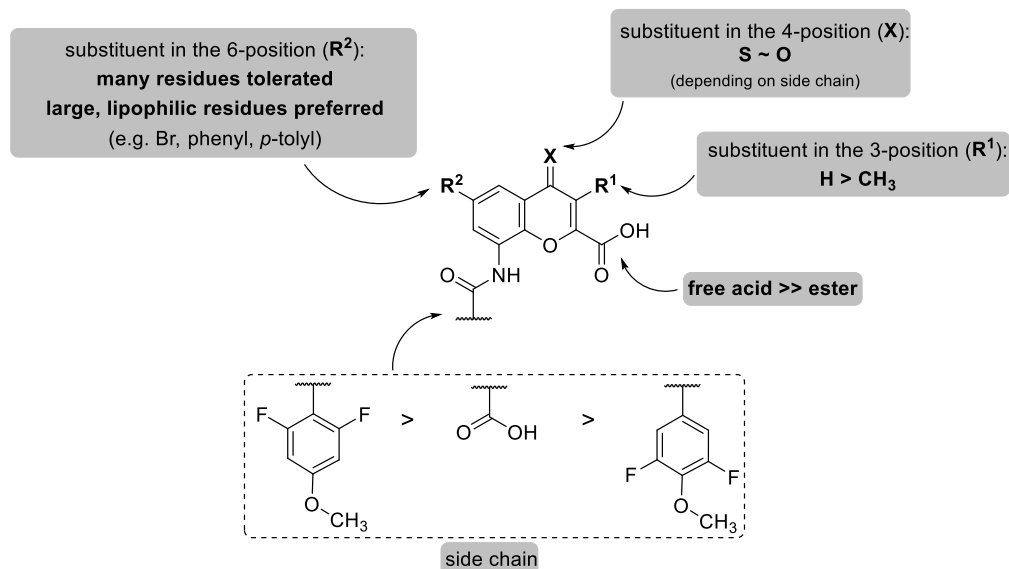


Figure 3.18. Structure-activity relationships of chromen-4-one derivatives determined for the human GPR35. See also previous works.¹

1,7-Phenanthroline derivatives generally displayed high potency at the human GPR35 ortholog, which tolerated many residues attached to the core scaffold. Large, lipophilic residues in the 6-position, such as bromine, unbranched alkyl chains, or *p*-substituted phenyl rings were particularly favored by the receptor. A hydrogen bond donor in the 4-position was not required for potency, and esterification of the carboxylic acid moieties was not accepted. However, methylation of the 5-position increased potency. The observed SARs for 1,7-phenanthroline derivatives are summarized in **Figure 3.19**.

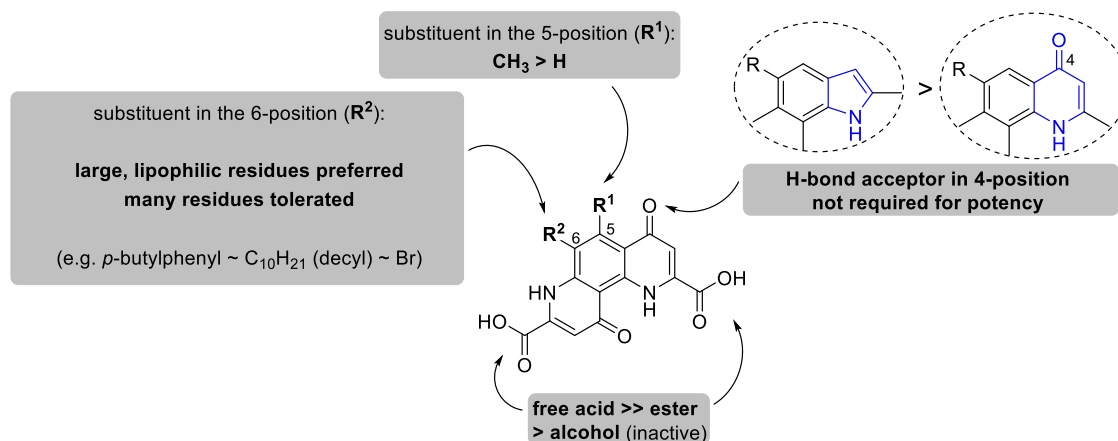


Figure 3.19. Structure-activity relationships of 1,7-phenanthroline derivatives determined for human GPR35.

Affinity of GPR35 agonists

The affinity of the GPR35 agonists developed for the human receptor ortholog was determined in radioligand binding assays versus the radioligand [^3H]PSB-13253.⁹² The measured affinity was largely comparable to the potency determined in β -arrestin assays, and EC_{50} values from arrestin assays generally correlated well with K_i values from binding experiments (see **Figure 3.20**).

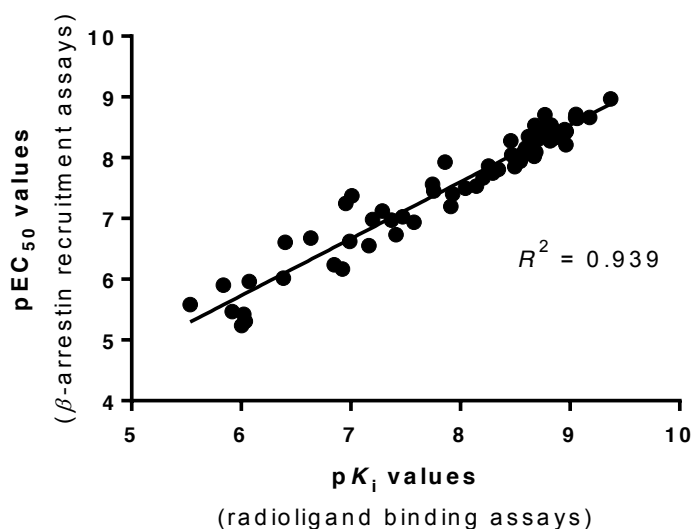


Figure 3.20. Scatter plot of pEC_{50} values plotted against their respective pK_i values to test for correlation. R^2 was determined in a two-tailed Pearson test.

While K_i values were generally lower than EC_{50} values by a factor of three, the highest discrepancy between the EC_{50} value and K_i value was observed with **67m**, a diesterified 6-octyl phenanthroline derivative, which was inactive in arrestin assays, but displayed relatively high affinity in radioligand binding experiments (K_i 175 nM). A similar observation was made for **80**, which is also a diester compound. It displayed an EC_{50} value of 680 nM, but showed much higher affinity (K_i 119 nM). Some other compounds have also shown a significant discrepancy between affinity and potency (see **Figure 3.21**).

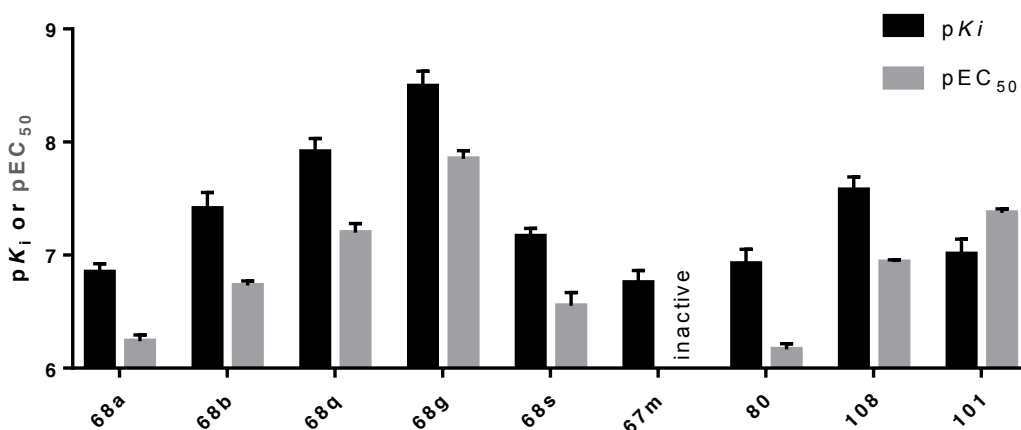


Figure 3.21. Bar chart of GPR35 agonists with significant discrepancy between affinity (pK_i) and potency (pEC_{50}).

In radioligand binding experiments, chromen-4-one derivatives and 1,7-phenanthroline derivatives generally displayed similar affinity and no superiority of one scaffold over the other could be demonstrated for the human GPR35 (see **Figure 3.22**). The chromen-4-one derivatives of this study, which showed the highest affinity for the receptor were **88c** (K_i 0.66 nM), **86b** (K_i 0.88 nM), **85a** (K_i 0.89 nM), **88a** (K_i 1.09 nM), and **88e** (K_i 1.38 nM). The 1,7-phenanthroline derivatives with the highest affinity were **68o** (K_i 0.863 nM), **68h** (K_i 1.08 nM), **68j** (K_i 1.12 nM), **68k** (K_i 1.12 nM), and **68m** (K_i 1.44 nM). The lead bufrolin displayed affinity in the same range with a K_i value of 1.22 nM.

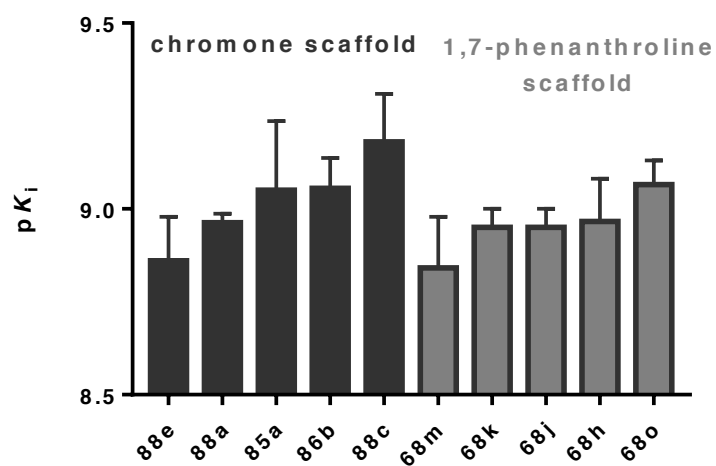


Figure 3.22. Chromen-4-one derivatives and 1,7-phenanthrolines with the highest affinity at the human GPR35.

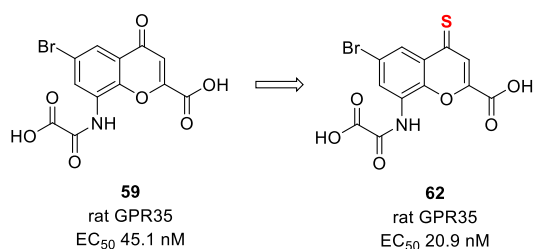
3.4.3.2 Rat GPR35

Potency of chromen-4-one derivatives

Important considerations concerning the SARs of chromone derivatives at the rat GPR35 have been reported in previous works by members of our group.^{1,92,108,186} By introducing chemical modifications at the 4-, 6-, and 8-positions of the chromone scaffold, it was possible to obtain highly potent derivatives for the human receptor ortholog with EC₅₀ values in the subnanomolar range. However, the most potent compounds at the human receptor were significantly less potent at the rat and mouse receptor orthologs. Compound **26**, which had displayed an EC₅₀ value of 1.08 nM at the human receptor (see above), showed a 145-fold reduced potency at the rat receptor ortholog.¹ Careful study and chemical optimization of a large library of chromen-4-one derivatives revealed that the rat receptor required ligands with a different substitution pattern than the human receptor. With the chromenone derivatives investigated herein, we attempted to expand the previously determined SARs for the rat receptor ortholog.

While human-optimized chromone derivatives were generally most potent with a 2,6-difluoro-4-methoxybenzamide moiety in the 8-position, the rat receptor ortholog required the presence of a second carboxylic acid moiety in that position for efficient activation. 8-Benzamidochromen-4-ones were generally less potent than the respective 8-carboxyformamido derivatives. Therefore, we initially focused on the development of smaller 8-carboxyformamidochromen-4-one derivatives bearing two carboxylic acid moieties.

In the previous study, the thionation of 6-bromo-8-(carboxyformamido)-4-oxo-4*H*-chromene-2-carboxylic acid (**59**, EC₅₀ 45.1 nM) led to a >2-fold increased potency at the rat receptor ortholog (**62**, EC₅₀ 20.9 nM).¹ In the present study, a similar increase in potency was observed upon thionation of the 4-position. The thionated 6-chloro-substituted **86a** showed a 3.7-fold increased potency compared to the 4-oxo derivative **115** (ANM296, EC₅₀ 80.0 nM) and thionation of 8-(carboxyformamido)-4-oxo-6-phenyl-4*H*-chromene-2-carboxylic acid (**60**, EC₅₀ 154 nM) even led to the 7.3-fold more potent **86b** (EC₅₀ 21.3 nM). We can therefore confirm the previous conclusion that thionation of 8-carboxyformamidochromen-4-ones indiscriminately increases their potency at the rat receptor (see **Figure 3.23**). A similar trend could be observed for the human receptor ortholog, although there, thionation generally led to a smaller increase in potency (see previous section).

previous work:¹

this work:

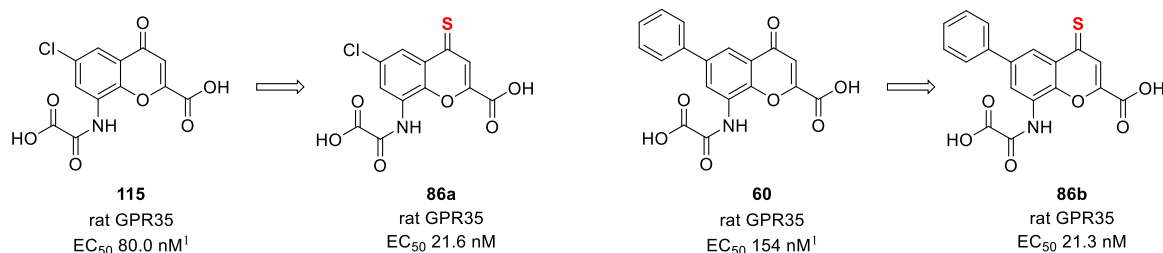


Figure 3.23. Thionation of 8-carboxyformamidochromenone derivatives increased rat receptor potency.¹

Interestingly and contrary to 4-oxo derivatives, the 6-phenyl chromen-4-thione derivative **86b** (EC₅₀ 21.3 nM) showed comparable potency to the 6-bromo derivative **62** (EC₅₀ 20.9 nM). Even more surprisingly, the 6-chloro derivative **86a** (EC₅₀ 21.6) was also similarly potent as the 6-bromo derivative **62**. This underlines the dominant effect of thionation at the 4-position.

The thionation of the larger 8-benzamidochromenones, on the other hand, quite surprisingly, led to a reduction in potency. In an effort to increase rodent receptor potency of the human-optimized 6-bromo-8-(2,6-difluoro-4-methoxybenzamido)-4-oxo-4*H*-chromene-2-carboxylic acid (**25**, EC₅₀ 199 nM) and 8-(2,6-difluoro-4-methoxybenzamido)-4-oxo-6-phenyl-4*H*-chromene-2-carboxylic acid (**26**, EC₅₀ 157 nM),¹ we replaced their 4-keto moieties with sulfur in a similar manner as performed with the 8-carboxyformamidochromenone derivatives above. However, while the human and mouse receptor orthologs tolerated **88a** and **88d** comparably well, they actually displayed lower potency (EC₅₀ 520 nM, 212 nM, respectively) than their 4-oxo counterparts at the rat receptor ortholog (see **Figure 3.24**).

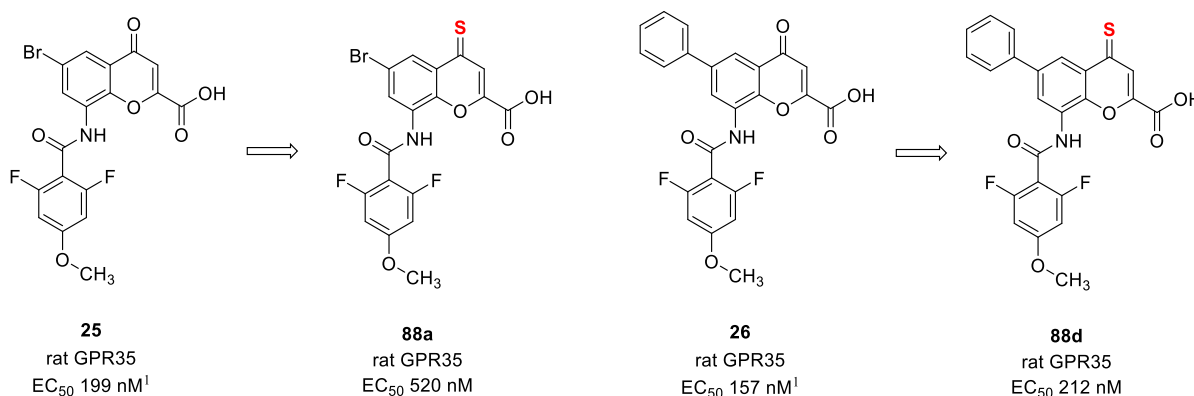


Figure 3.24. Thionation of 8-benzamidochromen-4-one derivatives decreased rat receptor potency.

Despite the somewhat weak potency of 8-benzamidochromen-4-one derivatives compared to the smaller 8-carboxyformidochromen-4-ones, the 6-*p*-tolyl-substituted 8-benzamidochromen-4-thione derivative **88e** displayed a relatively high potency with an EC_{50} value of 57.1 nM. It was the most potent one of the thionated 8-benzamidochromen-4-one derivatives. The closely related 6-phenyl derivative **88d** was already 3.7-fold less potent (EC_{50} 212), and the 6-bromo derivative **88a** showed 9-fold weaker potency (EC_{50} 520 nM). Interestingly, the 6-methyl derivative **88c**, which had been among the most potent derivatives at the human receptor (human GPR35: EC_{50} 2.18 nM), was among the weakest compounds at the rat receptor ortholog with an EC_{50} value of 615 nM. As with the human and mouse receptors, the best substitution pattern for the benzamide in the 8-position was 2,6-difluoro-4-methoxy, which had been identified in a previous study.⁹² The modification to a 3,5-difluoro-4-methoxy-substituted phenyl ring (**88b**, EC_{50} 1670 nM, E_{max} 60%) was not tolerated by the rat receptor (see **Figure 3.25**).

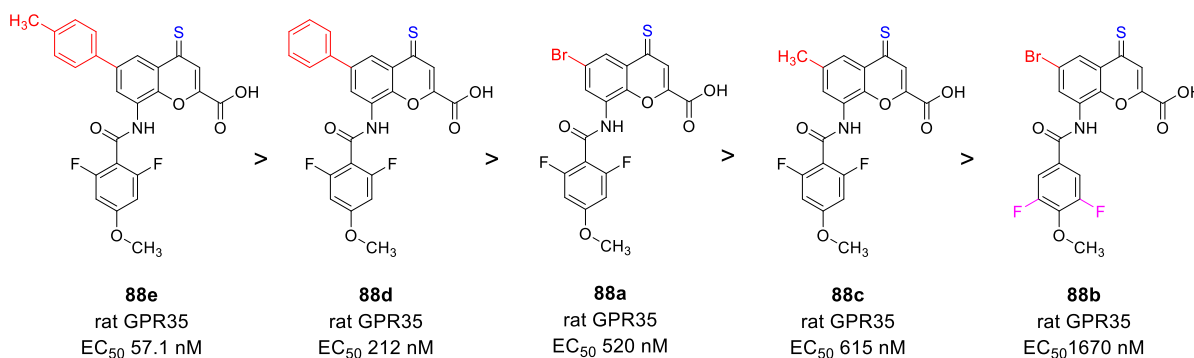


Figure 3.25. Rank order of potency of thionated 8-benzamidochromen-4-one derivatives at rat GPR35.

As mentioned above, unthionated 8-carboxyformamidochromen-4-one derivatives were generally less potent at this receptor than 4-thioxo derivatives, and the observed rank order of potency was different (see **Figure 3.26**). 6-Butyl-8-(carboxyformamido)-4-oxo-4*H*-chromene-2-carboxylic acid (**61**), which had been discovered in a previous work,¹ remained the most potent derivative with an EC₅₀ value of 29.7 nM. The 6-bromo derivative **59** was slightly less potent (EC₅₀ 45.1 nM). This was followed by 6-ethyl (**117**, ANM299, EC₅₀ 75.0 nM) and 6-chloro (**115**, ANM296, EC₅₀ 80.0 nM), which showed comparable potency to each other.¹ The new 6-*p*-butylphenyl derivative **85b** was the most potent of the 6-aryl derivatives (EC₅₀ 132 nM), however, its potency was not significantly different from the 6-*p*-tolyl derivative **85a** (EC₅₀ 142 nM) and the 6-phenyl derivative **60** (EC₅₀ 154 nM).¹ Therefore, it appears that alkylation of aryl moieties in the 6-position had no marked effect on potency. Our observations confirm that alkyl chains are the preferred substituent at the 6-position of this scaffold and that alkylation of aryl residues does not serve to improve potency at the rat GPR35.

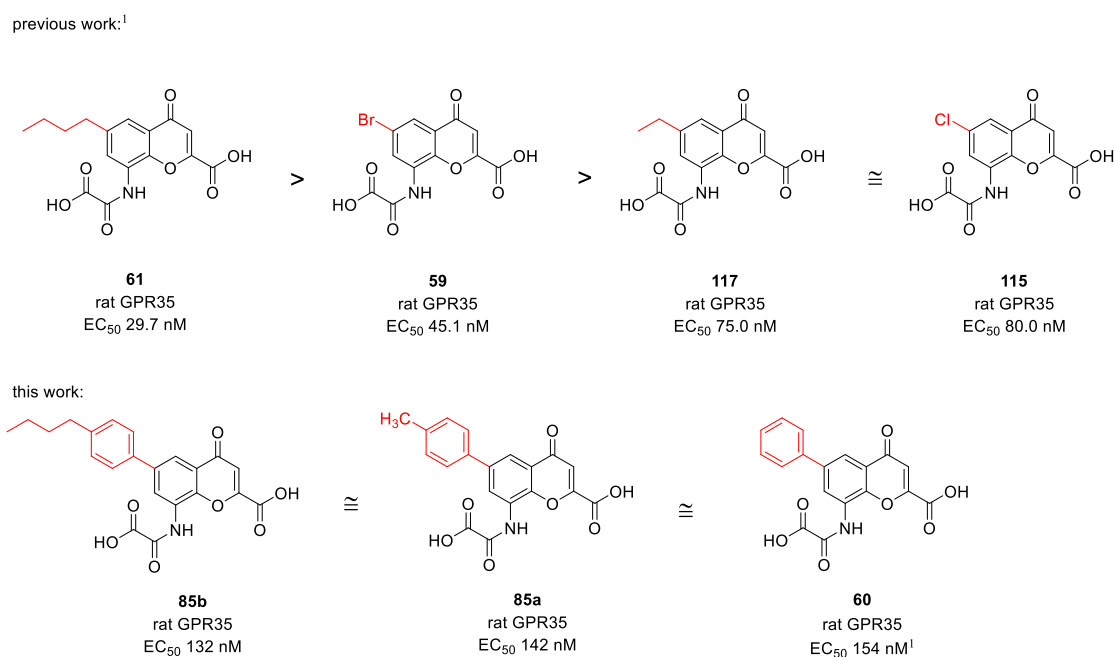


Figure 3.26. Rank order of potency of 8-carboxyformamidochromen-4-one derivatives.¹

Interestingly, the most potent chromone derivative of this work was the 3-methyl substituted **87** (EC₅₀ 12.2 nM). It was 3.7-fold more potent than the 3-position-unsubstituted **59** (EC₅₀ 45.1 nM).¹ It was even slightly more potent than the chromen-4-thione **62** (EC₅₀ 20.9 nM).¹ See **Figure 3.27**. A larger library of related 3-methyl chromen-4-ones and chromen-4-thiones differently substituted in the 6-position would be needed to explore this observation further. However, the 3-methyl residue only increased potency at the rat and mouse receptor orthologs

and reduced potency and affinity at the human GPR35 (see above), which is why it was not pursued further.

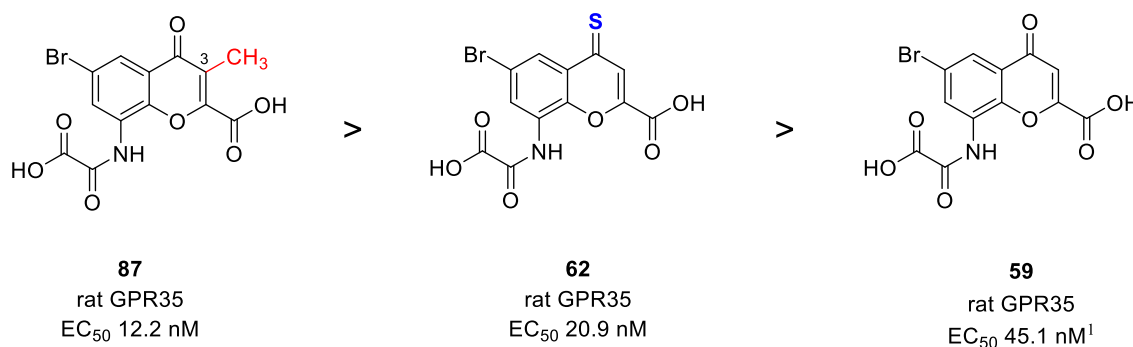


Figure 3.27. Methylation at the 3-position increased rat receptor potency significantly.

Potency of 1,7-phenanthroline derivatives

The lead structure bufrolin already displayed high potency at rat GPR35 with an EC₅₀ value of 1.86 nM in our β -arrestin assay. A reduction in potency at the rat receptor would be tolerated if potency at the mouse receptor increased. However, the previously described 6-methyl derivative **63** (EC₅₀ 26.3 nM) displayed ~14-fold reduced potency at this receptor ortholog without enhancing mouse GPR35 activity significantly.¹ Additional methylation at the 5-position resulted in the 5,6-dimethyl derivative **68z** (EC₅₀ 17.7 nM), which exhibited slightly increased potency (see **Figure 3.28**).

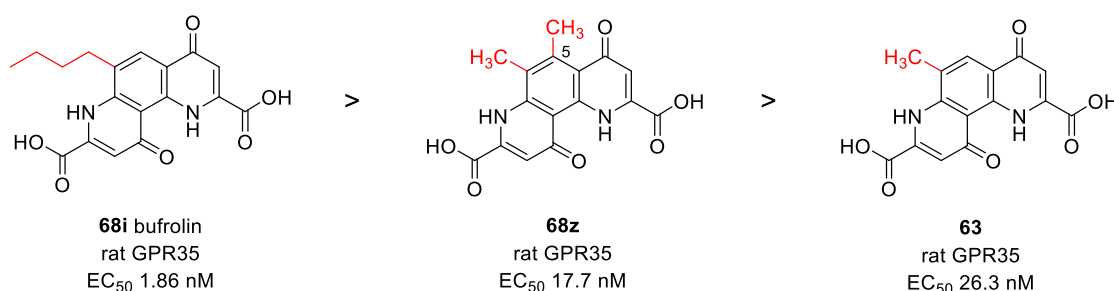


Figure 3.28. Alkylation of the 5-position increased potency at the rat GPR35 ortholog.

Our main focus was the optimization of the 6-position. Halogen substitution in the corresponding position of chromen-4-one derivatives had previously increased their potency at the human receptor ortholog.¹⁰⁸ Therefore, we investigated the impact of such substituents. First, we exchanged the butyl group of our lead compound bufrolin with hydrogen. With an

EC₅₀ value of 334 nM, the resulting **68a** showed ~180-fold reduced potency compared to the lead compound. Fluorination increased potency again and led to **68b** (EC₅₀ 170 nM), and the 6-chloro derivative **68c** was already active in the low nanomolar range again (EC₅₀ 21.6). The best halogen substituent in this position, however, was bromine, since **68d** exhibited single-digit nanomolar potency again, with an EC₅₀ value of 9.69 nM (see **Figure 3.29**). Replacement with a methoxy group did not significantly increase potency compared to hydrogen (**68q**, EC₅₀ 283 nM, **Figure 3.32**). Interestingly, the rat receptor ortholog was reasonably tolerant of a nitro group in the 6-position (**68e**, EC₅₀ 63.2, **Table 3.18**), which was not accepted by the mouse receptor (mouse GPR35: **68e**, EC₅₀ 706 nM).

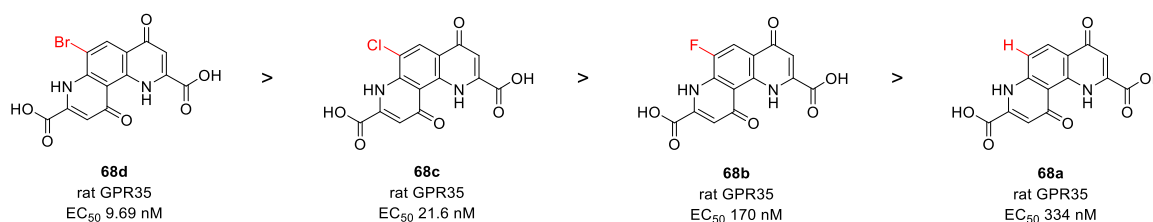


Figure 3.29. Rank order of potency for halogen-substituted 1,7-phenanthroline derivatives.

Considering that the most potent chromen-4-one derivatives at the human receptor had aromatic residues in their 6-positions, we introduced a number of different aryl moieties to the scaffold. A 6-phenyl ring was tolerated well (**68v**, EC₅₀ 31.7 nM) and displayed comparable potency to the previously described 6-methyl derivative **63** (EC₅₀ 26.3 nM). Methylation of the phenyl ring led to a significant increase in potency. The *p*-tolyl derivative **68w** showed an EC₅₀ value of 12.0 nM. Elongation of the alkyl group to *p*-butylphenyl increased potency further (**68y**, EC₅₀ 7.81 nM). However, the bulkier *p*-*tert*-butylphenyl derivative **68x** displayed 5-fold decreased potency (EC₅₀ 39.2 nM). The most potent 6-aryl-substituted 1,7-phenanthroline at the rat receptor was the thiophen-2-yl derivative **68u** (EC₅₀ 5.90 nM). Interestingly, it was tolerated very well by all investigated GPR35 orthologs even though the bioisosteric 6-phenyl derivative **68v** was not (see below). For the rank order of potency of 6-aryl derivatives at the rat GPR35 see **Figure 3.30**.

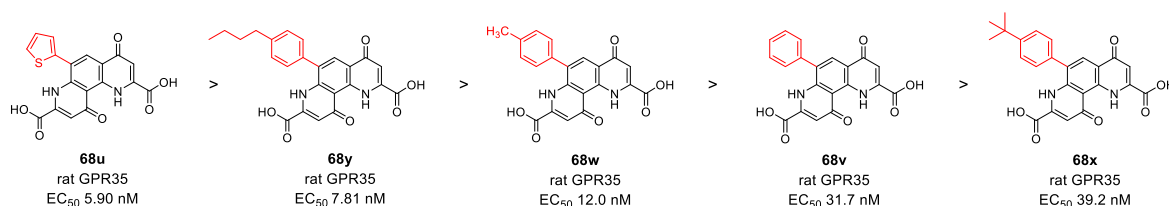


Figure 3.30. Rank order of potency of 6-aryl phenanthroline derivatives at the rat GPR35.

Modifying the alkyl chain length in the 6-position had the largest influence on potency. The 6-ethyl derivative **68g** (EC₅₀ 15.0 nM) was slightly more potent than the 6-methyl derivative **63**.¹ The 6-propyl derivative **68h** (EC₅₀ 3.22 nM) was ~4.7-fold more potent than **68g**. The 6-pentyl derivative **68j** (EC₅₀ 1.46 nM) was even slightly more potent than the lead compound bufrolin, and the trend continued upon further elongation. The 6-hexyl (**68k**, EC₅₀ 0.846 nM), 6-heptyl (**68l**, EC₅₀ 0.871 nM), 6-octyl (**68m**, EC₅₀ 0.780 nM), 6-nonyl (**68n**, EC₅₀ 0.671 nM), and 6-decyl (**68o**, EC₅₀ 0.723 nM) derivatives all exhibited EC₅₀ values in the subnanomolar range. Since all of these derivatives were so highly potent, a rank order of potency could not be determined. However, increasing the length of the alkyl chain to more than 10 carbon atoms reduced potency again, with the 6-dodecyl derivative **68p** (EC₅₀ 1.87 nM) being about as potent as the lead compound bufrolin. We also investigated the impact of branched alkyl chains by comparing the EC₅₀ values of the 6-*tert*-butyl derivative **68s** (EC₅₀ 68.2 nM, **Figure 3.31**), the 6-*sec*-butyl derivative **68r** (EC₅₀ 20.3 nM), and the 6-cyclohexyl derivative **68t** (EC₅₀ 11.8 nM) with the *n*-butyl-substituted lead bufrolin (EC₅₀ 1.86 nM). Considering that none of the branched side chains led to improved potency (see **Figure 3.31**), we concluded that the rat receptor prefers linear alkyl chains over branched ones.

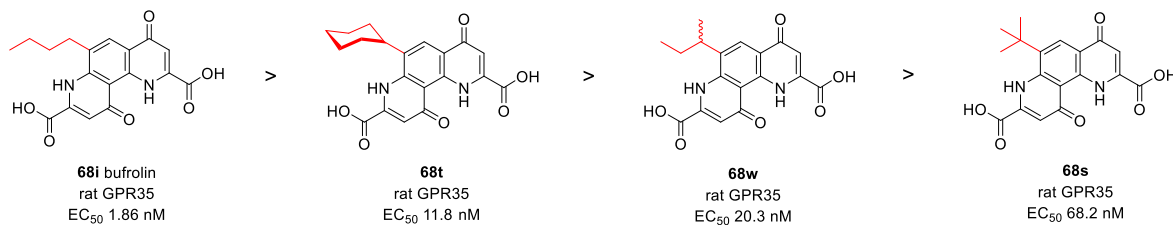


Figure 3.31. Linear alkyl chains in the 6-position were tolerated better than branched ones.

A number of 2,8-diester derivatives were also examined for their potency at the rat receptor ortholog in order to investigate the role of the carboxylic acid moieties. Unsurprisingly, the esterified compounds were generally much less potent than their free acid counterparts. The esterified heptyl derivative **67i** (EC₅₀ 63.0 nM) displayed a 72-fold reduction in potency compared to the 2,8-diacid **68l** (EC₅₀ 0.871 nM). The pentyl derivative **67j** (EC₅₀ 65.0 nM) showed ~45-fold weaker potency compared to **68j** (EC₅₀ 1.46 nM). The *sec*-butyl derivative **67r** (EC₅₀ 499 nM) was ~25-fold weaker than **68r** (EC₅₀ 20,3 nM). With a ~124-fold decreased potency, the esterified octyl derivative **67m** (EC₅₀ 96.4 nM) showed one of the largest differences in potency compared to its free acid equivalent (**68m**, EC₅₀ 0.78 nM). Only the potency discrepancy of the 6-bromo derivative **68d** (EC₅₀ 9.69 nM) and its dimethyl ester **67d** (EC₅₀ 1450 nM) was larger (~150-fold difference). Interestingly, the examined diester

compounds were comparably more potent at the rat receptor ortholog than at the other investigated orthologs (e.g. **67l**: rat GPR35, EC_{50} 63.0 nM; human GPR35, EC_{50} 239 nM; mouse GPR35, EC_{50} 881 nM). The 2,6-diol derivative **111** was completely inactive.

Potency of further scaffolds

We also examined other structures related to the abovementioned chromen-4-one and 1,7-phenanthroline scaffolds for their potency at the rat GPR35. Despite their high potency at the human receptor ortholog, these compounds generally displayed relatively weak potency at the rat receptor.

The pyrido[3,2-*g*]quinolone **105** showed an EC_{50} value of 320 nM (see **Table 3.19**). The pyrrolo[2,3-*f*]quinolone **110** was less potent with an EC_{50} value of 423 nM. This derivative was slightly less potent than its 1,7-phenanthroline-derived counterpart **68q** (EC_{50} 283 nM), which indicates that a hydrogen bond acceptor in ring A is beneficial for potency (see **Figure 3.32**).

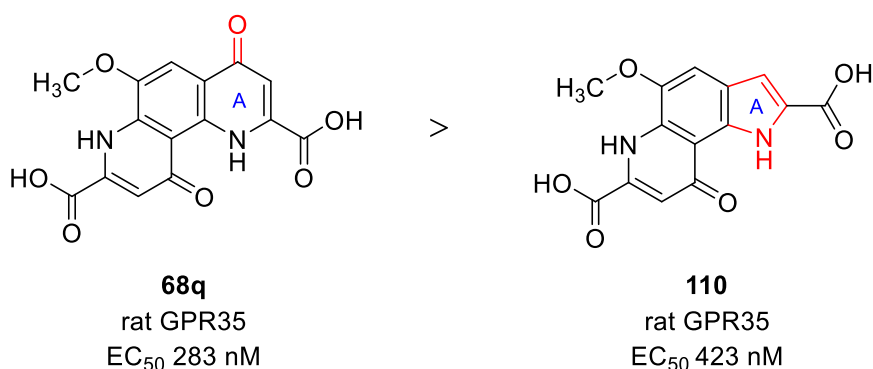


Figure 3.32. A hydrogen-bond acceptor in ring A improves potency slightly.

Smaller quinoline derivatives, such as **96a**, **96b**, and **99** were comparatively more potent at the rat receptor than at the other receptor orthologs, however, their EC_{50} values were still in the low micromolar range (EC_{50} 1210 nM, 550 nM, 974 nM, respectively). Unsurprisingly, the introduction of a second carboxylic acid moiety in **102** (EC_{50} 511 nM) instead of the bioisosteric nitro group in the 5-position of **96a** (EC_{50} 1210 nM) led to a ~2.4-fold increased potency (see **Figure 3.33**). Curiously, the diesterified **101** (EC_{50} 377) appeared even more potent. However, the difference was not statistically significant (compare **Table 3.19**), which could be due to poor solubility during the bioassay. It should be noted that **102** was less potent than the related phenanthroline derivative **68c**. This could be due to the higher rigidity of the latter, which fixes the active conformation of the compound.

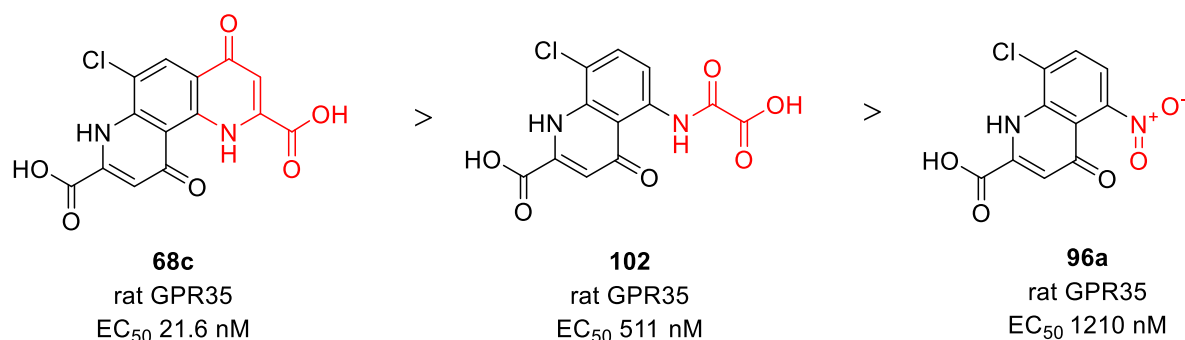


Figure 3.33. Quinoline derivatives display lower potency than related phenanthrolines.

The indole derivatives **108**, **107**, and **106** were not tolerated well by the receptor. The 2,5-dicarboxylic acid derivative **108** displayed an EC₅₀ value of 3930 nM. Surprisingly, the corresponding 2-monoethyl ester **107** was slightly more potent (EC₅₀ 1130 nM). However, the analogous 2,5-diethyl ester **106** was completely inactive. Considering that the tricyclic **110** was 9-fold more potent than the more flexible **108**, it is evident that the rat GPR35 does not tolerate the cleavage of ring C (see **Figure 3.34**).

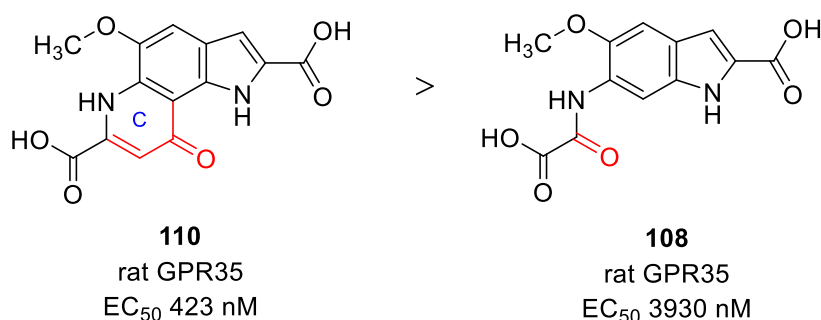


Figure 3.34. Cleavage of the ring C was not tolerated by the rat receptor.

Summary: Rat GPR35

We evaluated a library of potential GPR35 agonists with enhanced potency at the rodent receptor orthologs. Upon comparing EC₅₀ values of various scaffolds, we observed that the rat receptor generally tolerated the 1,7-phenanthroline scaffold best (see **Figure 3.35**).

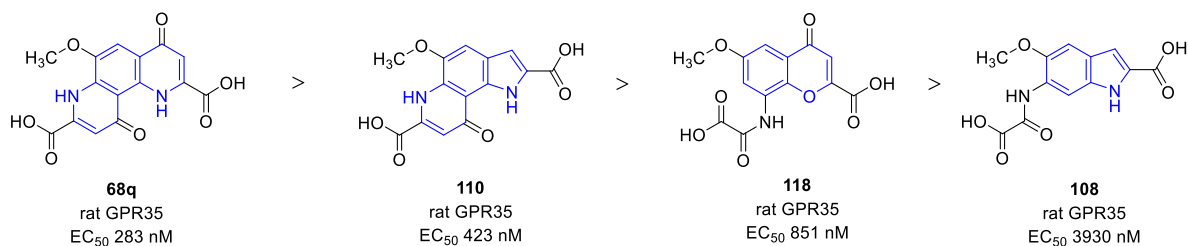


Figure 3.35. Comparison between different scaffolds at rat GPR35.

On the whole, however, the rat GPR35 ortholog accepted a wide range of substituents at the investigated positions. At the chromen-4-one scaffold, smaller derivatives of the 8-carboxyformamido type were more potent than the larger 8-benzamidochromen-4-ones. Alkylation of the 3-position increased potency, as well as thionation of the 4-keto moiety. The most potent derivatives of this ligand class had a large, lipophilic residue in their respective 6-positions, such as an alkyl, bromine, or aryl moiety. **Figure 3.36** provides a summary of important chromen-4-one structure-activity relationships at the rat GPR35.

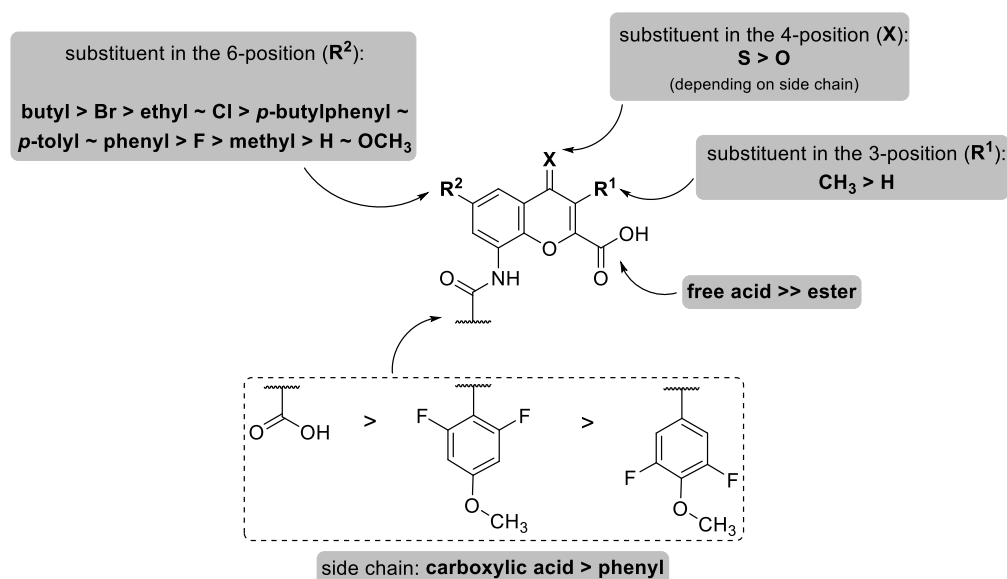


Figure 3.36. Structure-activity relationships of chromen-4-one derivatives determined for rat GPR35. See also previous works.¹

The potency of phenanthroline derivatives could be increased by elongation of the alkyl chain in the 6-position of the lead compound bufrolin. Other modifications at the scaffold (esterification, removal of hydrogen bond acceptors, and ring cleavage) did not improve potency. The alkylation of the 5-position could enhance the activity of one compound, but a larger set of derivatives would be needed to make generalizations. Numerically, the 6-nonyl-substituted compound **68n** was the most potent derivative of this study displaying an EC₅₀ value

in the subnanomolar range (EC_{50} 0.671 nM), however, the 6-decyl, and 6-octyl derivatives were not significantly less potent. The observed SARs for 1,7-phenanthroline derivatives are summarized in **Figure 3.37**.

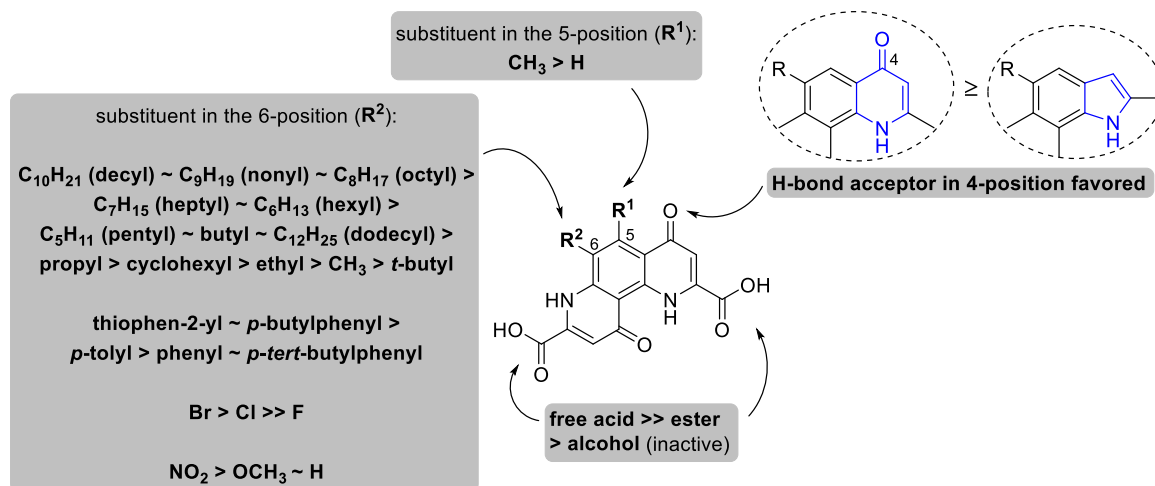


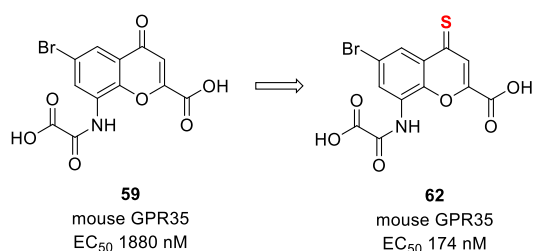
Figure 3.37. Structure-activity relationships of 1,7-phenanthroline derivatives determined for rat GPR35.

3.4.3.3 Mouse GPR35

Potency of chromen-4-one derivatives

The most potent chromone derivative at the mouse receptor of the previous work was 6-bromo-8-(carboxyformamido)-4-thioxo-4*H*-chromene-2-carboxylic acid (**62**).¹ With a potency of 174 nM the 4-thione derivative was more than 10-fold more potent than the 4-keto derivative **59**.¹ This was the reason why we decided to investigate a library of chromene-4-thione derivatives. Interestingly (and contrary to the rat receptor), these derivatives were consistently more potent at the mouse receptor than their 4-keto equivalents. **86b** (EC_{50} 127 nM) was 4-fold more potent than **60** (EC_{50} 494 nM). Compound **88d** (EC_{50} 169 nM) was almost twice as potent as **26** (EC_{50} 293 nM). Compound **86a** (EC_{50} 249 nM) was almost 7-fold more potent than its unthionated equivalent **115** (ANM296, EC_{50} 1710 nM).¹ An increase in potency could also be demonstrated for the thionation of the weakly active **25** (EC_{50} 2850 nM), which led to the slightly more potent compound **88a** (EC_{50} 1800 nM). For structures see **Figure 3.38**.

previous work:¹



this work:

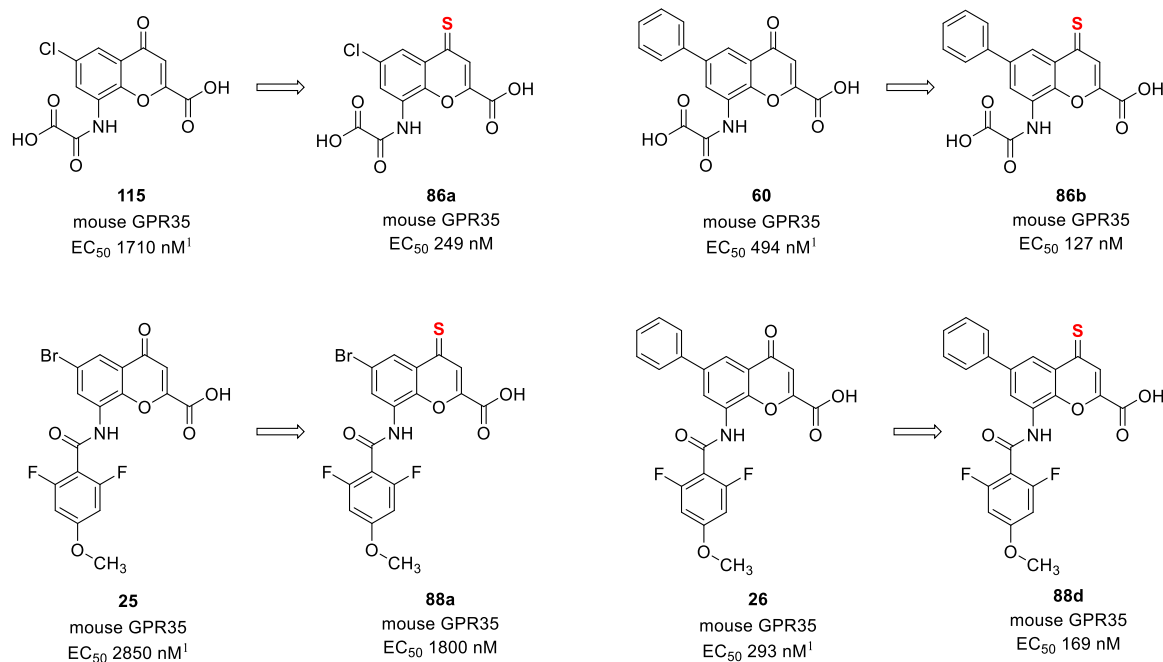


Figure 3.38. Thionation of the 4-position generally increases potency at mouse GPR35. See also previous works.¹

It appears that the mouse GPR35 prefers the larger, more lipophilic thioketone moiety instead of the strong H-bond acceptor oxygen in position 4. However, the pyrroloquinolone **110** (**Figure 3.47**), which lacks a hydrogen bond acceptor in this position, showed lower potency (EC₅₀ 2480 nM) than its phenanthroline-4,10-dione equivalent **68q** (EC₅₀ 1760 nM). This could be due to a slightly different binding mode of the other scaffolds compared to the chromone derivatives. Surprisingly, **87** – the 3-methyl derivative of **59** – showed an 11-fold greater potency than the unmethylated parent compound (**59**: EC₅₀ 1880 nM vs. **87**: EC₅₀ 167 nM).¹ For structures see **Figure 3.39**.

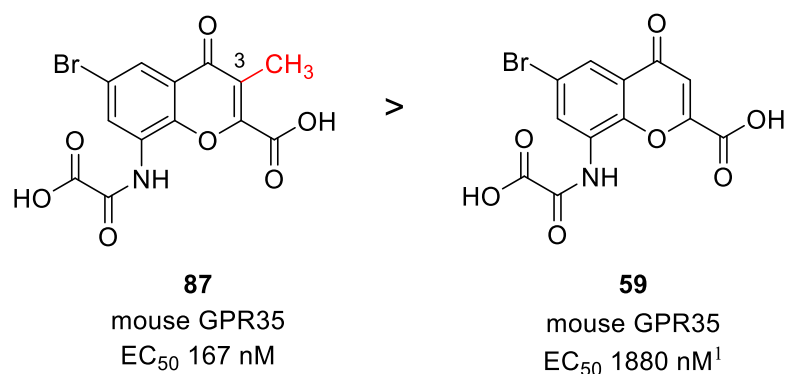


Figure 3.39. Methylation in the 3-position increased mouse GPR35 potency.

Taken together with the greater potency of 4-thione derivatives compared to their 4-keto counterparts, this is indicative of an additional lipophilic interaction of the mouse receptor. Interestingly, this additional interaction appears to be only present in the rodent GPR35 orthologs and is missing at the human receptor, seeing as the 3-position-unmethylated **59** has both greater potency (EC_{50} 11.8 nM) as well as affinity (K_i 13.8 nM) at the human receptor than **87** (EC_{50} 75.0 nM, K_i 51.6 nM).

One of the most important sites to introduce chemical modifications was the 6-position, which has already been noted in previous works.¹ Herein, we could confirm the previous observation that large lipophilic residues in the 6-position of the chromen-4-one or chromen-4-thione core increase mouse receptor potency, with aromatic moieties having the largest effect. The most potent chromen-4-thione derivative of the present study at the mouse GPR35, **86b** (EC_{50} 127 nM), bears a 6-phenyl moiety and was slightly more potent than the respective 6-bromo-substituted **62** (EC_{50} 174 nM), which in turn was more potent than the 6-chloro derivative **86a** (EC_{50} 249 nM). A similar rank order of potency was observed for the larger 8-benzamidochromen-4-thiones, where the 6-phenyl- and 6-*p*-tolyl-substituted **88d** and **88e**, respectively, were markedly more potent than the 6-methyl- or 6-bromo-substituted **88c** and **88a**, respectively (**88d**: EC_{50} 169 nM, **88e**: EC_{50} 171 nM, vs. **88c**: EC_{50} 984 nM, **88a**: EC_{50} 1800 nM). The potencies of variably 6-substituted chromen-4-one derivatives (e.g. **85a**: 6-*p*-tolyl, **61**: 6-butyl, **85b**: 6-*p*-butylphenyl, and **60**: 6-phenyl) were generally low at the mouse receptor (EC_{50} ~400-500 nM, see **Table 3.17** for exact values). However, they still performed better than their counterparts with smaller, less lipophilic residues in the 6-position (e.g. 6-ethyl: **117**, 6-chloro: **115**, and 6-bromo: **59**),¹ which displayed EC_{50} values in the range of 1000-2000 nM. Generally, the side chain in the 8-position was important for species selectivity, but while a second carboxylic acid moiety in addition to the one in the 2-position was highly important for rat receptor activity (see above), the difference between the 8-benzamido and the 8-

carboxyformamido moieties was not as pronounced at the mouse receptor ortholog (**Figure 3.40**). 8-(Carboxyformamido)-4-thioxo-6-phenyl-4*H*-chromene-2-carboxylic acid (**86b**, EC₅₀ 127 nM) was only slightly more potent than its 8-(2,6-difluoro-4-methoxybenzamido)-substituted equivalent **88d** (EC₅₀ 169 nM). In a previous work, the human-GPR35-optimized 8-benzamidochromen-4-one derivative **26** (EC₅₀ 293 nM) actually performed somewhat better than the rodent-optimized equivalent **60** (EC₅₀ 494 nM).¹ This indicates that the role of the 8-substitution is dependent on the 4-position. It is therefore tempting to assume a different binding mode depending on the substitution pattern in these two positions.

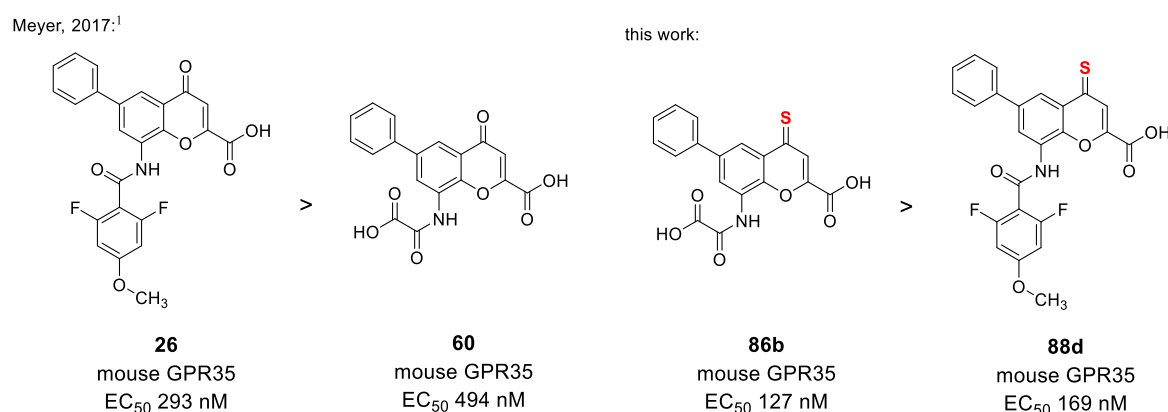


Figure 3.40. Thionation changes the previously observed rank order of potency.¹

Potency of 1,7-phenanthroline derivatives

Considering that the mast-cell stabilizer bufrolin had displayed high potency at both the human and the rat GPR35,² our group attempted to optimize it to increase mouse receptor potency. The 6-methyl derivative **63** was developed by our group and displayed an EC₅₀ value of 105 nM.¹ In our β -arrestin assay system, bufrolin (**30**, EC₅₀ 90.6 nM) was not significantly more potent than **63**. We therefore decided to investigate the 6-position further in the present study by introducing a variety of moieties. Firstly, we investigated the impact of its substitution with hydrogen (**68a**), which resulted in a dramatic reduction in potency (EC₅₀ 996 nM) compared to bufrolin (~11-fold). Next, we explored substitution with various halogen atoms, which had increased potency of chromen-4-one derivatives at the human and rat receptor orthologs in previous studies. The introduction of a fluorine moiety in the 6-position, however, decreased potency >35-fold (**68b**: EC₅₀ 3180 nM) compared to bufrolin (**30**) and shifted half-maximal effective concentrations into the micromolar range. Even compared to the unsubstituted **68a**, the reduction in potency was >3-fold. The introduction of a larger and less electronegative chlorine moiety in the 6-position, on the other hand, was better tolerated than the hydrogen

atom in this position. The 6-chloro derivative **68c** displayed an EC₅₀ value of 427 nM, and was thus more potent than the unsubstituted **68a** and the 6-fluoro derivative **68b**, but it was still almost 5-fold less potent than the lead structure **30** at this receptor ortholog. Even the larger 6-bromo-substituted **68d**, which had comparable potency to bufrolin at the human and rat receptor orthologs (see above), only showed an EC₅₀ value of 268 nM at the mouse GPR35 (see **Figure 3.41**).

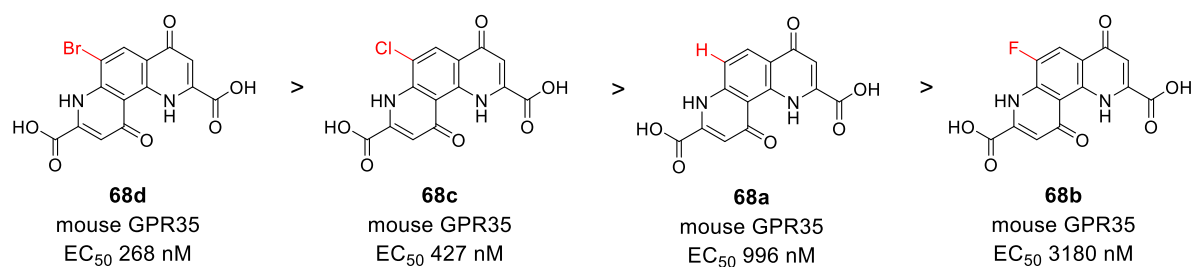


Figure 3.41. Impact of halogen substitution on mouse receptor potency.

Other more polar functional groups, such as 6-methoxy or 6-nitro were not tolerated by the mouse receptor either. The 6-methoxy derivative **68q** (EC₅₀ 1760 nM) was even less potent than the unsubstituted **68a** (EC₅₀ 996 nM). The 6-nitro derivative **68e** was not significantly more potent than **68a** with an EC₅₀ value of 706 nM, which supported the theory that larger, more lipophilic residues were needed to form additional interactions with the receptor at that position.

Keeping in mind that the 6-phenyl- and 6-*p*-tolyl-substituted chromone derivatives **88d** and **88e** had displayed some activity at the mouse GPR35, we wanted to explore the effects of aromatic residues in the 6-position of the phenanthroline scaffold. We first introduced a phenyl ring. The resulting **68v** (EC₅₀ 121 nM) was significantly more potent than the unsubstituted **68a** and even more than twice as potent as the 6-bromo derivative **68d**, which is indicative of an additional interaction with the mouse receptor. Moreover, **68v** was equally potent as the previous study's 6-methyl derivative **63** (EC₅₀ 105 nM)¹ and MacKenzie's bufrolin (**30**: EC₅₀ 90.6 nM). The 6-*p*-tolyl derivative **68w** was even slightly more potent with an EC₅₀ value of 74.8 nM. The elongation of the *p*-alkyl chain led to the development of an even more potent derivative at the mouse receptor (**68y**: EC₅₀ 60.2 nM). Making the aliphatic chain bulkier by changing it to *tert*-butyl was not tolerated, however, the resulting **68x** (EC₅₀ 268 nM) being more than 4-fold less potent than its linear counterpart **68y**. Studying the effect of aromatic residues at the 6-position, we also exchanged the phenyl moiety for the bioisosteric thiophen-2-yl residue. Interestingly, **68u** was about twice as potent (EC₅₀ 51.7 nM) as the lead compounds bufrolin (**30**) and **63**, as

well as the 6-phenyl derivative **68v**. Evidently, the mouse receptor tolerated some aromatic residues – especially in the presence of an unbranched aliphatic chain – but the maximally reached potency was not dramatically higher than that of our lead compounds. The observed rank order of potency for aromatic residues at the 6-position was thiophen-2-yl > *p*-butylphenyl > *p*-tolyl > phenyl > *p*-*tert*-butylphenyl at the mouse receptor (see **Figure 3.42**).

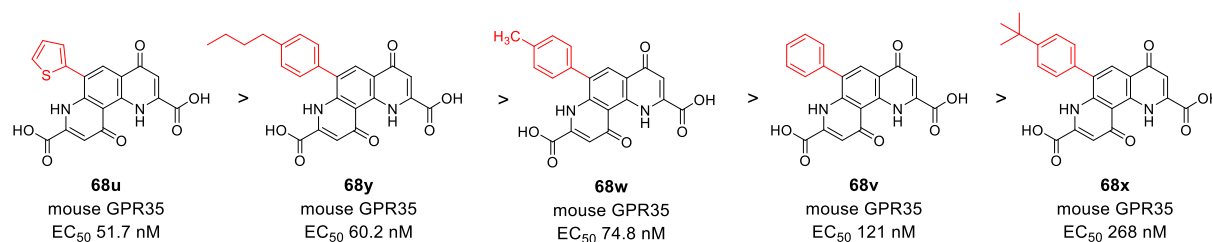


Figure 3.42. Rank order of potency of 6-aryl-substituted 1,7-phenanthroline derivatives.

Since neither the introduction of halogen substituents nor aromatic residues led to a substantial increase in potency at the mouse receptor, we decided to optimize the carbon chain of the lead structure bufrolin (**30**). First, we investigated whether the receptor prefers branched or linear alkyl chains. Similar to the human and rat receptors, the mouse GPR35 did not tolerate the bulky *tert*-butyl residue in position 6: **68s** showed an EC₅₀ value of 381 nM, which is 3.5-fold lower than the *n*-butyl-containing lead compound bufrolin. However, its potency was still in the range of the 6-chloro and 6-bromo derivatives (EC₅₀ 427 nM and 268 nM, respectively). The 6-*sec*-butyl derivative **68r** (EC₅₀ 135 nM) was significantly more potent than the *t*-butyl-substituted compound, but slightly less potent than the unbranched lead compound. Considering that similar observations had been made for the human and rat receptors, we concluded that GPR35 generally prefers unbranched alkyl chains to branched ones in this position (see **Figure 3.43**).

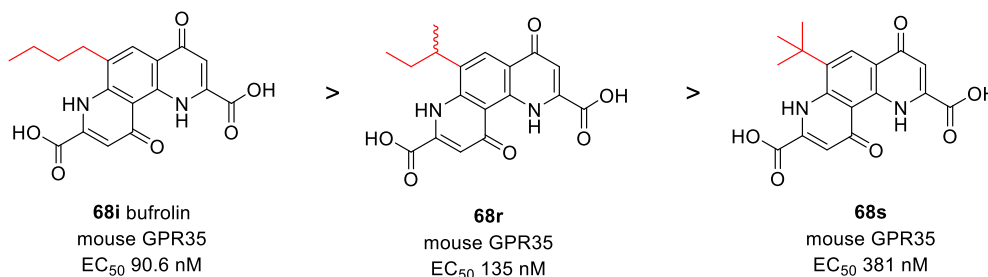


Figure 3.43. Linear alkyl chains in the 6-position led to higher potency than branched ones.

Next, we investigated the alkyl chain length. Starting from our previous study's 6-methyl derivative **63** (EC_{50} 105 nM),¹ we systematically elongated the alkyl chain. Although the initial step to the 6-ethyl compound **68g** (EC_{50} 322 nM) led to a 3-fold reduced potency, the addition of a carbon atom to 6-propyl (**68h**: EC_{50} 31.6 nM) increased potency significantly (see **Figure 3.44**). The 6-pentyl and hexyl derivatives showed EC_{50} values in the same range as **68h** (EC_{50} 34.1 nM and 33.8 nM, respectively). Cyclization of the hexyl chain provided the 6-cyclohexyl derivative **68t** (EC_{50} 37.0 nM) with equally high potency as the uncyclized counterpart. However, further elongation gradually increased potency again in the following rank order of potency: heptyl (**68l**: EC_{50} 20.5 nM) < octyl (**68m**: EC_{50} 14.3 nM) < nonyl (**68n**: EC_{50} 11.7 nM) < decyl (**68o**: EC_{50} 8.18 nM) < dodecyl (**68p**: EC_{50} 6.12 nM). Compounds **68o** and **68p** represent the most potent compounds of the present series and the first compounds ever described with single-digit nanomolar potency at the mouse receptor ortholog.

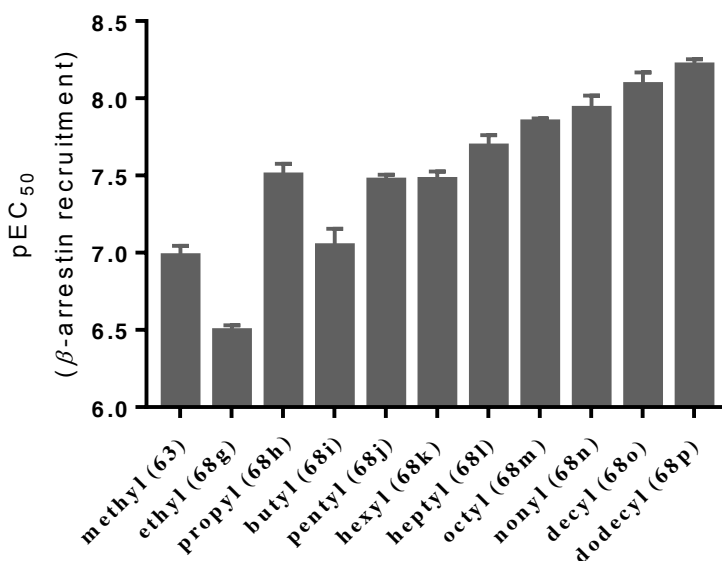


Figure 3.44. Potency of 6-alkyl-substituted 1,7-phenanthroline derivatives at mouse GPR35.

We also examined other positions of the phenanthroline scaffold apart from the 6-position. Firstly, we introduced a methyl group at the 5-position, which led to the 5,6-dimethylated **68z** (EC_{50} 61.5 nM). Interestingly, this compound was almost twice as potent as the 6-monomethylated **63** at the mouse GPR35 (see **Figure 3.45**). This indicates that the 5-position offers another promising location for future modifications.

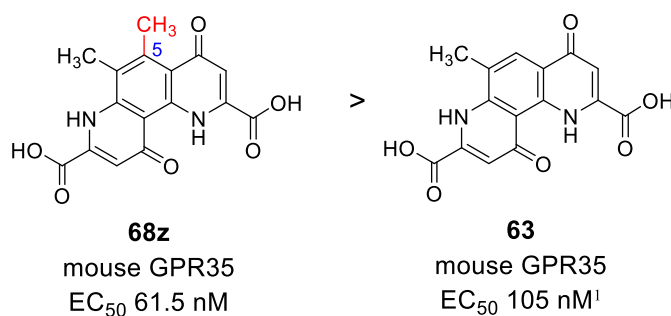


Figure 3.45. Methylation of the 5-position increased mouse receptor potency.

The impact of methylation of the free carboxylic acid moieties has already been discussed above for the human and rat GPR35. Similar results were observed at the mouse receptor ortholog (see **Figure 3.46**). Esterification generally decreased the compounds' potency dramatically also at this receptor and the measured activity could be due to hydrolysis mediated by esterases. The 2,8-diesterified 6-pentyl derivative **67j** displayed a >17-fold reduced potency (EC₅₀ 588 nM) compared to the free acid **68j** (EC₅₀ 34.1 nM). Similarly, the diesterified 6-octyl compound **67m** showed a 44-fold decreased potency compared to the free acid **68m** (EC₅₀ 14.3 nM). For the 6-*sec*-butyl derivatives, the reduction was less pronounced with a mere 6-fold decreased potency for the diesterified **67r** (EC₅₀ 849 nM). The 2,8-dimethylated 6-bromo derivative **67d** (EC₅₀ 3880 nM) was >14-fold less potent than the unprotected **68d** (EC₅₀ 268 nM). The 2,6-diol derivative **111** was inactive.

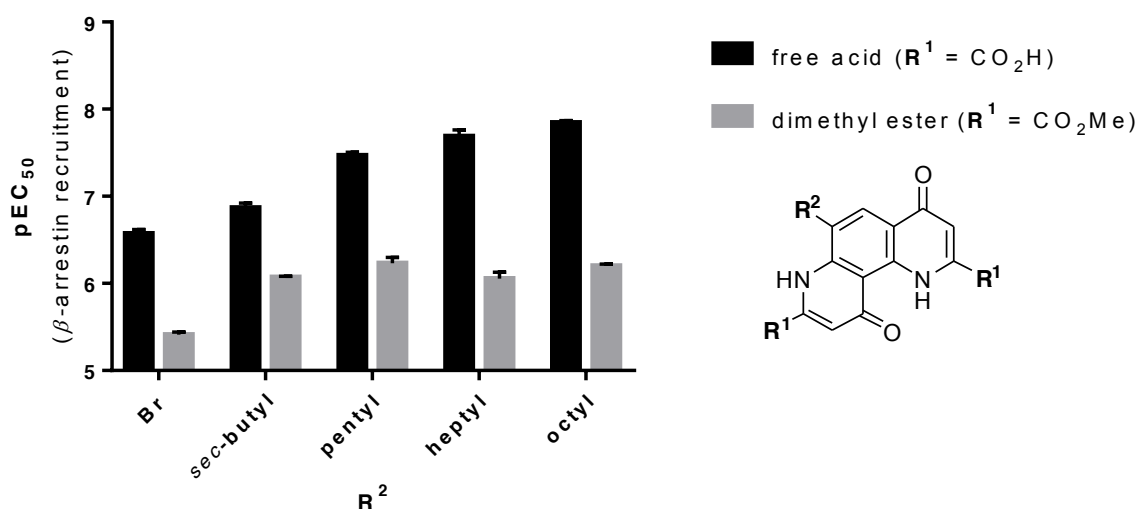


Figure 3.46. Esterification of carboxylic acid moieties resulted in decreased potency.

Potency of further scaffolds

In addition to chromones and phenanthrolines, we investigated other scaffolds for their activity at the mouse GPR35. While these scaffolds provided powerful tool compounds for the human receptor ortholog they were generally much less potent at the mouse receptor ortholog (see **Figure 3.47**). The pyrido[3,2-*g*]quinolone **105**, which had shown high potency at the human GPR35 (EC_{50} 11.4 nM), only displayed moderate activity at the mouse receptor ortholog (EC_{50} 518 nM). The pyrrolo[2,3-*f*]quinolone derivative **110**, which had displayed an EC_{50} value of 4.48 nM at the human receptor, only showed weak, micromolar potency at the mouse receptor (EC_{50} 2480 nM). Quinoline derivatives, such as **99** (EC_{50} 2750 nM) and **96b** (EC_{50} 4490 nM) exhibited similarly low activity at the mouse GPR35. The quinoline derivative **96a** was entirely inactive. It would be tempting to speculate that the lack of a second carboxylic acid moiety is responsible for the low activity of these quinolone derivatives, however, compound **102**, which possesses two carboxylic acid moieties (see **Figure 3.47**) and which was about as active as its phenanthroline counterpart **68c** at the human receptor, displays equally low activity at the mouse receptor (EC_{50} 2930 nM). We suspect a different binding mode for quinolone derivatives at rodent receptors, but a larger number of such derivatives accompanied by computational studies – ideally supported by crystallography – would be necessary to elucidate the exact manner of binding. The indole derivative **108** showed surprisingly low activity at the mouse GPR35 with an EC_{50} value of 5840 nM, considering its high activity at the human receptor ortholog.

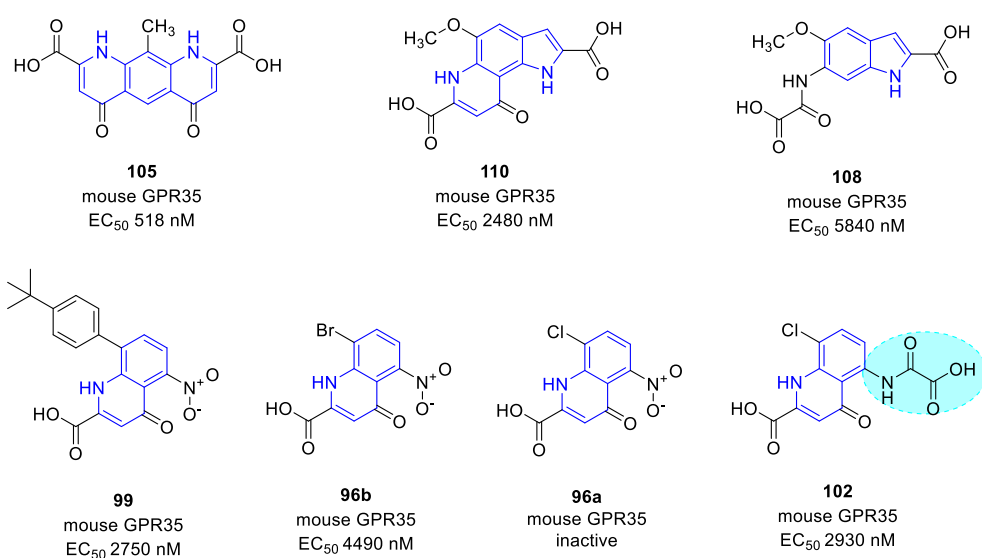


Figure 3.47. Quinolone and indole derivatives generally displayed weak potency at the mouse GPR35.

Summary: Mouse GPR35

The development of potent GPR35 agonists for the mouse receptor ortholog was more challenging than for the rat and especially the human receptor orthologs. While the human GPR35 tolerated practically all examined scaffolds and a wide range of highly diverse residues in the 6-position of chromone and phenanthroline derivatives (see above), the mouse receptor ortholog was very particular about accepted agonists. Although the 1,7-phenanthroline scaffold was its most favored ligand class, it was potently activated only by relatively few representatives of it. EC_{50} values below 50 nM were reached exclusively by derivatives with a linear alkyl chain in the 6-position. Other residues, such as aryls, halogens, a nitro or methoxy group led to derivatives with considerably lower potency. Methyl substitution in the 5-position was tolerated well, while the elimination of the 4-keto moiety or the esterification of the carboxylic acid groups was not. A summary of SARs of phenanthroline derivatives at the mouse receptor is provided in **Figure 3.48**.

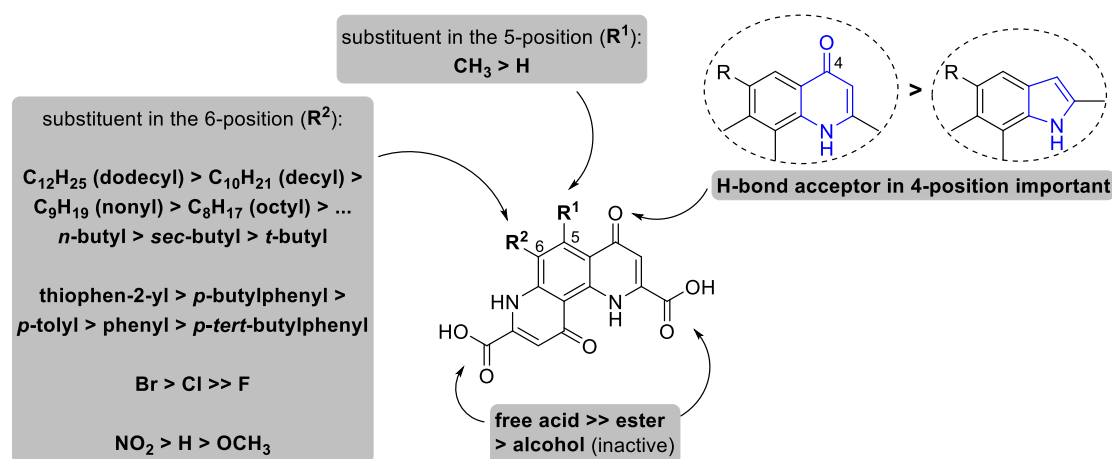


Figure 3.48. Structure-activity relationships of 1,7-phenanthroline derivatives with different substituents determined for mouse GPR35.

Derivatives with a chromenone scaffold were generally weaker than phenanthrolines at the mouse GPR35, however, their activity could be significantly enhanced by thionation of the 4-keto moiety. The total removal of an interaction partner in that position abolished agonist activity, whereas methylation of the 3-position was tolerated well. Large residues in the 6-position, such as phenyl, were generally preferred by the receptor. If the substituent in the 6-position was bulky enough (e.g. phenyl or *p*-tolyl), a benzamide in the 8-position was tolerated to some extent. Smaller residues in the 6-position required the presence of a second carboxylic acid group in the 8-position for potent receptor activation. The 8-benzamide had previously

been optimized for the human GPR35 ortholog,⁹² however, it appears that the mouse receptor also preferred a 2,6-difluoro-4-methoxybenzamide to a 3,5-difluoro-substituted ring (see above). A summary of important SARs of chromenone derivatives of this work is provided in **Figure 3.49**.

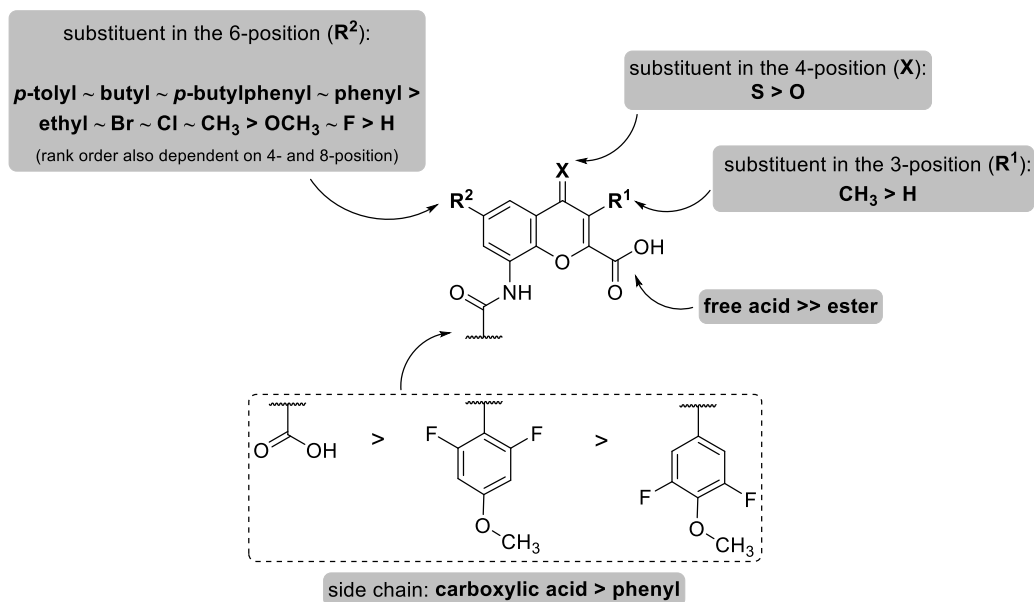


Figure 3.49. Structure-activity relationships of chromen-4-one derivatives with different substituents determined for mouse GPR35; contains considerations from previous works.¹

3.4.3.4 GPR35 ortholog selectivity

In line with previous studies, most compounds of the present study display profound ortholog selectivity. The discrepancy in potency is particularly noticeable at the mouse receptor ortholog, where only few derivatives of any scaffold reach high potency. The most equipotent compounds at the human, rat, and mouse GPR35 orthologs of this study were **68p** and **68o**, which both belong to the 1,7-phenanthroline class of ligands (**Figure 3.50**). The most equipotent chromone derivative **86b** was considerably less active at rodent GPR35 orthologs.

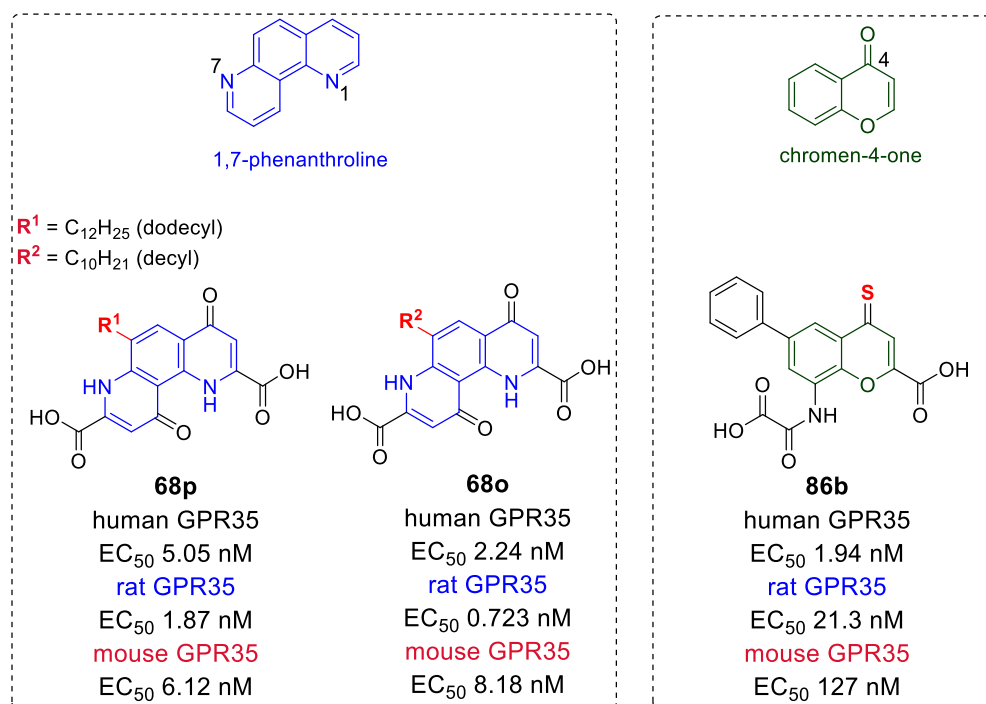


Figure 3.50. Most equipotent GPR35 agonists of this study.

Upon comparing the EC_{50} values of 1,7-phenanthroline derivatives, it is evident that the human receptor ortholog is highly tolerant of a large variety of substituents in the 6-position of the scaffold. The heat map in **Figure 3.51** illustrates that the majority of derivatives displayed EC_{50} values in the low nanomolar range at the human receptor (depicted in blue and purple). Only very few compounds showed EC_{50} values above 100 nM (green or yellow). The functional group tolerance at the rat receptor appears equally high, however, derivatives with long alkyl chains in the 6-position displayed extremely high potency with EC_{50} values in the subnanomolar range (magenta). At the mouse GPR35, the majority of derivatives showed relatively high EC_{50} values, which accounts for more green and yellow color in **Figure 3.51**. Only **68p** and **68o** reached single-digit nanomolar potency. Additionally, some compounds exhibited extremely low potency (depicted in red or orange).

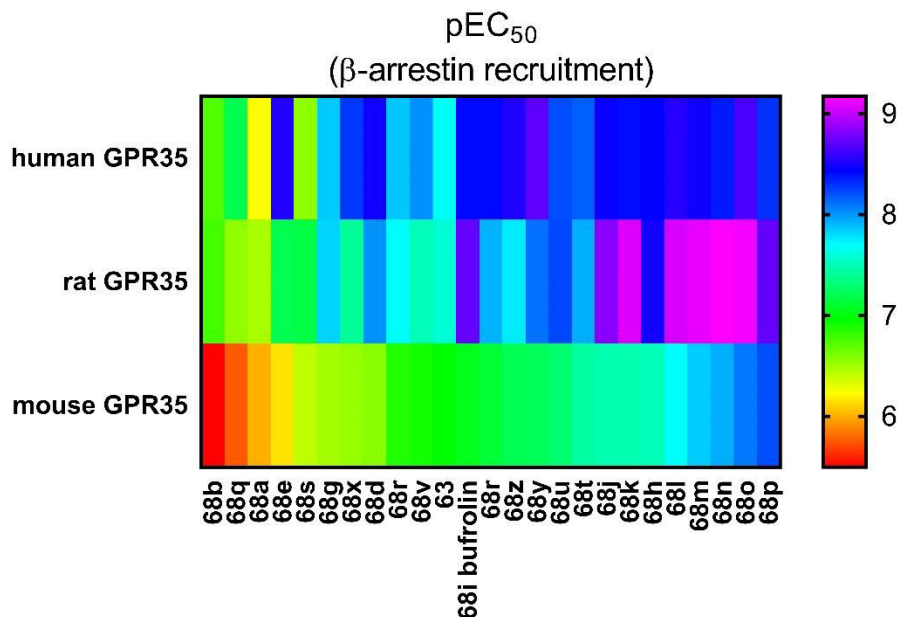


Figure 3.51. Heat map comparing potency (pEC₅₀) of 1,7-phenanthroline derivatives at the human, rat, and mouse GPR35.

In conclusion, it was possible to boost the potency of the lead compound bufrolin for all three investigated orthologs of GPR35. By elongating the alkyl chain in the scaffold's 6-position, potency gradually increased for all receptors until reaching a saturation state (**Figure 3.52**). Thus, we obtained the compounds with the highest potency at the human, rat, and mouse GPR35 known to date.

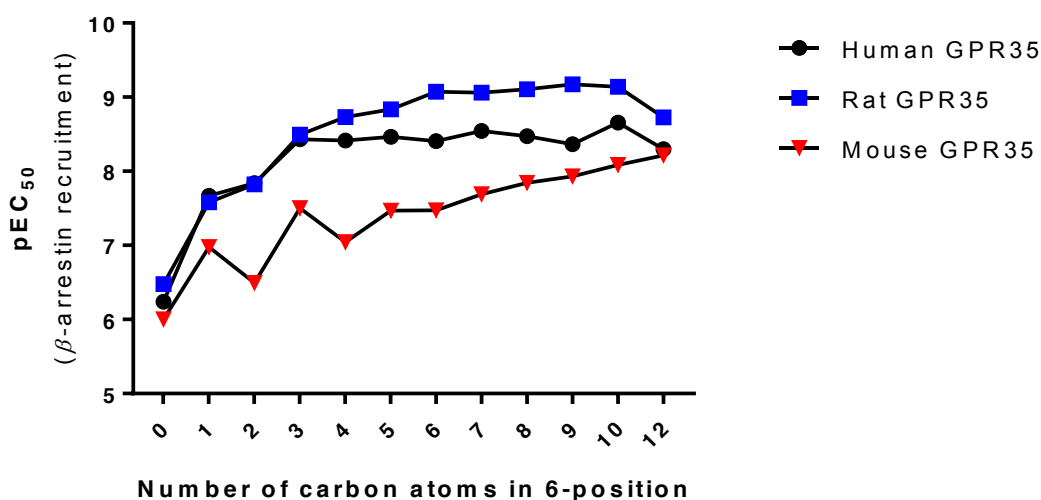


Figure 3.52. Potency of 6-alkyl-substituted 1,7-phenanthroline derivatives in relation to chain length.

3.5 Pharmacological evaluation at GPR84

3.5.1 Introduction

In previous studies, our group investigated the pharmacology of a variety of chromen-4-one derivatives at the human GPR84.^{1,186} In an effort to develop potent GPR84 antagonists, a large library of chromen-4-one derivatives had been synthesized and characterized in different assay systems.¹ The most potent derivatives of the previous study are depicted in **Figure 3.53**.

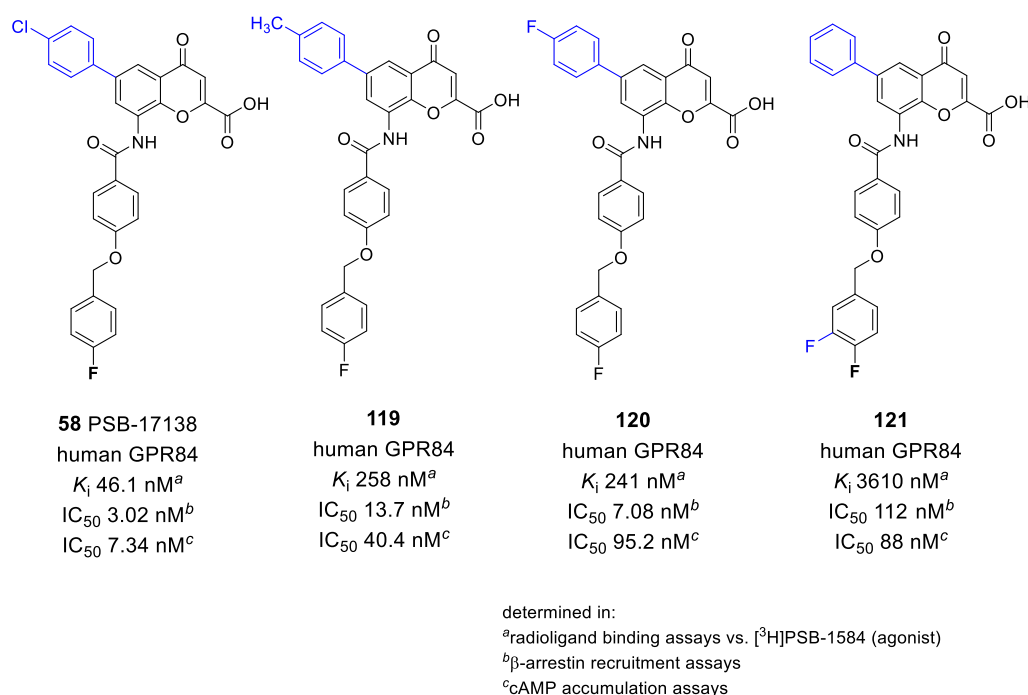
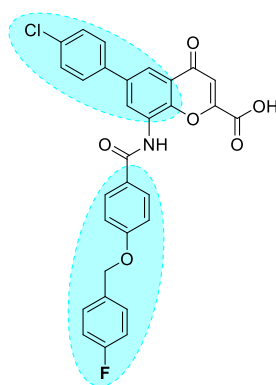


Figure 3.53. Most potent GPR84 antagonists described by Meyer (2017).¹

The most potent derivative of the previous work was PSB-17138 (**58**), which showed an inhibition constant (K_i) of 46.1 nM in radioligand binding experiments versus the radioligand [³H]PSB-1584.⁴⁹ The compound also displayed high potency in β-arrestin recruitment assays (IC₅₀ 3.02 nM) and cyclic adenosine monophosphate (cAMP) accumulation assays (IC₅₀ 7.34 nM).¹ Despite its excellent potency and affinity at GPR84, and an advantageous selectivity profile against related (orphan) GPCRs, PSB-17138 is a highly nonpolar compound with unfavorable physicochemical properties (see **Figure 3.54**).

**58** PSB-17138

MW: 543,9 g/mol

log D: 2.83 (pH 7.4)

log P: 5.08

HBD: 2

HBA: 7

tPSA: 101.9 Å²

Figure 3.54. PSB-17138 contains highly lipophilic structural elements (highlighted) and displays poor physicochemical properties.* HBA, hydrogen-bond acceptor; HBD, hydrogen-bond donor; log D, distribution coefficient; log P, partition coefficient; MW, molecular weight; tPSA, topological polar surface area.

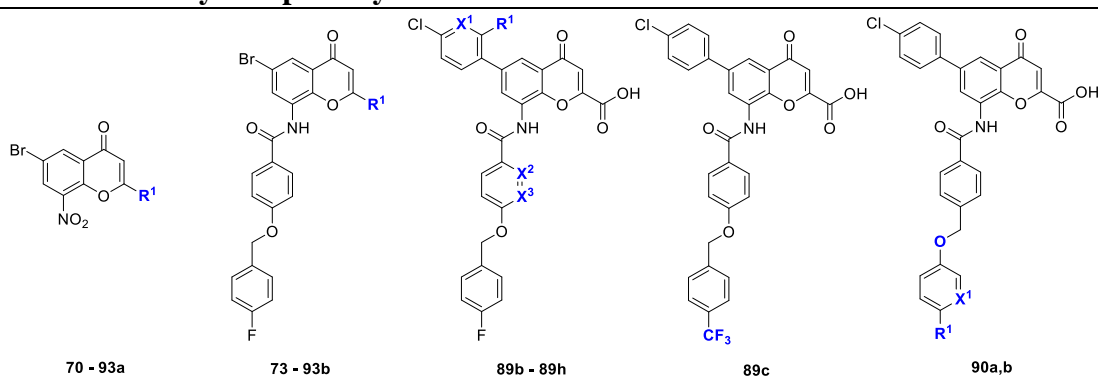
The aim of this study was to improve the physicochemical properties of the lead compound PSB-17138 by introducing polar residues to the scaffold. However, a substantial decrease in antagonist potency or affinity would not be acceptable. Therefore, synthetic modifications were carefully evaluated in radioligand binding assays versus [³H]PSB-1584 in membrane preparations of Chinese hamster ovary (CHO) cells recombinantly expressing human GPR84.⁴⁹ Additionally, a selection of promising compounds was evaluated in cAMP assays using CHO-human-GPR84 cells and PSB-17365 as agonist.¹⁶² In short, cells are incubated with forskolin, a stimulator of adenylate cyclase, which increases cytosolic cAMP concentrations. The addition of agonist causes the Gα_{i/o}-coupled GPR84 to inhibit the production of cAMP. Subsequent addition of antagonist blocks this inhibition and increases cAMP concentrations again, which can be measured radiometrically. The determined cAMP concentration is proportional to antagonist potency at a given antagonist concentration. Measurements at various antagonist concentrations allows for the calculation of half-maximal inhibitory concentration (IC₅₀) values, which can be used to compare individual compounds.

* Calculated by PerkinElmer's ChemDraw Professional (V: 17.0.0.206) and MarvinSketch 6.2.0

3.5.2 Results

The K_i and IC_{50} values for affinity and potency of individual compounds determined at the human GPR84 are provided in **Table 3.20**. The assays were performed by Katharina Sylvester as described previously.¹

Table 3.20. Affinity and potency of chromen-4-ones at human GPR84



compd	substitution pattern				radioligand binding assays ^a		cAMP assays ^b
	R ¹	X ¹	X ²	X ³	$K_i \pm SEM^c$ (nM)	(% inhibition \pm SEM)	$IC_{50} \pm SEM^c$ (nM)
70	CO ₂ H	-	-	-	1760 \pm 1360	(30 \pm 5)	126000 \pm 6520
92a	CN	-	-	-	44200 \pm 8170		n.d.
93a	tetrazol-5-yl	-	-	-	87100 \pm 14900		n.d.
73	CO ₂ Et	-	-	-	(-30 \pm 4)		n.d.
89a^d	CO ₂ H	-	-	-	2640 \pm 307		3890 \pm 2400
91b	CONH	-	-	-	(-20 \pm 7)		n.d.
92b	CN	-	-	-	78400 \pm 28700		n.d.
93b	tetrazol-5-yl	-	-	-	16300 \pm 2270		66000 \pm 14100
89b^d (58) PSB-17138	H	-	-	-	46.1 \pm 12.9		2050 \pm 1090
89d	Cl	-	-	-	137 \pm 21		n.d.
89e	H	N	-	-	31.3 \pm 6.2		285 \pm 117
89f	H	-	N	-	4.47 \pm 0.57		622 \pm 159
89g	H	-	-	N	1820 \pm 492		n.d.
89h	H	N	N	-	4.68 \pm 1.93		175 \pm 37
89c	<i>see above for structure</i>				275 \pm 45		n.d.
90a	F	N	-	-	84.9 \pm 10.9		n.d.
90b	OH	-	-	-	2418 \pm 702		n.d.

^aAffinities were determined in competition binding experiments using 5 nM [³H]PSB-1584 and membrane preparations of CHO cells recombinantly expressing human GPR84 (% inhibition at 10 μ M). ^bPotencies in cAMP accumulation assays were determined using CHO- β -arrestin-GPR84 cells (% inhibition of PSB-17365 (30 nM) response at 10 μ M). ^cConcentration-inhibition curves were performed in 3 independent experiments. ^dCompounds have previously been reported, but were synthesized and characterized again for comparison.^{1,186} n.d., not determined.

3.5.3 Structure-activity relationships

Important considerations regarding the structure-activity relationships of 8-benzamidochromen-4-one derivatives have been reported by Meyer in the previous study.¹ The work explored the significance of several positions of the chromone core scaffold, including the 4-, 6-, and 8-position. At the 4-position, the keto moiety was superior to a 4-thioketone. At the 6-position, a *p*-chlorophenyl residue was superior to other phenyl rings with variously substituted para-positions, including *p*-tolyl, *p*-fluorophenyl, and *p*-methoxyphenyl. And at the 8-position, *p,p*-fluorobenzoyloxybenzamide was the best substituent (see **Figure 3.55**).¹

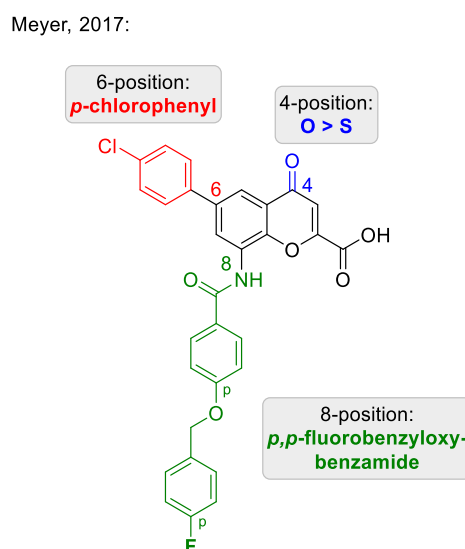


Figure 3.55. Previously optimized residues in the 4-, 6-, and 8-positions of the scaffold.¹

In this study, special focus lay on the carboxylic acid moiety in the 2-position, which had not been investigated previously. The esterification of the carboxyl group was not tolerated by the receptor. The ethyl ester derivative **73** showed no affinity for GPR84, while its free acid counterpart **89a** displayed a K_i value of 2640 nM. The primary amide derivative **91b** was also not accepted by the receptor. However, the 2-nitrile derivative **92b** displayed very weak affinity for GPR84 (K_i 78400 nM). A negative charge at this position seemed to be necessary for affinity, since the tetrazolyl derivative **93b** displayed a K_i value of 16300 nM. Considering that the free carboxyl derivative **89a** showed more than 6-fold increased affinity, it is still the best substituent for the 2-position (see **Figure 3.56**). The carboxylic acid was also superior to a

tetrazole moiety in functional assays. **89a** showed an IC_{50} value of 3890 nM, whereas the potency of **93b** was ~17-fold weaker (IC_{50} 66000 nM).

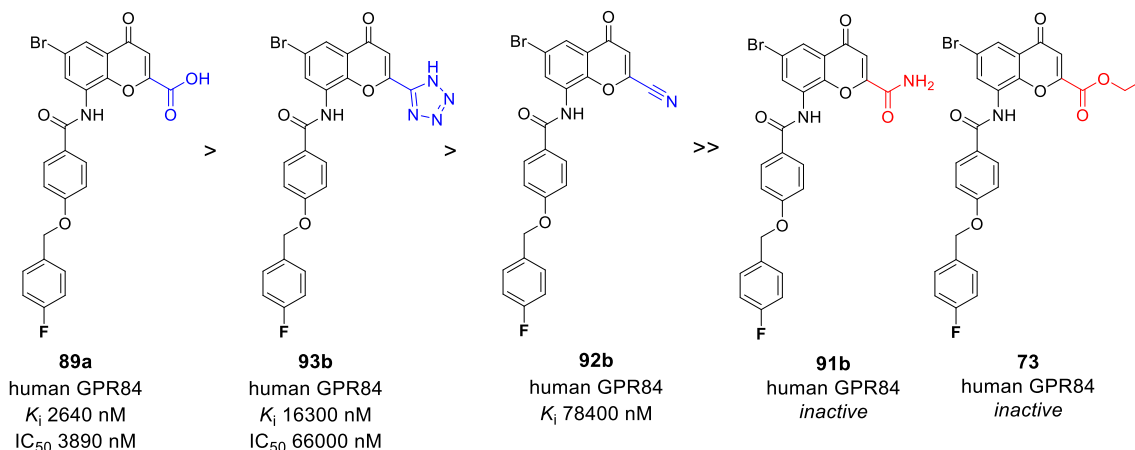


Figure 3.56. A carboxylic acid moiety in the 2-position was superior to other investigated substituents.

A similar observation was made for the smaller chromone derivatives **70**, **92a**, and **93a**. Contrary to the aforementioned larger derivatives, all of the evaluated small chromones showed affinity for GPR84. With a K_i value of 1760 nM the carboxylic acid derivative **70** was 25-fold more potent than the 2-nitrile **92a** (K_i 44200 nM) and ~50-fold more potent than the tetrazole derivative **93a** (K_i 87100 nM). See **Figure 3.57**.

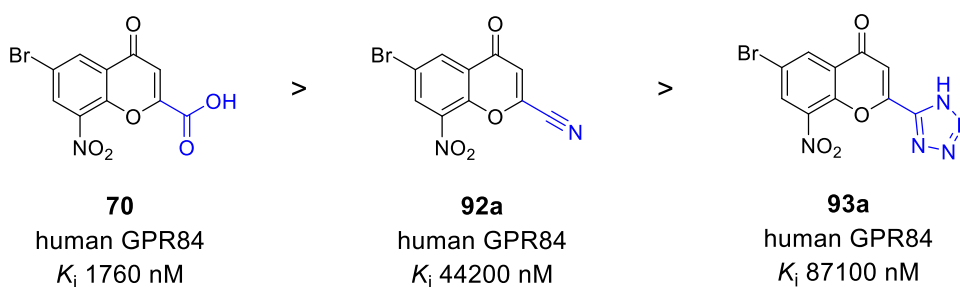


Figure 3.57. A carboxylic acid moiety was the best substituent in the 2-position of 8-nitro derivatives.

When we investigated the substituent in the 6-position of the chromen-4-one core, we obtained mixed results. The introduction of a second chlorine atom to the *p*-chlorophenyl resulted in the 2,4-dichlorophenyl derivative **89d**, which displayed a K_i value of 137 nM. Thus, it was ~3-fold weaker than the lead **89b** (K_i 46.1 nM). However, when we introduced a nitrogen atom at the 3'-position, the ensuing compound displayed comparable affinity to the lead structure. Compound **89e** showed a K_i value of 31.3 nM (see **Figure 3.58**). Additionally, the potency of **89e** in cAMP accumulation assays (IC_{50} 285 nM) was ~7-fold higher than that of the lead compound (**89b**: IC_{50} 2050 nM).

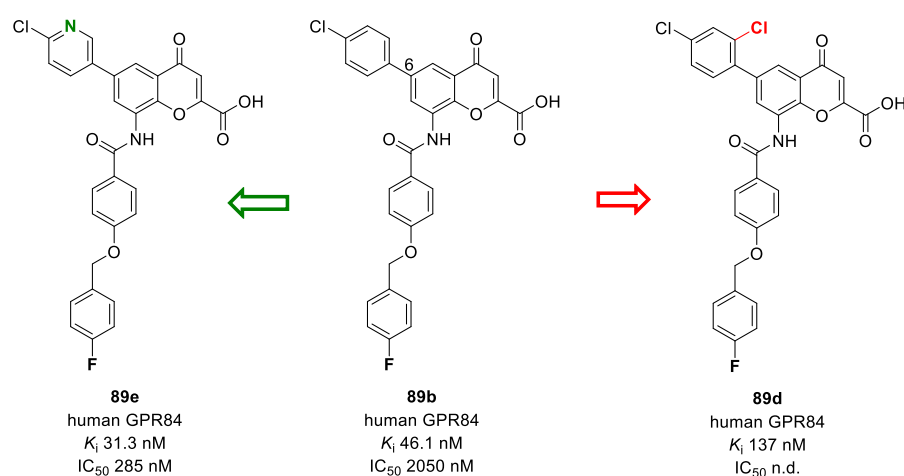


Figure 3.58. Potency and affinity increased with the introduction of a chloropyridine in the 6-position.

A trifluoromethyl residue instead of a fluorine moiety in the *p*-position of the side chain did not increase affinity. The resulting **89c** displayed a K_i value of 275 nM and was therefore ~6-fold weaker than the lead structure **89b**. A hydroxy group in this position was absolutely not tolerated by the receptor, indicated by the fact that **90b** showed affinity in the micromolar range (K_i 2418 nM). However, a nitrogen atom in the *meta*-position of the ring decreased affinity only slightly (**90a**: K_i 84.9 nM) compared to the lead structure **89b** (K_i 46.1 nM). Thus, the position of the ether oxygen appeared not be particularly critical (see **Figure 3.59**).

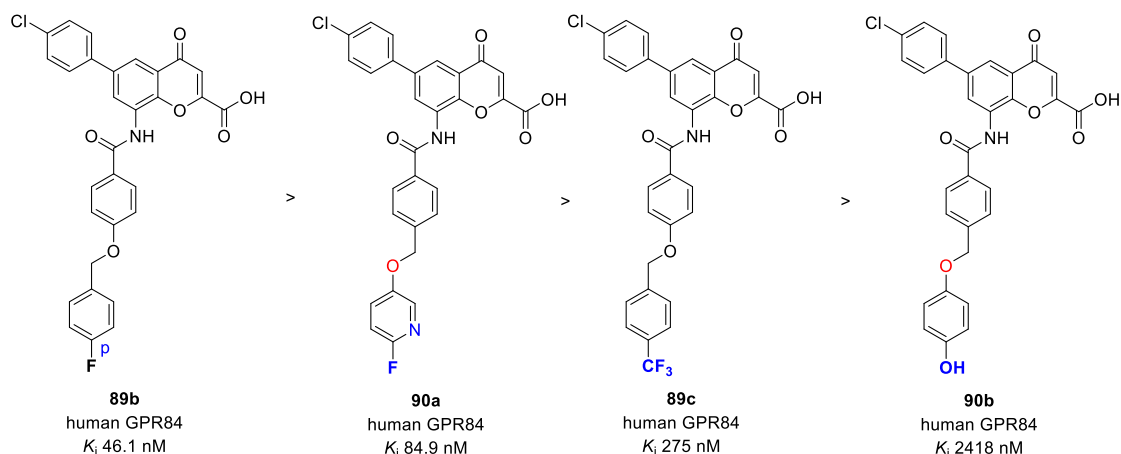


Figure 3.59. Modifications at the benzyl moiety did not improve affinity for GPR84.

The largest impact on affinity was observed when we introduced a nitrogen atom to the benzamide ring in the 8-position of the chromone core (see **Figure 3.60**). The introduction of a picolinamide residue led to a ~10-fold increased affinity (**89f**: K_i 4.47 nM) versus the lead structure **89b**. The picolinamide derivative **89f** was also 3-fold more potent than the lead structure in cAMP assays (**89f**: IC_{50} 622 nM vs. **89b**: IC_{50} 2050 nM). On the other hand, the substitution with nicotinamide as in **89g** decreased affinity dramatically (~40-fold, K_i 1820 nM).

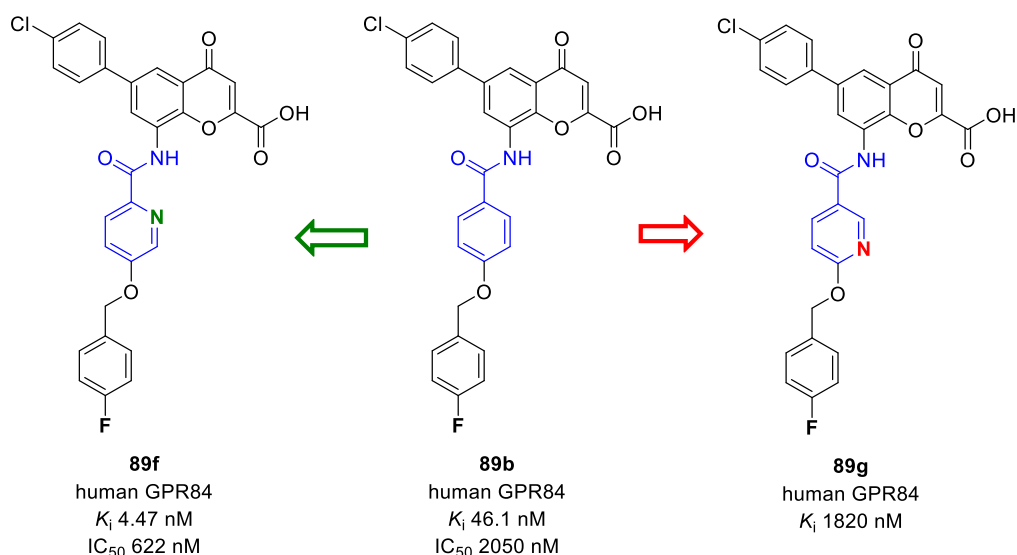


Figure 3.60. A picolinamide moiety in the 8-position was superior to the benzamide.

Finally, we combined the most advantageous alterations we had found so far. Compound **89h** incorporated the 6-chloropyridin-3-yl moiety of **89e** in the 6-position and the picolinamide residue of **89f** in the 8-position. With a K_i value of 4.68 nM, it displayed ~10-fold increased affinity compared to the lead compound **89b** (K_i 46.1 nM). In cAMP accumulation assays, **89h** showed an IC_{50} value of 175 nM. Thus, it was 12-fold more potent than the lead structure **89b** and even slightly more potent than either of its precursors **89e** and **89f** (see **Figure 3.61**).

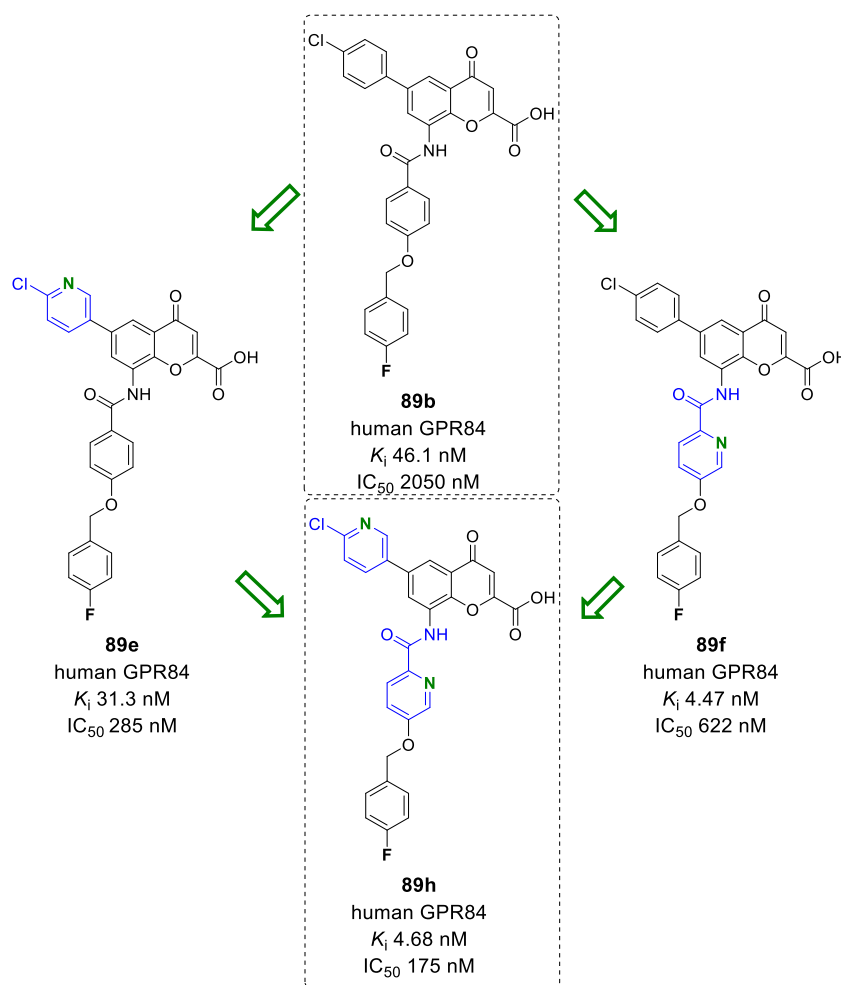


Figure 3.61. Compound **89h** contains structural elements of **89e** and **89f**.

The updated structure-activity relationships for chromen-4-one-based GPR84 antagonists are summarized in **Figure 3.62**.

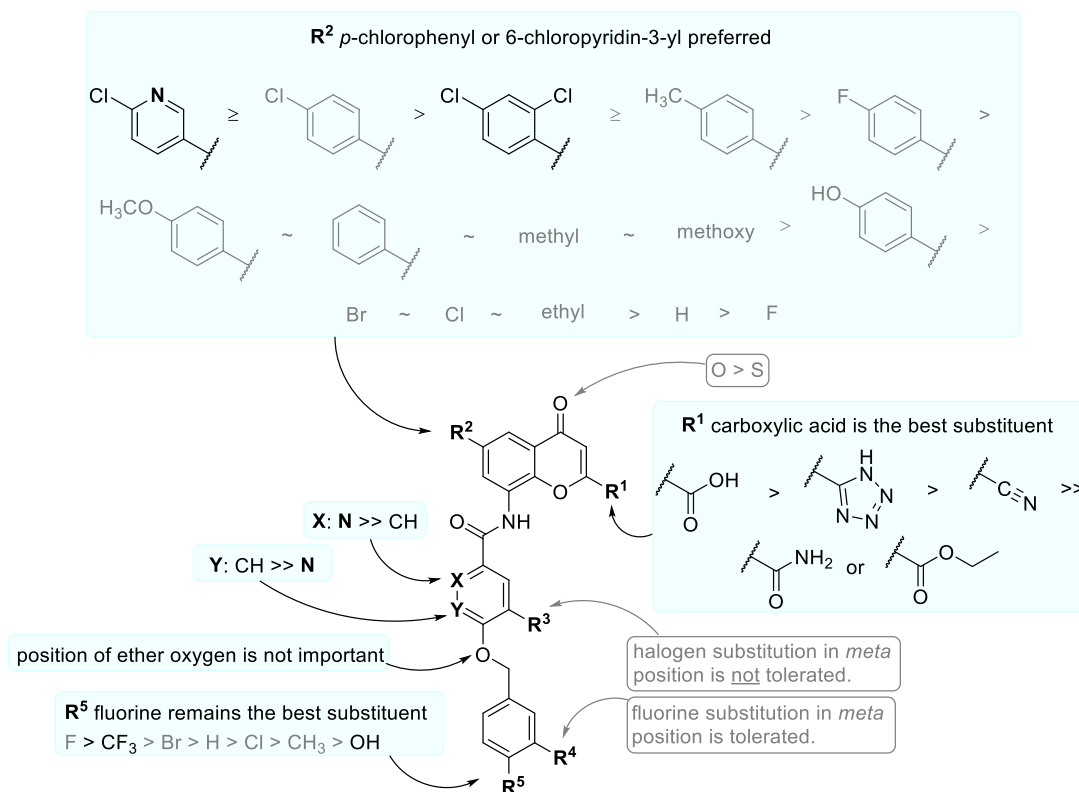


Figure 3.62. Updated structure-activity relationships (SARs) of chromen-4-one derivatives at GPR84. Previously reported SARs in gray.¹

Compound **89h** also outperformed the lead compound PSB-17138 regarding physicochemical properties (see **Figure 3.63**). The molecular weight of **89h** was only insignificantly higher than the lead structure's, however, two additional hydrogen bond acceptors increased its polarity markedly. In contrast to the lead compound, the partition coefficient (logP) of **89h** was well below five, and the distribution coefficient (logD) was significantly reduced (**89h**: logD_{7.5} 1.00), which is indicative of reasonable aqueous solubility.¹⁹⁰ The topological polar surface area (tPSA) of **89h** was increased, however, the threshold of 140 Å² was not exceeded. Therefore, we expect increased solubility and acceptable cell-permeability.¹⁹¹

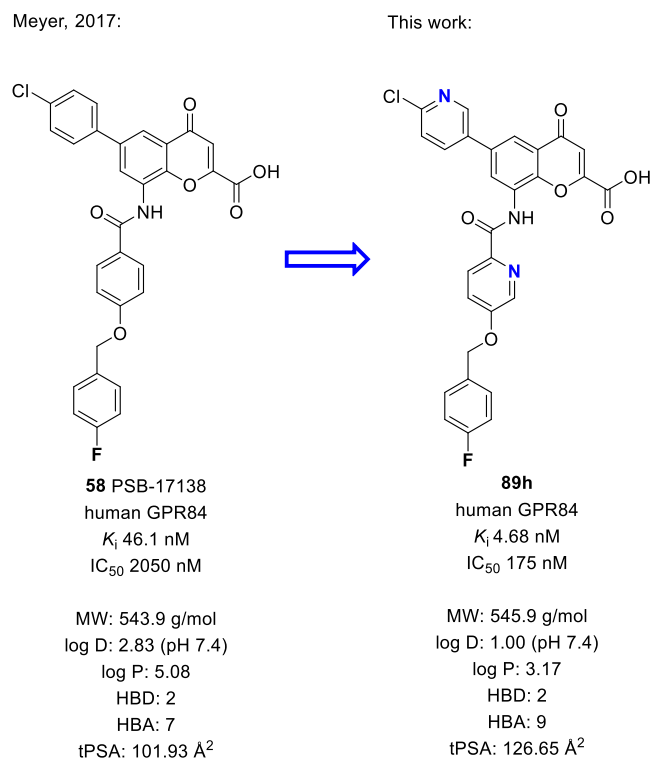


Figure 3.63. Comparison between PSB-17138 and **89h**. HBA, hydrogen bond acceptor; HBD, hydrogen bond donor; log D, distribution coefficient; log P, partition coefficient; MW, molecular weight; tPSA, topological polar surface area.*

In conclusion, we successfully optimized the physicochemical properties of the lead PSB-17138. To this end, we synthesized a variety of derivatives with increased polarity. Carefully monitoring the effects of hydrophilic substituents on potency and affinity, we combined the most beneficial modifications. The resulting **89h** not only showed higher polarity but also displayed superior potency and affinity compared to the lead structure.

* Calculated by PerkinElmer's ChemDraw Professional (V: 17.0.0.206) and MarvinSketch 6.2.0

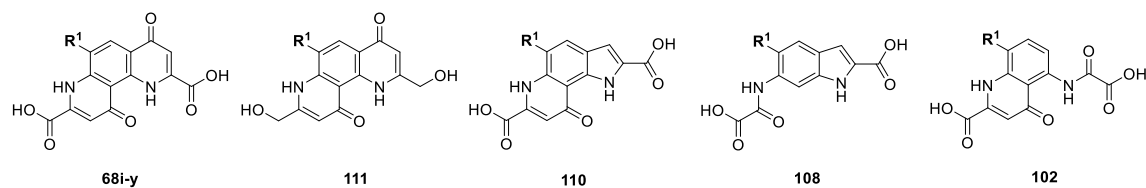
3.6 Selectivity studies

3.6.1 Introduction

A number of GPR35 agonists and GPR84 antagonists discussed herein were evaluated for their potential to activate or block other (orphan) GPCRs than their intended targets. Promising GPR35 agonists were tested at GPR18, GPR55, GPR84, and MAS-related G-protein coupled receptors (MRGPR) X2 and MRGPRX4. The selectivity of GPR84 antagonists versus GPR17, GPR18, GPR55, FFAR1, and FFAR4 has been demonstrated in a previous study.¹ Considering that GPR35 was activated by structurally related chromen-4-one derivatives, new GPR84 antagonists were evaluated at the human, rat, and mouse GPR35 orthologs to demonstrate selectivity.

3.6.2 Selectivity of GPR35 agonists

Firstly, we investigated the selectivity of a variety of GPR35 agonists versus GPR84 (see **Tables 3.21-22**). The compounds' ability to displace the radioligand [³H]PSB-1584 was measured in radioligand binding assays using human GPR84-expressing CHO cells. Assays were performed by Katharina Sylvester. The binding affinity data of 1,7-phenanthroline, quinoline, and indole derivatives at the human GPR84 is summarized in **Table 3.21**.

Table 3.21. Affinity of GPR35 agonists for the human GPR84: 1,7-phenanthroline, indole, and quinoline derivatives

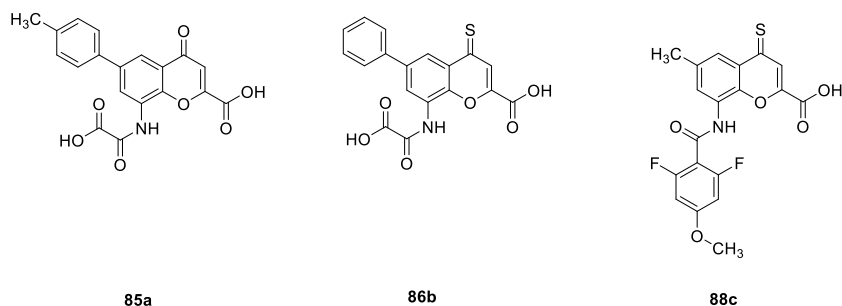
compound	substitution pattern	radioligand binding assays ^a $K_i \pm \text{SEM}^b$ (nM) (% inhibition \pm SEM)
	R ¹	
68i	butyl	>10000 (-5 \pm 12)
68k	hexyl	4990 \pm 1030
68o	decyl	3900 \pm 1550
68y	4-butylphenyl	7050 \pm 1530
111	heptyl	>10000 (10 \pm 2)
110	OCH ₃	>10000 (-16 \pm 10)
108	OCH ₃	>10000 (-1 \pm 10)
102	Cl	>10000 (-4 \pm 22)

^aAffinities were determined in competition binding experiments using 5 nM [³H]PSB-1584 and membrane preparations of CHO cells recombinantly expressing human GPR84 (% inhibition at 10 μ M).

^bConcentration-inhibition curves were performed in 3 independent experiments.

None of the investigated compounds could bind to GPR84 with high affinity. The 6-decyl derivative **68o** displayed the highest affinity for the receptor with a K_i value of 3900 nM. At the human GPR35, the compound showed 4500-fold higher affinity with a K_i value of 0.863 nM vs. the radioligand [³H]PSB-13253. The 6-hexyl derivative **68k** displayed similarly low affinity for GPR84 (K_i 4990 nM), thus it was also ~4500-fold less active compared to GPR35 (K_i 1.12 nM). The 6-*p*-butylphenyl derivative **68y** was ~4200-fold less active at GPR84 compared to GPR35.

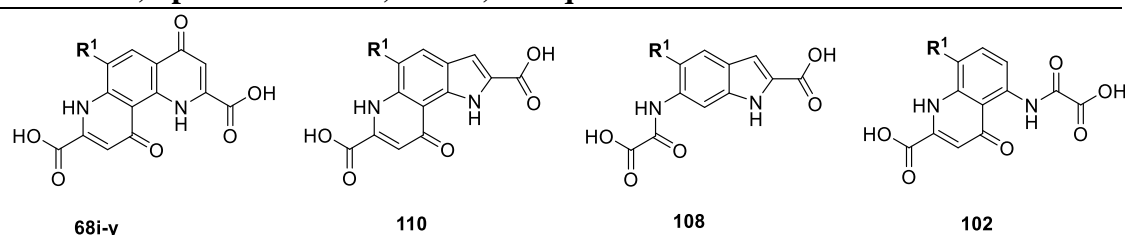
The measured affinity of investigated chromen-4-one-derived GPR35 agonists for GPR84 was even smaller (see **Table 3.22**). The 6-*p*-tolyl derivative **85a**, which had shown extremely high affinity for the human GPR35 (K_i 0.89 nM), was ~91000-fold less active at GPR84 (K_i 81100 nM). The 6-phenyl-substituted chromen-4-thione derivative **86b** displayed 71000-fold less affinity for GPR84 compared to GPR35 (K_i 0.88 nM). And the affinity of **88c** for GPR84 was ~61000-fold reduced (K_i 40500 nM) compared to GPR35 (K_i 0.66 nM).

Table 3.22. Affinity of GPR35 agonists for the human GPR84: chromen-4-one derivatives

compound	radioligand binding assays ^a <i>K</i> _i ± SEM ^b (nM)
85a	81100 ± 6450
86b	62700 ± 3530
88c	40500 ± 13300

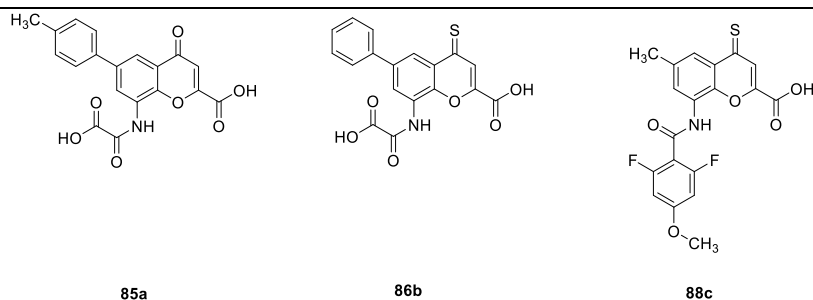
^aAffinities were determined in competition binding experiments using 5 nM [³H]PSB-1584 and membrane preparations of CHO cells recombinantly expressing human GPR84 (% inhibition at 10 μM). ^bConcentration-inhibition curves were performed in 3 independent experiments.

Moreover, a selection of GPR35 agonists with different scaffolds was tested for their activity at the human GPR18 and the human GPR55 (see **Tables 3.23-24**). None of the compounds induced the recruitment of β-arrestin to either receptor, nor could they block the effects of standard agonists when tested for antagonism in high concentrations of 10 μM. The assays were performed by Andhika Mahardhika.

Table 3.23. Activity of GPR35 agonists at the human GPR18 and the human GPR55: 1,7-phenanthroline, indole, and quinoline derivatives

compd	substitution pattern R ¹	human GPR18		human GPR55	
		β -arrestin recruitment assays ^a EC ₅₀ ± SEM ^c (nM) (% effect)	IC ₅₀ ± SEM ^d (nM) (% inhibition)	β -arrestin recruitment assays ^b EC ₅₀ ± SEM ^e (nM) (% effect)	IC ₅₀ ± SEM ^f (nM) (% inhibition)
68i	butyl	>10000 (15)	>10000 (-12)	>10000 (22)	>10000 (3)
68k	hexyl	>10000 (8)	>10000 (24)	>10000 (7)	>10000 (4)
68o	decyl	>10000 (13)	>10000 (13)	>10000 (10)	>10000 (0)
68y	4-butylphenyl	>10000 (7)	>10000 (8)	>10000 (4)	>10000 (0)
110	OCH ₃	>10000 (18)	>10000 (-1)	>10000 (20)	>10000 (-11)
108	OCH ₃	>10000 (13)	>10000 (11)	>10000 (13)	>10000 (-1)
102	Cl	>10000 (12)	>10000 (18)	>10000 (1)	>10000 (59)

^{a,b}Potencies were determined in functional β -arrestin recruitment assays using β -arrestin CHO K1 cells (DiscoverX) recombinantly expressing (a) the human GPR18 or (b) the human GPR55. Screenings were performed at a concentration of 10 μ M. ^cEffects were normalized to the signal induced by 10 μ M THC corresponding to a maximal response at GPR18. ^dPercent inhibition of PSB-KK-1415 (internal code: MZ-1415) activation (0.1 μ M) induced β -arrestin recruitment by test compound (10 μ M). ^eEffects were normalized to the signal induced by 10 μ M LPI corresponding to a maximal response at GPR55. ^fPercent inhibition of LPI activation (2 μ M) induced β -arrestin recruitment by test compound (10 μ M).

Table 3.24. Activity of GPR35 agonists at the human GPR18 and the human GPR55: chromen-4-one derivatives

compound	human GPR18		human GPR55	
	β -arrestin recruitment assays ^a		β -arrestin recruitment assays ^b	
	EC ₅₀ ± SEM ^c (nM) (% effect)	IC ₅₀ ± SEM ^d (nM) (% inhibition)	EC ₅₀ ± SEM ^e (nM) (% effect)	IC ₅₀ ± SEM ^f (nM) (% inhibition)
85a	>10000 (16)	>10000 (4)	>10000 (0)	>10000 (-6)
86b	>10000 (4)	>10000 (18)	>10000 (-20)	>10000 (30)
88c	>10000 (-1)	>10000 (29)	>10000 (-14)	>10000 (20)

^{a,b}Potencies were determined in functional β -arrestin recruitment assays using β -arrestin CHO K1 cells (DiscoverX) recombinantly expressing (a) the human GPR18 or (b) the human GPR55. Screenings were performed at a concentration of 10 μ M. ^cEffects were normalized to the signal induced by 10 μ M THC corresponding to a maximal response at GPR18. ^dPercent inhibition of PSB-KK-1415 (internal code: MZ-1415) activation (0.1 μ M) induced β -arrestin recruitment by test compound (10 μ M). ^eEffects were normalized to the signal induced by 10 μ M LPI corresponding to a maximal response at GPR55. ^fPercent inhibition of LPI activation (2 μ M) induced β -arrestin recruitment by test compound (10 μ M).

Selected 1,7-phenanthroline- and chromen-4-one-based GPR35 agonists were also investigated at the human MRGPRX2 and MRGPRX4 in β -arrestin recruitment assays (see **Table 3.25**). No activity was observed. Assays were performed by Yvonne K. Riedel.

Table 3.25. Potency of GPR35 agonists at human MRGPRX2 and MRGPRX4 in β -arrestin assays

MRGPRX2			
<i>β-arrestin recruitment assays^a</i>			
compd	EC ₅₀ ± SEM (nM) ^c	E _{max} ^c (%)	IC ₅₀ ± SEM (nM) ^d
68i	>10000	-	>10000
68d	>10000	-	>10000
105	>10000	-	>10000
85b	>10000	-	>10000
MRGPRX4			
<i>β-arrestin recruitment assays^b</i>			
compd	EC ₅₀ ± SEM (nM) ^e	E _{max} ^e (%)	IC ₅₀ ± SEM (nM) ^f
68i	>10000	-	>10000
68d	>10000	-	>10000
105	>10000	-	>10000
85b	>10000	-	>10000

^{a,b}Potency was determined in functional β -arrestin recruitment assays using β -arrestin CHO cells recombinantly expressing (a) the human MRGPRX2 or (b) the human MRGPRX4. Screening was performed at a concentration of 10 μ M. The results are the means of three to four independent effects. ^cEffects based on the effect of 5 μ M CST-14 (corresponding to the maximum effect). ^dInhibition of the effect of 1 μ M CST-14 (corresponding to its EC₈₀ value). ^eEffects based on the effect of 10 μ M PSB-18061 (corresponding to its maximum effect). ^fInhibition of the effect of 2.6 μ M PSB-18061 (corresponding to its EC₈₀ value).

New GPR35 agonists were also screened for their activity at the human MRGPRX4 using calcium mobilization assays (see **Table 3.26**). However, none of the investigated compounds increased intracellular calcium levels at high concentrations.

Table 3.26. Potency of GPR35 agonists at human MRGPRX4 in calcium mobilization assays

MRGPRX4		
compd	substitution pattern R ¹	calcium mobilization assay ^a EC ₅₀ ± SEM (nM) ^b (% effect ± SEM)
68o	decyl	>10000 (0 ± 1)
68w	<i>p</i> -tolyl	>10000 (0 ± 1)
68y	<i>p</i> -butylphenyl	>10000 (0 ± 1)
68x	4- <i>tert</i> -butylphenyl	>10000 (1 ± 1)
85b	<i>see above for structure</i>	>10000 (-1 ± 2)

^aPotency was determined in functional calcium mobilization assays using 1321N1 astrocytoma cells recombinantly expressing the human MRGPRX4. Screening was performed at a concentration of 10 μM. The results are the means of three independent effects. ^bEffects based on the effect of 1 μM PSB-18061 (corresponding to its maximum effect).

Summary: Selectivity of GPR35 agonists

In general, the probed GPR35 agonists were selective against a variety of G protein-coupled receptors. The selectivity profile of the most potent GPR35 agonists is provided in **Figure 3.64**. Most compounds did not display any measurable activity at the investigated receptors. Some 1,7-phenanthroline derivatives displayed affinity for GPR84 with *K_i* values in the micromolar range. A number of chromen-4-one derivatives also showed weak affinity for GPR84, however, this was expected, since the most potent GPR84 antagonists are based on this scaffold as well. Naturally, it is not possible to establish absolute selectivity of a ligand for a particular receptor, however, all compounds were substantially more potent at GPR35 compared to the other investigated, closely related targets. Therefore, we predict reasonable selectivity for GPR35.

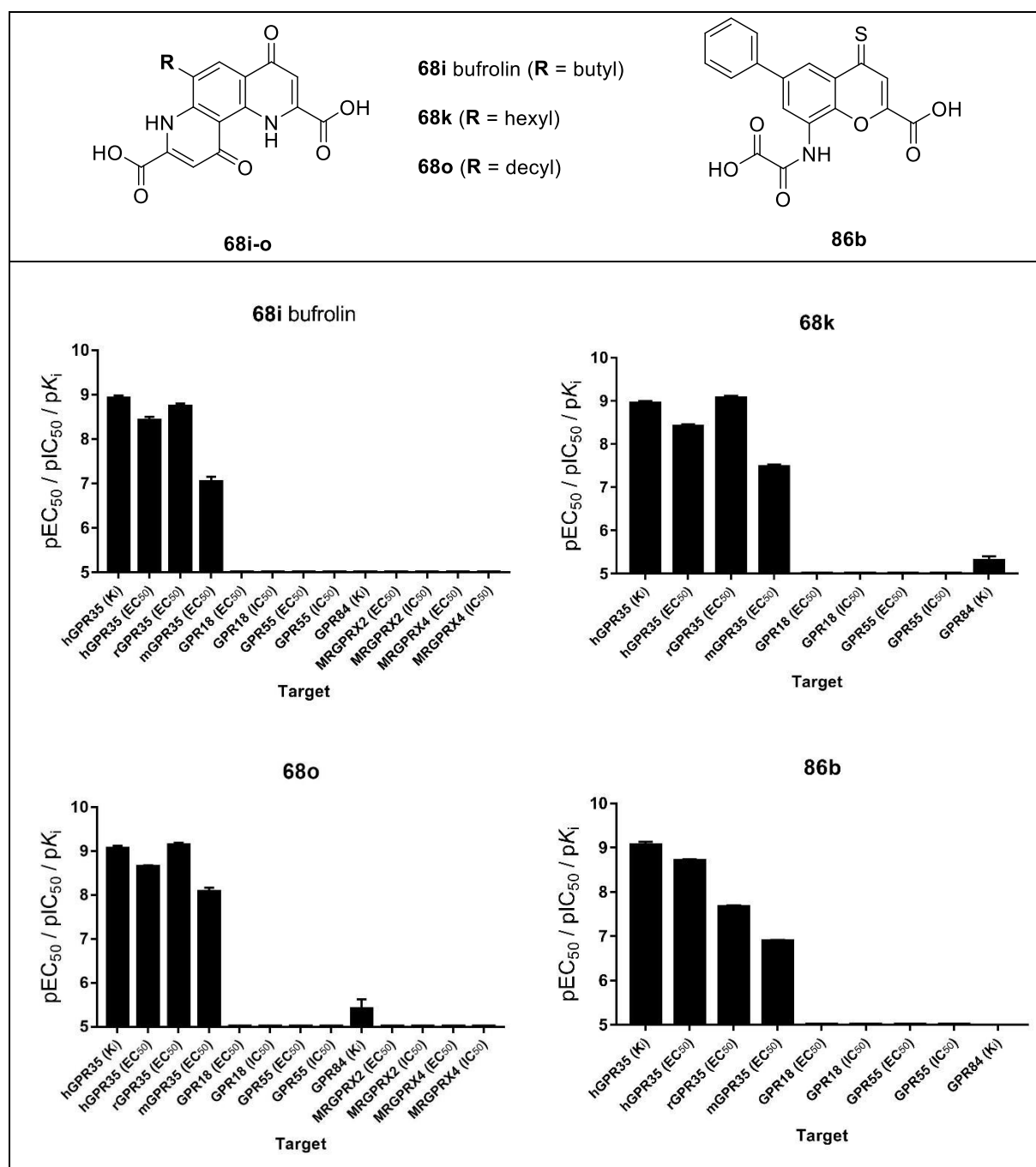


Figure 3.64. The most potent GPR35 agonists were selective versus related (orphan) GPCRs. h, human; m, mouse; r, rat. (If not otherwise indicated, the values pertain to the human receptor orthologs)

3.6.3 Selectivity of GPR84 antagonists

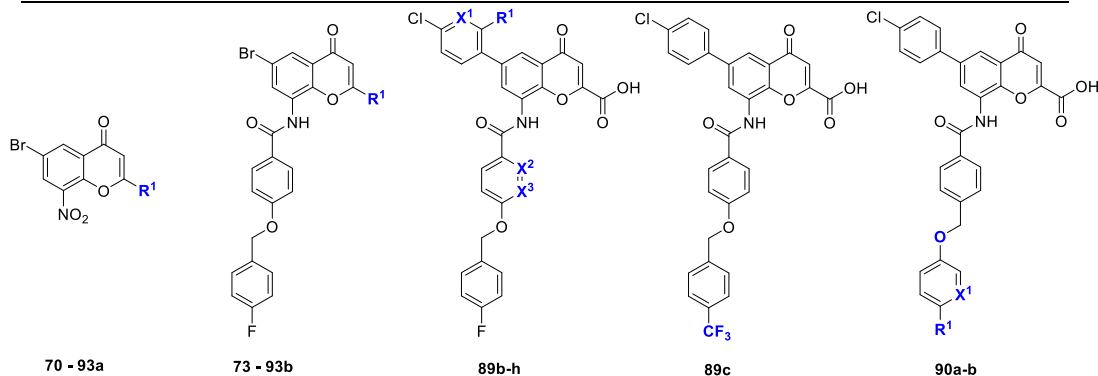
Next, we investigated the potency of GPR84 antagonists at the human, rat, and mouse GPR35 (see **Tables 3.27-29**). The selectivity of the scaffold against other receptors was demonstrated in a previous work.¹ Since these compounds were originally derived from GPR35 agonists, we expected a certain degree of activity. The assays were performed by Miriam Dielt.

Table 3.27. Affinity and potency of GPR84 antagonists at the human GPR35

compd	substitution pattern				radioligand binding assays ^a $K_i \pm$ SEM (nM) (% inhibition \pm SEM)	β -arrestin recruitment assays ^b		
	R ¹	X ¹	X ²	X ³		EC ₅₀ \pm SEM (nM) (% effect ^c \pm SEM)	E _{max} ^c	IC ₅₀ \pm SEM (nM) (%inhibition ^d \pm SEM)
70	CO ₂ H	-	-	-	1980 \pm 460	11100 \pm 2900	101	-
93a	tetrazol-5-yl	-	-	-	389 \pm 56	1980 \pm 90	99	-
73	CO ₂ Et	-	-	-	>10000 (-319 \pm 36)	>10000 (0 \pm 1)	-	(9 \pm 4)
89a	CO ₂ H	-	-	-	224 \pm 30	>10000 (50 \pm 3)	-	(24 \pm 2)
91b	CONH	-	-	-	>10000 (-345 \pm 145)	>10000 (3 \pm 3)	-	(3 \pm 11)
92b	CN	-	-	-	>10000 (-17 \pm 10)	>10000 (-2 \pm 1)	-	(31 \pm 9)
93b	tetrazol-5-yl	-	-	-	250 \pm 8	>10000 (11 \pm 1)	-	(29 \pm 10)
89b	H	-	-	-	>10000 (23 \pm 1)	>10000 (32 \pm 3)	-	(18 \pm 1)
89d	Cl	-	-	-	>10000 (14 \pm 7)	>10000 (35 \pm 3)	-	(17 \pm 4)
89e	H	N	-	-	>10000 (38 \pm 5)	>10000 (49 \pm 4)	-	(7 \pm 0)
89f	H	-	N	-	2640 \pm 210	2100 \pm 110	99	-
89g	H	-	-	N	>10000 (30 \pm 3)	>10000 (13 \pm 1)	-	(9 \pm 6)
89h	H	N	N	-	>10000 (45 \pm 5)	>10000 (37 \pm 4)	-	(13 \pm 11)
89c	<i>see above for structure</i>				1370 \pm 430	3030 \pm 80	79	-
90a	F	N	-	-	>10000 (48 \pm 1)	2350 \pm 180	61	-
90b	OH	-	-	-	317 \pm 58	2850 \pm 280	56	-

^aAffinities were determined in competition binding experiments using 5 nM [³H]PSB-13253 and membrane preparations of CHO cells recombinantly expressing human GPR35. ^bPotencies were determined in functional β -arrestin recruitment assays using β -arrestin CHO cells (DiscoverX) recombinantly expressing the GPR35 orthologs. Screenings were performed at a concentration of 10 μ M. Effects were normalized to the signal induced by 30 μ M, corresponding to a maximal response at the respective receptor. ^dInhibition of the effect of 5 μ M zaprinast (corresponding to its EC₈₀ value).

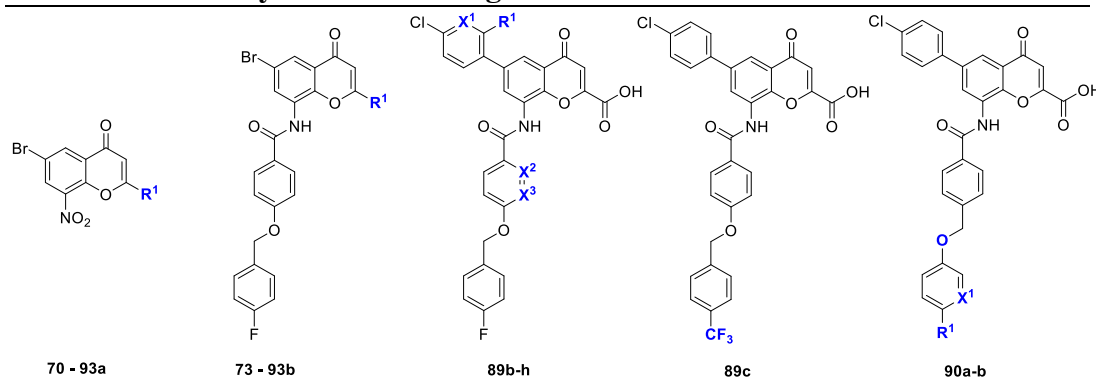
In general, GPR84 antagonists displayed only very weak affinity for the human GPR35 ortholog or none at all. The compounds with the highest affinity for GPR35 were **93a** (K_i 389 nM), **89a** (K_i 224 nM), **93b** (K_i 250 nM), and **90b** (K_i 317 nM). Interestingly, their activity in β -arrestin recruitment assays was significantly lower with EC₅₀ values in the micromolar range. Compounds **89a** and **93b** failed to induce the recruitment of β -arrestins at all, and the maximum efficacy of **90b** was only 56% of that of the standard agonist.

Table 3.28. Potency of GPR84 antagonists at the rat GPR35

compd	substitution pattern				β -arrestin recruitment assays ^a		
	R ¹	X ¹	X ²	X ³	EC ₅₀ ± SEM (nM) (% effect ^b ± SEM)	E _{max} ^b	IC ₅₀ ± SEM (nM) (%inhibition ^c ± SEM)
70	CO ₂ H	-	-	-	4900 ± 720	74	-
93a	tetrazol-5-yl	-	-	-	898 ± 151	84	-
73	CO ₂ Et	-	-	-	>10000 (-1 ± 2)	-	(1 ± 5)
89a	CO ₂ H	-	-	-	1070 ± 220	83	-
91b	CONH	-	-	-	>10000 (5 ± 1)	-	(-5 ± 0)
92b	CN	-	-	-	>10000 (1 ± 0)	-	(42 ± 3)
93b	tetrazol-5-yl	-	-	-	228 ± 38	95	-
89b	H	-	-	-	803 ± 73	53	-
89d	Cl	-	-	-	919 ± 127	54	-
89e	H	N	-	-	2690 ± 1050	97	-
89f	H	-	N	-	2330 ± 310	84	-
89g	H	-	-	N	358 ± 88	84	-
89h	H	N	N	-	385 ± 67*	68	-
89c	<i>see above for structure</i>				>10000 (38 ± 2)	-	(-4 ± 8)
90a	F	N	-	-	904 ± 80	60	-
90b	OH	-	-	-	843 ± 103	71	-

^aPotencies were determined in functional β -arrestin recruitment assays using β -arrestin CHO cells (DiscoverX) recombinantly expressing the GPR35 orthologs. Screenings were performed at a concentration of 10 μ M. Effects were normalized to the signal induced by ^b10 μ M zaprinast, corresponding to a maximal response at the respective receptor. ^cInhibition of the effect of 3 μ M zaprinast (corresponding to its EC₈₀ value). *extrapolated

Most of the investigated GPR84 antagonists also weakly activated the rat GPR35 ortholog, however, EC₅₀ values tended to be in the micromolar range. The most potent derivatives at rat GPR35 were **93b**, which exhibited an EC₅₀ value of 228 nM, **89g** (EC₅₀ 358 nM), and **89h** (EC₅₀ 385 nM). Nevertheless, only **93b** acted as a full agonist at the receptor, whereas **89g** and **89h** were only partial agonists with a maximum efficacy of 84 and 68 percent, respectively.

Table 3.29. Potency of GPR84 antagonists at the mouse GPR35

compd	substitution pattern				β -arrestin recruitment assays ^a		
	R ¹	X ¹	X ²	X ³	EC ₅₀ ± SEM (nM) (% effect ^b ± SEM)	E _{max} ^b	IC ₅₀ ± SEM (nM) (%inhibition ^c ± SEM)
70	CO ₂ H	-	-	-	>10000 (49 ± 2)	-	(1 ± 6)
93a	tetrazol-5-yl	-	-	-	2290 ± 350	106	-
73	CO ₂ Et	-	-	-	>10000 (-1 ± 2)	-	(3 ± 3)
89a	CO ₂ H	-	-	-	2720 ± 80	98	-
91b	CONH	-	-	-	>10000 (2 ± 2)	-	(-19 ± 5)
92b	CN	-	-	-	>10000 (2 ± 1)	-	(1 ± 4)
93b	tetrazol-5-yl	-	-	-	1960 ± 140	89	-
89b	H	-	-	-	>10000 (49 ± 2)	-	(8 ± 2)
89d	Cl	-	-	-	3560 ± 300	73	-
89e	H	N	-	-	>10000 (39 ± 4)	-	(2 ± 2)
89f	H	-	N	-	>10000 (38 ± 2)	-	(1 ± 0)
89g	H	-	-	N	2190 ± 430	73	-
89h	H	N	N	-	233 ± 54	76	-
89c	<i>see above for structure</i>				>10000 (29 ± 0)	-	(24 ± 6)
90a	F	N	-	-	>10000 (44 ± 1)	-	(-10 ± 5)
90b	OH	-	-	-	2500 ± 550	88	-

^aPotencies were determined in functional β -arrestin recruitment assays using β -arrestin CHO cells (DiscoverX) recombinantly expressing the GPR35 orthologs. Screenings were performed at a concentration of 10 μ M. Effects were normalized to the signal induced by ^b30 μ M zaprinast, corresponding to a maximal response at the respective receptor. ^cInhibition of the effect of 5 μ M zaprinast (corresponding to its EC₈₀ value).

Most GPR84 antagonists were inactive at the mouse GPR35 ortholog, while some derivatives showed EC₅₀ values in the low micromolar range. Compound **89h** was the only derivative to activate the receptor with nanomolar potency, however, its EC₅₀ value was relatively high (EC₅₀ 233 nM). Moreover, it failed to elicit a maximum response at the receptor (E_{max} 76%) compared to the standard agonist zaprinast (at 30 μM).

Summary: Selectivity of GPR84 antagonists

In general, chromen-4-one-based GPR84 antagonists of this study displayed very low potency or affinity at the various GPR35 orthologs. The compounds with the highest affinity for the human receptor failed to potently induce the recruitment of β-arrestins. The rat GPR35 was the most tolerant ortholog, since most derivatives displayed some activity there, however, the majority of compounds were only weak partial agonists. At the mouse receptor ortholog, most compounds were inactive. However, one compound (**89h**) displayed nanomolar potency. A comparison of the activity of selected compounds at GPR35 is provided in **Figure 3.64**.

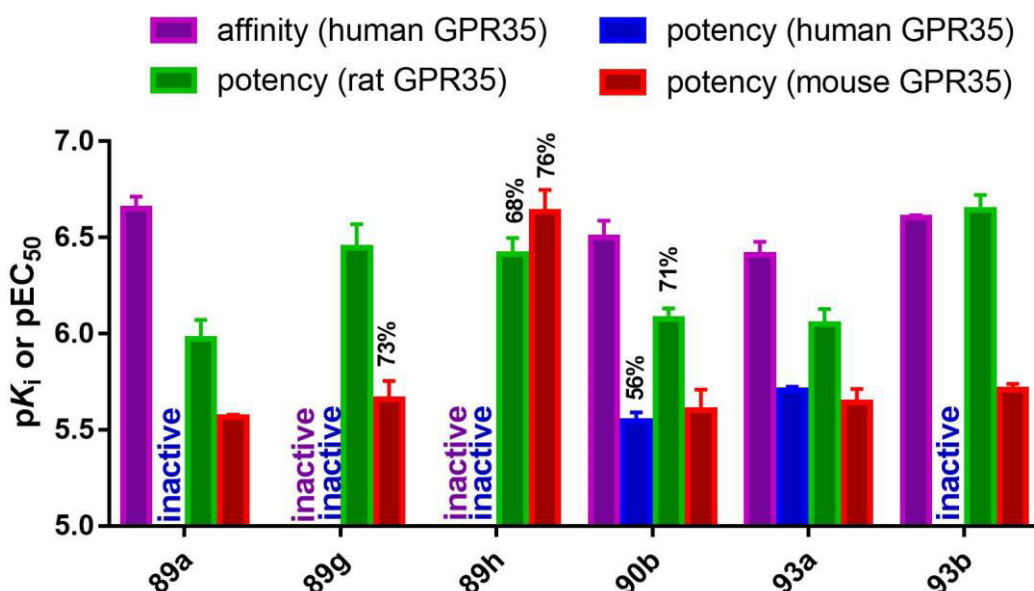


Figure 3.65. Affinity and potency of selected GPR84 antagonists at human, rat, and mouse GPR35. Percentages reflect maximum efficacy compared to zaprinast.

The selectivity profile of the most potent GPR84 antagonists of this study is summarized in **Figure 3.66**.

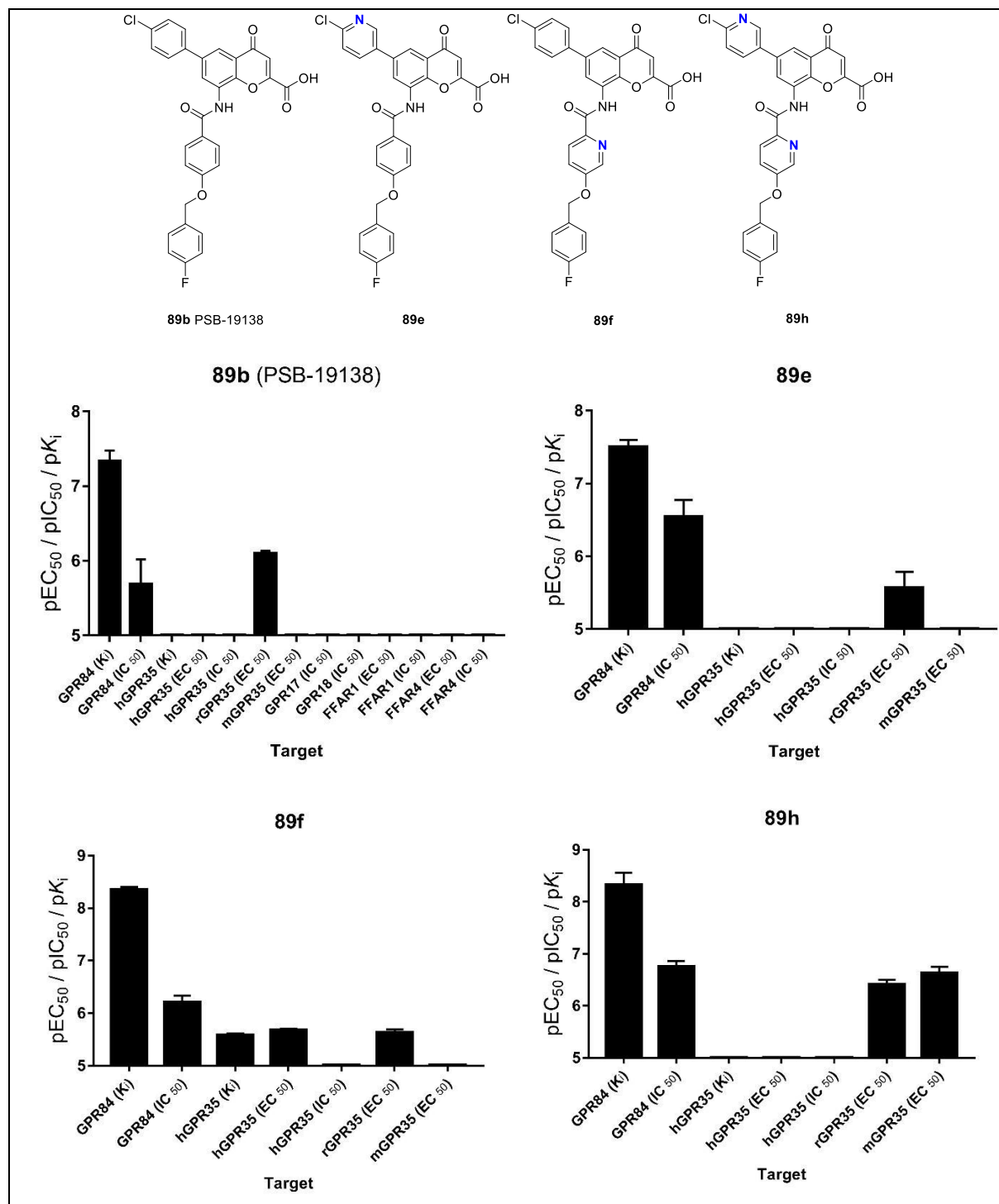


Figure 3.66. The most potent GPR84 antagonists were selective versus related (orphan) GPCRs. h, human; m, mouse; r, rat. (If not otherwise indicated, the values pertain to the human receptor orthologs)

3.7 Drug metabolism and pharmacokinetics

Selected molecules of this study were tested for their pharmacokinetic and metabolic properties at a contract research organization (Pharmacelsus GmbH, Saarbrücken, Germany). The examined in-vitro properties included plasma protein binding (PPB), microsomal stability (using human or mouse liver microsomes), aqueous solubility, and Caco2 transport (membrane permeability).

3.7.1 Results

The results are presented in **Table 3.30**.

Table 3.30. In vitro drug metabolism and pharmacokinetics of selected compounds

compound	substitution pattern		plasma protein binding (human) PPB [%]	microsomal stability (human, mouse) CL ^{int} [μ l/min/mg protein]	aqueous solubility (99% PBS [pH 7.4], 1% DMSO) solubility [μ M]	Caco2 transport (uni-directional) P _{app} *10 ⁻⁶ [cm/s]
	R ¹	X				
<u>Reference compounds:</u>						
warfarin	-	-	97.9	n.d. human: 140.2 (t _{1/2} 9.89 min)	n.d.	n.d.
verapamil	-	-	n.d.	mouse: 224.3 (t _{1/2} 6.18 min)	n.d.	n.d.
atenolol	-	-	n.d.	n.d.	n.d.	0.6
testosterone	-	-	n.d.	n.d.	n.d.	13.9
68d	Br	-	n.d.	human: 1.0 (t _{1/2} > 60 min)	94 ± 24	0.9 ± 0.1

				mouse: 2.2 ($t_{1/2} > 60$ min)		
68i bufrolin	butyl	-	95.3	human: < 0 ($t_{1/2} > 60$ min)	95.5 ± 4.2	n.d.
110	OCH ₃	-	99.6	human: < 0 ($t_{1/2} > 60$ min) mouse: < 0 ($t_{1/2} > 60$ min)	102 ± 5	n.d.
62^a PSB-21300	Br	S	100.0	human: 5.2 ($t_{1/2} > 60$ min) mouse: 3.0 ($t_{1/2} > 60$ min)	169 ± 8	n.d.
25^a PSB-13007	Br	O	99.9	human: 7.2 ($t_{1/2} > 60$ min) mouse: 1.0 ($t_{1/2} > 60$ min)	n.d.	n.d.
26^a PSB-21028	phenyl	O	100.0	n.d.	192 ± 29	n.d.
88a	Br	S	100.0	human: 22 ($t_{1/2} > 60$ min) mouse: 85 ($t_{1/2}$ 16.31 min)	n.d.	n.d.

^aCompounds **25** (PSB-13007), **26** (PSB-21028), and **62** (PSB-21300) have been synthesized by another member of our research group for a previous study.^{1,186} CL^{int}, intrinsic clearance; n.d., not determined; P_{app}, apparent permeability coefficient; PBS, phosphate buffered saline; PPB, plasma protein binding; $t_{1/2}$, half-life.

3.7.2 Discussion

When we investigated our compounds for their in-vitro pharmacokinetic and metabolic properties, we observed mixed results. Plasma protein binding (PPB) was generally high. Especially chromen-4-one derivatives, including chromen-4-thiones, were strongly bound to plasma proteins with bound proportions of over 99%. Compounds **26** (PSB-21028) and **88a** displayed the highest plasma protein binding rates with 0% in the unbound state. The pyrrolo[2,3-*f*]quinoline derivative **110** also displayed strong binding of 99.6%. The only 1,7-phenanthroline derivative whose PPB was investigated showed weaker binding. With a fraction of 95.3%, bufrolin (**68i**) was bound less strongly to plasma proteins than the reference compound warfarin (97.9%).

As far as microsomal stability was concerned, our compounds performed very well. All compounds except one (**88a**) were metabolically stable over the observed time period when subjected to human or mouse liver microsomes. Except for **88a**, which was metabolized by mouse liver microsomes at a half-life ($t_{1/2}$) of 16.3 min, all compounds displayed a half-life of >60 min. Especially the 1,7-phenanthroline derivatives **68d** and **68i** and the pyrrolo[2,3-*f*]quinoline derivative **110** displayed an extremely low intrinsic clearance.

The examined derivatives all exhibited relatively high semi-thermodynamic solubility at pH 7.4, with most compounds reaching aqueous concentrations of approximately 100 μM or more. The solubility of the chromen-4-one derivative **26** was highest with a final concentration of 192 μM , and the 1,7-phenanthroline derivatives' **68d** and **68i** was the lowest (94 μM and 95.5 μM , respectively).

Only **68d** was investigated in membrane permeability assays using Caco2 cells. The compound's permeability was low (0.9 cm/s), seeing as it performed about as well as the poorly permeable reference compound atenolol (0.6 cm/s).

In conclusion, the examined compounds showed favorable in-vitro pharmacokinetic and metabolic properties. They demonstrated especially high metabolic stability and satisfactory aqueous solubility. The low membrane permeability of **68d** suggests that this compound class might be most suited for local application.

4 Summary and outlook

4.1 Development of potent and selective ligands for orphan GPCRs

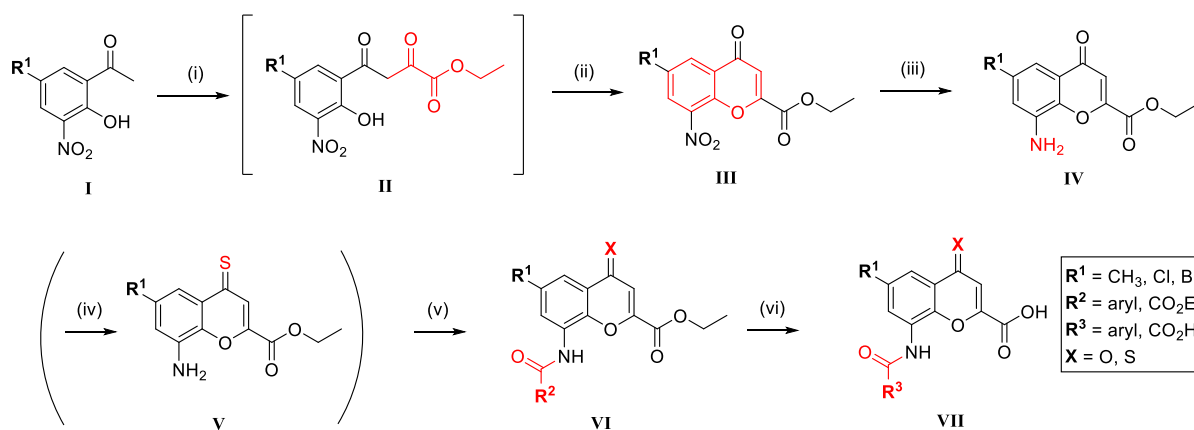
G protein-coupled receptors (GPCRs) are a superfamily of specialized transmembrane proteins with the ability to be activated by a tremendous variety of signaling molecules, ions, and even light. Not only are they indispensable for vision and olfaction but they also regulate countless physiological processes, such as blood pressure, immune responses, and cell differentiation. While some GPCRs have been extensively studied and as a consequence could be targeted by pharmaceutical drugs, the so-called “orphan” receptors are often poorly characterized. The inadequate understanding of their endogenous activators and a lack of surrogate tool compounds hamper basic research and drug development. With this study, we intended to facilitate the exploitation of two orphan GPCRs as drug targets. Both GPR35 and GPR84 are orphan receptors and insufficiently characterized despite mounting evidence of their involvement in major diseases. Therefore, we designed, synthesized, and optimized new pharmacological tool compounds based on promising lead structures of previous studies. Many of the herein described molecules were among the most potent known ligands for their respective receptor. This section summarizes the most important results of the study.

4.1.1 Synthesis

Among the most powerful tool compounds for GPR35 and GPR84, the chromen-4-one scaffold occupies a special position. Previous studies have demonstrated the scaffold’s versatility and potential for synthetic optimization.^{1,186,189} In this study, a variety of chromen-4-one derivatives have been prepared based on the synthetic procedures displayed in **Scheme 4.1**. The appropriate 5'-position-substituted 2'-hydroxy-3'-nitroacetophenone (**I**) reacted with diethyl oxalate in a crossed Claisen condensation giving the intermediate diketone **II**. We optimized the reaction employing tetrahydrofuran (THF) instead of the high-boiling dimethylformamide, which reduced reaction times significantly. A subsequent acid-catalyzed intramolecular condensation afforded the cyclized 8-nitrochromen-4-one **III** within 10 minutes, contrary to the reported 12 hours,¹ accelerating the workflow additionally. Reduction using the mild reducing agent SnCl₂ furnished the 8-aminochromen-4-one **IV**, which was optionally thionated to **V** using Lawesson’s reagent in toluene. This reaction was followed by various amide coupling reactions

affording **VI**. Compounds **VII** were prepared via an optimized mild hydrolysis reaction, using K_2CO_3 in a water/THF mixture. The 6-bromochromen-4-one derivative of **IV** was a valuable intermediate to introduce a wide range of aromatic residues (e.g. phenyl, *p*-tolyl, *p*-butylphenyl, 6-chloropyridin-3-yl, etc.) via a Suzuki coupling protocol in high yields.

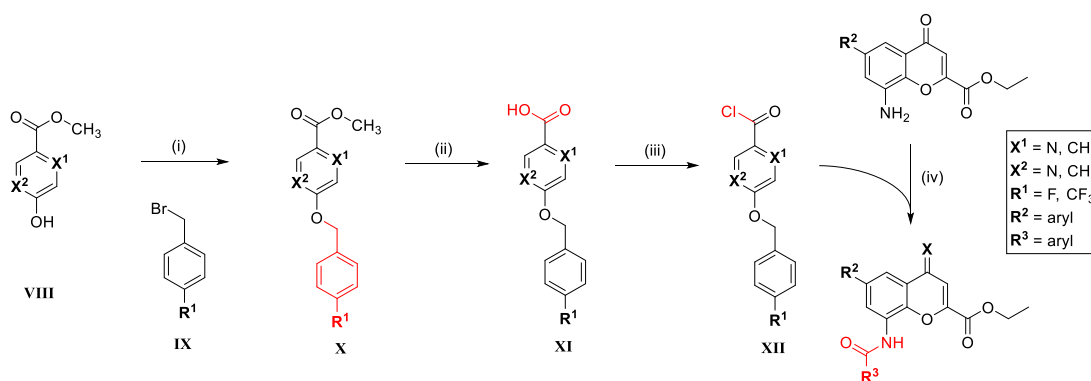
Scheme 4.1. Preparation of chromen-4-one and chromen-4-thione derivatives.^a



^aReagents and conditions: (i) diethyl oxalate, $KOtBu$, THF, 0 °C, 20 min; (ii) EtOH, HCl conc., reflux, 10 min, 62-84% yield for 2 steps; (iii) $\text{SnCl}_2 \cdot 2\text{H}_2\text{O}$, HCl (2M), EtOH, 65 °C, 40 min, 79-100% yield; (iv) Lawesson's reagent, toluene, reflux, 2 h, 17-58% yield; (v) acid chloride, THF/DCM, DIPEA, 0 °C, 1 h, Ar; rt, 24 h, 34-91% yield; (vi) K_2CO_3 , H_2O , THF, rt, 24 h, 45-99% yield.

Amide coupling reactions were performed using acid chlorides, which were either commercially available or prepared shortly before the reaction (**Scheme 4.2**). Generally, suitable methyl 4-hydroxybenzoates **VIII** reacted with benzyl bromides **IX** in a Williamson ether synthesis affording **X** in excellent yields, which was followed by hydrolysis to the carboxylic acid **XI** and chlorination to **XII**. The subsequent Schotten-Baumann reaction gave the desired amides in good to excellent yields.

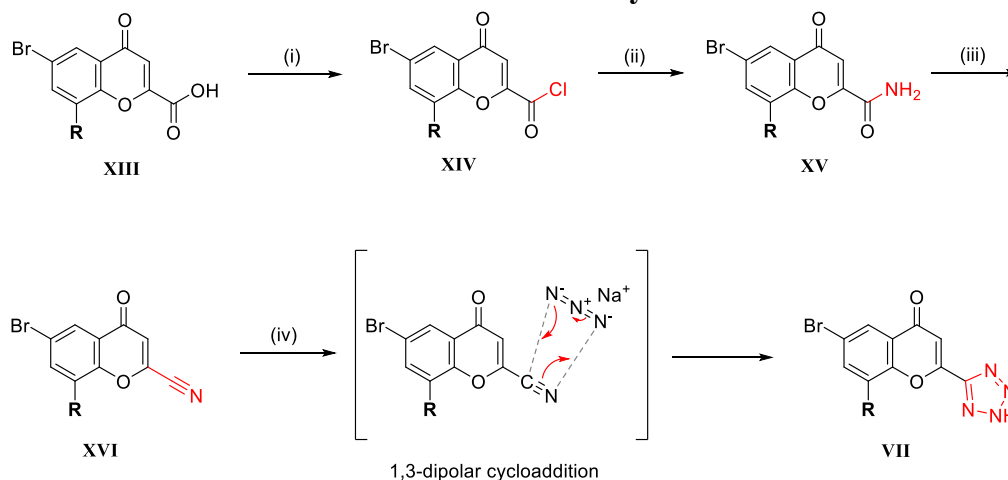
Scheme 4.2. Preparation of 4-(benzyloxy)benzoic acid derivatives used for amide coupling reactions.^a



^aReagents and conditions: (i) K_2CO_3 , acetone, reflux, 30 min; reflux, 3 h, 55-99% yield; (ii) aq NaOH (10%), MeOH, H_2O , reflux, 30 min; HCl conc, 70-100% yield; (iii) SOCl_2 neat or in DCM, reflux, 1-2 h, 99% yield; (iv) THF/DCM, DIPEA, 0 °C, 1 h, Ar; rt, 24 h, 34-91% yield.

We also developed a procedure to functionalize the carboxylic acid in the 2-position of chromones (**Scheme 4.3**). First, the 2-carboxylic acid moiety of **XIII** was chlorinated to **XIV**. The subsequent amide coupling, using gaseous ammonia both as reactant and as base, yielded the primary amide **XV**. Dehydration with phosphoryl chloride provided the respective nitriles **XVI** in good yields. The reaction of nitriles with sodium azide and pyridinium hydrochloride gave the 2-(tetrazol-5-yl)-chromenones **XVII** via a 1,3-dipolar cycloaddition in excellent yields and purity after filtration.

Scheme 4.3. Functionalization of chromone-2-carboxylic acids.^a



^aReagents and conditions: (i) SOCl_2 , DCM, DMF cat., reflux, 1 h; (ii) NH_3 , DCM, 0 °C, 1 h, 50-56% yield (2 steps); (iii) POCl_3 , DMF, 0 °C, overnight, Ar, 57-88% yield; (iv) NaN_3 , pyridinium-HCl, DMF, 100 °C, 1 h, Ar; aq HCl (2M), 0 °C, 84-94% yield.

With the synthetic methodologies described herein, we could explore a large variety of substituents at chromen-4-one-based GPR35 agonists and GPR84 antagonists (**Figure 4.1**). Regarding chromen-4-one-based GPR35 agonists, special focus lay on the 4- and 6-positions, which we modified extensively. GPR84 antagonists were mostly modified by replacing lipophilic phenyl rings with more polar heterocycles, but the 2-position was also analyzed in more detail.

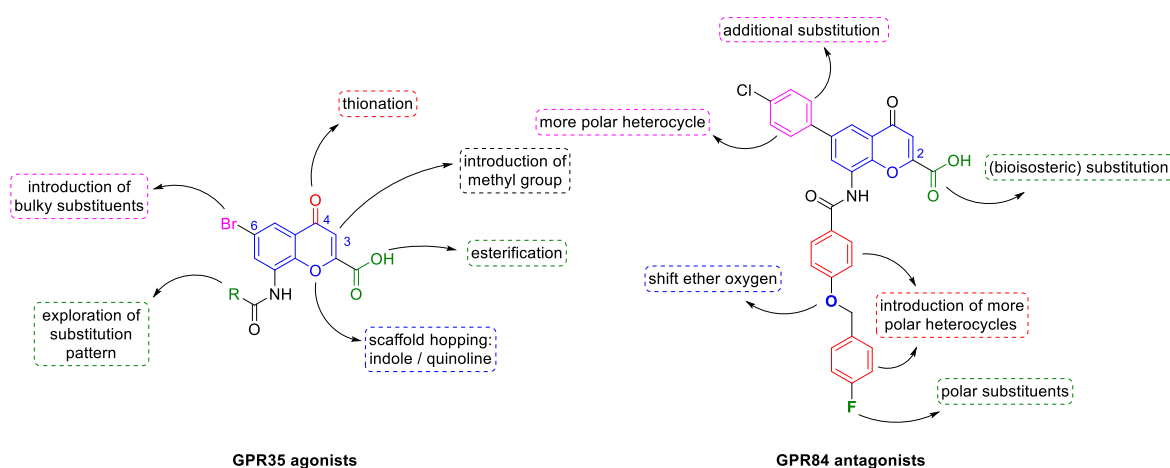
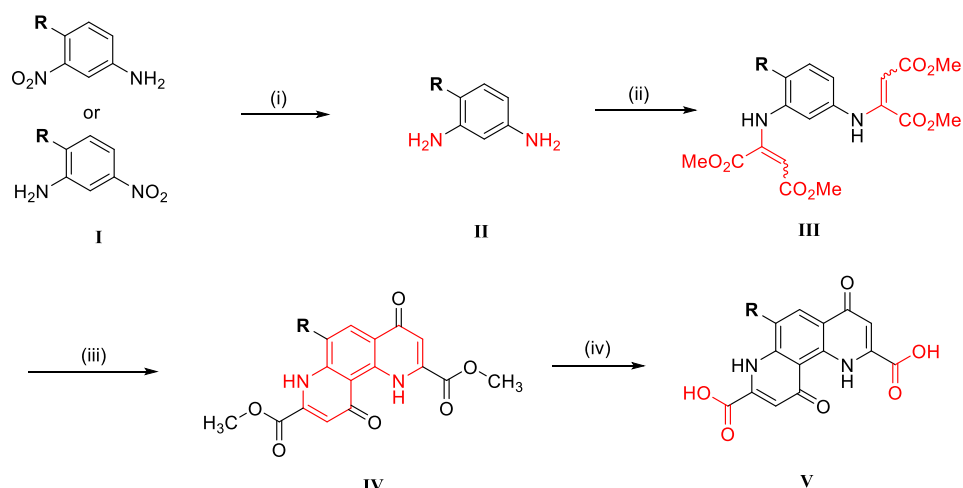


Figure 4.1. The lead structures' structure-activity relationships were investigated by introducing various synthetic modifications.

1,7-Phenanthroline derivatives were prepared using appropriately 4-position-substituted 1,3-phenylenediamines (**II**, **Scheme 4.4**), which were either commercially available or prepared from their respective nitroanilines (**I**) by catalytic reduction. Hydroamination reactions of dimethyl acetylenedicarboxylate afforded the enamine derivatives **III**, which were subsequently cyclized in a Conrad-Limpach reaction to give **IV**. Hydrolysis furnished 2,8-dicarboxylic acid derivatives **V**.

Scheme 4.4. Preparation of 1,7-phenanthroline derivatives.^a

^aReagents and conditions: (i) MeOH:THF (1:1), Pd/C (10%), H₂, 3.1 bar, rt, 2 h, 90-100% yield; (ii) DMAD, MeOH, rt, 12-24 h, Ar, 25-92% yield; (iii) Ph₂O, 250 °C, ~15 min, 4-67% yield; (iv) procedure A: NaOH aq, reflux, 1 h; HCl conc., 50-100% yield; procedure B: HCl (6M):HAc (1:1), reflux, 3-6 h, 65-100% yield.

We implemented a large variety of structural modifications at the scaffold's 6-position, which was in the focus of this study. However, we also probed the significance of the carboxylic acid moieties in the 2- and 8-positions, as well as the importance of the ketone in the 4-position. One compound was synthesized starting from 3,4-dimethyl-5-nitroaniline, furnishing a 5,6-dimethylphenanthroline derivative. By scaffold hopping, we also generated a library of structurally diverse, related derivatives to investigate their biological activity. **Figure 4.2** provides an overview of the structural modifications to the 1,7-phenanthroline scaffold of this study.

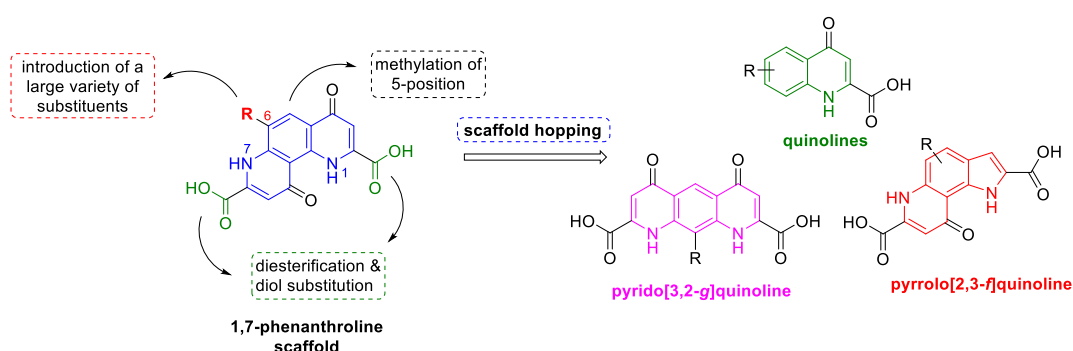


Figure 4.2. The 1,7-phenanthroline scaffold was extensively modified.

Thus, we successfully prepared and characterized a library of mostly novel chromen-4-one and 1,7-phenanthroline derivatives, as well as some structurally related indole and quinoline derivatives. The resulting molecules were evaluated for their potential to activate or block their intended targets. Selected compounds were also tested for off-target effects at related orphan receptors.

4.1.2 GPR35

The preparation and optimization of new GPR35 agonists was a major focus of this study. The receptor is highly expressed in the gastrointestinal tract with strong expression in the stomach and throughout colonic crypts. It is present on cells associated with the immune system, including monocytes, dendritic cells, and natural killer T cells. In line with being associated with several types of cancer, including gastric and colon cancers, GPR35 is strongly linked to immune regulation. It was implicated in the pathogenesis of ulcerative colitis and other inflammation-related diseases. Interestingly, the receptor was also found to control blood pressure and cardiac remodeling associated with hypoxia. Thus, GPR35 agonists and antagonists show potential for the treatment of many diseases. Some agonists have demonstrated antiallergic properties in humans, and animal studies suggest their use for the treatment of inflammatory bowel diseases and (neuropathic) pain. GPR35 antagonists, on the other hand, might protect from high blood pressure and prevent cardiac hypertrophy associated with heart failure. Additionally, they could mitigate cancer growth in GPR35-overexpressing tumors. However, no currently available pharmaceutical drug intentionally targets GPR35 due to most ligands' pronounced receptor ortholog selectivity. The overwhelming majority of recognized GPR35 ligands are virtually inactive at rodent orthologs of GPR35, which hampers basic research and preclinical target validation and efficacy studies. Aiming to bridge this gap, we optimized our group's chromen-4-one-based GPR35 agonists to increase their potency at the rat and mouse receptor orthologs. Using β -arrestin recruitment assays to determine the potency of new derivatives, we carefully studied their structure-activity relationships at each receptor ortholog (**Figure 4.3**).

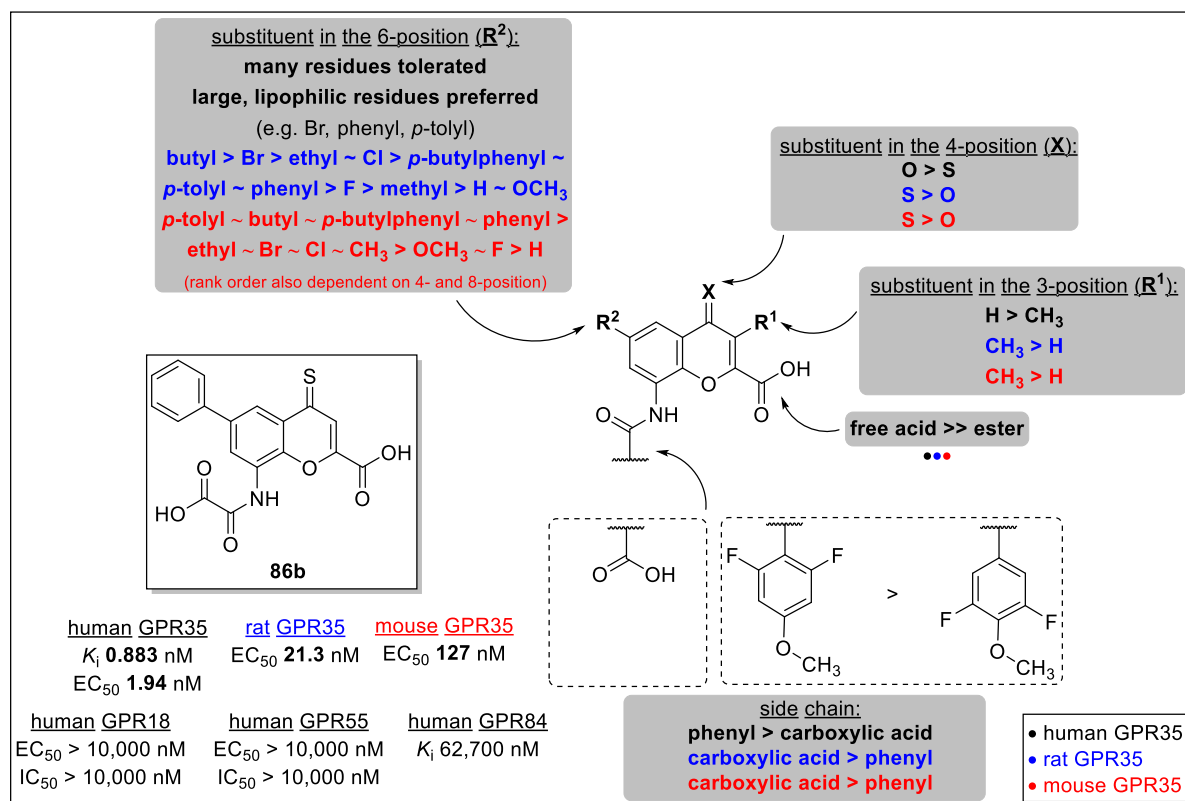


Figure 4.3. Structure-activity relationships for chromenones at GPR35. The most potent compound (**86b**) with the lowest GPR35 ortholog selectivity was further evaluated at related targets.

Apart from large, lipophilic groups in the 6-position, the potency at rodent receptor orthologs could be increased by thionation of the 4-position. Also, the introduction of a carboxyformamide moiety at the 8-position enhanced rodent receptor activity without decreasing potency at the human receptor ortholog. Methylation of the 3-position was beneficial for potency at rat and mouse GPR35, but curbed potency and affinity for the human receptor ortholog. Compound **86b** was the most potent derivative of this series, displaying EC₅₀ values in the nanomolar range at all three investigated GPR35 orthologs. With an EC₅₀ value of 1.94 nM it is among the most potent agonists at the human receptor known to date. It was selective versus the closely related GPR55 and other related GPCRs.

Based on a report about the high potency of bufrolin at the human and rat GPR35, we also optimized its 1,7-phenanthroline-based scaffold. The observed structure-activity relationships for this scaffold are summarized in **Figure 4.4**. While most derivatives were highly potent at the human and rat receptor orthologs, only those bearing long, unbranched alkyl chains in their 6-positions reached single-digit nanomolar potency at the mouse receptor ortholog. With EC₅₀

values of 8.18 nM and 6.12 nM, respectively, compounds **68o** and **68p** were the most potent derivatives at the mouse GPR35, and they displayed similarly high potency at the human and rat receptor orthologs (**Figure 4.4**). Both derivatives also showed high affinity for the human GPR35 versus the agonist radioligand [³H]PSB-13253 (**68o**: K_i 0.863 nM, **68p**: K_i 1.48 nM). The ability of **68o** to activate or block related GPCRs was investigated, and the compound was selective for GPR35 against GPR18, GPR55, and GPR84.

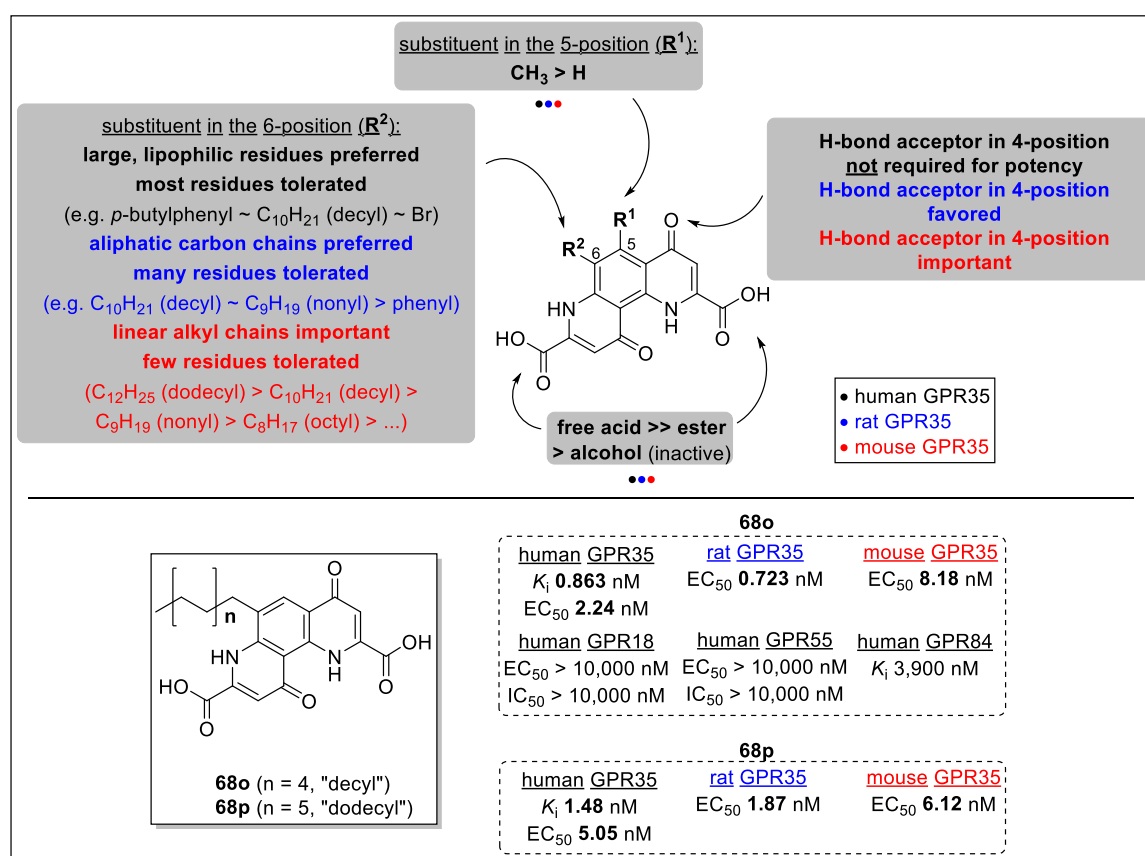


Figure 4.4. Structure-activity relationships for 1,7-phenanthrolines at GPR35. Compounds **68o** and **68p** displayed the lowest ortholog selectivity of all investigated compounds.

It was possible to boost the potency of the lead compound bufrolin for all three investigated orthologs of GPR35. By elongating the alkyl chain in the scaffold's 6-position, potency gradually increased for all receptors until reaching a saturation state. Thus, we obtained the compounds with the highest potency at the human, rat, and mouse GPR35 known to date. We also identified the 5-position as a promising location for future optimization of the scaffold. Additional future efforts will focus on the bioisosteric replacement of the carboxylic acid moieties in the 2- and 8-positions.

4.1.3 GPR84

The second orphan G protein-coupled receptor in the spotlight of this study was GPR84. It is strongly linked to immune regulation and has been described as a pro-inflammatory receptor. Being mainly expressed on immune cells with expression upregulated during infection or stress, it has recently garnered interest as a potential drug target for the treatment of inflammation-related diseases, such as ulcerative colitis and fibrosis. However, it has also been linked to the pathogenesis of Alzheimer's disease, atherosclerosis, and neuropathic pain. Agonists of the receptor have powerful immunostimulatory effects, which could be exploited for the treatment of cancer (immuno-oncology) or infections by boosting the endogenous immune response. The focus of this study was the optimization of GPR84 antagonists. These antagonists have the potential to elicit powerful anti-inflammatory and antifibrotic effects. Antagonists have also been proposed for the treatment of chronic pain. While medium-chain fatty acids (MCFA), such as decanoic acid, can activate the receptor with weak, micromolar potency, surrogate agonists, such as 6-hexylaminouracil (PSB-1584), are highly potent with EC_{50} values in the low nanomolar range. The first GPR84 antagonists sharing the receptor's ("orthosteric") MCFA binding site were recently developed in our group. PSB-17138 was the most potent derivative with a K_i value of 46.1 nM (determined versus [3 H]PSB-1584). These compounds were generally highly potent and selective, however, their poor physicochemical properties, especially low solubility ($\log D_{7.4}$ 2.83), had to be addressed. Considering that solubility and cell permeability are major factors for the success of drug development efforts, we carefully analyzed the reported structure-activity relationships of PSB-17138. In this study, we introduced polar groups into the structure to improve its properties without impairing its antagonistic potency at GPR84. After studying the effects of individual structural modifications on potency and affinity, we expanded the available structure-activity relationships and combined the most favorable changes. Compound **89h** (**Figure 4.5**) is dramatically less lipophilic ($\log D_{7.4}$ 1.00) and exhibited ~10-fold higher affinity for GPR84 (K_i 4.68 nM) than the lead structure. The structure-activity relationships are summarized in **Figure 4.5**.

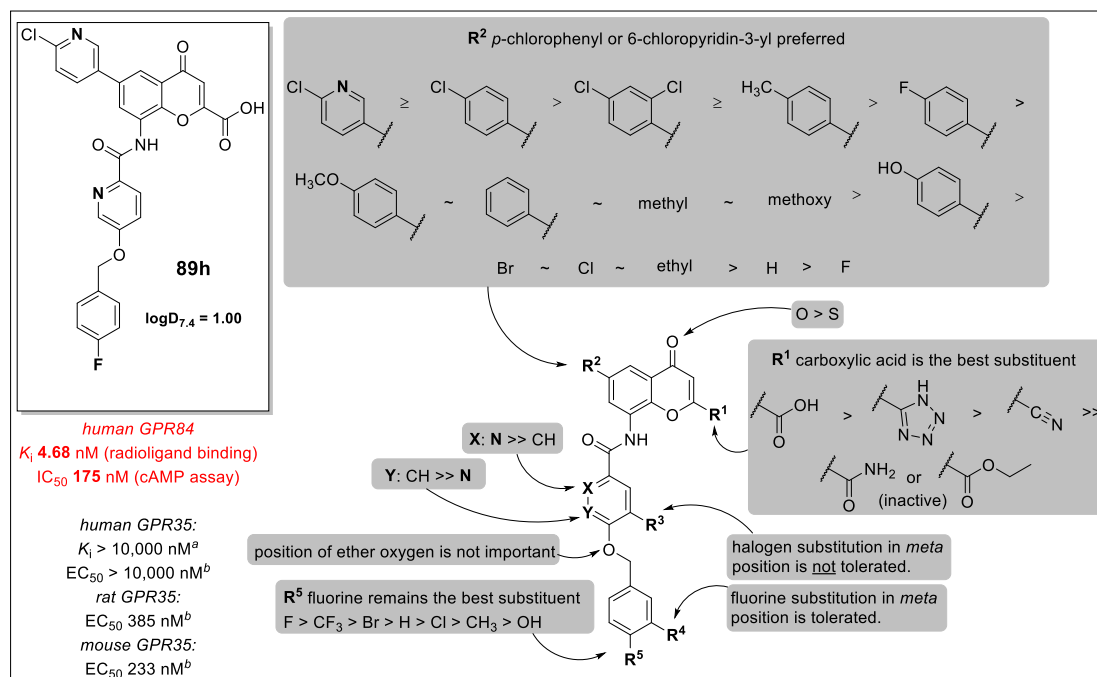


Figure 4.5. Structure-activity relationships for chromenones at the human GPR84. ^adetermined in radioligand binding assays versus [³H]PSB-13253. ^bdetermined in β -arrestin recruitment assays. log D_{7.4}, distribution coefficient at pH 7.4.

Focusing on the 6-position, the exchange of the *p*-chlorophenyl ring of the lead compound to the more polar 6-chloropyridin-3-yl moiety was tolerated well by GPR84 and increased polarity. The introduction of a picolinamide residue in the 8-position enhanced affinity ~10-fold compared to the lead compound's benzamide in that position. We also probed a number of other positions, however, neither the bioisosteric substitution of the carboxyl group with tetrazole in the 2-position nor the introduction of further halogen atoms or a hydroxy group was accepted by the receptor. Future optimizations could include further investigation of the 2-position for bioisosteric replacement, modification of the amide linker in the 8-position, and the exchange of the chromone core for related scaffolds (e.g. quinolone, indole, benzimidazole, etc.).

In conclusion, we synthesized, optimized, and characterized powerful new ligands for two orphan GPCRs with promising attributes of future drug targets. The tool compounds investigated herein are among the most potent hitherto described for their respective receptor. We also expanded the previously reported structure-activity relationships (SARs) for chromen-4-one derivatives substantially at both receptors and established new SARs for 1,7-phenanthrolines at GPR35. Although GPR35 and GPR84 were discovered over 20 years ago, their unique properties have so far been left unexploited. We are confident that this work provides important new insights that will facilitate drug development and expand the medicinal arsenal, offering improved treatment options for patients.

5 Experimental section

5.1 General remarks

All commercially available reagents were used as purchased (ABCR, Acros, Alfa Aesar, Sigma-Aldrich, or TCI). Solvents were used without additional purification or drying except for dichloromethane, which was distilled over calcium hydride. The reactions were monitored by thin layer chromatography (TLC) using aluminum sheets with silica gel 60 F₂₅₄ (Merck). Column chromatography was performed with silica gel 0.060-0.200 mm, pore diameter ca. 6 nm. All synthesized compounds were finally dried in vacuum at 8–12 Pa (0.08–0.12 mbar) using a sliding vane rotary vacuum pump (Vacuubrand GmbH). ¹H- and ¹³C NMR data were collected on a Bruker Avance 500 MHz NMR spectrometer at 500 MHz (¹H), or 126 MHz (¹³C), respectively. If indicated, NMR data were collected on a Bruker Ascend 600 MHz NMR spectrometer at 600 MHz (¹H), or 151 MHz (¹³C), respectively. DMSO-*d*₆ was employed as a solvent at 303 K, unless otherwise noted. Chemical shifts are reported in parts per million (ppm) relative to the deuterated solvent; that is, DMSO, $\delta(^1\text{H})$ 2.49 ppm; $\delta(^{13}\text{C})$ 39.7 ppm. In some cases, CDCl₃ was used as a solvent ($\delta(^1\text{H})$ 7.26 ppm, $\delta(^{13}\text{C})$ 77.0 ppm). Coupling constants *J* are given in Hertz, and spin multiplicities are given as s (singlet), d (doublet), t (triplet), q (quartet), sext. (sextet), m (multiplet), br (broad). Melting points were determined on a Büchi 530 melting point apparatus and are uncorrected. The purities of isolated products were determined by ESI-mass spectra obtained on an LCMS instrument (Applied Biosystems API 2000 LCMS/MS, HPLC Agilent 1100) using the following procedure: the compounds were dissolved at a concentration of 1.0 mg/mL in acetonitrile containing 2 mM ammonium acetate. Then, 10 μL of the sample were injected into an HPLC column (Macherey-Nagel Nucleodur[®] 3 μ C18, 50 x 2.00 mm). Elution was performed with a gradient of water/acetonitrile (containing 2 mM ammonium acetate) from 90:10 to 0:100 for 20 min at a flow rate of 300 $\mu\text{L}/\text{min}$, starting the gradient after 10 min. UV absorption was detected from 200 to 950 nm using a diode array detector (DAD). Purity of all compounds was determined at 254 nm. The purity of the compounds was generally $\geq 95\%$.

5.2 Preparation of phenanthrolines, quinolones, and indole derivatives

5.2.1 General Procedures

General procedure for the synthesis of compounds 64a-i and 64k-m. The appropriate 2-alkylaniline (for **64k-m**) or 4-alkylaniline (for **64a-i**) (12.3 mmol) was added dropwise to a stirred solution of concd. H₂SO₄ (50 mL) at rt. The mixture was cooled to -10 °C and an ice-cold solution of HNO₃ (65%, 940 μL, 13.5 mmol, 1.1 equiv.) in concd. H₂SO₄ (2.4 mL, 44.3 mmol, 3.6 equiv.) was added dropwise without the temperature rising above -5 °C. After that, the mixture was kept stirring at -5 °C for 10 min. Then, the solution was poured onto crushed ice and neutralized using a cold aq NaOH solution (20%). The mixture was extracted with DCM (3 × 100 mL). The organic layers were combined and dried over anhydrous Na₂SO₄, concentrated under reduced pressure, and the residue was further purified by column chromatography on a column of silica gel (8:2 petroleum ether/EtOAc).

General procedure for the synthesis of compounds 64j and 64n-q. 2-Bromo-5-nitroaniline (for **64n-q**) or 4-bromo-3-nitroaniline (for **64j**) (4.6 mmol), the appropriate boronic acid (9.2 mmol, 2 equiv.), K₂CO₃ (1.30 g, 9.2 mmol, 2 equiv.), and tetrakis(triphenylphosphine)palladium(0) (530 mg, 0.46 mmol, 0.1 equiv.) were mixed with anhydrous toluene (15 mL) and anhydrous DMF (5 mL) under inert gas atmosphere. The mixture was heated to 130 °C in a pressure tube with stirring for 3 h. After that, the solvents were removed under reduced pressure, and the residue was purified by column chromatography on a column of silica gel (8:2 petroleum ether/EtOAc).

General procedure for the synthesis of compounds 65g-z. The appropriate nitroaniline (9.0 mmol) was dissolved in a mixture of MeOH and THF (1:1, 20 mL), and palladium on carbon (10 wt.%) was added. The mixture was hydrogenated for 3 h at 3.1 bar and rt with stirring. After that, the catalyst was removed by filtration, and the solvents were evaporated under reduced pressure. The solid residue was directly used for the following step without further purification.

General procedure for the synthesis of compounds 66a-d, 66f, 66i-z, 103. Dimethyl acetylenedicarboxylate (2.4 mL, 19.8 mmol, 2.2 equiv.) was added dropwise to a stirred solution of the appropriate *m*-phenylenediamine (9.0 mmol) in MeOH (15 mL) at rt under argon atmosphere. Then, the mixture was refluxed for 1 h. After that, the solvent was removed under reduced pressure, and the residue was purified by column chromatography on a column of silica gel (8:2 petroleum ether/EtOAc).

General procedure for the synthesis of compounds 94a,b, 97, and LW319. Dimethyl acetylenedicarboxylate (310 μL, 2.53 mmol, 1.1 equiv.) was added dropwise to a stirred solution of the appropriate amine (2.30 mmol) in MeOH (10 mL) at rt. The mixture was stirred at that temperature for 12 h. After that, the resulting precipitate was collected by filtration, recrystallized from MeOH, and dried at 50 °C.

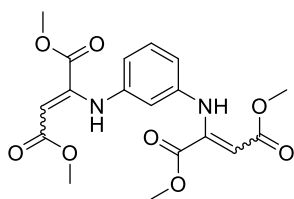
General procedure for the synthesis of compounds 67a-z, 95a,b, 98, 104, and 109. The appropriate enamine was dissolved in diphenyl ether (10 mL per gram) and refluxed for 15 min. After that, the mixture was cooled to rt and poured into petroleum ether (100 mL). The resulting precipitate was collected by filtration, and washed with petroleum ether (3 × 50 mL) and acetone. In some cases, further purification was necessary (see individual compounds).

General procedure for the synthesis of compounds 101 and 106. The appropriate amine (0.60 mmol) and Et₃N (170 μ L, 1.20 mmol, 2 equiv.) were dissolved in dry DCM (5 mL) and cooled to 0 °C under inert gas atmosphere. At this temperature, ethoxalyl chloride (75 μ L, 0.66 mmol, 1.1 equiv.) was added dropwise with stirring. The mixture was kept stirring at 0 °C for 1 h. Then, stirring continued at rt for 24 h. After that, the solvent was removed under reduced pressure, and the residue was purified by column chromatography.

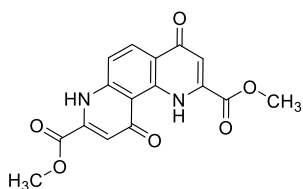
General procedure for the synthesis of compounds 68a-e, 68h,i,q,s,t,v,y, 96a,b, 99, 105, 110. The appropriate carboxylate ester (0.27 mmol) was mixed with MeOH (5 mL) and aq NaOH solution (10%, 3 mL) was added. After that, the mixture was refluxed for 30 min. Then, MeOH was removed under reduced pressure, and the mixture was acidified using concd. aq HCl. The precipitate was collected by filtration, washed with water, and dried at 50 °C.

General procedure for the synthesis of compounds 68f,g,j,r,u,w,x, 68k-p. The appropriate carboxylate ester (0.56 mmol) was dissolved in a mixture of aq acetic acid (50%) and concd. aq HCl (1:1, 5 mL). After that, the mixture was refluxed for 3 h. Then, it was cooled to rt and mixed with water (3 mL). The precipitate was collected by filtration, washed with water, and dried at 50 °C.

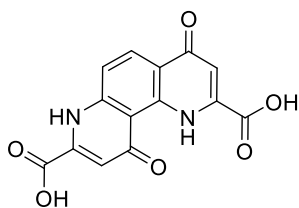
Preparation of 68a



Tetramethyl 2,2'-(1,3-phenylenebis(azanediyl))bis(but-2-enedioate) (66a, Yazh-K83). The compound was synthesized using benzene-1,3-diamine (1.20 g, 11.1 mmol). The product was isolated as a yellow solid (2.00 g, 46% yield). ¹H NMR (600 MHz, CDCl₃) δ 3.73 (s, 6H, 2 \times CO₂CH₃), 3.74 (s, 6H, 2 \times CO₂CH₃), 5.43 (s, 2H, 3'-H, 3''-H), 6.44 (t, *J* = 2.0 Hz, 1H, 2-H), 6.62 (dd, *J* = 2.1, 8.0 Hz, 2H, 4-H, 6-H), 7.17 (t, *J* = 8.0 Hz, 1H, 5-H), 9.57 (s, 2H, 2 \times NH). ¹³C NMR (151 MHz, CDCl₃) δ 51.3 (2 \times CO₂CH₃), 52.9 (2 \times CO₂CH₃), 94.6 (C-3', C-3''), 113.3 (C-2), 116.6 (C-4, C-6), 129.7 (C-5), 141.3 (C-2', C-2''), 147.5 (C-1, C-3), 164.6 (2 \times CO₂Me), 169.7 (2 \times CO₂Me). LC-MS (*m/z*): positive mode 393 [M + H]⁺. Purity by HPLC-UV (254 nm)-ESI-MS: 96.5%.

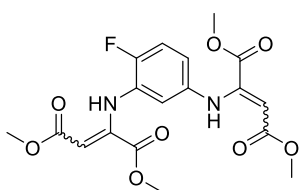


Dimethyl 4,10-dioxo-1,4,7,10-tetrahydro-1,7-phenanthroline-2,8-dicarboxylate (67a, Yazh-K85). The compound was synthesized using 66a (2.00 g, 5.11 mmol). The product was isolated as a white solid (880 mg, 53% yield). ¹H NMR (600 MHz, TFA-*d*₁) δ 4.30 (s, 3H, CO₂CH₃), 4.35 (s, 3H, CO₂CH₃), 7.91 (s, 1H, 3-H or 9-H), 8.29 (s, 1H, 3-H or 9-H), 8.43 (d, *J* = 9.2 Hz, 1H, 6-H), 8.91 (d, *J* = 9.2 Hz, 1H, 5-H). ¹³C NMR (151 MHz, TFA-*d*₁) δ 57.0 (CO₂CH₃), 57.1 (CO₂CH₃), 111.7 (C-3 or C-9), 113.3 (C-10a), 118.0 (C-3 or C-9), 120.1 (C-4a), 124.0 (C-6), 131.5 (C-5), 141.4 (C-2 or C-8), 142.6 (C-2 or C-8), 142.8 (C-6a or C-10b), 147.4 (C-6a or C-10b), 162.1 (CO₂Me), 164.6 (CO₂Me), 172.4 (C-4 or C-10), 183.7 (C-4 or C-10). LC-MS (*m/z*): positive mode 329 [M + H]⁺. Purity by HPLC-UV (254 nm)-ESI-MS: 95.3%.

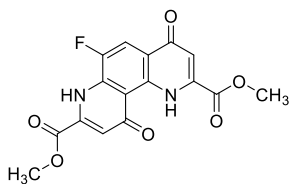


4,10-Dioxo-1,4,7,10-tetrahydro-1,7-phenanthroline-2,8-dicarboxylic acid (68a, LW26). The compound was synthesized using **67a** (200 mg, 0.61 mmol). The product was isolated as a white solid (165 mg, 85% yield). ^1H NMR (600 MHz, D_2O , ND_3) δ 6.47 – 6.66 (m, 2H, 3-H, 9-H), 7.07 (s, 1H, 6-H), 7.64 (s, 1H, 5-H). ^{13}C NMR (151 MHz, D_2O , ND_3) δ 113.2 (C-10a), 113.6 (C-3 or C-9), 114.8 (C-3 or C-9), 118.2 (C-6), 121.6 (C-4a), 131.2 (C-5), 141.0 (C-2 or C-8), 144.9 (C-2 or C-8), 145.8 (C-6a or C-10b), 146.7 (C-6a or C-10b), 168.3 ($\underline{\text{C}}\text{O}_2\text{H}$), 168.4 ($\underline{\text{C}}\text{O}_2\text{H}$), 180.8 (C-4 or C-10), 183.7 (C-4 or C-10). LC–MS (m/z): positive mode 301 [$\text{M} + \text{H}$] $^+$. Purity by HPLC–UV (254 nm)–ESI–MS: 96.0%. Mp: >300 °C dec. (Lit. mp: >320 °C)¹⁸⁵

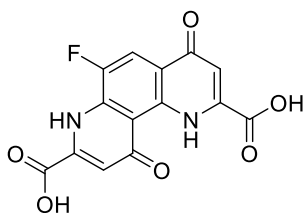
Preparation of 68b



Tetramethyl 2,2'-((4-fluoro-1,3-phenylene)bis(azanediyl))bis(but-2-enedioate) (66b, LW_YK104). The compound was synthesized using 4-fluorobenzene-1,3-diamine (5.0 g, 39.6 mmol). The product was isolated as a yellow oil (9.7 g, 60% yield). ^1H NMR (600 MHz, CDCl_3) δ 3.72 (s, 3H, $\text{CO}_2\text{C}\underline{\text{H}}_3$), 3.73 (s, 3H, $\text{CO}_2\text{C}\underline{\text{H}}_3$), 3.75 (s, 3H, $\text{CO}_2\text{C}\underline{\text{H}}_3$), 3.78 (s, 3H, $\text{CO}_2\text{C}\underline{\text{H}}_3$), 5.41 (s, 1H, 3'-H or 3''-H), 5.56 (s, 1H, 3'-H or 3''-H), 6.44 – 6.51 (m, 1H, 2-H), 6.55 – 6.62 (m, 1H, 6-H), 6.93 – 7.00 (m, 1H, 5-H), 9.44 – 9.57 (m, 2H, 2 \times $\underline{\text{N}}\underline{\text{H}}$). ^{13}C NMR (151 MHz, CDCl_3) δ 51.3 ($\text{CO}_2\text{C}\underline{\text{H}}_3$), 51.4 ($\text{CO}_2\text{C}\underline{\text{H}}_3$), 52.9 ($\text{CO}_2\text{C}\underline{\text{H}}_3$), 53.0 ($\text{CO}_2\text{C}\underline{\text{H}}_3$), 94.2 (C-3' or C-3''), 95.5 (C-3' or C-3''), 115.7 (C-2), 116.1 (d, $J = 21.2$ Hz, C-5), 117.7 (d, $J = 7.6$ Hz, C-6), 129.0 (d, $J = 12.9$ Hz, C-3), 136.8 (d, $J = 3.0$ Hz, C-1), 146.6 (C-2' or C-2''), 147.9 (C-2' or C-2''), 151.9 (d, $J = 243.4$ Hz, C-4), 163.7 ($\underline{\text{C}}\text{O}_2\text{Me}$), 164.3 ($\underline{\text{C}}\text{O}_2\text{Me}$), 169.7 ($\underline{\text{C}}\text{O}_2\text{Me}$), 169.8 ($\underline{\text{C}}\text{O}_2\text{Me}$). LC–MS (m/z): positive mode 411 [$\text{M} + \text{H}$] $^+$. Purity by HPLC–UV (254 nm)–ESI–MS: 98.4%.

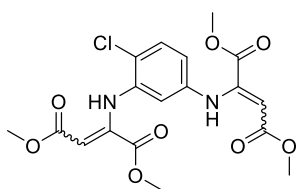


Dimethyl 6-fluoro-4,10-dioxo-1,4,7,10-tetrahydro-1,7-phenanthroline-2,8-dicarboxylate (67b). The compound was synthesized using **66b** (9.48 g, 23.1 mmol). The product was isolated as a white solid (560 mg, 7% yield). ^1H NMR (600 MHz, CDCl_3) δ 4.07 (s, 3H, $\text{CO}_2\text{C}\underline{\text{H}}_3$), 4.11 (s, 3H, $\text{CO}_2\text{C}\underline{\text{H}}_3$), 7.14 – 7.21 (m, 2H, 3-H, 9-H), 8.27 – 8.38 (m, 1H, 5-H), 14.20 (br, 1H, $\underline{\text{N}}\underline{\text{H}}$). ^{13}C NMR (151 MHz, CDCl_3) δ 53.8 ($\text{CO}_2\text{C}\underline{\text{H}}_3$), 54.4 ($\text{CO}_2\text{C}\underline{\text{H}}_3$), 114.0 (C-3 or C-9), 114.1 (C-3 or C-9), 114.2 (C-10a), 115.4 (C-5), 121.1 (d, $J = 5.1$ Hz, C-4a), 133.9 (d, $J = 16.1$ Hz, C-6a), 136.0 (C-10b), 137.0 (C-2 or C-8), 137.0 (C-2 or C-8), 148.0 (d, $J = 248.8$ Hz, C-6), 161.9 ($\underline{\text{C}}\text{O}_2\text{Me}$), 162.2 ($\underline{\text{C}}\text{O}_2\text{Me}$), 176.8 (C-4 or C-10), 180.7 (C-4 or C-10). LC–MS (m/z): positive mode 347 [$\text{M} + \text{H}$] $^+$. Purity by HPLC–UV (254 nm)–ESI–MS: 99.1%.

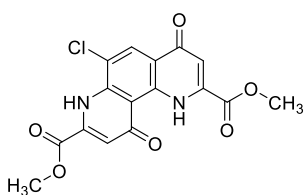


6-Fluoro-4,10-dioxo-1,4,7,10-tetrahydro-1,7-phenanthroline-2,8-dicarboxylic acid (68b, LW22). The compound was synthesized using **67b** (35 mg, 0.101 mmol). The product was isolated as a white solid (23 mg, 72% yield). ^1H NMR (600 MHz, D_2O , ND_3) δ 7.07 (s, 1H, 3-H or 9-H), 7.17 (s, 1H, 3-H or 9-H), 7.76 – 7.89 (m, 1H, 5-H). ^{13}C NMR (151 MHz, D_2O , ND_3) δ 108.9 (d, $J = 22.0$ Hz, C-5), 112.7 (C-3 or C-9), 114.9 (C-3 or C-9), 117.7 (C-10a), 121.5 (d, $J = 7.9$ Hz, C-4a), 140.3 (C-2 or C-8), 145.1 (C-2 or C-8), 145.8 (d, $J = 14.2$ Hz, C-6a), 158.1 (d, $J = 251.3$ Hz, C-6), 159.1 (C-10b), 169.9 (CO_2H), 176.7 (CO_2H), 179.8 (C-4 or C-10), 180.6 (C-4 or C-10). LC–MS (m/z): positive mode 319 [$\text{M} + \text{H}$] $^+$. Purity by HPLC–UV (254 nm)–ESI–MS: 99.8%. Mp: >300 °C dec.

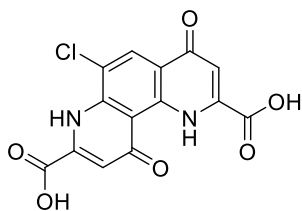
Preparation of 68c



Tetramethyl 2,2'-((4-chloro-1,3-phenylene)bis(azanediyl))bis(but-2-enedioate) (66c, LW24). The compound was synthesized using 4-chlorobenzene-1,3-diamine (2.0 g, 14 mmol). The product was isolated as a yellow oil (3.9 g, 66% yield). ^1H NMR (500 MHz, $\text{DMSO}-d_6$) δ 3.65 (s, 3H, CO_2CH_3), 3.69 (s, 3H, CO_2CH_3), 3.69 (s, 3H, CO_2CH_3), 3.73 (s, 3H, CO_2CH_3), 5.39 (s, 1H, 3'-H or 3''-H), 5.52 (s, 1H, 3'-H or 3''-H), 6.52 (d, $J = 2.5$ Hz, 1H, 2-H), 6.61 (dd, $J = 2.6, 8.6$ Hz, 1H, 6-H), 7.37 (d, $J = 8.6$ Hz, 1H, 5-H), 9.47 (s, 1H, NH), 9.65 (s, 1H, NH). ^{13}C NMR (126 MHz, $\text{DMSO}-d_6$) δ 51.3 (CO_2CH_3), 51.6 (CO_2CH_3), 53.2 (CO_2CH_3), 53.3 (CO_2CH_3), 96.1 (C-3' or C-3''), 96.3 (C-3' or C-3''), 112.9 (C-2), 116.4 (C-6), 118.8 (C-4), 130.0 (C-5), 137.3 (C-2' or C-2''), 140.5 (C-2' or C-2''), 145.8 (C-1 or C-3), 146.1 (C-1 or C-3), 163.3 (CO_2Me), 164.3 (CO_2Me), 167.8 (CO_2Me), 168.8 (CO_2Me). LC–MS (m/z): positive mode 427 [$\text{M} + \text{H}$] $^+$. Purity by HPLC–UV (254 nm)–ESI–MS: 96.5%.

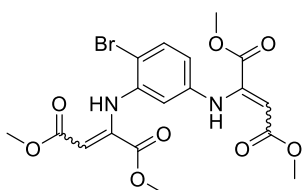


Dimethyl 6-chloro-4,10-dioxo-1,4,7,10-tetrahydro-1,7-phenanthroline-2,8-dicarboxylate (67c, LW25). The compound was synthesized using **66c** (3.60 g, 8.43 mmol). The product was isolated as a white solid (0.90 g, 30% yield). ^1H NMR (600 MHz, CDCl_3) δ 4.07 (s, 3H, CO_2CH_3), 4.12 (s, 3H, CO_2CH_3), 7.17 (s, 1H, 3-H or 9-H), 7.19 (s, 1H, 3-H or 9-H), 8.64 (s, 1H, 5-H), 9.81 (br, 1H, NH), 14.37 (s, 1H, NH). ^{13}C NMR (151 MHz, CDCl_3) δ 53.8 (CO_2CH_3), 54.4 (CO_2CH_3), 113.8 (C-10a), 114.9 (C-3 or C-9), 115.2 (C-3 or C-9), 118.3 (C-4a), 121.5 (C-6), 130.6 (C-5), 136.0 (C-2 or C-8), 137.1 (C-2 or C-8), 139.2 (C-6a or C-10b), 139.2 (C-6a or C-10b), 161.8 (CO_2Me), 162.0 (CO_2Me), 176.4 (C-4 or C-10), 181.2 (C-4 or C-10). LC–MS (m/z): positive mode 363 [$\text{M} + \text{H}$] $^+$. Purity by HPLC–UV (254 nm)–ESI–MS: 93.1%.

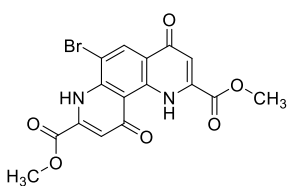


6-Chloro-4,10-dioxo-1,4,7,10-tetrahydro-1,7-phenanthroline-2,8-dicarboxylic acid (68c, LW212). The compound was synthesized using **67c** (100 mg, 0.30 mmol). The product was isolated as a yellow solid (55 mg, 50% yield). ^1H NMR (600 MHz, D_2O) δ 7.02 (s, 1H, 3-H or 9-H), 7.14 (s, 1H, 3-H or 9-H), 8.18 (s, 1H, 5-H). ^{13}C NMR (151 MHz, D_2O) δ 111.2 (C-3 or C-9), 112.8 (C-3 or C-9), 114.7 (C-10a), 119.5 (C-4a, C-6), 124.4 (C-5), 140.2 (C-2, C-8), 143.3 (C-6a, C-10b), 167.6 ($2 \times \text{CO}_2\text{H}$), 178.1 (C-4, C-10). LC-MS (m/z): positive mode 335 [$\text{M} + \text{H}$] $^+$. Purity by HPLC-UV (254 nm)-ESI-MS: 99.3%. Mp: >300 °C dec.

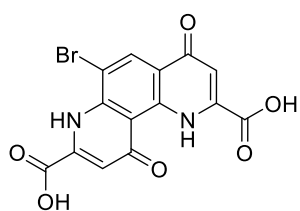
Preparation of 67d and 68d



Tetramethyl 2,2'-((4-bromo-1,3-phenylene)bis(azanediyl))bis(but-2-enedioate) (66d, LW11). The compound was synthesized using 4-bromobenzene-1,3-diamine (2.30 g, 12.3 mmol). The product was isolated as a yellow oil (2.20 g, 38% yield). ^1H NMR (600 MHz, CDCl_3) δ 3.73 (s, 3H, CO_2CH_3), 3.75 (s, 3H, CO_2CH_3), 3.76 (s, 3H, CO_2CH_3), 3.79 (s, 3H, CO_2CH_3), 5.46 (s, 1H, 3'-H or 3''-H), 5.59 (s, 1H, 3'-H or 3''-H), 6.28 (d, $J = 2.4$ Hz, 1H, 2-H), 6.48 (dd, $J = 2.5, 8.5$ Hz, 1H, 6-H), 7.43 (d, $J = 8.5$ Hz, 1H, 5-H), 9.48 (s, 1H, NH), 9.65 (s, 1H, NH). ^{13}C NMR (151 MHz, CDCl_3) δ 51.3 (CO_2CH_3), 51.5 (CO_2CH_3), 53.0 (CO_2CH_3), 53.1 (CO_2CH_3), 95.5 (C-3' or C-3''), 97.1 (C-3' or C-3''), 110.5 (C-4), 113.6 (C-2), 117.3 (C-6), 133.2 (C-5), 139.4 (C-2' or C-2''), 140.4 (C-2' or C-2''), 145.9 (C-1 or C-3), 147.1 (C-1 or C-3), 163.9 (CO_2Me), 164.2 (CO_2Me), 169.3 (CO_2Me), 169.6 (CO_2Me). LC-MS (m/z): positive mode 473 [$\text{M} + \text{H}$] $^+$. Purity by HPLC-UV (254 nm)-ESI-MS: 68.4%.

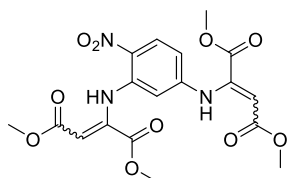


Dimethyl 6-bromo-4,10-dioxo-1,4,7,10-tetrahydro-1,7-phenanthroline-2,8-dicarboxylate (67d, LW151). The compound was synthesized using **66d** (2.20 g, 4.67 mmol). The product was isolated as a yellow solid (456 mg, 24% yield). ^1H NMR (600 MHz, CDCl_3) δ 4.07 (s, 3H, CO_2CH_3), 4.12 (s, 3H, CO_2CH_3), 7.17 (s, 1H, 3-H or 9-H), 7.19 (s, 1H, 3-H or 9-H), 8.64 (s, 1H, 5-H), 9.81 (br, 1H, NH), 14.37 (s, 1H, NH). ^{13}C NMR (151 MHz, CDCl_3) δ 53.8 (CO_2CH_3), 54.4 (CO_2CH_3), 113.8 (C-10a), 114.9 (C-3 or C-9), 115.2 (C-3 or C-9), 118.3 (C-4a), 121.5 (C-6), 130.6 (C-5), 136.0 (C-2 or C-8), 137.1 (C-2 or C-8), 139.2 (C-6a or C-10b), 139.2 (C-6a or C-10b), 161.8 (CO_2Me), 162.0 (CO_2Me), 176.4 (C-4 or C-10), 181.2 (C-4 or C-10). LC-MS (m/z): positive mode 407 [$\text{M} + \text{H}$] $^+$. Purity by HPLC-UV (254 nm)-ESI-MS: 96.4%. Mp: >290 °C dec.

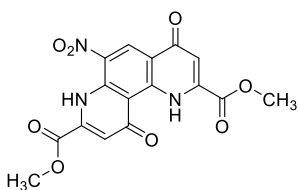


6-Bromo-4,10-dioxo-1,4,7,10-tetrahydro-1,7-phenanthroline-2,8-dicarboxylic acid (68d, LW23). The compound was synthesized using **67d** (42 mg, 0.103 mmol). The product was isolated as a brown solid (29 mg, 74% yield). ^1H NMR (600 MHz, D_2O , ND_3) δ 7.19 (s, 1H, 3-H or 9-H), 7.27 (s, 1H, 3-H or 9-H), 8.66 (s, 1H, 5-H). ^{13}C NMR (151 MHz, D_2O , ND_3) δ 113.5 (C-3 or C-9), 115.0 (C-3 or C-9), 117.0 (C-10a), 122.5 (C-6), 123.7 (C-4a), 130.4 (C-5), 143.3 (C-2 or C-8), 145.8 (C-2 or C-8), 151.5 (C-10b), 159.6 (C-6a), 169.9 ($\text{C}=\text{O}$), 176.8 ($\text{C}=\text{O}$), 180.4 (C-4 or C-10), 180.4 (C-4 or C-10). LC-MS (m/z): positive mode 379 $[\text{M} + \text{H}]^+$. Purity by HPLC-UV (254 nm)-ESI-MS: 95.7%. Mp: >300 °C dec.

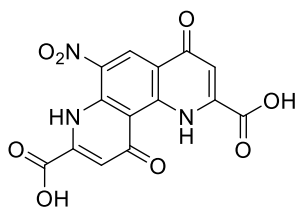
Preparation of 68e



Tetramethyl 2,2'-((4-nitro-1,3-phenylene)bis(azanediy))bis(but-2-enedioate) (66e, LW334). 4-Nitrobenzene-1,3-diamine (2.0 g, 13 mmol) was mixed with MeOH (25 mL) and DMAD (4.8 mL, 39 mmol, 3 equiv.) was added dropwise at rt while stirring. Then, the mixture was refluxed for 24 h. After that, MeOH was removed under reduced pressure, and the residue was purified by column chromatography (4:1 petroleum ether/EtOAc). The product was isolated as a yellow solid (3.9 g, 68% yield). ^1H NMR (600 MHz, CDCl_3) δ 3.76 (s, 3H, CO_2CH_3), 3.80 (s, 3H, CO_2CH_3), 3.83 (s, 3H, CO_2CH_3), 3.84 (s, 3H, CO_2CH_3), 5.69 (s, 1H, 3'-H or 3''-H), 5.88 (s, 1H, 3'-H or 3''-H), 6.04 (d, $J = 2.2$ Hz, 1H, 2-H), 6.44 (dd, $J = 2.3, 9.1$ Hz, 1H, 6-H), 8.10 (d, $J = 9.1$ Hz, 1H, 5-H), 9.62 (s, 1H, NH), 11.15 (s, 1H, NH). ^{13}C NMR (151 MHz, CDCl_3) δ 51.8 (CO_2CH_3), 51.9 (CO_2CH_3), 53.4 ($2 \times \text{CO}_2\text{CH}_3$), 100.3 (C-3' or C-3''), 104.6 (C-3' or C-3''), 108.7 (C-2), 112.6 (C-5), 128.0 (C-6), 132.6 (C-3), 138.9 (C-2' or C-2''), 142.7 (C-2' or C-2''), 144.8 (C-1), 146.2 (C-4), 163.6 ($\text{C}=\text{O}$), 164.1 ($\text{C}=\text{O}$), 167.5 ($\text{C}=\text{O}$), 169.0 ($\text{C}=\text{O}$). LC-MS (m/z): positive mode 438 $[\text{M} + \text{H}]^+$. Purity by HPLC-UV (254 nm)-ESI-MS: 80.4%.



Dimethyl 6-nitro-4,10-dioxo-1,4,7,10-tetrahydro-1,7-phenanthroline-2,8-dicarboxylate (67e, LW339). The compound was synthesized using **66e** (3.80 g, 8.70 mmol). The product was further purified by column chromatography on a column of silica gel (99:1 DCM/MeOH) and isolated as a yellow solid (140 mg, 4% yield). ^1H NMR (600 MHz, CDCl_3) δ 4.09 (s, 3H, CO_2CH_3), 4.13 (s, 3H, CO_2CH_3), 7.15 (s, 1H, 3-H or 9-H), 7.24 (s, 1H, 3-H or 9-H), 9.57 (s, 1H, 5-H), 12.58 (s, 1H, NH), 14.81 (s, 1H, NH). ^{13}C NMR (151 MHz, CDCl_3) δ 54.0 (CO_2CH_3), 54.5 (CO_2CH_3), 113.6 (C-10a), 116.0 (C-3 or C-9), 116.4 (C-3 or C-9), 119.1 (C-4a), 131.2 (C-6), 132.1 (C-5), 136.8 (C-2 or C-8), 137.3 (C-2 or C-8), 138.0 (C-10b), 144.8 (C-6a), 161.3 ($\text{C}=\text{O}$), 161.7 ($\text{C}=\text{O}$), 177.1 (C-4 or C-10), 180.9 (C-4 or C-10). LC-MS (m/z): positive mode 374 $[\text{M} + \text{H}]^+$. Purity by HPLC-UV (254 nm)-ESI-MS: 92.6%.



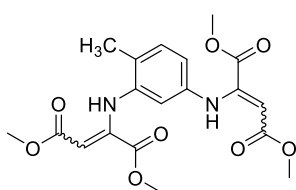
6-Nitro-4,10-dioxo-1,4,7,10-tetrahydro-1,7-phenanthroline-2,8-dicarboxylic acid (68e, LW347). The compound was synthesized using **67e** (15 mg, 0.04 mmol).

The product was isolated as a brown solid (10 mg, 72% yield). ^1H NMR (600 MHz, D_2O , ND_3) δ 6.96 (s, 1H, 3-H or 9-H), 7.07 (s, 1H, 3-H or 9-H), 8.76 (s, 1H, 5-H).

^{13}C NMR (151 MHz, D_2O , ND_3) δ 114.3 (C-3 or C-9), 115.5 (C-3 or C-9), 116.3 (C-10a), 119.3 (C-4a), 127.6 (C-5), 143.2 (C-6), 145.3 (C-2, C-8), 147.2 (C-6a, C-

10b), 168.8 (CO_2H), 172.8 (CO_2H), 181.5 (C-4 or C-10), 181.9 (C-4 or C-10). LC-MS (m/z): positive mode 346 $[\text{M} + \text{H}]^+$. Purity by HPLC-UV (254 nm)-ESI-MS: 99.6%. Mp: >300 °C dec.

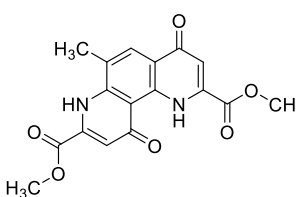
Preparation of 68f



Tetramethyl 2,2'-((4-methyl-1,3-phenylene)bis(azanediyl))bis(but-2-enedioate) (66f, LW409). The compound was synthesized using 4-methylbenzene-

1,3-diamine (1.00 g, 8.18 mmol). The product was isolated as a yellow oil (2.62 g, 79% yield). ^1H NMR (600 MHz, CDCl_3) δ 2.28 (s, 3H, ArCH_3), 3.71 (m, 6H, $2 \times \text{CO}_2\text{CH}_3$), 3.73 (s, 6H, $2 \times \text{CO}_2\text{CH}_3$), 5.35 (s, 1H, 3-H or 9-H), 5.43 (s, 1H, 3-H or

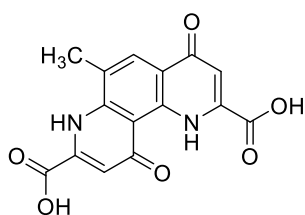
9-H), 6.30 (d, $J = 1.9$ Hz, 1H, 2-H), 6.58 (dd, $J = 2.1, 8.0$ Hz, 1H, 6-H), 7.07 (d, $J = 8.1$ Hz, 1H, 5-H), 9.46 (s, 1H, NH), 9.50 (s, 1H, NH). ^{13}C NMR (151 MHz, CDCl_3) δ 17.3 (ArCH_3), 51.1 (CO_2CH_3), 51.2 (CO_2CH_3), 52.8 (CO_2CH_3), 52.9 (CO_2CH_3), 93.5 (C-3' or C-3''), 93.8 (C-3' or C-3''), 114.4 (C-2), 117.4 (C-6), 126.4 (C-4), 131.1 (C-5), 138.8 (C-2' or C-2''), 139.6 (C-2' or C-2''), 148.0 (C-1 or C-3), 148.2 (C-1 or C-3), 164.3 (CO_2Me), 164.4 (CO_2Me), 169.8 (CO_2Me), 170.0 (CO_2Me). LC-MS (m/z): positive mode 407 $[\text{M} + \text{H}]^+$. Purity by HPLC-UV (254 nm)-ESI-MS: 87.9%.



Dimethyl 6-methyl-4,10-dioxo-1,4,7,10-tetrahydro-1,7-phenanthroline-2,8-dicarboxylate (67f, LW410). The compound was synthesized using **66f** (2.62 g,

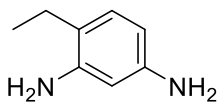
6.45 mmol). The product was isolated as a white solid (580 mg, 26% yield). ^1H NMR (600 MHz, CDCl_3) δ 2.57 (s, 3H, ArCH_3), 4.03 (s, 3H, CO_2CH_3), 4.07 (s, 3H, CO_2CH_3), 6.98 – 7.16 (m, 2H, 3-H, 9-H), 8.34 (s, 1H, 5-H), 9.24 (br, 1H, NH),

14.37 (s, 1H, NH). ^{13}C NMR (151 MHz, CDCl_3) δ 16.5 (ArCH_3), 53.6 (CO_2CH_3), 54.3 (CO_2CH_3), 112.8 (C-10a), 114.6 (C-3, C-9), 121.0 (C-4a), 121.3 (C-6), 131.2 (C-5), 135.5 (C-2 or C-8), 136.6 (C-2 or C-8), 139.2 (C-6a or C-10b), 141.8 (C-6a or C-10b), 162.3 (CO_2Me), 162.5 (CO_2Me), 177.3 (C-4 or C-10), 181.7 (C-4 or C-10). LC-MS (m/z): positive mode 343 $[\text{M} + \text{H}]^+$. Purity by HPLC-UV (254 nm)-ESI-MS: 96.1%.

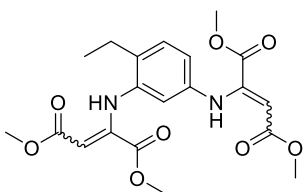


6-Methyl-4,10-dioxo-1,4,7,10-tetrahydro-1,7-phenanthroline-2,8-dicarboxylic acid (68f, LW412). The compound was synthesized using **67f** (200 mg, 0.584 mmol). The product was isolated as a white solid (183 mg, 100% yield). ^1H NMR (600 MHz, D_2O , ND_3) δ 2.01 (s, 3H, ArCH_3), 6.29 (s, 1H, 3-H or 9-H), 6.30 (s, 1H, 3-H or 9-H), 7.04 (s, 1H, 5-H). ^{13}C NMR (151 MHz, D_2O , ND_3) δ 18.3 (ArCH_3), 112.2 (C-10a), 112.7 (C-3 or C-9), 114.0 (C-3 or C-9), 120.7 (C-4a), 125.5 (C-6), 130.1 (C-5), 138.8 (C-2 or C-8), 142.8 (C-2 or C-8), 144.9 (C-6a or C-10b), 145.1 (C-6a or C-10b), 167.4 (CO_2H), 167.8 (CO_2H), 179.6 (C-4 or C-10), 183.2 (C-4 or C-10). LC-MS (m/z): positive mode 315 $[\text{M} + \text{H}]^+$. Purity by HPLC-UV (254 nm)-ESI-MS: 99.1%. Mp: >300 °C dec. (Lit. mp. > 300 °C dec.¹)

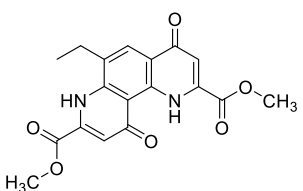
Preparation of 68g



4-Ethylbenzene-1,3-diamine (65g, LW96). The compound was synthesized using 2-ethyl-5-nitroaniline (675 mg, 4.07 mmol). The product was isolated as a white solid (554 mg, 100% yield) and directly used for the next step.

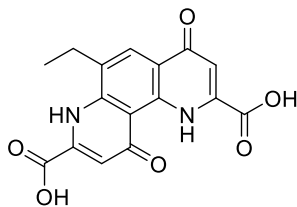


Tetramethyl 2,2'-((4-ethyl-1,3-phenylene)bis(azanediyl))bis(but-2-enedioate) (66g, LW99). The compound was synthesized using **65g** (554 mg, 4.07 mmol). The product was isolated as a yellow oil (1.47 g, 86% yield). ^1H NMR (600 MHz, CDCl_3) δ 1.24 (t, $J = 7.5$ Hz, 3H, ArCH_2CH_3), 2.65 (q, $J = 7.5$ Hz, 2H, ArCH_2CH_3), 3.71 – 3.72 (m, 6H, $2 \times \text{CO}_2\text{CH}_3$), 3.73 (s, 3H, CO_2CH_3), 3.74 (s, 3H, CO_2CH_3), 5.36 (s, 1H, 3'-H or 3''-H), 5.44 (s, 1H, 3'-H or 3''-H), 6.28 – 6.32 (m, 1H, 2-H), 6.61 – 6.66 (m, 1H, 6-H), 7.10 (d, $J = 8.1$ Hz, 1H, 5-H), 9.48 – 9.54 (m, 2H, $2 \times \text{NH}$). ^{13}C NMR (151 MHz, CDCl_3) δ 13.9 (ArCH_2CH_3), 24.1 (ArCH_2CH_3), 51.2 (CO_2CH_3), 51.2 (CO_2CH_3), 52.9 (CO_2CH_3), 52.9 (CO_2CH_3), 93.6 (C-3' or C-3''), 93.8 (C-3' or C-3''), 114.9 (C-2), 117.8 (C-6), 129.4 (C-5), 132.5 (C-4), 138.7 (C-2' or C-2''), 139.2 (C-2' or C-2''), 147.9 (C-1 or C-3), 148.5 (C-1 or C-3), 164.3 (CO_2Me), 164.4 (CO_2Me), 169.8 (CO_2Me), 170.1 (CO_2Me). LC-MS (m/z): positive mode 421 $[\text{M} + \text{H}]^+$. Purity by HPLC-UV (254 nm)-ESI-MS: 95.0%.



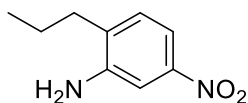
Dimethyl 6-ethyl-4,10-dioxo-1,4,7,10-tetrahydro-1,7-phenanthroline-2,8-dicarboxylate (67g, LW103). The compound was synthesized using **66g** (1.48 g, 3.52 mmol). The product was isolated as a yellow solid (370 mg, 30% yield). ^1H NMR (600 MHz, CDCl_3) δ 1.47 (t, $J = 7.4$ Hz, 3H, ArCH_2CH_3), 2.93 (q, $J = 7.3$ Hz, 2H, ArCH_2CH_3), 4.06 (s, 3H, CO_2CH_3), 4.10 (s, 3H, CO_2CH_3), 7.09 (s, 1H, 3-H or 9-H), 7.19 (s, 1H, 3-H or 9-H), 8.38 (s, 1H, 5-H), 14.55 (s, 1H, NH). ^{13}C NMR (151 MHz, CDCl_3) δ 12.6 (ArCH_2CH_3), 23.0 (ArCH_2CH_3), 53.7 (CO_2CH_3), 54.3 (CO_2CH_3), 112.8 (C-10a), 114.2 (C-3 or C-9), 114.5 (C-3 or C-9), 121.1 (C-4a), 127.0 (C-6), 128.9 (C-5), 135.6 (C-2 or C-8), 136.7 (C-2 or C-8), 139.1 (C-6a or C-10b),

141.4 (C-6a or C-10b), 162.2 (CO₂Me), 162.5 (CO₂Me), 177.0 (C-4 or C-10), 181.7 (C-4 or C-10). LC–MS (*m/z*): positive mode 357 [M + H]⁺. Purity by HPLC–UV (254 nm)–ESI–MS: 99.1%.

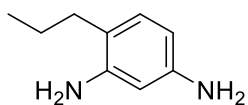


6-Ethyl-4,10-dioxo-1,4,7,10-tetrahydro-1,7-phenanthroline-2,8-dicarboxylic acid (68g, LW128). The compound was synthesized using **67g** (200 mg, 0.562 mmol). The product was isolated as a white solid (160 mg, 87% yield). ¹H NMR (600 MHz, D₂O, ND₃) δ 0.96 (t, *J* = 7.0 Hz, 3H, ArCH₂CH₃), 2.06 (s, 2H, ArCH₂CH₃), 6.19 (s, 1H, 3-H or 9-H), 6.22 (s, 1H, 3-H or 9-H), 6.84 (s, 1H, 5-H). ¹³C NMR (151 MHz, D₂O, ND₃) δ 12.5 (ArCH₂CH₃), 23.8 (ArCH₂CH₃), 111.8 (C-10a), 112.6 (C-3 or C-9), 113.8 (C-3 or C-9), 120.4 (C-4a), 126.5 (C-5), 129.4 (C-6), 138.4 (C-2 or C-8), 142.0 (C-2 or C-8), 144.6 (C-6a or C-10b), 144.8 (C-6a or C-10b), 167.1 (CO₂H), 167.7 (CO₂H), 179.5 (C-4 or C-10), 183.1 (C-4 or C-10). LC–MS (*m/z*): positive mode 329 [M + H]⁺. Purity by HPLC–UV (254 nm)–ESI–MS: 99.9%. Mp: >300 °C dec.

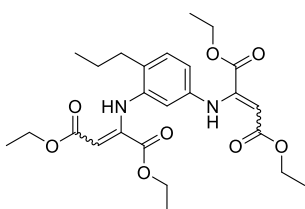
Preparation of 68h



5-Nitro-2-propylaniline (64k, LW243). The compound was synthesized using 2-propylaniline (3.5 g, 26 mmol). The product was isolated as a yellow solid (3.0 g, 64% yield). ¹H NMR (600 MHz, CDCl₃) δ 1.01 (t, *J* = 7.4 Hz, 3H, Ar(CH₂)₂CH₃), 1.67 (h, *J* = 7.4 Hz, 2H, ArCH₂CH₂CH₃), 2.51 (t, *J* = 7.7 Hz, 2H, ArCH₂CH₂CH₃), 3.95 (br, 2H, NH₂), 7.13 (d, *J* = 8.3 Hz, 1H, 3-H), 7.49 (d, *J* = 2.4 Hz, 1H, 6-H), 7.55 (dd, *J* = 2.4, 8.4 Hz, 1H, 4-H). ¹³C NMR (151 MHz, CDCl₃) δ 14.0 (Ar(CH₂)₂CH₃), 21.2 (ArCH₂CH₂CH₃), 33.2 (ArCH₂CH₂CH₃), 109.3 (C-6), 113.3 (C-4), 129.7 (C-3), 133.6 (C-2), 144.9 (C-5), 147.1 (C-1). LC–MS (*m/z*): positive mode 181 [M + H]⁺. Purity by HPLC–UV (254 nm)–ESI–MS: 99.1%.

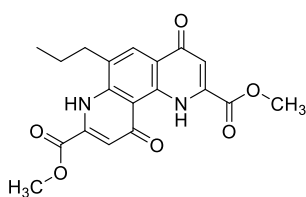


4-Propylbenzene-1,3-diamine (65h, LW246). The compound was synthesized using **64h** (2.9 g, 16 mmol). The product was isolated as a white solid (2.4 g, 100% yield) and used directly for the next step.

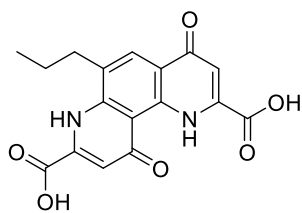


Tetraethyl 2,2'-((4-propyl-1,3-phenylene)bis(azanediyl))bis(but-2-enedioate) (66h, LW247). **65h** (2.39 g, 15.9 mmol) was dissolved in MeOH, and diethyl acetylenedicarboxylate (5.4 mL, 33.4 mmol, 2.1 equiv.) was added dropwise while stirring under argon at rt. The mixture was stirred at rt for overnight. After that, the solvent was removed under reduced pressure and the residue purified by column chromatography on a column of silica gel (8:2 petroleum ether/EtOAc). The product was isolated as a yellow oil (7.79 g, 100% yield). ¹H NMR (600 MHz, CDCl₃) δ 0.95 (t, *J* = 7.3 Hz, 3H,

Ar(CH₂)₂CH₃), 1.08 – 1.14 (m, 6H, 2 × CO₂CH₂CH₃), 1.26 – 1.32 (m, 6H, 2 × CO₂CH₂CH₃), 1.63 (h, *J* = 7.4 Hz, 2H, ArCH₂CH₂CH₃), 2.57 – 2.62 (m, 2H, ArCH₂CH₂CH₃), 4.13 – 4.21 (m, 8H, 4 × CO₂CH₂CH₃), 5.34 (s, 1H, 3'-H or 3''-H), 5.41 (s, 1H, 3'-H or 3''-H), 6.33 – 6.37 (m, 1H, 2-H), 6.61 (dd, *J* = 2.2, 8.1 Hz, 1H, 6-H), 7.05 (d, *J* = 8.1 Hz, 1H, 5-H), 9.44 – 9.55 (m, 2H, 2 × NH). ¹³C NMR (151 MHz, CDCl₃) δ 13.6 (CO₂CH₂CH₃), 13.7 (CO₂CH₂CH₃), 13.8 (Ar(CH₂)₂CH₃), 14.3 (CO₂CH₂CH₃), 14.3 (CO₂CH₂CH₃), 22.9 (ArCH₂CH₂CH₃), 33.1 (ArCH₂CH₂CH₃), 59.9 (CO₂CH₂CH₃), 59.9 (CO₂CH₂CH₃), 62.0 (CO₂CH₂CH₃), 62.0 (CO₂CH₂CH₃), 93.8 (C-3' or C-3''), 93.9 (C-3' or C-3''), 115.4 (C-2), 117.6 (C-6), 130.2 (C-5), 131.2 (C-4), 138.8 (C-2' or C-2''), 139.5 (C-2' or C-2''), 148.3 (C-1), 149.0 (C-3), 163.9 (CO₂Et), 164.0 (CO₂Et), 169.5 (CO₂Et), 169.7 (CO₂Et). LC-MS (*m/z*): positive mode 491 [M + H]⁺. Purity by HPLC-UV (254 nm)-ESI-MS: 98.0%.

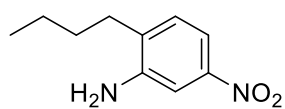


Diethyl 4,10-dioxo-6-propyl-1,4,7,10-tetrahydro-1,7-phenanthroline-2,8-dicarboxylate (67h, LW249). The compound was synthesized using **66h** (4.50 g, 9.18 mmol). The product was isolated as a beige solid (1.27 g, 35% yield). ¹H NMR (600 MHz, CDCl₃) δ 1.09 (t, *J* = 7.3 Hz, 3H, Ar(CH₂)₂CH₃), 1.45 – 1.51 (m, 6H, 2 × CO₂CH₂CH₃), 1.86 (h, *J* = 7.3 Hz, 2H, ArCH₂CH₂CH₃), 2.90 (t, *J* = 7.6 Hz, 2H, ArCH₂CH₂CH₃), 4.49 – 4.57 (m, 4H, 2 × CO₂CH₂CH₃), 7.16 (s, 1H, 3-H or 9-H), 7.26 (s, 1H, 3-H or 9-H), 8.43 (s, 1H, 5-H), 9.44 (br, 1H, NH), 14.67 (br, 1H, NH). ¹³C NMR (151 MHz, CDCl₃) δ 14.0 (CH₃), 14.1 (CH₃), 14.1 (CH₃), 21.9 (ArCH₂CH₂CH₃), 32.3 (ArCH₂CH₂CH₃), 63.1 (CO₂CH₂CH₃), 64.0 (CO₂CH₂CH₃), 113.0 (C-10a), 114.2 (C-3 or C-9), 114.4 (C-3 or C-9), 121.1 (C-4a), 125.7 (C-6), 130.2 (C-5), 135.8 (C-2 or C-8), 137.1 (C-2 or C-8), 139.2 (C-6a or C-10b), 141.5 (C-6a or C-10b), 161.7 (CO₂Et), 162.1 (CO₂Et), 177.2 (C-4 or C-10), 182.0 (C-4 or C-10). LC-MS (*m/z*): positive mode 399 [M + H]⁺. Purity by HPLC-UV (254 nm)-ESI-MS: 90.8%.

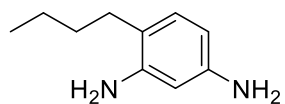


4,10-Dioxo-6-propyl-1,4,7,10-tetrahydro-1,7-phenanthroline-2,8-dicarboxylic acid (68h, LW257, PSB-20257). The compound was synthesized using **67h** (1.0 g, 2.5 mmol). The product was isolated as a white solid (600 mg, 70% yield). ¹H NMR (600 MHz, D₂O, ND₃) δ 0.95 (t, *J* = 7.1 Hz, 3H, Ar(CH₂)₂CH₃), 1.27 – 1.39 (m, 2H, ArCH₂CH₂CH₃), 2.01 – 2.14 (m, 2H, ArCH₂CH₂CH₃), 6.42 (s, 1H, 3-H or 9-H), 6.49 (s, 1H, 3-H or 9-H), 7.05 (s, 1H, 5-H). ¹³C NMR (151 MHz, D₂O, ND₃) δ 15.9 (Ar(CH₂)₂CH₃), 22.3 (ArCH₂CH₂CH₃), 33.1 (ArCH₂CH₂CH₃), 112.4 (C-10a), 112.9 (C-3 or C-9), 114.0 (C-3 or C-9), 120.8 (C-4a), 127.4 (C-5), 129.1 (C-6), 138.9 (C-2 or C-8), 142.5 (C-2 or C-8), 145.1 (C-6a or C-10b), 145.3 (C-6a or C-10b), 167.5 (CO₂H), 168.0 (CO₂H), 180.0 (C-4 or C-10), 183.5 (C-4 or C-10). LC-MS (*m/z*): positive mode 343 [M + H]⁺. Purity by HPLC-UV (254 nm)-ESI-MS: 96.4%. Mp: >300 °C dec.

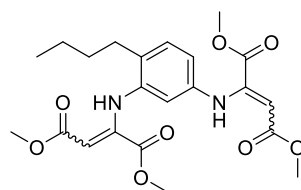
Preparation of 68i (bufrolin)



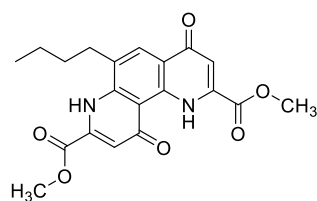
2-Butyl-5-nitroaniline (64i, LW9). The compound was synthesized using 2-butylaniline (5.0 g, 34 mmol). The product was isolated as a yellow solid (6.0 g, 91% yield). ^1H NMR (600 MHz, CDCl_3) δ 0.96 (t, $J = 7.3$ Hz, 3H, $\text{Ar}(\text{CH}_2)_3\text{CH}_3$), 1.42 (h, $J = 7.3$ Hz, 2H, $\text{Ar}(\text{CH}_2)_2\text{CH}_2\text{CH}_3$), 1.63 (p, $J = 7.6$ Hz, 2H, $\text{ArCH}_2\text{CH}_2\text{CH}_2\text{CH}_3$), 2.53 – 2.59 (m, 2H, $\text{ArCH}_2(\text{CH}_2)_2\text{CH}_3$), 7.16 (d, $J = 8.3$ Hz, 1H, 3-H), 7.54 (d, $J = 2.2$ Hz, 1H, 6-H), 7.58 (dd, $J = 2.2, 8.2$ Hz, 1H, 4-H). ^{13}C NMR (151 MHz, CDCl_3) δ 13.9 ($\text{Ar}(\text{CH}_2)_3\text{CH}_3$), 22.6 ($\text{Ar}(\text{CH}_2)_2\text{CH}_2\text{CH}_3$), 30.2 ($\text{ArCH}_2\text{CH}_2\text{CH}_2\text{CH}_3$), 31.0 ($\text{ArCH}_2(\text{CH}_2)_2\text{CH}_3$), 109.8 (C-6), 113.8 (C-4), 129.8 (C-3), 134.3 (C-2), 144.1 (C-1 or C-5), 147.1 (C-1 or C-5). LC-MS (m/z): positive mode 195 [$\text{M} + \text{H}$] $^+$. Purity by HPLC-UV (254 nm)-ESI-MS: 99.2%.



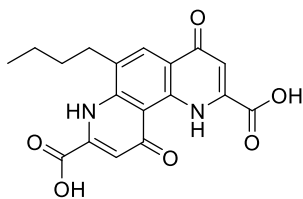
4-Butylbenzene-1,3-diamine (65i, LWX). The compound was synthesized using **64i** (1.50 g, 7.72 mmol). The product was isolated as a white solid (1.26 g, 99% yield) and directly used for the next step.



Tetramethyl 2,2'-((4-butyl-1,3-phenylene)bis(azanediyl))bis(but-2-enedioate) (66i, LW15). The compound was synthesized using **65i** (1.26 g, 7.67 mmol). The product was isolated as a yellow oil (1.78 g, 52% yield) and used directly for the next step. LC-MS (m/z): positive mode 449 [$\text{M} + \text{H}$] $^+$. Purity by HPLC-UV (254 nm)-ESI-MS: 89.9%.

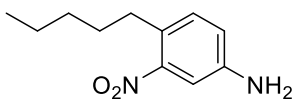


Dimethyl 6-butyl-4,10-dioxo-1,4,7,10-tetrahydro-1,7-phenanthroline-2,8-dicarboxylate (67i, LW16). The compound was synthesized using **66i** (1.50 g, 3.34 mmol). The product was isolated as a gray solid (450 mg, 35% yield). ^1H NMR (600 MHz, CDCl_3) δ 1.01 (t, $J = 7.3$ Hz, 3H, $\text{Ar}(\text{CH}_2)_3\text{CH}_3$), 1.49 (h, $J = 7.2$ Hz, 2H, $\text{Ar}(\text{CH}_2)_2\text{CH}_2\text{CH}_3$), 1.77 (p, $J = 7.7$ Hz, 2H, $\text{ArCH}_2\text{CH}_2\text{CH}_2\text{CH}_3$), 2.89 (t, $J = 7.7$ Hz, 2H, $\text{ArCH}_2(\text{CH}_2)_2\text{CH}_3$), 4.06 (s, 3H, CO_2CH_3), 4.10 (s, 3H, CO_2CH_3), 7.09 (s, 1H, 3-H or 9-H), 7.18 (s, 1H, 3-H or 9-H), 8.37 (s, 1H, 5-H), 9.38 (br, 1H, NH), 14.53 (s, 1H, NH). ^{13}C NMR (151 MHz, CDCl_3) δ 13.8 ($\text{Ar}(\text{CH}_2)_3\text{CH}_3$), 22.5 ($\text{Ar}(\text{CH}_2)_2\text{CH}_2\text{CH}_3$), 29.9 ($\text{ArCH}_2\text{CH}_2\text{CH}_2\text{CH}_3$), 30.7 ($\text{ArCH}_2(\text{CH}_2)_2\text{CH}_3$), 53.6 (CO_2CH_3), 54.3 (CO_2CH_3), 112.9 (C-10a), 114.4 (C-3, C-9), 121.2 (C-4a), 125.8 (C-6), 130.1 (C-5), 135.5 (C-2 or C-8), 136.6 (C-2 or C-8), 139.1 (C-6a or C-10b), 141.4 (C-6a or C-10b), 162.2 (CO_2Me), 162.6 (CO_2Me), 177.1 (C-4 or C-10), 181.8 (C-4 or C-10). LC-MS (m/z): positive mode 385 [$\text{M} + \text{H}$] $^+$. Purity by HPLC-UV (254 nm)-ESI-MS: 97.2%.

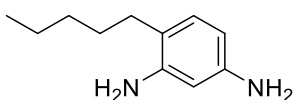


6-Butyl-4,10-dioxo-1,4,7,10-tetrahydro-1,7-phenanthroline-2,8-dicarboxylic acid (68i, LW19N, bufrolin). The compound was synthesized using **67i** (270 mg, 0.702 mmol). The product was isolated as a beige solid (219 mg, 88% yield). ^1H NMR (600 MHz, D_2O , ND_3) δ 1.02 (t, $J = 7.3$ Hz, 3H, $\text{Ar}(\text{CH}_2)_3\text{CH}_3$), 1.45 (h, $J = 7.3$ Hz, 2H, $\text{Ar}(\text{CH}_2)_2\text{CH}_2\text{CH}_3$), 1.57 (p, $J = 7.5$ Hz, 2H, $\text{ArCH}_2\text{CH}_2\text{CH}_2\text{CH}_3$), 2.56 – 2.62 (m, 2H, $\text{ArCH}_2(\text{CH}_2)_2\text{CH}_3$), 6.82 (s, 1H, 3-H or 9-H), 6.86 (s, 1H, 3-H or 9-H), 7.62 (s, 1H, 5-H). ^{13}C NMR (151 MHz, D_2O , ND_3) δ 16.0 ($\text{Ar}(\text{CH}_2)_3\text{CH}_3$), 24.7 ($\text{Ar}(\text{CH}_2)_2\text{CH}_2\text{CH}_3$), 31.6 ($\text{ArCH}_2\text{CH}_2\text{CH}_2\text{CH}_3$), 32.1 ($\text{ArCH}_2(\text{CH}_2)_2\text{CH}_3$), 113.3 (C-3 or C-9), 113.7 (C-10a), 114.2 (C-3 or C-9), 121.6 (C-4a), 128.0 (C-5), 131.4 (C-6), 140.1 (C-2 or C-8), 144.5 (C-2 or C-8), 145.7 (C-6a or C-10b), 147.2 (C-6a or C-10b), 168.8 (CO_2H), 169.0 (CO_2H), 180.6 (C-4 or C-10), 183.8 (C-4 or C-10). LC-MS (m/z): positive mode 357 [$\text{M} + \text{H}$] $^+$. Purity by HPLC-UV (254 nm)-ESI-MS: 99.6%. Mp: >300 °C dec. (Lit. mp: 300 °C dec.,¹⁸⁴ 305 – 310 °C¹⁸⁵)

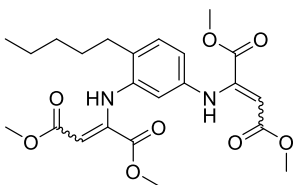
Preparation of 67j and 68j



3-Nitro-4-pentylaniline (64a, LW442). The compound was synthesized using 4-pentylaniline (2.0 g, 12.3 mmol). The product was isolated as an orange solid (2.5 g, 98% yield). ^1H NMR (600 MHz, CDCl_3) δ 0.88 (t, $J = 6.9$ Hz, 3H, $\text{Ar}(\text{CH}_2)_4\text{CH}_3$), 1.28 – 1.36 (m, 4H, $\text{Ar}(\text{CH}_2)_2(\text{CH}_2)_2\text{CH}_3$), 1.57 (p, $J = 7.4$ Hz, 2H, $\text{ArCH}_2\text{CH}_2(\text{CH}_2)_2\text{CH}_3$), 2.71 – 2.75 (m, 2H, $\text{ArCH}_2(\text{CH}_2)_3\text{CH}_3$), 6.82 (dd, $J = 2.5, 8.3$ Hz, 1H, 6-H), 7.09 (d, $J = 8.3$ Hz, 1H, 5-H), 7.18 (d, $J = 2.5$ Hz, 1H, 2-H). ^{13}C NMR (151 MHz, CDCl_3) δ 14.0 ($\text{Ar}(\text{CH}_2)_4\text{CH}_3$), 22.4 ($\text{Ar}(\text{CH}_2)_3\text{CH}_2\text{CH}_3$), 30.5 ($\text{Ar}(\text{CH}_2)_2\text{CH}_2\text{CH}_2\text{CH}_3$), 31.6 ($\text{ArCH}_2\text{CH}_2(\text{CH}_2)_2\text{CH}_3$), 32.1 ($\text{ArCH}_2(\text{CH}_2)_3\text{CH}_3$), 110.2 (C-2), 119.6 (C-6), 127.3 (C-4), 132.6 (C-5), 144.8 (C-1), 149.7 (C-3). LC-MS (m/z): positive mode 209 [$\text{M} + \text{H}$] $^+$. Purity by HPLC-UV (254 nm)-ESI-MS: 98.4%.

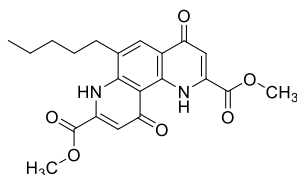


4-Pentylbenzene-1,3-diamine (65j, LW444). The compound was synthesized using **64a** (1.90 g, 9.13 mmol). The product was isolated as a white solid (1.63 g, 98% yield) and directly used for the next step.



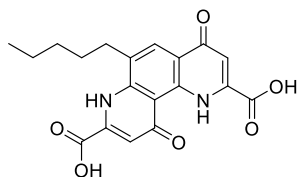
Tetramethyl 2,2'-((4-pentyl-1,3-phenylene)bis(azanediyl))bis(but-2-enedioate) (66j, LW445). The compound was synthesized using **65j** (1.63 g, 9.13 mmol). The product was isolated as a yellow oil (1.97 g, 47% yield). ^1H NMR (600 MHz, CDCl_3) δ 0.88 (t, $J = 6.9$ Hz, 3H, $\text{Ar}(\text{CH}_2)_4\text{CH}_3$), 1.28 – 1.38 (m, 4H, $\text{Ar}(\text{CH}_2)_2(\text{CH}_2)_2\text{CH}_3$), 1.61 (p, $J = 7.4$ Hz, 2H, $\text{ArCH}_2\text{CH}_2(\text{CH}_2)_2\text{CH}_3$), 2.58 – 2.63 (m, 2H, $\text{ArCH}_2(\text{CH}_2)_3\text{CH}_3$), 3.71 (s, 3H, CO_2CH_3), 3.71 (s, 3H, CO_2CH_3), 3.72 (s, 3H, CO_2CH_3), 3.73 (s, 3H, CO_2CH_3), 5.36 (s, 1H, 3'-H or 3''-H), 5.43 (s, 1H, 3'-H or 3''-H), 6.29 (d, $J = 2.0$ Hz, 1H, 2-H), 6.61 (dd, $J = 2.1, 8.1$ Hz, 1H, 6-H), 7.07 (d, $J = 8.1$ Hz, 1H, 5-H), 9.44 – 9.55 (m, 2H, 2 \times NH). ^{13}C NMR (151 MHz, CDCl_3) δ 14.0 ($\text{Ar}(\text{CH}_2)_4\text{CH}_3$), 22.4 ($\text{Ar}(\text{CH}_2)_3\text{CH}_2\text{CH}_3$), 29.2 ($\text{Ar}(\text{CH}_2)_2\text{CH}_2\text{CH}_2\text{CH}_3$), 31.0 ($\text{ArCH}_2\text{CH}_2(\text{CH}_2)_2\text{CH}_3$), 31.5 ($\text{ArCH}_2(\text{CH}_2)_3\text{CH}_3$), 51.1 (CO_2CH_3), 51.2 (CO_2CH_3), 52.8 (CO_2CH_3), 52.8 (CO_2CH_3), 93.6 (C-3' or C-3''), 93.7

(C-3' or C-3"), 115.1 (C-2), 117.6 (C-6), 130.3 (C-5), 131.3 (C-4), 138.7 (C-2' or C-2"), 139.3 (C-2' or C-2"), 147.9 (C-1), 148.5 (C-3), 164.3 (CO_2Me), 164.4 (CO_2Me), 169.8 (CO_2Me), 170.0 (CO_2Me). LC–MS (m/z): positive mode 463 $[\text{M} + \text{H}]^+$. Purity by HPLC–UV (254 nm)–ESI–MS: 86.2%.



Dimethyl 4,10-dioxo-6-pentyl-1,4,7,10-tetrahydro-1,7-phenanthroline-2,8-dicarboxylate (67j, LW450P).

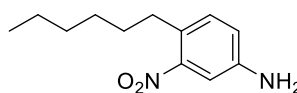
The compound was synthesized using **66j** (1.92 g, 4.16 mmol). The product was further purified by column chromatography on a column of silica gel (99:1 DCM/MeOH) and isolated as a beige solid (468 mg, 28% yield). ^1H NMR (600 MHz, CDCl_3) δ 0.92 (t, $J = 7.1$ Hz, 3H, $\text{Ar}(\text{CH}_2)_4\text{CH}_3$), 1.35 – 1.50 (m, 4H, $\text{Ar}(\text{CH}_2)_2(\text{CH}_2)_2\text{CH}_3$), 1.79 (p, $J = 7.7$ Hz, 2H, $\text{ArCH}_2\text{CH}_2(\text{CH}_2)_2\text{CH}_3$), 2.87 (t, $J = 7.8$ Hz, 2H, $\text{ArCH}_2(\text{CH}_2)_3\text{CH}_3$), 4.06 (s, 3H, CO_2CH_3), 4.10 (s, 3H, CO_2CH_3), 7.08 (s, 1H, 3-H or 9-H), 7.15 (s, 1H, 3-H or 9-H), 8.37 (s, 1H, 5-H), 9.38 (br, 1H, NH), 14.49 (s, 1H, NH). ^{13}C NMR (151 MHz, CDCl_3) δ 13.9 ($\text{Ar}(\text{CH}_2)_4\text{CH}_3$), 22.4 ($\text{Ar}(\text{CH}_2)_3\text{CH}_2\text{CH}_3$), 28.3 ($\text{Ar}(\text{CH}_2)_2\text{CH}_2\text{CH}_2\text{CH}_3$), 30.2 ($\text{ArCH}_2\text{CH}_2(\text{CH}_2)_2\text{CH}_3$), 31.6 ($\text{ArCH}_2(\text{CH}_2)_3\text{CH}_3$), 53.6 (CO_2CH_3), 54.3 (CO_2CH_3), 113.0 (C-10a), 114.3 (C-3 or C-9), 114.5 (C-3 or C-9), 121.2 (C-4a), 125.7 (C-6), 130.1 (C-5), 135.4 (C-2 or C-8), 136.6 (C-2 or C-8), 139.1 (C-6a or C-10b), 141.3 (C-6a or C-10b), 162.3 (CO_2Me), 162.6 (CO_2Me), 177.2 (C-4 or C-10), 181.8 (C-4 or C-10). LC–MS (m/z): positive mode 399 $[\text{M} + \text{H}]^+$. Purity by HPLC–UV (254 nm)–ESI–MS: 98.2%. Mp: 190–191 °C.



4,10-Dioxo-6-pentyl-1,4,7,10-tetrahydro-1,7-phenanthroline-2,8-dicarboxylic acid (68j, LW458).

The compound was synthesized using **67j** (100 mg, 0.25 mmol). The product was isolated as a white solid (60 mg, 65% yield). ^1H NMR (600 MHz, D_2O , ND_3) δ 0.90 (t, $J = 7.2$ Hz, 3H, $\text{Ar}(\text{CH}_2)_4\text{CH}_3$), 1.23 (s, 4H, $\text{Ar}(\text{CH}_2)_2(\text{CH}_2)_2\text{CH}_3$), 1.31 (p, $J = 5.9, 6.9$ Hz, 2H, $\text{ArCH}_2\text{CH}_2(\text{CH}_2)_2\text{CH}_3$), 2.03 (s, 2H, $\text{ArCH}_2(\text{CH}_2)_3\text{CH}_3$), 6.49 (d, $J = 1.3$ Hz, 1H, 3-H or 9-H), 6.57 (d, $J = 1.2$ Hz, 1H, 3-H or 9-H), 7.12 (s, 1H, 5-H). ^{13}C NMR (151 MHz, D_2O , ND_3) δ 16.1 ($\text{Ar}(\text{CH}_2)_4\text{CH}_3$), 24.7 ($\text{Ar}(\text{CH}_2)_3\text{CH}_2\text{CH}_3$), 28.9 ($\text{Ar}(\text{CH}_2)_2\text{CH}_2\text{CH}_2\text{CH}_3$), 31.2 ($\text{ArCH}_2\text{CH}_2(\text{CH}_2)_2\text{CH}_3$), 33.7 ($\text{ArCH}_2(\text{CH}_2)_3\text{CH}_3$), 112.7 (C-10a), 113.1 (C-3 or C-9), 114.1 (C-3 or C-9), 121.0 (C-4a), 127.7 (C-5), 129.2 (C-6), 139.2 (C-2 or C-8), 142.5 (C-2 or C-8), 145.2 (C-6a or C-10b), 145.5 (C-6a or C-10b), 167.4 (CO_2H), 168.1 (CO_2H), 180.1 (C-4 or C-10), 183.7 (C-4 or C-10). LC–MS (m/z): positive mode 371 $[\text{M} + \text{H}]^+$. Purity by HPLC–UV (254 nm)–ESI–MS: 99.5%. Mp: >300 °C dec. (Lit. mp: 297 – 300 °C,¹⁸⁴ 300 – 305 °C¹⁸⁵)

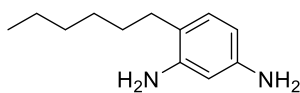
Preparation of 68k



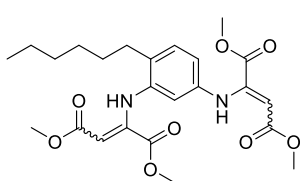
3-Nitro-4-hexylaniline (64b, LW418).

The compound was synthesized using 4-hexylaniline (2.2 mL, 11.2 mmol). The product was isolated as an orange solid (2.0 g, 80% yield). ^1H NMR (600 MHz, CDCl_3) δ 0.87 (t, $J = 6.9$ Hz, 3H, $\text{Ar}(\text{CH}_2)_5\text{CH}_3$), 1.26 – 1.36 (m, 6H, $\text{Ar}(\text{CH}_2)_2(\text{CH}_2)_3\text{CH}_3$), 1.56 (p, $J = 7.5$ Hz, 2H, $\text{ArCH}_2\text{CH}_2(\text{CH}_2)_3\text{CH}_3$), 2.73 (t, $J = 7.8$ Hz, 3H,

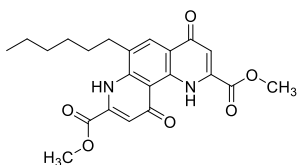
ArCH₂(CH₂)₄CH₃), 6.84 (dd, $J = 2.3, 8.2$ Hz, 1H, 6-H), 7.09 (d, $J = 8.2$ Hz, 1H, 5-H), 7.20 (d, $J = 2.2$ Hz, 1H, 2-H). ¹³C NMR (151 MHz, CDCl₃) δ 14.0 (Ar(CH₂)₅CH₃), 22.6 (Ar(CH₂)₄CH₂CH₃), 29.2 (Ar(CH₂)₃CH₂CH₂CH₃), 30.8 (Ar(CH₂)₂CH₂(CH₂)₂CH₃), 31.5 (ArCH₂CH₂(CH₂)₃CH₃), 32.2 (ArCH₂(CH₂)₄CH₃), 110.5 (C-2), 119.9 (C-6), 127.7 (C-4), 132.6 (C-5), 144.4 (C-1), 149.7 (C-3). LC–MS (m/z): positive mode 223 [M + H]⁺. Purity by HPLC–UV (254 nm)–ESI-MS: 98.0%.



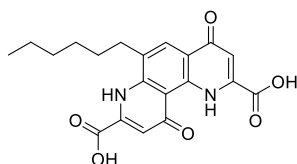
4-Hexylbenzene-1,3-diamine (65k, LW420). The compound was synthesized using **64b** (2.0 g, 9.0 mmol). The product was isolated as a white solid (1.7 g, 99% yield).



Tetramethyl 2,2'-((4-hexyl-1,3-phenylene)bis(azanediyl))bis(but-2-enedioate) (66k, LW423). The compound was synthesized using **65k** (1.7 g, 9.0 mmol). The product was isolated as a yellow oil (2.7 g, 63% yield). ¹H NMR (600 MHz, CDCl₃) δ 0.87 (t, $J = 7.0$ Hz, 3H, Ar(CH₂)₅CH₃), 1.27 – 1.32 (m, 4H, Ar(CH₂)₃(CH₂)₂CH₃), 1.32 – 1.38 (m, 2H, Ar(CH₂)₂CH₂(CH₂)₂CH₃), 1.60 (p, $J = 7.5$ Hz, 2H, ArCH₂CH₂(CH₂)₃CH₃), 2.57 – 2.64 (m, 2H, ArCH₂(CH₂)₄CH₃), 3.71 (s, 3H, CO₂CH₃), 3.72 (s, 3H, CO₂CH₃), 3.72 (s, 3H, CO₂CH₃), 3.74 (s, 3H, CO₂CH₃), 5.36 (s, 1H, 3'-H or 3''-H), 5.43 (s, 1H, 3'-H or 3''-H), 6.30 (d, $J = 2.1$ Hz, 1H, 2-H), 6.61 (dd, $J = 2.2, 8.1$ Hz, 1H, 6-H), 7.07 (d, $J = 8.1$ Hz, 1H, 5-H), 9.50 (s, 2H, 2 × NH). ¹³C NMR (151 MHz, CDCl₃) δ 14.0 (Ar(CH₂)₅CH₃), 22.6 (Ar(CH₂)₄CH₂CH₃), 29.0 (Ar(CH₂)₃CH₂CH₂CH₃), 29.5 (Ar(CH₂)₂CH₂(CH₂)₂CH₃), 31.1 (ArCH₂CH₂(CH₂)₃CH₃), 31.6 (ArCH₂(CH₂)₄CH₃), 51.2 (CO₂CH₃), 51.2 (CO₂CH₃), 52.8 (CO₂CH₃), 52.9 (CO₂CH₃), 93.6 (C-3' or C-3''), 93.7 (C-3' or C-3''), 115.1 (C-2), 117.7 (C-6), 130.3 (C-5), 131.4 (C-4), 138.7 (C-2' or C-2''), 139.3 (C-2' or C-2''), 147.9 (C-1), 148.5 (C-3), 164.4 (CO₂Me), 164.4 (CO₂Me), 169.8 (CO₂Me), 170.0 (CO₂Me). LC–MS (m/z): positive mode 477 [M + H]⁺. Purity by HPLC–UV (254 nm)–ESI-MS: 95.7%.

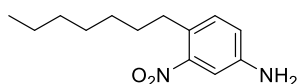


Dimethyl 4,10-dioxo-6-hexyl-1,4,7,10-tetrahydro-1,7-phenanthroline-2,8-dicarboxylate (67k, LW425). The compound was synthesized using **66k** (2.63 g, 5.52 mmol). The product was isolated as a white solid (640 mg, 28% yield). ¹H NMR (600 MHz, CDCl₃) δ 0.89 (t, $J = 7.0$ Hz, 3H, Ar(CH₂)₅CH₃), 1.29 – 1.40 (m, 4H, Ar(CH₂)₃(CH₂)₂CH₃), 1.47 (p, $J = 7.2$ Hz, 2H, Ar(CH₂)₂CH₂(CH₂)₂CH₃), 1.79 (p, $J = 7.7$ Hz, 2H, ArCH₂CH₂(CH₂)₃CH₃), 2.86 – 2.92 (m, 2H, ArCH₂(CH₂)₄CH₃), 4.06 (s, 3H, CO₂CH₃), 4.10 (s, 3H, CO₂CH₃), 7.11 (s, 1H, 3-H or 9-H), 7.16 (s, 1H, 3-H or 9-H), 8.39 (s, 1H, 5-H). ¹³C NMR (151 MHz, CDCl₃) δ 14.0 (Ar(CH₂)₅CH₃), 22.5 (Ar(CH₂)₄CH₂CH₃), 28.6 (Ar(CH₂)₃CH₂CH₂CH₃), 29.1 (Ar(CH₂)₂CH₂(CH₂)₂CH₃), 30.3 (ArCH₂CH₂(CH₂)₃CH₃), 31.5 (ArCH₂(CH₂)₄CH₃), 53.6 (CO₂CH₃), 54.3 (CO₂CH₃), 113.0 (C-10a), 114.4 (C-3 or C-9), 114.5 (C-3 or C-9), 121.3 (C-4a), 125.7 (C-6), 130.2 (C-5), 135.5 (C-2 or C-8), 136.6 (C-2 or C-8), 139.2 (C-6a or C-10b), 141.4 (C-6a or C-10b), 162.3 (CO₂Me), 162.6 (CO₂Me), 177.3 (C-4 or C-10), 181.9 (C-4 or C-10). LC–MS (m/z): positive mode 413 [M + H]⁺. Purity by HPLC–UV (254 nm)–ESI-MS: 89.3%.

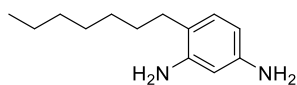


6-Hexyl-4,10-dioxo-1,4,7,10-tetrahydro-1,7-phenanthroline-2,8-dicarboxylic acid (68k, LW428). The compound was synthesized using **67k** (100 mg, 0.24 mmol). The product was isolated as a white solid (88 mg, 95% yield). ^1H NMR (600 MHz, D_2O , ND_3) δ 0.89 (t, $J = 6.7$ Hz, 3H, $\text{Ar}(\text{CH}_2)_5\text{CH}_3$), 1.17 – 1.36 (m, 8H, $\text{ArCH}_2(\text{CH}_2)_4\text{CH}_3$), 2.14 (s, 2H, $\text{ArCH}_2(\text{CH}_2)_4\text{CH}_3$), 6.57 (s, 1H, 3-H or 9-H), 6.62 (s, 1H, 3-H or 9-H), 7.25 (s, 1H, 5-H). ^{13}C NMR (151 MHz, D_2O , ND_3) δ 16.2 ($\text{Ar}(\text{CH}_2)_5\text{CH}_3$), 24.7 ($\text{Ar}(\text{CH}_2)_4\text{CH}_2\text{CH}_3$), 29.3 ($\text{Ar}(\text{CH}_2)_3\text{CH}_2\text{CH}_2\text{CH}_3$), 31.1 ($\text{Ar}(\text{CH}_2)_2\text{CH}_2(\text{CH}_2)_2\text{CH}_3$), 31.4 ($\text{ArCH}_2\text{CH}_2(\text{CH}_2)_3\text{CH}_3$), 33.7 ($\text{ArCH}_2(\text{CH}_2)_4\text{CH}_3$), 112.9 (C-10a), 113.2 (C-3 or C-9), 114.2 (C-3 or C-9), 121.2 (C-4a), 128.0 (C-5), 129.4 (C-6), 139.4 (C-2 or C-8), 142.7 (C-2 or C-8), 145.3 (C-6a or C-10b), 145.6 (C-6a or C-10b), 167.5 (CO_2H), 168.2 (CO_2H), 180.3 (C-4 or C-10), 183.9 (C-4 or C-10). LC-MS (m/z): positive mode 385 $[\text{M} + \text{H}]^+$. Purity by HPLC-UV (254 nm)-ESI-MS: 99.4%. Mp: >300 °C dec.

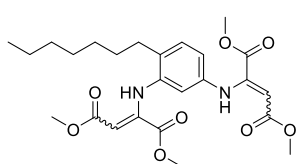
Preparation of 671 and 681



3-Nitro-4-heptylaniline (64c, LW443). The compound was synthesized using 4-heptylaniline (2.0 mg, 10.5 mmol). The product was isolated as an orange solid (2.45 mg, 99% yield). ^1H NMR (600 MHz, CDCl_3) δ 0.87 (t, $J = 7.0$ Hz, 3H, $\text{Ar}(\text{CH}_2)_6\text{CH}_3$), 1.24 – 1.34 (m, 8H, $\text{Ar}(\text{CH}_2)_2(\text{CH}_2)_4\text{CH}_3$), 1.56 (p, $J = 7.6$ Hz, 2H, $\text{ArCH}_2\text{CH}_2(\text{CH}_2)_4\text{CH}_3$), 2.68 – 2.76 (m, 2H, $\text{ArCH}_2(\text{CH}_2)_5\text{CH}_3$), 6.80 (dd, $J = 2.5$ Hz, 8.2 Hz, 1H, 6-H), 7.08 (d, $J = 8.3$ Hz, 1H, 5-H), 7.16 (d, $J = 2.5$ Hz, 1H, 2-H). ^{13}C NMR (151 MHz, CDCl_3) δ 14.1 ($\text{Ar}(\text{CH}_2)_6\text{CH}_3$), 22.6 ($\text{Ar}(\text{CH}_2)_5\text{CH}_2\text{CH}_3$), 29.0 ($\text{Ar}(\text{CH}_2)_4\text{CH}_2\text{CH}_2\text{CH}_3$), 29.4 ($\text{Ar}(\text{CH}_2)_3\text{CH}_2(\text{CH}_2)_2\text{CH}_3$), 30.9 ($\text{Ar}(\text{CH}_2)_2\text{CH}_2(\text{CH}_2)_3\text{CH}_3$), 31.8 ($\text{ArCH}_2\text{CH}_2(\text{CH}_2)_4\text{CH}_3$), 32.2 ($\text{ArCH}_2(\text{CH}_2)_5\text{CH}_3$), 110.1 (C-2), 119.5 (C-6), 127.2 (C-4), 132.6 (C-5), 145.0 (C-1), 149.7 (C-3). LC-MS (m/z): positive mode 237 $[\text{M} + \text{H}]^+$. Purity by HPLC-UV (254 nm)-ESI-MS: 94.3%.

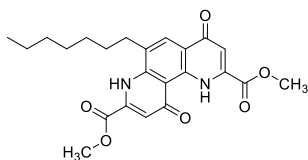


4-Heptylbenzene-1,3-diamine (65o, LW448). The compound was synthesized using **64c** (2.2 g, 9.3 mmol). The product was isolated as a white solid (1.9 g, 99% yield) and directly used for the next step.

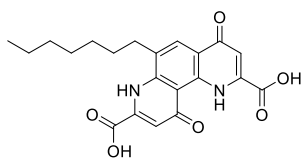


Tetramethyl 2,2'-((4-heptyl-1,3-phenylene)bis(azanediyl))bis(but-2-enedioate) (661, LW449). The compound was synthesized using **651** (1.9 g, 9.3 mmol). The product was isolated as a yellow oil (3.0 g, 66% yield). ^1H NMR (600 MHz, CDCl_3) δ 0.87 (t, $J = 7.0$ Hz, 3H, $\text{Ar}(\text{CH}_2)_6\text{CH}_3$), 1.22 – 1.39 (m, 8H, $\text{Ar}(\text{CH}_2)_2(\text{CH}_2)_4\text{CH}_3$), 1.60 (p, $J = 7.4$ Hz, 2H, $\text{ArCH}_2\text{CH}_2(\text{CH}_2)_4\text{CH}_3$), 2.56 – 2.65 (m, 2H, $\text{ArCH}_2(\text{CH}_2)_5\text{CH}_3$), 3.71 (s, 3H, CO_2CH_3), 3.72 (s, 3H, CO_2CH_3), 3.73 (s, 3H, CO_2CH_3), 3.74 (s, 3H, CO_2CH_3), 5.36 (s, 1H, 3'-H or 3''-H), 5.43 (s, 1H, 3'-H or 3''-H), 6.16 – 6.41 (m, 1H, 2-H), 6.62 (dd, $J = 2.1$, 8.1 Hz, 1H, 6-H), 7.07 (d, $J = 8.1$ Hz, 1H, 5-H), 9.50 (s, 2H, $2 \times \text{NH}$). ^{13}C NMR (151 MHz, CDCl_3) δ 14.1 ($\text{Ar}(\text{CH}_2)_6\text{CH}_3$), 22.6 ($\text{Ar}(\text{CH}_2)_5\text{CH}_2\text{CH}_3$), 29.1 ($\text{Ar}(\text{CH}_2)_4\text{CH}_2\text{CH}_2\text{CH}_3$), 29.3 ($\text{Ar}(\text{CH}_2)_3\text{CH}_2(\text{CH}_2)_2\text{CH}_3$), 29.6 ($\text{Ar}(\text{CH}_2)_2\text{CH}_2(\text{CH}_2)_3\text{CH}_3$), 31.1

(ArCH₂CH₂(CH₂)₄CH₃), 31.8 (ArCH₂(CH₂)₅CH₃), 51.2 (CO₂CH₃), 51.2 (CO₂CH₃), 52.9 (CO₂CH₃), 52.9 (CO₂CH₃), 93.6 (C-3' or C-3''), 93.7 (C-3' or C-3''), 115.1 (C-2), 117.7 (C-6), 130.3 (C-5), 131.4 (C-4), 138.7 (C-2' or C-2''), 139.4 (C-2' or C-2''), 147.9 (C-1), 148.5 (C-3), 164.4 (CO₂Me), 164.4 (CO₂Me), 169.9 (CO₂Me), 170.0 (CO₂Me). LC–MS (*m/z*): positive mode 491 [M + H]⁺. Purity by HPLC–UV (254 nm)–ESI–MS: 89.3%.

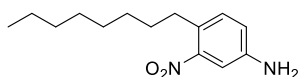


Dimethyl 4,10-dioxo-6-heptyl-1,4,7,10-tetrahydro-1,7-phenanthroline-2,8-dicarboxylate (67i, LW454). The compound was synthesized using **66i** (3.0 g, 6.1 mmol). The product was isolated as a white solid (1.0 g, 38% yield). ¹H NMR (600 MHz, CDCl₃) δ 0.87 (t, *J* = 6.2 Hz, 3H, Ar(CH₂)₆CH₃), 1.25 – 1.40 (m, 6H, Ar(CH₂)₃(CH₂)₃CH₃), 1.45 (p, *J* = 7.2 Hz, 2H, Ar(CH₂)₂CH₂(CH₂)₃CH₃), 1.77 (p, *J* = 7.2 Hz, 2H, ArCH₂CH₂(CH₂)₄CH₃), 2.86 (t, *J* = 7.4 Hz, 2H, ArCH₂(CH₂)₅CH₃), 4.05 (s, 3H, CO₂CH₃), 4.09 (s, 3H, CO₂CH₃), 7.06 (s, 1H, 3-H or 9-H), 7.12 (s, 1H, 3-H or 9-H), 8.34 (s, 1H, 5-H), 9.35 (br, 1H, NH), 14.45 (br, 1H, NH). ¹³C NMR (151 MHz, CDCl₃) δ 14.0 (Ar(CH₂)₆CH₃), 22.5 (Ar(CH₂)₅CH₂CH₃), 28.6 (Ar(CH₂)₄CH₂CH₂CH₃), 29.0 (Ar(CH₂)₃CH₂(CH₂)₂CH₃), 29.4 (Ar(CH₂)₂CH₂(CH₂)₃CH₃), 30.2 (ArCH₂CH₂(CH₂)₄CH₃), 31.6 (ArCH₂(CH₂)₅CH₃), 53.6 (CO₂CH₃), 54.3 (CO₂CH₃), 112.9 (C-10a), 114.3 (C-3 or C-9), 114.4 (C-3 or C-9), 121.2 (C-4a), 125.7 (C-6), 130.0 (C-5), 135.4 (C-2 or C-8), 136.5 (C-2 or C-8), 139.1 (C-6a or C-10b), 141.3 (C-6a or C-10b), 162.3 (CO₂Me), 162.5 (CO₂Me), 177.2 (C-4 or C-10), 181.8 (C-4 or C-10). LC–MS (*m/z*): positive mode 427 [M + H]⁺. Purity by HPLC–UV (254 nm)–ESI–MS: 97.6%. Mp: 172–173 °C.



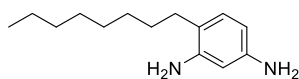
4,10-Dioxo-6-heptyl-1,4,7,10-tetrahydro-1,7-phenanthroline-2,8-dicarboxylic acid (68i, LW456). The compound was synthesized using **67i** (566 mg, 1.33 mmol). The product was isolated as a gray solid (344 mg, 65% yield). ¹H NMR (600 MHz, D₂O, ND₃) δ 0.87 (t, *J* = 6.6 Hz, 3H, Ar(CH₂)₆CH₃), 1.18 – 1.39 (m, 8H, Ar(CH₂)₂(CH₂)₄CH₃), 1.41 – 1.60 (m, 2H, ArCH₂CH₂(CH₂)₄CH₃), 2.41 – 2.54 (m, 2H, ArCH₂(CH₂)₅CH₃), 6.78 (s, 1H, 3-H or 9-H), 6.81 (s, 1H, 3-H or 9-H), 7.60 (s, 1H, 5-H). ¹³C NMR (151 MHz, D₂O, ND₃) δ 16.2 (Ar(CH₂)₆CH₃), 24.7 (Ar(CH₂)₅CH₂CH₃), 29.8 (Ar(CH₂)₄CH₂CH₂CH₃), 31.0 (Ar(CH₂)₃CH₂(CH₂)₂CH₃), 31.3 (Ar(CH₂)₂CH₂(CH₂)₃CH₃), 31.8 (ArCH₂CH₂(CH₂)₄CH₃), 33.8 (ArCH₂(CH₂)₅CH₃), 113.3 (C-3 or C-9), 113.6 (C-10a), 114.3 (C-3 or C-9), 121.6 (C-4a), 128.6 (C-5), 130.5 (C-6), 140.0 (C-2 or C-8), 143.7 (C-2 or C-8), 145.8 (C-6a or C-10b), 146.2 (C-6a or C-10b), 168.2 (CO₂H), 168.7 (CO₂H), 180.7 (C-4 or C-10), 184.2 (C-4 or C-10). LC–MS (*m/z*): positive mode 399 [M + H]⁺. Purity by HPLC–UV (254 nm)–ESI–MS: 98.2%. Mp: >300 °C dec.

Preparation of 67m and 68m

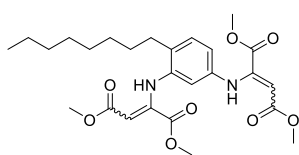


3-Nitro-4-octylaniline (64d, LW468). The compound was synthesized using 4-octylaniline (2.1 mL, 9.8 mmol). The product was isolated as an orange solid (2.0 g, 82% yield). ¹H NMR (600 MHz, CDCl₃) δ 0.87 (t, *J* = 7.0 Hz, 3H, Ar(CH₂)₇CH₃), 1.22 – 1.35 (m, 10H, Ar(CH₂)₂(CH₂)₅CH₃), 1.56 (p, *J* = 7.6 Hz, 2H, ArCH₂CH₂(CH₂)₅CH₃), 2.71 – 2.76 (m, 2H, ArCH₂(CH₂)₆CH₃),

3.81 (br, 2H, NH₂), 6.81 (dd, $J = 2.5, 8.2$ Hz, 1H, 6-H), 7.08 (d, $J = 8.3$ Hz, 1H, 5-H), 7.17 (d, $J = 2.4$ Hz, 1H, 2-H). ¹³C NMR (151 MHz, CDCl₃) δ 14.1 (Ar(CH₂)₇CH₃), 22.6 (Ar(CH₂)₆CH₂CH₃), 29.2 (Ar(CH₂)₅CH₂CH₂CH₃), 29.3 (Ar(CH₂)₄CH₂(CH₂)₂CH₃), 29.5 (Ar(CH₂)₃CH₂(CH₂)₃CH₃), 30.8 (Ar(CH₂)₂CH₂(CH₂)₄CH₃), 31.8 (ArCH₂CH₂(CH₂)₅CH₃), 32.2 (ArCH₂(CH₂)₆CH₃), 110.2 (C-2), 119.6 (C-6), 127.3 (C-4), 132.6 (C-5), 144.8 (C-1), 149.7 (C-3). LC-MS (m/z): positive mode 251 [M + H]⁺. Purity by HPLC-UV (254 nm)-ESI-MS: 95.4%.

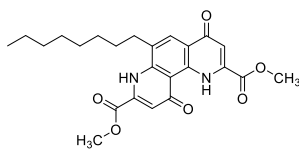


4-Octylbenzene-1,3-diamine (65m, LW469). The compound was synthesized using **64d** (1.82 g, 7.27 mmol). The product was isolated as a white solid (1.60 g, 100% yield) and directly used for the next step.



Tetramethyl 2,2'-((4-octyl-1,3-phenylene)bis(azanediyl))bis(but-2-enedioate) (66m, LW471). The compound was synthesized using **65m** (1.60 g, 7.27 mmol).

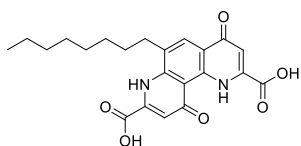
The product was isolated as a yellow oil (2.52 g, 69% yield). ¹H NMR (600 MHz, CDCl₃) δ 0.87 (t, $J = 6.9$ Hz, 3H, Ar(CH₂)₇CH₃), 1.24 – 1.36 (m, 10H, Ar(CH₂)₂(CH₂)₅CH₃), 1.60 (p, $J = 7.6$ Hz, 2H, ArCH₂CH₂(CH₂)₅CH₃), 2.58 – 2.63 (m, 2H, ArCH₂(CH₂)₆CH₃), 3.71 (s, 3H, CO₂CH₃), 3.71 (s, 3H, CO₂CH₃), 3.72 (s, 3H, CO₂CH₃), 3.73 (s, 3H, CO₂CH₃), 5.36 (s, 1H, 3'-H or 3''-H), 5.43 (s, 1H, 3'-H or 3''-H), 6.30 (d, $J = 1.9$ Hz, 1H, 2-H), 6.61 (dd, $J = 2.1, 8.1$ Hz, 1H, 6-H), 7.07 (d, $J = 8.1$ Hz, 1H, 5-H), 9.50 (s, 2H, 2 × NH). ¹³C NMR (151 MHz, CDCl₃) δ 14.1 (Ar(CH₂)₇CH₃), 22.6 (Ar(CH₂)₆CH₂CH₃), 29.2 (Ar(CH₂)₅CH₂CH₂CH₃), 29.3 (Ar(CH₂)₄CH₂(CH₂)₂CH₃), 29.3 (Ar(CH₂)₃CH₂(CH₂)₃CH₃), 29.6 (Ar(CH₂)₂CH₂(CH₂)₄CH₃), 31.1 (ArCH₂CH₂(CH₂)₅CH₃), 31.8 (ArCH₂(CH₂)₆CH₃), 51.2 (CO₂CH₃), 51.2 (CO₂CH₃), 52.8 (CO₂CH₃), 52.9 (CO₂CH₃), 93.6 (C-3' or C-3''), 93.7 (C-3' or C-3''), 115.1 (C-2), 117.7 (C-6), 130.3 (C-5), 131.4 (C-4), 138.7 (C-2' or C-2''), 139.3 (C-2' or C-2''), 147.9 (C-1), 148.5 (C-3), 164.3 (CO₂Me), 164.4 (CO₂Me), 169.8 (CO₂Me), 170.0 (CO₂Me). LC-MS (m/z): positive mode 505 [M + H]⁺. Purity by HPLC-UV (254 nm)-ESI-MS: 88.9%.



Dimethyl 4,10-dioxo-6-octyl-1,4,7,10-tetrahydro-1,7-phenanthroline-2,8-dicarboxylate (67m, LW473A). The compound was synthesized using **66m** (2.52 g, 4.99 mmol). The product was further purified by column chromatography on a column of silica gel (99:1 DCM/MeOH) and isolated as a yellow solid (563 mg,

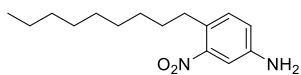
26% yield). ¹H NMR (600 MHz, CDCl₃) δ 0.88 (t, $J = 6.9$ Hz, 3H, Ar(CH₂)₇CH₃), 1.25 – 1.32 (m, 6H, Ar(CH₂)₄(CH₂)₃CH₃), 1.34 – 1.41 (m, 2H, Ar(CH₂)₃CH₂(CH₂)₃CH₃), 1.47 (p, $J = 7.2$ Hz, 2H, Ar(CH₂)₂CH₂(CH₂)₄CH₃), 1.79 (p, $J = 7.7$ Hz, 2H, ArCH₂CH₂(CH₂)₅CH₃), 2.87 – 2.93 (m, 2H, ArCH₂(CH₂)₆CH₃), 4.07 (s, 3H, CO₂CH₃), 4.11 (s, 3H, CO₂CH₃), 7.13 (s, 1H, 3-H or 9-H), 7.24 (s, 1H, 3-H or 9-H), 8.40 (s, 1H, 5-H), 9.41 (br, 1H, NH), 14.62 (br, 1H, NH). ¹³C NMR (151 MHz, CDCl₃) δ 14.1 (Ar(CH₂)₇CH₃), 22.6 (Ar(CH₂)₆CH₂CH₃), 28.7 (Ar(CH₂)₅CH₂CH₂CH₃), 29.1 (Ar(CH₂)₄CH₂(CH₂)₂CH₃), 29.3 (Ar(CH₂)₃CH₂(CH₂)₃CH₃), 29.5 (Ar(CH₂)₂CH₂(CH₂)₄CH₃), 30.3 (ArCH₂CH₂(CH₂)₅CH₃), 31.8 (ArCH₂(CH₂)₆CH₃), 53.7 (CO₂CH₃), 54.3 (CO₂CH₃), 113.0 (C-10a), 114.3 (C-3 or C-9), 114.5 (C-3 or C-9), 121.1 (C-4a), 126.0 (C-6), 130.1 (C-5), 135.5 (C-2 or C-8), 136.7 (C-2 or C-8), 139.2 (C-6a or C-10b), 141.5 (C-6a or

C-10b), 162.2 ($\underline{\text{CO}_2\text{Me}}$), 162.6 ($\underline{\text{CO}_2\text{Me}}$), 177.1 (C-4 or C-10), 181.9 (C-4 or C-10). LC-MS (m/z): positive mode 441 $[\text{M} + \text{H}]^+$. Purity by HPLC-UV (254 nm)-ESI-MS: 98.7%. Mp: 169–170 °C.

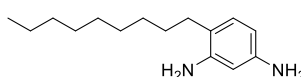


4,10-Dioxo-6-octyl-1,4,7,10-tetrahydro-1,7-phenanthroline-2,8-dicarboxylic acid (68m, LW474, PSB-19474). The compound was synthesized using **67m** (450 mg, 1.01 mmol). The product was isolated as a white solid (390 mg, 94% yield). ^1H NMR (600 MHz, D_2O , ND_3) δ 0.80 (t, $J = 6.8$ Hz, 3H, $\text{Ar}(\text{CH}_2)_7\underline{\text{CH}_3}$), 1.14 – 1.29 (m, 8H, $\text{Ar}(\text{CH}_2)_3(\underline{\text{CH}_2})_4\text{CH}_3$), 1.30 – 1.36 (m, 2H, $\text{Ar}(\text{CH}_2)_2\underline{\text{CH}_2}(\text{CH}_2)_4\text{CH}_3$), 1.56 – 1.64 (m, 2H, $\text{ArCH}_2\underline{\text{CH}_2}(\text{CH}_2)_5\text{CH}_3$), 2.70 (t, $J = 7.3$ Hz, 2H, $\text{Ar}\underline{\text{CH}_2}(\text{CH}_2)_6\text{CH}_3$), 6.90 (s, 1H, 3-H or 9-H), 6.91 (s, 1H, 3-H or 9-H), 7.82 (s, 1H, 5-H). ^{13}C NMR (151 MHz, D_2O , ND_3) δ 16.1 ($\text{Ar}(\text{CH}_2)_7\underline{\text{CH}_3}$), 24.7 ($\text{Ar}(\text{CH}_2)_6\underline{\text{CH}_2}\text{CH}_3$), 30.0 ($\text{Ar}(\text{CH}_2)_5\underline{\text{CH}_2}\text{CH}_2\text{CH}_3$), 31.0 ($\text{Ar}(\text{CH}_2)_4\underline{\text{CH}_2}(\text{CH}_2)_2\text{CH}_3$), 31.1 ($\text{Ar}(\text{CH}_2)_3\underline{\text{CH}_2}(\text{CH}_2)_3\text{CH}_3$), 31.2 ($\text{Ar}(\text{CH}_2)_2\underline{\text{CH}_2}(\text{CH}_2)_4\text{CH}_3$), 32.0 ($\text{ArCH}_2\underline{\text{CH}_2}(\text{CH}_2)_5\text{CH}_3$), 33.7 ($\text{Ar}\underline{\text{CH}_2}(\text{CH}_2)_6\text{CH}_3$), 113.4 (C-3 or C-9), 114.0 (C-10a), 114.4 (C-3 or C-9), 121.9 (C-4a), 129.1 (C-5), 131.1 (C-6), 140.3 (C-2 or C-8), 144.2 (C-2 or C-8), 145.9 (C-6a or C-10b), 146.6 (C-6a or C-10b), 168.6 ($\underline{\text{CO}_2\text{H}}$), 168.9 ($\underline{\text{CO}_2\text{H}}$), 180.9 (C-4 or C-10), 184.5 (C-4 or C-10). LC-MS (m/z): positive mode 413 $[\text{M} + \text{H}]^+$. Purity by HPLC-UV (254 nm)-ESI-MS: 97.4%. Mp: >300 °C dec.

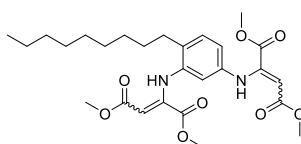
Preparation of 68n



3-Nitro-4-nonylaniline (64e, LW441). The compound was synthesized using 4-nonylaniline (3.0 g, 13.7 mmol). The product was isolated as an orange solid (2.5 g, 75% yield). ^1H NMR (600 MHz, CDCl_3) δ 0.87 (t, $J = 7.0$ Hz, 3H, $\text{Ar}(\text{CH}_2)_8\underline{\text{CH}_3}$), 1.24 – 1.34 (m, 12H, $\text{Ar}(\text{CH}_2)_2(\underline{\text{CH}_2})_6\text{CH}_3$), 1.52 – 1.59 (m, 2H, $\text{ArCH}_2\underline{\text{CH}_2}(\text{CH}_2)_6\text{CH}_3$), 2.70 – 2.75 (m, 2H, $\text{Ar}\underline{\text{CH}_2}(\text{CH}_2)_7\text{CH}_3$), 6.81 (dd, $J = 2.5, 8.2$ Hz, 1H, 6-H), 7.08 (d, $J = 8.3$ Hz, 1H, 5-H), 7.17 (d, $J = 2.4$ Hz, 1H, 2-H). ^{13}C NMR (151 MHz, CDCl_3) δ 14.1 ($\text{Ar}(\text{CH}_2)_8\underline{\text{CH}_3}$), 22.6 ($\text{Ar}(\text{CH}_2)_7\underline{\text{CH}_2}\text{CH}_3$), 29.3 ($\text{Ar}(\text{CH}_2)_6\underline{\text{CH}_2}\text{CH}_2\text{CH}_3$), 29.4 ($\text{Ar}(\text{CH}_2)_4(\underline{\text{CH}_2})_2(\text{CH}_2)_2\text{CH}_3$), 29.5 ($\text{Ar}(\text{CH}_2)_3\underline{\text{CH}_2}(\text{CH}_2)_4\text{CH}_3$), 30.9 ($\text{Ar}(\text{CH}_2)_2\underline{\text{CH}_2}(\text{CH}_2)_5\text{CH}_3$), 31.9 ($\text{ArCH}_2\underline{\text{CH}_2}(\text{CH}_2)_6\text{CH}_3$), 32.2 ($\text{Ar}\underline{\text{CH}_2}(\text{CH}_2)_7\text{CH}_3$), 110.2 (C-2), 119.5 (C-6), 127.2 (C-4), 132.6 (C-5), 145.0 (C-1), 149.7 (C-3). LC-MS (m/z): positive mode 265 $[\text{M} + \text{H}]^+$. Purity by HPLC-UV (254 nm)-ESI-MS: 94.4%.

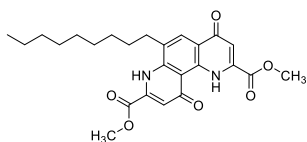


4-Nonylbenzene-1,3-diamine (65n, LW446). The compound was synthesized using **64e** (390 mg, 1.48 mmol). The product was isolated as a white solid (346 mg, 100% yield) and directly used for the next step.



Tetramethyl 2,2'-((4-nonyl-1,3-phenylene)bis(azanediyl))bis(but-2-enedioate) (66n, LW447). The compound was synthesized using **65n** (346 mg, 1.48 mmol). The product was isolated as a yellow oil (475 mg, 62% yield). ^1H NMR (600 MHz, CDCl_3) δ 0.87 (t, $J = 7.0$ Hz, 3H, $\text{Ar}(\text{CH}_2)_8\underline{\text{CH}_3}$), 1.23 – 1.37 (m, 12H,

Ar(CH₂)₂(CH₂)₆CH₃), 1.60 (p, *J* = 7.5 Hz, 2H, ArCH₂CH₂(CH₂)₆CH₃), 2.58 – 2.63 (m, 2H, ArCH₂(CH₂)₇CH₃), 3.71 (s, 3H, CO₂CH₃), 3.72 (s, 3H, CO₂CH₃), 3.72 (s, 3H, CO₂CH₃), 3.74 (s, 3H, CO₂CH₃), 5.36 (s, 1H, 3'-H or 3''-H), 5.43 (s, 1H, 3'-H or 3''-H), 6.30 (d, *J* = 2.0 Hz, 1H, 2-H), 6.62 (dd, *J* = 2.1, 8.1 Hz, 1H, 6-H), 7.07 (d, *J* = 8.1 Hz, 1H, 5-H), 9.50 (s, 2H, 2 × NH). ¹³C NMR (151 MHz, CDCl₃) δ 14.1 (Ar(CH₂)₈CH₃), 22.6 (Ar(CH₂)₇CH₂CH₃), 29.3 (Ar(CH₂)₆CH₂CH₂CH₃), 29.3 (Ar(CH₂)₅CH₂(CH₂)₂CH₃), 29.4 (Ar(CH₂)₄CH₂(CH₂)₃CH₃), 29.5 (Ar(CH₂)₃CH₂(CH₂)₄CH₃), 29.6 (Ar(CH₂)₂CH₂(CH₂)₅CH₃), 31.1 (ArCH₂CH₂(CH₂)₆CH₃), 31.9 (ArCH₂(CH₂)₇CH₃), 51.2 (CO₂CH₃), 52.8 (CO₂CH₃), 52.9 (CO₂CH₃), 53.4 (CO₂CH₃), 93.6 (C-3' or C-3''), 93.7 (C-3' or C-3''), 115.1 (C-2), 117.7 (C-6), 130.3 (C-5), 131.4 (C-4), 138.7 (C-2' or C-2''), 139.4 (C-2' or C-2''), 147.9 (C-1), 148.5 (C-3), 164.4 (CO₂Me), 164.4 (CO₂Me), 169.8 (CO₂Me), 170.0 (CO₂Me). LC–MS (*m/z*): positive mode 519 [M + H]⁺. Purity by HPLC–UV (254 nm)–ESI–MS: 86.4%.

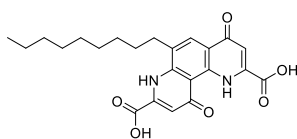


Dimethyl 4,10-dioxo-6-nonyl-1,4,7,10-tetrahydro-1,7-phenanthroline-2,8-

dicarboxylate (67n, LW452). The compound was synthesized using **66n** (460 mg, 0.89 mmol). The product was isolated as a white solid (200 mg, 49% yield). ¹H

NMR (600 MHz, CDCl₃) δ 0.87 (t, *J* = 6.8 Hz, 3H, Ar(CH₂)₈CH₃), 1.24 – 1.31 (m,

8H, Ar(CH₂)₄(CH₂)₄CH₃), 1.33 – 1.42 (m, 2H, Ar(CH₂)₃CH₂(CH₂)₄CH₃), 1.47 (p, *J* = 7.3 Hz, 2H, Ar(CH₂)₂CH₂(CH₂)₅CH₃), 1.79 (p, *J* = 7.7 Hz, 2H, ArCH₂CH₂(CH₂)₆CH₃), 2.90 (t, *J* = 7.7 Hz, 2H, ArCH₂(CH₂)₇CH₃), 4.06 (s, 3H, CO₂CH₃), 4.11 (s, 3H, CO₂CH₃), 7.13 (s, 1H, 3-H or 9-H), 7.21 (s, 1H, 3-H or 9-H), 8.42 (s, 1H, 5-H), 9.41 (br, 1H, NH), 14.57 (br, 1H, NH). ¹³C NMR (151 MHz, CDCl₃) δ 14.1 (Ar(CH₂)₈CH₃), 22.6 (Ar(CH₂)₇CH₂CH₃), 28.7 (Ar(CH₂)₆CH₂CH₂CH₃), 29.2 (Ar(CH₂)₅CH₂(CH₂)₂CH₃), 29.3 (Ar(CH₂)₄CH₂(CH₂)₃CH₃), 29.4 (Ar(CH₂)₃CH₂(CH₂)₄CH₃), 29.5 (Ar(CH₂)₂CH₂(CH₂)₅CH₃), 30.3 (ArCH₂CH₂(CH₂)₆CH₃), 31.8 (ArCH₂(CH₂)₇CH₃), 53.7 (CO₂CH₃), 54.3 (CO₂CH₃), 113.0 (C-10a), 114.4 (C-3 or C-9), 114.5 (C-3 or C-9), 121.3 (C-4a), 125.8 (C-6), 130.2 (C-5), 135.5 (C-2 or C-8), 136.7 (C-2 or C-8), 139.2 (C-6a or C-10b), 141.4 (C-6a or C-10b), 162.3 (CO₂Me), 162.6 (CO₂Me), 177.3 (C-4 or C-10), 181.9 (C-4 or C-10). LC–MS (*m/z*): positive mode 455 [M + H]⁺. Purity by HPLC–UV (254 nm)–ESI–MS: 98.6%.

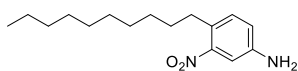


4,10-Dioxo-6-nonyl-1,4,7,10-tetrahydro-1,7-phenanthroline-2,8-dicarboxylic acid (68n, LW457P). The compound was synthesized using **67n** (38 mg, 0.084

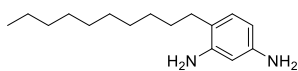
mmol). The product was isolated as a white solid (35 mg, 99% yield). ¹H NMR (600

MHz, D₂O, ND₃) δ 0.74 (t, *J* = 6.7 Hz, 3H, Ar(CH₂)₈CH₃), 1.04 – 1.16 (m, 8H, Ar(CH₂)₄(CH₂)₄CH₃), 1.18 – 1.25 (m, 2H, Ar(CH₂)₃CH₂(CH₂)₄CH₃), 1.27 – 1.39 (m, 2H, Ar(CH₂)₂CH₂(CH₂)₅CH₃), 1.61 – 1.79 (m, 2H, ArCH₂CH₂(CH₂)₆CH₃), 2.84 – 3.00 (m, 2H, ArCH₂(CH₂)₇CH₃), 7.03 (s, 2H, 3-H, 9-H), 8.04 (s, 1H, 5-H). ¹³C NMR (151 MHz, D₂O, ND₃) δ 16.7 (Ar(CH₂)₈CH₃), 25.4 (Ar(CH₂)₇CH₂CH₃), 31.0 (Ar(CH₂)₆CH₂CH₂CH₃), 31.4 (Ar(CH₂)₅CH₂(CH₂)₂CH₃), 31.6 (Ar(CH₂)₄CH₂(CH₂)₃CH₃), 31.7 (Ar(CH₂)₂(CH₂)₂(CH₂)₄CH₃), 33.2 (ArCH₂CH₂(CH₂)₆CH₃), 34.4 (ArCH₂(CH₂)₇CH₃), 114.1 (C-3 or C-9), 115.0 (C-3 or C-9), 115.4 (C-10a), 122.8 (C-4a), 129.5 (C-5), 133.8 (C-6), 141.6 (C-2, C-8), 146.5 (C-6a or C-10b), 146.8 (C-6a or C-10b), 170.0 (CO₂H), 171.0 (CO₂H), 181.8 (C-4 or C-10), 184.6 (C-4 or C-10). LC–MS (*m/z*): positive mode 427 [M + H]⁺. Purity by HPLC–UV (254 nm)–ESI–MS: 95.0%. Mp: >300 °C dec.

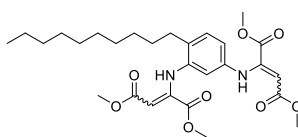
Preparation of 68o



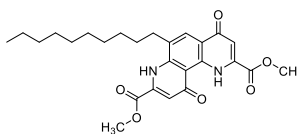
3-Nitro-4-decylaniline (64f, LW216). The compound was synthesized using 4-decylaniline (2.0 g, 8.6 mmol). The product was isolated as an orange solid (1.9 g, 79% yield). ^1H NMR (600 MHz, CDCl_3) δ 0.88 (t, $J = 7.0$ Hz, 3H, $\text{Ar}(\text{CH}_2)_9\text{CH}_3$), 1.23 – 1.35 (m, 14H, $\text{Ar}(\text{CH}_2)_2(\text{CH}_2)_7\text{CH}_3$), 1.56 (p, $J = 7.6$ Hz, 2H, $\text{ArCH}_2\text{CH}_2(\text{CH}_2)_7\text{CH}_3$), 2.71 – 2.76 (m, 2H, $\text{ArCH}_2(\text{CH}_2)_8\text{CH}_3$), 6.78 – 6.84 (m, 1H, 6-H), 7.08 (d, $J = 8.2$ Hz, 1H, 5-H), 7.14 – 7.19 (m, 1H, 2-H). ^{13}C NMR (151 MHz, CDCl_3) δ 14.1 ($\text{Ar}(\text{CH}_2)_9\text{CH}_3$), 22.6 ($\text{Ar}(\text{CH}_2)_8\text{CH}_2\text{CH}_3$), 29.3 ($\text{Ar}(\text{CH}_2)_7\text{CH}_2\text{CH}_2\text{CH}_3$), 29.4 ($\text{Ar}(\text{CH}_2)_6\text{CH}_2(\text{CH}_2)_2\text{CH}_3$), 29.5 ($\text{Ar}(\text{CH}_2)_5\text{CH}_2(\text{CH}_2)_3\text{CH}_3$), 29.5 ($\text{Ar}(\text{CH}_2)_4\text{CH}_2(\text{CH}_2)_4\text{CH}_3$), 29.6 ($\text{Ar}(\text{CH}_2)_3\text{CH}_2(\text{CH}_2)_5\text{CH}_3$), 30.9 ($\text{Ar}(\text{CH}_2)_2\text{CH}_2(\text{CH}_2)_6\text{CH}_3$), 31.9 ($\text{ArCH}_2\text{CH}_2(\text{CH}_2)_7\text{CH}_3$), 32.2 ($\text{ArCH}_2(\text{CH}_2)_8\text{CH}_3$), 110.2 (C-2), 119.5 (C-6), 127.2 (C-4), 132.6 (C-5), 145.0 (C-1), 149.7 (C-3). LC–MS (m/z): positive mode 279 $[\text{M} + \text{H}]^+$. Purity by HPLC–UV (254 nm)–ESI–MS: 81.4%.



4-Decylbenzene-1,3-diamine (65o, LW219). The compound was synthesized using **64f** (1.80 g, 6.47 mmol). The product was isolated as a white solid (1.60 g, 98% yield).

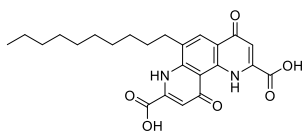


Tetramethyl 2,2'-((4-decyl-1,3-phenylene)bis(azanediyl))bis(but-2-enedioate) (66o, LW222). The compound was synthesized using **65o** (1.60 g, 6.44 mmol). The product was isolated as a yellow oil (1.43 g, 41% yield) and directly used for the next step. LC–MS (m/z): positive mode 533 $[\text{M} + \text{H}]^+$. Purity by HPLC–UV (254 nm)–ESI–MS: 61.5%.



Dimethyl 6-decyl-4,10-dioxo-1,4,7,10-tetrahydro-1,7-phenanthroline-2,8-dicarboxylate (67o, LW223). The compound was synthesized using **66o** (1.43 g, 2.68 mmol). The product was further purified by column chromatography on a column of silica gel (99:1 DCM/MeOH) and isolated as a beige solid (100 mg, 8% yield). ^1H NMR (600 MHz, CDCl_3) δ 0.84 – 0.89 (m, 3H, $\text{Ar}(\text{CH}_2)_9\text{CH}_3$), 1.21 – 1.32 (m, 10H, $\text{Ar}(\text{CH}_2)_4(\text{CH}_2)_5\text{CH}_3$), 1.33 – 1.40 (m, 2H, $\text{Ar}(\text{CH}_2)_3\text{CH}_2(\text{CH}_2)_5\text{CH}_3$), 1.46 (p, $J = 6.1$ Hz, 2H, $\text{Ar}(\text{CH}_2)_2\text{CH}_2(\text{CH}_2)_6\text{CH}_3$), 1.79 (p, $J = 6.8$ Hz, 2H, $\text{ArCH}_2\text{CH}_2(\text{CH}_2)_7\text{CH}_3$), 2.90 (t, $J = 6.9$ Hz, 2H, $\text{ArCH}_2(\text{CH}_2)_8\text{CH}_3$), 4.06 (s, 3H, CO_2CH_3), 4.10 (s, 3H, CO_2CH_3), 7.12 (s, 1H, 3-H or 9-H), 7.23 (s, 1H, 3-H or 9-H), 8.40 (s, 1H, 5-H), 9.40 (br, 1H, NH), 14.61 (br, 1H, NH). ^{13}C NMR (151 MHz, CDCl_3) δ 14.1 ($\text{Ar}(\text{CH}_2)_9\text{CH}_3$), 22.6 ($\text{Ar}(\text{CH}_2)_8\text{CH}_2\text{CH}_3$), 28.7 ($\text{Ar}(\text{CH}_2)_7\text{CH}_2\text{CH}_2\text{CH}_3$), 29.3 ($\text{Ar}(\text{CH}_2)_6\text{CH}_2(\text{CH}_2)_2\text{CH}_3$), 29.3 ($\text{Ar}(\text{CH}_2)_5\text{CH}_2(\text{CH}_2)_3\text{CH}_3$), 29.5 ($\text{Ar}(\text{CH}_2)_4\text{CH}_2(\text{CH}_2)_4\text{CH}_3$), 29.5 ($\text{Ar}(\text{CH}_2)_3\text{CH}_2(\text{CH}_2)_5\text{CH}_3$), 29.5 ($\text{Ar}(\text{CH}_2)_2\text{CH}_2(\text{CH}_2)_6\text{CH}_3$), 30.3 ($\text{ArCH}_2\text{CH}_2(\text{CH}_2)_7\text{CH}_3$), 31.8 ($\text{ArCH}_2(\text{CH}_2)_8\text{CH}_3$), 53.7 (CO_2CH_3), 54.3 (CO_2CH_3), 112.9 (C-10a), 114.3 (C-3 or C-9), 114.4 (C-3 or C-9), 121.1 (C-4a), 126.0 (C-6), 130.1 (C-5), 135.5 (C-2 or C-8), 136.7 (C-2 or C-8), 139.1 (C-6a or C-10b), 141.4 (C-6a or C-10b), 162.2 (CO_2Me), 162.6 (CO_2Me).

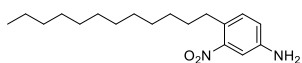
177.1 (C-4 or C-10), 181.9 (C-4 or C-10). LC–MS (m/z): positive mode 469 $[M + H]^+$. Purity by HPLC–UV (254 nm)–ESI–MS: 98.2%.



6-Decyl-4,10-dioxo-1,4,7,10-tetrahydro-1,7-phenanthroline-2,8-dicarboxylic acid (68o, LW241, PSB-18241). The compound was synthesized using **67o** (46 mg, 0.098 mmol). The product was isolated as a brown solid (43 mg, 99% yield).

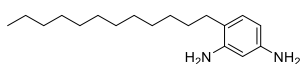
$^1\text{H NMR}$ (600 MHz, D_2O , $\text{C}_5\text{D}_5\text{N}$) δ 0.34 (t, $J = 7.3$ Hz, 3H, $\text{Ar}(\text{CH}_2)_9\text{CH}_3$), 0.55 (s, 6H, $\text{Ar}(\text{CH}_2)_6(\text{CH}_2)_3\text{CH}_3$), 0.60 – 0.69 (m, 4H, $\text{Ar}(\text{CH}_2)_4(\text{CH}_2)_2(\text{CH}_2)_3\text{CH}_3$), 0.79 (p, $J = 7.5$ Hz, 2H, $\text{Ar}(\text{CH}_2)_3\text{CH}_2(\text{CH}_2)_5\text{CH}_3$), 0.94 (p, $J = 7.7$ Hz, 2H, $\text{Ar}(\text{CH}_2)_2\text{CH}_2(\text{CH}_2)_6\text{CH}_3$), 1.36 (p, $J = 7.2$ Hz, 2H, $\text{ArCH}_2\text{CH}_2(\text{CH}_2)_7\text{CH}_3$), 2.61 (t, $J = 7.0$ Hz, 2H, $\text{ArCH}_2(\text{CH}_2)_8\text{CH}_3$), 6.87 (s, 1H, 3-H or 9-H), 6.89 (s, 1H, 3-H or 9-H), 7.88 (s, 1H, 5-H). $^{13}\text{C NMR}$ (151 MHz, D_2O , $\text{C}_5\text{D}_5\text{N}$) δ 16.2 ($\text{Ar}(\text{CH}_2)_9\text{CH}_3$), 24.8 ($\text{Ar}(\text{CH}_2)_8\text{CH}_2\text{CH}_3$), 30.8 ($\text{Ar}(\text{CH}_2)_7\text{CH}_2\text{CH}_2\text{CH}_3$), 31.2 ($\text{Ar}(\text{CH}_2)_6\text{CH}_2(\text{CH}_2)_2\text{CH}_3$), 31.4 ($\text{Ar}(\text{CH}_2)_5\text{CH}_2(\text{CH}_2)_3\text{CH}_3$), 31.6 ($\text{Ar}(\text{CH}_2)_3(\text{CH}_2)_2(\text{CH}_2)_4\text{CH}_3$), 31.6 ($\text{Ar}(\text{CH}_2)_2\text{CH}_2(\text{CH}_2)_6\text{CH}_3$), 32.3 ($\text{ArCH}_2\text{CH}_2(\text{CH}_2)_7\text{CH}_3$), 33.9 ($\text{ArCH}_2(\text{CH}_2)_8\text{CH}_3$), 113.8 (C-3 or C-9), 114.3 (C-10a), 114.5 (C-3 or C-9), 122.2 (C-4a), 129.6 (C-6), 130.8 (C-5), 140.4 (C-2 or C-8), 143.2 (C-2 or C-8), 145.9 (C-6a or C-10b), 146.4 (C-6a or C-10b), 167.5 (CO_2H), 168.7 (CO_2H), 181.2 (C-4 or C-10), 184.9 (C-4 or C-10). LC–MS (m/z): positive mode 441 $[M + H]^+$. Purity by HPLC–UV (254 nm)–ESI–MS: 97.5%. Mp: >300 °C dec.

Preparation of 68p



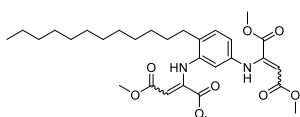
3-Nitro-4-dodecylaniline (64g, LW451). The compound was synthesized using 4-dodecylaniline (2.0 g, 7.7 mmol). The product was isolated as an orange solid (1.4

g, 60% yield). $^1\text{H NMR}$ (600 MHz, CDCl_3) δ 0.88 (t, $J = 7.0$ Hz, 3H, $\text{Ar}(\text{CH}_2)_{11}\text{CH}_3$), 1.24 – 1.34 (m, 18H, $\text{Ar}(\text{CH}_2)_2(\text{CH}_2)_9\text{CH}_3$), 1.51 – 1.61 (m, 2H, $\text{ArCH}_2\text{CH}_2(\text{CH}_2)_9\text{CH}_3$), 2.69 – 2.77 (m, 2H, $\text{ArCH}_2\text{CH}_2(\text{CH}_2)_9\text{CH}_3$), 6.80 (dd, $J = 2.5, 8.2$ Hz, 1H, 6-H), 7.08 (d, $J = 8.3$ Hz, 1H, 5-H), 7.16 (d, $J = 2.5$ Hz, 1H, 2-H). $^{13}\text{C NMR}$ (151 MHz, CDCl_3) δ 14.1 ($\text{Ar}(\text{CH}_2)_{11}\text{CH}_3$), 22.7 ($\text{Ar}(\text{CH}_2)_{10}\text{CH}_2\text{CH}_3$), 29.3 ($\text{Ar}(\text{CH}_2)_9\text{CH}_2\text{CH}_2\text{CH}_3$), 29.4 ($\text{Ar}(\text{CH}_2)_8\text{CH}_2(\text{CH}_2)_2\text{CH}_3$), 29.5 ($\text{Ar}(\text{CH}_2)_7\text{CH}_2(\text{CH}_2)_3\text{CH}_3$), 29.6 ($\text{Ar}(\text{CH}_2)_6\text{CH}_2(\text{CH}_2)_4\text{CH}_3$), 29.6 ($\text{Ar}(\text{CH}_2)_4(\text{CH}_2)_2(\text{CH}_2)_5\text{CH}_3$), 29.6 ($\text{Ar}(\text{CH}_2)_3\text{CH}_2(\text{CH}_2)_7\text{CH}_3$), 30.9 ($\text{Ar}(\text{CH}_2)_2\text{CH}_2(\text{CH}_2)_8\text{CH}_3$), 31.9 ($\text{ArCH}_2\text{CH}_2(\text{CH}_2)_9\text{CH}_3$), 32.2 ($\text{ArCH}_2(\text{CH}_2)_{10}\text{CH}_3$), 110.1 (C-2), 119.5 (C-6), 127.2 (C-4), 132.6 (C-5), 145.0 (C-1), 149.7 (C-3). LC–MS (m/z): positive mode 307 $[M + H]^+$. Purity by HPLC–UV (254 nm)–ESI–MS: 94.8%.

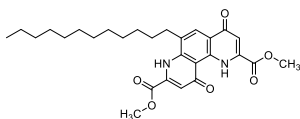


4-Dodecylbenzene-1,3-diamine (65p, LW459). The compound was synthesized using **64g** (1.3 g, 4.3 mmol). The product was isolated as a white solid (1.2 g, 100%

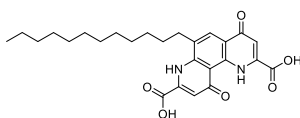
yield) and was directly used for the next step.



Tetramethyl 2,2'-((4-dodecyl-1,3-phenylene)bis(azanediy))bis(but-2-enedioate) (66p, LW460). The compound was synthesized using **65p** (1.2 g, 4.3 mmol). The product was isolated as a yellow oil (1.55 g, 67% yield). $^1\text{H NMR}$ (600 MHz, CDCl_3) δ 0.87 (t, $J = 7.0$ Hz, 3H, $\text{Ar}(\text{CH}_2)_{11}\text{CH}_3$), 1.21 – 1.37 (m, 18H, $\text{Ar}(\text{CH}_2)_2(\text{CH}_2)_9\text{CH}_3$), 1.60 (p, $J = 7.4$ Hz, 2H, $\text{ArCH}_2\text{CH}_2(\text{CH}_2)_9\text{CH}_3$), 2.57 – 2.67 (m, 2H, $\text{ArCH}_2(\text{CH}_2)_{10}\text{CH}_3$), 3.71 (s, 3H, CO_2CH_3), 3.72 (s, 3H, CO_2CH_3), 3.72 (s, 3H, CO_2CH_3), 3.74 (s, 3H, CO_2CH_3), 5.36 (s, 1H, 3'-H or 3''-H), 5.43 (s, 1H, 3'-H or 3''-H), 6.28 – 6.32 (m, 1H, 2-H), 6.62 (dd, $J = 1.9, 8.1$ Hz, 1H, 6-H), 7.07 (d, $J = 8.1$ Hz, 1H, 5-H), 9.50 (s, 2H, $2 \times \text{NH}$). $^{13}\text{C NMR}$ (151 MHz, CDCl_3) δ 14.1 ($\text{Ar}(\text{CH}_2)_{11}\text{CH}_3$), 22.7 (CH_2), 29.3 (CH_2), 29.4 (CH_2), 29.6 (CH_2), 29.6 (CH_2), 29.7 (CH_2), 31.1 (CH_2), 31.9 (CH_2), 51.2 (CO_2CH_3), 51.2 (CO_2CH_3), 52.8 (CO_2CH_3), 52.9 (CO_2CH_3), 93.6 (C-3' or C-3''), 93.7 (C-3' or C-3''), 115.1 (C-2), 117.7 (C-6), 130.3 (C-5), 131.4 (C-4), 138.7 (C-2' or C-2''), 139.4 (C-2' or C-2''), 147.9 (C-1), 148.5 (C-3), 164.4 (CO_2Me), 164.4 (CO_2Me), 169.8 (CO_2Me), 170.0 (CO_2Me). LC-MS (m/z): positive mode 561 $[\text{M} + \text{H}]^+$. Purity by HPLC-UV (254 nm)-ESI-MS: 91.6%.

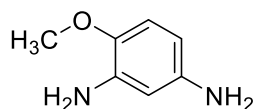


Dimethyl 6-dodecyl-4,10-dioxo-1,4,7,10-tetrahydro-1,7-phenanthroline-2,8-dicarboxylate (67p, LW462). The compound was synthesized using **66p** (1.48 g, 2.64 mmol). The product was isolated as a gray solid (450 mg, 35% yield). $^1\text{H NMR}$ (600 MHz, CDCl_3) δ 0.87 (t, $J = 7.0$ Hz, 3H, $\text{Ar}(\text{CH}_2)_{11}\text{CH}_3$), 1.22 – 1.33 (m, 14H, $\text{Ar}(\text{CH}_2)_4(\text{CH}_2)_7\text{CH}_3$), 1.38 (p, $J = 7.1$ Hz, 2H, $\text{Ar}(\text{CH}_2)_3\text{CH}_2(\text{CH}_2)_7\text{CH}_3$), 1.47 (p, $J = 7.4$ Hz, 2H, $\text{Ar}(\text{CH}_2)_2\text{CH}_2(\text{CH}_2)_8\text{CH}_3$), 1.80 (p, $J = 7.8$ Hz, 2H, $\text{ArCH}_2\text{CH}_2(\text{CH}_2)_9\text{CH}_3$), 2.91 (t, $J = 7.7$ Hz, 2H, $\text{ArCH}_2(\text{CH}_2)_{10}\text{CH}_3$), 4.07 (s, 3H, CO_2CH_3), 4.11 (s, 3H, CO_2CH_3), 7.15 (s, 1H, 3-H or 9-H), 7.29 (s, 1H, 3-H or 9-H), 8.42 (s, 1H, 5-H), 9.44 (s, 1H, NH), 14.70 (s, 1H, NH). $^{13}\text{C NMR}$ (151 MHz, CDCl_3) δ 14.1 ($\text{Ar}(\text{CH}_2)_{11}\text{CH}_3$), 22.7 (CH_2), 28.7 (CH_2), 29.3 (CH_2), 29.3 (CH_2), 29.5 (CH_2), 29.6 (CH_2), 29.6 (CH_2), 29.6 (CH_2), 30.3 (CH_2), 31.9 (CH_2), 53.7 (CO_2CH_3), 54.3 (CO_2CH_3), 112.9 (C-10a), 114.2 (C-3 or C-9), 114.5 (C-3 or C-9), 121.0 (C-4a), 126.1 (C-6), 130.1 (C-5), 135.5 (C-2 or C-8), 136.8 (C-2 or C-8), 139.2 (C-6a or C-10b), 141.5 (C-6a or C-10b), 162.2 (CO_2Me), 162.6 (CO_2Me), 177.0 (C-4 or C-10), 181.9 (C-4 or C-10). LC-MS (m/z): positive mode 497 $[\text{M} + \text{H}]^+$. Purity by HPLC-UV (254 nm)-ESI-MS: 94.0%.

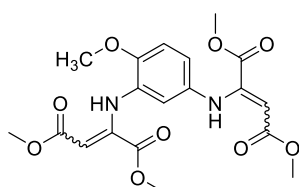


6-Dodecyl-4,10-dioxo-1,4,7,10-tetrahydro-1,7-phenanthroline-2,8-dicarboxylic acid (68p, LW463N, PSB-19463). The compound was synthesized using **67p** (110 mg, 0.22 mmol). The product was isolated as a white solid (73 mg, 70% yield). $^1\text{H NMR}$ (600 MHz, D_2O , $\text{C}_5\text{D}_5\text{N}$) δ 0.00 – 0.04 (m, 3H, $\text{Ar}(\text{CH}_2)_{11}\text{CH}_3$), 0.24 – 0.41 (m, 14H, $\text{Ar}(\text{CH}_2)_4(\text{CH}_2)_7\text{CH}_3$), 0.51 (s, 2H, $\text{Ar}(\text{CH}_2)_3\text{CH}_2(\text{CH}_2)_7\text{CH}_3$), 0.65 (s, 2H, $\text{Ar}(\text{CH}_2)_2\text{CH}_2(\text{CH}_2)_8\text{CH}_3$), 1.03 (s, 2H, $\text{ArCH}_2\text{CH}_2(\text{CH}_2)_9\text{CH}_3$), 2.28 (s, 2H, $\text{ArCH}_2(\text{CH}_2)_{10}\text{CH}_3$), 6.71 – 6.79 (m, 1H, 3-H or 9-H), 6.78 – 6.87 (m, 1H, 3-H or 9-H), 7.74 (s, 1H, 5-H). $^{13}\text{C NMR}$ (151 MHz, D_2O , $\text{C}_5\text{D}_5\text{N}$) δ 16.0 ($\text{Ar}(\text{CH}_2)_{11}\text{CH}_3$), 24.5 (CH_2), 30.7 (CH_2), 31.1 (CH_2), 31.2 (CH_2), 31.4 (CH_2), 31.4 (CH_2), 32.1 (CH_2), 33.7 (CH_2), 113.7 (C-3 or C-9), 114.2 (C-10a), 114.3 (C-3 or C-9), 122.1 (C-4a), 128.9 (C-6), 130.7 (C-5), 140.3 (C-2 or C-8), 142.9 (C-2 or C-8), 146.2 (C-6a or C-10b), 146.8 (C-6a or C-10b), 166.9 (CO_2H), 168.1 (CO_2H), 181.0 (C-4 or C-10), 184.7 (C-4 or C-10). LC-MS (m/z): positive mode 469 $[\text{M} + \text{H}]^+$. Purity by HPLC-UV (254 nm)-ESI-MS: 97.0%. Mp: >300 °C dec.

Preparation of 68q

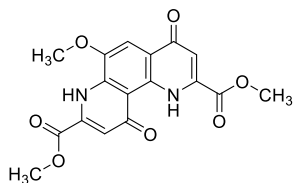


4-Methoxybenzene-1,3-diamine (65q, LW335). The compound was synthesized using 2-methoxy-5-nitroaniline (1.0 g, 5.9 mmol). The product was isolated as a white solid (815 mg, 100% yield) and used directly for the next step.



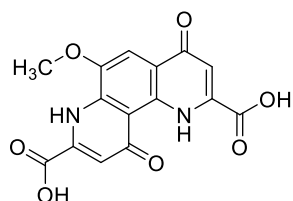
Tetramethyl 2,2'-((4-methoxy-1,3-phenylene)bis(azanediyl))bis(but-2-enedioate) (66q, LW336). The compound was synthesized using **65q** (815 mg, 5.90 mmol). The product was isolated as a yellow oil (1.90 g, 76% yield). ¹H NMR (600 MHz, CDCl₃) δ 3.70 (s, 3H, OCH₃), 3.72 (s, 3H, CO₂CH₃), 3.74 (s, 3H, CO₂CH₃), 3.78 (s, 3H, CO₂CH₃), 3.82 (s, 3H, CO₂CH₃), 5.32 (s, 1H, 3'-H or 3''-H),

5.43 (s, 1H, 3'-H or 3''-H), 6.38 (d, *J* = 2.5 Hz, 1H, 2-H), 6.60 (dd, *J* = 2.5, 8.6 Hz, 1H, 6-H), 6.76 (d, *J* = 8.6 Hz, 1H, 5-H), 9.46 (s, 1H, NH), 9.60 (s, 1H, NH). ¹³C NMR (151 MHz, CDCl₃) δ 51.1 (CO₂CH₃), 51.2 (CO₂CH₃), 52.8 (2 × CO₂CH₃), 55.8 (OCH₃), 92.5 (C-3' or C-3''), 93.9 (C-3' or C-3''), 111.2 (C-2), 114.3 (C-5), 117.5 (C-6), 130.0 (C-3), 133.6 (C-1), 147.0 (C-2' or C-2''), 147.9 (C-2' or C-2''), 148.8 (C-4), 164.3 (CO₂Me), 164.6 (CO₂Me), 169.7 (CO₂Me), 170.0 (CO₂Me). LC-MS (*m/z*): positive mode 423 [M + H]⁺. Purity by HPLC-UV (254 nm)-ESI-MS: 82.9%.



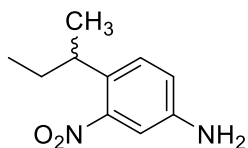
Dimethyl 6-methoxy-4,10-dioxo-1,4,7,10-tetrahydro-1,7-phenanthroline-2,8-dicarboxylate (67q, LW342). The compound was synthesized using **66q** (1.90 g, 4.50 mmol). The product was further purified by column chromatography on a column of silica gel (97:3 DCM/MeOH) and isolated as a yellow solid (180 mg, 11% yield). ¹H NMR (600 MHz, CDCl₃) δ 4.06 (s, 3H, CO₂CH₃), 4.09 (s, 3H, CO₂CH₃),

4.13 (s, 3H, OCH₃), 7.13 (s, 1H, 3-H or 9-H), 7.14 (m, 1H, 3-H or 9-H), 7.89 (s, 1H, 5-H), 9.81 (br, 1H, NH), 14.21 (s, 1H, NH). ¹³C NMR (151 MHz, CDCl₃) δ 53.6 (CO₂CH₃), 54.2 (CO₂CH₃), 56.8 (OCH₃), 106.7 (C-3 or C-9), 113.3 (C-3 or C-9), 113.4 (C-10a), 115.1 (C-5), 121.7 (C-4a), 134.6 (C-2 or C-8), 135.2 (C-2 or C-8), 135.6 (C-6a or C-10b), 135.9 (C-6a or C-10b), 144.5 (C-6), 162.0 (CO₂Me), 162.3 (CO₂Me), 176.8 (C-4 or C-10), 181.1 (C-4 or C-10). LC-MS (*m/z*): positive mode 359 [M + H]⁺. Purity by HPLC-UV (254 nm)-ESI-MS: 86.0%.

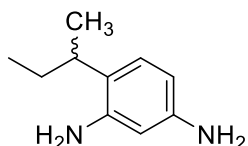


6-Methoxy-4,10-dioxo-1,4,7,10-tetrahydro-1,7-phenanthroline-2,8-dicarboxylic acid (68q, LW346). The compound was synthesized using **67q** (15 mg, 0.042 mmol). The product was isolated as a brown solid (13 mg, 94% yield). ¹H NMR (600 MHz, D₂O, ND₃) δ 3.97 (s, 3H, OCH₃), 6.85 (s, 1H, 3-H or 9-H), 6.91 (s, 1H, 3-H or 9-H), 7.14 (s, 1H, 5-H). ¹³C NMR (151 MHz, D₂O, ND₃) δ 58.6 (OCH₃), 104.5 (C-3 or C-9), 112.3 (C-3 or C-9), 115.0 (C-10a), 115.0 (C-5), 122.2 (C-4a), 136.5 (C-2 or C-8), 141.0 (C-2 or C-8), 144.3 (C-6a, C-10b), 150.5 (C-6), 169.2 (CO₂H), 171.4 (CO₂H), 179.7 (C-4 or C-10), 182.1 (C-4 or C-10). LC-MS (*m/z*): positive mode 331 [M + H]⁺. Purity by HPLC-UV (254 nm)-ESI-MS: 98.3%. Mp: >300 °C dec.

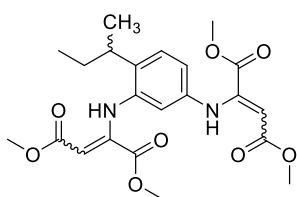
Preparation of 67r and 68r



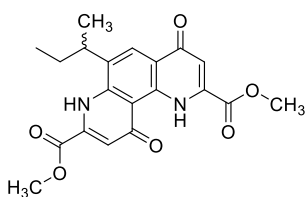
4-(*sec*-Butyl)-3-nitroaniline (64h, LW464). The compound was synthesized using 4-(*sec*-butyl)aniline (2.1 mL, 13.4 mmol). The product was isolated as an orange solid (2.6 g, 99% yield). $^1\text{H NMR}$ (600 MHz, CDCl_3) δ 0.80 (t, $J = 7.4$ Hz, 3H, 4'- CH_3), 1.21 (d, $J = 6.8$ Hz, 3H, 1'- CH_3), 1.47 – 1.67 (m, 2H, 3'- CH_2), 2.98 (h, $J = 7.0$ Hz, 1H, 2'- CH), 3.79 (br, 2H, NH_2), 6.84 (dd, $J = 2.5, 8.5$ Hz, 1H, 6-H), 6.96 (d, $J = 2.5$ Hz, 1H, 2-H), 7.16 (d, $J = 8.5$ Hz, 1H, 5-H). $^{13}\text{C NMR}$ (151 MHz, CDCl_3) δ 12.1 (C-4'), 21.6 (C-1'), 30.7 (C-3'), 34.6 (C-2'), 109.1 (C-2), 119.3 (C-6), 128.5 (C-5), 130.8 (C-4), 144.5 (C-1), 150.8 (C-3). LC-MS (m/z): positive mode 195 $[\text{M} + \text{H}]^+$. Purity by HPLC-UV (254 nm)-ESI-MS: 98.2%.



4-(*sec*-Butyl)benzene-1,3-diamine (65r, LW465). The compound was synthesized using **64h** (1.15 g, 5.93 mmol). The product was isolated as a white solid (974 mg, 100% yield) and was directly used for the next step.

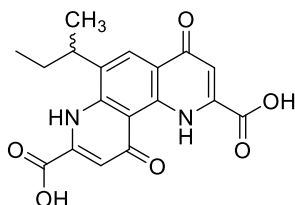


Tetramethyl 2,2'-((4-(*sec*-butyl)-1,3-phenylene)bis(azanediyl))bis(but-2-enedioate) (66r, LW466). The compound was synthesized using **65r** (974 mg, 5.93 mmol). The product was isolated as a yellow oil (1.66 g, 62% yield). $^1\text{H NMR}$ (600 MHz, CDCl_3) δ 0.85 (t, $J = 7.4$ Hz, 3H, 4'''- CH_3), 1.22 (d, $J = 6.9$ Hz, 3H, 1'''- CH_3), 1.57 – 1.66 (m, 2H, 3'''- CH_2), 2.96 (h, $J = 6.9$ Hz, 1H, 2'''- CH), 3.68 (s, 3H, CO_2CH_3), 3.72 (s, 3H, CO_2CH_3), 3.73 (s, 3H, CO_2CH_3), 3.74 (s, 3H, CO_2CH_3), 5.37 (s, 1H, 3'-H or 3''-H), 5.43 (s, 1H, 3'-H or 3''-H), 6.31 (d, $J = 2.2$ Hz, 1H, 2-H), 6.69 (dd, $J = 2.2, 8.3$ Hz, 1H, 6-H), 7.12 (d, $J = 8.3$ Hz, 1H, 5-H), 9.49 (s, 1H, NH), 9.51 (s, 1H, NH). $^{13}\text{C NMR}$ (151 MHz, CDCl_3) δ 11.9 (C-4'''), 20.9 (C-1'''), 30.0 (C-3'''), 34.8 (C-2'''), 51.2 (2 \times CO_2CH_3), 52.8 (CO_2CH_3), 52.9 (CO_2CH_3), 93.3 (C-3' or C-3''), 93.7 (C-3' or C-3''), 115.8 (C-2), 118.3 (C-6), 127.3 (C-5), 136.5 (C-4), 138.4 (C-2' or C-2''), 139.2 (C-2' or C-2''), 147.8 (C-1), 149.1 (C-3), 164.3 (CO_2Me), 164.4 (CO_2Me), 169.8 (CO_2Me), 170.2 (CO_2Me). LC-MS (m/z): positive mode 449 $[\text{M} + \text{H}]^+$. Purity by HPLC-UV (254 nm)-ESI-MS: 91.2%.



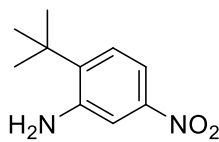
Dimethyl 6-(*sec*-butyl)-4,10-dioxo-1,4,7,10-tetrahydro-1,7-phenanthroline-2,8-dicarboxylate (67r, LW467). The compound was synthesized using **66r** (1.58 g, 3.52 mmol). The product was further purified by column chromatography on a column of silica gel (99:1 DCM/MeOH) and isolated as a gray solid (100 mg, 7% yield). $^1\text{H NMR}$ (600 MHz, CDCl_3) δ 0.97 (s, 3H, 4'- CH_3), 1.47 (s, 3H, 1'- CH_3), 1.71 – 1.99 (m, 2H, 3'- CH_2), 3.01 (s, 1H, 2'- CH), 3.99 – 4.17 (m, 6H, 2 \times CO_2CH_3), 7.14 (s, 1H, 3-H or 9-H), 7.22 (s, 1H, 3-H or 9-H), 8.49 (s, 1H, 5-H), 9.58 (br, 1H, NH), 14.68 (s, 1H, NH). $^{13}\text{C NMR}$ (151 MHz, CDCl_3) δ 12.1 (C-4'), 20.3 (C-1'), 29.7 (C-3'), 35.1 (C-2'), 53.6 (CO_2CH_3), 54.3 (CO_2CH_3), 113.1 (C-10a), 114.2 (C-3 or C-9),

114.4 (C-3 or C-9), 121.4 (C-4a), 128.1 (C-5), 130.7 (C-6), 135.4 (C-2 or C-8), 136.7 (C-2 or C-8), 139.0 (C-6a or C-10b), 141.1 (C-6a or C-10b), 162.3 ($\underline{\text{CO}}_2\text{Me}$), 162.7 ($\underline{\text{CO}}_2\text{Me}$), 177.3 (C-4 or C-10), 182.1 (C-4 or C-10). LC-MS (m/z): positive mode 385 $[\text{M} + \text{H}]^+$. Purity by HPLC-UV (254 nm)-ESI-MS: 98.2%. Mp: 198–199 °C dec.

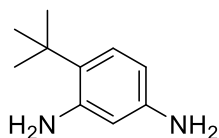


6-(*sec*-Butyl)-4,10-dioxo-1,4,7,10-tetrahydro-1,7-phenanthroline-2,8-dicarboxylic acid (68r, LW472). The compound was synthesized using **67r** (50 mg, 0.13 mmol). The product was isolated as a white solid (30 mg, 65% yield). ^1H NMR (600 MHz, D_2O , ND_3) δ 0.86 – 1.00 (m, 3H, 4'- $\underline{\text{CH}}_3$), 1.38 (d, $J = 6.7$ Hz, 3H, 1'- $\underline{\text{CH}}_3$), 1.52 – 1.77 (m, 2H, 3'- $\underline{\text{CH}}_2$), 3.08 (h, $J = 6.5$ Hz, 1H, 2'- $\underline{\text{CH}}$), 6.86 (s, 2H, 3-H, 9-H), 7.95 (s, 1H, 5-H). ^{13}C NMR (151 MHz, D_2O , ND_3) δ 13.8 (C-4'), 21.4 (C-1'), 31.9 (C-3'), 36.5 (C-2'), 113.2 (C-3 or C-9), 114.1 (C-3 or C-9), 114.2 (C-10a), 121.8 (C-4a), 127.0 (C-5), 136.6 (C-6), 140.2 (C-2 or C-8), 144.2 (C-2 or C-8), 145.9 (C-6a or C-10b), 147.0 (C-6a or C-10b), 168.9 ($\underline{\text{CO}}_2\text{H}$), 169.2 ($\underline{\text{CO}}_2\text{H}$), 180.9 (C-4 or C-10), 184.2 (C-4 or C-10). LC-MS (m/z): positive mode 357 $[\text{M} + \text{H}]^+$. Purity by HPLC-UV (254 nm)-ESI-MS: 98.9%. Mp: >300 °C dec.

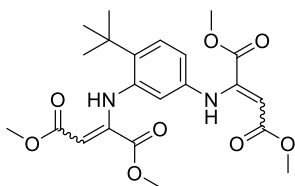
Preparation of 68s



2-(*tert*-Butyl)-5-nitroaniline (64m, LW137). The compound was synthesized using 2-(*tert*-butyl)aniline (5.2 mL, 34 mmol). The product was isolated as a yellow solid (5.2 g, 76% yield). ^1H NMR (600 MHz, CDCl_3) δ 1.44 (s, 9H, $\text{ArC}(\underline{\text{CH}}_3)_3$), 7.34 (d, $J = 8.7$ Hz, 1H, 3-H), 7.47 (d, $J = 2.4$ Hz, 1H, 6-H), 7.53 (dd, $J = 2.5, 8.6$ Hz, 1H, 4-H). ^{13}C NMR (151 MHz, CDCl_3) δ 29.1 ($\text{ArC}(\underline{\text{CH}}_3)_3$), 34.7 ($\text{ArC}(\underline{\text{CH}}_3)_3$), 111.4 (C-6), 113.1 (C-4), 127.3 (C-3), 140.5 (C-2), 145.3 (C-1), 146.9 (C-5). LC-MS (m/z): positive mode 195 $[\text{M} + \text{H}]^+$. Purity by HPLC-UV (254 nm)-ESI-MS: 90.0%.

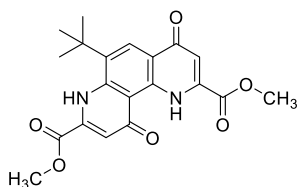


2-(*tert*-Butyl)benzene-1,3-diamine (65s, LW138). The compound was synthesized using **64m** (1.5 g, 7.7 mmol). The product was isolated as a white solid (1.2 g, 95% yield) and directly used for the next step.

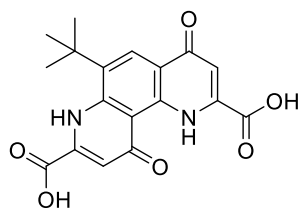


Tetramethyl 2,2'-((4-(*tert*-butyl)-1,3-phenylene)bis(azanediyl))bis(but-2-enedioate) (66s, LW140). The compound was synthesized using **65s** (1.2 g, 7.3 mmol). The product was isolated as a yellow oil (1.2 g, 36% yield). ^1H NMR (600 MHz, CDCl_3) δ 1.43 (s, 9H, $\text{ArC}(\underline{\text{CH}}_3)_3$), 3.67 (s, 3H, $\text{CO}_2\underline{\text{CH}}_3$), 3.72 (s, 3H, $\text{CO}_2\underline{\text{CH}}_3$), 3.74 (s, 3H, $\text{CO}_2\underline{\text{CH}}_3$), 3.76 (s, 3H, $\text{CO}_2\underline{\text{CH}}_3$), 5.38 (s, 1H, 3'-H or 3''-H), 5.45 (s, 1H, 3'-H or 3''-H), 6.28 (d, $J = 2.2$ Hz, 1H, 2-H), 6.63 (dd, $J = 2.3, 8.5$ Hz, 1H, 6-H), 7.27 (d, $J = 8.5$ Hz, 1H, 5-H), 9.50 (s, 1H, $\underline{\text{NH}}$), 9.69 (s, 1H, $\underline{\text{NH}}$). ^{13}C NMR (151 MHz, CDCl_3) δ 30.4 ($\text{ArC}(\underline{\text{CH}}_3)_3$), 34.7 ($\text{ArC}(\underline{\text{CH}}_3)_3$), 51.2 ($\text{CO}_2\underline{\text{CH}}_3$), 51.2 ($\text{CO}_2\underline{\text{CH}}_3$), 52.8 ($\text{CO}_2\underline{\text{CH}}_3$), 52.9 ($\text{CO}_2\underline{\text{CH}}_3$), 93.3 (C-3' or C-3''), 94.0 (C-3' or C-3''), 117.5

(C-2 or C-6), 117.6 (C-2 or C-6), 127.6 (C-5), 138.8 (C-4), 138.9 (C-2' or C-2''), 140.1 (C-2' or C-2''), 147.5 (C-1 or C-3), 148.7 (C-1 or C-3), 164.3 ($\underline{\text{CO}}_2\text{Me}$), 164.4 ($\underline{\text{CO}}_2\text{Me}$), 169.8 ($\underline{\text{CO}}_2\text{Me}$), 170.3 ($\underline{\text{CO}}_2\text{Me}$). LC–MS (m/z): positive mode 449 $[\text{M} + \text{H}]^+$. Purity by HPLC–UV (254 nm)–ESI–MS: 97.3%.

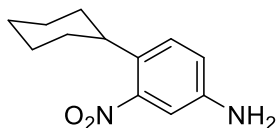


Dimethyl 6-(*tert*-butyl)-4,10-dioxo-1,4,7,10-tetrahydro-1,7-phenanthroline-2,8-dicarboxylate (67s, LW150). The compound was synthesized using **66s** (1.0 g, 2.23 mmol). The product was isolated as a gray solid (44 mg, 8% yield). ^1H NMR (600 MHz, CDCl_3) δ 1.66 (s, 9H, $\text{ArC}(\underline{\text{CH}}_3)_3$), 4.06 (s, 3H, $\text{CO}_2\underline{\text{CH}}_3$), 4.12 (s, 3H, $\text{CO}_2\underline{\text{CH}}_3$), 7.14 (s, 1H, 3-H or 9-H), 7.20 (s, 1H, 3-H or 9-H), 8.63 (s, 1H, 5-H), 10.03 (s, 1H, $\underline{\text{NH}}$), 14.73 (s, 1H, $\underline{\text{NH}}$). ^{13}C NMR (151 MHz, CDCl_3) δ 30.8 ($\text{ArC}(\underline{\text{CH}}_3)_3$), 34.5 ($\text{ArC}(\underline{\text{CH}}_3)_3$), 53.6 ($\text{CO}_2\underline{\text{CH}}_3$), 54.4 ($\text{CO}_2\underline{\text{CH}}_3$), 113.7 (C-3 or C-9), 114.1 (C-10a), 114.7 (C-3 or C-9), 121.1 (C-4a), 128.5 (C-5), 133.1 (C-6), 135.0 (C-2 or C-8), 136.7 (C-2 or C-8), 139.4 (C-6a or C-10b), 141.7 (C-6a or C-10b), 162.4 ($\underline{\text{CO}}_2\text{Me}$), 163.0 ($\underline{\text{CO}}_2\text{Me}$), 177.7 (C-4 or C-10), 182.4 (C-4 or C-10). LC–MS (m/z): positive mode 385 $[\text{M} + \text{H}]^+$. Purity by HPLC–UV (254 nm)–ESI–MS: 95.6%.

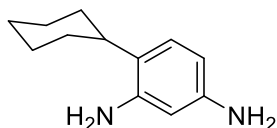


6-(*tert*-Butyl)-4,10-dioxo-1,4,7,10-tetrahydro-1,7-phenanthroline-2,8-dicarboxylic acid (68, LW153). The compound was synthesized using **67s** (30 mg, 0.078 mmol). The product was isolated as a white solid (15 mg, 54% yield). ^1H NMR (600 MHz, D_2O , ND_3) δ 1.54 (s, 9H, $\text{ArC}(\underline{\text{CH}}_3)_3$), 6.66 (s, 1H, 3-H or 9-H), 6.74 (s, 1H, 3-H or 9-H), 7.96 (s, 1H, 5-H). ^{13}C NMR (151 MHz, D_2O , ND_3) δ 32.4 ($\text{ArC}(\underline{\text{CH}}_3)_3$), 36.7 ($\text{ArC}(\underline{\text{CH}}_3)_3$), 113.4 (C-3 or C-9), 113.5 (C-3 or C-9), 114.5 (C-10a), 121.2 (C-4a), 128.1 (C-5), 137.7 (C-6), 140.1 (C-2 or C-8), 143.5 (C-2 or C-8), 144.7 (C-6a or C-10b), 145.8 (C-6a or C-10b), 168.2 ($\underline{\text{CO}}_2\text{H}$), 168.5 ($\underline{\text{CO}}_2\text{H}$), 180.8 (C-4 or C-10), 184.6 (C-4 or C-10). LC–MS (m/z): positive mode 357 $[\text{M} + \text{H}]^+$. Purity by HPLC–UV (254 nm)–ESI–MS: 97.8%. Mp: >300 °C dec.

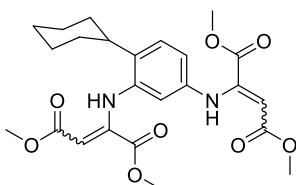
Preparation of 68t



4-Cyclohexyl-3-nitroaniline (64i, LW253). The compound was synthesized using 4-cyclohexylaniline (4.0 g, 23 mmol). The product was isolated as a yellow solid (4.3 g, 85% yield). ^1H NMR (600 MHz, CDCl_3) δ 1.18 – 1.27 (m, 1H, Cy), 1.34 – 1.41 (m, 4H, Cy), 1.71 – 1.76 (m, 1H, Cy), 1.78 – 1.86 (m, 4H, Cy), 2.85 (tt, $J = 3.3, 8.3$ Hz, 1H, Cy), 3.91 (s, 2H, $\underline{\text{NH}}_2$), 6.82 (dd, $J = 2.5, 8.5$ Hz, 1H, 6-H), 6.97 (d, $J = 2.5$ Hz, 1H, 2-H), 7.19 (d, $J = 8.5$ Hz, 1H, 5-H). ^{13}C NMR (151 MHz, CDCl_3) δ 26.0 (C-4'), 26.7 (C-3', C-5'), 34.1 (C-2', C-6'), 38.2 (C-1'), 109.4 (C-2), 119.2 (C-6), 128.8 (C-5), 131.0 (C-4), 144.6 (C-1), 150.2 (C-3). LC–MS (m/z): positive mode 221 $[\text{M} + \text{H}]^+$. Purity by HPLC–UV (254 nm)–ESI–MS: 98.7%.

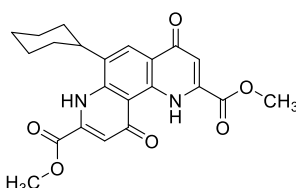


4-Cyclohexylbenzene-1,3-diamine (65t, LW263). The compound was synthesized using **64i** (1.25 g, 5.67 mmol). The product was isolated as a yellow solid (1.08 g, 100% yield) and was used directly for the next step.



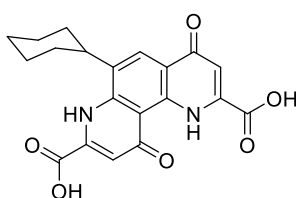
Tetramethyl 2,2'-((4-cyclohexyl-1,3-phenylene)bis(azanediyl))bis(but-2-enedioate) (66t, LW264). The compound was synthesized using **65t** (1.08 g, 5.67 mmol). The product was isolated as a yellow oil (1.89 g, 70% yield). ¹H NMR (600 MHz, CDCl₃) δ 1.23 – 1.29 (m, 1H, Cy), 1.33 – 1.48 (m, 4H, Cy), 1.71 – 1.79 (m, 1H, Cy), 1.81 – 1.89 (m, 4H, Cy), 2.70 – 2.83 (m, 1H, Cy), 3.70 (s, 3H, CO₂CH₃),

3.72 (s, 3H, CO₂CH₃), 3.73 (s, 3H, CO₂CH₃), 3.75 (s, 3H, CO₂CH₃), 5.36 (s, 1H, 3'-H or 3''-H), 5.45 (s, 1H, 3'-H or 3''-H), 6.30 (d, *J* = 1.9 Hz, 1H, 2-H), 6.67 (dd, *J* = 2.0, 8.3 Hz, 1H, 6-H), 7.14 (d, *J* = 8.3 Hz, 1H, 5-H), 9.45 – 9.57 (m, 2H, 2 × NH). ¹³C NMR (151 MHz, CDCl₃) δ 26.2 (C-4'''), 26.8 (C-3''', C-5'''), 33.3 (C-2''', C-6'''), 38.3 (C-1'''), 51.2 (CO₂CH₃), 51.2 (CO₂CH₃), 52.8 (CO₂CH₃), 52.9 (CO₂CH₃), 93.7 (C-3' or C-3''), 93.7 (C-3' or C-3''), 115.5 (C-2), 118.1 (C-6), 127.2 (C-5), 136.7 (C-4), 138.4 (C-2' or C-2''), 138.8 (C-2' or C-2''), 147.8 (C-1), 148.9 (C-3), 164.4 (CO₂Me), 164.4 (CO₂Me), 169.8 (CO₂Me), 170.1 (CO₂Me). LC–MS (*m/z*): positive mode 475 [M + H]⁺. Purity by HPLC–UV (254 nm)–ESI–MS: 91.0%.



Dimethyl 6-cyclohexyl-4,10-dioxo-1,4,7,10-tetrahydro-1,7-phenanthroline-2,8-dicarboxylate (67t, LW267). The compound was synthesized using **66t** (1.80 g, 3.80 mmol). The product was isolated as a brown solid (742 mg, 47% yield). ¹H NMR (600 MHz, CDCl₃) δ 1.32 – 1.43 (m, 1H, Cy), 1.50 – 1.62 (m, 2H, Cy), 1.63 – 1.75 (m, 2H, Cy), 1.84 – 1.91 (m, 1H, Cy), 1.95 – 2.06 (m, 4H, Cy), 2.75 – 2.86

(m, 1H, Cy), 4.06 (s, 3H, CO₂CH₃), 4.11 (s, 3H, CO₂CH₃), 7.12 (s, 1H, 3-H or 9-H), 7.24 (s, 1H, 3-H or 9-H), 8.47 (s, 1H, 5-H), 9.55 (br, 1H, NH). ¹³C NMR (151 MHz, CDCl₃) δ 25.9 (C-4'), 26.8 (C-3', C-5'), 33.1 (C-2', C-6'), 38.6 (C-1'), 53.7 (CO₂CH₃), 54.3 (CO₂CH₃), 113.0 (C-10a), 114.2 (C-3 or C-9), 114.3 (C-3 or C-9), 121.3 (C-4a), 127.7 (C-5), 131.0 (C-6), 135.4 (C-2 or C-8), 136.7 (C-2 or C-8), 139.0 (C-6a or C-10b), 140.8 (C-6a or C-10b), 162.2 (CO₂Me), 162.7 (CO₂Me), 177.2 (C-4 or C-10), 182.1 (C-4 or C-10). LC–MS (*m/z*): positive mode 411 [M + H]⁺. Purity by HPLC–UV (254 nm)–ESI–MS: 93.7%.

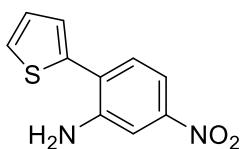


6-Cyclohexyl-4,10-dioxo-1,4,7,10-tetrahydro-1,7-phenanthroline-2,8-dicarboxylic acid (68t, LW268). The compound was synthesized using **67t** (600 mg, 1.46 mmol). The product was isolated as a yellow solid (540 mg, 97% yield). ¹H NMR (600 MHz, D₂O, ND₃) δ 1.05 – 1.28 (m, 4H, Cy), 1.37 – 1.52 (m, 2H, Cy), 1.58 – 1.68 (m, 2H, Cy), 1.70 – 1.88 (m, 2H, Cy), 2.29 – 2.45 (m, 1H, Cy), 6.66 (s, 1H, 3-

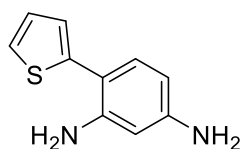
H or 9-H), 6.69 (s, 1H, 3-H or 9-H), 7.56 (s, 1H, 5-H). ¹³C NMR (151 MHz, D₂O, ND₃) δ 28.4 (C-4'), 28.9 (C-3', C-5'), 35.1 (C-2', C-6'), 40.1 (C-1'), 113.1 (C-3 or C-9), 113.4 (C-10a), 113.9 (C-3 or C-9), 121.5 (C-4a), 126.9 (C-5), 134.5 (C-6), 139.5 (C-2 or C-8), 142.3 (C-2 or C-8), 145.1 (C-6a or C-10b), 145.7 (C-6a or C-10b), 167.8

(CO₂H), 168.4 (CO₂H), 180.5 (C-4 or C-10), 184.3 (C-4 or C-10). LC-MS (*m/z*): positive mode 383 [M + H]⁺. Purity by HPLC-UV (254 nm)-ESI-MS: 96.4%. Mp: >300 °C dec.

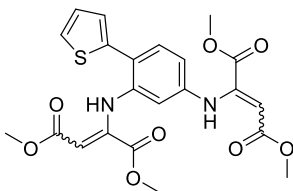
Preparation of 68u



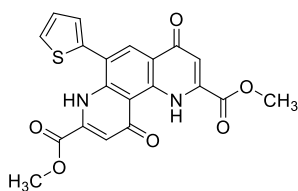
5-Nitro-2-(thiophen-2-yl)aniline (64n, LW183). The compound was synthesized using 2-Bromo-5-nitroaniline (2.0 g, 9.2 mmol). The product was isolated as a yellow solid (1.75 g, 86% yield). ¹H NMR (600 MHz, CDCl₃) δ 4.34 (s, 2H, NH₂), 7.14 – 7.18 (m, 1H, ArH), 7.30 (d, *J* = 3.4 Hz, 1H, ArH), 7.37 (d, *J* = 8.3 Hz, 1H, ArH), 7.44 (d, *J* = 5.1 Hz, 1H, ArH), 7.56 – 7.62 (m, 2H, 2 × ArH). ¹³C NMR (151 MHz, CDCl₃) δ 110.0 (C-6), 113.0 (C-4), 125.8 (C-2), 126.8 (Ar), 126.8 (Ar), 127.9 (Ar), 131.3 (C-3), 138.6 (C-1'), 144.7 (C-5), 148.0 (C-1). LC-MS (*m/z*): positive mode 221 [M + H]⁺. Purity by HPLC-UV (254 nm)-ESI-MS: 99.1%.



4-(Thiophen-2-yl)benzene-1,3-diamine (65u, LW185). The compound was synthesized using 2-Bromo-5-nitroaniline (1.6 g, 7.3 mmol). The product was isolated as a white solid (1.4 g, 100% yield).

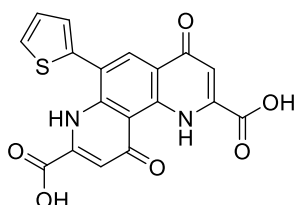


Tetramethyl 2,2'-((4-(thiophen-2-yl)-1,3-phenylene)bis(azanediyl))bis(but-2-enedioate) (66u, LW186). The compound was synthesized using **65u** (1.38 g, 7.25 mmol). The product was isolated as a yellow oil (855 mg, 25% yield). ¹H NMR (600 MHz, CDCl₃) δ 3.68 (s, 3H, CO₂CH₃), 3.69 (s, 3H, CO₂CH₃), 3.73 (s, 3H, CO₂CH₃), 3.77 (s, 3H, CO₂CH₃), 5.44 (s, 1H, 3'-H or 3''-H), 5.48 (s, 1H, 3'-H or 3''-H), 6.38 (d, *J* = 2.1 Hz, 1H, 2-H), 6.68 (dd, *J* = 2.2, 8.3 Hz, 1H, 6-H), 7.07 (dd, *J* = 3.7, 5.1 Hz, 1H, ArH), 7.23 – 7.25 (m, 1H, ArH), 7.31 – 7.33 (m, 1H, ArH), 7.39 (d, *J* = 8.3 Hz, 1H, 5-H), 9.44 (s, 1H, NH), 9.58 (s, 1H, NH). ¹³C NMR (151 MHz, CDCl₃) δ 51.2 (CO₂CH₃), 51.3 (CO₂CH₃), 52.9 (CO₂CH₃), 53.1 (CO₂CH₃), 95.0 (C-3' or C-3''), 95.1 (C-3' or C-3''), 115.3 (C-2), 117.4 (C-6), 124.1 (C-1'''), 126.0 (Ar), 126.4 (Ar), 127.4 (Ar), 130.8 (C-5), 138.6 (C-4), 139.2 (C-2' or C-2''), 140.3 (C-2' or C-2''), 147.0 (C-1 or C-3), 147.7 (C-1 or C-3), 164.1 (CO₂Me), 164.3 (CO₂Me), 169.6 (CO₂Me), 169.7 (CO₂Me). LC-MS (*m/z*): positive mode 475 [M + H]⁺. Purity by HPLC-UV (254 nm)-ESI-MS: 87.2%.



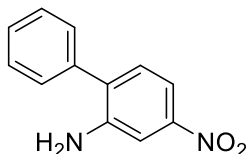
Dimethyl 4,10-dioxo-6-(thiophen-2-yl)-1,4,7,10-tetrahydro-1,7-phenanthroline-2,8-dicarboxylate (67u, LW191). The compound was synthesized using **66u** (695 mg, 1.47 mmol). The product was further purified by column chromatography on a column of silica gel (99:1 DCM/MeOH) and isolated as a yellow solid (170 mg, 28% yield). ¹H NMR (600 MHz, CDCl₃) δ 4.05 (s, 3H, CO₂CH₃), 4.08 (s, 3H, CO₂CH₃), 7.13 (s, 1H, ArH), 7.24 (s, 1H, ArH), 7.29 (s, 1H, ArH), 7.36 (s, 1H, ArH), 7.58

(d, $J = 5.0$ Hz, 1H, ArH), 8.59 (s, 1H, 5-H), 10.08 (br, 1H, NH), 14.66 (s, 1H, NH). ^{13}C NMR (151 MHz, CDCl_3) δ 53.8 (CO_2CH_3), 54.2 (CO_2CH_3), 113.1 (C-10a), 114.6 (C-3 or C-9), 114.8 (C-3 or C-9), 120.1 (C-6), 121.0 (C-4a), 127.8 (Ar), 128.4 (Ar), 128.7 (Ar), 132.2 (C-5), 135.5 (C-2 or C-8), 135.9 (C-1'), 137.0 (C-2 or C-8), 140.1 (C-6a or C-10b), 140.7 (C-6a or C-10b), 162.1 (CO_2Me), 162.2 (CO_2Me), 177.1 (C-4 or C-10), 181.7 (C-4 or C-10). LC-MS (m/z): positive mode 411 $[\text{M} + \text{H}]^+$. Purity by HPLC-UV (254 nm)-ESI-MS: 96.5%.

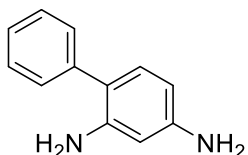


4,10-Dioxo-6-(thiophen-2-yl)-1,4,7,10-tetrahydro-1,7-phenanthroline-2,8-dicarboxylic acid (68u, LW204). The compound was synthesized using **67u** (55 mg, 0.13 mmol). The product was isolated as a beige solid (44 mg, 86% yield). ^1H NMR (600 MHz, D_2O , ND_3) δ 6.26 (s, 1H, 3-H or 9-H), 6.30 (s, 1H, 3-H or 9-H), 6.76 (d, $J = 2.7$ Hz, 1H, ArH), 6.99 (dd, $J = 3.2, 5.1$ Hz, 1H, ArH), 7.20 (s, 1H, 5-H), 7.37 (d, $J = 5.3$ Hz, 1H, ArH). ^{13}C NMR (151 MHz, D_2O , ND_3) δ 113.0 (C-10a), 113.2 (C-3 or C-9), 113.9 (C-3 or C-9), 120.6 (C-6), 122.3 (C-4a), 129.2 (C-5), 130.3 (Ar), 130.6 (Ar), 131.2 (Ar), 138.0 (C-1'), 139.6 (C-2 or C-8), 140.5 (C-2 or C-8), 145.2 (C-6a or C-10b), 145.6 (C-6a or C-10b), 167.1 (CO_2H), 167.8 (CO_2H), 179.9 (C-4 or C-10), 183.2 (C-4 or C-10). LC-MS (m/z): positive mode 383 $[\text{M} + \text{H}]^+$. Purity by HPLC-UV (254 nm)-ESI-MS: 95.0%. Mp: >300 °C dec.

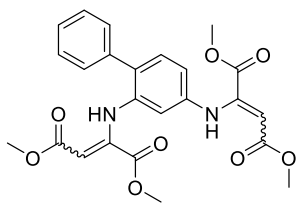
Preparation of 68v



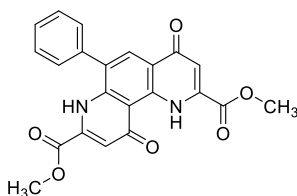
4-Nitro-[1,1'-biphenyl]-2-amine (64o, LW213). The compound was synthesized using 2-Bromo-5-nitroaniline (2.50 g, 11.5 mmol). The product was isolated as a yellow solid (2.34 g, 95% yield). ^1H NMR (600 MHz, CDCl_3) δ 7.24 (d, $J = 8.3$ Hz, 1H, ArH), 7.40 – 7.46 (m, 3H, ArH), 7.47 – 7.52 (m, 2H, ArH), 7.61 (d, $J = 2.2$ Hz, 1H, ArH), 7.65 (dd, $J = 2.2, 8.3$ Hz, 1H, ArH). ^{13}C NMR (151 MHz, CDCl_3) δ 109.8 (C-3), 113.4 (C-5), 128.4 (C-4'), 128.6 (C-2', C-6'), 129.2 (C-3', C-5'), 131.0 (C-6), 133.6 (C-1), 137.3 (C-1'), 144.2 (C-4), 148.1 (C-2). LC-MS (m/z): positive mode 215 $[\text{M} + \text{H}]^+$. Purity by HPLC-UV (254 nm)-ESI-MS: 98.2%.



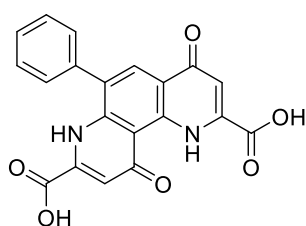
[1,1'-Biphenyl]-2,4-diamine (65v, LW217). The compound was synthesized using **64o** (2.00 g, 9.34 mmol). The product was isolated as a white solid (1.72 g, 100% yield) and directly used for the next step.



Tetramethyl 2,2'-([1,1'-biphenyl]-2,4-diylbis(azanediyl))bis(but-2-enedioate) (66u, LW218). The compound was synthesized using **65v** (1.72 g, 9.34 mmol). The product was isolated as a yellow oil (4.01 g, 92% yield). ^1H NMR (600 MHz, CDCl_3) δ 3.64 (s, 3H, CO_2CH_3), 3.72 (s, 3H, CO_2CH_3), 3.74 (s, 3H, CO_2CH_3), 3.79 (s, 3H, CO_2CH_3), 5.38 (s, 1H, 3''-H or 3'''-H), 5.45 (s, 1H, 3''-H or 3'''-H), 6.41 (d, $J = 2.1$ Hz, 1H, 3-H), 6.72 (dd, $J = 2.2, 8.2$ Hz, 1H, 5-H), 7.20 (d, $J = 8.2$ Hz, 1H, 6-H), 7.31 – 7.35 (m, 1H, 4'-H), 7.38 – 7.46 (m, 4H, 2'-H, 3'-H, 5'-H, 6'-H), 9.23 (s, 1H, NH), 9.61 (s, 1H, NH). ^{13}C NMR (151 MHz, CDCl_3) δ 51.1 (CO_2CH_3), 51.3 (CO_2CH_3), 52.9 (CO_2CH_3), 53.0 (CO_2CH_3), 94.7 (C-3'' or C-3'''), 94.7 (C-3'' or C-3'''), 114.6 (C-3), 117.2 (C-5), 127.5 (C-4'), 128.5 (C-2', C-6'), 129.3 (C-3', C-5'), 130.8 (C-1'), 131.3 (C-6), 137.8 (C-1), 138.7 (C-2'' or C-2'''), 140.2 (C-2'' or C-2'''), 147.3 (C-2 or C-4), 147.6 (C-2 or C-4), 164.2 (CO_2Me), 164.4 (CO_2Me), 169.4 (CO_2Me), 169.7 (CO_2Me). LC-MS (m/z): positive mode 469 $[\text{M} + \text{H}]^+$. Purity by HPLC-UV (254 nm)-ESI-MS: 85.0%.

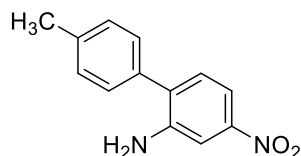


Dimethyl 4,10-dioxo-6-phenyl-1,4,7,10-tetrahydro-1,7-phenanthroline-2,8-dicarboxylate (67v, LW221). The compound was synthesized using **66v** (2.00 g, 4.27 mmol). The product was isolated as a gray solid (168 mg, 10% yield). ^1H NMR (600 MHz, CDCl_3) δ 4.01 (s, 3H, CO_2CH_3), 4.08 (s, 3H, CO_2CH_3), 7.09 (s, 1H, 3-H or 9-H), 7.21 (s, 1H, 3-H or 9-H), 7.50 – 7.57 (m, 3H, $3 \times \text{ArH}$), 7.58 – 7.64 (m, 2H, $2 \times \text{ArH}$), 8.49 (s, 1H, 5-H), 9.66 (br, 1H, NH), 14.64 (s, 1H, NH). ^{13}C NMR (151 MHz, CDCl_3) δ 53.7 (CO_2CH_3), 54.2 (CO_2CH_3), 113.0 (C-10a), 114.3 (C-3 or C-9), 114.6 (C-3 or C-9), 121.2 (C-4a), 127.4 (C-6), 129.1 (C-2', C-6'), 129.5 (C-5), 130.0 (C-3', C-5'), 131.4 (C-4'), 134.4 (C-2 or C-8), 135.7 (C-2 or C-8), 136.8 (C-1'), 139.8 (C-6a or C-10b), 140.6 (C-6a or C-10b), 162.2 (CO_2Me), 162.2 (CO_2Me), 177.3 (C-4 or C-10), 181.7 (C-4 or C-10). LC-MS (m/z): positive mode 405 $[\text{M} + \text{H}]^+$. Purity by HPLC-UV (254 nm)-ESI-MS: 97.5%.

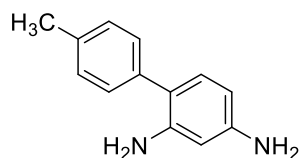


4,10-Dioxo-6-phenyl-1,4,7,10-tetrahydro-1,7-phenanthroline-2,8-dicarboxylic acid (68v, LW228). The compound was synthesized using **67v** (100 mg, 0.247 mmol). The product was isolated as a white solid (74 mg, 80% yield). ^1H NMR (600 MHz, D_2O , ND_3) δ 7.04 (s, 1H, 3-H or 9-H), 7.06 (s, 1H, 3-H or 9-H), 7.56 – 7.66 (m, 5H, $5 \times \text{ArH}$), 8.18 (s, 1H, 5-H). ^{13}C NMR (151 MHz, D_2O , ND_3) δ 113.6 (C-3 or C-9), 114.2 (C-3 or C-9), 115.3 (C-10a), 122.1 (C-4a), 130.0 (C-5), 131.4 (C-4'), 132.0 (C-2', C-6'), 132.3 (C-3', C-5'), 134.6 (C-6), 139.3 (C-2 or C-8), 142.1 (C-2 or C-8), 146.1 (C-1'), 146.6 (C-6a, C-10b), 150.8 (C-6a, C-10b), 169.4 (CO_2H), 171.5 (CO_2H), 181.5 (C-4 or C-10), 183.1 (C-4 or C-10). LC-MS (m/z): positive mode 377 $[\text{M} + \text{H}]^+$. Purity by HPLC-UV (254 nm)-ESI-MS: 98.8%. Mp: >300 °C dec.

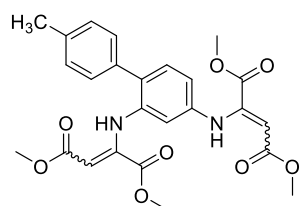
Preparation of 68w



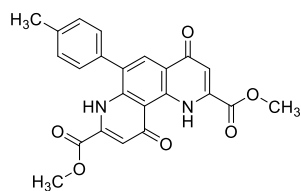
4'-Methyl-4-nitro-[1,1'-biphenyl]-2-amine (64p, LW417). The compound was synthesized using 2-bromo-5-nitroaniline (1.0 mg, 4.6 mmol). The product was isolated as a yellow solid (920 mg, 88% yield). ^1H NMR (600 MHz, CDCl_3) δ 2.42 (s, 3H, ArCH_3), 7.21 (d, $J = 8.3$ Hz, 1H, ArH), 7.30 (d, $J = 7.9$ Hz, 2H, 3'-H, 5'-H), 7.33 (d, $J = 8.0$ Hz, 2H, 2'-H, 6'-H), 7.58 (s, 1H, ArH), 7.62 (d, $J = 7.8$ Hz, 1H, ArH). ^{13}C NMR (151 MHz, CDCl_3) δ 21.2 (ArCH_3), 109.5 (C-3), 113.1 (C-5), 128.4 (C-2', C-6'), 129.8 (C-3', C-5'), 130.9 (C-6), 133.5 (C-1), 134.4 (C-1'), 138.3 (C-4'), 144.5 (C-4), 147.9 (C-2). LC-MS (m/z): positive mode 229 [$\text{M} + \text{H}$] $^+$. Purity by HPLC-UV (254 nm)-ESI-MS: 96.6%.



4'-Methyl-[1,1'-biphenyl]-2,4-diamine (65w, LW422). The compound was synthesized using **64q** (900 mg, 4.05 mmol). The product was isolated as a white solid (800 mg, 100% yield) and directly used for the next step.

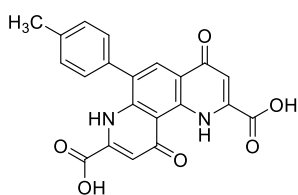


Tetramethyl 2,2'-((4'-methyl-[1,1'-biphenyl]-2,4-diyl)bis(azanediyl))bis(but-2-enedioate) (66w, LW421). The compound was synthesized using **65w** (800 mg, 4.04 mmol). The product was isolated as a yellow oil (522 mg, 27% yield). ^1H NMR (600 MHz, CDCl_3) δ 2.38 (s, 3H, ArCH_3), 3.65 (s, 3H, CO_2CH_3), 3.72 (s, 3H, CO_2CH_3), 3.74 (s, 3H, CO_2CH_3), 3.78 (s, 3H, CO_2CH_3), 5.39 (s, 1H, 3''-H or 3'''-H), 5.43 (s, 1H, 3''-H or 3'''-H), 6.39 (d, $J = 1.6$ Hz, 1H, 3-H), 6.70 (dd, $J = 1.9, 8.2$ Hz, 1H, 5-H), 7.19 (d, $J = 8.2$ Hz, 1H, 6-H), 7.21 (d, $J = 7.9$ Hz, 2H, 3'-H, 5'-H), 7.33 (d, $J = 7.9$ Hz, 2H, 2'-H, 6'-H), 9.22 (s, 1H, NH), 9.60 (s, 1H, NH). ^{13}C NMR (151 MHz, CDCl_3) δ 21.2 (ArCH_3), 51.1 (CO_2CH_3), 51.3 (CO_2CH_3), 52.9 (CO_2CH_3), 53.0 (CO_2CH_3), 94.5 (C-3'' or C-3'''), 94.6 (C-3'' or C-3'''), 114.5 (C-3), 117.2 (C-5), 129.1 (C-2', C-6'), 129.3 (C-3', C-5'), 130.8 (C-1'), 131.3 (C-6), 134.8 (C-4'), 137.1 (C-1), 138.7 (C-2'' or C-2'''), 140.0 (C-2'' or C-2'''), 147.4 (C-2 or C-4), 147.6 (C-2 or C-4), 164.3 (CO_2Me), 164.4 (CO_2Me), 169.5 (CO_2Me), 169.7 (CO_2Me). LC-MS (m/z): positive mode 483 [$\text{M} + \text{H}$] $^+$. Purity by HPLC-UV (254 nm)-ESI-MS: 79.6%.



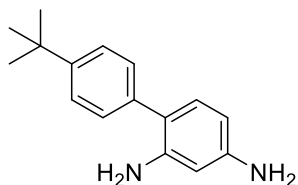
Dimethyl 4,10-dioxo-6-(p-tolyl)-1,4,7,10-tetrahydro-1,7-phenanthroline-2,8-dicarboxylate (67w, LW424). The compound was synthesized using **66w** (500 mg, 1.04 mmol). The product was isolated as a brown solid (125 mg, 29% yield). ^1H NMR (600 MHz, CDCl_3) δ 2.47 (s, 3H, ArCH_3), 4.01 (s, 3H, CO_2CH_3), 4.07 (s, 3H, CO_2CH_3), 7.09 (s, 1H, 3-H or 9-H), 7.19 (s, 1H, 3-H or 9-H), 7.40 (s, 4H, $4 \times \text{ArH}$), 8.48 (s, 1H, 5-H), 9.71 (s, 1H, NH), 14.62 (s, 1H, NH). ^{13}C NMR (151 MHz, CDCl_3) δ 21.3 (ArCH_3), 53.7 (CO_2CH_3), 54.1 (CO_2CH_3), 113.0 (C-10a), 114.2 (C-3 or C-9), 114.7 (C-3 or C-9), 121.3 (C-4a), 127.4 (C-6), 128.9 (C-2', C-6'), 130.7 (C-3', C-5'), 131.3 (C-5), 131.4 (C-4'), 135.7 (C-2 or C-8), 136.7 (C-2 or C-8), 139.5 (C-

1'), 139.7 (C-6a or C-10b), 140.7 (C-6a or C-10b), 162.2 ($\underline{\text{CO}}_2\text{Me}$), 162.3 ($\underline{\text{CO}}_2\text{Me}$), 177.4 (C-4 or C-10), 181.8 (C-4 or C-10). LC-MS (m/z): positive mode 419 $[\text{M} + \text{H}]^+$. Purity by HPLC-UV (254 nm)-ESI-MS: 94.0%.

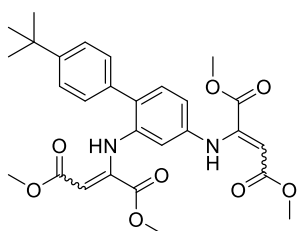


4,10-Dioxo-6-(*p*-tolyl)-1,4,7,10-tetrahydro-1,7-phenanthroline-2,8-dicarboxylic acid (68w, LW427). The compound was synthesized using **67w** (100 mg, 0.24 mmol). The product was isolated as a brown solid (90 mg, 96% yield). ^1H NMR (600 MHz, D_2O , ND_3) δ 2.39 (s, 3H, ArCH_3), 6.79 – 6.94 (m, 2H, 3-H, 9-H), 7.05 – 7.18 (m, 2H, 3'-H, 5'-H), 7.19 – 7.31 (m, 2H, 2'-H, 6'-H), 7.90 (s, 1H, 5-H). ^{13}C NMR (151 MHz, D_2O , ND_3) δ 23.1 (ArCH_3), 113.6 (C-3 or C-9), 114.1 (C-3 or C-9), 114.5 (C-10a), 121.9 (C-4a), 130.9 (C-5), 131.3 (C-2', C-6'), 131.6 (C-4'), 132.7 (C-3', C-5'), 134.5 (C-6), 141.1 (C-2 or C-8), 141.9 (C-2 or C-8), 143.5 (C-1'), 146.0 (C-6a or C-10b), 147.2 (C-6a or C-10b), 168.9 ($2 \times \underline{\text{CO}}_2\text{H}$), 181.1 (C-4 or C-10), 184.1 (C-4 or C-10). LC-MS (m/z): positive mode 391 $[\text{M} + \text{H}]^+$. Purity by HPLC-UV (254 nm)-ESI-MS: 95.0%. Mp: >300 °C dec.

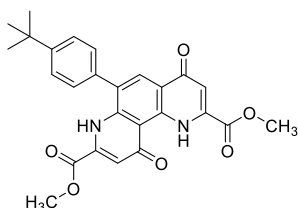
Preparation of 68x



4'-(*tert*-Butyl)-[1,1'-biphenyl]-2,4-diamine (65x, LW484). The compound was synthesized using **64q** (720 mg, 2.67 mmol). The product was isolated as a white solid (642 mg, 100% yield) and directly used for the next step.

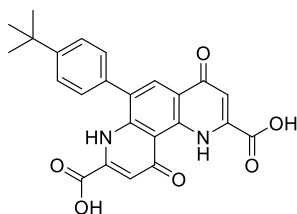


Tetramethyl 2,2'-((4'-(*tert*-butyl)-[1,1'-biphenyl]-2,4-diyl)bis(azanediyl))bis(but-2-enedioate) (66x, LW485). The compound was synthesized using **65x** (642 mg, 2.67 mmol). The product was isolated as a yellow oil (519 mg, 37% yield) and used directly for the next step.



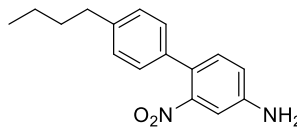
Dimethyl 6-(4-(*tert*-butyl)phenyl)-4,10-dioxo-1,4,7,10-tetrahydro-1,7-phenanthroline-2,8-dicarboxylate (67x, LW113). The compound was synthesized using **66x** (519 mg, 0.99 mmol). The product was further purified by column chromatography on a column of silica gel (99:1 DCM/MeOH) and isolated as a yellow solid (274 mg, 67% yield). ^1H NMR (600 MHz, CDCl_3) δ 1.40 (s, 9H, $\text{ArC}(\underline{\text{CH}}_3)_3$), 4.02 (s, 3H, $\text{CO}_2\underline{\text{CH}}_3$), 4.08 (s, 3H, $\text{CO}_2\underline{\text{CH}}_3$), 7.09 (s, 1H, 3-H or 9-H), 7.19 (s, 1H, 3-H or 9-H), 7.45 (d, $J = 8.2$ Hz, 2H, 2'-H, 6'-H), 7.61 (d, $J = 8.2$ Hz, 2H, 3'-H, 5'-H), 8.48 (s, 1H, 5-H), 9.76 (s, 1H, NH), 14.62 (s, 1H, NH). ^{13}C NMR (151 MHz, CDCl_3) δ 31.2 ($\text{ArC}(\underline{\text{CH}}_3)_3$), 34.8 ($\text{ArC}(\underline{\text{CH}}_3)_3$), 53.7 ($\text{CO}_2\underline{\text{CH}}_3$), 54.1 ($\text{CO}_2\underline{\text{CH}}_3$), 113.0 (C-10a), 114.3 (C-3 or C-9), 114.6 (C-3 or C-9), 121.3 (C-4a), 126.9 (C-3', C-5'), 127.4 (C-6), 128.8 (C-2',

C-6'), 131.3 (C-5), 131.5 (C-1'), 135.7 (C-2 or C-8), 136.7 (C-2 or C-8), 139.7 (C-6a or C-10b), 140.7 (C-6a or C-10b), 152.7 (C-4'), 162.2 ($\underline{\text{CO}}_2\text{Me}$), 162.3 ($\underline{\text{CO}}_2\text{Me}$), 177.3 (C-4 or C-10), 181.8 (C-4 or C-10). LC–MS (m/z): positive mode 461 $[\text{M} + \text{H}]^+$. Purity by HPLC–UV (254 nm)–ESI–MS: 97.3%.

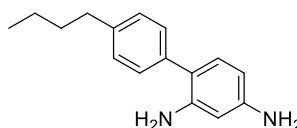


6-(4-(*tert*-Butyl)phenyl)-4,10-dioxo-1,4,7,10-tetrahydro-1,7-phenanthroline-2,8-dicarboxylic acid (68x, LW127P). The compound was synthesized using **67x** (54 mg, 0.118 mmol). The product was isolated as a yellow solid (42 mg, 82% yield). ^1H NMR (600 MHz, D_2O , ND_3) δ 1.33 (s, 9H, $\text{ArC}(\underline{\text{CH}}_3)_3$), 6.81 (s, 2H, 3-H, 9-H), 7.08 (s, 2H, 2'-H, 6'-H), 7.42 – 7.57 (m, 2H, 3'-H, 5'-H), 7.78 (s, 1H, 5-H). ^{13}C NMR (151 MHz, D_2O , ND_3) δ 33.2 ($\text{ArC}(\underline{\text{CH}}_3)_3$), 36.8 ($\text{ArC}(\underline{\text{CH}}_3)_3$), 113.6 (C-3 or C-9, C-10a), 114.2 (C-3 or C-9), 121.8 (C-4a), 129.3 (C-3', C-5'), 130.7 (C-1'), 130.9 (C-5), 131.1 (C-2', C-6'), 134.3 (C-6), 140.8 (C-2 or C-8), 142.7 (C-2 or C-8), 146.1 (C-6a or C-10b), 146.3 (C-6a or C-10b), 155.4 (C-4'), 168.0 ($\underline{\text{CO}}_2\text{H}$), 168.6 ($\underline{\text{CO}}_2\text{H}$), 181.0 (C-4 or C-10), 184.3 (C-4 or C-10). LC–MS (m/z): positive mode 433 $[\text{M} + \text{H}]^+$. Purity by HPLC–UV (254 nm)–ESI–MS: 98.4%. Mp: >300 °C dec.

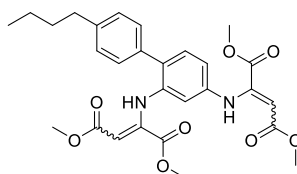
Preparation of 68y



4'-Butyl-2-nitro-[1,1'-biphenyl]-4-amine (64j, LW231). The compound was synthesized using 4-bromo-3-nitroaniline (2.50 g, 11.5 mmol). The product was isolated as an orange solid (2.53 g, 82% yield). ^1H NMR (600 MHz, CDCl_3) δ 0.96 (t, $J = 7.4$ Hz, 3H, $\text{Ar}(\underline{\text{CH}}_2)_3\underline{\text{CH}}_3$), 1.35 – 1.44 (m, 2H, $\text{Ar}(\underline{\text{CH}}_2)_2\underline{\text{CH}}_2\underline{\text{CH}}_3$), 1.61 – 1.67 (m, 2H, $\text{ArCH}_2\underline{\text{CH}}_2\underline{\text{CH}}_2\underline{\text{CH}}_3$), 2.63 – 2.69 (m, 2H, $\text{ArCH}_2(\underline{\text{CH}}_2)_2\underline{\text{CH}}_3$), 7.23 (d, $J = 8.3$ Hz, 1H, 6-H), 7.30 (d, $J = 8.1$ Hz, 2H, 3'-H, 5'-H), 7.35 (d, $J = 8.1$ Hz, 2H, 2'-H, 6'-H), 7.61 (d, $J = 2.2$ Hz, 1H, 3-H), 7.65 (dd, $J = 2.3$, 8.3 Hz, 1H, 5-H). ^{13}C NMR (151 MHz, CDCl_3) δ 13.9 ($\text{Ar}(\underline{\text{CH}}_2)_3\underline{\text{CH}}_3$), 22.4 ($\text{Ar}(\underline{\text{CH}}_2)_2\underline{\text{CH}}_2\underline{\text{CH}}_3$), 33.5 ($\text{ArCH}_2\underline{\text{CH}}_2\underline{\text{CH}}_2\underline{\text{CH}}_3$), 35.4 ($\text{Ar}\underline{\text{CH}}_2(\underline{\text{CH}}_2)_2\underline{\text{CH}}_3$), 109.7 (C-3), 113.4 (C-5), 128.4 (C-2', C-6'), 129.2 (C-3', C-5'), 131.0 (C-6), 133.7 (C-1), 134.5 (C-1'), 143.3 (C-4'), 144.2 (C-2), 147.9 (C-4). LC–MS (m/z): positive mode 271 $[\text{M} + \text{H}]^+$. Purity by HPLC–UV (254 nm)–ESI–MS: 97.8%.

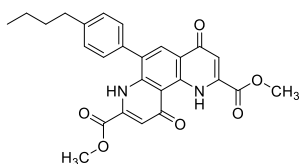


4'-Butyl-[1,1'-biphenyl]-2,4-diamine (65y, LW234). The compound was synthesized using **64j** (2.0 g, 11.5 mmol). The product was isolated as a white solid (1.6 g, 90% yield) and directly used for the next step.



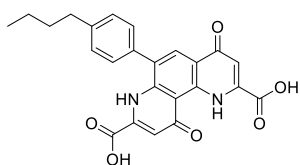
Tetramethyl 2,2'-((4'-butyl-[1,1'-biphenyl]-2,4-diyl)bis(azanediyl))bis(but-2-enedioate) (66y, LW235). The compound was synthesized using **65y** (1.60 g, 6.66 mmol). The product was isolated as a yellow oil (2.86 g, 82% yield). ^1H NMR (500 MHz, $\text{DMSO}-d_6$) δ 0.90 (t, $J = 7.4$ Hz, 3H, $\text{Ar}(\underline{\text{CH}}_2)_3\underline{\text{CH}}_3$), 1.28 – 1.36 (m, 2H,

Ar(CH₂)₂CH₂CH₃), 1.54 – 1.61 (m, 2H, ArCH₂CH₂CH₂CH₃), 2.58 – 2.62 (m, 2H, ArCH₂(CH₂)₂CH₃), 3.58 (s, 3H, CO₂CH₃), 3.64 (s, 3H, CO₂CH₃), 3.66 (s, 3H, CO₂CH₃), 3.72 (s, 3H, CO₂CH₃), 5.25 (s, 1H, 3"-H or 3'''-H), 5.36 (s, 1H, 3"-H or 3'''-H), 6.50 (d, *J* = 2.2 Hz, 1H, 3-H), 6.72 (dd, *J* = 2.3, 8.2 Hz, 1H, 5-H), 7.19 (d, *J* = 8.2 Hz, 1H, 6-H), 7.23 – 7.26 (m, 2H, 3'-H, 5'-H), 7.27 – 7.31 (m, 2H, 2'-H, 6'-H), 9.28 (s, 1H, NH), 9.55 (s, 1H, NH). ¹³C NMR (126 MHz, DMSO-*d*₆) δ 13.9 (Ar(CH₂)₃CH₃), 21.8 (Ar(CH₂)₂CH₂CH₃), 33.1 (ArCH₂CH₂CH₂CH₃), 34.6 (ArCH₂(CH₂)₂CH₃), 51.2 (CO₂CH₃), 51.3 (CO₂CH₃), 53.1 (CO₂CH₃), 53.2 (CO₂CH₃), 93.4 (C-3" or C-3'''), 95.2 (C-3" or C-3'''), 113.7 (C-3), 116.5 (C-5), 128.7 (C-2', C-6'), 128.9 (C-3', C-5'), 129.4 (C-1'), 131.2 (C-6), 134.9 (C-4'), 138.0 (C-1), 140.4 (C-2" or C-2'''), 141.7 (C-2" or C-2'''), 146.4 (C-2 or C-4), 147.7 (C-2 or C-4), 163.7 (CO₂Me), 164.4 (CO₂Me), 168.2 (CO₂Me), 168.9 (CO₂Me). LC–MS (*m/z*): positive mode 525 [M + H]⁺. Purity by HPLC–UV (254 nm)–ESI–MS: 98.9%.



Dimethyl 6-(4-butylphenyl)-4,10-dioxo-1,4,7,10-tetrahydro-1,7-phenanthroline-2,8-dicarboxylate (67y, LW239). The compound was synthesized using **66y** (2.86 g, 5.45 mmol). The product was further purified by column chromatography on a column of silica gel (99:1 DCM/MeOH) and isolated as a gray solid (267 mg, 11% yield). ¹H NMR (600 MHz, CDCl₃) δ 0.97 (t, *J* = 7.4

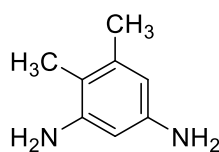
Hz, 3H, Ar(CH₂)₃CH₃), 1.42 (h, *J* = 7.4 Hz, 2H, Ar(CH₂)₂CH₂CH₃), 1.69 (p, *J* = 7.6 Hz, 2H, ArCH₂CH₂CH₂CH₃), 2.65 – 2.77 (m, 2H, ArCH₂(CH₂)₂CH₃), 4.01 (s, 3H, CO₂CH₃), 4.08 (s, 3H, CO₂CH₃), 7.10 (s, 1H, 3-H or 9-H), 7.21 (s, 1H, 3-H or 9-H), 7.41 (s, 4H, 4 × ArH), 8.49 (s, 1H, 5-H), 9.73 (s, 1H, NH), 14.64 (s, 1H, NH). ¹³C NMR (151 MHz, CDCl₃) δ 13.9 (Ar(CH₂)₃CH₃), 22.4 (Ar(CH₂)₂CH₂CH₃), 33.4 (ArCH₂CH₂CH₂CH₃), 35.4 (ArCH₂(CH₂)₂CH₃), 53.7 (CO₂CH₃), 54.1 (CO₂CH₃), 113.0 (C-10a), 114.3 (C-3 or C-9), 114.6 (C-3 or C-9), 121.3 (C-4a), 127.6 (C-6), 128.9 (C-2', C-6'), 130.0 (C-3', C-5'), 131.2 (C-5), 131.6 (C-1'), 135.7 (C-2 or C-8), 136.8 (C-2 or C-8), 139.7 (C-6a or C-10b), 140.7 (C-6a or C-10b), 144.5 (C-4'), 162.2 (CO₂Me), 162.2 (CO₂Me), 177.3 (C-4 or C-10), 181.8 (C-4 or C-10). LC–MS (*m/z*): positive mode 461 [M + H]⁺. Purity by HPLC–UV (254 nm)–ESI–MS: 98.2%.



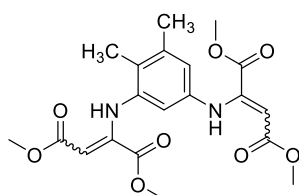
6-(4-Butylphenyl)-4,10-dioxo-1,4,7,10-tetrahydro-1,7-phenanthroline-2,8-dicarboxylic acid (68y, LW250). The compound was synthesized using **67y** (30 mg, 0.065 mmol). The product was isolated as a beige solid (27 mg, 98% yield). ¹H NMR (600 MHz, D₂O, ND₃) δ 0.95 (t, *J* = 7.3 Hz, 3H, Ar(CH₂)₃CH₃), 1.32 – 1.44

(m, 2H, Ar(CH₂)₂CH₂CH₃), 1.47 – 1.68 (m, 2H, ArCH₂CH₂CH₂CH₃), 2.47 – 2.72 (m, 2H, ArCH₂(CH₂)₂CH₃), 6.96 (d, *J* = 7.7 Hz, 2H, 3-H, 9-H), 7.20 – 7.49 (m, 4H, 4 × ArH), 8.01 (s, 1H, 5-H). ¹³C NMR (151 MHz, D₂O, ND₃) δ 16.0 (Ar(CH₂)₃CH₃), 24.5 (Ar(CH₂)₂CH₂CH₃), 35.5 (ArCH₂CH₂CH₂CH₃), 37.2 (ArCH₂(CH₂)₂CH₃), 113.6 (C-3 or C-9), 114.2 (C-3 or C-9), 114.8 (C-10a), 122.1 (C-4a), 130.6 (C-5), 131.6 (C-2', C-6'), 132.1 (C-3', C-5'), 132.4 (C-4'), 135.3 (C-6), 141.4 (C-2 or C-8), 144.4 (C-2 or C-8), 146.1 (C-1'), 146.9 (C-6a or C-10b), 148.1 (C-6a or C-10b), 169.1 (2 × CO₂H), 181.3 (C-4 or C-10), 184.0 (C-4 or C-10). LC–MS (*m/z*): positive mode 433 [M + H]⁺. Purity by HPLC–UV (254 nm)–ESI–MS: 99.0%. Mp: >300 °C dec.

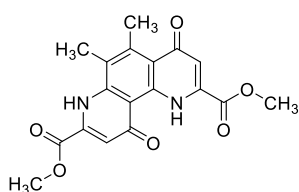
Preparation of 68z



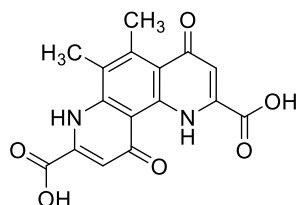
4,5-Dimethylbenzene-1,3-diamine (65z, LW291). The compound was synthesized using 3,4-dimethyl-5-nitroaniline (1.0 g, 6.0 mmol). The product was isolated as a white solid (817 mg, 100% yield) and directly used for the next step.



Tetramethyl 2,2'-((4,5-dimethyl-1,3-phenylene)bis(azanediyl))bis(but-2-enedioate) (66z, LW295). The compound was synthesized using **65z** (817 mg, 6.00 mmol). The product was isolated as a yellow oil (2.30 g, 92% yield). ^1H NMR (600 MHz, CDCl_3) δ 2.18 (s, 3H, ArCH_3), 2.24 (s, 3H, ArCH_3), 3.71 – 3.72 (m, 6H, $2 \times \text{CO}_2\text{CH}_3$), 3.73 (s, 6H, $2 \times \text{CO}_2\text{CH}_3$), 5.33 (s, 1H, 3'-H or 3''-H), 5.40 (s, 1H, 3'-H or 3''-H), 6.17 – 6.20 (m, 1H, ArH), 6.54 (d, $J = 1.6$ Hz, 1H, ArH), 9.43 – 9.48 (m, 2H, $2 \times \text{NH}$). ^{13}C NMR (151 MHz, CDCl_3) δ 13.4 (ArCH_3), 20.5 (ArCH_3), 51.1 (CO_2CH_3), 51.2 (CO_2CH_3), 52.9 ($2 \times \text{CO}_2\text{CH}_3$), 93.1 (C-3' or C-3''), 93.3 (C-3' or C-3''), 112.9 (C-2), 119.6 (C-6), 125.7 (C-4), 137.9 (C-2' or C-2''), 138.6 (C-2' or C-2''), 139.6 (C-5), 148.0 (C-1 or C-3), 148.8 (C-1 or C-3), 164.3 (CO_2Me), 164.5 (CO_2Me), 169.8 (CO_2Me), 170.1 (CO_2Me). LC-MS (m/z): positive mode 421 $[\text{M} + \text{H}]^+$. Purity by HPLC-UV (254 nm)-ESI-MS: 82.6%.

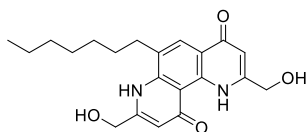


Dimethyl 5,6-dimethyl-4,10-dioxo-1,4,7,10-tetrahydro-1,7-phenanthroline-2,8-dicarboxylate (67z, LW297). The compound was synthesized using **66z** (2.20 g, 5.24 mmol). The product was isolated as a white solid (750 mg, 41% yield). ^1H NMR (600 MHz, CDCl_3) δ 2.42 (s, 3H, ArCH_3), 2.92 (s, 3H, ArCH_3), 4.03 (s, 3H, CO_2CH_3), 4.07 (s, 3H, CO_2CH_3), 6.96 – 7.06 (m, 2H, $2 \times \text{NH}$). ^{13}C NMR (151 MHz, CDCl_3) δ 12.4 (ArCH_3), 18.9 (ArCH_3), 53.5 (CO_2CH_3), 54.2 (CO_2CH_3), 110.4 (C-10a), 113.9 (C-3 or C-9), 116.3 (C-3 or C-9), 118.9 (C-4a), 120.2 (C-6), 134.9 (C-2 or C-8), 135.2 (C-2 or C-8), 140.4 (C-6a or C-10b), 140.8 (C-6a or C-10b), 145.2 (C-5), 162.2 (CO_2Me), 162.4 (CO_2Me), 179.7 (C-4 or C-10), 181.3 (C-4 or C-10). LC-MS (m/z): positive mode 357 $[\text{M} + \text{H}]^+$. Purity by HPLC-UV (254 nm)-ESI-MS: 92.4%.



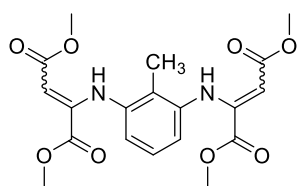
5,6-Dimethyl-4,10-dioxo-1,4,7,10-tetrahydro-1,7-phenanthroline-2,8-dicarboxylic acid (68z, LW299B). The compound was synthesized using **67z** (100 mg, 0.28 mmol). The product was isolated as a white solid (92 mg, 100% yield). ^1H NMR (600 MHz, D_2O , ND_3) δ 2.00 (s, 3H, ArCH_3), 2.35 (s, 3H, ArCH_3), 6.46 (s, 1H, 3-H or 9-H), 6.51 (s, 1H, 3-H or 9-H). ^{13}C NMR (151 MHz, D_2O , ND_3) δ 14.3 (ArCH_3), 20.9 (ArCH_3), 110.7 (C-10a), 113.3 (C-3 or C-9), 115.6 (C-3 or C-9), 120.7 (C-4a), 122.6 (C-6), 141.0 (C-2 or C-8), 142.2 (C-2 or C-8), 143.4 (C-5), 144.7 (C-6a or C-10b), 144.8 (C-6a or C-10b), 167.8 (CO_2H), 168.8 (CO_2H), 182.9 (C-4 or C-10), 183.2 (C-4 or C-10). LC-MS (m/z): positive mode 329 $[\text{M} + \text{H}]^+$. Purity by HPLC-UV (254 nm)-ESI-MS: 95.0%. Mp: >300 °C dec.

Preparation of 111

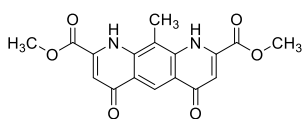


6-Heptyl-2,8-bis(hydroxymethyl)-1,7-phenanthroline-4,10(1H,7H)-dione (111, LW517). **671** (200 mg, 0.469 mmol) was dissolved in a mixture of dichloromethane (5 mL) and methanol (5 mL). The solution was cooled to 0°C, and NaBH₄ (816 mg, 21.6 mmol, 46 equiv.) was added. The mixture was kept stirring at that temperature for 2 h. After that, stirring continued at rt for 2 h. Then, EtOAc (5 mL) and methanol (5 mL) were added at 0°C. The solvents were evaporated under reduced pressure, and the residue was purified by column chromatography (4:1 DCM/MeOH). **111** was isolated as a white solid (40 mg, 23% yield). ¹H NMR (600 MHz, DMSO-*d*₆) δ 0.82 (t, *J* = 6.9 Hz, 3H, Ar(CH₂)₆CH₃), 1.17 – 1.25 (m, 4H, Ar(CH₂)₄(CH₂)₂CH₃), 1.26 – 1.38 (m, 4H, Ar(CH₂)₂(CH₂)₂(CH₂)₂CH₃), 1.63 (p, *J* = 7.7 Hz, 2H, ArCH₂CH₂(CH₂)₄CH₃), 2.91 (t, *J* = 7.6 Hz, 2H, ArCH₂(CH₂)₅CH₃), 4.57 (d, *J* = 5.0 Hz, 2H, CH₂OH), 4.63 (d, *J* = 4.7 Hz, 2H, CH₂OH), 5.78 – 5.87 (m, 1H, CH₂OH), 5.94 (t, *J* = 5.5 Hz, 1H, CH₂OH), 6.09 (s, 1H, 3-H or 9-H), 6.40 (s, 1H, 3-H or 9-H), 8.05 (s, 1H, 5-H), 10.72 (s, 1H, NH), 14.46 (s, 1H, NH). ¹³C NMR (151 MHz, DMSO-*d*₆) δ 14.1 (Ar(CH₂)₆CH₃), 22.3 (Ar(CH₂)₅CH₂CH₃), 28.8 (Ar(CH₂)₄CH₂CH₂CH₃), 28.9 (Ar(CH₂)₃CH₂(CH₂)₂CH₃), 28.9 (Ar(CH₂)₂CH₂(CH₂)₃CH₃), 29.8 (ArCH₂CH₂(CH₂)₄CH₃), 31.5 (ArCH₂(CH₂)₅CH₃), 59.7 (CH₂OH), 59.9 (CH₂OH), 106.9 (C-3 or C-9), 108.7 (C-3 or C-9), 111.3 (C-10a), 119.2 (C-6), 125.6 (C-4a), 127.7 (C-5), 138.9 (C-6a or C-10b), 141.4 (C-6a or C-10b), 151.8 (C-2 or C-8), 154.0 (C-2 or C-8), 175.6 (C-4 or C-10), 180.6 (C-4 or C-10). LC–MS (*m/z*): positive mode 371 [M + H]⁺. Purity by HPLC–UV (254 nm)–ESI–MS: 97.5%. Mp: 265–266 °C.

Preparation of 104 and 105

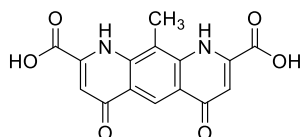


Tetramethyl 2,2'-((2-methyl-1,3-phenylene)bis(azanediyl))bis(but-2-enedioate) (103, LW154). The compound was synthesized using 2-methylbenzene-1,3-diamine (2.00 g, 16.4 mmol). The product was isolated as a yellow solid (3.55 g, 55% yield). ¹H NMR (600 MHz, CDCl₃) δ 2.32 (s, 3H, ArCH₃), 3.64 (s, 6H, 2 × CO₂CH₃), 3.75 (s, 6H, 2 × CO₂CH₃), 5.42 (s, 2H, 3'-H, 3''-H), 6.58 (d, *J* = 7.9 Hz, 2H, 4-H, 6-H), 6.98 (t, *J* = 8.0 Hz, 1H, 5-H), 9.53 (s, 2H, 2 × NH). ¹³C NMR (151 MHz, CDCl₃) δ 12.3 (ArCH₃), 51.2 (2 × CO₂CH₃), 52.7 (2 × CO₂CH₃), 93.2 (C-3', C-3''), 118.7 (C-4, C-6), 123.9 (C-2), 126.0 (C-5), 140.0 (C-1), 148.9 (C-3), 164.6 (2 × CO₂Me), 170.2 (2 × CO₂Me). LC–MS (*m/z*): positive mode 407 [M + H]⁺. Purity by HPLC–UV (254 nm)–ESI–MS: 98.7%.



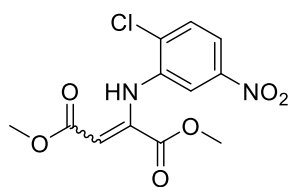
Dimethyl 10-methyl-4,6-dioxo-1,4,6,9-tetrahydropyrido[3,2-g]quinoline-2,8-dicarboxylate (104, LW156). The compound was synthesized using **103** (3.50 g, 8.62 mmol). The product was isolated as a yellow solid (1.30 g, 44% yield). ¹H NMR (600 MHz, TFA-*d*₁) δ 3.29 (s, 3H, ArCH₃), 4.33 (s, 6H, 2 × CO₂CH₃), 7.98 (s, 2H, 3-H, 7-H), 9.93 (s, 1H, 5-H). ¹³C NMR (151 MHz, TFA-*d*₁) δ 11.5 (ArCH₃), 57.3 (2 × CO₂CH₃), 108.3 (C-3, C-7), 120.2 (C-10), 123.1

(C-4a, C-5a), 126.9 (C-5), 140.9 (C-2, C-8), 146.6 (C-9a, C-10a), 162.6 ($2 \times \text{CO}_2\text{Me}$), 180.2 (C-4, C-6). LC–MS (m/z): positive mode 343 $[\text{M} + \text{H}]^+$. Purity by HPLC–UV (254 nm)–ESI–MS: 97.7%. Mp: $>300^\circ\text{C}$ dec.

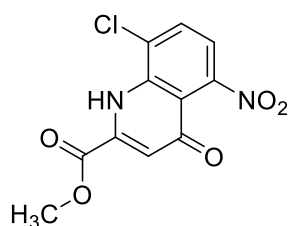


10-Methyl-4,6-dioxo-1,4,6,9-tetrahydropyrido[3,2-g]quinoline-2,8-dicarboxylic acid (105, LW162). The compound was synthesized using **104** (165 mg, 0.48 mmol). The product was isolated as a yellow solid (148 mg, 98% yield). ^1H NMR (600 MHz, D_2O , ND_3) δ 2.41 (s, 3H, ArCH_3), 6.42 (s, 2H, 3-H, 7-H), 8.09 (s, 1H, 5-H). ^{13}C NMR (151 MHz, D_2O , ND_3) δ 12.0 (ArCH_3), 109.0 (C-3, C-7), 115.8 (C-10), 123.0 (C-5), 123.2 (C-4a, C-5a), 140.6 (C-2, C-8), 148.7 (C-9a, C-10a), 168.7 ($2 \times \text{CO}_2\text{H}$), 183.7 (C-4, C-6). LC–MS (m/z): positive mode 315 $[\text{M} + \text{H}]^+$. Purity by HPLC–UV (254 nm)–ESI–MS: 99.9%. Mp: $>300^\circ\text{C}$ dec.

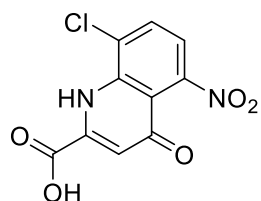
Preparation of 96a



Dimethyl 2-((2-chloro-5-nitrophenyl)amino)but-2-enedioate (94a, LW36). The compound was synthesized using 2-chloro-5-nitroaniline (1.5 g, 6.7 mmol). The product was isolated as a yellow solid (2.1 g, 100% yield). ^1H NMR (600 MHz, CDCl_3) δ 3.79 (s, 3H, CO_2CH_3), 3.83 (s, 3H, CO_2CH_3), 5.77 (s, 1H, 3'-H), 7.54 (d, $J = 8.7$ Hz, 1H, 4-H), 7.58 (s, 1H, 6-H), 7.83 (d, $J = 7.8$ Hz, 1H, 3-H), 9.92 (s, 1H, NH). ^{13}C NMR (151 MHz, CDCl_3) δ 51.8 (CO_2CH_3), 53.3 (CO_2CH_3), 99.6 (C-3'), 114.5 (C-6), 118.2 (C-4), 130.3 (C-3), 131.3 (C-2), 138.3 (C-1), 144.5 (C-2'), 146.6 (C-5), 163.4 (CO_2Me), 169.2 (CO_2Me). LC–MS (m/z): positive mode 315 $[\text{M} + \text{H}]^+$. Purity by HPLC–UV (254 nm)–ESI–MS: 87.4%.



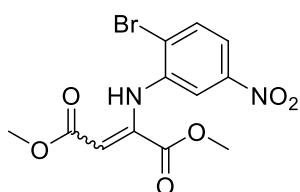
Methyl 8-chloro-5-nitro-4-oxo-1,4-dihydroquinoline-2-carboxylate (95a, LW42). The compound was synthesized using **94a** (2.0 g, 6.4 mmol). The product was isolated as a yellow solid (1.4 g, 78% yield). ^1H NMR (600 MHz, CDCl_3) δ 4.08 (s, 3H, CO_2CH_3), 6.99 (s, 1H, 3-H), 7.29 (d, $J = 8.2$ Hz, 1H, 6-H), 7.80 (d, $J = 8.2$ Hz, 1H, 7-H), 9.41 (br, 1H, NH). ^{13}C NMR (151 MHz, CDCl_3) δ 54.3 (CO_2CH_3), 113.7 (C-3), 117.9 (C-4a), 117.9 (C-6), 124.9 (C-8), 132.0 (C-7), 136.2 (C-2 or C-8a), 136.7 (C-2 or C-8a), 147.5 (C-5), 162.3 (CO_2Me), 175.4 (C-4). LC–MS (m/z): positive mode 283 $[\text{M} + \text{H}]^+$. Purity by HPLC–UV (254 nm)–ESI–MS: 99.3%.



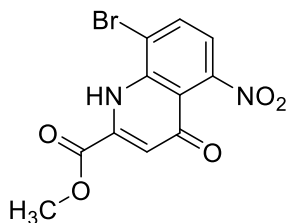
6-Chloro-5-nitro-4-oxo-1,4-dihydroquinoline-2-carboxylic acid (96a, LW48). The compound was synthesized using **95a** (20 mg, 0.071 mmol). The product was isolated as a white solid (14 mg, 73% yield). ^1H NMR (600 MHz, D_2O , ND_3) δ 6.83 (s, 1H, 3-H), 7.27 (d, $J = 8.1$ Hz, 1H, 6-H), 7.64 (d, $J = 8.1$ Hz, 1H, 7-H). ^{13}C NMR (151 MHz, D_2O , ND_3) δ 110.1 (C-3), 117.4 (C-4a), 117.9 (C-6), 129.6 (C-7), 131.1 (C-8), 141.9

(C-2 or C-5), 145.9 (C-2 or C-5), 152.4 (C-8a), 170.6 ($\underline{\text{CO}_2\text{H}}$), 174.6 (C-4). LC-MS (m/z): positive mode 269 [$\text{M} + \text{H}$] $^+$. Purity by HPLC-UV (254 nm)-ESI-MS: 99.7%. Mp: >300 °C dec.

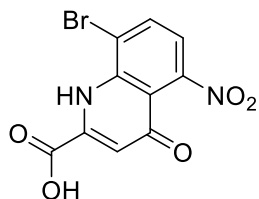
Preparation of 96b



Dimethyl 2-((2-bromo-5-nitrophenyl)amino)but-2-enedioate (94b, LW63). The compound was synthesized using 2-bromo-5-nitroaniline (500 mg, 2.30 mmol). The product was isolated as a yellow solid (347 mg, 42% yield). ^1H NMR (600 MHz, CDCl_3) δ 3.80 (s, 3H, CO_2CH_3), 3.83 (s, 3H, CO_2CH_3), 5.78 (s, 1H, 3'-H), 7.54 (d, $J = 2.3$ Hz, 1H, 6-H), 7.73 (d, $J = 8.7$ Hz, 1H, 3-H), 7.76 (dd, $J = 2.3, 8.7$ Hz, 1H, 4-H), 9.90 (s, 1H, NH). ^{13}C NMR (126 MHz, $\text{DMSO}-d_6$) δ 51.8 (CO_2CH_3), 53.5 (CO_2CH_3), 98.2 (C-3'), 115.2 (C-6), 119.2 (C-4), 122.1 (C-2), 134.1 (C-3), 139.4 (C-1), 144.9 (C-2'), 147.2 (C-5), 163.3 ($\underline{\text{CO}_2\text{Me}}$), 168.5 ($\underline{\text{CO}_2\text{Me}}$). LC-MS (m/z): positive mode 359 [$\text{M} + \text{H}$] $^+$. Purity by HPLC-UV (254 nm)-ESI-MS: 86.7%.

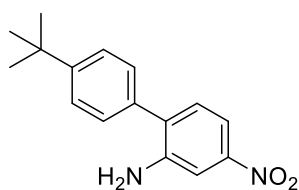


Methyl 8-bromo-5-nitro-4-oxo-1,4-dihydroquinoline-2-carboxylate (95b, LW65). The compound was synthesized using 94b (200 mg, 0.56 mmol). The product was isolated as a white solid (41 mg, 23% yield). ^1H NMR (600 MHz, CDCl_3) δ 4.08 (s, 3H, CO_2CH_3), 6.98 (s, 1H, 3-H), 7.23 (d, $J = 8.2$ Hz, 1H, 6-H), 7.97 (d, $J = 8.2$ Hz, 1H, 7-H), 9.47 (br, 1H, NH). ^{13}C NMR (151 MHz, CDCl_3) δ 54.3 (CO_2CH_3), 113.5 (C-3), 114.6 (C-8), 117.8 (C-4a), 118.4 (C-6), 135.5 (C-7), 136.4 (C-2 or C-5), 137.6 (C-2 or C-5), 148.1 (C-8a), 162.3 ($\underline{\text{CO}_2\text{Me}}$), 175.4 (C-4). LC-MS (m/z): positive mode 327 [$\text{M} + \text{H}$] $^+$. Purity by HPLC-UV (254 nm)-ESI-MS: 99.4%.

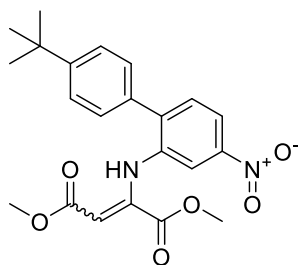


6-Bromo-5-nitro-4-oxo-1,4-dihydroquinoline-2-carboxylic acid (96b, LW72). The compound was synthesized using 95b (20 mg, 0.061 mmol). The product was isolated as a white solid (10 mg, 52% yield). ^1H NMR (600 MHz, D_2O , ND_3) δ 6.83 (s, 1H, 3-H), 7.27 (d, $J = 8.1$ Hz, 1H, 6-H), 7.64 (d, $J = 8.1$ Hz, 1H, 7-H). ^{13}C NMR (151 MHz, D_2O , ND_3) δ 112.8 (C-3), 120.5 (C-4a), 120.8 (C-6), 126.7 (C-8), 135.1 (C-7), 147.5 (C-5 or C-2), 149.4 (C-5 or C-2), 157.7 (C-8a), 175.1 ($\underline{\text{CO}_2\text{H}}$), 176.5 (C-4). LC-MS (m/z): positive mode 313 [$\text{M} + \text{H}$] $^+$. Purity by HPLC-UV (254 nm)-ESI-MS: 99.5%. Mp: >300 °C dec.

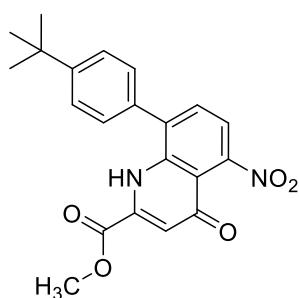
Preparation of 99



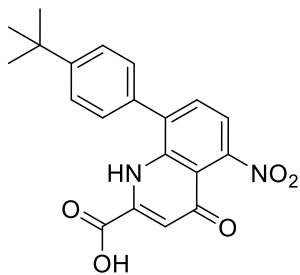
4'-(*tert*-Butyl)-4-nitro-[1,1'-biphenyl]-2-amine (64q, LW69). The compound was synthesized using 2-bromo-5-nitroaniline (1.50 g, 6.91 mmol). The product was isolated as a yellow solid (1.38 g, 74% yield). $^1\text{H NMR}$ (600 MHz, CDCl_3) δ 1.37 (s, 9H, $\text{ArC}(\text{CH}_3)_3$), 7.24 (d, $J = 8.3$ Hz, 1H, 6-H), 7.38 (d, $J = 8.3$ Hz, 2H, 2'-H, 6'-H), 7.51 (d, $J = 8.3$ Hz, 2H, 3'-H, 5'-H), 7.61 (d, $J = 2.2$ Hz, 1H, 3-H), 7.64 (dd, $J = 2.2, 8.3$ Hz, 1H, 5-H). $^{13}\text{C NMR}$ (151 MHz, CDCl_3) δ 31.3 ($\text{ArC}(\text{CH}_3)_3$), 34.7 ($\text{ArC}(\text{CH}_3)_3$), 109.7 (C-3), 113.4 (C-5), 126.1 (C-3', C-5'), 128.3 (C-2', C-6'), 131.0 (C-6), 133.7 (C-1), 134.3 (C-1'), 144.2 (C-2 or C-4), 147.9 (C-2 or C-4), 151.5 (C-4'). LC-MS (m/z): positive mode 271 $[\text{M} + \text{H}]^+$. Purity by HPLC-UV (254 nm)-ESI-MS: 97.1%.



Dimethyl 2-((4'-(*tert*-butyl)-4-nitro-[1,1'-biphenyl]-2-yl)amino)but-2-enedioate (97, LW69N). The compound was synthesized using **64q** (410 mg, 1.52 mmol). The product was isolated as a yellow solid (517 mg, 82% yield). $^1\text{H NMR}$ (600 MHz, CDCl_3) δ 1.37 (s, 9H, $\text{ArC}(\text{CH}_3)_3$), 3.67 (s, 3H, CO_2CH_3), 3.74 (s, 3H, CO_2CH_3), 5.56 (s, 1H, 3''-H), 7.40 – 7.45 (m, 3H, 2'-H, 6'-H, 6-H), 7.48 – 7.51 (m, 2H, 3'-H, 5'-H), 7.68 (d, $J = 2.2$ Hz, 1H, 3-H), 7.98 (dd, $J = 2.2, 8.4$ Hz, 1H, 5-H), 9.37 (s, 1H, NH). $^{13}\text{C NMR}$ (151 MHz, CDCl_3) δ 31.2 ($\text{ArC}(\text{CH}_3)_3$), 34.7 ($\text{ArC}(\text{CH}_3)_3$), 51.4 (CO_2CH_3), 53.1 (CO_2CH_3), 97.2 (C-3''), 116.1 (C-3), 118.9 (C-5), 125.9 (C-3', C-5'), 128.7 (C-2', C-6'), 131.4 (C-6), 133.4 (C-1), 139.0 (C-1'), 140.4 (C-2), 146.1 (C-2''), 147.2 (C-4), 151.9 (C-4'), 163.8 (CO_2Me), 169.1 (CO_2Me). LC-MS (m/z): positive mode 413 $[\text{M} + \text{H}]^+$. Purity by HPLC-UV (254 nm)-ESI-MS: 87.5%.

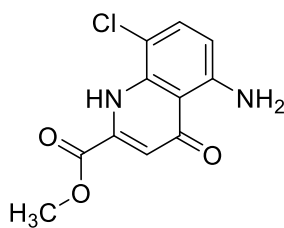


Methyl 8-(4-(*tert*-butyl)phenyl)-5-nitro-4-oxo-1,4-dihydroquinoline-2-carboxylate (98, LW89). The compound was synthesized using **97** (450 mg, 1.09 mmol). The product was isolated as a white solid (300 mg, 72% yield). $^1\text{H NMR}$ (600 MHz, CDCl_3) δ 1.41 (s, 9H, $\text{ArC}(\text{CH}_3)_3$), 3.99 (s, 3H, CO_2CH_3), 6.96 (s, 1H, 3-H), 7.38 (d, $J = 7.8$ Hz, 1H, 7-H), 7.41 (d, $J = 8.2$ Hz, 2H, 2'-H, 6'-H), 7.60 – 7.67 (m, 3H, 6-H, 3'-H, 5'-H). $^{13}\text{C NMR}$ (151 MHz, CDCl_3) δ 31.2 ($\text{ArC}(\text{CH}_3)_3$), 34.9 ($\text{ArC}(\text{CH}_3)_3$), 54.1 (CO_2CH_3), 112.8 (C-3), 117.4 (C-4a), 118.1 (C-6), 127.1 (C-3', C-5'), 128.5 (C-2', C-6'), 131.2 (C-8), 132.8 (C-7), 134.4 (C-5 or C-1'), 136.0 (C-5 or C-1'), 137.5 (C-2), 148.0 (C-8a), 153.2 (C-4'), 162.8 (CO_2Me), 176.0 (C-4). LC-MS (m/z): positive mode 381 $[\text{M} + \text{H}]^+$. Purity by HPLC-UV (254 nm)-ESI-MS: 98.1%.

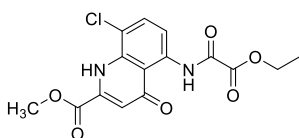


8-(4-(*tert*-Butyl)phenyl)-5-nitro-4-oxo-1,4-dihydroquinoline-2-carboxylic acid (99, LW94). The compound was synthesized using **98** (30 mg, 0.079 mmol). The product was isolated as a white solid (20 mg, 69% yield). ^1H NMR (600 MHz, D_2O , ND_3) δ 1.32 (s, 9H, $\text{ArC}(\text{CH}_3)_3$), 6.88 (s, 1H, 3-H), 7.28 (d, $J = 7.7$ Hz, 2H, 2'-H, 6'-H), 7.44 – 7.50 (m, 2H, 6-H, 7-H), 7.58 (d, $J = 7.9$ Hz, 2H, 3'-H, 5'-H). ^{13}C NMR (151 MHz, D_2O , ND_3) δ 33.1 ($\text{ArC}(\text{CH}_3)_3$), 36.8 ($\text{ArC}(\text{CH}_3)_3$), 112.0 (C-3), 119.3 (C-4a), 121.3 (C-6), 129.0 (C-3', C-5'), 131.6 (C-2', C-6'), 134.0 (C-7), 135.5 (C-8), 140.1 (C-2 or C-1'), 142.8 (C-2 or C-1'), 149.3 (C-5 or C-8a), 151.0 (C-5 or C-8a), 155.4 (C-4'), 170.9 (CO_2H), 179.1 (C-4). LC-MS (m/z): positive mode 367 [$\text{M} + \text{H}$] $^+$. Purity by HPLC-UV (254 nm)-ESI-MS: 99.1%. Mp: >300 °C dec.

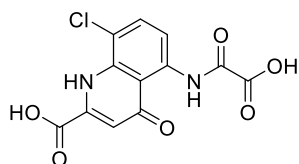
Preparation of 101 and 102



Methyl 5-amino-8-chloro-4-oxo-1,4-dihydroquinoline-2-carboxylate (100, LW147). **95a** (520 mg, 1.84 mmol) was suspended in a mixture of EtOH (30 mL) and dilute HCl (2 M, 30 mL). Tin(II) chloride dihydrate (1.66 g, 7.35 mmol, 4 equiv.) was added at rt, and the mixture was heated to 70 °C for 40 min. After that, EtOH was removed under reduced pressure, and the residue was extracted with DCM (3 \times 50 mL). The organic layer was washed with saturated aq K_2CO_3 solution, dried over anhydrous Na_2SO_4 solution, concentrated under reduced pressure and dried at 50 °C. The product was isolated as an orange solid (324 mg, 70% yield). ^1H NMR (600 MHz, CDCl_3) δ 4.03 (s, 3H, CO_2CH_3), 6.34 (d, $J = 8.6$ Hz, 1H, ArH), 6.80 (s, 1H, 3-H), 7.34 (d, $J = 8.6$ Hz, 1H, ArH), 9.11 (br, 1H, NH). ^{13}C NMR (151 MHz, CDCl_3) δ 53.8 (CO_2CH_3), 106.3 (C-4a), 108.3 (C-3), 112.5 (C-6), 113.4 (C-8), 133.3 (C-7), 135.3 (C-2), 137.1 (C-8a), 149.1 (C-5), 162.7 (CO_2Me), 182.5 (C-4). LC-MS (m/z): positive mode 253 [$\text{M} + \text{H}$] $^+$. Purity by HPLC-UV (254 nm)-ESI-MS: 97.2%.



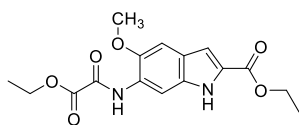
Methyl 8-chloro-5-(2-ethoxy-2-oxoacetamido)-4-oxo-1,4-dihydroquinoline-2-carboxylate (101, LW160). The compound was synthesized using **100** (150 mg, 0.6 mmol). The product was isolated as a yellow solid (170 mg, 80% yield). ^1H NMR (600 MHz, CDCl_3) δ 1.45 (t, $J = 7.1$ Hz, 3H, $\text{CO}_2\text{CH}_2\text{CH}_3$), 4.08 (s, 3H, CO_2CH_3), 4.46 (q, $J = 7.1$ Hz, 2H, $\text{CO}_2\text{CH}_2\text{CH}_3$), 6.98 (s, 1H, 3-H), 7.71 (d, $J = 8.8$ Hz, 1H, 6-H), 8.63 (d, $J = 8.8$ Hz, 1H, 7-H), 9.49 (s, 1H, NH), 14.53 (s, 1H, NH). ^{13}C NMR (151 MHz, CDCl_3) δ 14.0 ($\text{CO}_2\text{CH}_2\text{CH}_3$), 54.2 (CO_2CH_3), 63.5 ($\text{CO}_2\text{CH}_2\text{CH}_3$), 113.0 (C-3), 114.4 (C-6), 115.6 (C-4a), 116.6 (C-6), 133.6 (C-7), 135.9 (C-2), 136.4 (C-5), 138.5 (C-8a), 155.5 (CONH), 160.0 (CO_2Et), 162.2 (CO_2Me), 182.3 (C-4). LC-MS (m/z): positive mode 353 [$\text{M} + \text{H}$] $^+$. Purity by HPLC-UV (254 nm)-ESI-MS: 97.7%. Mp: 254–255 °C dec.



5-(Carboxyformamido)-8-chloro-4-oxo-1,4-dihydroquinoline-2-carboxylic acid (102, LW168).

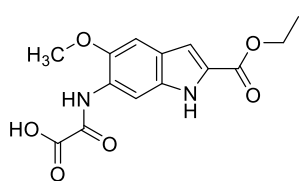
101 (50 mg, 0.14 mmol) was mixed with methanol (10 mL) and aq NaOH (0.6M, 0.5 mL) was added at rt. The mixture was heated to 70 °C with stirring for 1 h. Water (3 mL) was added at that temperature. Then, the solution was cooled to rt and acidified using concd. HCl. The precipitate was collected by filtration, washed consecutively with water, acetone, and petroleum ether (5 mL each) and dried at 50 °C for overnight. The product was isolated as a yellow solid (38 mg, 86% yield). ¹H NMR (600 MHz, D₂O, ND₃) δ 6.38 (s, 1H, 3-H), 7.28 (s, 1H, ArH), 7.87 (s, 1H, ArH). ¹³C NMR (151 MHz, D₂O, ND₃) δ 112.3 (C-3), 115.5 (C-6), 116.3 (C-4a), 119.0 (C-8), 135.3 (C-7), 137.9 (C-2), 139.4 (C-5), 145.4 (C-8a), 164.8 (CONH), 167.9 (2 × CO₂H), 184.5 (C-4). LC-MS (*m/z*): positive mode 311 [M + H]⁺. Purity by HPLC-UV (254 nm)-ESI-MS: 99.9%. Mp: 270–271 °C dec.

Preparation of 106, 107, and 108



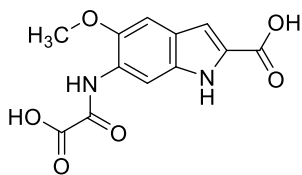
Ethyl 6-(2-ethoxy-2-oxoacetamido)-5-methoxy-1H-indole-2-carboxylate (106, LW314N).

The compound was synthesized using ethyl 6-amino-5-methoxy-1H-indole-2-carboxylate (200 mg, 0.854 mmol). The product was isolated as a white solid (190 mg, 67% yield). ¹H NMR (600 MHz, CDCl₃) δ 1.38 – 1.47 (m, 6H, 2 × CO₂CH₂CH₃), 3.96 (s, 3H, OCH₃), 4.35 – 4.51 (m, 4H, 2 × CO₂CH₂CH₃), 7.08 (s, 1H, ArH), 7.12 (s, 1H, ArH), 8.61 (s, 1H, ArH), 9.05 (s, 1H, NH), 9.75 (s, 1H, NH). ¹³C NMR (151 MHz, CDCl₃) δ 14.0 (CO₂CH₂CH₃), 14.4 (CO₂CH₂CH₃), 56.1 (OCH₃), 61.0 (CO₂CH₂CH₃), 63.6 (CO₂CH₂CH₃), 101.4 (Ar), 103.1 (Ar), 108.2 (Ar), 123.7 (Ar), 125.7 (Ar), 127.9 (Ar), 131.5 (Ar), 144.8 (C-5), 153.7 (CONH), 160.8 (CO₂Et), 161.6 (CO₂Et). LC-MS (*m/z*): positive mode 335 [M + H]⁺. Purity by HPLC-UV (254 nm)-ESI-MS: 99.3%. Mp: 234–235 °C dec.



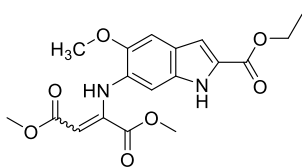
2-((2-(Ethoxycarbonyl)-5-methoxy-1H-indol-6-yl)amino)-2-oxoacetic acid (107, LW316Et).

106 (60 mg, 0.18 mmol) was dissolved in THF (4 mL) and a solution of K₂CO₃ (50 mg, 0.36 mmol, 2 equiv.) in H₂O (1 mL) was added dropwise at rt. The mixture was stirred at this temperature for 48 h. After that, concd. HCl (1 drop) was added, THF was evaporated under reduced pressure, and the resulting precipitate was collected by filtration, washed with water and dried at 50 °C. The product was isolated as a yellow solid (54 mg, 100% yield). ¹H NMR (600 MHz, DMSO-*d*₆) δ 1.32 (t, *J* = 7.1 Hz, 3H, CO₂CH₂CH₃), 3.90 (s, 3H, OCH₃), 4.30 (q, *J* = 7.1 Hz, 2H, CO₂CH₂CH₃), 7.05 (s, 1H, ArH), 7.25 (s, 1H, ArH), 8.40 (s, 1H, ArH), 9.71 (s, 1H, NH), 11.78 (s, 1H, NH). ¹³C NMR (151 MHz, DMSO-*d*₆) δ 14.5 (CO₂CH₂CH₃), 56.4 (OCH₃), 60.5 (CO₂CH₂CH₃), 102.0 (Ar), 103.2 (Ar), 107.8 (Ar), 123.2 (Ar), 125.3 (Ar), 127.7 (Ar), 132.1 (Ar), 144.7 (C-5), 155.5 (CONH), 161.2 (CO₂Et), 162.0 (CO₂H). LC-MS (*m/z*): positive mode 307 [M + H]⁺. Purity by HPLC-UV (254 nm)-ESI-MS: 99.7%. Mp: 223–224 °C dec.

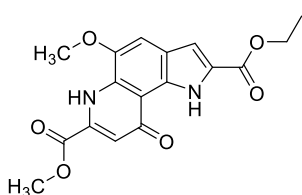


6-(Carboxyformamido)-5-methoxy-1H-indole-2-carboxylic acid (108, LW341B). **108** (30 mg, 0.090 mmol) was suspended in MeOH (5 mL) and an aq solution of NaOH (1M, 1 mL) was added while stirring at rt. After that, the mixture was heated to 70 °C for 1 h. Then, H₂O (3 mL) was added, MeOH was evaporated under reduced pressure, and the mixture was acidified using concd. HCl. The precipitate was collected by filtration, washed with water and dried at 50 °C. The product was isolated as a gray solid (24 mg, 96% yield). ¹H NMR (600 MHz, D₂O, ND₃) δ 3.95 (s, 3H, OCH₃), 6.98 (s, 1H, ArH), 7.32 (s, 1H, ArH), 8.09 (s, 1H, ArH). ¹³C NMR (151 MHz, D₂O, ND₃) δ 59.1 (OCH₃), 105.3 (Ar), 107.5 (Ar), 107.9 (Ar), 126.5 (Ar), 127.1 (Ar), 133.4 (Ar), 137.1 (Ar), 148.3 (C-5), 164.9 (CONH), 168.4 (CO₂H), 172.1 (CO₂H). LC–MS (*m/z*): positive mode 279 [M + H]⁺. Purity by HPLC–UV (254 nm)–ESI–MS: 98.6%. Mp: 253–254 °C dec.

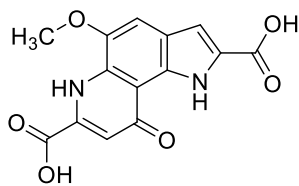
Preparation of 109 and 110



Dimethyl 2-((2-(ethoxycarbonyl)-5-methoxy-1H-indol-6-yl)amino)but-2-enedioate (LW319). The compound was synthesized using ethyl 6-amino-5-methoxy-1H-indole-2-carboxylate (600 mg, 2.56 mmol). The product was isolated as a yellow solid (978 mg, 100% yield). ¹H NMR (600 MHz, CDCl₃) δ 1.40 (t, *J* = 7.1 Hz, 3H, CO₂CH₂CH₃), 3.72 (s, 3H, CO₂CH₃), 3.75 (s, 3H, CO₂CH₃), 3.89 (s, 3H, OCH₃), 4.39 (q, *J* = 7.1 Hz, 2H, CO₂CH₂CH₃), 5.43 (s, 1H, 3'-H), 6.79 (s, 1H, ArH), 7.03 (s, 1H, ArH), 7.10 (d, *J* = 1.8 Hz, 1H, ArH), 8.84 (s, 1H, NH), 9.78 (s, 1H, NH). ¹³C NMR (151 MHz, CDCl₃) δ 14.4 (CO₂CH₂CH₃), 51.2 (CO₂CH₃), 52.7 (CO₂CH₃), 55.9 (OCH₃), 60.9 (CO₂CH₂CH₃), 93.6 (C-3'), 102.0 (C-4 or C-7), 102.2 (C-4 or C-7), 108.5 (C-3), 123.7 (Ar), 127.2 (Ar), 129.9 (Ar), 131.7 (Ar), 147.1 (C-5 or C-2'), 147.5 (C-5 or C-2'), 161.7 (CO₂Et), 165.0 (CO₂Me), 169.7 (CO₂Me). LC–MS (*m/z*): positive mode 377 [M + H]⁺. Purity by HPLC–UV (254 nm)–ESI–MS: 95.3%.



2-Ethyl 7-methyl 5-methoxy-9-oxo-6,9-dihydro-1H-pyrrolo[2,3-f]quinoline-2,7-dicarboxylate (109, LW322P). The compound was synthesized using LW319 (500 mg, 1.33 mmol). The product was further purified by column chromatography on a column of silica gel (97:3 DCM/MeOH) and isolated as a yellow solid (260 mg, 57% yield). ¹H NMR (600 MHz, CDCl₃) δ 1.42 (t, *J* = 7.1 Hz, 3H, CO₂CH₂CH₃), 4.05 (s, 3H, OCH₃ or CO₂CH₃), 4.06 (s, 3H, OCH₃ or CO₂CH₃), 4.42 (q, *J* = 7.1 Hz, 2H, CO₂CH₂CH₃), 7.11 (s, 1H, ArH), 7.22 (d, *J* = 2.3 Hz, 1H, ArH), 7.27 (s, 1H, ArH), 9.70 (br, 1H, NH), 11.12 (s, 1H, NH). ¹³C NMR (151 MHz, CDCl₃) δ 14.4 (CO₂CH₂CH₃), 53.8 (CO₂CH₃), 56.2 (OCH₃), 60.8 (CO₂CH₂CH₃), 105.2 (C-8), 108.4 (C-3), 113.1 (C-4), 113.5 (C-8a), 121.2 (Ar), 126.9 (Ar), 127.6 (Ar), 130.3 (Ar), 134.4 (Ar), 143.1 (C-5), 161.0 (CO₂Et), 162.9 (CO₂Me), 178.8 (C-9). LC–MS (*m/z*): positive mode 345 [M + H]⁺. Purity by HPLC–UV (254 nm)–ESI–MS: 99.3%. Mp: 240–241 °C dec.



5-Methoxy-9-oxo-6,9-dihydro-1H-pyrrolo[2,3-f]quinoline-2,7-dicarboxylic acid (110, LW324B). The compound was synthesized using **109** (50 mg, 0.145 mmol). The product was isolated as a yellow solid (40 mg, 91% yield). ^1H NMR (600 MHz, D_2O , ND_3) δ 3.83 (s, 3H, OCH_3), 6.65 – 6.72 (m, 1H, ArH), 6.84 – 6.89 (m, 1H, ArH), 6.97 (s, 1H, ArH). ^{13}C NMR (151 MHz, D_2O , ND_3) δ 58.4 (OCH_3), 107.3 (C-3), 109.0 (C-8), 112.0 (C-4), 114.5 (C-9a), 124.0 (Ar), 127.7 (Ar), 131.5 (Ar), 134.5 (Ar), 144.0 (Ar), 144.9 (C-5), 169.1 (CO_2H), 171.6 (CO_2H), 181.8 (C-9). LC-MS (m/z): positive mode 303 [$\text{M} + \text{H}$] $^+$. Purity by HPLC-UV (254 nm)-ESI-MS: 99.6%. Mp: >300 °C dec.

5.3 Preparation of chromen-4-one derivatives

5.3.1 General Procedures

General procedure for the synthesis of compounds 69a-c. The appropriate 5'-substituted 2'-hydroxy-3'-nitroacetophenone (23 mmol) and diethyl oxalate (7.8 mL, 58 mmol, 2.5 equiv.) were dissolved in THF (100 mL). The mixture was added dropwise to a stirred suspension of potassium *tert*-butoxide (10.3 g, 92 mmol, 4 equiv.) in THF (100 mL) at 0 °C. After completed addition, the reaction mixture was kept stirring at that temperature for 10 min. Then, the solvent was removed under reduced pressure at 45 °C. Water (100 mL) was added, and the solution was acidified using dilute aq HCl (2 M, 100 mL, 8 equiv.). The mixture was extracted using DCM (3 × 100 mL). The combined organic layers were dried over anhydrous Na₂SO₄ and concentrated under reduced pressure. The liquid residue was dissolved in EtOH (200 mL), concd. aq HCl (10 mL) was added, and the mixture was refluxed for 20 min until the formation of a precipitate. After that, the mixture was cooled to 0 °C, and the precipitate was collected by filtration. The product was recrystallized from EtOH, washed with EtOH and petroleum ether, and dried at 50 °C for overnight.

General procedure for the synthesis of compounds 71a-c and LW327. The appropriate nitro derivative (17 mmol) was suspended in a mixture of EtOH (70 mL) and dilute HCl (2 M, 70 mL). Tin(II) chloride dihydrate (15.8 g, 69 mmol, 4 equiv.) was added at rt, and the mixture was heated to 70 °C for 40 min. After that, EtOH was removed under reduced pressure, and the residue was extracted with DCM (3 × 50 mL). The organic layer was washed with a saturated aq K₂CO₃ solution, dried over anhydrous Na₂SO₄, and concentrated under reduced pressure. The resulting solid was dried at 50 °C for overnight.

General procedure for the synthesis of compounds 75a-f. Ethyl 8-amino-6-bromo-4-oxo-4*H*-chromene-2-carboxylate (**71b**, 1.0 g, 3.2 mmol), the appropriate boronic acid derivative (6.4 mmol, 2 equiv.), K₂CO₃ (880 mg, 6.4 mmol, 2 equiv.), and tetrakis(triphenylphosphine)palladium(0) (370 mg, 0.32 mmol, 0.1 equiv.) were mixed with anhydrous toluene (15 mL) and anhydrous DMF (5 mL) under inert gas atmosphere. The mixture was heated to 130 °C in a pressure tube with stirring for 3 h. After that, the solvents were removed under reduced pressure, and the residue was purified by column chromatography on a column of silica gel (7:3 petroleum ether/acetone).

General procedure for the synthesis of compounds 72a-c, 76a,b. The appropriate ethyl 8-amino-4-oxo-4*H*-chromene-2-carboxylate (10 mmol) was dissolved in toluene (50 mL), and Lawesson's reagent (8.6 g, 20 mmol, 2 equiv.) was added. The mixture was refluxed for 2 h. After that, the solvent was removed under reduced pressure, and the residue was purified by column chromatography on a column of silica gel (7:3 petroleum ether/acetone).

General procedure for the synthesis of compounds 74a, 77a,b, 78a, 80. The appropriate amine (0.7 mmol) and DIPEA (0.24 mL, 1.4 mmol, 2 equiv.) were dissolved in dry DCM (5 mL) and cooled to 0 °C under inert gas atmosphere. At this temperature, ethoxalyl chloride (0.09 mL, 0.8 mmol, 1.1 equiv.) was added dropwise with stirring. The mixture was kept stirring at 0 °C for 1 h. Then, stirring continued at rt for 24 h. After that, the solvent was removed under reduced pressure, and the residue was purified by column chromatography.

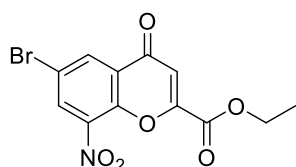
General procedure for the synthesis of compounds 74c-d, 78b,c. The appropriate difluoro-4-methoxybenzoic acid (0.34 mmol) was mixed with SOCl_2 (5 mL) and refluxed for 2 h. After that, the solvent was removed under reduced pressure. The residue was added dropwise to a stirred solution of the appropriate amine (0.30 mmol) and DIPEA (160 μL , 0.90 mmol) in dry THF (5 mL) at 0 °C under inert gas atmosphere. The mixture was kept stirring for 1 h at that temperature. After that, stirring continued at rt for 24 h. Then, the solvent was removed under reduced pressure, and the residue was purified by column chromatography.

General procedure for the synthesis of compounds 85a,b, 86a,b, 87, 88a-e, 89a-h, 90a. A solution of K_2CO_3 (50 mg, 0.36 mmol) in water (2 mL) was added slowly to a suspension of the appropriate ester (0.12 mmol) in THF. The reaction mixture was stirred at rt for 24 h. After that, water (2 mL) was added, and THF was evaporated under reduced pressure. Then, the mixture was acidified using few drops of concd. HCl. The precipitate was collected by filtration and washed with water (5 mL). In some cases, further purification was necessary (see individual compounds).

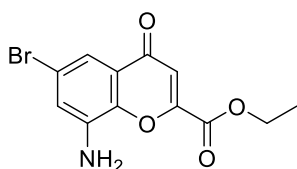
General procedure for the synthesis of compounds 81a-d, 83a,b. The appropriate phenol derivative (20 mmol) was dissolved in acetone (50 mL), and K_2CO_3 (60 mmol, 3 equiv.) was added at rt. Then, the mixture was refluxed for 30 min. After that, the appropriate benzyl bromide derivative (30 mmol, 1.5 equiv.) was added at rt, and the mixture was refluxed for 3 h. The mixture was cooled to rt and filtrated. The filtrate was collected and concentrated under reduced pressure. The resulting residue was collected. In some cases, further purification was necessary (see individual compounds).

General procedure for the synthesis of compounds 82a,b, 84a,b. The appropriate ester (10.4 mmol) was mixed with methanol (20 mL) and aq NaOH solution (10%, 2 mL) was added at rt. Then, the mixture was refluxed for 30 min. After that, the organic solvent was removed under reduced pressure, water (20 mL) was added, and the mixture was acidified using concd. aq HCl. The precipitate was collected by filtration and washed with water. In some cases, further purification was necessary (see individual compounds).

Preparation of 71b

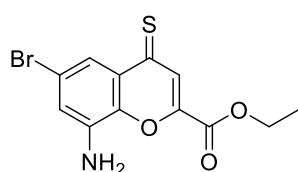


Ethyl 6-bromo-8-nitro-4-oxo-4H-chromene-2-carboxylate (69b, LW273). The compound was synthesized using 1-(5-bromo-2-hydroxy-3-nitrophenyl)ethanone (6.0 g, 23 mmol) and was isolated as a white solid (6.1 g, 78% yield). ^1H NMR (600 MHz, CDCl_3) δ 1.45 (t, $J = 7.1$ Hz, 3H, CH_2CH_3), 4.49 (q, $J = 7.1$ Hz, 2H, CH_2CH_3), 7.21 (s, 1H, 3-H), 8.48 (d, $J = 2.4$ Hz, 1H, 7-H), 8.58 (d, $J = 2.4$ Hz, 1H, 5-H). ^{13}C NMR (151 MHz, CDCl_3) δ 14.0 (CH_2CH_3), 63.6 (CH_2CH_3), 115.1 (C-3), 118.2 (C-4a), 127.0 (C-6), 133.5 (C-7), 134.0 (C-5), 139.7 (C-8), 147.0 (C-8a), 152.9 (C-2), 159.3 (CO_2Et), 174.9 (C-4). LC-MS (m/z): positive mode 342 [$\text{M} + \text{H}$] $^+$. Purity by HPLC-UV (254 nm)-ESI-MS: 94.0%.

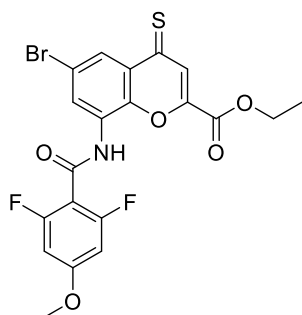


Ethyl 8-amino-6-bromo-4-oxo-4H-chromene-2-carboxylate (71b, LW275). The compound was synthesized using **69b** (6.0 g, 18 mmol) and was isolated as a yellow solid (5.6 g, 100% yield). ^1H NMR (600 MHz, CDCl_3) δ 1.42 (t, $J = 7.1$ Hz, 3H, CH_2CH_3), 4.45 (q, $J = 7.1$ Hz, 2H, CH_2CH_3), 7.07 (s, 1H, 3-H), 7.15 (d, $J = 2.2$ Hz, 1H, 7-H), 7.61 (d, $J = 2.1$ Hz, 1H, 5-H). ^{13}C NMR (151 MHz, CDCl_3) δ 14.1 (CH_2CH_3), 63.1 (CH_2CH_3), 114.5 (C-3), 116.1 (C-7), 119.7 (C-4a), 120.8 (C-5), 125.6 (C-6), 137.9 (C-8), 143.6 (C-8a), 151.3 (C-2), 160.2 (CO_2Et), 177.4 (C-4). LC-MS (m/z): positive mode 314 [$\text{M} + \text{H}$] $^+$. Purity by HPLC-UV (254 nm)-ESI-MS: 97.4%.

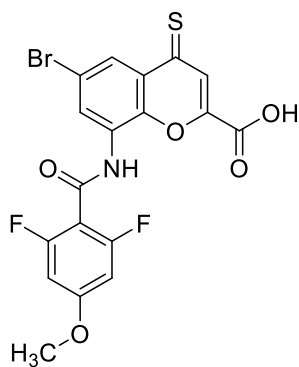
Preparation of 88a



Ethyl 8-amino-6-bromo-4-thioxo-4H-chromene-2-carboxylate (72b, LW276). The compound was synthesized using **71b** (3.3 g, 10 mmol). The product was isolated as a brown solid (1.9 g, 58% yield). ^1H NMR (600 MHz, $(\text{CD}_3)_2\text{CO}$) δ 1.42 (t, $J = 7.1$ Hz, 3H, CH_2CH_3), 4.46 (q, $J = 7.1$ Hz, 2H, CH_2CH_3), 7.32 (s, 1H, 7-H), 7.68 (s, 1H, 3-H), 7.70 (s, 1H, 5-H). ^{13}C NMR (151 MHz, $(\text{CD}_3)_2\text{CO}$) δ 14.3 (CH_2CH_3), 63.6 (CH_2CH_3), 116.7 (C-7), 120.3 (C-3), 121.8 (C-6), 125.7 (C-5), 133.1 (C-4a), 139.6 (C-8), 141.6 (C-8a), 142.9 (C-2), 161.4 (CO_2Et), 203.4 (C-4). LC-MS (m/z): positive mode 330 [$\text{M} + \text{H}$] $^+$. Purity by HPLC-UV (254 nm)-ESI-MS: 96.2%.

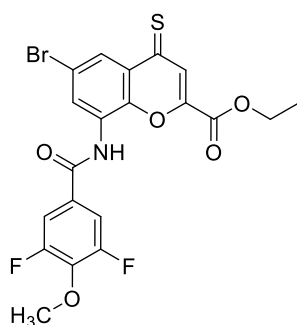


Ethyl 6-bromo-8-(2,6-difluoro-4-methoxybenzamido)-4-thioxo-4H-chromene-2-carboxylate (74b, LW294). The compound was synthesized using 2,6-difluoro-4-methoxybenzoic acid (108 mg, 0.57 mmol) and **72b** (170 mg, 0.52 mmol). The amide was isolated as a green solid (129 mg, 50% yield). ^1H NMR (600 MHz, CDCl_3) δ 1.44 (t, $J = 7.1$ Hz, 3H, CH_2CH_3), 3.88 (s, 3H OCH_3), 4.46 (q, $J = 7.0$ Hz, 2H, CH_2CH_3), 6.57 – 6.69 (m, 2H, 3'-H, 5'-H), 7.81 (s, 1H, 3-H), 8.21 – 8.41 (m, 1H, 7-H), 8.84 (s, 1H, 5-H), 9.15 (s, 1H, NH). ^{13}C NMR (151 MHz, CDCl_3) δ 14.0 (CH_2CH_3), 56.2 (OCH_3), 63.2 (CH_2CH_3), 98.9 – 99.4 (m, C-3', C-5'), 105.0 (t, $J = 16.3$ Hz, C-1'), 121.4 (C-6), 124.5 (C-7), 125.8 (C-3), 127.2 (C-5), 129.5 (C-8), 131.7 (C-4a), 139.6 (C-8a), 140.6 (C-2), 158.5 (C-4'), 160.7 (CO_2Et), 162.2 (dd, $J = 9.0, 253.2$ Hz, C-2', C-6'), 163.5 (t, $J = 14.8$ Hz, CONH), 201.7 (C-4). LC-MS (m/z): positive mode 498 [$\text{M} + \text{H}$] $^+$. Purity by HPLC-UV (254 nm)-ESI-MS: 89.7%.

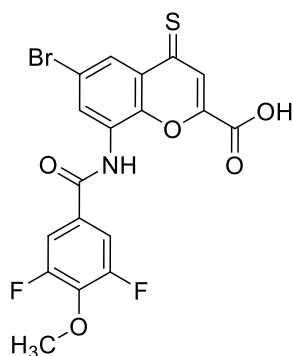


6-Bromo-8-(2,6-difluoro-4-methoxybenzamido)-4-thioxo-4H-chromene-2-carboxylic acid (88a, LW296). The product was synthesized using **74b** (62 mg, 0.12 mmol). The precipitate was collected by filtration and further purified by column chromatography on a column of silica gel (94:5:1 DCM/MeOH/TFA). The product was isolated as a brown solid (34 mg, 60% yield). ^1H NMR (600 MHz, CDCl_3 , MeOD) δ 3.78 (s, 3H, OCH_3), 6.48 (d, $J = 9.9$ Hz, 2H, 3'-H, 5'-H), 7.81 (s, 1H, 7-H), 8.32 (s, 1H, 3-H), 9.04 (s, 1H, 5-H). ^{13}C NMR (151 MHz, CDCl_3 , MeOD) δ 55.9 (OCH_3), 97.9 – 98.2 (m, C-3', C-5'), 107.3 (t, $J = 21.1$ Hz, C-1'), 120.5 (C-6), 124.9 (C-7), 125.0 (C-3), 128.4 (C-5), 129.8 (C-8), 129.9 (C-4a), 131.5 (C-8a), 141.0 (C-2), 160.3 (CO_2H , C-4'), 160.9 (dd, $J = 9.9$, 250.8 Hz, C-2', C-6'), 162.4 (t, $J = 14.1$ Hz, CONH), 202.5 (C-4). LC-MS (m/z): positive mode 472 [$\text{M} + \text{H}$] $^+$. Purity by HPLC-UV (254 nm)-ESI-MS: 98.8%. Mp: 165–166 $^\circ\text{C}$ dec.

Preparation of 88b



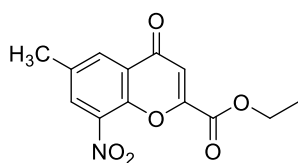
Ethyl 6-bromo-8-(3,5-difluoro-4-methoxybenzamido)-4-thioxo-4H-chromene-2-carboxylate (74c, LW281). The compound was synthesized using 3,5-difluoro-4-methoxybenzoic acid (64 mg, 0.34 mmol) and **72b** (100 mg, 0.30 mmol). The amide was isolated as a green solid (50 mg, 34% yield). ^1H NMR (600 MHz, CDCl_3) δ 1.48 (t, $J = 7.0$ Hz, 3H, CH_2CH_3), 4.14 (s, 3H, OCH_3), 4.51 (q, $J = 7.0$ Hz, 2H, CH_2CH_3), 7.55 (d, $J = 7.7$ Hz, 2H, 2'-H, 6'-H), 7.82 (s, 1H, 7-H), 8.28 (s, 1H, 3-H), 8.67 (s, 1H, 5-H), 9.06 (s, 1H, NH). ^{13}C NMR (151 MHz, CDCl_3) δ 14.1 (CH_2CH_3), 61.8 (t, $J = 3.7$ Hz, OCH_3), 63.5 (CH_2CH_3), 111.7 (dd, $J = 6.3$, 18.3 Hz, C-2', C-6'), 121.4 (C-6), 124.7 (C-7), 125.8 (C-3), 126.9 (C-5), 127.33 – 127.59 (m, C-1'), 129.3 (C-8), 131.7 (C-4a), 139.6 (C-4'), 140.4 (C-2, C-8a), 155.2 (dd, $J = 5.9$, 251.0 Hz, C-3', C-5'), 160.7 (CO_2Et), 162.3 (CONH), 201.6 (C-4). LC-MS (m/z): positive mode 498 [$\text{M} + \text{H}$] $^+$. Purity by HPLC-UV (254 nm)-ESI-MS: 72.2%.



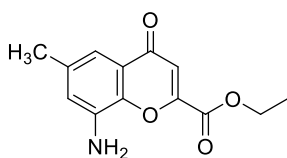
6-Bromo-8-(3,5-difluoro-4-methoxybenzamido)-4-thioxo-4H-chromene-2-carboxylic acid (88b, LW283). The product was synthesized using **74c** (40 mg, 0.08 mmol). The precipitate was collected by filtration and further purified by column chromatography on a column of silica gel (94:5:1 DCM/MeOH/TFA). The product was isolated as a green solid (17 mg, 45% yield). ^1H NMR (600 MHz, $\text{DMSO}-d_6$) δ 4.05 (s, 3H, OCH_3), 7.67 (s, 1H, 3-H), 7.79 (d, $J = 8.6$ Hz, 2H, 2'-H, 6'-H), 8.26 – 8.33 (m, 2H, 5-H, 7-H), 10.58 (s, 1H, NH). ^{13}C NMR (151 MHz, $\text{DMSO}-d_6$) δ 61.8 – 62.0 (m, OCH_3), 112.6 (dd, $J = 5.5$, 18.8 Hz, C-2', C-6'), 119.3 (C-6), 124.7 (C-7), 126.0 (C-3), 128.0 (t, $J = 7.8$ Hz, C-1'), 130.3 (C-8), 131.9 (C-4a), 133.1 (C-5), 139.2 (t, $J = 13.5$ Hz, C-4'), 144.2 (C-8a), 144.5 (C-2), 154.5 (dd, $J = 5.9$, 247.6 Hz, C-3', C-5'),

161.5 (CO₂H), 163.0 (CONH), 201.5 (C-4). LC–MS (*m/z*): positive mode 472 [M + H]⁺. Purity by HPLC–UV (254 nm)–ESI-MS: 96.5%. Mp: 240–241 °C dec.

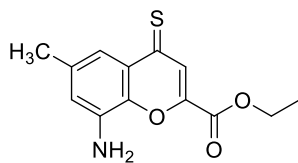
Preparation of 88c



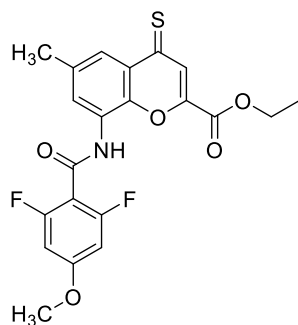
Ethyl 6-methyl-8-nitro-4-oxo-4H-chromene-2-carboxylate (69c, LW309). The compound was synthesized using 1-(2-hydroxy-5-methyl-3-nitrophenyl)ethanone (2.0 g, 10 mmol). The product was isolated as a white solid (2.3 g, 84% yield). ¹H NMR (600 MHz, CDCl₃) δ 1.44 (t, *J* = 7.1 Hz, 3H, CH₂CH₃), 2.55 (s, 3H, ArCH₃), 4.47 (q, *J* = 7.1 Hz, 2H, CH₂CH₃), 7.17 (s, 1H, 3-H), 8.20 (d, *J* = 2.2 Hz, 1H, 5-H), 8.26 (d, *J* = 2.0 Hz, 1H, 7-H). ¹³C NMR (151 MHz, CDCl₃) δ 14.0 (CH₂CH₃), 20.8 (ArCH₃), 63.4 (CH₂CH₃), 114.9 (C-3), 125.6 (C-4a), 131.1 (C-7), 131.5 (C-5), 136.0 (C-6), 138.8 (C-8), 146.3 (C-8a), 152.6 (C-2), 159.6 (CO₂Et), 176.3 (C-4). LC–MS (*m/z*): positive mode 278 [M + H]⁺. Purity by HPLC–UV (254 nm)–ESI-MS: 99.4%.



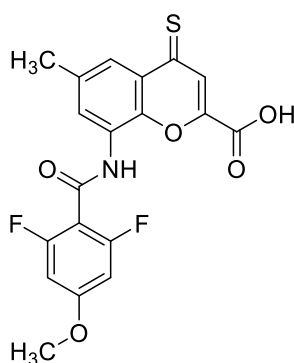
Ethyl 8-amino-4-oxo-6-methyl-4H-chromene-2-carboxylate (71c, LW312). The compound was synthesized using **69c** (1.0 g, 3.6 mmol). The product was isolated as a yellow solid (700 mg, 79% yield). ¹H NMR (600 MHz, CDCl₃) δ 1.42 (t, *J* = 7.1 Hz, 3H, CH₂CH₃), 2.35 (s, 3H, ArCH₃), 4.44 (q, *J* = 7.1 Hz, 2H, CH₂CH₃), 6.90 (d, *J* = 1.8 Hz, 1H, 7-H), 7.05 (s, 1H, 3-H), 7.31 (s, 1H, 5-H). ¹³C NMR (151 MHz, CDCl₃) δ 14.1 (CH₂CH₃), 21.2 (ArCH₃), 62.8 (CH₂CH₃), 113.7 (C-3), 114.3 (C-7), 119.9 (C-5), 124.5 (C-4a), 136.1 (C-8), 136.3 (C-6), 143.2 (C-8a), 151.1 (C-2), 160.6 (CO₂Et), 178.8 (C-4). LC–MS (*m/z*): positive mode 248 [M + H]⁺. Purity by HPLC–UV (254 nm)–ESI-MS: 96.2%.



Ethyl 8-amino-6-methyl-4-thioxo-4H-chromene-2-carboxylate (72c, LW321). The compound was synthesized using **71c** (600 mg, 2.4 mmol). The product was isolated as a brown solid (110 mg, 17% yield). ¹H NMR (600 MHz, CDCl₃) δ 1.42 (t, *J* = 6.9 Hz, 3H, CH₂CH₃), 2.35 (s, 3H, ArCH₃), 4.44 (q, *J* = 6.8 Hz, 2H, CH₂CH₃), 6.90 (s, 1H, 7-H), 7.60 (s, 1H, 5-H), 7.80 (s, 1H, 3-H). ¹³C NMR (151 MHz, CDCl₃) δ 14.1 (CH₂CH₃), 21.3 (ArCH₃), 62.8 (CH₂CH₃), 116.2 (C-7), 119.9 (C-3), 125.4 (C-5), 131.5 (C-4a), 136.8 (C-8), 137.4 (C-6), 138.3 (C-8a), 141.0 (C-2), 161.3 (CO₂Et), 203.8 (C-4). LC–MS (*m/z*): positive mode 264 [M + H]⁺. Purity by HPLC–UV (254 nm)–ESI-MS: 96.7%.

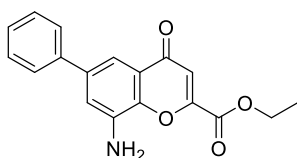


Ethyl 8-(2,6-difluoro-4-methoxybenzamido)-6-methyl-4-thioxo-4H-chromene-2-carboxylate (74d, LW332). The compound was synthesized using 2,6-difluoro-4-methoxybenzoic acid (71 mg, 0.38 mmol) and **72c** (90 mg, 0.34 mmol). The amide was isolated as a green solid (94 mg, 64% yield). ^1H NMR (600 MHz, CDCl_3) δ 1.43 (t, $J = 7.1$ Hz, 3H, CH_2CH_3), 2.49 (s, 3H, ArCH_3), 3.87 (s, 3H, OCH_3), 4.45 (q, $J = 7.1$ Hz, 2H, CH_2CH_3), 6.59 (d, $J = 10.6$ Hz, 2H, 3'-H, 5'-H), 7.81 (s, 1H, 3-H), 7.97 (s, 1H, 7-H), 8.77 (s, 1H, NH), 8.81 (s, 1H, 5-H). ^{13}C NMR (151 MHz, CDCl_3) δ 14.0 (CH_2CH_3), 21.6 (ArCH_3), 56.1 (OCH_3), 63.0 (CH_2CH_3), 98.8 – 99.3 (m, C-3', C-5'), 105.5 (t, $J = 16.5$ Hz, C-1'), 122.0 (C-7), 125.6 (C-3), 126.3 (C-5), 127.9 (C-8), 130.7 (C-4a), 137.6 (C-6), 139.1 (C-8a), 140.6 (C-2), 158.6 (C-4'), 161.0 (CO_2Et), 162.1 (dd, $J = 9.1, 252.9$ Hz, C-2', C-6'), 163.1 (t, $J = 14.9$ Hz, CONH), 203.2 (C-4). LC-MS (m/z): positive mode 434 [$\text{M} + \text{H}$] $^+$. Purity by HPLC-UV (254 nm)-ESI-MS: 93.3%.

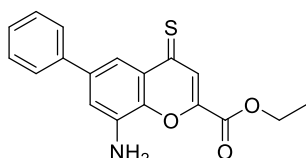


8-(2,6-Difluoro-4-methoxybenzamido)-6-methyl-4-thioxo-4H-chromene-2-carboxylic acid (88c, LW337). The product was synthesized using **74d** (70 mg, 0.16 mmol). The precipitate was collected by filtration and further purified by column chromatography on a column of silica gel (90:9:1 DCM/MeOH/TFA). The product was isolated as a brown solid (60 mg, 93% yield). ^1H NMR (600 MHz, CDCl_3 , MeOD) δ 2.44 (s, 3H, ArCH_3), 3.80 (s, 3H, OCH_3), 6.51 (d, $J = 9.8$ Hz, 2H, 3'-H, 5'-H), 7.79 (s, 1H, 3-H), 7.97 (s, 1H, 7-H), 8.70 (s, 1H, 5-H). ^{13}C NMR (151 MHz, CDCl_3 , MeOD) δ 21.3 (ArCH_3), 55.9 (OCH_3), 97.7 – 99.1 (m, C-3', C-5'), 106.5 (t, $J = 19.1$ Hz, C-1'), 122.3 (C-7), 125.8 (C-3), 127.4 (C-5), 127.8 (C-8), 130.8 (C-4a), 137.2 (C-6), 139.8 (C-8a), 141.0 (C-2), 159.6 (C-4'), 161.3 (dd, $J = 9.7, 251.7$ Hz, C-2', C-6'), 162.6 (t, $J = 14.3$ Hz, CONH), 163.4 (CO_2H), 203.4 (C-4). LC-MS (m/z): positive mode 406 [$\text{M} + \text{H}$] $^+$. Purity by HPLC-UV (254 nm)-ESI-MS: 97.6%. Mp: 250–251 °C dec.

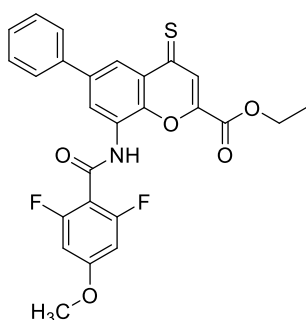
Preparation of 88d



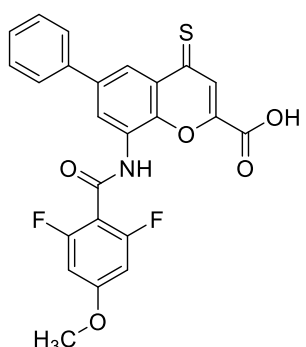
Ethyl 8-amino-4-oxo-6-phenyl-4H-chromene-2-carboxylate (75a, LW284). The compound was synthesized using **71b** (1.0 g, 3.2 mmol) and phenylboronic acid (780 mg, 6.4 mmol). The product was isolated as a yellow solid (950 mg, 96% yield). ^1H NMR (600 MHz, CDCl_3) δ 1.43 (t, $J = 7.4$ Hz, 3H, CH_2CH_3), 4.45 (q, $J = 7.1$ Hz, 2H, CH_2CH_3), 7.09 (s, 1H, 3-H), 7.28 (d, $J = 1.9$ Hz, 1H, 5-H), 7.35 (t, $J = 7.4$ Hz, 1H, 4'-H), 7.42 (t, $J = 7.6$ Hz, 2H, 3'-H, 5'-H), 7.59 (d, $J = 7.5$ Hz, 2H, 2'-H, 6'-H), 7.72 (d, $J = 2.0$ Hz, 1H, 7-H). ^{13}C NMR (151 MHz, CDCl_3) δ 14.1 (CH_2CH_3), 62.9 (CH_2CH_3), 111.8 (C-7), 114.3 (C-3), 117.2 (C-5), 124.9 (C-4a), 127.1 (C-2', C-6'), 127.8 (C-4'), 128.8 (C-3', C-5'), 137.0 (C-8), 139.2 (C-1'), 139.6 (C-8a), 144.1 (C-6), 151.2 (C-2), 160.5 (CO_2Et), 178.8 (C-4). LC-MS (m/z): positive mode 310 [$\text{M} + \text{H}$] $^+$. Purity by HPLC-UV (254 nm)-ESI-MS: 96.0%.

**Ethyl 8-amino-6-phenyl-4-thioxo-4H-chromene-2-carboxylate (76a, LW287).**

The compound was synthesized using **75a** (940 mg, 3.0 mmol). The product was isolated as a brown solid (585 mg, 56% yield). ^1H NMR (600 MHz, CDCl_3) δ 1.44 (t, $J = 7.1$ Hz, 3H, CH_2CH_3), 4.46 (q, $J = 7.1$ Hz, 2H, CH_2CH_3), 7.32 (d, $J = 2.0$ Hz, 1H, 3-H), 7.37 (t, $J = 7.3$ Hz, 1H, 4'-H), 7.44 (t, $J = 7.6$ Hz, 2H, 3'-H, 5'-H), 7.60 – 7.64 (m, 2H, 2'-H, 6'-H), 7.84 (s, 1H, 5-H), 8.02 (d, $J = 2.0$ Hz, 1H, 7-H). ^{13}C NMR (151 MHz, CDCl_3) δ 14.1 (CH_2CH_3), 62.9 (CH_2CH_3), 114.7 (C-7), 117.5 (C-3), 125.5 (C-5), 127.2 (C-2', C-6'), 127.9 (C-4'), 128.8 (C-3', C-5'), 131.8 (C-4a), 137.3 (C-8), 139.5 (C-8a), 139.6 (C-1'), 140.2 (C-6), 141.0 (C-2), 161.3 (CO_2Et), 204.0 (C-4). LC-MS (m/z): positive mode 326 $[\text{M} + \text{H}]^+$. Purity by HPLC-UV (254 nm)-ESI-MS: 85.8%.

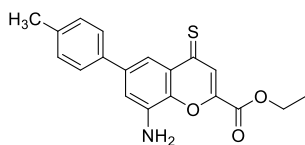
**Ethyl 8-(2,6-difluoro-4-methoxybenzamido)-6-phenyl-4-thioxo-4H-chromene-2-carboxylate (78b, LW289).**

The compound was synthesized using 2,6-difluoro-4-methoxybenzoic acid (126 mg, 0.67 mmol) and **76a** (200 mg, 0.61 mmol). The amide was isolated as a yellow solid (144 mg, 48% yield). ^1H NMR (600 MHz, CDCl_3) δ 1.45 (t, $J = 7.2$ Hz, 3H, CH_2CH_3), 3.88 (s, 3H, OCH_3), 4.48 (q, $J = 7.1$ Hz, 2H, CH_2CH_3), 6.61 (d, $J = 10.7$ Hz, 2H, 3''-H, 5''-H), 7.40 (t, $J = 7.4$ Hz, 1H, 4'-H), 7.47 (t, $J = 7.6$ Hz, 2H, 3'-H, 5'-H), 7.74 (d, $J = 7.4$ Hz, 2H, 2'-H, 6'-H), 7.85 (s, 1H, 3-H), 8.40 (d, $J = 2.1$ Hz, 1H, 7-H), 8.90 (s, 1H, 5-H), 9.29 (s, 1H, NH). ^{13}C NMR (151 MHz, CDCl_3) δ 14.1 (CH_2CH_3), 56.2 (OCH_3), 63.1 (CH_2CH_3), 99.0 – 99.2 (m, C-3'', C-5''), 105.4 (t, $J = 16.1$ Hz, C-1''), 120.1 (C-7), 124.0 (C-3), 125.7 (C-5), 127.5 (C-2', C-6'), 128.2 (C-4'), 128.7 (C-8), 128.9 (C-3', C-5'), 131.1 (C-4a), 139.0 (C-1'), 140.2 (C-8a), 140.6 (C-6), 158.6 (C-2), 158.7 (C-4''), 161.0 (CO_2Et), 162.1 (dd, $J = 9.0, 252.9$ Hz, C-2'', C-6''), 163.2 (t, $J = 14.9$ Hz, CONH), 203.3 (C-4). LC-MS (m/z): positive mode 496 $[\text{M} + \text{H}]^+$. Purity by HPLC-UV (254 nm)-ESI-MS: 85.1%.

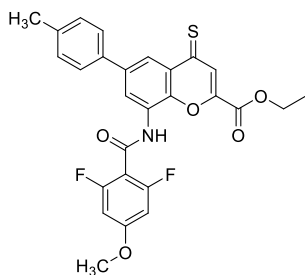
**8-(2,6-Difluoro-4-methoxybenzamido)-6-phenyl-4-thioxo-4H-chromene-2-carboxylic acid (88d, LW302).**

The product was synthesized using **78b** (65 mg, 0.13 mmol). The precipitate was filtered off, and purified by column chromatography. The product was isolated as a brown solid (40 mg, 66% yield). ^1H NMR (600 MHz, $\text{DMSO}-d_6$) δ 3.85 (s, 3H, OCH_3), 6.90 (d, $J = 10.1$ Hz, 2H, 3''-H, 5''-H), 7.45 (t, $J = 7.3$ Hz, 1H, 4'-H), 7.54 (t, $J = 7.6$ Hz, 2H, 3'-H, 5'-H), 7.68 (s, 1H, 3-H), 7.72 (d, $J = 7.4$ Hz, 2H, 2'-H, 6'-H), 8.39 (d, $J = 1.8$ Hz, 1H, 7-H), 8.51 (s, 1H, 5-H), 10.63 (s, 1H, NH). ^{13}C NMR (151 MHz, $\text{DMSO}-d_6$) δ 56.6 (OCH_3), 98.8 (d, $J = 28.3$ Hz, C-3'', C-5''), 107.1 (t, $J = 21.3$ Hz, C-1''), 121.3 (C-7), 124.9 (C-3), 127.1 (C-2', C-6'), 128.3 (C-5), 128.6 (C-4'), 128.7 (C-8), 129.5 (C-3', C-5'), 131.3 (C-4a), 138.2 (C-1'), 138.7 (C-8a), 143.4 (C-6), 143.7 (C-2), 159.1 (C-4''), 160.5 (dd, $J = 248.9, 10.4$ Hz, C-2'', C-6''), 161.7 (CO_2H), 162.4 (t, $J = 14.2$ Hz, CONH), 202.8 (C-4). LC-MS (m/z): positive mode 468 $[\text{M} + \text{H}]^+$. Purity by HPLC-UV (254 nm)-ESI-MS: 97.2%. Mp: 165–166 °C dec.

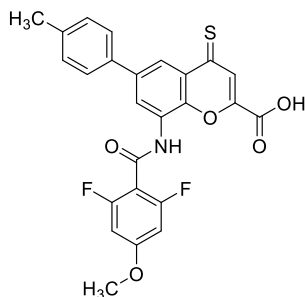
Preparation of 88e



Ethyl 8-amino-4-thioxo-6-(*p*-tolyl)-4*H*-chromene-2-carboxylate (76b, LW307). The compound was synthesized using **75b** (350 mg, 1.1 mmol). The product was isolated as a brown solid (122 mg, 33% yield). ¹H NMR (600 MHz, CDCl₃) δ 1.44 (t, $J = 7.1$ Hz, 3H, CH₂CH₃), 2.40 (s, 3H, ArCH₃), 4.45 (q, $J = 7.1$ Hz, 2H, CH₂CH₃), 7.25 (d, $J = 7.7$ Hz, 2H, 3'-H, 5'-H), 7.30 (s, 1H, 7-H), 7.52 (d, $J = 7.8$ Hz, 2H, 2'-H, 6'-H), 7.83 (s, 1H, 5-H), 8.00 (s, 1H, 3-H). ¹³C NMR (151 MHz, CDCl₃) δ 14.1 (CH₂CH₃), 21.1 (ArCH₃), 62.9 (CH₂CH₃), 114.4 (C-7), 117.3 (C-3), 125.5 (C-5), 127.0 (C-2', C-6'), 129.5 (C-3', C-5'), 131.8 (C-4a), 136.6 (C-8), 137.3 (C-1'), 137.8 (C-4'), 139.4 (C-8a), 140.1 (C-6), 141.0 (C-2), 161.3 (CO₂Et), 203.9 (C-4). LC-MS (m/z): positive mode 340 [M + H]⁺. Purity by HPLC-UV (254 nm)-ESI-MS: 93.0%.

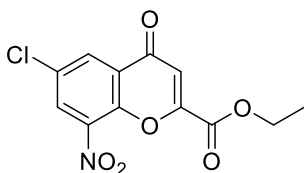


Ethyl 8-(2,6-difluoro-4-methoxybenzamido)-6-(*p*-tolyl)-4-thioxo-4*H*-chromene-2-carboxylate (78c, LW338). The compound was synthesized using 2,6-difluoro-4-methoxybenzoic acid (56 mg, 0.30 mmol) and **76b** (90 mg, 0.27 mmol). The amide was isolated as a green solid (96 mg, 70% yield). ¹H NMR (600 MHz, CDCl₃) δ 1.45 (t, $J = 7.1$ Hz, 3H, CH₂CH₃), 2.41 (s, 3H, ArCH₃), 3.88 (s, 3H, OCH₃), 4.47 (q, $J = 7.1$ Hz, 2H, CH₂CH₃), 6.58 – 6.64 (m, 2H, 3''-H, 5''-H), 7.28 (d, $J = 7.8$ Hz, 2H, 3'-H, 5'-H), 7.64 (d, $J = 7.9$ Hz, 2H, 2'-H, 6'-H), 7.85 (s, 1H, 3-H), 8.39 (d, $J = 2.2$ Hz, 1H, 7-H), 8.82 – 8.90 (m, 1H, 5-H), 9.28 (d, $J = 2.2$ Hz, 1H, NH). ¹³C NMR (151 MHz, CDCl₃) δ 14.1 (CH₂CH₃), 21.2 (ArCH₃), 56.2 (OCH₃), 63.1 (CH₂CH₃), 98.8 – 99.3 (m, C-3'', C-5''), 105.4 (t, $J = 16.4$ Hz, C-1''), 119.8 (C-7), 123.8 (C-3), 125.7 (C-2', C-6'), 127.3 (C-5), 128.6 (C-8), 129.6 (C-3', C-5'), 131.1 (C-4a), 136.0 (C-4'), 138.2 (C-1'), 140.0 (C-8a), 140.1 (C-6), 140.6 (C-2), 158.6 (C-4''), 161.0 (CO₂Et), 162.0 (dd, $J = 9.1, 252.9$ Hz, C-2'', C-6''), 163.3 (t, $J = 15.0$ Hz, CONH), 203.3 (C-4). LC-MS (m/z): positive mode 510 [M + H]⁺. Purity by HPLC-UV (254 nm)-ESI-MS: 91.1%.

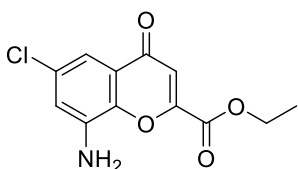


8-(2,6-Difluoro-4-methoxybenzamido)-6-(*p*-tolyl)-4-thioxo-4*H*-chromene-2-carboxylic acid (88e, LW345). The product was synthesized using **78c** (40 mg, 0.08 mmol). The precipitate was collected by filtration and further purified by column chromatography on a column of silica gel (94:5:1 DCM/MeOH/TFA). The product was isolated as a brown solid (34 mg, 90% yield). ¹H NMR (600 MHz, DMSO-*d*₆) δ 2.37 (s, 3H, ArCH₃), 3.86 (s, 3H, OCH₃), 6.90 (d, $J = 10.2$ Hz, 2H, 3''-H, 5''-H), 7.35 (d, $J = 8.1$ Hz, 2H, 3'-H, 5'-H), 7.62 (d, $J = 7.7$ Hz, 2H, 2'-H, 6'-H), 7.68 (s, 1H, 3-H), 8.39 (s, 1H, 7-H), 8.50 (s, 1H, 5-H), 10.69 (s, 1H, NH). ¹³C NMR (151 MHz, DMSO-*d*₆) δ 20.9 (ArCH₃), 56.6 (OCH₃), 98.4 – 99.3 (m, C-3'', C-5''), 107.1 (C-1''), 120.9 (C-7), 124.9 (C-3), 126.9 (C-2', C-6'), 128.1 (C-5), 128.8 (C-8), 130.1 (C-3', C-5'), 131.3 (C-4a), 135.3 (C-4'), 138.2 (C-1'), 138.7 (C-8a), 143.6 (C-6), 143.8 (C-2), 159.2 (C-4''), 160.6 (dd, $J = 11.1, 248.7$ Hz, C-2'', C-6''), 161.7 (CO₂H), 162.4 (t, $J = 14.3$ Hz, CONH), 202.8 (C-4). LC-MS (m/z): positive mode 482 [M + H]⁺. Purity by HPLC-UV (254 nm)-ESI-MS: 97.3%. Mp: 166–167 °C dec.

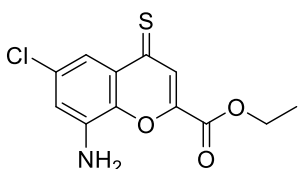
Preparation of 86a



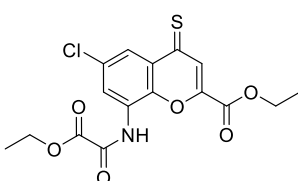
Ethyl 6-chloro-8-nitro-4-oxo-4H-chromene-2-carboxylate (69a, LW197). The compound was synthesized using 1-(5-chloro-2-hydroxy-3-nitrophenyl)ethanone (3.0 g, 14 mmol) and was isolated as a white solid (2.6 g, 62% yield). ^1H NMR (500 MHz, DMSO- d_6) δ 1.34 (t, $J = 7.1$ Hz, 3H, CH_2CH_3), 4.40 (q, $J = 7.1$ Hz, 2H, CH_2CH_3), 7.09 (s, 1H, 3-H), 8.29 (d, $J = 2.6$ Hz, 1H, 7-H), 8.68 (d, $J = 2.6$ Hz, 1H, 5-H). ^{13}C NMR (126 MHz, DMSO- d_6) δ 13.9 (CH_2CH_3), 63.2 (CH_2CH_3), 114.5 (C-3), 126.6 (C-4a), 129.6 (C-7), 129.9 (C-6), 130.6 (C-5), 140.0 (C-8), 146.4 (C-8a), 152.4 (C-2), 159.3 (CO_2Et), 175.1 (C-4). LC-MS (m/z): positive mode 298 $[\text{M} + \text{H}]^+$. Purity by HPLC-UV (254 nm)-ESI-MS: 92.5%.



Ethyl 8-amino-6-chloro-4-oxo-4H-chromene-2-carboxylate (71a, LW226). The compound was synthesized using **69a** (2.5 g, 8.4 mmol) and was isolated as a yellow solid (1.8 g, 80% yield). ^1H NMR (600 MHz, CDCl_3) δ 1.41 (t, $J = 7.1$ Hz, 3H, CH_2CH_3), 4.21 (br, 2H, NH_2), 4.44 (q, $J = 7.1$ Hz, 2H, CH_2CH_3), 6.99 (s, 1H, 7-H), 7.05 (s, 1H, 3-H), 7.42 (s, 1H, 5-H). ^{13}C NMR (151 MHz, CDCl_3) δ 14.0 (CH_2CH_3), 63.0 (CH_2CH_3), 112.7 (C-7), 114.3 (C-3), 117.9 (C-5), 125.3 (C-4a), 132.1 (C-6), 138.0 (C-8), 143.1 (C-8a), 151.3 (C-2), 160.2 (CO_2Et), 177.5 (C-4). LC-MS (m/z): positive mode 268 $[\text{M} + \text{H}]^+$. Purity by HPLC-UV (254 nm)-ESI-MS: 95.7%.

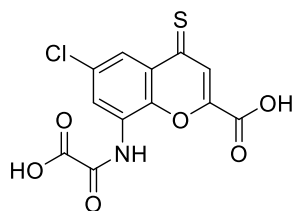


Ethyl 8-amino-6-chloro-4-thioxo-4H-chromene-2-carboxylate (72a, LW229). The compound was synthesized using **71a** (1.7 g, 6.3 mmol). The product was isolated as a brown solid (310 mg, 17% yield). ^1H NMR (600 MHz, CDCl_3) δ 1.42 (t, $J = 7.1$ Hz, 3H, CH_2CH_3), 4.44 (q, $J = 7.1$ Hz, 2H, CH_2CH_3), 7.04 (s, 1H, 3-H), 7.72 – 7.77 (m, 1H, 7-H), 7.79 (s, 1H, 5-H). ^{13}C NMR (151 MHz, CDCl_3) δ 14.1 (CH_2CH_3), 63.0 (CH_2CH_3), 115.7 (C-7), 118.2 (C-3), 125.6 (C-5), 132.1 (C-8), 133.4 (C-6), 137.9 (C-4a), 138.6 (C-8a), 141.1 (C-2), 161.0 (CO_2Et), 202.5 (C-4). LC-MS (m/z): positive mode 284 $[\text{M} + \text{H}]^+$. Purity by HPLC-UV (254 nm)-ESI-MS: 97.6%.



Ethyl 6-chloro-8-(2-ethoxy-2-oxoacetamido)-4-thioxo-4H-chromene-2-carboxylate (74a, LW232). The compound was synthesized using **72a** (200 mg, 0.7 mmol). The amide was isolated as a green solid (200 mg, 75% yield). ^1H NMR (600 MHz, CDCl_3) δ 1.47 (t, $J = 7.2$ Hz, 6H, $2 \times \text{CH}_2\text{CH}_3$), 4.42 – 4.56 (m, 4H, $2 \times \text{CH}_2\text{CH}_3$), 7.76 (s, 1H, 3-H), 8.11 (d, $J = 2.4$ Hz, 1H, 7-H), 8.78 (d, $J = 2.4$ Hz, 1H, 5-H), 9.79 (s, 1H, NH). ^{13}C NMR (151 MHz, CDCl_3) δ 14.0 (CH_2CH_3), 14.0 (CH_2CH_3), 63.3 (CH_2CH_3), 64.2 (CH_2CH_3), 122.4 (C-7), 123.9 (C-3), 125.6 (C-5), 128.1 (C-8), 131.3 (C-6), 133.6 (C-4a), 139.2 (C-8a), 140.7 (C-

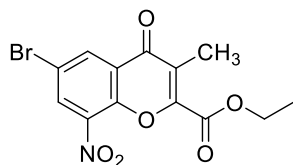
2), 154.0 (CONH), 159.7 (CO₂Et), 160.4 (CO₂Et), 201.5 (C-4). LC–MS (*m/z*): positive mode 384 [M + H]⁺. Purity by HPLC–UV (254 nm)–ESI–MS: 98.8%.



8-(Carboxyformamido)-6-chloro-4-thioxo-4H-chromene-2-carboxylic acid (86a, LW236). The compound was synthesized using **74a** (62 mg, 0.12 mmol). The product was isolated as a brown solid (34 mg, 60% yield). ¹H NMR (500 MHz, DMSO-*d*₆) δ 7.66 (s, 1H, 3-H), 8.07 (d, *J* = 2.5 Hz, 1H, 7-H), 8.43 (d, *J* = 2.2 Hz, 1H, 5-H), 10.34 (s, 1H, NH). ¹³C NMR (126 MHz, DMSO-*d*₆) δ 121.9 (C-7), 124.9 (C-3), 126.2 (C-5), 129.5 (C-8), 131.4 (C-6), 131.6 (C-4a), 141.8 (C-8a), 143.4 (C-

2), 156.9 (CONH), 161.0 (CO₂H), 161.5 (CO₂H), 201.7 (C-4). LC–MS (*m/z*): positive mode 328 [M + H]⁺. Purity by HPLC–UV (254 nm)–ESI–MS: 95.6%. Mp: 231–232 °C dec.

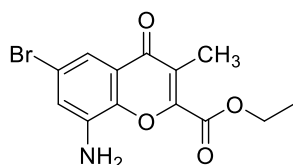
Preparation of 80 and 87



Ethyl 6-bromo-3-methyl-8-nitro-4-oxo-4H-chromene-2-carboxylate (79, LW318).

1-(5-Bromo-2-hydroxy-3-nitrophenyl)propan-1-one (2.0 g, 7.3 mmol) was dissolved in dry pyridine (15 mL) and ethoxalyl chloride (1.6 mL, 14.6 mmol, 2 equiv.) was added dropwise at rt. The mixture was refluxed for 6 h. After that, water (50 mL) was added, and the mixture was extracted with EtOAc (3 × 50 mL).

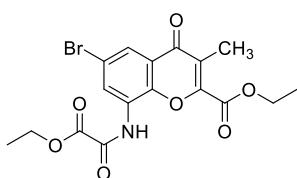
The organic layers were combined, washed with brine, dried over anhydrous Na₂SO₄, and concentrated under reduced pressure. The residue was purified by column chromatography on a column of silica gel (7:3 petroleum ether/EtOAc). The product was isolated as a yellow solid (953 mg, 37% yield). ¹H NMR (600 MHz, CDCl₃) δ 1.45 (t, *J* = 7.1 Hz, 3H, CH₂CH₃), 2.39 (s, 3H, ArCH₃), 4.47 (q, *J* = 7.1 Hz, 2H, CH₂CH₃), 8.46 (d, *J* = 2.5 Hz, 1H, 7-H), 8.57 (d, *J* = 2.5 Hz, 1H, 5-H). ¹³C NMR (151 MHz, CDCl₃) δ 10.1 (ArCH₃), 14.0 (CH₂CH₃), 63.0 (CH₂CH₃), 117.3 (C-3), 125.1 (C-4a), 125.5 (C-6), 133.2 (C-7), 134.3 (C-5), 139.1 (C-8), 146.5 (C-8a), 148.9 (C-2), 160.5 (CO₂Et), 175.8 (C-4). LC–MS (*m/z*): positive mode 356 [M + H]⁺. Purity by HPLC–UV (254 nm)–ESI–MS: 98.8%.



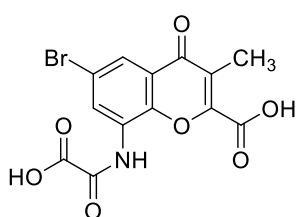
Ethyl 8-amino-6-bromo-3-methyl-4-oxo-4H-chromene-2-carboxylate (LW327).

The compound was synthesized using **79** (800 mg, 2.25 mmol) and was isolated as a yellow solid (705 mg, 96% yield). ¹H NMR (600 MHz, CDCl₃) δ 1.44 (t, *J* = 7.1 Hz, 3H, CH₂CH₃), 2.36 (s, 3H, ArCH₃), 4.46 (q, *J* = 7.1 Hz, 2H, CH₂CH₃), 7.10 (d, *J* = 1.9 Hz, 1H, 7-H), 7.61 (d, *J* = 1.8 Hz, 1H, 5-H). ¹³C NMR (151 MHz, CDCl₃) δ

10.3 (ArCH₃), 14.2 (CH₂CH₃), 62.6 (CH₂CH₃), 116.1 (C-7), 119.0 (C-3), 119.9 (C-5), 123.6 (C-4a), 124.5 (C-6), 137.7 (C-8), 143.1 (C-8a), 147.8 (C-2), 161.5 (CO₂Et), 177.8 (C-4). LC–MS (*m/z*): positive mode 326 [M + H]⁺. Purity by HPLC–UV (254 nm)–ESI–MS: 90.7%.

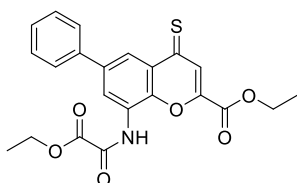


Ethyl 6-bromo-8-(2-ethoxy-2-oxoacetamido)-3-methyl-4-oxo-4H-chromene-2-carboxylate (80, LW328). The product was synthesized using **LW327** (80 mg, 0.25 mmol). The amide was isolated as a white solid (90 mg, 85% yield). $^1\text{H NMR}$ (600 MHz, CDCl_3) δ 1.46 (t, $J = 7.2$ Hz, 3H, CH_2CH_3), 1.51 (t, $J = 7.2$ Hz, 3H, CH_2CH_3), 2.42 (s, 3H, Ar CH_3), 4.45 – 4.51 (m, 4H, $2 \times \text{CH}_2\text{CH}_3$), 8.06 (d, $J = 2.3$ Hz, 1H, 7-H), 8.89 (d, $J = 2.3$ Hz, 1H, 5-H), 9.77 (s, 1H, NH). $^{13}\text{C NMR}$ (151 MHz, CDCl_3) δ 10.2 (Ar CH_3), 14.0 (CH_2CH_3), 14.0 (CH_2CH_3), 62.9 (CH_2CH_3), 64.1 (CH_2CH_3), 119.1 (C-3), 123.0 (C-4a), 123.6 (C-7), 125.9 (C-6), 126.3 (C-5), 127.4 (C-8), 143.7 (C-8a), 147.2 (C-2), 154.0 (CONH), 160.0 (CO_2Et), 160.8 (CO_2Et), 176.9 (C-4). LC–MS (m/z): positive mode 426 $[\text{M} + \text{H}]^+$. Purity by HPLC–UV (254 nm)–ESI-MS: 97.1%. Mp: 140–141 °C.

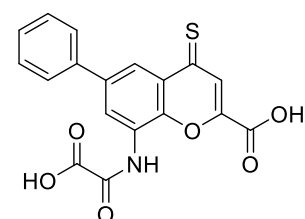


6-Bromo-8-(carboxyformamido)-3-methyl-4-oxo-4H-chromene-2-carboxylic acid (87, LW329). The compound was synthesized using **80** (60 mg, 0.14 mmol). The product was isolated as a white solid (47 mg, 90% yield). $^1\text{H NMR}$ (600 MHz, CDCl_3 , MeOD) δ 2.36 (s, 3H, CH_3), 8.02 (d, $J = 2.2$ Hz, 1H, 7-H), 8.81 (d, $J = 2.2$ Hz, 1H, 5-H). $^{13}\text{C NMR}$ (151 MHz, CDCl_3 , MeOD) δ 10.1 (CH_3), 118.8 (C-3), 123.0 (C-4a), 123.5 (C-7), 125.4 (C-6), 126.5 (C-5), 127.3 (C-8), 144.0 (C-8a), 148.2 (C-2), 155.5 (CONH), 160.9 (CO_2H), 162.6 (CO_2H), 177.4 (C-4). LC–MS (m/z): positive mode 370 $[\text{M} + \text{H}]^+$. Purity by HPLC–UV (254 nm)–ESI-MS: 98.8%. Mp: 243–244 °C dec.

Preparation of 86b



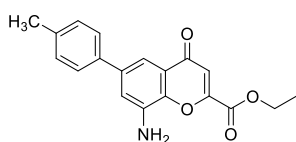
Ethyl 8-(2-ethoxy-2-oxoacetamido)-6-phenyl-4-thioxo-4H-chromene-2-carboxylate (78a, LW368). The compound was synthesized using **76a** (50 mg, 0.15 mmol). The amide was isolated as a green solid (48 mg, 75% yield). $^1\text{H NMR}$ (600 MHz, CDCl_3) δ 1.46 – 1.51 (m, 6H, $2 \times \text{CH}_2\text{CH}_3$), 4.45 – 4.53 (m, 4H, $2 \times \text{CH}_2\text{CH}_3$), 7.41 (t, $J = 7.4$ Hz, 1H, 4'-H), 7.49 (t, $J = 7.6$ Hz, 2H, 3'-H, 5'-H), 7.70 (d, $J = 7.3$ Hz, 2H, 2'-H, 6'-H), 7.85 (s, 1H, 5-H), 8.42 (d, $J = 2.1$ Hz, 1H, 3-H), 9.12 (d, $J = 2.1$ Hz, 1H, 7-H), 9.86 (s, 1H, NH). $^{13}\text{C NMR}$ (151 MHz, CDCl_3) δ 14.0 (CH_2CH_3), 14.1 (CH_2CH_3), 63.2 (CH_2CH_3), 64.1 (CH_2CH_3), 121.2 (C-7), 123.2 (C-3), 125.7 (C-5), 127.4 (C-8), 127.4 (C-2', C-6'), 128.4 (C-4'), 129.1 (C-3', C-5'), 131.1 (C-4a), 138.7 (C-1'), 140.2 (C-8a), 140.3 (C-6), 140.7 (C-2), 154.2 (CONH), 160.1 (CO_2Et), 160.8 (CO_2Et), 203.1 (C-4). LC–MS (m/z): positive mode 426 $[\text{M} + \text{H}]^+$. Purity by HPLC–UV (254 nm)–ESI-MS: 96.4%.



8-(Carboxyformamido)-6-phenyl-4-thioxo-4H-chromene-2-carboxylic acid (86b, LW372). The product was synthesized using **78a** (24 mg, 0.06 mmol). The product was isolated as a brown solid (21 mg, 99% yield). $^1\text{H NMR}$ (600 MHz, $\text{DMSO}-d_6$) δ 7.27 – 7.60 (m, 3H, 3-H, 2'-H, 6'-H), 7.66 (s, 3H, 3'-H, 4'-H, 5'-H), 8.30 (s, 1H, 7-H), 8.69 (s, 1H, 5-H), 10.38 (s, 1H, NH). $^{13}\text{C NMR}$ (151 MHz,

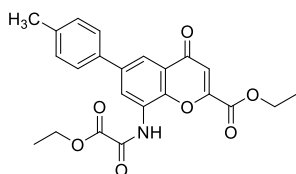
DMSO-*d*₆ δ 120.6 (C-7), 124.8 (C-3), 125.5 (C-5), 127.0 (C-2', C-6'), 128.4 (C-8), 128.6 (C-4'), 129.5 (C-3', C-5'), 130.9 (C-4a), 138.3 (C-1'), 138.7 (C-8a), 142.5 (C-6), 143.6 (C-2), 157.5 (CONH), 161.4 (CO₂Et), 161.7 (CO₂Et), 202.8 (C-4). LC–MS (*m/z*): positive mode 370 [M + H]⁺. Purity by HPLC–UV (254 nm)–ESI–MS: 96.4%. Mp: 250–251 °C dec.

Preparation of 85a



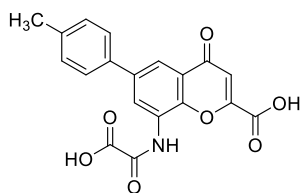
Ethyl 8-amino-4-oxo-6-(*p*-tolyl)-4*H*-chromene-2-carboxylate (75b, LW304).

The compound was synthesized using **71b** (1.0 g, 3.2 mmol) and potassium *p*-tolyltrifluoroborate (1.3 g, 6.4 mmol). The product was isolated as a yellow solid (842 mg, 81% yield). ¹H NMR (600 MHz, CDCl₃) δ 1.43 (t, *J* = 7.1 Hz, 3H, CH₂CH₃), 2.39 (s, 3H, ArCH₃), 4.46 (q, *J* = 7.1 Hz, 2H, CH₂CH₃), 7.10 (s, 1H, 3-H), 7.24 (d, *J* = 7.9 Hz, 2H, 3'-H, 5'-H), 7.28 (d, *J* = 2.0 Hz, 1H, 5-H), 7.51 (d, *J* = 8.1 Hz, 2H, 2'-H, 6'-H), 7.72 (d, *J* = 2.0 Hz, 1H, 7-H). ¹³C NMR (151 MHz, CDCl₃) δ 14.1 (CH₂CH₃), 21.1 (ArCH₃), 62.9 (CH₂CH₃), 111.6 (C-7), 114.4 (C-3), 117.1 (C-5), 124.9 (C-4a), 127.0 (C-2', C-6'), 129.6 (C-3', C-5'), 136.7 (C-8), 137.0 (C-1'), 137.7 (C-4'), 139.2 (C-8a), 144.0 (C-6), 151.2 (C-2), 160.5 (CO₂Et), 178.9 (C-4). LC–MS (*m/z*): positive mode 324 [M + H]⁺. Purity by HPLC–UV (254 nm)–ESI–MS: 95.9%.



Ethyl 8-(2-ethoxy-2-oxoacetamido)-4-oxo-6-(*p*-tolyl)-4*H*-chromene-2-carboxylate (77a, LW308).

The compound was synthesized using **75b** (50 mg, 0.15 mmol). The amide was isolated as a white solid (45 mg, 71% yield). ¹H NMR (600 MHz, CDCl₃) δ 1.44 – 1.56 (m, 6H, 2 × CH₂CH₃), 2.41 (s, 3H, ArCH₃), 4.42 – 4.56 (m, 4H, 2 × CH₂CH₃), 7.16 (s, 1H, 3-H), 7.28 (d, *J* = 8.0 Hz, 2H, 3'-H, 5'-H), 7.59 (d, *J* = 8.0 Hz, 2H, 2'-H, 6'-H), 8.15 (d, *J* = 2.1 Hz, 1H, 5-H), 9.08 (d, *J* = 2.1 Hz, 1H, 7-H), 9.83 (s, 1H, NH). ¹³C NMR (151 MHz, CDCl₃) δ 14.0 (CH₂CH₃), 14.0 (CH₂CH₃), 21.1 (ArCH₃), 63.2 (CH₂CH₃), 64.0 (CH₂CH₃), 114.8 (C-3), 118.3 (C-7), 123.0 (C-5), 124.3 (C-4a), 126.9 (C-8), 127.1 (C-2', C-6'), 129.8 (C-3', C-5'), 135.7 (C-1'), 138.3 (C-4'), 139.3 (C-8a), 144.7 (C-6), 151.1 (C-2), 154.2 (CONH), 159.9 (CO₂Et), 160.1 (CO₂Et), 177.7 (C-4). LC–MS (*m/z*): positive mode 424 [M + H]⁺. Purity by HPLC–UV (254 nm)–ESI–MS: 97.4%.

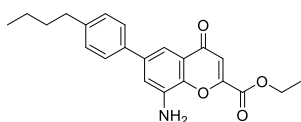


8-(Carboxyformamido)-4-oxo-6-(*p*-tolyl)-4*H*-chromene-2-carboxylic acid (85a, LW317).

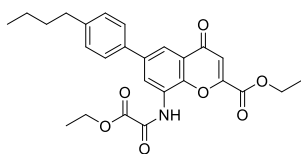
The compound was synthesized using **77a** (18 mg, 0.04 mmol). The product was isolated as a yellow solid (13 mg, 82% yield). ¹H NMR (500 MHz, DMSO-*d*₆) δ 2.36 (s, 3H, ArCH₃), 6.97 (s, 1H, 3-H), 7.33 (d, *J* = 8.1 Hz, 2H, 3'-H, 5'-H), 7.61 (d, *J* = 8.2 Hz, 2H, 2'-H, 6'-H), 8.02 (d, *J* = 2.3 Hz, 1H, 5-H), 8.57 (d, *J* = 2.2 Hz, 1H, 7-H), 10.38 (s, 1H, NH). ¹³C NMR (126 MHz, DMSO-*d*₆) δ 20.9 (ArCH₃), 113.6 (C-3), 118.1 (C-7), 124.6 (C-8), 125.7 (C-5), 126.9 (C-2', C-6'), 127.7 (C-4a), 130.1 (C-3', C-5'), 135.4 (C-1'), 137.7 (C-4'), 138.1

(C-8a), 147.0 (C-6), 153.0 (C-2), 157.0 (CONH), 161.3 (CO₂H), 161.4 8 (CO₂H), 177.5 (C-4). LC–MS (*m/z*): positive mode 368 [M + H]⁺. Purity by HPLC–UV (254 nm)–ESI-MS: 97.4%. Mp: 250–251 °C.

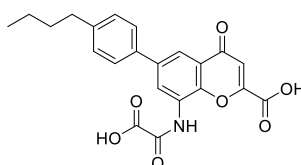
Preparation of 85b



Ethyl 8-amino-6-(4-butylphenyl)-4-oxo-4H-chromene-2-carboxylate (75c, LW415). The compound was synthesized using **71b** (500 mg, 1.6 mmol) and 4-butylboronic acid (570 mg, 3.2 mmol). The product isolated as a yellow solid (470 mg, 80% yield). ¹H NMR (600 MHz, CDCl₃) δ 0.95 (t, *J* = 7.4 Hz, 3H, ArCH₂CH₂CH₂CH₃), 1.35 – 1.40 (m, 2H, ArCH₂CH₂CH₂CH₃), 1.42 (t, *J* = 7.1 Hz, 3H, CO₂CH₂CH₃), 1.63 (p, *J* = 7.6 Hz, 2H, ArCH₂CH₂CH₂CH₃), 2.60 – 2.69 (m, 2H, ArCH₂CH₂CH₂CH₃), 4.43 (q, *J* = 7.1 Hz, 2H, CO₂CH₂CH₃), 7.09 (s, 1H, 3-H), 7.24 (d, *J* = 8.0 Hz, 2H, 3'-H, 5'-H), 7.33 (s, 1H, 5-H), 7.53 (d, *J* = 8.1 Hz, 2H, 2'-H, 6'-H), 7.75 (s, 1H, 7-H). ¹³C NMR (151 MHz, CDCl₃) δ 13.9 (CH₃), 14.1 (CH₃), 22.4 (ArCH₂CH₂CH₂CH₃), 33.5 (ArCH₂CH₂CH₂CH₃), 35.2 (ArCH₂CH₂CH₂CH₃), 62.9 (CO₂CH₂CH₃), 112.0 (C-7), 114.4 (C-3), 117.5 (C-5), 124.9 (C-4a), 126.9 (C-2', C-6'), 128.9 (C-3', C-5'), 136.4 (C-8), 136.8 (C-1'), 139.2 (C-8a), 142.8 (C-4'), 144.2 (C-6), 151.2 (C-2), 160.4 (CO₂Et), 178.8 (C-4). LC–MS (*m/z*): positive mode 366 [M + H]⁺. Purity by HPLC–UV (254 nm)–ESI-MS: 94.5%.



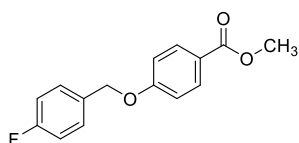
Ethyl 6-(4-butylphenyl)-8-(2-ethoxy-2-oxoacetamido)-4-oxo-4H-chromene-2-carboxylate (77b, LW416). The compound was synthesized using **75c** (100 mg, 0.27 mmol). The amide was isolated as a white solid (115 mg, 91% yield). ¹H NMR (600 MHz, CDCl₃) δ 0.94 (t, *J* = 7.4 Hz, 3H, ArCH₂CH₂CH₂CH₃), 1.38 (h, *J* = 7.3 Hz, 2H, ArCH₂CH₂CH₂CH₃), 1.43 – 1.52 (m, 6H, 2 × CO₂CH₂CH₃), 1.63 (p, *J* = 7.6 Hz, 2H, ArCH₂CH₂CH₂CH₃), 2.58 – 2.68 (m, 2H, ArCH₂CH₂CH₂CH₃), 4.38 – 4.55 (m, 4H, 2 × CO₂CH₂CH₃), 7.15 (s, 1H, 3-H), 7.28 (d, *J* = 8.0 Hz, 2H, 3'-H, 5'-H), 7.60 (d, *J* = 8.0 Hz, 2H, 2'-H, 6'-H), 8.14 (d, *J* = 2.0 Hz, 1H, 5-H), 9.07 (d, *J* = 2.0 Hz, 1H, 7-H), 9.81 (s, 1H, NH). ¹³C NMR (151 MHz, CDCl₃) δ 13.9 (CH₃), 14.0 (CH₃), 14.0 (CH₃), 22.3 (ArCH₂CH₂CH₂CH₃), 33.5 (ArCH₂CH₂CH₂CH₃), 35.3 (ArCH₂CH₂CH₂CH₃), 63.2 (CO₂CH₂CH₃), 64.0 (CO₂CH₂CH₃), 114.8 (C-3), 118.3 (C-7), 122.9 (C-5), 124.3 (C-4a), 126.9 (C-8), 127.1 (C-2', C-6'), 129.1 (C-3', C-5'), 135.8 (C-1'), 139.3 (C-8a), 143.4 (C-6), 144.6 (C-4'), 151.1 (C-2), 154.1 (CONH), 159.9 (CO₂Et), 160.0 (CO₂Et), 177.7 (C-4). LC–MS (*m/z*): positive mode 466 [M + H]⁺. Purity by HPLC–UV (254 nm)–ESI-MS: 96.1%.



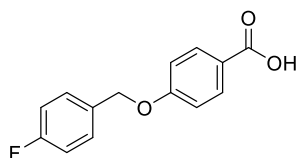
6-(4-Butylphenyl)-8-(carboxyformamido)-4-oxo-4H-chromene-2-carboxylic acid (85b, LW419). The compound was synthesized using **77b** (100 mg, 0.22 mmol). The product was isolated as a yellow solid (74 mg, 84% yield). ¹H NMR (600 MHz, DMSO-*d*₆) δ 0.90 (t, *J* = 7.4 Hz, 3H, ArCH₂CH₂CH₂CH₃), 1.32 (h, *J* = 7.4 Hz, 2H, ArCH₂CH₂CH₂CH₃), 1.58 (p, *J* = 7.6 Hz, 2H, ArCH₂CH₂CH₂CH₃), 2.62 (t, *J* = 7.7 Hz, 2H, ArCH₂CH₂CH₂CH₃), 6.96 (s, 1H, 3-H), 7.32 (d, *J* = 8.1 Hz, 2H, 3'-H, 5'-H), 7.61 (d, *J* = 8.1 Hz, 2H, 2'-H, 6'-H),

8.01 (d, $J = 2.2$ Hz, 1H, 5-H), 8.57 (d, $J = 2.0$ Hz, 1H, 7-H), 10.35 (s, 1H, NH). ^{13}C NMR (151 MHz, DMSO- d_6) δ 13.9 (ArCH₂CH₂CH₂CH₃), 21.9 (ArCH₂CH₂CH₂CH₃), 33.1 (ArCH₂CH₂CH₂CH₃), 34.6 (ArCH₂CH₂CH₂CH₃), 113.7 (C-3), 118.1 (C-7), 124.6 (C-4a), 125.6 (C-5), 126.9 (C-2', C-6'), 127.7 (C-8), 129.4 (C-3', C-5'), 135.6 (C-1'), 137.7 (C-8a), 142.9 (C-6), 146.9 (C-4'), 152.9 (C-2), 156.9 (CONH), 161.3 (CO₂H), 161.4 (CO₂H), 177.4 (C-4). LC-MS (m/z): positive mode 410 [M + H]⁺. Purity by HPLC-UV (254 nm)-ESI-MS: 98.8%. Mp: 250–251 °C.

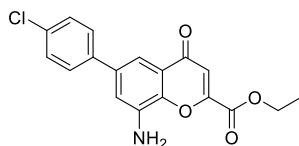
Preparation of 89b



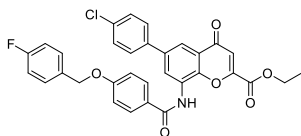
Methyl 4-((4-fluorobenzyl)oxy)benzoate (81a, LW351). The compound was synthesized using methyl 4-hydroxybenzoate (3.0 g, 20 mmol) and 4-fluorobenzylbromide (5.7 g, 30 mmol). The resulting solid was washed with water and cold ethanol. **81a** was isolated as a white solid (2.7 g, 55% yield). ^1H NMR (600 MHz, CDCl₃) δ 3.86 (s, 3H, CO₂CH₃), 5.05 (s, 2H, OCH₂), 6.93 – 6.98 (m, 2H, 3-H, 5-H), 7.04 – 7.09 (m, 2H, 3'-H, 5'-H), 7.36 – 7.41 (m, 2H, 2'-H, 6'-H), 7.96 – 8.00 (m, 2H, 2-H, 6-H). ^{13}C NMR (151 MHz, CDCl₃) δ 51.9 (CO₂CH₃), 69.4 (OCH₂), 114.4 (C-3, C-5), 115.6 (d, $J = 21.9$ Hz, C-3', C-5'), 122.9 (C-1), 129.4 (d, $J = 8.5$ Hz, C-2', C-6'), 131.6 (C-2, C-6), 132.0 (d, $J = 3.2$ Hz, C-1'), 162.2 (C-4), 162.6 (d, $J = 246.6$ Hz, C-4'), 166.7 (CO₂Me). LC-MS (m/z): positive mode 261 [M + H]⁺. Purity by HPLC-UV (254 nm)-ESI-MS: 97.9%.



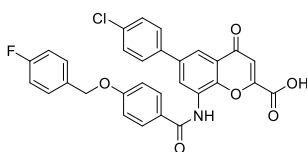
4-((4-Fluorobenzyl)oxy)benzoic acid (82a, LW352). The compound was synthesized using **81a** (2.7 g, 10.4 mmol) and was isolated as a white solid (2.55 g, 100% yield). ^1H NMR (600 MHz, DMSO- d_6) δ 5.13 (s, 2H, OCH₂), 6.94 – 7.08 (m, 2H, 3-H, 5-H), 7.16 – 7.28 (m, 2H, 3'-H, 5'-H), 7.41 – 7.57 (m, 2H, 2'-H, 6'-H), 7.82 – 7.93 (m, 2H, 2-H, 6-H). ^{13}C NMR (151 MHz, DMSO- d_6) δ 68.8 (OCH₂), 114.3 (C-3, C-5), 115.4 (d, $J = 21.7$ Hz, C-3', C-5'), 126.6 (C-1), 130.2 (d, $J = 8.6$ Hz, C-2', C-6'), 131.2 (C-2, C-6), 133.2 (d, $J = 3.0$ Hz, C-1'), 161.0 (C-4), 162.1 (d, $J = 244.0$ Hz, C-4'), 167.9 (CO₂H). LC-MS (m/z): positive mode 247 [M + H]⁺. Purity by HPLC-UV (254 nm)-ESI-MS: 98.8%.



Ethyl 8-amino-6-(4-chlorophenyl)-4-oxo-4H-chromen-2-carboxylate (75d, LW348N). The compound was synthesized using **71b** (3.0 g, 9.6 mmol) and 4-chlorophenylboronic acid (3.0 g, 19.2 mmol). The product was isolated as a yellow solid (1.68 g, 55% yield). ^1H NMR (600 MHz, CDCl₃) δ 1.41 (t, $J = 7.1$ Hz, 3H, CO₂CH₂CH₃), 4.43 (q, $J = 7.1$ Hz, 2H, CO₂CH₂CH₃), 7.07 (s, 1H, 3-H), 7.17 – 7.22 (m, 1H, 7-H), 7.34 – 7.39 (m, 2H, 3'-H, 5'-H), 7.45 – 7.52 (m, 2H, 2'-H, 6'-H), 7.60 – 7.65 (m, 1H, 5-H). ^{13}C NMR (151 MHz, CDCl₃) δ 14.1 (CO₂CH₂CH₃), 62.9 (CO₂CH₂CH₃), 111.6 (C-3), 114.4 (C-7), 116.7 (C-5), 124.9 (C-4a), 128.3 (C-3', C-5'), 129.0 (C-2', C-6'), 134.0 (C-6), 137.2 (C-4'), 137.9 (C-1'), 138.0 (C-8), 144.2 (C-8a), 151.3 (C-2), 160.4 (CO₂Et), 178.7 (C-4). LC-MS (m/z): positive mode 344 [M + H]⁺. Purity by HPLC-UV (254 nm)-ESI-MS: 94.1%.

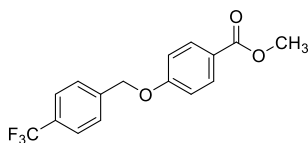


Ethyl 6-(4-chlorophenyl)-8-(4-((4-fluorobenzyl)oxy)benzamido)-4-oxo-4H-chromene-2-carboxylate (77c, LW439). To a mixture of **75d** (558 mg, 1.62 mmol) and **82a** (400 mg, 1.62 mmol, 1 equiv.) in anhydrous DCM (15 mL) was added Et₃N (680 μ L, 4.86 mmol, 3 equiv.) while stirring under inert gas atmosphere. Thionyl chloride (120 μ L, 1.62 mmol, 1 equiv.) was added at rt and the mixture was kept stirring for 72 h. After that, the mixture was dried, and the residue was purified by column chromatography on a column of silica gel (9:1 DCM/ethyl acetate). The product was isolated as a white solid (163 mg, 18% yield). No suitable solvent could be determined for NMR analysis. LC-MS (m/z): positive mode 572 [M + H]⁺. Purity by HPLC-UV (254 nm)-ESI-MS: not determined due to low solubility.

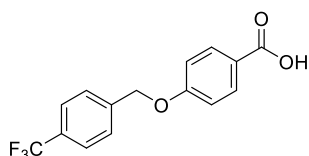


6-(4-Chlorophenyl)-8-(4-((4-fluorobenzyl)oxy)benzamido)-4-oxo-4H-chromene-2-carboxylic acid (89b, LW440). The compound was synthesized using **77c** (150 mg, 0.26 mmol) and was isolated as a slightly yellow solid (98 mg, 69% yield). ¹H NMR (600 MHz, DMSO-*d*₆) δ 5.20 (s, 2H, OCH₂), 6.98 (s, 1H, 3-H), 7.16 – 7.21 (m, 2H, 3''-H, 5''-H), 7.21 – 7.27 (m, 2H, 3'''-H, 5'''-H), 7.51 – 7.55 (m, 2H, 2''-H, 6'''-H), 7.55 – 7.59 (m, 2H, 3'-H, 5'-H), 7.78 – 7.83 (m, 2H, 2'-H, 6'-H), 8.01 – 8.05 (m, 2H, 2''-H, 6''-H), 8.09 (d, J = 2.3 Hz, 1H, 7-H), 8.41 (d, J = 2.2 Hz, 1H, 5-H), 10.19 (s, 1H, CONH). ¹³C NMR (151 MHz, DMSO-*d*₆) δ 68.9 (OCH₂), 113.6 (C-3), 114.8 (C-3'', C-5''), 115.5 (d, J = 21.1 Hz, C-3''', C-5'''), 118.6 (C-7), 124.7 (C-4a), 126.4 (C-1''), 128.9 (C-2'', C-6''), 129.0 (C-5), 129.3 (C-8), 129.4 (C-2', C-6'), 129.9 (C-3', C-5'), 130.3 (d, J = 8.0 Hz, C-2''', C-6'''), 133.0 (d, J = 3.0 Hz, C-1'''), 133.3 (C-6), 136.2 (C-4'), 137.2 (C-1'), 149.0 (C-8a), 153.1 (C-2), 161.3 (C-4''), 161.4 (CO₂H), 162.0 (d, J = 244.1 Hz, C-4'''), 165.1 (CONH), 177.5 (C-4). LC-MS (m/z): positive mode 544 [M + H]⁺. Purity by HPLC-UV (254 nm)-ESI-MS: 98.1%. Mp: 265–266 °C. (Lit. mp: 264 – 265 °C)¹

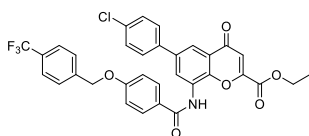
Preparation of 89c



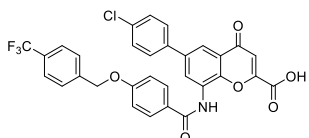
Methyl 4-((4-(trifluoromethyl)benzyl)oxy)benzoate (81b, LW477). The compound was synthesized using methyl 4-hydroxybenzoate (1.0 g, 6.6 mmol) and 4-fluorobenzylbromide (2.4 g, 9.9 mmol). The resulting solid was washed with water. **81b** was isolated as a white solid (2.04 g, 99% yield). ¹H NMR (600 MHz, CDCl₃) δ 3.89 (s, 3H, CO₂CH₃), 5.17 (s, 2H, OCH₂), 6.99 (d, J = 8.7 Hz, 2H, 3-H, 5-H), 7.55 (d, J = 8.0 Hz, 2H, 2'-H, 6'-H), 7.65 (d, J = 8.0 Hz, 2H, 3'-H, 5'-H), 8.01 (d, J = 8.7 Hz, 2H, 2-H, 6-H). ¹³C NMR (151 MHz, CDCl₃) δ 51.9 (CO₂CH₃), 69.1 (OCH₂), 114.4 (C-3, C-5), 123.2 (C-1), 124.0 (q, J = 271.5 Hz, C-F₃), 125.6 (q, J = 3.6 Hz, C-3', C-5'), 127.4 (C-2', C-6'), 130.3 (q, J = 32.3 Hz, C-4'), 131.7 (C-2, C-6), 140.3 (C-1'), 162.0 (C-4), 166.7 (CO₂Me). LC-MS (m/z): positive mode 311 [M + H]⁺. Purity by HPLC-UV (254 nm)-ESI-MS: 97.4%.



4-((4-(Trifluoromethyl)benzyl)oxy)benzoic acid (82b, LW478). The compound was synthesized from **81b** (1.0 g, 3.23 mmol) and isolated as a white solid (940 mg, 98 % yield). $^1\text{H NMR}$ (600 MHz, $\text{DMSO-}d_6$) δ 5.30 (s, 2H, OCH_2), 7.10 (d, $J = 8.8$ Hz, 2H, 3-H, 5-H), 7.67 (d, $J = 8.1$ Hz, 2H, 2'-H, 6'-H), 7.75 (d, $J = 8.2$ Hz, 2H, 3'-H, 5'-H), 7.90 (d, $J = 8.8$ Hz, 2H, 2-H, 6-H), 12.62 (br, 1H, CO_2H). $^{13}\text{C NMR}$ (151 MHz, $\text{DMSO-}d_6$) δ 68.7 (OCH_2), 114.8 (C-3, C-5), 123.6 (C-1), 124.4 (q, $J = 271.2$ Hz, CF_3), 125.5 (q, $J = 3.5$ Hz, C-3', C-5'), 128.2 (C-2', C-6'), 128.6 (q, $J = 31.7$ Hz, C-4'), 131.6 (C-2, C-6), 141.6 (C-1'), 161.8 (C-4), 167.1 (CO_2H). LC-MS (m/z): positive mode 297 [$\text{M} + \text{H}$] $^+$. Purity by HPLC-UV (254 nm)-ESI-MS: 98.4%.

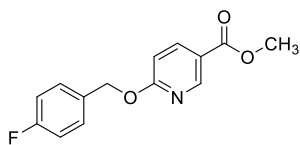


Ethyl 6-(4-chlorophenyl)-4-oxo-8-(4-((4-(trifluoromethyl)benzyl)oxy)benzamido)-4H-chromene-2-carboxylate (77d, LW479). **82b** (150 mg, 0.510 mmol) was mixed with thionyl chloride (5 mL) and refluxed for 2 h. After that, excess thionyl chloride was removed under reduced pressure, and the residue was dissolved in dry DCM (3 mL). This solution was added dropwise to a mixture of **75d** (117 mg, 0.340 mmol) and Et_3N (140 μL , 1.02 mmol) in dry THF (10 mL) under argon at 0 °C. After 1 h, stirring continued at rt for another 72 h. After that, the solvent was evaporated, and the residue was purified by column chromatography on a column of silica gel (3:1:1 DCM/petroleum ether/ EtOAc). **77d** was isolated as a white solid (100 mg, 47 % yield). $^1\text{H NMR}$ (600 MHz, $\text{DMF-}d_7$) δ 1.37 (t, $J = 7.1$ Hz, 3H, $\text{CO}_2\text{CH}_2\text{CH}_3$), 4.44 (q, $J = 7.1$ Hz, 2H, $\text{CO}_2\text{CH}_2\text{CH}_3$), 5.45 (s, 2H, OCH_2), 7.05 (s, 1H, 3-H), 7.26 – 7.34 (m, 2H, $2 \times \text{ArH}$), 7.64 (d, $J = 8.4$ Hz, 2H, $2 \times \text{ArH}$), 7.78 – 7.86 (m, 4H, $4 \times \text{ArH}$), 7.88 (d, $J = 8.5$ Hz, 2H, $2 \times \text{ArH}$), 8.14 (d, $J = 2.1$ Hz, 1H, 5-H), 8.20 (d, $J = 8.7$ Hz, 2H, $2 \times \text{ArH}$), 8.71 (d, $J = 2.0$ Hz, 1H, 7-H), 10.16 (s, 1H, NH). $^{13}\text{C NMR}$ (151 MHz, $\text{DMF-}d_7$) δ 14.1 (CH_2CH_3), 63.6 (CH_2CH_3), 69.6 (OCH_2), 114.5 (C-3), 115.5 (C-3'', C-5''), 118.7 (C-7), 124.3 (CF_3), 125.6 (C-4a), 126.2 (q, $J = 3.4$ Hz, C-3''', C-5'''), 127.5 (C-8), 128.1 (C-5), 128.9 (C-2', C-6'), 129.5 (C-2''', C-6'''), 129.6 (C-4'''), 130.0 (C-3', C-5'), 130.3 (C-1'''), 130.5 (C-2'', C-6''), 134.3 (C-4'), 137.5 (C-6), 138.4 (C-1'), 142.6 (C-1'''), 149.0 (C-8a), 152.7 (C-2), 160.7 (CO_2Et), 162.4 (C-4''), 165.7 (CONH), 177.9 (C-4). LC-MS (m/z): positive mode 622 [$\text{M} + \text{H}$] $^+$. Purity by HPLC-UV (254 nm)-ESI-MS: 97.7%.

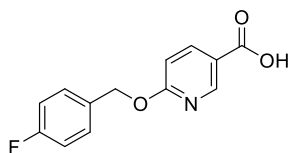


6-(4-Chlorophenyl)-4-oxo-8-(4-((4-(trifluoromethyl)benzyl)oxy)benzamido)-4H-chromene-2-carboxylic acid (89c, LW480). The compound was synthesized using **77d** (40 mg, 0.064 mmol) and isolated as a yellow solid (32 mg, 84% yield). $^1\text{H NMR}$ (600 MHz, $\text{DMSO-}d_6$) δ 5.35 (s, 2H, OCH_2), 6.97 (s, 1H, 3-H), 7.20 (d, $J = 8.2$ Hz, 2H, 3''-H, 5''-H), 7.55 (d, $J = 8.0$ Hz, 2H, 3'''-H, 5'''-H), 7.70 (d, $J = 7.5$ Hz, 2H, 3'-H, 5'-H), 7.78 (d, $J = 7.3$ Hz, 4H, 2'-H, 6'-H, 2'''-H, 6'''-H), 8.04 (d, $J = 8.2$ Hz, 2H, 2''-H, 6''-H), 8.07 (s, 1H, 5-H), 8.41 (s, 1H, 7-H), 10.18 (s, 1H, NH). $^{13}\text{C NMR}$ (151 MHz, $\text{DMSO-}d_6$) δ 68.7 (OCH_2), 113.6 (C-3), 114.9 (C-3'', C-5''), 118.6 (C-7), 124.2 (q, $J = 272.1$ Hz, CF_3), 124.7 (C-4a), 125.6 (C-3''', C-5'''), 126.6 (C-8), 128.3 (C-5, C-2', C-6'), 128.4 – 129.1 (m, C-4'''), 128.8 (C-2'', C-6''), 129.3 (C-1'''), 129.3 (C-3', C-5'), 129.9 (C-2'', C-6''), 133.3 (C-4'), 136.2 (C-6), 137.1 (C-1'), 141.7 (C-1'''), 149.0 (C-8a), 153.1 (C-2), 161.2 (C-4''), 161.3 (CO_2H), 165.1 (CONH), 177.5 (C-4). LC-MS (m/z): positive mode 594 [$\text{M} + \text{H}$] $^+$. Purity by HPLC-UV (254 nm)-ESI-MS: 97.1 %. Mp: 282–283 °C.

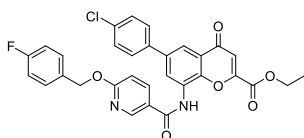
Preparation of 89g



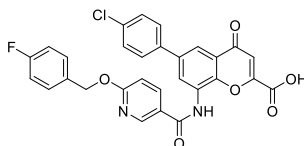
Methyl 6-((4-fluorobenzyl)oxy)nicotinate (81d, LW519). The product was synthesized using methyl 6-hydroxynicotinate (1.5 g, 9.8 mmol) and 4-fluorobenzylbromide (1.8 mL, 14.7 mmol). The product was isolated as a white solid (2.32 g, 91% yield). ^1H NMR (600 MHz, $\text{DMSO-}d_6$) δ 3.77 (s, 3H, CO_2CH_3), 5.18 (s, 2H, OCH_2), 6.46 (d, $J = 9.5$ Hz, 1H, 5-H), 7.03 – 7.24 (m, 2H, 3'-H, 5'-H), 7.26 – 7.50 (m, 2H, 2'-H, 6'-H), 7.79 (dd, $J = 2.6, 9.5$ Hz, 1H, 4-H), 8.66 (d, $J = 2.5$ Hz, 1H, 2-H). ^{13}C NMR (151 MHz, $\text{DMSO-}d_6$) δ 51.2 (OCH_2), 52.0 (CO_2CH_3), 108.9 (C-3), 115.6 (d, $J = 21.6$ Hz, C-3', C-5'), 119.3 (C-5), 130.3 (d, $J = 8.3$ Hz, C-2', C-6'), 133.1 (d, $J = 3.1$ Hz, C-1'), 138.7 (C-4), 144.3 (C-2), 161.5 (C-6), 161.6 (d, $J = 243.8$ Hz, C-4'), 164.4 (CO_2Me). ^{19}F NMR (565 MHz, $\text{DMSO-}d_6$) δ -114.5. LC-MS (m/z): positive mode 262 [$\text{M} + \text{H}$] $^+$. Purity by HPLC-UV (254 nm)-ESI-MS: 99.1%.



6-((4-Fluorobenzyl)oxy)nicotinic acid (82d, LW520). 81d (1.0 g, 3.83 mmol) was mixed with aq NaOH solution (10%, 15 mL) and refluxed for 1 h. After that, the mixture was cooled to rt and acidified using concd. aq HCl. The precipitate was collected by filtration, washed with water (20 mL), and dried at 60°C. The product was isolated as a white solid (890 mg, 94% yield). ^1H NMR (600 MHz, $\text{DMSO-}d_6$) δ 5.16 (s, 2H, OCH_2), 6.44 (d, $J = 9.5$ Hz, 1H, 5-H), 7.08 – 7.22 (m, 2H, 3'-H, 5'-H), 7.33 – 7.45 (m, 2H, 2'-H, 6'-H), 7.78 (dd, $J = 2.5, 9.5$ Hz, 1H, 4-H), 8.58 (d, $J = 2.5$ Hz, 1H, 2-H), 12.85 (br, 1H, CO_2H). ^{13}C NMR (151 MHz, $\text{DMSO-}d_6$) δ 51.1 (OCH_2), 109.8 (C-3), 115.5 (d, $J = 21.4$ Hz, C-3', C-5'), 119.1 (C-5), 130.3 (d, $J = 8.6$ Hz, C-2', C-6'), 133.2 (d, $J = 2.9$ Hz, C-1'), 139.1 (C-4), 144.1 (C-2), 161.6 (C-6), 161.9 (d, $J = 244.0$ Hz, C-4'), 165.4 (CO_2H). ^{19}F NMR (565 MHz, $\text{DMSO-}d_6$) δ -114.6. LC-MS (m/z): positive mode 248 [$\text{M} + \text{H}$] $^+$. Purity by HPLC-UV (254 nm)-ESI-MS: 98.1%.



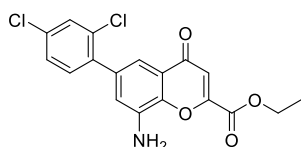
Ethyl 6-(4-chlorophenyl)-8-(6-((4-fluorobenzyl)oxy)nicotinamido)-4-oxo-4H-chromene-2-carboxylate (77h, LW521). LW520 (245 mg, 0.989 mmol) was mixed with dry DCM and thionyl chloride (1.4 mL, 19.8 mmol) and refluxed for 2 h. After that, excess thionyl chloride was removed under reduced pressure, and the residue was dissolved in dry DCM (3 mL). This solution was added dropwise to a mixture of 75d (170 mg, 0.495 mmol) and Et_3N (345 μL , 2.48 mmol) in dry THF (10 mL) under argon at 0 °C. After 1 h, stirring continued at rt for another 24 h. After that, the solvent was evaporated, and the residue was purified by column chromatography on a column of silica gel (8:2 DCM/EtOAc). 77h was isolated as a white solid (150 mg, 53% yield). No suitable solvent found for NMR analysis. LC-MS (m/z): positive mode 573 [$\text{M} + \text{H}$] $^+$. Purity by HPLC-UV (254 nm)-ESI-MS: 99.6%.



6-(4-Chlorophenyl)-8-(6-((4-fluorobenzyl)oxy)nicotinamido)-4-oxo-4H-chromene-2-carboxylic acid (89g, LW522). The compound was synthesized using 77h (76 mg, 0.133 mmol) and isolated as a slightly yellow solid (57 mg, 79% yield). ^1H NMR (600 MHz, $\text{DMSO-}d_6$) δ 5.19 (s, 2H, OCH_2), 6.56 (d, $J = 9.5$ Hz, 1H, 5'-H),

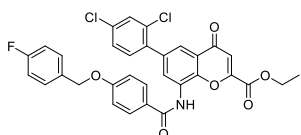
6.97 (s, 1H, 3-H), 7.16 – 7.23 (m, 2H, 3'''-H, 5'''-H), 7.42 – 7.47 (m, 2H, 2'''-H, 6'''-H), 7.53 – 7.59 (m, 2H, 3'-H, 5'-H), 7.75 – 7.81 (m, 2H, 2'-H, 6'-H), 8.03 (dd, $J = 2.6, 9.5$ Hz, 1H, 4''-H), 8.10 (d, $J = 2.3$ Hz, 1H, 7-H), 8.33 (d, $J = 2.3$ Hz, 1H, 5-H), 8.72 (d, $J = 2.5$ Hz, 1H, 2''-H), 10.24 (s, 1H, CONH). ^{13}C NMR (151 MHz, DMSO- d_6) δ 51.6 (OCH₂), 112.6 (C-4a), 113.5 (C-3), 115.6 (d, $J = 21.8$ Hz, C-3''', C-5'''), 118.9 (C-7), 119.1 (C-5''), 124.8 (C-8), 128.8 (C-2', C-6', C-5), 128.9 (C-3''), 129.4 (C-3', C-5'), 130.4 (d, $J = 8.1$ Hz, C-2''', C-6'''), 133.1 (d, $J = 3.0$ Hz, C-1'''), 133.4 (C-4'), 136.2 (C-1'), 137.1 (C-8a), 138.2 (C-4''), 142.5 (C-2''), 149.1 (C-6), 153.5 (C-2), 161.3 (CO₂H), 161.4 (C-6''), 161.9 (d, $J = 243.8$ Hz, C-4'''), 162.9 (CONH), 177.5 (C-4). ^{19}F NMR (565 MHz, DMSO- d_6) δ -114.5. LC-MS (m/z): positive mode 545 [M + H]⁺. Purity by HPLC-UV (254 nm)-ESI-MS: 96.3 %. Mp: >300 °C.

Preparation of 89d



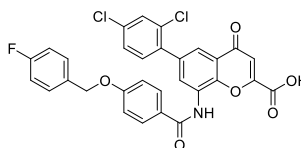
Ethyl 8-amino-6-(2,4-dichlorophenyl)-4-oxo-4H-chromen-2-carboxylate (89d, LW392). The compound was synthesized using **71b** (500 mg, 1.6 mmol) and 2,4-dichlorophenylboronic acid (610 mg, 3.2 mmol). The product was isolated as a yellow solid (480 mg, 80% yield). ^1H NMR (600 MHz, DMSO- d_6) δ 1.36 (t, $J = 7.1$

Hz, 3H, CO₂CH₂CH₃), 4.40 (q, $J = 7.0$ Hz, 2H, CO₂CH₂CH₃), 5.70 (s, 2H, NH₂), 6.91 (s, 1H, 3-H), 7.14 (s, 2H, 7-H, 3'-H), 7.43 (d, $J = 8.2$ Hz, 1H, 6'-H), 7.49 (d, $J = 8.1$ Hz, 1H, 5'-H), 7.71 (s, 1H, 5-H). ^{13}C NMR (151 MHz, DMSO- d_6) δ 14.0 (CO₂CH₂CH₃), 62.8 (CO₂CH₂CH₃), 111.0 (C-3), 113.4 (C-7), 118.4 (C-5), 124.2 (C-4a), 127.9 (C-5'), 129.4 (C-6'), 132.4 (C-2'), 132.7 (C-3'), 133.3 (C-4'), 135.7 (C-8), 138.2 (C-1'), 138.8 (C-6), 143.5 (C-8a), 151.8 (C-2), 160.2 (CO₂Et), 177.7 (C-4). LC-MS (m/z): positive mode 378 [M + H]⁺. Purity by HPLC-UV (254 nm)-ESI-MS: 91.3%.



Ethyl 6-(2,4-dichlorophenyl)-8-(4-((4-fluorobenzyl)oxy)benzamido)-4-oxo-4H-chromene-2-carboxylate (77e, LW399). **82a** (148 mg, 0.60 mmol) was mixed with dry toluene and thionyl chloride (67 μL , 0.90 mmol) and refluxed for 2 h. After that,

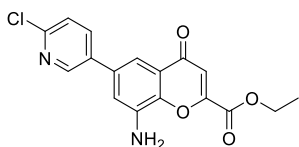
excess thionyl chloride was removed under reduced pressure, and the residue was dissolved in dry toluene (3 mL). This solution was added dropwise to a mixture of **75e** (200 mg, 0.53 mmol), DIPEA (270 μL , 1.6 mmol), and dry THF (5 mL) at 0°C under inert gas atmosphere. The mixture was stirred at that temperature for 1 h. After that, stirring continued at rt for 24 h. Then, the solvents were evaporated under reduced pressure, and the residue was purified by column chromatography on a column of silica gel (8:2 DCM/EtOAc). **77e** was isolated as a white solid (100 mg, 31 % yield). No suitable solvent could be determined for NMR analysis. LC-MS (m/z): negative mode 604 [M + H]⁺; positive mode 606 [M + H]⁺. Purity by HPLC-UV (254 nm)-ESI-MS: 90.0 %.



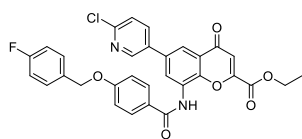
6-(2,4-Dichlorophenyl)-8-(4-((4-fluorobenzyl)oxy)benzamido)-4-oxo-4H-chromene-2-carboxylic acid (89d, LW404). The compound was synthesized using **77e** (81 mg, 0.13 mmol) and isolated as a yellow solid (60 mg, 80% yield). ^1H NMR (500 MHz, DMSO- d_6) δ 5.20 (s, 2H), 6.98 (s, 1H), 7.16 – 7.19 (m, 2H),

7.20 – 7.25 (m, 2H), 7.51 – 7.55 (m, 2H), 7.56 (s, 2H), 7.78 (s, 1H), 7.88 (d, $J = 1.8$ Hz, 1H), 7.98 – 8.04 (m, 2H), 8.19 (d, $J = 2.0$ Hz, 2H), 10.18 (s, 1H). ^{13}C NMR (126 MHz, DMSO- d_6) δ 69.0, 113.7, 114.9, 115.5 (d, $J = 21.3$ Hz), 121.6, 124.2, 125.1, 126.3, 128.2, 128.7, 129.7, 129.9, 130.3 (d, $J = 8.3$ Hz), 131.0, 132.5, 133.0, 133.0, 133.9, 134.9, 137.0, 148.9, 153.3, 161.4, 161.5, 162.2 (d, $J = 243.9$ Hz), 165.1, 177.5. (Low solubility.) LC–MS (m/z): positive mode 578 $[\text{M} + \text{H}]^+$. Purity by HPLC–UV (254 nm)–ESI–MS: 96.1%. Mp: 253–254 °C.

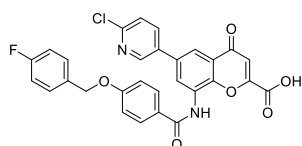
Preparation of 89e



Ethyl 8-amino-6-(6-chloropyridin-3-yl)-4-oxo-4H-chromen-2-carboxylate (75f, LW413). The compound was synthesized using **71b** (1.2 g, 3.85 mmol) and 6-chloro-3-pyridinylboronic acid (1.2 g, 7.7 mmol). The product was isolated as a yellow solid (392 mg, 30% yield). ^1H NMR (600 MHz, CDCl_3) δ 1.43 (t, $J = 7.0$ Hz, 3H, $\text{CO}_2\text{CH}_2\text{CH}_3$), 4.47 (q, $J = 6.9$ Hz, 2H, $\text{CO}_2\text{CH}_2\text{CH}_3$), 7.11 (s, 1H, 3-H), 7.20 (s, 1H, 7-H), 7.39 (d, $J = 8.2$ Hz, 1H, 3'-H), 7.64 (s, 1H, 5-H), 7.87 (d, $J = 6.3$ Hz, 1H, 4'-H), 8.60 (s, 1H, 6'-H). ^{13}C NMR (151 MHz, CDCl_3) δ 14.1 ($\text{CO}_2\text{CH}_2\text{CH}_3$), 63.0 ($\text{CO}_2\text{CH}_2\text{CH}_3$), 111.8 (C-3), 114.5 (C-7), 116.2 (C-3'), 124.3 (C-5), 125.1 (C-4a), 134.3 (C-5'), 134.5 (C-8), 137.2 (C-4'), 137.7 (C-6), 144.5 (C-8a), 147.8 (C-6'), 150.9 (C-2'), 151.4 (C-2), 160.3 (CO_2Et), 178.4 (C-4). LC–MS (m/z): positive mode 345 $[\text{M} + \text{H}]^+$. Purity by HPLC–UV (254 nm)–ESI–MS: 95.4%.



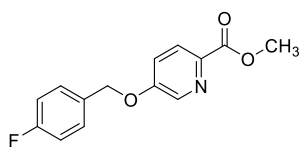
Ethyl 6-(6-chloropyridin-3-yl)-8-((4-fluorobenzyl)oxy)benzamido)-4-oxo-4H-chromene-2-carboxylate (77f, LW432). **82a** (492 mg, 2.0 mmol) was mixed with dry toluene and thionyl chloride (443 μL , 6.0 mmol), and DMF (5 drops), and the mixture was refluxed for 3 h. After that, excess thionyl chloride was removed under reduced pressure, and the residue was dissolved in dry DCM (3 mL). This solution was added dropwise to a mixture of **75f** (350 mg, 1.0 mmol), DIPEA (520 μL , 3.0 mmol), and dry THF (10 mL) at 0°C under inert gas atmosphere. The mixture was stirred at that temperature for 1 h. After that, stirring continued at rt for 24 h. Then, the solvents were evaporated under reduced pressure, and the residue was purified by column chromatography on a column of silica gel (8:2 DCM/EtOAc). **77f** was isolated as a yellow solid (75 mg, 13% yield). No suitable solvent could be determined for NMR or LC–MS analysis.



6-(6-Chloropyridin-3-yl)-8-((4-fluorobenzyl)oxy)benzamido)-4-oxo-4H-chromene-2-carboxylic acid (89e, LW435B). The compound was synthesized using **77f** (45 mg, 0.078 mmol) and isolated as a yellow solid (19 mg, 45% yield). ^1H NMR (600 MHz, DMSO- d_6) δ 5.20 (s, 2H, OCH_2), 6.99 (s, 1H, 3-H), 7.18 (d, $J = 8.8$ Hz, 2H, 3'''-H, 5'''-H), 7.21 – 7.26 (m, 2H, 2'''-H, 6'''-H), 7.51 – 7.56 (m, 2H, 3''-H, 5''-H), 7.65 (d, $J = 8.3$ Hz, 1H, 5'-H), 8.04 (d, $J = 8.5$ Hz, 2H, 2''-H, 6''-H), 8.16 (d, $J = 2.2$ Hz, 1H, 7-H), 8.27 (dd, $J = 2.6, 8.3$ Hz, 1H, 4'-H), 8.44 (d, $J = 2.2$ Hz, 1H, 5-H), 8.82 (d, $J = 2.6$ Hz, 1H, 2'-H), 10.27 (s, 1H, CONH). ^{13}C NMR (151 MHz, DMSO- d_6) δ 68.9 (OCH_2), 113.6 (C-3), 114.8 (C-3', C-5'), 115.5 (d, $J = 21.2$ Hz, C-3''', C-5'''), 119.4 (C-7), 124.7 (C-5'), 124.8 (C-4a), 126.3 (C-8), 129.3 (C-5), 129.6 (C-1''), 129.9 (C-2', C-6'), 130.3 (d, $J = 8.6$ Hz, C-2''', C-6'''), 133.0

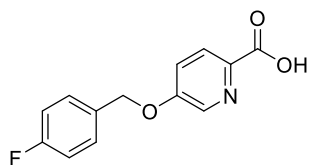
(d, $J = 2.9$ Hz, C-1'''), 133.2 (C-3'), 133.5 (C-6), 138.3 (C-4'), 148.2 (C-2'), 149.5 (C-8a), 150.1 (C-2), 153.3 (C-6'), 161.3 (CO₂H), 161.4 (C-4''), 162.1 (d, $J = 244.0$ Hz, C-4'''), 165.1 (CONH), 177.5 (C-4). LC-MS (m/z): positive mode 545 [M + H]⁺. Purity by HPLC-UV (254 nm)-ESI-MS: 96.7 %. Mp: 290-291 °C.

Preparation of 89f



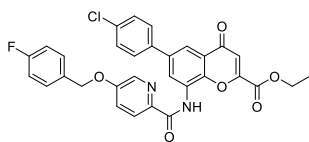
Methyl 5-((4-fluorobenzyl)oxy)picolinate (81c, LW390N). The compound was synthesized using methyl 5-hydroxypicolinate (300 mg, 1.96 mmol) and 4-fluorobenzylbromide (360 μ L, 2.94 mmol). The resulting solid was washed with water and cold ethanol. **81c** was isolated as a white solid (425 mg, 83 % yield). ¹H

NMR (600 MHz, CDCl₃) δ 3.97 (s, 3H, CO₂CH₃), 5.12 (s, 2H, OCH₂), 7.03 – 7.13 (m, 2H, 3'-H, 5'-H), 7.32 (dd, $J = 2.8, 8.7$ Hz, 1H, 4-H), 7.37 – 7.43 (m, 2H, 2'-H, 6'-H), 8.10 (d, $J = 8.7$ Hz, 1H, 3-H), 8.45 (d, $J = 2.7$ Hz, 1H, 6-H). ¹³C NMR (151 MHz, CDCl₃) δ 52.7 (CO₂CH₃), 69.9 (OCH₂), 115.8 (d, $J = 21.3$ Hz, C-3', C-5'), 121.1 (C-3), 126.5 (C-4), 129.5 (d, $J = 8.7$ Hz, C-2', C-6'), 131.0 (d, $J = 3.2$ Hz, C-1'), 138.4 (C-6), 140.3 (C-2), 157.2 (C-5), 162.9 (d, $J = 247.5$ Hz, C-4'), 165.1 (CO₂Me). LC-MS (m/z): positive mode 262 [M + H]⁺. Purity by HPLC-UV (254 nm)-ESI-MS: 99.0 %.



5-((4-Fluorobenzyl)oxy)picolinic acid (82c, LW433). **81c** (570 mg, 2.18 mmol) was mixed with methanol (20 mL) and a solution of K₂CO₃ (906 mg, 6.55 mmol, 3 equiv.) in water (10 mL). The mixture was heated to 70°C for 30 min. After that, methanol was evaporated and the mixture acidified with concd. aq HCl. The precipitate was collected by filtration, washed with water, and dried at 50°C for overnight. **82c** was isolated as a white solid (375 mg, 70 % yield). ¹H

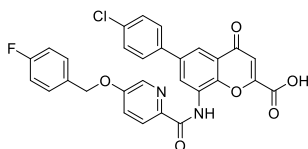
NMR (600 MHz, DMSO-*d*₆) δ 5.23 (s, 2H, OCH₂), 7.22 (t, $J = 8.8$ Hz, 2H, 3'-H, 5'-H), 7.53 (dd, $J = 5.8, 8.1$ Hz, 2H, 2'-H, 6'-H), 7.56 (dd, $J = 2.7, 8.7$ Hz, 1H, 4-H), 8.02 (d, $J = 8.7$ Hz, 1H, 3-H), 8.41 (d, $J = 2.5$ Hz, 1H, 6-H). ¹³C NMR (151 MHz, DMSO-*d*₆) δ 69.4 (OCH₂), 115.6 (d, $J = 21.3$ Hz, C-3', C-5'), 121.4 (C-3), 126.3 (C-4), 130.5 (d, $J = 8.1$ Hz, C-2', C-6'), 132.4 (d, $J = 3.0$ Hz, C-1'), 138.3 (C-6), 141.2 (C-2), 156.9 (C-5), 162.2 (d, $J = 244.3$ Hz, C-4'), 166.0 (CO₂H). LC-MS (m/z): positive mode 248 [M + H]⁺. Purity by HPLC-UV (254 nm)-ESI-MS: 80.8 %.



Ethyl 6-(4-chlorophenyl)-8-(5-((4-fluorobenzyl)oxy)picolinamido)-4-oxo-4H-chromene-2-carboxylate (77g, LW437). **75d** (100 mg, 0.29 mmol), **82c** (72 mg, 0.29 mmol, 1 equiv.), and Et₃N (121 μ L, 0.87 mmol, 3 equiv.) were mixed with 10 mL of dry DCM under argon atmosphere. Thionyl chloride (20 μ L, 0.29 mmol, 1

equiv.) was added at rt. The mixture was stirred for overnight at this temperature. After that, the solvent was evaporated, and the residue was purified by column chromatography (8:2 DCM/EtOAc). **77g** was isolated as a greenish solid (49 mg, 31 % yield). ¹H NMR (600 MHz, CDCl₃) δ 1.38 – 1.67 (m, 3H), 4.33 – 4.64 (m, 2H), 5.12 (s, 2H), 7.05 – 7.18 (m, 2H), 7.31 – 7.40 (m, 2H), 7.42 (s, 2H), 7.61 (s, 2H), 7.96 (s, 1H), 8.18 (s, 1H), 8.28 (s, 1H), 9.22 (s, 1H), 10.68 (s, 1H). Resolution too low for assignment. ¹³C NMR (151 MHz, CDCl₃) δ 14.1 (CO₂CH₂CH₃), 63.0 (CO₂CH₂CH₃), 69.9 (OCH₂), 114.6 (C-3), 115.8 (d, $J = 21.7$ Hz, C-3''', C-5'''), 116.6 (C-7),

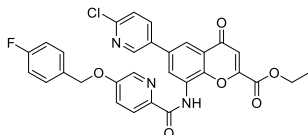
121.3 (C-5), 122.0 (C-3"), 123.8 (C-4"), 124.2 (C-4a), 128.4 (C-2', C-6'), 128.8 (C-4'), 129.0 (C-3', C-5'), 129.5 (d, $J = 8.5$ Hz, C-2"', C-6"',), 131.0 (C-1'''), 134.2 (C-8), 137.3 (C-6''), 137.4 (C-1'), 137.6 (C-8a), 141.9 (C-2''), 145.0 (C-6), 151.2 (C-2), 157.4 (C-5''), 160.0 ($\underline{\text{CONH}}$), 162.2 ($\underline{\text{CO}_2\text{Et}}$), 162.8 (d, $J = 247.5$ Hz, C-4'''), 177.7 (C-4). LC-MS (m/z): positive mode 573 [$\text{M} + \text{H}$]⁺. Purity by HPLC–UV (254 nm)–ESI-MS: 98.2 %.



6-(4-Chlorophenyl)-8-(5-((4-fluorobenzyl)oxy)picolinamido)-4-oxo-4H-chromene-2-carboxylic acid (89f, LW453, PSB-19453). The compound was synthesized using **77g** (30 mg, 0.05 mmol) and isolated as a yellow solid (18 mg, 64 % yield).

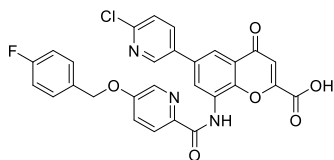
¹H NMR (600 MHz, DMSO-*d*₆) δ 5.29 (s, 2H, $\underline{\text{OCH}_2}$), 6.96 (s, 1H, ArH), 7.26 (s, 2H, 2 \times ArH), 7.57 (s, 4H, 4 \times ArH), 7.74 (s, 3H, 3 \times ArH), 7.92 (s, 1H, ArH), 8.17 (s, 1H, ArH), 8.40 (s, 1H, ArH), 8.99 (s, 1H, ArH), 10.65 (s, 1H, $\underline{\text{NH}}$). ¹³C NMR (151 MHz, DMSO-*d*₆) δ 69.6 ($\underline{\text{OCH}_2}$), 113.7 (C-3), 115.6 (d, $J = 21.5$ Hz, C-3''', C-5'''), 116.6 (C-7), 122.6 (C-4''), 122.8 (C-3''), 124.0 (C-5), 124.3 (C-4a), 128.8 (C-2', C-6'), 128.9 (C-8), 129.4 (C-3', C-5'), 130.5 (d, $J = 8.2$ Hz, C-2''', C-6'''), 132.3 (C-1'''), 133.3 (C-6), 136.4 (C-4'), 137.3 (C-6''), 137.5 (C-1'), 141.4 (C-2''), 146.1 (C-8a), 152.8 (C-5''), 157.6 (C-2), 161.2 ($\underline{\text{CONH}}$), 162.1 ($\underline{\text{CO}_2\text{H}}$), 162.1 (d, $J = 244.6$ Hz, C-4'''), 177.4 (C-4). LC–MS (m/z): positive mode 545 [$\text{M} + \text{H}$]⁺. Purity by HPLC–UV (254 nm)–ESI-MS: 97.7 %. Mp: 246–247 °C.

Preparation of 89h



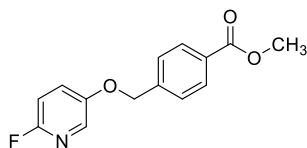
Ethyl 6-(6-chloropyridin-3-yl)-8-(5-((4-fluorobenzyl)oxy)picolinamido)-4-oxo-4H-chromene-2-carboxylate (77i, LW497). **82c** (329 mg, 1.33 mmol) was mixed with dry DCM (20 mL), and thionyl chloride (950 μL , 13.3 mmol) was added. The mixture was refluxed for 2 h. After that, the solvent and excess SOCl_2

were evaporated, and a cooled solution of **75** (230 mg, 0.667 mmol) and DIPEA (580 μL , 3.34 mmol) in dry THF (10 mL) was added dropwise to the residue, while stirring at 0°C under inert gas atmosphere. The mixture was kept at this temperature for 1 h. After that, stirring continued at rt for overnight. Then, the solvents were removed under reduced pressure and the residue was purified by column chromatography on a column of silica gel (8:1:1 DCM/petroleum ether/EtOAc). **77i** was isolated as a white solid (150 mg, 39 % yield). ¹H NMR (600 MHz, CDCl_3) δ 1.52 (t, $J = 7.1$ Hz, 3H, $\text{CO}_2\text{CH}_2\text{CH}_3$), 4.52 (q, $J = 7.1$ Hz, 2H, $\text{CO}_2\text{CH}_2\text{CH}_3$), 5.17 (s, 2H, $\underline{\text{OCH}_2}$), 7.12 (t, $J = 8.5$ Hz, 2H, 3'''-H, 5'''-H), 7.18 (s, 1H, 3-H), 7.37 – 7.49 (m, 4H, 7-H, 5'-H, 2'''-H, 6'''-H), 7.97 (dd, $J = 2.2, 8.2$ Hz, 1H, 4''-H), 8.02 – 8.07 (m, 1H, 5-H), 8.24 (d, $J = 8.6$ Hz, 1H, 4'-H), 8.38 (d, $J = 2.1$ Hz, 1H, 6''-H), 8.68 – 8.79 (m, 1H, 3''-H), 9.27 (s, 1H, 2'-H), 10.82 (s, 1H, $\underline{\text{CONH}}$). ¹³C NMR (151 MHz, CDCl_3) δ 14.1 ($\text{CO}_2\text{CH}_2\text{CH}_3$), 63.2 ($\text{CO}_2\text{CH}_2\text{CH}_3$), 70.0 ($\underline{\text{OCH}_2}$), 114.9 (C-3), 115.8 (d, $J = 21.9$ Hz, C-3''', C-5'''), 117.1 (C-7), 121.4 (C-5' or C-3''), 122.0 (C-5' or C-3''), 124.0 (C-5), 124.3 (C-4''), 124.5 (C-4a), 129.3 (C-8), 129.5 (d, $J = 8.5$ Hz, C-2''', C-6'''), 131.0 (d, $J = 3.1$ Hz, C-1'''), 133.8 (C-6 or C-3'), 134.5 (C-6 or C-3'), 137.4 (C-4' or C-6''), 137.4 (C-4' or C-6''), 141.9 (C-8a), 145.5 (C-2''), 148.1 (C-2'), 151.2 (C-6'), 151.4 (C-5''), 157.5 (C-2), 160.0 ($\underline{\text{CO}_2\text{Et}}$), 162.4 ($\underline{\text{CONH}}$), 162.9 (d, $J = 247.7$ Hz, C-4'''), 177.6 (C-4). ¹⁹F NMR (565 MHz, CDCl_3) δ -112.8. LC–MS (m/z): positive mode 575 [$\text{M} + \text{H}$]⁺. Purity by HPLC–UV (254 nm)–ESI-MS: not determined due to low solubility.

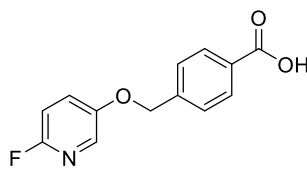


6-(6-Chloropyridin-3-yl)-8-(5-((4-fluorobenzyl)oxy)picolinamido)-4-oxo-4H-chromene-2-carboxylic acid (89h, LW500, PSB-19500). The compound was synthesized using **77i** (50 mg, 0.087 mmol) and was isolated as a white solid (31 mg, 65% yield). ^1H NMR (600 MHz, $\text{DMSO-}d_6$) δ 5.27 (s, 2H, OCH_2), 6.92 (s, 1H, 3-H), 7.14 – 7.34 (m, 2H, 3''-H, 5''-H), 7.55 (s, 2H, 2'''-H, 6'''-H), 7.60 (d, $J = 7.9$, 1H, 5'-H), 7.69 (d, $J = 7.0$ Hz, 1H, 4''-H), 7.92 (s, 1H, 7-H), 8.11 (d, $J = 8.1$ Hz, 1H, 4'-H), 8.15 (d, $J = 6.5$ Hz, 1H, 6''-H), 8.34 (s, 1H, 5-H), 8.72 (s, 1H, 3''-H), 8.94 (s, 1H, 2'-H), 10.58 (s, 1H, CONH). ^{13}C NMR (151 MHz, $\text{DMSO-}d_6$) δ 69.6 (OCH_2), 113.7 (C-3), 115.6 (d, $J = 21.6$ Hz, C-3''', C-5'''), 117.1 (C-7), 122.5 (C-5' or C-3''), 122.6 (C-5' or C-3''), 124.0 (C-5), 124.3 (C-4a), 124.7 (C-4''), 129.0 (C-8), 130.5 (d, $J = 8.4$ Hz, C-2''', C-6'''), 132.3 (d, $J = 2.5$ Hz, C-1'''), 133.2 (C-6 or C-3'), 133.7 (C-6 or C-3'), 137.2 (C-4' or C-6''), 138.1 (C-4' or C-6''), 141.2 (C-8a), 146.2 (C-2''), 148.0 (C-2'), 150.1 (C-6'), 152.9 (C-5''), 157.6 (C-2), 161.1 (CO_2H), 162.0 (CONH), 162.1 (d, $J = 244.4$ Hz, C-4'''), 177.2 (C-4). ^{19}F NMR (565 MHz, $\text{DMSO-}d_6$) δ -113.8. LC-MS (m/z): positive mode 546 [$\text{M} + \text{H}$] $^+$. Purity by HPLC-UV (254 nm)-ESI-MS: 96.9 %. Mp: 257-258 $^\circ\text{C}$.

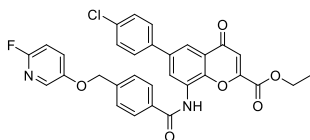
Preparation of 90a



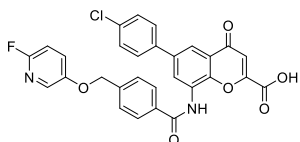
Methyl 4-(((6-fluoropyridin-3-yl)oxy)methyl)benzoate (83a, LW505). The compound was synthesized using 6-fluoropyridin-3-ol (1.0 g, 8.8 mmol) and methyl 4-(bromomethyl)benzoate (3.1 g, 13.3 mmol). The resulting solid was further purified by column chromatography (4:1 petroleum ether/EtOAc). **83a** was isolated as a white solid (2.1 g, 90% yield). ^1H NMR (600 MHz, CDCl_3) δ 3.91 (s, 3H, CO_2CH_3), 5.13 (s, 2H, OCH_2), 6.85 (dd, $J = 3.5, 8.9$ Hz, 1H, 5'-H), 7.32 – 7.41 (m, 1H, 4'-H), 7.45 – 7.51 (m, 2H, 3-H, 5-H), 7.84 – 7.90 (m, 1H, 2'-H), 8.01 – 8.09 (m, 2H, 2-H, 6-H). ^{13}C NMR (151 MHz, CDCl_3) δ 52.2 (CO_2CH_3), 70.4 (OCH_2), 109.7 (d, $J = 40.3$ Hz, C-5'), 127.0 (C-3, C-5), 128.1 (d, $J = 8.1$ Hz, C-4'), 130.0 (C-2, C-6), 130.0 (C-1), 133.3 (d, $J = 15.5$ Hz, C-2'), 140.9 (C-4), 152.6 (d, $J = 4.2$ Hz, C-3'), 158.1 (d, $J = 233.3$ Hz, C-6'), 166.6 (CO_2Me). LC-MS (m/z): positive mode 262 [$\text{M} + \text{H}$] $^+$. Purity by HPLC-UV (254 nm)-ESI-MS: 97.6 %.



4-(((6-Fluoropyridin-3-yl)oxy)methyl)benzoic acid (84a, LW506N). The compound was synthesized using **83a** (1.5 g, 5.74 mmol) and was isolated as a white solid (825 mg, 87% yield). ^1H NMR (600 MHz, $\text{DMSO-}d_6$) δ 5.25 (s, 2H, OCH_2), 7.11 (dd, $J = 3.3, 8.9$ Hz, 1H, 5'-H), 7.55 (d, $J = 8.1$ Hz, 2H, 3-H, 5-H), 7.63 – 7.70 (m, 1H, 4'-H), 7.91 – 8.02 (m, 3H, 2-H, 6-H, 2'-H), 12.95 (s, 1H, CO_2H). ^{13}C NMR (151 MHz, $\text{DMSO-}d_6$) δ 69.9 (OCH_2), 110.0 (d, $J = 40.8$ Hz, C-5'), 127.7 (C-3, C-5), 128.8 (d, $J = 8.3$ Hz, C-4'), 129.7 (C-2, C-6), 130.6 (C-1), 133.8 (d, $J = 15.7$ Hz, C-2'), 141.5 (C-4), 153.0 (d, $J = 4.1$ Hz, C-3'), 157.5 (d, $J = 229.3$ Hz, C-6'), 167.2 (CO_2H). ^{19}F NMR (565 MHz, $\text{DMSO-}d_6$) δ -78.0. LC-MS (m/z): positive mode 248 [$\text{M} + \text{H}$] $^+$. Purity by HPLC-UV (254 nm)-ESI-MS: 99.0 %.

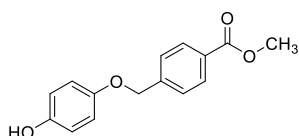


Ethyl 6-(4-chlorophenyl)-8-(4-(((6-fluoropyridin-3-yl)oxy)methyl)benzamido)-4-oxo-4H-chromene-2-carboxylate (77j, LW507). **84a** (144 mg, 0.582 mmol) was mixed with dry DCM (5 mL), and thionyl chloride (850 μ L, 11.64 mmol) was added at rt. Then, the mixture was refluxed for 2 h. After that, the residue was suspended in dry DCM (3 mL) and added dropwise to a cooled solution of **75d** (100 mg, 0.291 mmol) and DIPEA (253 μ L, 1.455 mmol) in dry THF (5 mL) at 0 °C under inert gas atmosphere. The mixture was stirred at that temperature for 1 h. After that, stirring continued at rt for 24 h. After that, the solvents were evaporated under reduced pressure and the residue was purified by column chromatography (9:1 DCM/EtOAc). **77j** was isolated as a white solid (145 mg, 87% yield). ^1H NMR (600 MHz, DMF- d_7) δ 1.37 (t, J = 7.1 Hz, 3H, $\text{CO}_2\text{CH}_2\text{CH}_3$), 4.44 (q, J = 7.1 Hz, 2H, $\text{CO}_2\text{CH}_2\text{CH}_3$), 5.41 (s, 2H, OCH_2), 7.05 (s, 1H, 3-H), 7.17 (dd, J = 3.4, 8.9 Hz, 1H, 5'''-H), 7.61 – 7.65 (m, 2H, 3''-H, 5''-H), 7.74 – 7.80 (m, 3H, 5-H, 3'-H, 5'-H), 7.85 – 7.89 (m, 2H, 2''-H, 6''-H), 8.04 – 8.09 (m, 1H, 7-H), 8.15 (d, J = 2.3 Hz, 1H, 4'''-H), 8.23 (d, J = 8.2 Hz, 2H, 2'-H, 6'-H), 8.70 (d, J = 2.3 Hz, 1H, 2'''-H), 10.29 (s, 1H, CONH). ^{13}C NMR (151 MHz, DMF- d_7) δ 14.1 ($\text{CO}_2\text{CH}_2\text{CH}_3$), 63.6 ($\text{CO}_2\text{CH}_2\text{CH}_3$), 70.8 (OCH_2), 110.4 (d, J = 41.0 Hz, C-5'''), 114.5 (C-3), 119.0 (C-4'''), 125.6 (C-4a), 128.4 (C-5), 128.4 (C-3'', C-5''), 128.7 (C-2', C-6'), 129.3 (d, J = 8.4 Hz, C-2'''), 129.5 (C-2'', C-6''), 130.0 (C-3', C-5'), 130.1 (C-8), 134.4 (C-6), 134.5 (C-7), 134.6 (C-4'), 137.5 (C-1''), 138.3 (C-4''), 141.8 (C-1'), 149.1 (C-8a), 152.7 (C-2), 153.9 (d, J = 4.2 Hz, C-3'''), 158.9 (d, J = 229.8 Hz, C-6'''), 160.7 (CO_2Et), 166.1 (CONH), 177.9 (C-4). ^{19}F NMR (565 MHz, DMF- d_7) δ -79.2. LC-MS (m/z): positive mode 573 [$\text{M} + \text{H}$] $^+$. Purity by HPLC-UV (254 nm)-ESI-MS: 97.6 %.

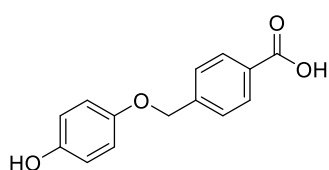


6-(4-Chlorophenyl)-8-(4-(((6-fluoropyridin-3-yl)oxy)methyl)benzamido)-4-oxo-4H-chromene-2-carboxylic acid (90a, LW509). The compound was synthesized using **77j** (50 mg, 0.087 mmol). The precipitate further purified by column chromatography on a column of silica gel (4:1 DCM/MeOH). **90a** was isolated as a yellow solid (43 mg, 91% yield). ^1H NMR (600 MHz, DMSO- d_6) δ 5.27 (s, 2H, OCH_2), 6.74 (s, 1H, 3-H), 7.13 (dd, J = 3.4, 8.9 Hz, 1H, 5'''-H), 7.54 (d, J = 8.5 Hz, 2H, 3''-H, 5''-H), 7.58 (d, J = 8.1 Hz, 2H, 3'-H, 5'-H), 7.64 – 7.72 (m, 1H, 4'''-H), 7.74 (d, J = 8.5 Hz, 2H, 2''-H, 6''-H), 7.96 – 8.02 (m, 2H, 5-H, 2'''-H), 8.08 (d, J = 8.1 Hz, 2H, 2'-H, 6'-H), 8.37 (d, J = 2.2 Hz, 1H, 7-H), 10.46 (s, 1H, CONH). ^{13}C NMR (151 MHz, DMSO- d_6) δ 69.9 (OCH_2), 110.0 (d, J = 40.8 Hz, C-5'''), 110.3 (C-3), 118.3 (C-7), 124.5 (C-4a), 127.5 (C-5), 127.6 (C-3'', C-5''), 128.2 (C-3', C-5'), 128.7 (C-2'', C-6''), 128.8 (d, J = 8.2 Hz, C-4'''), 129.0 (C-8), 129.3 (C-2', C-6'), 133.0 (C-4''), 133.8 (C-4'), 133.8 (d, J = 15.8 Hz, C-2'''), 135.2 (C-1'), 137.6 (C-1''), 140.5 (C-8a), 148.8 (C-6), 153.0 (d, J = 4.0 Hz, C-3'''), 157.4 (d, J = 229.5 Hz, C-6'''), 161.6 (C-2), 161.7 (CO_2H), 165.4 (CONH), 178.4 (C-4). ^{19}F NMR (565 MHz, DMSO) δ -78.1. LC-MS (m/z): positive mode 545 [$\text{M} + \text{H}$] $^+$. Purity by HPLC-UV (254 nm)-ESI-MS: 98.2 %. Mp: 269-270 °C.

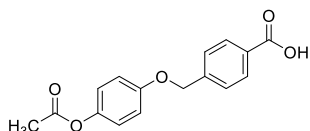
Preparation of 90b



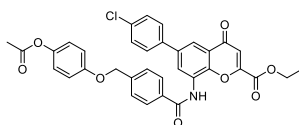
Methyl 4-((4-hydroxyphenoxy)methyl)benzoate (83b, LW481). The compound was synthesized using deoxyarbutin (3.0 g, 13.1 mmol) and methyl 4-(bromomethyl)benzoate (3.8 g, 19.7 mmol). The crude white solid (3.4 g yield) was collected and directly used for the next step. ^1H NMR (600 MHz, CDCl_3) δ 3.92 (s, 3H, CO_2CH_3), 5.06 (s, 2H, OCH_2), 6.77 (d, $J = 8.9$ Hz, 2H, 2'-H, 6'-H), 6.84 (d, $J = 8.9$ Hz, 2H, 3'-H, 5'-H), 7.49 (d, $J = 8.2$ Hz, 2H, 3-H, 5-H), 8.04 (d, $J = 8.2$ Hz, 2H, 2-H, 6-H). ^{13}C NMR (151 MHz, CDCl_3) δ 52.2 (CO_2CH_3), 70.1 (OCH_2), 116.0 (C-2', C-6'), 116.1 (C-3', C-5'), 127.0 (C-3, C-5), 129.5 (C-1), 129.8 (C-2, C-6), 142.6 (C-4), 150.0 (C-4'), 152.5 (C-1'), 167.0 (CO_2Me).



4-((4-Hydroxyphenoxy)methyl)benzoic acid (84b, LW482). The compound was synthesized using **83b** (2.0 g, 7.7 mmol). The precipitate was collected by filtration, dried, and purified by column chromatography on a column of silica gel (4:1 DCM/MeOH). **84b** was isolated as a white solid (1.7 g, 92% yield). ^1H NMR (600 MHz, $\text{DMSO}-d_6$) δ 5.06 (s, 2H, OCH_2), 6.67 (d, $J = 8.9$ Hz, 2H, 2'-H, 6'-H), 6.82 (d, $J = 8.9$ Hz, 2H, 3'-H, 5'-H), 7.52 (d, $J = 8.1$ Hz, 2H, 3-H, 5-H), 7.94 (d, $J = 8.1$ Hz, 2H, 2-H, 6-H), 8.92 (br, 1H, ArOH), 12.90 (br, 1H, CO_2H). ^{13}C NMR (151 MHz, $\text{DMSO}-d_6$) δ 69.4 (OCH_2), 115.9 (C-2', C-6'), 116.0 (C-3', C-5'), 127.4 (C-3, C-5), 129.6 (C-2, C-6), 130.2 (C-1), 142.8 (C-4), 151.1 (C-4'), 151.7 (C-1'), 167.3 (CO_2H). LC-MS (m/z): positive mode: 262 [$\text{M}+18$]. Purity by HPLC-UV (254 nm)-ESI-MS: 98.0%.

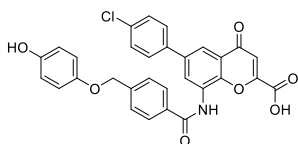


4-((4-Acetoxyphenoxy)methyl)benzoic acid (LW501). **84b** (1.10 g, 4.50 mmol) was suspended in dry THF (20 mL), and dry pyridine (360 μL , 4.50 mmol, 1 equiv.) was added. Then, acetic anhydride (470 μL , 4.95 mmol, 1.1 equiv.) was added dropwise, and the mixture was stirred for 4 h at rt. After that, the solvent was removed under reduced pressure, and the residue was purified by column chromatography (9:1 DCM/MeOH). **LW501** was isolated as a white solid (480 mg, 37% yield). ^1H NMR (600 MHz, $\text{DMSO}-d_6$) δ 2.22 (s, 3H, CH_3), 5.17 (s, 2H, OCH_2), 6.92 – 7.13 (m, 4H, 2'-H, 3'-H, 5'-H, 6'-H), 7.55 (d, $J = 8.2$ Hz, 2H, 3-H, 5-H), 7.96 (d, $J = 8.2$ Hz, 2H, 2-H, 6-H). ^{13}C NMR (151 MHz, $\text{DMSO}-d_6$) δ 20.9 (CH_3), 69.2 (OCH_2), 115.5 (C-2', C-6'), 122.8 (C-3', C-5'), 127.5 (C-3, C-5), 129.7 (C-2, C-6), 130.5 (C-1), 142.2 (C-4), 144.4 (C-4'), 155.9 (C-1'), 167.3 (CO_2H), 169.6 (MeCO_2). LC-MS (m/z): positive mode 287 [$\text{M} + \text{H}$] $^+$. Purity by HPLC-UV (254 nm)-ESI-MS: 98.2%.



Ethyl 8-(4-((4-acetoxyphenoxy)methyl)benzamido)-6-(4-chlorophenyl)-4-oxo-4H-chromene-2-carboxylate (77k, LW503). **LW501** (553 mg, 1.93 mmol) was suspended in dry DCM (20 mL), and thionyl chloride (1.40 mL, 19.30 mmol) was added at rt. Then, the mixture was refluxed for 2 h. After that, the solvent and excess SOCl_2 were removed under reduced pressure. The residue was suspended in dry DCM (10 mL). To this mixture was added dropwise a cooled solution of **75d** (333 mg, 0.97 mmol) and DIPEA (840 μL , 4.83 mmol) in dry THF (10 mL) at 0 $^\circ\text{C}$ under inert

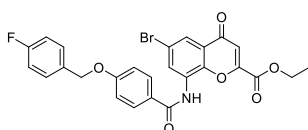
gas atmosphere. The mixture was stirred at this temperature for 1 h. After that, stirring continued at rt for 24 h. Then, the solvents were evaporated, and the residue was purified by column chromatography on a column of silica gel (8:1:1 DCM/EtOAc/petroleum ether). **77k** was isolated as a white solid (581 mg, 98% yield). ^1H NMR (600 MHz, DMF- d_7) δ 1.37 (t, $J = 7.1$ Hz, 3H, $\text{CO}_2\text{CH}_2\text{CH}_3$), 2.28 (s, 3H, CH_3), 4.44 (q, $J = 7.0$ Hz, 2H, $\text{CO}_2\text{CH}_2\text{CH}_3$), 5.31 (s, 2H, OCH_2), 7.05 (s, 1H, 3-H), 7.13 (s, 4H), 7.64 (d, $J = 8.2$ Hz, 2H, 2''-H, 6'''-H), 7.76 (d, $J = 7.9$ Hz, 2H, 3''-H, 5''-H), 7.88 (d, $J = 8.3$ Hz, 2H, 3'''-H, 5'''-H), 8.15 (s, 1H, 7-H), 8.23 (d, $J = 7.9$ Hz, 2H, 2'-H, 6''-H), 8.70 (s, 1H, 5-H), 10.35 (s, 1H, CONH). ^{13}C NMR (151 MHz, DMF- d_7) δ 14.1 ($\text{CO}_2\text{CH}_2\text{CH}_3$), 20.9 ($\text{CH}_3\text{CO}_2\text{Ar}$), 63.6 ($\text{CO}_2\text{CH}_2\text{CH}_3$), 70.0 (OCH_2), 114.5 (C-3), 116.1 (C-2'', C-6'''), 119.0 (C-7), 123.4 (C-3''', C-5'''), 125.6 (C-4a), 128.3 (C-3'', C-5''), 128.5 (C-5), 128.7 (C-2', C-6'), 129.5 (C-2'', C-6''), 130.0 (C-3', C-5'), 130.1 (C-8), 134.3 (C-4''), 134.4 (C-4'), 137.5 (C-1'), 138.3 (C-1''), 142.6 (C-8a), 145.5 (C-6), 149.2 (C-4'''), 152.7 (C-2), 156.9 (C-1'''), 160.7 (CO_2Et), 166.1 (CONH), 170.2 (MeCO_2Ar), 177.9 (C-4). LC-MS (m/z): positive mode 613 $[\text{M} + \text{H}]^+$. Purity by HPLC-UV (254 nm)-ESI-MS: not determined due to low solubility.



6-(4-Chlorophenyl)-8-(4-((4-hydroxyphenoxy)methyl)benzamido)-4-oxo-4H-chromene-2-carboxylic acid (90b, LW504N). **77k** (200 mg, 0.327 mmol) was mixed with THF (10 mL), and a solution of K_2CO_3 (225 mg, 1.634 mmol, 5 equiv.) in water (5 mL) was added dropwise while stirring at rt. After 72 h of stirring at rt,

THF was evaporated under reduced pressure, and water (2 mL) was added. The mixture was acidified using aq HCl (2 M, 1 mL). The precipitate was collected, washed with water, and dried (74 mg yield). Due to an incomplete reaction, 40 mg of the solid were suspended in THF (5 mL), and a solution of NaOH (1 mg) in water (1 mL) was added while stirring. The mixture was stirred at rt for 1 h. After that, THF was evaporated, and the mixture was acidified using concd. aq HCl (1 drop). The precipitate was collected by filtration, washed with water and cold ethanol, and was dried at 60 °C. **90b** was isolated as a yellow solid (25 mg yield). ^1H NMR (600 MHz, DMSO- d_6) δ 5.11 (s, 2H, OCH_2), 6.68 (d, $J = 8.9$ Hz, 2H, 2''-H, 6'''-H), 6.85 (d, $J = 8.9$ Hz, 2H, 3''-H, 5'''-H), 6.98 (s, 1H, 3-H), 7.56 (d, $J = 8.5$ Hz, 2H, 3''-H, 5''-H), 7.61 (d, $J = 8.1$ Hz, 2H, 3'-H, 5'-H), 7.80 (d, $J = 8.5$ Hz, 2H, 2''-H, 6''-H), 8.05 (d, $J = 8.1$ Hz, 2H, 2'-H, 6'-H), 8.10 (d, $J = 2.2$ Hz, 1H, 7-H), 8.41 (d, $J = 2.1$ Hz, 1H, 5-H), 8.93 (br, 1H, ArOH), 10.35 (s, 1H, CONH). ^{13}C NMR (151 MHz, DMSO- d_6) δ 69.4 (OCH_2), 113.6 (C-3), 115.9 (C-2'', C-6'''), 116.0 (C-3''', C-5'''), 118.9 (C-7), 124.8 (C-4a), 127.5 (C-3'', C-5''), 128.0 (C-2', C-6'), 128.9 (C-2'', C-6''), 129.1 (C-5), 129.1 (C-8), 129.4 (C-3', C-5'), 133.3 (C-4''), 133.4 (C-4'), 136.2 (C-1''), 137.1 (C-1'), 142.0 (C-8a), 149.1 (C-6), 151.1 (C-4'''), 151.7 (C-1'''), 153.1 (C-2), 161.3 (CO_2H), 165.5 (CONH), 177.5 (C-4). LC-MS (m/z): positive mode 542 $[\text{M} + \text{H}]^+$. Purity by HPLC-UV (254 nm)-ESI-MS: 97.1%. Mp: 272-273 °C.

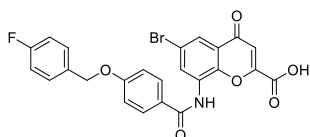
Preparation of 73, 89a, 91b, 92b, and 93b



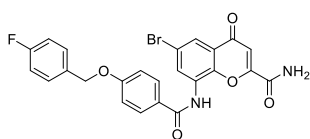
Ethyl 6-bromo-8-(4-((4-fluorobenzyl)oxy)benzamido)-4-oxo-4H-chromene-2-carboxylate (73, LW546). **82a** (1.18 g, 4.8 mmol) was mixed with dry toluene (10 mL), and thionyl chloride (7.0 mL, 96 mmol) was added at rt. Then, the mixture

was refluxed for 1 h. After that, the residue was suspended in dry DCM (5 mL) and added dropwise to a cooled solution of **71b** (1.0 g, 0.32 mmol) and Et_3N (443 μL , 3.2 mmol) in dry DCM (10 mL) at 0 °C under inert gas

atmosphere. The mixture was stirred at that temperature for 1 h and at rt for additional 24 h. After that, the solvents were evaporated under reduced pressure, and the residue was purified by column chromatography (99:1 DCM/EtOAc). **73** was isolated as a white solid (1.06 g, 61% yield). ¹H NMR (500 MHz, DMSO-*d*₆) δ 1.29 (t, *J* = 7.1 Hz, 3H, CO₂CH₂CH₃), 4.37 (q, *J* = 7.1 Hz, 2H, CO₂CH₂CH₃), 5.22 (s, 2H, OCH₂), 7.00 (s, 1H, 3-H), 7.16 – 7.24 (m, 4H, 3'-H, 5'-H, 3''-H, 5''-H), 7.52 (ddd, *J* = 2.5, 5.3, 8.4 Hz, 2H, 2''-H, 6''-H), 7.93 (d, *J* = 2.3 Hz, 1H, 7-H), 7.96 – 8.02 (m, 2H, 2'-H, 6'-H), 8.38 (d, *J* = 2.3 Hz, 1H, 5-H), 9.88 (s, 1H, CONH). ¹³C NMR (126 MHz, DMSO-*d*₆) δ 13.5 (CO₂CH₂CH₃), 62.6 (OCH₂), 68.9 (CO₂CH₂CH₃), 113.5 (C-3), 114.7 (C-3', C-5'), 115.0 (d, *J* = 21.6 Hz, C-3'', C-5''), 117.7 (C-6), 122.4 (C-7), 125.2 (C-4a), 125.9 (C-1'), 129.4 (C-2', C-6'), 129.7 (d, *J* = 8.3 Hz, C-2'', C-6''), 130.3 (C-8), 131.0 (C-5), 132.7 (d, *J* = 2.7 Hz, C-1''), 147.5 (C-8a), 151.8 (C-2), 159.4 (CO₂Et), 161.4 (C-4'), 162.1 (d, *J* = 244.0 Hz, C-4''), 164.6 (CONH), 175.7 (C-4). LC-MS (*m/z*): positive mode 542 [M + H]⁺. Purity by HPLC-UV (254 nm)-ESI-MS: 98.0 %. Mp: 223-224 °C.

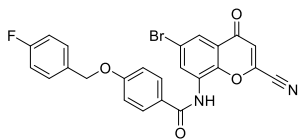


6-Bromo-8-(4-((4-fluorobenzyl)oxy)benzamido)-4-oxo-4H-chromene-2-carboxylic acid (89a, LW547). The compound was synthesized using **73** (625 mg, 1.16 mmol) and was isolated as a white solid (561 mg, 95% yield). ¹H NMR (500 MHz, DMSO-*d*₆) δ 5.20 (s, 2H, OCH₂), 6.97 (s, 1H, 3-H), 7.16 – 7.20 (m, 2H, 3'-H, 5'-H), 7.20 – 7.26 (m, 2H, 3''-H, 5''-H), 7.50 – 7.56 (m, 2H, 2''-H, 6''-H), 7.95 (d, *J* = 2.4 Hz, 1H, 7-H), 7.97 – 8.02 (m, 2H, 2'-H, 6'-H), 8.32 (d, *J* = 2.4 Hz, 1H, 5-H), 10.15 (s, 1H, CONH). ¹³C NMR (126 MHz, DMSO-*d*₆) δ 69.0 (OCH₂), 113.6 (C-3), 114.9 (C-3', C-5'), 115.5 (d, *J* = 21.3 Hz, C-3'', C-5''), 117.8 (C-6), 123.0 (C-7), 125.6 (C-4a), 126.1 (C-1'), 129.9 (C-2', C-6'), 130.2 (d, *J* = 8.4 Hz, C-2'', C-6''), 130.5 (C-8), 132.1 (C-5), 133.0 (d, *J* = 2.8 Hz, C-1''), 148.2 (C-8a), 153.4 (C-2), 161.1 (C-4'), 161.6 (CO₂H), 162.1 (d, *J* = 243.9 Hz, C-4''), 165.0 (CONH), 176.4 (C-4). ¹⁹F NMR (565 MHz, DMSO-*d*₆) δ -114.2. LC-MS (*m/z*): positive mode 514 [M + H]⁺. Purity by HPLC-UV (254 nm)-ESI-MS: 98.9 %. Mp: 252-253 °C. (Lit. mp: 239 – 240 °C)¹⁸⁶



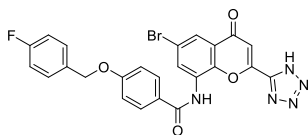
6-Bromo-8-(4-((4-fluorobenzyl)oxy)benzamido)-4-oxo-4H-chromene-2-carboxamide (91b, LW550). **89a** (300 mg, 0.59 mmol) was mixed with dry DCM (20 mL), thionyl chloride (425 μL, 5.9 mmol, 10 equiv.), and DMF (5 drops). After that, the mixture was refluxed for 30 min. Then, the solvents and excess SOCl₂ were removed under reduced pressure. The residue was dissolved in dry DCM (10 mL) and cooled to 0°C under inert gas atmosphere. Gaseous ammonia was bubbled through the solution for 1 h at that temperature. Then, the solvent was removed under reduced pressure, and the residue was washed with water (10 mL) and methanol (10 mL), and dried at 60°C. **91b** was isolated as a white solid (150 mg, 50% yield). ¹H NMR (600 MHz, DMSO-*d*₆) δ 5.21 (s, 2H, OCH₂), 6.88 (s, 1H, 3-H), 7.14 – 7.19 (m, 2H, 3'-H, 5'-H), 7.20 – 7.27 (m, 2H, 3''-H, 5''-H), 7.48 – 7.56 (m, 2H, 2''-H, 6''-H), 7.88 (d, *J* = 2.3 Hz, 1H, 7-H), 7.93 – 8.00 (m, 2H, 2'-H, 6'-H), 8.23 (s, 1H, CONH₂), 8.64 (d, *J* = 2.3 Hz, 1H, 5-H), 8.67 (s, 1H, CONH₂). ¹³C NMR (151 MHz, DMSO-*d*₆) δ 68.9 (OCH₂), 111.1 (C-3), 114.7 (C-3', C-5'), 115.5 (d, *J* = 21.3 Hz, C-3'', C-5''), 117.9 (C-6), 121.9 (C-7), 125.5 (C-4a), 126.7 (C-1'), 129.9 (C-5), 130.2 (d, *J* = 8.0 Hz, C-2'', C-6''), 130.3 (C-8), 130.3 (C-2', C-6'), 133.0 (d, *J* = 3.1 Hz, C-1''), 146.1 (C-8a), 156.2 (C-2), 160.7 (C-4'), 161.5 (CONH), 162.0 (d, *J* = 243.6 Hz, C-4''), 166.0 (CONH₂), 176.0 (C-4). ¹⁹F NMR (565 MHz, DMSO-*d*₆) δ -

115.0. LC–MS (m/z): positive mode 513 $[M + H]^+$. Purity by HPLC–UV (254 nm)–ESI-MS: 96.6 %. Mp: 295–296 °C.



6-Bromo-8-((4-(4-fluorobenzyl)oxy)benzamido)-4-oxo-4H-chromene-2-carbonitrile (92b, LW551). **91b** (100 mg, 0.196 mmol) was mixed with dry DMF (5 mL) and cooled to 0 °C. At this temperature, POCl₃ (91 μL, 0.978 mmol, 5 equiv.) was added while stirring under inert gas atmosphere. After that, the mixture was stirred

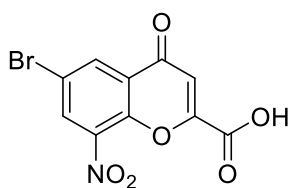
at rt for overnight. Then, it was poured onto crushed ice and extracted using DCM (3 × 50 mL). The organic layers were combined, dried using Na₂SO₄, and concentrated under reduced pressure. The resulting residue was further purified by column chromatography on a column of silica gel (4:1 petroleum ether/EtOAc). **92b** was isolated as a yellow solid (55 mg, 57% yield). ¹H NMR (600 MHz, DMSO-*d*₆) δ 5.20 (s, 2H, OCH₂), 7.17 – 7.20 (m, 2H, 3'-H, 5'-H), 7.21 – 7.27 (m, 2H, 3''-H, 5''-H), 7.45 (s, 1H, 3-H), 7.50 – 7.56 (m, 2H, 2''-H, 6''-H), 7.91 (d, *J* = 2.4 Hz, 1H, 7-H), 7.96 – 8.00 (m, 2H, 2'-H, 6'-H), 8.42 (d, *J* = 2.4 Hz, 1H, 5-H), 10.35 (s, 1H, CONH). ¹³C NMR (151 MHz, DMSO-*d*₆) δ 68.9 (OCH₂), 112.4 (CN), 114.9 (C-3', C-5'), 115.5 (d, *J* = 21.6 Hz, C-3'', C-5''), 118.4 (C-6), 120.5 (C-3), 122.7 (C-7), 125.7 (C-4a), 126.0 (C-1'), 130.1 (C-8), 130.2 (C-2', C-6'), 130.2 (d, *J* = 8.8 Hz, C-2'', C-6''), 132.0 (C-5), 133.0 (d, *J* = 3.1 Hz, C-1''), 137.2 (C-2), 148.0 (C-8a), 161.6 (C-4'), 162.0 (d, *J* = 244.2 Hz, C-4''), 165.5 (CONH), 174.5 (C-4). ¹⁹F NMR (565 MHz, DMSO-*d*₆) δ -115.0. LC–MS (m/z): positive mode 495 $[M + H]^+$. Purity by HPLC–UV (254 nm)–ESI-MS: 97.3 %. Mp: 229–230 °C.



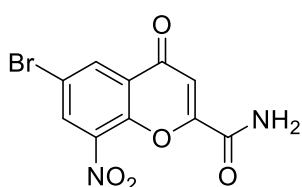
N-(6-Bromo-4-oxo-2-(1H-tetrazol-5-yl)-4H-chromen-8-yl)-4-((4-fluorobenzyl)oxy)benzamide (93b, LW552). **92b** (22 mg, 0.0446 mmol) was dissolved in DMF (3 mL) and pyridinium hydrochloride (26 mg, 0.223 mmol, 5 equiv.) and

NaN₃ (14 mg, 0.223 mmol, 5 equiv.) were added while stirring at rt. Then, the mixture was heated to 100 °C for 1 h under inert gas atmosphere. After that, the mixture was cooled to 0 °C and acidified using aq HCl solution (2 M, 10 mL). (*Caution: formation of hydrazoic acid!*) The resulting precipitate was collected by filtration and washed with water. **93b** was isolated as a white solid (20 mg, 84% yield). ¹H NMR (600 MHz, DMSO-*d*₆) δ 5.22 (s, 2H, OCH₂), 7.17 (s, 1H, 3-H), 7.17 – 7.21 (m, 2H, 3'-H, 5'-H), 7.22 – 7.27 (m, 2H, 3''-H, 5''-H), 7.51 – 7.56 (m, 2H, 2''-H, 6''-H), 7.95 (d, *J* = 2.4 Hz, 1H, 7-H), 8.01 – 8.06 (m, 2H, 2'-H, 6'-H), 8.49 – 8.54 (m, 1H, 5-H), 10.11 (s, 1H, CONH). ¹³C NMR (151 MHz, DMSO-*d*₆) δ 68.9 (OCH₂), 110.6 (C-3), 114.8 (C-3', C-5'), 115.5 (d, *J* = 21.7 Hz, C-3'', C-5''), 118.0 (C-6), 122.4 (C-7), 125.5 (C-4a), 126.3 (C-1'), 130.2 (d, *J* = 8.5 Hz, C-2'', C-6''), 130.3 (C-2', C-6'), 130.4 (C-8), 130.6 (C-5), 133.0 (d, *J* = 2.9 Hz, C-1''), 147.3 (C-8a), 152.1 (C-2), 152.8 (C-tetrazole), 161.6 (C-4'), 161.7 (d, *J* = 244.1 Hz, C-4''), 165.5 (CONH), 175.2 (C-4). ¹⁹F NMR (565 MHz, DMSO-*d*₆) δ -115.0. LC–MS (m/z): positive mode 538 $[M + H]^+$. Purity by HPLC–UV (254 nm)–ESI-MS: 98.4 %. Mp: 230–231 °C.

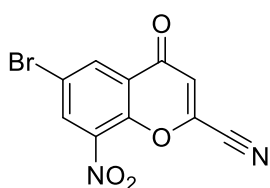
Preparation of 70, 92a, and 93a



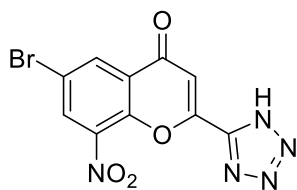
6-Bromo-8-nitro-4-oxo-4H-chromene-2-carboxylic acid (70, LW538N). **69b** (3.72 g, 11 mmol) was mixed with glacial acetic acid (25 mL) and aq HCl (6M, 25 mL). The mixture was refluxed for 2 h until a clear solution formed. After that, heating and stirring was stopped and the mixture was allowed to reach rt slowly. The crystallized product was collected by filtration, washed with water, and dried at 50 °C. **70** was isolated as a white solid (2.77 g, 80%). ¹H NMR (600 MHz, DMSO-*d*₆) δ 7.04 (s, 1H, 3-H), 8.40 (d, *J* = 2.5 Hz, 1H, 7-H), 8.74 (d, *J* = 2.5 Hz, 1H, 5-H). ¹³C NMR (151 MHz, DMSO-*d*₆) δ 114.4 (C-3), 117.2 (C-6), 126.8 (C-4a), 132.5 (C-7), 133.0 (C-5), 140.1 (C-8), 146.8 (C-8a), 153.6 (C-2), 160.8 (C=O), 175.3 (C-4). LC-MS (*m/z*): positive mode 316 [M + H]⁺. Purity by HPLC-UV (254 nm)-ESI-MS: 95.6 %. Mp: 228-229 °C.



6-Bromo-8-nitro-4-oxo-4H-chromene-2-carboxamide (91a, LW540N). **70** (3.04 g, 9.67 mmol) was mixed with dry DCM (50 mL), thionyl chloride (14 mL, 193.5 mmol, 20 equiv.), and dry DMF (10 drops), and refluxed for 1 h. Then, the solvents and excess SOCl₂ were evaporated under reduced pressure, and the residue was dissolved in dry DCM (20 mL). The solution was cooled to 0 °C and gaseous ammonia was bubbled through it for 1 h while stirring. After that, the solvent was removed, and the residue was washed with water (20 mL) and ethanol (20 mL). **91a** was isolated as a white solid (1.68 g, 56% yield). ¹H NMR (600 MHz, DMSO-*d*₆) δ 6.97 (s, 1H, 3-H), 7.96 (s, 1H, CONH₂), 8.28 (s, 1H, CONH₂), 8.41 (d, *J* = 2.3 Hz, 1H, 7-H), 8.73 (d, *J* = 2.4 Hz, 1H, 5-H). ¹³C NMR (151 MHz, DMSO-*d*₆) δ 111.6 (C-3), 117.1 (C-6), 126.7 (C-4a), 132.7 (C-7), 133.1 (C-5), 139.9 (C-8), 146.5 (C-8a), 156.0 (C-2), 160.2 (C=O), 175.0 (C-4). LC-MS (*m/z*): positive mode 315 [M + H]⁺. Purity by HPLC-UV (254 nm)-ESI-MS: 96.1 %.



6-Bromo-8-nitro-4-oxo-4H-chromene-2-carbonitrile (92a, LW541C). **91a** (1.1 g, 3.2 mmol) was suspended in dry DMF (30 mL) and cooled to 0 °C under inert gas atmosphere while stirring. Then, POCl₃ was added at that temperature, and the mixture was stirred overnight at rt. After that, the solution was poured onto crushed ice and neutralized using K₂CO₃. The resulting precipitate was collected by filtration and further purified by column chromatography (4:1 petroleum ether/EtOAc). **92a** was isolated as a white solid (825 mg, 88% yield). ¹H NMR (600 MHz, DMSO-*d*₆) δ 7.61 (s, 1H, 3-H), 8.43 (d, *J* = 2.5 Hz, 1H, 7-H), 8.80 (d, *J* = 2.5 Hz, 1H, 5-H). ¹³C NMR (151 MHz, DMSO-*d*₆) δ 112.1 (C≡N), 117.8 (C-6), 121.1 (C-3), 126.9 (C-4a), 132.9 (C-7), 133.6 (C-5), 137.5 (C-2), 139.3 (C-8), 147.2 (C-8a), 173.5 (C-4). LC-MS (*m/z*): no mass detected (not ionizable). Purity by HPLC-UV (254 nm)-ESI-MS: 97.8%. Mp: 150-151 °C.



6-Bromo-8-nitro-2-(1H-tetrazol-5-yl)-4H-chromen-4-one (93a, LW542). **92a** (1.0 g, 3.39 mmol) was mixed with DMF (30 mL), pyridinium chloride (1.95 g, 16.9 mmol, 5 equiv.), and NaN₃ (1.10 g, 16.9 mmol, 5 equiv.). The mixture was heated to 100 °C for 1 h while stirring. After that, the solution was cooled to 0 °C and mixed with aq HCl (2 M, 30 mL). (*Caution: formation of hydrazoic acid!*) The

resulting solid was collected by filtration and washed with water. **93a** was isolated as a white solid (1.08 g, 94% yield). ¹H NMR (600 MHz, DMSO-*d*₆) δ 7.22 (s, 1H, 3-H), 8.44 (d, *J* = 2.4 Hz, 1H, 7-H), 8.76 (d, *J* = 2.4 Hz, 1H, 5-H). ¹³C NMR (151 MHz, DMSO-*d*₆) δ 111.0 (C-3), 117.2 (C-6), 126.9 (C-4a), 132.5 (C-7), 132.7 (C-5), 140.0 (C-8), 146.9 (C-8a), 153.3 (C-2), 154.4 (C-tetrazole), 174.0 (C-4). LC-MS (*m/z*): positive mode 338 [M + H]⁺. Purity by HPLC-UV (254 nm)-ESI-MS: 99.0%. Mp: 250-251 °C.

5.4 Biological experiments

5.4.1 G protein-coupled receptor 35

β -Arrestin recruitment assays

The experiments were performed by Dr. Dominik Thimm, MSc Beatriz Büschbell, and Miriam Diett using the PathHunter β -arrestin recruitment system (DiscoverX). Chinese hamster ovary (CHO) cells expressing a fusion protein of β -arrestin and a deletion mutant of β -galactosidase were used to express the receptor in question (human, rat, or mouse GPR35). The cell lines were either commercially available or prepared in our group. For each experiment, 20000 cells were plated in 90 μ L cell plating 2 reagent or F12 medium supplemented with fetal calf serum (FCS, 10%), penicillin G (100 U/mL) and streptomycin (100 μ g/mL) on a 96 well plate one day in advance. The F12 medium was exchanged for a medium without FCS after 24 h incubation at 37 °C and 5% CO₂ (~ 3 h before the assay). The assay was started by adding 10 μ L of agonist solution to each well (10% DMSO in cell plating 2 reagent). For antagonist assays, 5 μ L of the antagonist solution (10% in DMSO in cell plating 2 reagent) was added 30 min before 5 μ L of standard agonist (human, mouse GPR35: 5 μ M, rat GPR35: 3 μ M) was added. After 90 min of incubation, 50 μ L of detection reagent (PathHunter Detection Kit) was added followed by further incubation for 60 min. Luminescence was measured for 1 min (Berthold Mithras Plate Reader). Concentration-inhibition curves were generated in 3-4 independent experiments using GraphPad Prism 4.

Radioligand binding assay

These assays were performed using [³H]PSB-13253 in a final volume of 400 μ L (10 μ L DMSO or test compound dissolved in 100% DMSO, 190 μ L buffer (sterile 50 mM Tris-HCl, 10 mM MgCl₂, pH 7.4), 100 μ L radioligand solution (5 nM final concentration), 100 μ L membrane preparation (10 μ g protein)). The membrane preparations were diluted with a sterile buffer (50 mM Tris-HCl, 10 mM MgCl₂, pH 7.4). For competition studies, the assay solution was incubated for 100 min followed by filtration through a GF/B filter using a Brandel Harvester (Brandel, Gaithersburg, MD). Filters were washed three times (2-3 mL of ice-cold 50 mM Tris-HCl buffer (pH 7.4)) and the radioactivity was measured by scintillation counting using a Tri-

Carb 1810 TR (Perkin-Elmer, Waltham, MA). Three to four independent experiments were performed in duplicates by Dr. Dominik Thimm and Miriam Dielt.

5.4.2 G protein-coupled receptor 84

cAMP accumulation assay

These experiments were performed by Katharina Sylvester. On 24 well plates, CHO cells expressing the human GPR84 were cultured for 2 days. The medium was removed and cells were washed with Hanks' balanced salt solution (HBSS, pH 7.4). Then, the cAMP assay was performed at a final assay volume of 500 μ L. After the addition of 300 μ L HBSS to each well, 50 μ L of Ro20-1724 (phosphodiesterase inhibitor) were pipetted. After incubation for 10 min at 37°C, 50 μ L of the antagonist solution (100% DMSO) were added and incubation continued for another 60 min. To the controls with forskolin or decanoic acid, 50 μ L of HBSS was added instead. Then, 50 μ L of decanoic acid were added as agonist (or 50 μ L HBSS containing 10% DMSO as control with forskolin). After exactly 5 min of incubation, 50 μ L of forskolin were added for increased intracellular cAMP production. After another 15 min of incubation, the reaction was stopped by removing the reaction buffer and adding hot lysis buffer (500 μ L, 90 °C, 4 mM EDTA, 0.01% Triton X-100, pH 7.4, Sigma, Munich). After cooling down for 5 min, the 24 well plates were frozen at -20 °C. Then, the cell lysate was thawed and homogenized with the pipette. The lysate (50 μ L) was incubated with 30 μ L of [³H]cAMP (3 nM) and 40 μ L of cAMP binding protein (cAMP dependent protein kinase) diluted in lysis buffer for 1 h at 4 °C. After that, the mixture was filtrated using a GF/B filter and a Brandel Harvester (Brandel, Gaithersburg, MD). The radioactivity was measured by scintillation counting using a Tri-Carb 1810 TR (Perkin-Elmer, Waltham, MA). For determining cAMP concentrations, three to four independent experiments were performed.

Radioligand binding assay

The desired concentrations of the test substances were prepared, taking into account the final DMSO final concentration and dilution in the assay were prepared. Of these, 10 μ l each were placed in duplicates in prepared 3.5 ml reaction tubes, as well as 10 μ l DMSO for the determination of total binding and 10 μ l of [³H]PSB1584 in DMSO (10 μ M) for the determination of nonspecific binding. To each reaction tube, 190 μ l of assay buffer was added

followed by 100 μ l of radioligand dissolved in 50 mM Tris-buffer, 10 mM $MgCl_2$, pH 7.4 with a concentration of 1-10 nM. The CHO- β -arrestin-GPR84 membrane preparation was diluted with 50 mM Tris-buffer, 10 mM $MgCl_2$, pH 7.4, such that 10-50 μ g of protein was used per reaction tube, depending on the grade of the membrane preparation. The reaction mixtures were incubated for 2.5 hours at 25°C in a water bath. The incubation time was 3.5 hours. Subsequent filtration through GF-C filters separated the bound radioligand from the free one. The filters were washed three times with 2 ml ice-cold 50 mM Tris-buffer, pH 7.4. The filter discs were transferred to scintillation vials, mixed with 2.5 ml of scintillation cocktail and measured in the LSC counter after 9 h of incubation. For the evaluation of the experiment, the specific binding of the radioligand in the presence of the different concentrations of the test substances was determined and displayed graphically. To determine the specific binding of the radioligand, the values of non-specific binding (cpm) obtained in the experiment were subtracted from the values of total binding and the values obtained for the different concentrations of the test substances. The program Graph Pad Prism was used to generate a sigmoidal inhibition curve from which an IC_{50} or K_i values was calculated corresponding to affinity of the test substance for the receptor. Assays were performed by Katharina Sylvester.

6 List of abbreviations

[³⁵ S]GTP γ S	[³⁵ S]guanosine 5'- <i>O</i> -(γ -thio)triphosphate
2'FL	2- <i>O</i> -fucosyllactose
6-OAU	6-octylaminouracil
6'SL	6'- <i>O</i> -sialyllactose
7TM	seven transmembrane
AC	adenylate cyclase
AD	Alzheimer's disease
AhR	arylhydrocarbon receptor
Akt	protein kinase B
AMPK	AMP-activated protein kinase
aq	aqueous
BRET	bioluminescence resonance energy transfer
cAMP	3',5'-cyclic adenosine monophosphate
Cas9	CRISPR-associated protein-9
cGMP	3',5'-cyclic guanosine monophosphate
CHO	Chinese hamster ovary
CL _{int}	intrinsic clearance
compd	compound
conc	concentrated
CRISPR	clustered regularly interspaced short palindromic repeat
CST-14	cortistatin-14
CXCL	chemokine (C-X-C motif) ligand
CXCR	CXC-chemokine receptor
DAG	diacylglycerol
DCM	dichloromethane
dec.	decomposition
DHICA	5,6-dihydroxyindole-2-carboxylic acid
DIPEA	<i>N,N</i> -diisopropylethylamine
DMAD	dimethyl acetylenedicarboxylate
DMF	dimethylformamide
DMR	dynamic mass redistribution
DMSO	dimethyl sulfoxide
DSS	dextran sulfate sodium
EC ₅₀	half-maximal effective concentration
ECL	extracellular loop
E _{max}	maximal efficacy
ERK	extracellular signal-kinases
ESI-MS	electrospray ionization mass spectrometry
Et ₃ N	triethylamine
EtOAc	ethyl acetate
EtOH	ethanol
FFAR	free fatty acid receptor
FRET	fluorescence resonance energy transfer
GDP	guanosine diphosphate
GI	gastrointestinal
GPCR	G protein-coupled receptor
GPR	G protein-coupled receptor

GRAFS	glutamate, rhodopsin, adhesion, frizzled/taste, secretin
GRK	G protein-coupled receptor kinase
GTP	guanosine triphosphate
HA	hemagglutinin
HAc	acetic acid
HBA	hydrogen-bond acceptor
HBD	hydrogen-bond donor
HEK293	human embryonic kidney 293
HMO	human milk oligosaccharide
HPLC	high-performance liquid chromatography
HTS	high-throughput screening
IBD	inflammatory bowel disease
IC ₅₀	half-maximal inhibitory concentration
ICL	intracellular loop
IL	interleukin
IP ₃	inositol trisphosphate
K _D	dissociation constant
K _i	inhibitory constant
KO ^t Bu	potassium <i>tert</i> -butoxide
Lit. m.p.	literature melting point
LKB ₁	liver kinase B ₁
LNT	lacto- <i>N</i> -tetrose
LogD	distribution coefficient
LogP	partition coefficient (octanol:water)
LPA	lysophosphatidic acid
LPAR	lysophosphatidic acid receptor
LPI	lysophosphatidylinositol
LPS	lipopolysaccharides
MCFA	medium-chain fatty acid
MeOH	methanol
mp	melting point
MRGPRX	MAS-related G protein-coupled receptor member
mRNA	messenger ribonucleic acid
mTOR	mammalian target of rapamycin
MW	molecular weight
n.d.	not determined
NMDA	<i>N</i> -methyl-D-aspartate
NMR	nuclear magnetic resonance
o.n.	overnight
PAINS	pan assay interference structure
P _{app}	apparent permeability coefficient
PBS	phosphate buffered saline
PCA	passive cutaneous anaphylaxis
PCR	polymerase chain reaction
Pd/C	palladium on activated charcoal
PDE	phosphodiesterase
PGE	prostaglandin E
Ph ₂ O	diphenyl ether
PIP ₂	phosphatidylinositol 4,5-bisphosphate
PLC	phospholipase C
PPB	plasma protein binding

PTX	pertussis toxin
qRT-PCR	quantitative real-time polymerase chain reaction
RGS	regulators of G protein signaling
SAR	structure-activity relationship
SEM	standard error of the mean
SNP	single nucleotide polymorphism
$t_{1/2}$	half-life
T3	3,3',5-triiodothyronine
TGF	transforming growth factor
THC	tetrahydrocannabinol
THF	tetrahydrofuran
TLC	thin layer chromatography
TM	transmembrane domain
TNF	tumor necrosis factor
tPSA	topological polar surface area
XIAP	X-linked inhibitor of apoptosis protein

7 Literature

- (1) Meyer, A. Chromen-4-ones as novel potent and selective ligands for purinoceptor-related class A δ -branch orphan G protein-coupled receptors, Rheinische Friedrich-Wilhelms-Universität Bonn, Germany, 2017.
- (2) MacKenzie, A. E.; Caltabiano, G.; Kent, T. C.; Jenkins, L.; McCallum, J. E.; Hudson, B. D.; Nicklin, S. a; Fawcett, L.; Markwick, R.; Charlton, S. J.; Milligan, G. The antiallergic mast cell stabilizers lodoxamide and bufrolin as the first high and equipotent agonists of human and rat GPR35. *Mol. Pharmacol.* **2014**, *85*, 91–104.
- (3) Jenkins, L.; Brea, J.; Smith, N. J.; Hudson, B. D.; Reilly, G.; Bryant, N. J.; Castro, M.; Loza, M.-I.; Milligan, G. Identification of novel species-selective agonists of the G-protein-coupled receptor GPR35 that promote recruitment of β -arrestin-2 and activate $G\alpha_{13}$. *Biochem. J.* **2010**, *432*, 451–459.
- (4) Fredriksson, R.; Lagerström, M. C.; Lundin, L.-G.; Schiöth, H. B. The G-protein-coupled receptors in the human genome form five main families. Phylogenetic analysis, paralogon groups, and fingerprints. *Mol. Pharmacol.* **2003**, *63*, 1256–1272.
- (5) Venkatakrisnan, A. J.; Deupi, X.; Lebon, G.; Tate, C. G.; Schertler, G. F.; Babu, M. M. Molecular signatures of G-protein-coupled receptors. *Nature* **2013**, *494*, 185–194.
- (6) Milligan, G.; Kostenis, E. Heterotrimeric G-proteins: a short history. *Br. J. Pharmacol.* **2006**, *147*, 46–55.
- (7) Hendriks-Balk, M. C.; Peters, S. L. M.; Michel, M. C.; Alewijnse, A. E. Regulation of G protein-coupled receptor signalling: focus on the cardiovascular system and regulator of G protein signalling proteins. *Eur. J. Pharmacol.* **2008**, *585*, 278–291.
- (8) Lefkowitz, R. J. The superfamily of heptahelical receptors. *Nat. Cell Biol.* **2000**, *2*, 133–136.
- (9) Hill, S. J. G-protein-coupled receptors: past, present and future. *Br. J. Pharmacol.* **2006**, *147*, 27–37.
- (10) Rosenbaum, D. M.; Rasmussen, S. G. F.; Kobilka, B. K. The structure and function of G-protein-coupled receptors. *Nature* **2009**, *459*, 356–363.
- (11) Lappano, R.; Maggiolini, M. G protein-coupled receptors: novel targets for drug

- discovery in cancer. *Nat. Rev. Drug Discov.* **2011**, *10*, 47–60.
- (12) Hauser, A. S.; Attwood, M. M.; Rask-Andersen, M.; Schiöth, H. B.; Gloriam, D. E. Trends in GPCR drug discovery: new agents, targets and indications. *Nat. Rev. Drug Discov.* **2017**, *16*, 829–842.
- (13) Stapleton, M. P. Sir James Black and propranolol. The role of the basic sciences in the history of cardiovascular pharmacology. *Texas Hear. Inst. J.* **1997**, *24*, 336–342.
- (14) Rang, H. P. The receptor concept: pharmacology's big idea. *Br. J. Pharmacol.* **2006**, *147*, 9–16.
- (15) Dixon, R. A. F.; Kobilka, B. K.; Strader, D. J.; Benovic, J. L.; Dohlman, H. G.; Frielle, T.; Bolanowski, M. A.; Bennett, C. D.; Rands, E.; Diehl, R. E.; Mumford, R. A.; Slater, E. E.; Sigal, I. S.; Caron, M. G.; Lefkowitz, R. J.; Strader, C. D. Cloning of the gene and cDNA for mammalian β -adrenergic receptor and homology with rhodopsin. *Nature* **1986**, *321*, 75–79.
- (16) Lefkowitz, R. J. Seven transmembrane receptors: a brief personal retrospective. *Biochim. Biophys. Acta* **2007**, *1768*, 748–755.
- (17) Attwood, T. K.; Findlay, J. B. C. Fingerprinting G-protein-coupled receptors. *Protein Eng. Des. Sel.* **1994**, *7*, 195–203.
- (18) Kolakowski, L. F. J. GCRDb: a G-protein-coupled receptor database. *Receptors Channels* **1994**, *2*, 1–7.
- (19) Hu, G.-M.; Mai, T.-L.; Chen, C.-M. Visualizing the GPCR Network: Classification and Evolution. *Sci. Rep.* **2017**, *7*, 15495.
- (20) Fredriksson, R.; Schiöth, H. B. The repertoire of G-protein-coupled receptors in fully sequenced genomes. *Mol. Pharmacol.* **2005**, *67*, 1414–1425.
- (21) Schiöth, H. B.; Fredriksson, R. The GRAFS classification system of G-protein coupled receptors in comparative perspective. *Gen. Comp. Endocrinol.* **2005**, *142*, 94–101.
- (22) Lagerström, M. C.; Schiöth, H. B. Structural diversity of G protein-coupled receptors and significance for drug discovery. *Nat. Rev. Drug Discov.* **2008**, *7*, 339–357.
- (23) Katritch, V.; Cherezov, V.; Stevens, R. C. Structure-function of the G protein-coupled receptor superfamily. *Annu. Rev. Pharmacol. Toxicol.* **2013**, *53*, 531–556.

-
- (24) Bjarnadottir, T. K.; Gloriam, D. E.; Hellstrand, S. H.; Kristiansson, H.; Fredriksson, R.; Schioth, H. B. Comprehensive repertoire and phylogenetic analysis of the G protein-coupled receptors in human and mouse. *Genomics* **2006**, *88*, 263–273.
- (25) Palczewski, K.; Kumasaka, T.; Hori, T.; Behnke, C. A.; Motoshima, H.; Fox, B. A.; Trong, I. Le; Teller, D. C.; Okada, T.; Stenkamp, R. E.; Yamamoto, M.; Miyano, M. Crystal structure of rhodopsin: a G protein-coupled receptor. *Science* **2000**, *289*, 739–745.
- (26) Oldham, W. M.; Hamm, H. E. Heterotrimeric G protein activation by G-protein-coupled receptors. *Nat. Rev. Mol. Cell Biol.* **2008**, *9*, 60–71.
- (27) Katritch, V.; Cherezov, V.; Stevens, R. C. Diversity and modularity of G protein-coupled receptor structures. *Trends Pharmacol. Sci.* **2012**, *33*, 17–27.
- (28) Neumann, E.; Khawaja, K.; Müller-Ladner, U. G protein-coupled receptors in rheumatology. *Nat. Rev. Rheumatol.* **2014**, *10*, 429–436.
- (29) Rodbell, M. Signal transduction: evolution of an idea (Nobel Lecture). *Angew. Chemie* **1995**, *34*, 1420–1428.
- (30) Gilman, A. G. G proteins and regulation of adenylate cyclase (Nobel Lecture). *Angew. Chemie* **1995**, *34*, 1406–1419.
- (31) Simon, M. I.; Strathmann, M. P.; Gautam, N. Diversity of G proteins in signal transduction. *Science* **1991**, *252*, 802–808.
- (32) Downes, G. B.; Gautam, N. The G protein subunit gene families. *Genomics* **1999**, *62*, 544–552.
- (33) Pierce, K. L.; Premont, R. T.; Lefkowitz, R. J. Seven-transmembrane receptors. *Nat. Rev. Mol. Cell Biol.* **2002**, *3*, 639–650.
- (34) Rhee, S. G.; Bae, Y. S. Regulation of phosphoinositide-specific phospholipase C isozymes. *J. Biol. Chem.* **1997**, *272*, 15045–15048.
- (35) Kozasa, T.; Jiang, X.; Hart, M. J.; Sternweis, P. M.; Singer, W. D.; Gilman, A. G.; Bollag, G.; Sternweis, P. C. P115 RhoGEF, a GTPase activating protein for G α_{12} and G α_{13} . *Science* **1998**, *280*, 2109–2111.
- (36) Wettschureck, N.; Offermanns, S. Mammalian G proteins and their cell type specific functions. *Physiological Rev.* **2005**, *85*, 1159–1204.

- (37) Pflieger, J.; Gresham, K.; Koch, W. J. G protein-coupled receptor kinases as therapeutic targets in the heart. *Nat. Rev. Cardiol.* **2019**, *16*, 612–622.
- (38) Winstel, R.; Freund, S.; Krasel, C.; Hoppe, E.; Lohse, M. J. Protein kinase cross-talk: membrane targeting of the β -adrenergic receptor kinase by protein kinase C. *Proc. Natl. Acad. Sci. U. S. A.* **1996**, *93*, 2105–2109.
- (39) Cong, M.; Perry, S. J.; Lin, F. T.; Fraser, I. D.; Hu, L. A.; Chen, W.; Pitcher, J. A.; Scott, J. D.; Lefkowitz, R. J. Regulation of membrane targeting of the G protein-coupled receptor kinase 2 by protein kinase A and its anchoring protein AKAP79. *J. Biol. Chem.* **2001**, *276*, 15192–15199.
- (40) Khan, S. M.; Sleno, R.; Gora, S.; Zylbergold, P.; Laverdure, J.-P.; Labbé, J.-C.; Miller, G. J.; Hébert, T. E. The expanding roles of $G_{\beta\gamma}$ subunits in G protein-coupled receptor signaling and drug action. *Pharmacol. Rev.* **2013**, *65*, 545–577.
- (41) Claing, A.; Laporte, S. A.; Caron, M. G.; Lefkowitz, R. J. Endocytosis of G protein-coupled receptors: roles of G protein-coupled receptor kinases and β -arrestin proteins. *Prog. Neurobiol.* **2002**, *66*, 61–79.
- (42) Reiter, E.; Lefkowitz, R. J. GRKs and beta-arrestins: roles in receptor silencing, trafficking and signaling. *Trends Endocrinol. Metab.* **2006**, *17*, 159–165.
- (43) Cabrera-Vera, T. M.; Vanhauwe, J.; Thomas, T. O.; Medkova, M.; Preininger, A.; Mazzoni, M. R.; Hamm, H. E. Insights into G protein structure, function, and regulation. *Endocr. Rev.* **2003**, *24*, 765–781.
- (44) Gilman, A. G. G proteins: transducers of receptor-generated signals. *Annu. Rev. Biochem.* **1987**, *56*, 615–649.
- (45) De Vries, L.; Zheng, B.; Fischer, T.; Elenko, E.; Farquhar, M. G. The regulator of G protein signaling family. *Annu. Rev. Pharmacol. Toxicol.* **2000**, *40*, 235–271.
- (46) Ross, E. M.; Wilkie, T. M. GTPase-activating proteins for heterotrimeric G proteins: regulators of G protein signaling (RGS) and RGS-like proteins. *Annu. Rev. Biochem.* **2000**, *69*, 795–827.
- (47) Krupnick, J. G.; Benovic, J. L. The role of receptor kinases and arrestins in G protein-coupled receptor regulation. *Annu. Rev. Pharmacol. Toxicol.* **1998**, *38*, 289–319.
- (48) Grundmann, M.; Merten, N.; Malfacini, D.; Inoue, A.; Preis, P.; Simon, K.; Rüttiger, N.;

- Ziegler, N.; Benkel, T.; Schmitt, N. K.; Ishida, S.; Müller, I.; Reher, R.; Kawakami, K.; Inoue, A.; Rick, U.; Kühl, T.; Imhof, D.; Aoki, J.; König, G. M.; Hoffmann, C.; Gomeza, J.; Wess, J.; Kostenis, E. Lack of β -arrestin signaling in the absence of active G proteins. *Nat. Commun.* **2018**, *9*, 341.
- (49) Köse, M.; Pillaiyar, T.; Namasivayam, V.; De Filippo, E.; Sylvester, K.; Ulven, T.; Von Kügelgen, I.; Müller, C. E. An agonist radioligand for the proinflammatory lipid-activated G protein-coupled receptor GPR84 providing structural insights. *J. Med. Chem.* **2020**, *63*, 2391–2410.
- (50) O’Dowd, B. F.; Nguyen, T.; Marchese, A.; Cheng, R.; Lynch, K. R.; Heng, H. H. Q.; Kolakowski, L. F.; George, S. R. Discovery of three novel G-protein-coupled receptor genes. *Genomics* **1998**, *47*, 310–313.
- (51) Marti-Solano, M.; Crilly, S. E.; Malinverni, D.; Munk, C.; Harris, M.; Pearce, A.; Quon, T.; Mackenzie, A. E.; Wang, X.; Peng, J.; Tobin, A. B.; Ladds, G.; Milligan, G.; Gloriam, D. E.; Puthenveedu, M. A.; Babu, M. M. Combinatorial expression of GPCR isoforms affects signalling and drug responses. *Nature* **2020**, *587*, 650–656.
- (52) Okumura, S. I.; Baba, H.; Kumada, T.; Nanmoku, K.; Nakajima, H.; Nakane, Y.; Hioki, K.; Ikenaka, K. Cloning of a G-protein-coupled receptor that shows an activity to transform NIH3T3 cells and is expressed in gastric cancer cells. *Cancer Sci.* **2004**, *95*, 131–135.
- (53) Quon, T.; Lin, L.-C.; Ganguly, A.; Tobin, A. B.; Milligan, G. Therapeutic opportunities and challenges in targeting the orphan G protein-coupled receptor GPR35. *ACS Pharmacol. Transl. Sci.* **2020**, *3*, 801–812.
- (54) Ali, H.; AbdelMageed, M.; Olsson, L.; Israelsson, A.; Lindmark, G.; Hammarström, M.-L.; Hammarström, S.; Sitohy, B. Utility of G protein-coupled receptor 35 expression for predicting outcome in colon cancer. *Tumor Biol.* **2019**, *41*.
- (55) Milligan, G. Orthologue selectivity and ligand bias: translating the pharmacology of GPR35. *Trends Pharmacol. Sci.* **2011**, *32*, 317–325.
- (56) MacKenzie, A. E.; Lappin, J. E.; Taylor, D. L.; Nicklin, S. A.; Milligan, G. GPR35 as a novel therapeutic target. *Front. Endocrinol.* **2011**, *2*, 68.
- (57) Taniguchi, Y.; Tonai-Kachi, H.; Shinjo, K. Zaprinast, a well-known cyclic guanosine monophosphate-specific phosphodiesterase inhibitor, is an agonist for GPR35. *FEBS*

- Lett.* **2006**, *580*, 5003–5008.
- (58) Fallarini, S.; Magliulo, L.; Paoletti, T.; de Lalla, C.; Lombardi, G. Expression of functional GPR35 in human iNKT cells. *Biochem. Biophys. Res. Commun.* **2010**, *398*, 420–425.
- (59) Cosi, C.; Mannaioni, G.; Cozzi, A.; Carlà, V.; Sili, M.; Cavone, L.; Maratea, D.; Moroni, F. G-protein coupled receptor 35 (GPR35) activation and inflammatory pain: studies on the antinociceptive effects of kynurenic acid and zaprinast. *Neuropharmacology* **2011**, *60*, 1227–1231.
- (60) Mackenzie, A. E.; Milligan, G. The emerging pharmacology and function of GPR35 in the nervous system. *Neuropharmacology* **2017**, *113*, 661–671.
- (61) Jenkins, L.; Alvarez-Curto, E.; Campbell, K.; de Munnik, S.; Canals, M.; Schlyer, S.; Milligan, G. Agonist activation of the G protein-coupled receptor GPR35 involves transmembrane domain III and is transduced via $G\alpha_{13}$ and β -arrestin-2. *Br. J. Pharmacol.* **2011**, *162*, 733–748.
- (62) McCallum, J. E.; Mackenzie, A. E.; Divorcy, N.; Clarke, C.; Delles, C.; Milligan, G.; Nicklin, S. A. G-protein-coupled receptor 35 mediates human saphenous vein vascular smooth muscle cell migration and endothelial cell proliferation. *J. Vasc. Res.* **2015**, *52*, 383–395.
- (63) Mackenzie, A. E.; Quon, T.; Lin, L.-C.; Hauser, A. S.; Jenkins, L.; Inoue, A.; Tobin, A. B.; Gloriam, D. E.; Hudson, B. D.; Milligan, G. Receptor selectivity between the G proteins $G\alpha_{12}$ and $G\alpha_{13}$ is defined by a single leucine-to-isoleucine variation. *FASEB J.* **2019**, *33*, 5005–5017.
- (64) Oka, S.; Ota, R.; Shima, M.; Yamashita, A.; Sugiura, T. GPR35 is a novel lysophosphatidic acid receptor. *Biochem. Biophys. Res. Commun.* **2010**, *395*, 232–237.
- (65) Maravillas-Montero, J. L.; Burkhardt, A. M.; Hevezi, P. A.; Carnevale, C. D.; Smit, M. J.; Zlotnik, A. Cutting edge: GPR35/CXCR8 is the receptor of the mucosal chemokine CXCL17. *J. Immunol.* **2015**, *194*, 29–33.
- (66) Horikawa, Y.; Oda, N.; Cox, N. J.; Li, X.; Orho-Melander, M.; Hara, M.; Hinokio, Y.; Lindner, T. H.; Mashima, H.; Schwarz, P. E.; del Bosque-Plata, L.; Horikawa, Y.; Oda, Y.; Yoshiuchi, I.; Colilla, S.; Polonsky, K. S.; Wei, S.; Concannon, P.; Iwasaki, N.; Schulze, J.; Baier, L. J.; Bogardus, C.; Groop, L.; Boerwinkle, E.; Hanis, C. L.; Bell, G.

- I. Genetic variation in the gene encoding calpain-10 is associated with type 2 diabetes mellitus. *Nat. Genet.* **2000**, *26*, 163–175.
- (67) Sun, Y. V.; Bielak, L. F.; Peyser, P. A.; Turner, S. T.; Sheedy II, P. F.; Boerwinkle, E.; Kardia, S. L. R. Application of machine learning algorithms to predict coronary artery calcification with a sibship-based design. *Genet. Epidemiol.* **2008**, *32*, 350–360.
- (68) Imielinski, M.; Baldassano, R. N.; Griffiths, A.; Russell, R. K.; Annese, V.; Dubinsky, M.; Kugathasan, S.; Bradfield, J. P.; Walters, T. D.; Sleiman, P.; Kim, C. E.; Muise, A.; Wang, K.; Glessner, J. T.; Saeed, S.; Zhang, H.; Frackelton, E. C.; Hou, C.; Flory, J. H.; Otieno, G.; Hakonarson, H.; et al. Common variants at five new loci associated with early-onset inflammatory bowel disease. *Nat. Genet.* **2009**, *41*, 1335–1340.
- (69) Ellinghaus, D.; Folseraas, T.; Holm, K.; Ellinghaus, E.; Melum, E.; Balschun, T.; Laerdahl, J. K.; Shiryayev, A.; Gotthardt, D. N.; Weismüller, T. J.; Schramm, C.; Wittig, M.; Bergquist, A.; Björnsson, E.; Marschall, H.-U.; Vatn, M.; Teufel, A.; Rust, C.; Gieger, C.; Wichmann, H.-E.; Runz, H.; Sterneck, M.; Rupp, C.; Braun, F.; Weersma, R. K.; Wijmenga, C.; Ponsioen, C. Y.; Mathew, C. G.; Rutgeerts, P.; Vermeire, S.; Schrupf, E.; Hov, J. R.; Manns, M. P.; Boberg, K. M.; Schreiber, S.; Franke, A.; Karlsen, T. H. Genome-wide association analysis in Primary sclerosing cholangitis and ulcerative colitis identifies risk loci at GPR35 and TCF4. *Hepatology* **2013**, *58*, 1074–1083.
- (70) Ellinghaus, D.; Jostins, L.; Spain, S. L.; Cortes, A.; Bethune, J.; Han, B.; Park, Y. R.; Raychaudhuri, S.; Pouget, J. G.; Hübenthal, M.; Folseraas, T.; Wang, Y.; Esko, T.; Metspalu, A.; Westra, H.-J.; Franke, L.; Pers, T. H.; Weersma, R. K.; Collij, V.; D’Amato, M.; Halfvarson, J.; Jensen, A. B.; Lieb, W.; Degenhardt, F.; Forstner, A. J.; Hofmann, A.; Schreiber, S.; Mrowietz, U.; Juran, B. D.; Lazaridis, K. N.; Brunak, S.; Dale, A. M.; Trembath, R. C.; Weidinger, S.; Weichenthal, M.; Ellinghaus, E.; Elder, J. T.; Barker, J. N. W. N.; Andreassen, O. A.; McGovern, D. P.; Karlsen, T. H.; Barrett, J. C.; Parkes, M.; Brown, M. A.; Franke, A. Analysis of five chronic inflammatory diseases identifies 27 new associations and highlights disease-specific patterns at shared loci. *Nat. Genet.* **2016**, *48*, 510–518.
- (71) Liu, J. Z.; van Sommeren, S.; Huang, H.; Ng, S. C.; Alberts, R.; Takahashi, A.; Ripke, S.; Lee, J. C.; Jostins, L.; Shah, T.; Abedian, S.; Cheon, J. H.; Cho, J.; Daryani, N. E.; Franke, L.; Fuyuno, Y.; Hart, A.; Juyal, R. C.; Juyal, G.; Kim, W. H.; Morris, A. P.;

- Poustchi, H.; Newman, W. G.; Midha, V.; Orchard, T. R.; Vahedi, H.; Sood, A.; Sung, J. J. Y.; Malekzadeh, R.; Westra, H.-J.; Yamazaki, K.; Yang, S.-K.; Barrett, J. C.; Franke, A.; Alizadeh, B. Z.; Parkes, M.; B K, T.; Daly, M. J.; Kubo, M.; Anderson, C. A.; Weersma, R. K.; Consortium, I. M. S. G.; Consortium, I. I. B. D. G. Association analyses identify 38 susceptibility loci for inflammatory bowel disease and highlight shared genetic risk across populations. *Nat. Genet.* **2015**, *47*, 979–986.
- (72) Cortes, A.; Hadler, J.; Pointon, J. P.; Robinson, P. C.; Karaderi, T.; Leo, P.; Cremin, K.; Pryce, K.; Harris, J.; Lee, S.; Joo, K. Bin; Shim, S.-C.; Weisman, M.; Ward, M.; Zhou, X.; Garchon, H.-J.; Chiocchia, G.; Nossent, J.; Lie, B. A.; Førre, Ø.; Brown, M. A.; et al. Identification of multiple risk variants for ankylosing spondylitis through high-density genotyping of immune-related loci. *Nat. Genet.* **2013**, *45*, 730–738.
- (73) Wang, J.; Simonavicius, N.; Wu, X.; Swaminath, G.; Reagan, J.; Tian, H.; Ling, L. Kynurenic acid as a ligand for orphan G protein-coupled receptor GPR35. *J. Biol. Chem.* **2006**, *281*, 22021–22028.
- (74) Egerod, K. L.; Petersen, N.; Timshel, P. N.; Rekling, J. C.; Wang, Y.; Liu, Q.; Schwartz, T. W.; Gautron, L. Profiling of G protein-coupled receptors in vagal afferents reveals novel gut-to-brain sensing mechanisms. *Mol. Metab.* **2018**, *12*, 62–75.
- (75) Farooq, S. M.; Hou, Y.; Li, H.; O’Meara, M.; Wang, Y.; Li, C.; Wang, J.-M. Disruption of GPR35 exacerbates dextran sulfate sodium-induced colitis in mice. *Dig. Dis. Sci.* **2018**, *63*, 2910–2922.
- (76) Guo, Y. J.; Zhou, Y. J.; Yang, X. L.; Shao, Z. M.; Ou, Z. L. The role and clinical significance of the CXCL17-CXCR8 (GPR35) axis in breast cancer. *Biochem. Biophys. Res. Commun.* **2017**, *493*, 1159–1167.
- (77) Wang, W.; Han, T.; Tong, W.; Zhao, J.; Qiu, X. Overexpression of GPR35 confers drug resistance in NSCLC cells by β -arrestin/Akt signaling. *Oncotargets Ther.* **2018**, *11*, 6249–6257.
- (78) Schneditz, G.; Elias, J. E.; Pagano, E.; Zaeem Cader, M.; Saveljeva, S.; Long, K.; Mukhopadhyay, S.; Arasteh, M.; Lawley, T. D.; Dougan, G.; Bassett, A.; Karlsen, T. H.; Kaser, A.; Kaneider, N. C. GPR35 promotes glycolysis, proliferation, and oncogenic signaling by engaging with the sodium potassium pump. *Sci. Signal.* **2019**, *12*, eaau9048.
- (79) Min, K.-D.; Asakura, M.; Liao, Y.; Nakamaru, K.; Okazaki, H.; Takahashi, T.; Fujimoto,

- K.; Ito, S.; Takahashi, A.; Asanuma, H.; Yamazaki, S.; Minamino, T.; Sanada, S.; Seguchi, O.; Nakano, A.; Ando, Y.; Otsuka, T.; Furukawa, H.; Isomura, T.; Takashima, S.; Mochizuki, N.; Kitakaze, M. Identification of genes related to heart failure using global gene expression profiling of human failing myocardium. *Biochem. Biophys. Res. Commun.* **2010**, *393*, 55–60.
- (80) Ronkainen, V.-P.; Tuomainen, T.; Huusko, J.; Laidinen, S.; Malinen, M.; Palvimo, J. J.; Ylä-Herttuala, S.; Vuolteenaho, O.; Tavi, P. Hypoxia-inducible factor 1-induced G protein-coupled receptor 35 expression is an early marker of progressive cardiac remodelling. *Cardiovasc. Res.* **2014**, *101*, 69–77.
- (81) Divorcy, N.; Milligan, G.; Graham, D.; Nicklin, S. A. The orphan receptor GPR35 contributes to angiotensin II-induced hypertension and cardiac dysfunction in mice. *Am. J. Hypertens.* **2018**, *31*, 1049–1058.
- (82) Ohshiro, H.; Tonai-Kachi, H.; Ichikawa, K. GPR35 is a functional receptor in rat dorsal root ganglion neurons. *Biochem. Biophys. Res. Commun.* **2008**, *365*, 344–348.
- (83) Berlinguer-Palmini, R.; Masi, A.; Narducci, R.; Cavone, L.; Maratea, D.; Cozzi, A.; Sili, M.; Moroni, F.; Mannaioni, G. GPR35 activation reduces Ca²⁺ transients and contributes to the kynurenic acid-dependent reduction of synaptic activity at CA3-CA1 synapses. *PLoS One* **2013**, *8*, e82180.
- (84) Alkondon, M.; Pereira, E. F. R.; Todd, S. W.; Randall, W. R.; Lane, M. V; Albuquerque, E. X. Functional G-protein-coupled receptor 35 is expressed by neurons in the CA1 field of the hippocampus. *Biochem. Pharmacol.* **2015**, *93*, 506–518.
- (85) Usoskin, D.; Furlan, A.; Islam, S.; Abdo, H.; Lönnnerberg, P.; Lou, D.; Hjerling-Leffler, J.; Haeggström, J.; Kharchenko, O.; Kharchenko, P. V; Linnarsson, S.; Ernfors, P. Unbiased classification of sensory neuron types by large-scale single-cell RNA sequencing. *Nat. Neurosci.* **2015**, *18*, 145–153.
- (86) Resta, F.; Masi, A.; Sili, M.; Laurino, A.; Moroni, F.; Mannaioni, G. Kynurenic acid and zaprinast induce analgesia by modulating HCN channels through GPR35 activation. *Neuropharmacology* **2016**, *108*, 136–143.
- (87) Rojewska, E.; Ciapała, K.; Mika, J. Kynurenic acid and zaprinast diminished CXCL17-evoked pain-related behaviour and enhanced morphine analgesia in a mouse neuropathic pain model. *Pharmacol. Reports* **2019**, *71*, 139–148.

- (88) Guo, J.; Williams, D. J.; Puhl, H. L.; Ikeda, S. R. Inhibition of N-Type calcium channels by activation of GPR35, an orphan receptor, heterologously expressed in rat sympathetic neurons. *J. Pharmacol. Exp. Ther.* **2008**, *324*, 342–351.
- (89) Alexander, S. P. H.; Christopoulos, A.; Davenport, A. P.; Kelly, E.; Mathie, A.; Peters, J. A.; Veale, E. L.; Armstrong, J. F.; Faccenda, E.; Harding, S. D.; Pawson, A. J.; Sharman, J. L.; Southan, C.; Davies, J. A.; Collaborators, C. THE CONCISE GUIDE TO PHARMACOLOGY 2019/20: G protein-coupled receptors. *Br. J. Pharmacol.* **2019**, *176* (S1), S21–S141.
- (90) Stone, T. W. Does kynurenic acid act on nicotinic receptors? An assessment of the evidence. *J. Neurochem.* **2020**, *152*, 627–649.
- (91) Divorty, N.; Mackenzie, A. E.; Nicklin, S. A.; Milligan, G. G protein-coupled receptor 35: an emerging target in inflammatory and cardiovascular disease. *Front. Pharmacol.* **2015**, *6*, 41.
- (92) Thimm, D.; Funke, M.; Meyer, A.; Müller, C. E. 6-Bromo-8-(4-[³H]methoxybenzamido)-4-oxo-4H-chromene-2-carboxylic acid: a powerful tool for studying orphan G protein-coupled receptor GPR35. *J. Med. Chem.* **2013**, *56*, 7084–7099.
- (93) Deng, H.; Hu, H.; Fang, Y. Multiple tyrosine metabolites are GPR35 agonists. *Sci Rep* **2012**, *2*, 373.
- (94) Southern, C.; Cook, J. M.; Neetoo-Isseljee, Z.; Taylor, D. L.; Kettleborough, C. A.; Merritt, A.; Bassoni, D. L.; Raab, W. J.; Quinn, E.; Wehrman, T. S.; Davenport, A. P.; Brown, A. J.; Green, A.; Wigglesworth, M. J.; Rees, S. Screening β -arrestin recruitment for the identification of natural ligands for orphan G-protein-coupled receptors. *J. Biomol. Screen.* **2013**, *18*, 599–609.
- (95) Davis, P. J.; Goglia, F.; Leonard, J. L. Nongenomic actions of thyroid hormone. *Nat. Rev. Endocrinol.* **2016**, *12*, 111–121.
- (96) Park, S. J.; Lee, S. J.; Nam, S. Y.; Im, D. S. GPR35 mediates Iodoxamide-induced migration inhibitory response but not CXCL17-induced migration stimulatory response in THP-1 cells; is GPR35 a receptor for CXCL17? *Br. J. Pharmacol.* **2018**, *175*, 154–161.
- (97) Binti Mohd Amir, N. A. S.; Mackenzie, A. E.; Jenkins, L.; Boustani, K.; Hillier, M. C.;

- Tsuchiya, T.; Milligan, G.; Pease, J. E. Evidence for the existence of a CXCL17 receptor distinct from GPR35. *J. Immunol.* **2018**, *201*, 714–724.
- (98) Foata, F.; Sprenger, N.; Rochat, F.; Damak, S. Activation of the G-protein coupled receptor GPR35 by human milk oligosaccharides through different pathways. *Sci. Rep.* **2020**, *10*, 16117.
- (99) Gibson, A. Phosphodiesterase 5 inhibitors and nitrenergic transmission—from zaprinast to sildenafil. *Eur. J. Pharmacol.* **2001**, *411*, 1–10.
- (100) Neetoo-Isseljee, Z.; MacKenzie, A. E.; Southern, C.; Jerman, J.; McIver, E. G.; Harries, N.; Taylor, D. L.; Milligan, G. High-throughput identification and characterization of novel, species-selective GPR35 agonists. *J. Pharmacol. Exp. Ther.* **2013**, *344*, 568–578.
- (101) Zhao, P.; Sharir, H.; Kapur, A.; Cowan, A.; Geller, E. B.; Adler, M. W.; Seltzman, H. H.; Reggio, P. H.; Heynen-Genel, S.; Sauer, M.; Chung, T. D. Y.; Bai, Y.; Chen, W.; Caron, M. G.; Barak, L. S.; Abood, M. E. Targeting of the orphan receptor GPR35 by pamoic acid: a potent activator of extracellular signal-regulated kinase and β -arrestin2 with antinociceptive activity. *Mol. Pharmacol.* **2010**, *78*, 560–568.
- (102) Jenkins, L.; Harries, N.; Lappin, J. E.; MacKenzie, A. E.; Neetoo-Isseljee, Z.; Southern, C.; McIver, E. G.; Nicklin, S. A.; Taylor, D. L.; Milligan, G. Antagonists of GPR35 display high species ortholog selectivity and varying modes of action. *J. Pharmacol. Exp. Ther.* **2012**, *343*, 683–695.
- (103) Yang, Y.; Lu, J. Y. L.; Wu, X.; Summer, S.; Whoriskey, J.; Saris, C.; Reagan, J. D. G-protein-coupled receptor 35 is a target of the asthma drugs cromolyn disodium and nedocromil sodium. *Pharmacology* **2010**, *86*, 1–5.
- (104) Deng, H.; Hu, H.; He, M.; Hu, J.; Niu, W.; Ferrie, A. M.; Fang, Y. Discovery of 2-(4-methylfuran-2(5H)-ylidene)malononitrile and thieno[3,2-*b*]thiophene-2-carboxylic acid derivatives as G protein-coupled receptor 35 (GPR35) agonists. *J. Med. Chem.* **2011**, *2*, 7385–7396.
- (105) Deng, H.; Fang, Y. Synthesis and agonistic activity at the GPR35 of 5,6-dihydroxyindole-2-carboxylic acid analogues. *ACS Med. Chem. Lett.* **2012**, *3*, 550–554.
- (106) Yang, Y.; Fu, A.; Wu, X.; Reagan, J. D. GPR35 is a target of the loop diuretic drugs bumetanide and furosemide. *Pharmacology* **2012**, *89*, 13–17.

- (107) Willis, E. F.; Clough, G.; Church, M. Investigation into the mechanisms by which nedocromil sodium, frusemide and bumetanide inhibit the histamine-induced itch and flare response in human skin in vivo. *Clin. Exp. Allergy* **2004**, *34*, 450–455.
- (108) Funke, M.; Thimm, D.; Schiedel, A. C.; Müller, C. E. 8-Benzamidochromen-4-one-2-carboxylic acids: potent and selective agonists for the orphan G protein-coupled receptor GPR35. *J. Med. Chem.* **2013**, *56*, 5182–5197.
- (109) Wei, L.; Wang, J.; Zhang, X.; Wang, P.; Zhao, Y.; Li, J.; Hou, T.; Qu, L.; Shi, L.; Liang, X.; Fang, Y. Discovery of 2*H*-chromen-2-one derivatives as G protein-coupled receptor-35 agonists. *J. Med. Chem.* **2017**, *60*, 362–372.
- (110) Wei, L.; Hou, T.; Lu, C.; Wang, J.; Zhang, X.; Fang, Y.; Zhao, Y.; Feng, J.; Li, J.; Qu, L.; Piao, H.; Liang, X. SAR studies of N-[2-(1*H*-tetrazol-5-yl)phenyl]benzamide derivatives as potent G protein-coupled receptor-35 agonists. *ACS Med. Chem. Lett.* **2018**, *9*, 422–427.
- (111) Mackenzie, A. E. An investigation of the molecular pharmacology of G protein-coupled receptor 35, University of Glasgow, Scotland, 2015.
- (112) Heynen-Genel, S.; Dahl, R.; Shi, S.; Sauer, M.; Hariharan, S.; Sergienko, E.; Dad, S.; Chung, T.; Stonich, D.; Su, Y.; Caron, M.; Zhao, P.; Abood, M.; Barak, L. *Selective GPR35 Antagonists - Probes 1 & 2*; NIH Molecular Libraries Program, 2010.
- (113) Heynen-Genel, S.; Dahl, R.; Shi, S.; Sauer, M.; Hariharan, S.; Sergienko, E.; Dad, S.; Chung, T. D. Y.; Stonich, D.; Su, Y.; Zhao, P.; Caron, M. G.; Abood, M. E.; Barak, L. S. *Selective GPR35 Antagonists - Probe 3*; NIH Molecular Libraries Program, 2011.
- (114) Tsukahara, T.; Hamouda, N.; Utsumi, D.; Matsumoto, K.; Amagase, K.; Kato, S. G protein-coupled receptor 35 contributes to mucosal repair in mice via migration of colonic epithelial cells. *Pharmacol. Res.* **2017**, *123*, 27–39.
- (115) Kim, M.-J.; Park, S.-J.; Nam, S.-Y.; Im, D.-S. Lodoxamide attenuates hepatic fibrosis in mice: involvement of GPR35. *Biomol. Ther.* **2020**, *28*, 92–97.
- (116) Chen, K.; He, L.; Li, Y.; Li, X.; Qiu, C.; Pei, H.; Yang, D. Inhibition of GPR35 preserves mitochondrial function after myocardial infarction by targeting calpain 1/2. *J. Cardiovasc. Pharmacol.* **2020**, *75*, 556–563.
- (117) Yousefi, S.; Cooper, P. P. R.; Potter, S. L.; Mueck, B.; Jarai, G. Cloning and expression

- analysis of a novel G-protein-coupled receptor selectively expressed on granulocytes. *J. Leukoc. Biol.* **2001**, *69*, 1045–1052.
- (118) Wittenberger, T.; Schaller, H. C.; Hellebrand, S. An expressed sequence tag (EST) data mining strategy succeeding in the discovery of new G-protein coupled receptors. *J. Mol. Biol.* **2001**, *307*, 799–813.
- (119) Venkataraman, C.; Kuo, F. The G-protein coupled receptor, GPR84 regulates IL-4 production by T lymphocytes in response to CD3 crosslinking. *Immunol. Lett.* **2005**, *101*, 144–153.
- (120) Gaidarov, I.; Anthony, T.; Gatlin, J.; Chen, X.; Mills, D.; Solomon, M.; Han, S.; Semple, G.; Unett, D. J. Embelin and its derivatives unravel the signaling, proinflammatory and antiatherogenic properties of GPR84 receptor. *Pharmacol. Res.* **2018**, *131*, 158–198.
- (121) Wang, J.; Wu, X.; Simonavicius, N.; Tian, H.; Ling, L. Medium-chain fatty acids as ligands for orphan G protein-coupled receptor GPR84. *J. Biol. Chem.* **2006**, *281*, 34457–34464.
- (122) Bouchard, C.; Pagé, J.; Bédard, A.; Tremblay, P.; Vallières, L. G protein-coupled receptor 84, a microglia-associated protein expressed in neuroinflammatory conditions. *Glia* **2007**, *55*, 790–800.
- (123) Lattin, J. E.; Schroder, K.; Su, A. I.; Walker, J. R.; Zhang, J.; Wiltshire, T.; Saijo, K.; Glass, C. K.; Hume, D. A.; Kellie, S.; Sweet, M. J. Expression analysis of G protein-coupled receptors in mouse macrophages. *Immunome Res.* **2008**, *4*, 5.
- (124) Wojciechowicz, M. L.; Ma'ayan, A. GPR84: an immune response dial? *Nat. Rev. Drug Discov.* **2020**, *19*, 374.
- (125) Recio, C.; Lucy, D.; Purvis, G. S. D.; Iveson, P.; Zeboudj, L.; Iqbal, A. J.; Lin, D.; O'Callaghan, C.; Davison, L.; Griesbach, E.; Russell, A. J.; Wynne, G. M.; Dib, L.; Monaco, C.; Greaves, D. R. Activation of the immune-metabolic receptor GPR84 enhances inflammation and phagocytosis in macrophages. *Front. Immunol.* **2018**, *9*, 1419.
- (126) Mancini, S. J.; Mahmud, Z. Al; Jenkins, L.; Bolognini, D.; Newman, R.; Barnes, M.; Edye, M. E.; McMahan, S. B.; Tobin, A. B.; Milligan, G. On-target and off-target effects of novel orthosteric and allosteric activators of GPR84. *Sci. Rep.* **2019**, *9*, 1861.

- (127) Muredda, L.; Kępczyńska, M. A.; Zaibi, M. S.; Alomar, S. Y.; Trayhurn, P. IL-1 β and TNF α inhibit GPR120 (FFAR4) and stimulate GPR84 (EX33) and GPR41 (FFAR3) fatty acid receptor expression in human adipocytes: implications for the anti-inflammatory action of n-3 fatty acids. *Arch. Physiol. Biochem.* **2018**, *124*, 97–108.
- (128) Zaibi, M. S.; Kępczyńska, M. A.; Harikumar, P.; Alomar, S. Y.; Trayhurn, P. IL-33 stimulates expression of the GPR84 (EX33) fatty acid receptor gene and of cytokine and chemokine genes in human adipocytes. *Cytokine* **2018**, *110*, 189–193.
- (129) Nikaido, Y.; Koyama, Y.; Yoshikawa, Y.; Furuya, T.; Takeda, S. Mutation analysis and molecular modeling for the investigation of ligand-binding modes of GPR84. *J. Biochem.* **2015**, *157*, 311–320.
- (130) Mahmud, Z. A.; Jenkins, L.; Ulven, T.; Labéguère, F.; Gosmini, R.; De Vos, S.; Hudson, B. D.; Tikhonova, I. G.; Milligan, G. Three classes of ligands each bind to distinct sites on the orphan G protein-coupled receptor GPR84. *Sci. Rep.* **2017**, *7*, 17953–17967.
- (131) Ichimura, A.; Hirasawa, A.; Hara, T.; Tsujimoto, G. Free fatty acid receptors act as nutrient sensors to regulate energy homeostasis. *Prostaglandins Other Lipid Mediat.* **2009**, *89*, 82–88.
- (132) Tikhonova, I. G. Application of GPCR structures for modelling of free fatty acid receptors - Free fatty acid receptors. In *Handbook of experimental pharmacology*; Milligan, G., Kimura, I., Eds.; Springer: Cham, 2016; pp 57–77.
- (133) Hara, T.; Kashihara, D.; Ichimura, A.; Kimura, I.; Tsujimoto, G.; Hirasawa, A. Role of free fatty acid receptors in the regulation of energy metabolism. *Biochim. Biophys. Acta* **2014**, *1841*, 1292–1300.
- (134) Cornish, J.; MacGibbon, A.; Lin, J.-M.; Watson, M.; Callon, K. E.; Tong, P. C.; Dunford, J. E.; van der Does, Y.; Williams, G. A.; Grey, A. B.; Naot, D.; Reid, I. R. Modulation of osteoclastogenesis by fatty acids. *Endocrinology* **2008**, *149*, 5688–5695.
- (135) Wauquier, F.; Philippe, C.; Léotoing, L.; Mercier, S.; Davicco, M.-J.; Lebecque, P.; Guicheux, J.; Pilet, P.; Miot-Noirault, E.; Poitout, V.; Alquier, T.; Coxam, V.; Wittrant, Y. The free fatty acid receptor G protein-coupled receptor 40 (GPR40) protects from bone loss through inhibition of osteoclast differentiation. *J. Biol. Chem.* **2013**, *288*, 6542–6551.
- (136) Cartoni, C.; Yasumatsu, K.; Ohkuri, T.; Shigemura, N.; Yoshida, R.; Godinot, N.; le

- Coutre, J.; Ninomiya, Y.; Damak, S. Taste preference for fatty acids is mediated by GPR40 and GPR120. *J. Neurosci.* **2010**, *30*, 8376–8382.
- (137) Hong, Y.-H.; Nishimura, Y.; Hishikawa, D.; Tsuzuki, H.; Miyahara, H.; Gotoh, C.; Choi, K.-C.; Feng, D. D.; Chen, C.; Lee, H.-G.; Katoh, K.; Roh, S.-G.; Sasaki, S. Acetate and propionate short chain fatty acids stimulate adipogenesis via GPCR43. *Endocrinology* **2005**, *146*, 5092–5099.
- (138) Nøhr, M. K.; Pedersen, M. H.; Gille, A.; Egerod, K. L.; Engelstoft, M. S.; Husted, A. S.; Sichlau, R. M.; Grunddal, K. V; Poulsen, S. S.; Han, S.; Jones, R. M.; Offermanns, S.; Schwartz, T. W. GPR41/FFAR3 and GPR43/FFAR2 as cosensors for short-chain fatty acids in enteroendocrine cells vs FFAR3 in enteric neurons and FFAR2 in enteric leukocytes. *Endocrinology* **2013**, *154*, 3552–3564.
- (139) Hirasawa, A.; Tsumaya, K.; Awaji, T.; Katsuma, S.; Adachi, T.; Yamada, M.; Sugimoto, Y.; Miyazaki, S.; Tsujimoto, G. Free fatty acids regulate gut incretin glucagon-like peptide-1 secretion through GPR120. *Nat. Med.* **2005**, *11*, 90–94.
- (140) Nagasaki, H.; Kondo, T.; Fuchigami, M.; Hashimoto, H.; Sugimura, Y.; Ozaki, N.; Arima, H.; Ota, A.; Oiso, Y.; Hamada, Y. Inflammatory changes in adipose tissue enhance expression of GPR84, a medium-chain fatty acid receptor: TNF α enhances GPR84 expression in adipocytes. *FEBS Lett.* **2012**, *286*, 368–372.
- (141) Suzuki, M.; Takaishi, S.; Nagasaki, M.; Onozawa, Y.; Iino, I.; Maeda, H.; Komai, T.; Oda, T. Medium-chain fatty acid-sensing receptor, GPR84, is a proinflammatory receptor. *J. Biol. Chem.* **2013**, *288*, 10684–10691.
- (142) Kaspersen, M. H.; Jenkins, L.; Dunlop, J.; Milligan, G.; Ulven, T. Succinct synthesis of saturated hydroxy fatty acids and in vitro evaluation of all hydroxylauric acids on FFA1, FFA4 and GPR84. *Medchemcomm* **2017**, *8*, 1360–1365.
- (143) Peters, A.; Rabe, P.; Krumbholz, P.; Kalwa, H.; Kraft, R.; Schöneberg, T.; Stäubert, C. Natural biased signaling of hydroxycarboxylic acid receptor 3 and G protein-coupled receptor 84. *Cell Commun. Signal.* **2020**, *18*, 31.
- (144) Suckow, A. T.; Briscoe, C. P. Key questions for translation of FFA receptors: from pharmacology to medicines BT - free fatty acid receptors; Milligan, G., Kimura, I., Eds.; Springer International Publishing: Cham, 2017; pp 101–131.
- (145) Ulven, T.; Christiansen, E. Dietary fatty acids and their potential for controlling

- metabolic diseases through activation of FFA4/GPR120. *Annu. Rev. Nutr.* **2015**, *35*, 239–263.
- (146) Nicol, L. S. C.; Dawes, J. M.; La Russa, F.; Didangelos, A.; Clark, A. K.; Gentry, C.; Grist, J.; Davies, J. B.; Malcangio, M.; McMahon, S. B. The role of G-protein receptor 84 in experimental neuropathic pain. *J. Neurosci.* **2015**, *35*, 8959–8969.
- (147) Sundqvist, M.; Christenson, K.; Holdfeldt, A.; Gabl, M.; Mårtensson, J.; Björkman, L.; Dieckmann, R.; Dahlgren, C.; Forsman, H. Similarities and differences between the responses induced in human phagocytes through activation of the medium chain fatty acid receptor GPR84 and the short chain fatty acid receptor FFA2R. *Biochim. Biophys. acta. Mol. cell Res.* **2018**, *1865*, 695–708.
- (148) Pillaiyar, T.; Köse, M.; Sylvester, K.; Weighardt, H.; Thimm, D.; Borges, G.; Förster, I.; Von Kügelgen, I.; Müller, C. E. Diindolylmethane derivatives: potent agonists of the immunostimulatory orphan G protein-coupled receptor GPR84. *J. Med. Chem.* **2017**, *60*, 3636–3655.
- (149) Huang, Q.; Feng, D.; Liu, K.; Wang, P.; Xiao, H.; Wang, Y.; Zhang, S.; Liu, Z. A medium-chain fatty acid receptor Gpr84 in zebrafish: expression pattern and roles in immune regulation. *Dev. Comp. Immunol.* **2014**, *45*, 252–258.
- (150) Dupont, S.; Arijis, I.; Blanque, R.; Laukens, D.; Nys, K.; Ceccotti, M. C.; Merciris, D.; De Vos, S.; Mate, O.; Parent, I.; De Vriendt, V.; Labeguere, F.; Galien, R.; Devos, M.; Rutgeerts, P.; Vandeghinste, N.; Vermeire, S.; Brys, R. GPR84 inhibition as a novel therapeutic approach in IBD: mechanistic and translational studies. *J. Crohn's Colitis* **2015**, *9*, S92–S93.
- (151) Puengel, T.; De Vos, S.; Hundertmark, J.; Kohlhepp, M.; Guldiken, N.; Pujuguet, P.; Auberval, M.; Marsais, F.; Shoji, K. F.; Saniere, L.; Trautwein, C.; Luedde, T.; Strnad, P.; Brys, R.; Clément-Lacroix, P.; Tacke, F. The medium-chain fatty acid receptor GPR84 mediates myeloid cell infiltration promoting steatohepatitis and fibrosis. *J. Clin. Med.* **2020**, *9*, 1140.
- (152) Gagnon, L.; Leduc, M.; Thibodeau, J. F.; Zhang, M. Z.; Grouix, B.; Sarra-Bournet, F.; Gagnon, W.; Hince, K.; Tremblay, M.; Geerts, L.; Kennedy, C. R. J.; Hébert, R. L.; Gutsol, A.; Holterman, C. E.; Kamto, E.; Gervais, L.; Ouboudinar, J.; Richard, J.; Felton, A.; Laverdure, A.; Simard, J. C.; Létourneau, S.; Cloutier, M. P.; Leblond, F. A.; Abbott, S. D.; Penney, C.; Duceppe, J. S.; Zacharie, B.; Dupuis, J.; Calderone, A.; Nguyen, Q.

- T.; Harris, R. C.; Laurin, P. A newly discovered antifibrotic pathway regulated by two fatty acid receptors: GPR40 and GPR84. *Am. J. Pathol.* **2018**, *188*, 1132–1148.
- (153) Abdel-Aziz, H.; Schneider, M. GPR84 and TREM-1 signaling contribute to the pathogenesis of reflux esophagitis. *Mol. Med.* **2016**, *21*, 1011–1024.
- (154) Audoy-Rémus, J.; Bozoyan, L.; Dumas, A.; Filali, M.; Lecours, C.; Lacroix, S.; Rivest, S.; Tremblay, M. E.; Vallières, L. GPR84 deficiency reduces microgliosis, but accelerates dendritic degeneration and cognitive decline in a mouse model of Alzheimer's disease. *Brain Behav. Immun.* **2015**, *46*, 112–120.
- (155) Dietrich, P. A.; Yang, C.; Leung, H. H. L.; Lynch, J. R.; Gonzales, E.; Liu, B.; Haber, M.; Norris, M. D.; Wang, J.; Wang, J. Y. GPR84 sustains aberrant β -catenin signaling in leukemic stem cells for maintenance of MLL leukemogenesis. *Blood* **2014**, *124*, 3284–3294.
- (156) Park, J.-W.; Yoon, H.-J.; Kang, W. Y.; Cho, S.; Seong, S. J.; Lee, H. W.; Yoon, Y.-R.; Kim, H.-J. G protein-coupled receptor 84 controls osteoclastogenesis through inhibition of NF- κ B and MAPK signaling pathways. *J. Cell. Physiol.* **2018**, *233*, 1481–1489.
- (157) Khalil, N.; Manganas, H.; Ryerson, C. J.; Shapera, S.; Cantin, A. M.; Hernandez, P.; Turcotte, E. E.; Parker, J. M.; Moran, J. E.; Albert, G. R.; Sawtell, R.; Hagerimana, A.; Laurin, P.; Gagnon, L.; Cesari, F.; Kolb, M. Phase 2 clinical trial of PBI-4050 in patients with idiopathic pulmonary fibrosis. *Eur. Respir. J.* **2019**, *53*, 1800663.
- (158) Vermeire, S.; Reinisch, W.; Wasko-Czopnik, D.; Van Kaem, T.; Desrivot, J.; Vanhoutte, F.; Beets, J. P610 Efficacy and safety of GLPG1205, a GPR84 antagonist, in ulcerative colitis: multi-centre proof-of-concept study. *J. Crohn's Colitis* **2017**, *11* (suppl_1), S390–S391.
- (159) Labéguère, F.; Dupont, S.; Alvey, L.; Soulas, F.; Newsome, G.; Tirera, A.; Quenehen, V.; Mai, T. T. T.; Deprez, P.; Blanqué, R.; Oste, L.; Le Tallec, S.; De Vos, S.; Hagers, A.; Vandeveld, A.; Nelles, L.; Vandervoort, N.; Conrath, K.; Christophe, T.; van der Aar, E.; Wakselman, E.; Merciris, D.; Cottreaux, C.; da Costa, C.; Saniere, L.; Clement-Lacroix, P.; Jenkins, L.; Milligan, G.; Fletcher, S.; Brys, R.; Gosmini, R. Discovery of 9-cyclopropylethynyl-2-((S)-1-[1,4]dioxan-2-ylmethoxy)-6,7-dihydropyrimido[6,1-a]isoquinolin-4-one (GLPG1205), a unique GPR84 negative allosteric modulator undergoing evaluation in a phase II clinical trial. *J. Med. Chem.* **2020**.

- (160) Gamo, K.; Kiryu-Seo, S.; Konishi, H.; Aoki, S.; Matsushima, K.; Wada, K.; Kiyama, H. G-protein-coupled receptor screen reveals a role for chemokine receptor CCR5 in suppressing microglial neurotoxicity. *J. Neurosci.* **2008**, *28*, 11980–11988.
- (161) Marsango, S.; Barki, N.; Jenkins, L.; Tobin, A. B.; Milligan, G. Therapeutic validation of an orphan G protein-coupled receptor: The case of GPR84. *Br. J. Pharmacol.* **2020**.
- (162) Pillaiyar, T.; Köse, M.; Namasivayam, V.; Sylvester, K.; Borges, G.; Thimm, D.; Von Kügelgen, I.; Müller, C. E. 6-(Ar)alkylamino-substituted uracil derivatives: lipid mimetics with potent activity at the orphan G protein-coupled receptor 84 (GPR84). *ACS Omega* **2018**, *3*, 3365–3383.
- (163) Du Toit, E.; Browne, L.; Irving-Rodgers, H.; Massa, H. M.; Fozzard, N.; Jennings, M. P.; Peak, I. R. Effect of GPR84 deletion on obesity and diabetes development in mice fed long chain or medium chain fatty acid rich diets. *Eur. J. Nutr.* **2018**, *57*, 1737–1746.
- (164) Montgomery, M. K.; Osborne, B.; Brandon, A. E.; O'Reilly, L.; Fiveash, C. E.; Brown, S. H. J.; Wilkins, B. P.; Samsudeen, A.; Yu, J.; Devanapalli, B.; Hertzog, A.; Tolun, A. A.; Kavanagh, T.; Cooper, A. A.; Mitchell, T. W.; Biden, T. J.; Smith, N. J.; Cooney, G. J.; Turner, N. Regulation of mitochondrial metabolism in murine skeletal muscle by the medium-chain fatty acid receptor Gpr84. *FASEB J.* **2019**, *33*, 12264–12276.
- (165) Zhang, Q.; Yang, H.; Li, J.; Xie, X. Discovery and characterization of a novel small-molecule agonist for medium-chain free fatty acid receptor G protein-coupled receptor 84. *J. Pharmacol. Exp. Ther.* **2016**, *357*, 337–344.
- (166) Liu, Y.; Zhang, Q.; Chen, L. H.; Yang, H.; Lu, W.; Xie, X.; Nan, F. J. Design and synthesis of 2-alkylpyrimidine-4,6-diol and 6-alkylpyridine-2,4-diol as potent GPR84 agonists. *ACS Med. Chem. Lett.* **2016**, *7*, 579–583.
- (167) Hakak, Y.; Unett, D.; Gatlin, J.; Liaw, C. W. Human G protein-coupled receptor and modulators thereof for the treatment of atherosclerosis and atherosclerotic disease and for the treatment of conditions related to MCP-1 expression. WO2007027661 A3, 2007.
- (168) Lu, H.; Wang, J.; Wang, Y.; Quiao, L.; Zhou, Y. Embelin and its role in chronic diseases. *Adv. Exp. Med. Biol.* **2016**, *928*, 397–418.
- (169) Nikolovska-Coleska, Z.; Xu, L.; Hu, Z.; Tomita, Y.; Li, P.; Roller, P. P.; Wang, R.; Fang, X.; Guo, R.; Zhang, M.; Lippman, M. E.; Yang, D.; Wang, S. Discovery of embelin as a cell-permeable, small-molecular weight inhibitor of XIAP through structure-based

- computational screening of a traditional herbal medicine three-dimensional structure database. *J. Med. Chem.* **2004**, *47*, 2430–2440.
- (170) Lee, H.; Ko, J. H.; Baek, S. H.; Nam, D.; Lee, S. G.; Lee, J.; Yang, W. M.; Um, J. Y.; Kim, S. H.; Shim, B. S.; Ahn, K. S. Embelin inhibits invasion and migration of MDA-MB-231 breast cancer cells by suppression of CXC chemokine receptor 4, matrix metalloproteinases-9/2, and epithelial-mesenchymal transition. *Phyther. Res.* **2016**, *30*, 1021–1032.
- (171) Manglik, A.; Lin, H.; Aryal, D. K.; McCorvy, J. D.; Dengler, D.; Corder, G.; Levit, A.; Kling, R. C.; Bernat, V.; Hübner, H.; Huang, X.-P.; Sassano, M. F.; Giguère, P. M.; Löber, S.; Duan, D.; Scherrer, G.; Kobilka, B. K.; Gmeiner, P.; Roth, B. L.; Shoichet, B. K. Structure-based discovery of opioid analgesics with reduced side effects. *Nature* **2016**, *537*, 185–190.
- (172) Lucy, D.; Purvis, G. S. D.; Zeboudj, L.; Chatzopoulou, M.; Recio, C.; Bataille, C. J. R.; Wynne, G. M.; Greaves, D. R.; Russell, A. J. A biased agonist at immunometabolic receptor GPR84 causes distinct functional effects in macrophages. *ACS Chem. Biol.* **2019**, *14*, 2055–2064.
- (173) Takeda, S.; Yamamoto, A.; Okada, T.; Matsumura, E.; Nose, E.; Kogure, K.; Kojima, S.; Haga, T. Identification of surrogate ligands for orphan G protein-coupled receptors. *Life Sci.* **2003**, *74*, 367–377.
- (174) Wang, T. T. Y.; Schoene, N. W.; Milner, J. A.; Kim, Y. S. Broccoli-derived phytochemicals indole-3-carbinol and 3,3'-diindolylmethane exerts concentration-dependent pleiotropic effects on prostate cancer cells: comparison with other cancer preventive phytochemicals. *Mol. Carcinog.* **2012**, *51*, 244–256.
- (175) Yin, X.-F.; Chen, J.; Mao, W.; Wang, Y.-H.; Chen, M.-H. A selective aryl hydrocarbon receptor modulator 3,3'-diindolylmethane inhibits gastric cancer cell growth. *J. Exp. Clin. Cancer Res.* **2012**, *31*, 46.
- (176) Seo, S. gwon; Shin, S. ho; Min, S.; Kwon, J. Y.; Kim, K.-H.; Lee, K. W.; Lee, H. J. 3,3'-diindolylmethane inhibits adipogenesis of 3T3-L1 preadipocytes by proteosomal degradation of cyclin D1. *FASEB J.* **2011**, *25*, 581.15.
- (177) Marques, M.; Laflamme, L.; Benassou, I.; Cissokho, C.; Guillemette, B.; Gaudreau, L. Low levels of 3,3'-diindolylmethane activate estrogen receptor α and induce

- proliferation of breast cancer cells in the absence of estradiol. *BMC Cancer* **2014**, *14*, 524.
- (178) Yin, H.; Chu, A.; Li, W.; Wang, B.; Shelton, F.; Otero, F.; Nguyen, D. G.; Caldwell, J. S.; Chen, Y. A. Lipid G protein-coupled receptor ligand identification using beta-arrestin PathHunter assay. *J. Biol. Chem.* **2009**, *284*, 12328–12338.
- (179) Labéguère, F. G.; Newsome, G. J. R.; Alvey, L. J.; Sanière, L. R. M.; Fletcher, S. R. Novel dihydropyrimidinoisoquinolinones and pharmaceutical compositions thereof for the treatment of inflammatory disorders and their preparation. WO 2013092791 A1, Jun 27, 2013.
- (180) Grouix, B.; Sarra-Bournet, F.; Leduc, M.; Simard, J.-C.; Hince, K.; Geerts, L.; Blais, A.; Gervais, L.; Laverdure, A.; Felton, A.; Richard, J.; Ouboudinar, J.; Gagnon, W.; Leblond, F. A.; Laurin, P.; Gagnon, L. PBI-4050 reduces stellate cell activation and liver fibrosis through modulation of intracellular ATP levels and the liver kinase B1/AMP-activated protein kinase/mammalian target of rapamycin pathway. *J. Pharmacol. Exp. Ther.* **2018**, *367*, 71–81.
- (181) Zheng, X.; Hu, M.; Zang, X.; Fan, Q.; Liu, Y.; Che, Y.; Guan, X.; Hou, Y.; Wang, G.; Hao, H. Kynurenic acid/GPR35 axis restricts NLRP3 inflammasome activation and exacerbates colitis in mice with social stress. *Brain Behav. Immun.* **2019**, *79*, 244–255.
- (182) Agudelo, L. Z.; Ferreira, D. M. S.; Cervenka, I.; Bryzgalova, G.; Dadvar, S.; Jannig, P. R.; Pettersson-Klein, A. T.; Lakshmikanth, T.; Sustarsic, E. G.; Porsmyr-Palmertz, M.; Correia, J. C.; Izadi, M.; Martínez-Redondo, V.; Ueland, P. M.; Midttun, Ø.; Gerhart-Hines, Z.; Brodin, P.; Pereira, T.; Berggren, P. O.; Ruas, J. L. Kynurenic acid and GPR35 regulate adipose tissue energy homeostasis and inflammation. *Cell Metab.* **2018**, *27*, 378–392.e5.
- (183) Nguyen, Q. T.; Nsaibia, M. J.; Sirois, M. G.; Calderone, A.; Tardif, J.-C.; Fen Shi, Y.; Ruiz, M.; Daneault, C.; Gagnon, L.; Grouix, B.; Laurin, P.; Dupuis, J. PBI-4050 reduces pulmonary hypertension, lung fibrosis, and right ventricular dysfunction in heart failure. *Cardiovasc. Res.* **2020**, *116*, 171–182.
- (184) Waring, W. S. Pyridoquinoline dicarboxylic acid derivatives. US3,790,577, 1974.
- (185) Hall, C. M.; Wright, J. B.; Johnson, H. G.; Taylor, A. J. Quinoline derivatives as antiallergy agents. 2. Fused-ring quinaldic acids. *J. Med. Chem.* **1977**, *20*, 1337–1343.

- (186) Funke, M. Medizinische Chemie G-Protein-gekoppelter P2Y- und verwandter Waisen-Rezeptoren: Synthese, Optimierung und Charakterisierung selektiver Liganden als pharmakologische Tools, Rheinische Friedrich-Wilhelms-Universität Bonn, Germany, 2014.
- (187) Lee, K. S.; Seo, S. H.; Lee, Y. H.; Kim, H. D.; Son, M. H.; Chung, B. Y.; Lee, J. Y.; Jin, C.; Lee, Y. S. Synthesis and biological evaluation of chromone carboxamides as calpain inhibitors. *Bioorg. Med. Chem. Lett.* **2005**, *15*, 2857—2860.
- (188) Nakai, H.; Konno, M.; Kosuge, S.; Sakuyama, S.; Toda, M.; Arai, Y.; Obata, T.; Katsube, N.; Miyamoto, T. New potent antagonists of leukotrienes C4 and D4. 1. Synthesis and structure-activity relationships. *J. Med. Chem.* **1988**, *31*, 84–91.
- (189) Thimm, D. Medizinische Chemie und molekulare Pharmakologie G-Protein-gekoppelter Purin- und verwandter Waisen-Rezeptoren. (Medicinal chemistry and molecular pharmacology of G protein-coupled purinergic and related orphan receptors.), Rheinische Friedrich-Wilhelms Universität Bonn, Germany, 2014.
- (190) Lipinski, C. A. Drug-like properties and the causes of poor solubility and poor permeability. *J. Pharmacol. Toxicol. Methods* **2000**, *44*, 235–249.
- (191) Clark, D. E. Rapid calculation of polar molecular surface area and its application to the prediction of transport phenomena. 1. Prediction of intestinal absorption. *J. Pharm. Sci.* **1999**, *88*, 807–814.

8 Acknowledgements

Firstly, I would like to express the sincerest gratitude to my doctoral advisor and committee chair, Prof. Christa Müller, who created an interdisciplinary work environment that fosters scientific creativity and personal growth. I thank her for an exciting and rewarding Ph.D. project and the countless fruitful discussions about it. I would also like to thank all of my committee members for the time invested in the evaluation of my Ph.D. thesis.

I am especially grateful to the Bonn International Graduate School of Drug Sciences (BIGS DrugS) and the German Federal Ministry of Education and Research (BMBF) for twice awarding me a generous scholarship and various travel grants to present our research at international conferences.

I would like to thank all colleagues at the Department of Medicinal and Pharmaceutical Chemistry of the University of Bonn, especially those directly involved in my main projects. Special thanks go to Dr. Thanigaimalai Pillaiyar and Dr. Anton Ivanov for sharing their invaluable expertise in chemistry with me, which has never failed to impress me. I also thank all technical assistants for their professional competence and their patience with inexperienced Ph.D. students.

I want to thank my long-term lab mate Georg Rolshoven, a skilled pharmacist and chemist, whose limitless energy was a constant source of motivation. I am also grateful to my office mates, Sophie Clemens, Jessica Nagel, and Dr. Ahmed Temirak, for their kind support during the writing of this manuscript amidst a global pandemic. I also thank my fellow assistants of the 4th semester practical courses for their reliable proficiency and stimulating discussions.

Last but not least, I would like to express my heartfelt gratitude to my family for their continuous support, frequent encouragements, and their confidence in me.

Publications

- 2021: [Pillaiyar, T.](#); [Wendt, L. L.](#); [Manickam, M.](#); Easwaran, M. The recent outbreaks of human coronaviruses: a medicinal chemistry perspective. *Med. Res. Rev.* **2021**, *41*, 72–135.
- 2019: [Wendt, L. L.](#); Thimm D.; Müller C. E. Development of potent GPR35 agonists with activity at human and rodent receptors. (Posterpräsentation, ACS National Meeting, Orlando, USA)
- 2017: [Wendt, L. L.](#); Pillaiyar, T.; Müller C. E. Synthesis of 6-substituted 1,7-phenanthroline derivatives as agonists for the orphan G protein-coupled receptor GPR35. (Posterpräsentation, International Symposium on Synthesis and Catalysis, Évora, Portugal)